



**Thermoplastic Natural Rubbers based on Natural Rubber (NR) and Ethylene Vinyl
Acetate Copolymer (EVA) with Natural Rubber-*graft*-
Poly(dimethyl(methacryloyloxymethyl)phosphonate)
(NR-*g*-PDMMMP) as Compatibilizer**

Punyanich Intharapat

**A Thesis Submitted in Fulfillment of the Requirements for
the Degree of Doctor of Philosophy
(Polymer Technology)
Graduate School
Prince of Songkla University
Pattani, Thailand**

and

**Le Grade de Docteur de l'Université du Maine
(Spécialité: Chimie et Physicochimie des Polymères)
Faculté des Sciences et Techniques
Université du Maine
Le Mans, France
2009**

Copyright of Prince of Songkla University

วิทยานิพนธ์เรื่อง	เทอร์โมพลาสติกยางธรรมชาติจากการเบลนดระหว่างยางธรรมชาติกับเอทิลีน ไวนิลอะซิเตท โดยใช้กราฟต์โคพอลิเมอร์ของยางธรรมชาติกับพอลิไคเมทิลเมทาคริไลต์ลอกซีเมทิลฟอสโฟเนตเป็นสารเพิ่มความเข้ากันได้
ผู้แต่ง	นางสาวปชญานิช อินทรพัฒน์
สาขาวิชา	เทคโนโลยีพอลิเมอร์
ปีการศึกษา	2552

บทคัดย่อ

กราฟต์โคพอลิเมอร์ของยางธรรมชาติกับพอลิไคเมทิลอะคริไลต์ลอกซีเมทิลฟอสโฟเนต พอลิไคเอทิลเมทาคริไลต์ลอกซีเมทิลฟอสโฟเนต และพอลิไคเมทิลเมทาคริไลต์ลอกซีเมทิลฟอสโฟเนตสังเคราะห์ได้โดยใช้เทคนิค"กราฟต์จาก"ในสภาวะน้ำยาง โดยใช้แสงยูวีก่อให้เกิดการเริ่มของปฏิกิริยากราฟต์โคพอลิเมอร์ไรเซชันและมีหมู่โคเอทิลไดโซโอบคาร์บาเมตเป็นตัวริเริ่มปฏิกิริยาในกระบวนการเกิดกราฟต์โคพอลิเมอร์ งานวิจัยนี้เป็นการศึกษาปัจจัยต่างๆ ที่มีผลต่อปฏิกิริยาการกราฟต์โคพอลิเมอร์ไรเซชัน ได้แก่ อัตราส่วนโดยโมลของมอนอเมอร์ต่อตัวริเริ่ม และเวลาในการทำปฏิกิริยา ต่อสัดส่วนการกราฟต์ของยางธรรมชาติกราฟต์และการเปลี่ยนแปลงมอนอเมอร์ พบว่า สัดส่วนการกราฟต์และการเปลี่ยนแปลงมอนอเมอร์มีค่าเพิ่มขึ้นเมื่อเพิ่มความเข้มข้นของมอนอเมอร์และเวลาในการทำปฏิกิริยา โดยกราฟต์โคพอลิเมอร์ของยางธรรมชาติกับไคเมทิลอะคริไลต์ลอกซีเมทิลฟอสโฟเนตที่อัตราส่วนโดยโมลของมอนอเมอร์ต่อตัวริเริ่ม เท่ากับ 7 ที่เวลาในการทำปฏิกิริยา 180 นาที จะให้สัดส่วนการกราฟต์และการเปลี่ยนแปลงมอนอเมอร์สูงที่สุด ความยาวสายโซ่เฉลี่ยของสายโซ่กราฟต์อยู่ในช่วง 9-73 สันฐานวิทยาของอนุภาคน้ำยางกราฟต์ทั้ง 3 ชนิด ด้วยเครื่องทรานสมิซชันอิเล็กตรอนไมโครสโกปีพบว่า การกราฟต์โคพอลิเมอร์ไรเซชันเป็นแบบคอร์-เชลล์ ศึกษาสมบัติเชิงความร้อนของยางธรรมชาติกราฟต์ พบว่า การสลายตัวของยางธรรมชาติกราฟต์ปรากฏ 2 ช่วง กล่าวคือ การสลายตัวช่วงแรกที่ถูกอุณหภูมิต่ำเป็นการสลายตัวของยางธรรมชาติ และช่วงที่สองเกิดการสลายตัวที่อุณหภูมิสูงกว่ายางธรรมชาติ นอกจากนี้ยังพบว่าเกิดการเกิดเถ้าเพิ่มขึ้นเมื่อสัดส่วนการกราฟต์เพิ่มขึ้น ในงานวิจัยนี้ กราฟต์โคพอลิเมอร์ของยางธรรมชาติกับพอลิไคเมทิลเมทาคริไลต์ลอกซีเมทิลฟอสโฟเนต ถูกนำมาใช้เป็นสารเพิ่มความเข้ากันได้ในการเตรียมเทอร์โมพลาสติกยางธรรมชาติจากยางธรรมชาติกับเอทิลีนไวนิลอะซิเตท โดยใช้เทคนิคการเบลนดแบบปกติและการเบลนดโดยผ่านกระบวนการไดนามิกวัลคาไนซ์ โดยศึกษาอิทธิพลต่างๆ ได้แก่ ระดับการกราฟต์ ได้แก่ 71, 80, 89 และ 95% และปริมาณของยางธรรมชาติกราฟต์ ได้แก่ 1, 3, 5, 7, 9, 12 และ 15% โดยน้ำหนักของยางธรรมชาติ ที่ใช้เป็นสาร

เพิ่มความเข้ากันได้ต่อสมบัติการไหล สมบัติพลวัต สมบัติเชิงกล สัมฐานวิทยา และสมบัติเชิงความร้อน พบว่า การใช้ยางธรรมชาติกราฟต์ที่มีสัดส่วนการกราฟต์เท่ากับ 80% ในปริมาณ 7% โดยน้ำหนักของยางธรรมชาติในการเบลนด์แบบปกติ และ 9% โดยน้ำหนักของยางธรรมชาติ ในการเบลนด์แบบไดนามิกวัลคาไนเซชัน ให้ประสิทธิภาพในการเพิ่มความเข้ากันได้ที่ดีที่สุด โดยพบว่า การใช้สารเพิ่มความเข้ากันได้ที่สภาวะดังกล่าวส่งผลให้ ความเหนียวเหนียว สมบัติความต้านทานต่อแรงดึง ความสามารถในการยืดจนขาดสูงที่สุด ในขณะเดียวกัน การยืดอยู่ตัว และแทนเดลด้าต่ำที่สุด การศึกษาสัมฐานวิทยาของการเบลนด์ที่ใช้สารเพิ่มความเข้ากันได้พบว่า ขนาดของเฟสยางลดลง อุณหภูมิการสลายตัวของพอลิเมอร์เบลนด์มีค่าสูงขึ้น นอกจากนี้ อุณหภูมิกลาสทรานซิชันของพอลิเมอร์เบลนด์ มีการเลื่อนเข้าหากันส่วนปริมาณผลึกของเอทิลีนไวนิลอะซิเตทเฟสลดลง

Titre de la Thèse	Caoutchouc Naturel Thermoplastiques à base de Caoutchouc Naturel (NR) et de Copolymère d'Éthylène - Acétate de Vinyle (EVA), Compatibilisés avec des Caoutchoucs Naturels greffés Poly(méthacryloyloxyméthylphosphonate de diméthyle) (NR- <i>g</i> -PDMAMP)
Auteur	Miss Punyanich Intharapat
Major Program	Technologie des polymères
Année	2009

RÉSUMÉ

Des copolymères greffés à base de caoutchouc naturel (NR) et de poly(acryloyloxyméthylphosphonate de diméthyle) (NR-*g*-PDMAMP), de poly(méthacryloyloxyéthylphosphonate de diméthyle) (NR-*g*-PDMMEP) et de poly(méthacryloyloxyméthylphosphonate de diméthyle) (NR-*g*-PDMMMP) ont été synthétisés en milieu latex selon la méthode dite « grafting from ». La stratégie utilisée a consisté à photopolymériser des monomères porteurs de fonctions phosphonate de diméthyle, comme l'acryloyloxyméthylphosphonate de diméthyle (DMAMP), le méthacryloyloxyéthylphosphonate de diméthyle (DMMEP) et le méthacryloyloxyméthylphosphonate de diméthyle (DMMMP), à partir de sites amorceurs photosensibles *N,N*-diéthylthiocarbamate préalablement introduits le long des chaînes 1,4-polyisoprène du caoutchouc naturel. L'augmentation de la concentration en monomère et l'augmentation du temps de réaction ont pour effet d'augmenter à la fois le taux de conversion et le taux de greffage. Les meilleurs taux de conversion et de greffage ont été obtenus avec le DMAMP en utilisant un rapport molaire [DMAMP]/[unités polyisoprène fonctionnalisées *N,N*-diéthylthiocarbamate] = 7 et un temps de réaction de 180 min. Les degrés moyens de polymérisation (\overline{DP}_n) ont été calculés par spectroscopie RMN du proton (RMN 1H) : ils varient entre 9 et 73 selon le monomère utilisé. Les analyses par Microscopie Electronique à Transmission (MET) des NR-*g*-PDMAMP, NR-*g*-PDMMEP et NR-*g*-PDMMMP ont montré des morphologies de type « core-shell ». Les analyses thermogravimétriques (ATG) effectuées sur les NR-*g*-PDMAMP, NR-*g*-PDMMEP

et NR-*g*-PDMMMP, ont montré que ceux-ci se dégradent en deux étapes : la première correspond à la décomposition des greffons porteurs de fonctions phosphonate de diméthyle, la seconde à celle du squelette caoutchouc. Dans ce cas, la température de dégradation du squelette caoutchouc est toujours supérieure à celle du caoutchouc naturel pur. Le fait que le taux de résidu observé après dégradation du squelette caoutchouc augmente avec l'augmentation du taux de greffage est aussi significatif d'un renforcement de la tenue au feu. Des études de compatibilisation des mélanges caoutchouc naturel (NR) / copolymère d'éthylène - acétate de vinyle (EVA) ont par la suite été envisagées avec le copolymère NR-*g*-PDMMMP, choisi comme agent compatibilisant. Elles ont été effectuées sur des mélanges simples 50/50 NR/EVA incorporant le NR-*g*-PDMMMP, mais aussi des mélanges 40/60 NR/EVA dynamiquement vulcanisés. Dans les deux cas, les influences du taux de greffage (71, 80, 89, et 95%) et du taux de chargement (0, 1, 3, 5, 7, 9, 12, et 15 % en poids par rapport au NR du NR-*g*-PDMMMP sur les propriétés rhéologiques, dynamiques, mécaniques, morphologiques, et thermiques ont été étudiées. Les meilleurs effets de compatibilisation ont été observés avec le copolymère NR-*g*-PDMMMP ayant un taux de greffage de 80%, pour un taux de chargement de 7% dans le cas du mélange simple 50/50 NR/EVA et de 9% dans celui du mélange dynamiquement vulcanisé 40/60 NR/EVA. Dans ces conditions, la viscosité complexe des mélanges est optimale (déviations positives), de même que la résistance et l'élongation à la rupture, alors que $\tan \delta$ (facteur d'amortissement) est minimal tension set. Les études microscopiques par SEM des mélanges ont montré une réduction de la taille des domaines. Il a aussi été noté que la stabilité thermique du mélange NR/EVA se trouve renforcée avec l'incorporation du NR-*g*-PDMMMP en tant que compatibilisant. Cet effet compatibilisant du NR-*g*-PDMMMP pour les mélanges NR/EVA a également été démontré en DSC par le rapprochement l'une vers l'autre des températures de transition vitreuse (T_g) des phases NR et EVA, ainsi que par la diminution du degré de cristallinité de la phase EVA.

Mots clés: Copolymère greffé, mélange, photopolymérisation, méthacryloyloxyméthylphosphonate de diméthyle, méthacryloyloxyéthyl-

phosphonate de diméthyle, acryloyloxyméthylphosphonate de diméthyle, caoutchouc naturel, copolymère d'éthylène - acétate de vinyle, compatibilisation.

Thesis Title	Thermoplastic Natural Rubbers based on Natural Rubber (NR) and Ethylene Vinyl Acetate Copolymer (EVA), with Natural Rubber- <i>graft</i> -Poly(dimethyl(methacryloyloxymethyl)phosphonate) (NR- <i>g</i> -PDMMMP) as Compatibilizer
Author	Miss Punyanich Intharapat
Major Program	Polymer Technology
Academic Year	2009

ABSTRACT

Graft copolymers of natural rubber and poly(dimethyl(acryloyloxymethyl)phosphonate) (NR-*g*-PDMAMP), natural rubber and poly(dimethyl(methacryloyloxyethyl)phosphonate) (NR-*g*-PDMMEP), and natural rubber and poly(dimethyl(methacryloyloxymethyl)phosphonate) (NR-*g*-PDMMMP), were prepared in latex medium via a “grafting from” methodology based on the photopolymerization of dimethyl(acryloyloxymethyl)phosphonate (DMAMP), dimethyl(methacryloyloxyethyl)phosphonate (DMMEP), and dimethyl(methacryloyloxymethyl)phosphonate (DMMMP), respectively used as phosphorus-containing monomers. The grafting polymerization was initiated from *N,N*-diethyldithiocarbamate groups previously bound in side position of the rubber chains. The effects of monomer concentration on monomer conversion and grafting rate were investigated, showing that conversion and grafting rate increased with increasing monomer concentration and reaction time. Highest conversions and grafting rates were obtained with a molar ratio $[DMAMP] / [\text{initiating units}] = 7$ for a reaction time of 180 min. Calculation of the graft average length (\overline{DP}_n) from ¹H-NMR spectra of the synthesized graft copolymers showed \overline{DP}_n values in the range of 9-73. Visualizations of NR-*g*-PDMAMP, NR-*g*-PDMMEP, and NR-*g*-PDMMMP latices by Transmission Electron Microscopy (TEM) showed core-shell morphologies. Degradation of NR-*g*-PDMAMP, NR-*g*-PDMMEP, and NR-*g*-PDMMMP occurred in two steps: decomposition of dimethylphosphonate-functionalized grafts took place prior to the second step corresponding to the decomposition of NR backbone, but the degradation temperature of this last step was higher than that of pure NR. Moreover, these graft copolymer exhibited the flame resistance as evident by increase in char

residue with increasing of grafting rate. NR-*g*-PDMMMP was selected as blend compatibilizer for NR/EVA blends by two distinct techniques: simple and dynamically cured NR/EVA blends. Influence of NR-*g*-PDMMMP of varied grafting rates (i.e., 71, 80, 89, and 95%) and various loading levels of (i.e., 0, 1, 3, 5, 7, 9, 12, and 15 wt% of NR on rheological, dynamic, mechanical, morphological, and thermal properties were investigated in the case of uncured 50/50 and dynamically cured 40/60 NR/EVA blends. The best compatibilization effect was observed with a blend incorporating a NR-*g*-PDMMMP of grafting rate equal to 80%, with a loading level of 7 wt% for uncured blend and 9 wt% for dynamically cured blend. In these conditions, the highest complex viscosity (positive deviation), tensile strength, and elongation at break, as well as the lowest values of tension set and $\tan \delta$ (damping factor), were observed. SEM micrographs of compatibilized blend showed reducing of the size of the domains. It was also noted that the thermal stability of NR/EVA blends was improved by incorporating NR-*g*-PDMMMP as a blend compatibilizer. The compatibilizing effect of the NR-*g*-PDMMMP for NR/EVA blends was also shown by the shift toward each other of the glass transition temperatures (T_g) of NR and EVA blend components and the decrease of the crystallinity degree of the EVA phase.

Key words: graft copolymer, blend, photopolymerization, dimethyl(methacryloyloxymethyl)phosphonate, dimethyl(methacryloyloxyethyl)phosphonate, dimethyl(acryloyloxymethyl)phosphonate, natural rubber, ethylene vinyl acetate copolymer, compatibilization.

ACKNOWLEDGEMENTS

I would like to take this opportunity, first and foremost, to express my heartiest thanks and deep gratitude to my best supervisor, Assoc. Prof. Dr. Charoen Nakason for his helpful guidance, valuable discussions and for giving to change to study and support throughout this research. I also would like to express my gratitude sincere thanks and appreciation accorded to my kind co-supervisor, Dr. Daniel Derouet for spending his time and his thoughtful discussions, encouragement, patience and kindness in the preparation of this thesis and manuscripts as well as for all supports my living throughout the stay at l'Université du Maine, Le Mans, France.

I am extremely grateful to Assoc. Prof. Dr. Pairote Klinpitaksa for his kindness and advice for my thesis and who was the chairperson of thesis defense and his kind comments.

I am also gratefulness to Assoc. Prof. Dr. Pranee Phinyocheep, Faculty of Science, Mahidol University for her kind comments and encouragements.

I appreciate to thank Prof. Jean-François Pilard, l'Université du Maine for his helpful suggestions and comments of the thesis defense.

I feel deeply thank Dr. Laurent Vaysse from CIRAD ((PERSYST) UMR IATE Rubber Technology Laboratory for his kind comments and helpful suggestions and who was the external examiner of the thesis defense.

Special acknowledgement is accorded to Assis. Prof. Dr. Waeasae Waehama, Assis. Prof. Dr. Adisai Rungvichaniwat and Dr. Tulyapong Tulyapitak from Prince of Songkla University, for spending their time to review and give kind recommend to thesis prior to submission as well as their assistance towards the success of this undertaking.

Sincere thanks are also extended to all lecturers, staff, lab assistants and technical assistants in Faculté des Sciences, l'Université du Maine especially the Chimie des polymers (UCO2M N°6011) for their assistance towards the success of the project who had tremendously contributed to the smooth running of the project. These include Prof. Jean-Claude Brosse, Prof. Laurent Fontaine, Dr. Frédéric Gohier, Dr. Jean-Claude Soutif, Dr. Stéphanie Legoupy, Dr. Sagrario Pascual, Dr. Véronique Montembault, Dr. Michel Thomas, Anita Loiseau, Moneger Jean-Luc and Aline Lambert for their helps, support and encouragement when I worked in UCO2M at l'Université du Maine.

My sincere thanks are also extended to all my friendly colleagues for their powerful friendship and encouragement during my stay in Le Mans, France, especially Dr. Jean-Marc Cracowski, Dr. Quang Ngoc Tran, Dr. Chuanpit Khaokong, Dr. Anuwat Saetung, Dr. Rachid Jellali, Dr. Nasreddine Kébir, Dr. Gaëlle Morandi, Dr. Stéphanie Pican, Dr. Supinya Prakanrat, Dr. Lapporn Vayachuta, Dr. Thi Hong Nhung DOAN, Dien Pham Phuoc, Sandie Pioge, Faten Sadaka and Thomas Blin.

I am grateful to all staff and all my friends in Department of Rubber Technology and Polymer Science, Faculty of Science and Technology namely Mrs Absorn Jongrakwattana, Korthun Benyahiran, Inyars Kama, Hama Sulung and Haseumao Deorao, for their moral support and invaluable advice.

I am sincere grateful to the Thailand Research Fund (TRF): Grant no: PHD/0068/2547 and the French government via the embassy in Thailand for financial support research and superb facilities during my course of study in France 2005-2008. I am also thankful the Center of Excellence in Natural Rubber Technology (and Faculty of Graduate School and Faculty of Science and Technology, Prince of Songkla University for financial support research during working in Thailand.

Finally, I would like to send my sincere gratitude to both of my lovely parents, my sister and my brother for their patient support, motivation and encouragement. The usefulness of this thesis, I dedicate to my family and all the teachers who have taught me since my childhood.

Punyanich Intharapat

CONTENTS

	Page
ABSTRACT (THAI)	iii
ABSTRACT (FRENCH)	v
ABSTRACT (ENGLISH)	viii
ACKNOWLEDGEMENTS	x
LIST OF TABLES	xvi
LIST OF FIGURES	xx
LIST OF SCHEMES	xxxvi
LIST OF ABBREVIATIONS	xxxvii

CHAPTER

1. INTRODUCTION

1.1 Background.....	1
1.2 Objectives.....	3
1.3 Research Summary.....	4
1.4 Expectation of the research.....	5

2. LITERATURE SURVEY

2.1 Introduction.....	6
2.2 Chemical modification of natural rubber.....	8
2.3 Graft copolymer.....	12
2.4 Thermoplastic elastomers (TPEs).....	17
2.5 Thermoplastic natural rubber (TPNR).....	29
2.6 Compatibilization in polymer blends.....	30

CONTENTS (continued)

	Page
3. EXPERIMENT	
3.1 Materials.....	36
3.2 Instruments.....	43
3.3 Experiments.....	47
3.4 Preparation of test specimens.....	63
3.5 Testing and characterization.....	63
 4. RESULTS AND DISCUSSION	
PART A: SYNTHESIS AND CHARACTERIZATION OF NATURAL RUBBER SUPPORT OF DIMETHYLPHOSPHONATE POLYMER GRAFTS	
4.1 Monomer synthesis.....	71
4.2 Synthesis of NR- <i>g</i> -PDMAMP, NR- <i>g</i> -PDMMEP and..... NR- <i>g</i> -PDMMMP.....	76
4.2.1 Synthesis and characterization of..... NR- <i>g</i> -PDMAMP and NR- <i>g</i> -PDMMEP.....	78
4.2.2 Synthesis and characterization of NR- <i>g</i> -PDMMMP	100
 PART B: PREPARATION OF SIMPLE BLEND BASED ON NR/EVA	
4.3 Thermodynamic of NR/EVA blends.....	125
4.4 Effect of different types of compatibilizers on properties of NR/EVA blends.....	126
4.5 Effect of grafting rate of NR- <i>g</i> -PDMMMP on properties of NR/EVA blend.....	134
4.6 Effect of concentration of graft copolymer.....	149

CONTENTS (continued)

	Page
PART C: THERMOPLASTIC VULCANIZATES (TPVs)	
4.7 Effect of blend compositions on properties of NR/EVA.. TPVs.....	159
4.8 Effect of vulcanization systems on dynamically cured.... 40/60 NR/EVA blends.....	172
4.9 Effect of different types of compatibilizers.....	192
4.10 Effect of concentration of compatibilizer.....	200
4.11 Recyclability of dynamically cured NR/EVA blends....	217
5. CONCLUSION.....	222
REFERENCES.....	233
APPENDIX.....	249
BIOGRAPHY.....	296

LIST OF TABLES

Table	Page
3.1 Some properties of EVA grade N 8038.....	39
3.2 Properties of HRJ-10518.....	41
3.3 General properties of Petroleum oil (IRM 903)..... (ASTM D5964).....	42
3.4 Polymerization condition and grafting rate of..... NR- <i>g</i> -PDMMMP.....	53
3.5 Formulation and mixing schedule of 50/50 NR/EVA blends.. with different types of compatibilizers.....	54
3.6 Formulation and mixing schedule of 50/50 NR/EVA blends.. with different grafting rate of NR- <i>g</i> -PDMMMP.....	55
3.7 Formulation and mixing schedule of 50/50 NR/EVA blends.. with various loading levels of NR- <i>g</i> -PDMMMP..... compatibilizer.....	55
3.8 Formulation and mixing schedule for preparation of..... dynamically cured NR/EVA blends with variation of..... blend ratios.....	56
3.9 Formulation used to prepare NR compound with different.... curing systems.....	57
3.10 Mixing schedule used to prepare NR compound with..... different curing systems.....	58
3.11 Formulation used to prepare NR/EVA TPVs with..... different curing system.....	59
3.12 Mixing schedule used to prepare NR/EVA TPVs with..... different curing system.....	60
3.13 Formulation and mixing schedule used to prepare..... dynamically cured 40/60 NR/EVA blends with..... different types of NR- <i>g</i> -PDMMMP blend compatibilizer.....	61

LIST OF TABLES (continued)

Table	Page	
3.14	Formulation and mixing schedule used to prepare..... NR/EVA TPVs to investigate effect of loading level..... of NR- <i>g</i> -PDMMMP blend compatibilizer.....	62
3.15	Dimensions of dumbbell die C.....	65
4.1	Assignment of ¹ H-NMR, ¹³ C-NMR and ³¹ P-NMR of NR- <i>g</i> -PDMAMP and NR- <i>g</i> -PDMMEP.....	85
4.2	Assignment of FTIR absorption peaks of NR- <i>g</i> -PDMAMP... and NR- <i>g</i> -PDMMEP.....	86
4.3	Degrees of polymerization (\overline{DP}_n) and grafting rates (GR)... of the various graft copolymers obtained.....	94
4.4	TGA characteristics of NR, PDMAMP, PDMMEP,..... NR- <i>g</i> -PDMAMP after 60 min (GR = 83 %) and..... 180 min (GR = 86 %) of grafting, and NR- <i>g</i> -PDMMEP..... after 60 min (GR = 77 %) and 180 min (GR = 80 %). of grafting, in nitrogen and oxygen atmospheres,..... respectively. Grafting conditions:..... [monomer] / [DEDT-NR units] = 7.....	97
4.5	Estimation of epoxide content (mol%) of ENR by ¹ H-NMR..	101
4.6	Compositions in units% of the <i>N,N</i> -diethyldithiocarbamate-.. functionalized NRs (DEDT-NR) obtained after addition of... DEDT-Na onto oxirane rings of ENRs.....	103
4.7	Degrees of polymerization (\overline{DP}_n) and grafting rates (GR).... of the different NR- <i>g</i> -PDMMMP graft copolymers..... coming from 4% DEDT-NR , 7.2% DEDT-NR , and..... 12% DEDT-NR , respectively. Reaction time of 60..... and 180 min and [monomer]/[DEDT-NR unit] = 1.25.....	112
4.8	Mooney viscosity of pure NR and NR- <i>g</i> -PDMMMP with..... various grafting rates.....	115

LIST OF TABLES (continued)

Table	Page
4.9 TGA characteristics of NR, PDMMMP, NR- <i>g</i> -PDMMMP... with various grafting rates (i.e., 71, 80, 89 and 95%),..... in nitrogen and oxygen atmospheres.....	120
4.10 LOI values and char residue of NR and NR- <i>g</i> -PDMMMP... with various grafting rates.....	122
4.11 Tensile and hardness properties of 50/50 NR/EVA blends... without and with four types of blend compatibilizers.....	133
4.12 TGA characteristics under nitrogen atmosphere of NR, EVA, 50/50 NR/EVA blends without compatibilizer and with..... NR- <i>g</i> -PDMMMP containing various grafting rates..... (i.e., 71, 80, 89 and 95%) as a blend compatibilizer.....	146
4.13 Tensile properties of dynamically cured NR/EVA blends... with various blend ratios.....	162
4.14 TGA data of dynamically cured NR/EVA blends with..... various blend ratio.....	169
4.15 DMTA data of dynamically cured NR/EVA blends of..... various blend ratios.....	171
4.16 Curing characteristics of static vulcanizate NR carried out.... at 150°C using sulphur, peroxide, mixed (sulphur plus peroxide), and..... phenolic curing systems, respectively.....	173
4.17 Tensile properties of NR vulcanizates with various..... vulcanization systems.....	177
4.18 Tensile and hardness properties of uncured and..... dynamic cured 40/60 NR/EVA TPVs with various types..... of vulcanization systems.....	188
4.19 Tensile properties of dynamically cured 40/60 NR/EVA..... Blend with different types of compatibilizers.....	199

LIST OF TABLES (continued)

Table		Page
4.20	Mechanical properties of 40/60 NR/EVA blends with..... various quantities of NR-g-PDMMMP.....	210
4.21	Glass transition temperature (T_g) of pure EVA, pure NR..... and their blends with various loading levels of..... NR-g-PDMMMP.....	213
4.22	The melting temperature (T_m), degree of crystallinity (X_i)... and heat of fusion (ΔH) of EVA phase in EVA and their..... blend with various quantities of NR-g-PDMMMP.....	214
4.23	TGA data of NR, pure EVA, and dynamically cured..... 40/60 NR/EVA blend without and with 5, 9 and 15 wt%..... of NR-g-PDMMMP 80% compatibilizer.....	215

LIST OF FIGURES

Figure	Page
2.1 Hydrogenation of natural rubber.....	9
2.2 Mechanism of epoxidation NR with peracid.....	10
2.3 Dibutylphosphate reaction with epoxidized 1,4-polyisoprene units of ENR in latex medium.....	11
2.4 Grafting of a second polymer onto the NR backbone.....	12
2.5 Exact graft copolymers (1) random graft copolymer..... containing identical branches randomly distributed along.... the backbone; (2) regular graft copolymer containing..... identical branches equally spaced along the backbone;..... (3) simple graft copolymer; and (4) graft copolymer with.... two trifunctional branch points.....	13
2.6 Synthesis of randomly branched graft copolymers by..... “Grafting-onto” method.....	14
2.7 Synthesis of randomly branched graft copolymers by..... “Grafting-from” method.....	14
2.8 Synthesis of randomly branched graft copolymers by..... “Grafting- through” method.....	15
2.9 Classification of TPEs.....	18
2.10 Representation of different TPE structures:..... segmented block copolymer (a), ionomer (b), and..... hard polymer/elastomer blends (c).....	18
2.11 Co-continuous structure of TPE based on simple blend..... of rubber and plastic material.....	20
2.12 Relationship between the ratio of the viscosities..... of two components and their proportion in the mixture.....	22
2.13 Effect of particle size of rubber domains on..... stress-strain properties of TPVs (a), and effect of extent..... of cure on mechanical properties and oil swell of TPVs (b)...	24

LIST OF FIGURES (continued)

Figure	Page
2.14	Morphology development of dynamic vulcanizates.....
	during mixing operation..... 25
2.15	Crosslinking of diene rubbers using sulphur cured system.... 26
2.16	Crosslinking of diene rubbers using phenolic cured system... 27
2.17	Crosslinking of diene rubbers using peroxide cured system... 28
2.18	Possible morphologies of a blend of polymer A (solid lines).. and polymer B (dashed lines): (a) miscible, (b) immiscible,... (c) partially miscible..... 32
2.19	Penetration of block or grafted-copolymer compatilizers into the I and II phase of a heterogeneous polymer blend:..... (a) diblock; (b) triblock; (c) multigraft and (d) single graft... 34
3.1	Molecular structure of HRJ-10518..... 40
3.2	Standard Die shape for cutting dumbbell specimens..... 64
3.3	Standard specimen shape for testing flammability..... according to the ISO3582..... 70
4.1	Typical NMR spectra of DMAMP..... 73
4.2	Typical NMR spectra of DMMEP..... 74
4.3	Typical NMR spectra of DMMMP..... 75
4.4	Infrared spectra of DMAMP, DMMEP, and DMMMP..... 76
4.5	¹ H-NMR spectrum of epoxidized natural rubber with..... 20 mole% epoxide..... 78
4.6	¹ H NMR spectrum of NR support of..... N,N-diethyldithiocarbamate groups with 5.5 mol%..... DEDT-NR unit..... 80
4.7	Mechanism of the addition of DEDT-Na onto the cis isomer contained in 4,5-epoxy-4-methyloctane..... 80

LIST OF FIGURES (continued)

Figure		Page
4.8	Typical ^1H -NMR spectra of (a) NR- <i>g</i> -PDMAMP and..... (b) NR- <i>g</i> -PDMMEP.....	82
4.9	Typical ^{13}C -NMR spectra of (a) NR- <i>g</i> -PDMAMP and..... (b) NR- <i>g</i> -PDMMEP.....	83
4.10	Typical ^{31}P -NMR spectra of (a) NR- <i>g</i> -PDMAMP and..... (b) NR- <i>g</i> -PDMMEP.....	84
4.11	FTIR spectra of NR- <i>g</i> -PDMAMP and NR- <i>g</i> -PDMAMP.....	86
4.12	Progress of monomer conversion and monomer conversion... in grafts (determination by weighing) for..... the photopolymerizations of DMAMP and DMMEP..... initiated from DEDT-NR with..... [monomer] / [DEDT-NR units] = 3.5.....	88
4.13	Progress of grafting rate (determined by weighing) for the... photopolymerizations of DMAMP and DMMEP initiated... from DEDT-NR with [monomer] / [DEDT-NR units] = 3.5..	88
4.14	First-order kinetic plots for the photopolymerizations..... of DMAMP and DMMEP initiated from DEDT-NR..... with [monomer] / [DEDT-NR units] = 3.5.....	90
4.15	Dependence of molecular weight (\overline{M}_n) on monomer..... conversion for the photopolymerizations of DMAMP and... DMMEP initiated from DEDT-NR with..... [monomer]/[DEDT-NR units] = 7.....	90
4.16	Comparison of the progress of the grafting rates determined.. by weighing with the one of grafting rates obtained from.... ^1H NMR for the photopolymerizations of DMAMP and..... DMMEP initiated from DEDT-NR with..... [monomer] / [DEDT-NR units] = 3.5.....	91

LIST OF FIGURES (continued)

Figure	Page	
4.17	Influence of monomer concentration and monomer structure on the progress of (a) monomer conversion,..... (b) monomer conversion in grafts, (c) grafting rate, and..... (d) \overline{DP}_n , respectively.....	93
4.18	TGA curves under nitrogen atmosphere of NR, PDMAMP,... PDMMEP, NR- <i>g</i> -PDMMEP after 60 min (GR = 77 %) and... 180 min (GR = 80 %) of grafting, and NR- <i>g</i> -PDMAMP..... after 60 min (GR = 83 %) and 180 min (GR = 86 %) of..... grafting. Grafting conditions:..... [monomer] / [DEDT-NR units] = 7.....	96
4.19	TGA curves under oxygen atmosphere of NR, PDMAMP,... PDMMEP, NR- <i>g</i> -PDMMEP after 60 min (GR = 77 %) and.. 180 min (GR = 80 %) of grafting, and NR- <i>g</i> -PDMAMP..... after 60 min (GR = 83 %) and 180 min (GR = 86 %) of..... grafting. Grafting conditions:..... [monomer] / [DEDT-NR units] = 7.....	97
4.20	DSC curves of (a) NR, (b) PDMAMP, (c) PDMMEP,..... NR- <i>g</i> -PDMMEP after (d) 60 min and (e) 180 min of..... grafting, and NR- <i>g</i> -PDMAMP after (f) 60 min and..... (g) 180 min of grafting. Grafting conditions:..... [monomer] / [DEDT-NR units] = 7.....	99
4.21	TEM micrographs of (a) natural rubber, (b) NR- <i>g</i> -PDMAMP, and (c) NR- <i>g</i> -PDMMEP. Grafting conditions: 60 min with... [monomer]/[DEDT-NR units] =7.....	100
4.22	¹ H-NMR spectra of ENR with various epoxidation levels.....	101
4.23	¹ H-NMR spectra of <i>N,N</i> -diethyldithiocarbamate-..... functionalized natural rubbers (DEDT-NRs) with various..... contents in DEDR-NR units.....	103

LIST OF FIGURES (continued)

Figure	Page	
4.24	¹ H-NMR spectra of NR-g-PDMMMPs obtained after..... photopolymerization of DMMMP initiated from..... 4% DEDT-NR during 60 min, (b) 4% DEDT-NR during 180 min, (c) 7.2% DEDT-NR during 180 min,..... and (d) 12% DEDT-NR during 180 min.....	105
4.25	Typical ¹³ C-NMR spectrum of NR-g-PDMMMP.....	106
4.26	Typical ³¹ P-NMR spectrum of NR-g-PDMMMP.....	106
4.27	IR spectra of NR-g-PDMMMP obtained after photopolymerization of DMMMP initiated from..... (a) 4% DEDT-NR during 60 min, (b) 4% DEDT-NR during.. 180 min, (c) 7.2% DEDT-NR during 180 min and..... (d) 12% DEDT-NR during 180 min.....	107
4.28	Progress of monomer conversion and monomer conversion... in grafts (determination by weighing) for..... the photopolymerizations of DMMMP initiated from..... 4% DEDT-NR, 7.2% DEDT-NR, and 12% DEDT-NR, respectively. [monomer] / [DEDT-NR units] molar ratio = 1.25	109
4.29	Progress of grafting rate (determined by weighing..... and ¹ H-NMR technique) for the photopolymerizations..... of DMMMP initiated from 4% DEDT-NR, 7.2% DEDT-NR, and 12% DEDT-NR, respectively..... [monomer] / [DEDT-NR units] molar ratio = 1.25.....	109
4.30	First-order kinetic plots for the photopolymerization of DMMMP initiated from 4% DEDT-NR, 7.2% DEDT-NR, and 12% DEDT-NR, respectively..... [monomer] / [DEDT-NR units] molar ratio = 1.25.....	110

LIST OF FIGURES (continued)

Figure	Page	
4.31	Dependence of molecular weight (\overline{M}_n) on monomer conversion for the photopolymerization of DMMMP initiated from 4% DEDT-NR , 7.2% DEDT-NR , and 12% DEDT-NR , respectively, [monomer] / [DEDT-NR units] molar ratio = 1.25	111
4.32	Evolution of degree of polymerization (\overline{DP}_n) of NR- <i>g</i> -PDMMMP initiated from 4% DEDT-NR , 7.2% DEDT-NR , and 12% DEDT-NR , respectively	112
4.33	DSC thermograms of NR- <i>g</i> -PDMMMP with various grafting rates: (a) NR-<i>g</i>-PDMMMP 71%* , (b) NR-<i>g</i>-PDMMMP 80%* , (c) NR-<i>g</i>-PDMMMP 89%* , (d) NR-<i>g</i>-PDMMMP 95%* (e) pure NR (*grafting rate in wt%)	114
4.34	Mooney viscosity of NR- <i>g</i> -PDMMMP with various grafting rates: (a) NR-<i>g</i>-PDMMMP 71%* , (b) NR-<i>g</i>-PDMMMP 80%* , (c) NR-<i>g</i>-PDMMMP 89%* , (d) NR-<i>g</i>-PDMMMP 95%* and (e) pure NR (*grafting rate in wt%)	114
4.35	Tan δ as a function of frequency of pure NR and NR- <i>g</i> -PDMMMP with various grafting rates	116
4.36	TGA thermograms obtained under oxygen atmosphere of (a) NR-<i>g</i>-PDMMMP 71% , (b) NR-<i>g</i>-PDMMMP 80% , (c) NR-<i>g</i>-PDMMMP 89% , (d) NR-<i>g</i>-PDMMMP 89% , (e) pure NR, and (f) PDMMMP homopolymer	118

LIST OF FIGURES (continued)

Figure	Page	
4.37	TGA thermograms under nitrogen atmosphere of NR,..... PDMMP, NR- <i>g</i> -PDMMP with various grafting rates:..... (a) NR-<i>g</i>-PDMMP 71% , (b) NR-<i>g</i>-PDMMP 80% ,..... (c) NR-<i>g</i>-PDMMP 89% , (d) NR-<i>g</i>-PDMMP 89% ,..... (e) pure NR and (f) PDMMP.....	119
4.38	LOI of pure NR and NR- <i>g</i> -PDMMP with..... various grafting rates.....	122
4.39	Burning rate of pure NR and NR- <i>g</i> -PDMMP with..... various grafting rates.....	123
4.40	TEM micrographs of (a) natural rubber,..... (b) NR-<i>g</i>-PDMMP 71% , (c) NR-<i>g</i>-PDMMP 80% ,..... (d) NR-<i>g</i>-PDMMP 89% and (e) NR-<i>g</i>-PDMMP 95% ...	124
4.41	Complex viscosity as a function of frequency of..... 50/50 NR/EVA blends with four types of blend..... compatibilizers.....	127
4.42	Complex viscosity at a constant frequency of 6 rad/s of..... 50/50 NR/EVA blends with four types of blend..... compatibilizers.....	128
4.43	Storage modulus as a function of frequency of..... 50/50 NR/EVA blends with four types of blend..... compatibilizers.....	129
4.44	Storage modulus at a constant frequency of 0.16 rad/s..... of 50/50 NR/EVA blends with four types of blend..... compatibilizers.....	130
4.45	SEM micrographs of 50/50 NR/EVA blends with four types. of blend compatibilizers: (a) without compatibilizers,..... (b) NR- <i>g</i> -PDMMP, (c) NR- <i>g</i> -PDMMEP,..... (d) NR- <i>g</i> -PDMAMP and (e) ENR-30.....	130

LIST OF FIGURES (continued)

Figure	Page	
4.46	Tan δ at a constant frequency of 0.16 rad/s..... of 50/50 NR/EVA blends with four types of blend..... compatibilizers.....	131
4.47	Stress-strain behaviours of 50/50 NR/EVA blends with..... four types of blend compatibilizers.....	132
4.48	Complex viscosity as a function of frequency of..... 50/50 NR/EVA blends with NR-g-PDMMMP compatibilizer with various grafting rates of 71, 80, 89 and 95 %.....	135
4.49	Complex viscosity at a constant frequency of 0.16 rad/s..... of 50/50 NR/EVA blends with NR-g-PDMMMP..... compatibilizer with various grafting rates of 71, 80, 89..... and 95 %.....	135
4.50	Schematic illustrating the physical interaction of..... the graft copolymer at interfaces.....	136
4.51	Storage modulus as a function of frequency of..... 50/50 NR/EVA blends with NR-g-PDMMMP compatibilizer with various grafting rates of 71, 80, 89 and 95 %.....	137
4.52	Storage modulus at a constant frequency of 0.16 rad/s..... of 50/50 NR/EVA blends with NR-g-PDMMMP compatibilizer with various grafting rates of 71, 80, 89 and 95 %.....	137
4.53	Tan δ as a function of frequency of 50/50 NR/EVA blends... with NR-g-PDMMMP compatibilizer with various..... grafting rates of 71, 80, 89 and 95%.....	139
4.54	Tan δ at a constant frequency of 0.16 rad/s..... of 50/50 NR/EVA blends with NR-g-PDMMMP..... compatibilizer with various grafting rates of 71, 80, 89..... and 95 %.....	139

LIST OF FIGURES (continued)

Figure	Page	
4.55	Stress-strain behaviours of 50/50 NR/EVA blends..... with NR-g-PDMMMP compatibilizer with various..... grafting rates of 71, 80, 89 and 95 %.....	140
4.56	Tensile strength of 50/50 NR/EVA blends..... with NR-g-PDMMMP compatibilizer with..... various grafting rates of 71, 80, 89 and 95 %.....	142
4.57	Elongation at break of 50/50 NR/EVA blends..... with NR-g-PDMMMP compatibilizer with..... various grafting rates of 71, 80, 89 and 95 %.....	142
4.58	Tension set of 50/50 NR/EVA blends with NR-g-PDMMMP compatibilizer with various grafting rates of 71, 80, 89..... and 95 %.....	143
4.59	Degree of swelling of 50/50 NR/EVA blends..... with NR-g-PDMMMP compatibilizer with various..... grafting rates of 71, 80, 89 and 95 %.....	144
4.60	TGA curves under nitrogen atmosphere of..... 50/50 NR/EVA blends.....	145
4.61	SEM micrographs of 50/50 NR/EVA blends with..... NR-g-PDMMMP compatibilizer with various grafting rates: (a) without compatibilizer, (b) NR-g-PDMMMP 71%,..... (c) NR-g-PDMMMP 80%, (d) NR-g-PDMMMP 89% and.... (e) NR-g-PDMMMP 95%.....	148
4.62	Complex viscosity as a function of frequency..... of 50/50 NR/EVA blends with various loading levels of..... NR-g-PDMMMP compatibilizer.....	150
4.63	Complex viscosity at a constant frequencies of 0.06, 0.08.... and 0.16 rad/s of 50/50 NR/EVA blends with various..... loading levels of NR-g-PDMMMP compatibilizer.....	150

LIST OF FIGURES (continued)

Figure	Page
4.64 Schematic representation of the formation of micelles in..... 50/50 NR/EVA blend above the critical micelle concentration (CMC): (a) optimum level of blend compatibilizer and..... (b) concentration of blend compatibilizer higher than CMC..	151
4.65 Storage modulus as a function of frequency of..... 50/50 NR/EVA blends with various loading levels of..... NR-g-PDMMMP compatibilizer.....	152
4.66 Storage modulus at a constant frequencies of 0.06, 0.08..... and 0.16 rad/s of 50/50 NR/EVA blends with various..... loading levels of NR-g-PDMMMP compatibilizer.....	153
4.67 $\tan \delta$ as a function of frequency of 50/50 NR/EVA blends... with various loading levels of NR-g-PDMMMP..... compatibilizer.....	154
4.68 $\tan \delta$ at a constant frequencies of 0.06, 0.08 and 0.16 rad/s... of 50/50 NR/EVA blends with various loading levels of..... NR-g-PDMMMP compatibilizer.....	154
4.69 Stress-strain behaviours of 50/50 NR/EVA blends with..... various loading levels of NR-g-PDMMMP compatibilizer....	155
4.70 Tensile strength and elongation at break of 50/50 NR/EVA .. blends with various loading levels of NR-g-PDMMMP..... compatibilizer.....	156
4.71 Tension set of 50/50 NR/EVA blends with various..... loading levels of NR-g-PDMMMP compatibilizer.....	157
4.72 SEM micrographs of 50/50 NR/EVA blends with various.... loading levels of NR-g-PDMMMP compatibilizer : (a) without compatibilizer, (b) with 1%, (c) 3% , (d) 5%, (e) 7%, (f) 9%, (g) 12% and (h) 15% of NR-g-PDMMMP.....	158
4.73 Complex viscosity as a function of frequency of dynamically cured NR/EVA blends <i>versus</i> NR content	160

LIST OF FIGURES (continued)

Figure		Page
4.74	Complex viscosity at a constant frequencies of 6.28, 18.85... and 56.55 rad/s of dynamically cured NR/EVA blends..... <i>versus</i> NR content	160
4.75	Stress-strain curves of dynamically cured NR/EVA blends... as a function of NR content.	161
4.76	Tensile strength and elongation at break of dynamically..... cured NR/EVA blends <i>versus</i> NR content	163
4.77	SEM micrographs of dynamically cured NR/EVA blends..... with various blend ratios: (a) 75/25, (b) 60/40, (c) 50/50,..... (d) 40/60, (e) 25/75.....	164
4.78	Variation of vulcanized NR domain size and tensile strength of the dynamically cured 75/25, 60/40,..... 50/50, 40/60, 25/75 NR/EVA blend <i>versus</i> NR content.....	165
4.79	Variation of tension set and hardness of dynamically cured... NR/EVA blends <i>versus</i> NR content, and comparison..... the ones of pure EVA and static cured NR, respectively.....	166
4.80	Evolution of swelling degree of the dynamically cured..... NR/EVA blends <i>versus</i> NR content, and comparison..... the one of pure EVA and static cured NR, respectively.....	167
4.81	TGA thermograms of dynamically cured NR/EVA blends... with various blend ratios.....	168
4.82	Storage modulus (G') of dynamically cured NR/EVA blends of various compositions <i>versus</i> temperature, and comparison with that of pure EVA and static cured NR.....	170
4.83	Tan δ of dynamically cured NR/EVA blends of..... various compositions <i>versus</i> temperature, and comparison.... with that of pure EVA and static cured NR.....	171

LIST OF FIGURES (continued)

Figure	Page	
4.84	Curing curves of the static vulcanization of NR carried out... at 150°C using sulphur, peroxide,..... mixed (sulphur plus peroxide), and phenolic curing systems,.. respectively.....	172
4.85	Different torque value (MH-ML) of NR vulcanizates..... according to the curing system	174
4.86	Cure rate index (CRI) of NR vulcanizates according to..... the curing systems used.....	176
4.87	Stress-strain curves of NR vulcanizates as a function of the curing system used to vulcanizate NR.....	177
4.88	Schematic representation of the crosslinked structure of NR vulcanizates in relation with the cured system used	178
4.89	Tensile strength of NR vulcanizates according to..... the cured system used.....	179
4.90	Elongation at break of NR vulcanizates according to..... the cured system used.....	179
4.91	Hardness of NR vulcanizates according to the cured system... used.....	180
4.92	Complex viscosity as a function of frequency of..... the dynamically cured 40/60 NR/EVA blends with various... vulcanization systems.....	181
4.93	Complex viscosity at a constant frequency of 3.14 rad/s of.. dynamically cured 40/60 NR/EVA blends with various..... vulcanization systems.....	182
4.94	Storage modulus as a function of frequency of dynamically.. cured 40/60 NR/EVA blends with various vulcanization..... systems.....	183
4.95	Tan δ as a function of frequency of dynamically cured 40/60 NR/EVA blends with various vulcanization systems.....	184

LIST OF FIGURES (continued)

Figure	Page
4.96 Quantity of extractable NR phase of uncured and dynamically cured 40/60 NR/EVA blends with various vulcanization systems.....	185
4.97 Quantity of extractable EVA phase of uncured and dynamically cured 40/60 NR/EVA blends with various vulcanization systems.....	186
4.98 Degree of swelling of uncured and dynamically cured 40/60 NR/EVA blends with various vulcanization systems.....	187
4.99 Stress-strain behaviours of uncured and dynamically cured 40/60 NR/EVA blends with various vulcanization systems...	187
4.100 SEM micrographs of uncured and dynamic cured 40/60 NR/EVA blends with various types of vulcanization systems.....	191
4.101 Complex viscosity as a function of frequency for the dynamically cured 40/60 NR/EVA TPVs with four types of blend compatibilizers.....	193
4.102 Complex viscosity at a constant frequency of 6.25 rad/s for the dynamically cured 40/60 NR/EVA TPVs with four types of blend compatibilizers.....	194
4.103 Storage modulus as function of frequency in dynamically cured 40/60 NR/EVA TPVs with four types of blend Compatibilizers.....	195
4.104 Storage modulus at a constant frequency of 6.25 rad/s of dynamically cured NR/EVA TPVs with four types of blend compatibilizers.....	195
4.105 Tan δ as a function of frequency for the dynamically cured NR/EVA TPVs with four types of blend compatibilizers.....	196
4.106 SEM micrographs of dynamically cured 40/60 NR/EVA blends: (a) without compatibilizer, (b) NR-g-PDMMMP, (c) NR-g-PDMMEP, (d) NR-g-PDMAMP and (e) ENR-30....	197

LIST OF FIGURES (continued)

Figure	Page
4.107 Stress-strain behaviours of dynamically cured 40/60 NR/EVA blends with different types of compatibilizers.....	198
4.108 Storage modulus as a function of frequency of dynamically.. cured 40/60 NR/EVA blends with various loading levels of.. NR-g-PDMMMP compatibilizer.....	201
4.109 Storage modulus at a constant frequencies of 6, 19 and..... 57 rad/s of dynamically cured 40/60 NR/EVA blends with... various loading levels of NR-g-PDMMMP compatibilizer...	201
4.110 Possible chemical interaction of graft copolymer..... (NR-g-PDMMMP) and natural rubber and EVA in the blend component at the interfacial area.....	202
4.111 Schematic representation of a compatibilization..... NR-g-PDMMMP compatibilizer at the interface of NR and.. EVA.....	203
4.112 Tan δ at a constant frequencies of 6, 19 and 57 rad/s of..... dynamically cured 40/60 NR/EVA blends with various..... loading levels of NR-g-PDMMMP compatibilizer.....	204
4.113 Complex viscosity as a function of frequency of dynamically cured 40/60 NR/EVA blends with various loading levels of... NR-g-PDMMMP compatibilizer.....	205
4.114 Complex viscosity at a constant frequencies of 6, 19 and..... 57 rad/s of dynamically cured 40/60 NR/EVA blends with... various loading levels of NR-g-PDMMMP compatibilizer...	206
4.115 SEM micrographs of dynamically cured 40/60 NR/EVA..... blends: (a) without compatibilizer, (b) with NR-g-PDMMMP = 1%, (c) with NR-g-PDMMMP = 3%, (d) with..... NR-g-PDMMMP = 5%, (E) with NR-g-PDMMMP = 7%,... (f) with NR-g-PDMMMP = 9%, (g) with NR-g-PDMMMP.. = 12% and (h) with NR-g-PDMMMP = 15%.....	207

LIST OF FIGURES (continued)

Figure	Page
4.116 Relationship between average diameter of vulcanized rubber domains and complex viscosity at a frequency of 6 rad/s of.. dynamically cured 40/60 NR/EVA blends with various..... loading levels of NR- <i>g</i> -PDMMMP compatibilizer.....	208
4.117 Stress-strain behaviours of dynamically cured 40/60..... NR/EVA blends with various quantities of NR- <i>g</i> -PDMMMP	209
4.118 DSC thermograms of (a) EVA, (b) 40/60 NR/EVA without.. NR- <i>g</i> -PDMMMP, (c) 40/60 NR/EVA with 5 wt% of..... NR- <i>g</i> -PDMMMP, (d) 40/60 NR/EVA with 9 wt% of..... NR- <i>g</i> -PDMMMP, (e) 40/60 NR/EVA with 15 wt% of..... NR- <i>g</i> -PDMMMP, (f) NR.....	212
4.119 TGA thermograms of NR, EVA and 40/60 dynamically cured NR/EVA blends with different loading levels of..... NR- <i>g</i> -PDMMMP compatibilizer.....	215
4.120 Stress-strain behaviours of uncompatibilized recycled..... dynamically cured 40/60 NR/EVA blends compared with the virgin material.....	217
4.121 Stress-strain behaviours of compatibilized recycled..... dynamically cured 40/60 NR/EVA blends compared with the virgin material.....	218
4.122 Tensile strength of uncompatibilized and compatibilized..... recycled dynamically cured 40/60 NR/EVA blends compared with the virgin material.....	219
4.123 Hardness of uncompatibilized and compatibilized recycled... dynamically cured 40/60 NR/EVA blends compared with the virgin material.....	219
4.124 Elongation at break of uncompatibilized and compatibilized... recycled dynamically cured 40/60 NR/EVA blends compared with the virgin material.....	220

4.125	Tension set of uncompatibilized and compatibilized recycled dynamically cured 40/60 NR/EVA blends compared with the virgin material.....	220
4.126	SEM micrographs of dynamically cured 40/60 NR/EVA..... blend: (a) the virgin without compatibilizer,..... (b) after 5 cycles without compatibilizer, (c) the virgin with NR- <i>g</i> -PDMMMP and (d) after 5 cycles with..... NR- <i>g</i> -PDMMMP.....	221

LIST OF SCHEMES

Scheme		Page
2.1	Mechanism of “living” radical photopolymerization..... of vinyl monomers initiated from..... N,N-dialkyldithiocarbamate iniferters.....	17
4.1	Synthesis of DMAMP, DMMEP, and DMMMP monomers..	72
4.2	The reaction used to synthesize graft copolymer.....	77
4.3	The <i>in-situ</i> performic epoxidation of NR employing..... hydrogen peroxide and formic acid.....	79
4.4	Influence of DMAMP (1) and DMMEP (2) structures on.... reactivity.....	87

LIST OF ABBREVIATIONS

ADS	Air dried sheet
API	American Petroleum Institute
ASTM	American Society for Testing and Materials
BDC	Benzyl <i>N,N</i> -diethyldithiocarbamate
BT	Mercaptobenzothiazole
CRI	Cure rate index
DCP	Dicumyl peroxide
DEDT	<i>N,N</i> -diethyldithiocarbamate
DEDT-Na	Sodium <i>N,N</i> -diethyldithiocarbamate trihydrate
DEDT-NR	<i>N,N</i> -diethyldithiocarbamate functionalized natural rubber
DMAMP	Dimethyl(acryloyloxymethyl)phosphonate
DMMEP	Dimethyl(methacryloyloxymethyl)phosphonate
DMMMP	Dimethyl(methacryloyloxymethyl)phosphonate
DRC	Dry rubber content
\overline{DP}_n	Degree of Polymerization
DV	Dynamic vulcanizate
ENR	Epoxidized natural rubber
EPDM	Ethylene propylene diene monomer
EPDM- <i>g</i> -MA	Ethylene propylene diene monomer-graft-maleic anhydride
EVA	Ethylene vinyl acetate copolymer
EVASH	Mercapto-modified EVA
GR	Grafting rate
HDPE	High density polyethylene
iPP	Isotactic polypropylene
ISO	International Standards Organization
LLDPE	Linear Low Density Polyethylene
LOI	Limiting oxygen index
MA	Maleic anhydride
MNR	Maleated natural rubber

LIST OF ABBREVIATIONS (continued)

\overline{M}_n	Number average molecular weight
NBR	Nitrile butadiene rubber
NR	Natural rubber
NR- <i>g</i> -PDMAMP	NR-graft-poly(dimethyl(acryloyloxymethyl)phosphonate)
NR- <i>g</i> -PDMMEP	NR-graft-poly(dimethyl(acryloyloxymethyl)phosphonate)
NR- <i>g</i> -PDMMP	NR-graft-poly(dimethyl(acryloyloxymethyl)phosphonate)
NR- <i>g</i> -PMMP	NR-graft-poly(methyl methacrylate)
NR- <i>g</i> -PS	NR-graft-polystyrene
PA	Polyamide
PAN	Polyacrylonitrile
PDMAMP	Poly(dimethyl(acryloyloxymethyl)phosphonate)
PAMMEP	poly(dimethyl(acryloyloxymethyl)phosphonate)
PDMMP	NR-graft-poly(dimethyl(acryloyloxymethyl)phosphonate)
PE	Polyethylene
PI- <i>b</i> -PS	Polyisoprene-block-Polystyrene
Ph-PP	Phenolic modified polypropylene
PMMA	Poly(methyl methacrylate)
PP	Polypropylene
PP- <i>g</i> -MA	Polypropylene-graft-maleic anhydride
S	Sulphur
TAC	Triallyl cyanurate
TBAB	Tetrabutylammonium bromide
TC	Diethyldithiocarbamate
TDCA	N-(<i>p</i> -tolyl)- <i>N</i> ', <i>N</i> '-diethyldithiocarbamoylacetamide
TEA	Triethylamine
TMQ	Polymerized 2, 2, 4-trimethyl-1, 2-dihydroquinoline
TMS	Tetramethylsilane
TPE	Thermoplastic elastomer
TPE-A	Thermoplastic polyamide elastomers
TPE-E	Thermoplastic polyester elastomers

LIST OF ABBREVIATIONS (continued)

TPE-O	Thermoplastic polyolefin
TPE-V or TPV	Thermoplastic vulcanizate
TPNR	Thermoplastic natural rubber
TPR	Thermoplastic rubber
UV	Ultraviolet
ZnO	Zinc oxide
cm	Centimeter
°C	Degree Celsius
cst	Centistokes
°F	Degree Fahrenheit
G'	Storage modulus
G''	Loss modulus
g	Gram
h	Hour
ΔH	Heat of fusion
in	Inch
J	Joule
keV	Kilo electron volt
kJ	Kilojoule
kPa	Kilopascal
m ²	Square meter
MPa	Megapascal
ml	Milliliter
mm	Millimeter
min	Minute
μm	Micrometer
N	Newton
psi	Pound per square inch
phr	Part per hundred rubber
%	Percent

LIST OF ABBREVIATIONS (continued)

ppm	Parts per million
rpm	Round per minute
wt%	Percent by weight
η	Viscosity
η^*	Complex viscosity

CHAPTER 1

INTRODUCTION

1.1 Background

Thermoplastic elastomers (TPEs) play an important role in the polymer industry due to their good processability and their elastomeric properties (Ibrahim and Dahlan, 1998). There has been a growth of subcategories of TPEs to distinguish between different types of materials. Several examples are block copolymers, thermoplastic rubber blends, and ionomers. However, extensive studies have been carried out in the area of TPEs based on elastomer/thermoplastic blends (Abdou-Sabet and Patel, 1991). This is due to blending technology is less expensive than the synthesis of new polymer or copolymer, including development of monomer preparation and polymerization technology. TPEs based on NR/thermoplastic blends are called “thermoplastic natural rubber” (TPNR) blends. This type of blend has grown along two distinctly different product classes. That is, simple blend based on blending of natural rubber with polyolefin that is commonly designated as thermoplastic elastomeric olefins (TEOs) or thermoplastic polyolefins (TPOs), and another class is thermoplastic vulcanizates (TPVs) or dynamic vulcanizates (DVs). The dynamically vulcanized thermoplastic elastomer blends have attracted more interest than the simple blend because of their important technical advantages in processing of the dynamic vulcanization from the peculiar morphological features, and because they tolerate elevated temperature (Mousa *et al.*, 1998; Wang *et al.*, 2002; Nakason *et al.*, 2006). Furthermore, it has been well-established that the dynamic vulcanization of the rubber causes the improvement of its mechanical, thermal, and impact properties by comparison with the uncured or partially crosslinked composition (Kim *et al.*, 1996, Gosh *et al.*, 1996; Mousa *et al.*, 1998; Hailongjin *et al.*, 2002; Wang *et al.*, 2002). A great number of known thermoplastics were used to prepare TPNRs based on blending of NR. The most consideration were polystyrene (PS) (Asaletha *et al.*, 1999), polypropylene (PP) (Suryadiansyah, 2002; Varghese *et al.*, 2004; Ismail; Nakason *et al.*, 2006), high

density polyethylene (HDPE) (Nakason *et al.*, 2006a), linear low density polyethylene (LLDPE) (Abdullah *et al.*, 1995; Dahlan *et al.*, 2000), poly(methyl methacrylate) (PMMA) (Oommen and Thomas, 1996; Mina *et al.*, 2004), and polyamide 6 (PA-6) (Carone *et al.*, 2000). Among the various types of thermoplastics, EVA is one of the interested materials because of some superior properties including excellent ozone resistance, weather resistance, thermal resistance (Jansen and Soares, 1996; Koshy *et al.*, 1992; Chowdhury *et al.*, 2000; Jansen *et al.*, 1996), mechanical behavior (Doak, 1986; Mohamad *et al.*, 2006; Varghese, 1995), and halogen-free thermoplasticity. Also, NR provides to the blend high elasticity and resistance to impact (Derouet *et al.*, 2007; Asaletha *et al.*, 1999).

Melt blending of elastomers and thermoplastics leads normally to immiscible blends due to the difference between intrinsic properties of the blend components. This causes the formation of TPV materials that are characterized by two-phase morphologies with high interfacial tension, poor interface adhesion, and poor mechanical properties, which limits the usage of the materials. The compatibility of the rubber-thermoplastic blends has been improved by means of blend compatibilizers. To obtain blends with convenient properties, one accessible route consists to incorporate a graft copolymer as blend compatibilizer.

Graft copolymers of NR are well known products coming from chemical modification of NR macromolecules. This is a route to prepare new materials that are possible to be used as blend compatibilizers to promote compatibility between NR and thermoplastic components. Some well-known modified NR products that have been used as blend compatibilizers include natural rubber-*g*-PMMA (Oommen *et al.*, 1997; Oommen and Thomas, 1997), natural rubber-*g*-glycidyl methacrylate/polystyrene (Suriyachai *et al.*, 2004), and natural rubber-*g*- polystyrene (Chuayjuljit *et al.*, 2005; Asaletha *et al.*, 1995 and 1998). Numerous reviews dealing with the compatibilization of polymer blend based on natural rubber and thermoplastic blend by addition of graft copolymers indicated an improvement of blend properties in these conditions (Choudhury and Bhowmick, 1989; Taha., 1996; Oommen *et al.*, 1997; Asaletha *et al.*, 1998; Nakason *et al.*, 2006; Botros *et al.*, 2006; Thitithammawong., 2008).

In the present work, the purpose is to synthesize new graft copolymers of NR with the aim to improve some of its intrinsic properties and to use them as blend compatibilizers for NR/EVA blends. The idea was to create polymer grafts bearing phosphonate groups along the rubber chains. To synthesize this type of graft copolymer, a “grafting from” methodology will be considered. It will consist in the photopolymerization of acrylate and methacrylate monomers bearing dialkylphosphonate groups, i.e., dimethyl(acryloyloxymethyl)phosphonate (DMAMP), dimethyl(methacryloyloxyethyl)phosphonate (DMMEP), and dimethyl(methacryloyloxymethyl)phosphonate (DMMMP), from active initiating groups previously introduced on the rubber chains.

1.2 Objectives

The objective of the present research work is to develop graft copolymers of NR by incorporating phosphorus-containing monomers onto NR chains *via* a graft copolymerization methodology, in order to improve some properties of NR (i.e., flame-retardancy and oil resistance). Moreover, the work is aimed to prepare new NR derivatives able to be used as blend compatibilizers to promote the compatibility between NR and some polar thermoplastics such as EVA, as well as to increase the added value of NR and its area of applications. The main objectives are listed below:

To graft polymers bearing dialkylphosphonate groups onto NR chains *via* a graft copolymerization procedure performed in appropriate conditions, and to characterize the graft copolymer structures obtained and to determine their physical, physico-chemical, and rheological properties.

To investigate the effect of the graft copolymer concentration on the properties of simple 50/50 NR/EVA blends. Rheological, dynamic, mechanical, thermal, and morphological properties will be investigated.

To investigate the effect of various blend ratios of NR/EVA on properties of the TPVs.

To investigate the effect of different curing systems, i.e. sulphur, peroxide, and mixed systems, on properties of 40/60 NR/EVA TPVs.

To investigate the compatibilizing capability of NR-*g*-PDMMMP compared with the other types such as NR-*g*-PDMAMP, NR-*g*-PDMMEP, and epoxidized natural rubber (ENR).

To explore various properties of compatibilized NR/EVA TPVs using a graft copolymer (i.e., NR-*g*-PDMMMP) with different concentrations.

1.3 Research Summary

The research covered details as follow:

1. Synthesis and characterization of the phosphorus-containing monomers, i.e., dimethyl(acryloyloxymethyl)phosphonate (DMAMP), dimethyl(methacryloyloxyethyl)phosphonate (DMMEP) and (dimethyl(methacryloyloxymethyl)phosphonate) (DMMMP)
2. Synthesis and charecterization of graft copolymers of NR and poly(dimethyl(acryloyloxymethyl)phosphonate) (NR-*g*-PDMAMP), NR and poly(dimethyl(methacryloyloxyethyl)phosphonate) (NR-*g*-PDMMEP), and NR and poly(dimethyl(methacryloyloxymethyl)phosphonate) (NR-*g*-PDMMMP), respectively.
3. Investigation of the compatibilizing capability of different types of compatibilizer such as NR-*g*-PDMMMP, NR-*g*-PDMAMP, NR-*g*-PDMMEP, and epoxidized natural rubber (ENR) on the properties of 50/50 NR/EVA blends.
4. Investigation of the influence of grafting rate and graft copolymer concentration of NR-*g*-PDMMMP on properties of 50/50 NR/EVA blends.
5. Investigation of the influence of NR-*g*-PDMMMP concentrations and grafting rates on properties of 40/60 NR/EVA TPVs using sulphur as curing agent.
6. Investigation of the influence of blend ratios on properties of NR/EVA TPVs.
7. Investigation of the influence of different curing system (sulphur, peroxide, and mixed cured systems) on properties of 40/60 NR/EVA TPVs.
8. Investigation of the influence of different types of compatibilizers (i.e., NR-*g*-PDMMMP, NR-*g*-PDMAMP, NR-*g*-PDMMEP, and epoxidized natural rubber on properties of 40/60 NR/EVA TPVs.
9. Investigation of the influence of loading level of NR40/60 NR/EVA TPVs on properties of 40/60 NR/EVA TPVs.

10. Investigation of the influence of recyclability of 40/60 NR/EVA TPVs with and without on properties of 40/60 NR/EVA TPVs.

1.4 Expectation of the research

1. Increasing consumption of NR.
2. Improving some properties of NR (i.e., flame-retardancy and oil resistance), as well as obtaining new NR derivatives able to be used as blend compatibilizers to promote the blend compatibility between NR and polar thermoplastics.
3. Knowledge of introducing the phosphorus-containing monomers onto NR by graft polymerization procedure. This is an alternative way to apply with other compounds in order to extend a modified natural rubber with desired properties.

CHAPTER 2

LITERATURE SURVEY

2.1 Introduction

Natural rubber (NR) is an interesting material with commercial success due to its excellent physical properties (i.e. high mechanical strength, low heat build up, excellent flexibility, and resistance to impact and tear). Also, NR has the advantage to be a renewable resource. However, NR has some drawbacks, for instance low flame resistance, sensitivity to chemicals and solvents, and poor ozone resistance and weathering. This is mainly due to its unsaturated hydrocarbon chain structure and non-polar character, which causes limitation in variety of applications. Therefore, chemical modification of NR has been widely developed to improve various properties for instance gas permeability, oil resistance, and flame resistance (Brosse *et al.*, 2000). Well-known modified NR products include epoxidized natural rubbers (ENR) (Bradbury and Perera, 1985; Perera, 1987), maleated natural rubbers (MNR) (Derouet *et al.*, 1990; Nakason *et al.*, 2004 and 2006), dibutylphosphate supported natural rubber (DSNR) (Derouet *et al.*, 1994 and 2001), graft copolymers of NR and PMMA (NR-g-PMMA) (Thiraphattaraphun *et al.*, 2001; Arayapranee *et al.*, 2003), graft copolymers of NR and polystyrene (NR-g-PS) (Prasassarakich *et al.*, 2001; Chuayjuljit *et al.*, 2005) and graft copolymers of NR and glycidyl methacrylate/styrene (Suriyachai *et al.*, 2004). The chemical modification of NR macromolecules is not only considered to compensate its drawback properties, but also to prepare new materials such as thermoplastic natural rubber (TPNR) by blending modified NR with polar thermoplastics. Furthermore, utilization of modified natural rubber as blend compatibilizer is a route to prepare new materials with unique properties. The modified products such as, NR-g-PMMA (Oommen *et al.*, 1997; Oommen and Thomas, 1997), NR-g-glycidyl methacrylate/styrene (Suriyachai *et al.*, 2004), NR-g-polystyrene (Chuayjuljit *et al.*, 2005; Asaletha *et al.*, 1995 and 1998), liquid natural rubber (Dahlan *et al.*, 2000 and 2002), and epoxidized natural rubber (Nakason *et al.*, 2001; El-Sayed and Afifi, 2002; Xie *et al.*, 2003) have been used as blend compatibilizers to promote compatibility of polymer blends of NR and thermoplastics.

In recent years, blends of elastomers and thermoplastics have become technologically useful as thermoplastic elastomers (TPEs). They have properties of elastomers, but they are processable as thermoplastics. TPEs based on natural rubber and thermoplastic blends, which are called “thermoplastic natural rubber” (TPNR) blends, are a family of materials prepared by blending natural rubber and thermoplastics. TPNR blends have grown along two distinctly different product classes. That is, simple blend which is commonly designated as thermoplastic elastomeric olefins (TEOs) or thermoplastic polyolefins (TPOs), and thermoplastic vulcanizates (TPVs) or dynamic vulcanizates (DVs). NR is considered to be a good component for blending with thermoplastic due to its excellent flexibility and impact resistance. Therefore, NR has an inherent affinity to many thermoplastics such as polypropylene (Ismail and Suryadiansyah, 2002; Jeong Seok *et al.*, 2003; Varghese *et al.*, 2004; Nakason *et al.*, 2006 and 2008), low-density polyethylene (Akhtar *et al.*, 1986; Abdullah *et al.*, 1995), and polystyrene (Asaletha *et al.*, 1999). Modified NR in forms of epoxidized natural rubber (Ramesh and De, 1993; Mohanty *et al.*, 1996; Nakason *et al.*, 2004), NR-g-poly(methyl methacrylate) (Oommen *et al.*, 1997; Thiraphattaraphun *et al.*, 2001; Nakason *et al.*, 2005), and maleated natural rubber (MNR) (Carone *et al.*, 2000; Nakason *et al.*, 2006) have been also used to prepare TPNRs by blending with polar thermoplastics. However, most polymer pairs in blends are thermodynamically incompatible which gives rise to poor mechanical properties. This is due to lack of interaction at the interface, which leads to poor interfacial adhesion. Compatibilization of polymer blends is becoming a rapidly growing field since it provides a convenient procedure to enhance mechanical, thermal, or chemical properties of existing materials without the expense of synthesis of new polymer. There are two important routes to improve the blend compatibility of different polymers. One is the incorporation of a third component (i.e. a blend compatibilizer), typically a block or graft copolymer, or a polymer with reactive functional groups (Braun *et al.*, 1996; Oommen *et al.*, 1997; George *et al.*, 1999). The compatibilizers consist of segments that are chemically identical to their respective counterparts in the polymer pairs and are thought to be located preferentially at the interface (Oh *et al.*, 2003). The other is to perform a chemical

reaction between the blend components or modification of interfaces, i.e. reactive blending (Mohanty *et al.*, 1996; Nakason *et al.*, 2001).

2.2 Chemical modification of natural rubber

Natural rubber is a polymer that has been commercially available for over a hundred year. NR shows a very uniform microstructure that provides unique and important characteristics to the material, namely the ability to crystallize under strain, a phenomenon known as “strain induced crystallization”, and very low hysteresis. From these properties (i.e., good tensile strength, high resilience, excellent flexibility, and resistance to impact and tear) NR is very useful in many applications. However, NR shows low resistance to oxidation, UV radiation, weathering, and a wide range of chemicals and solvents, mainly due to its unsaturated chain structure and low polarity. These inherent drawbacks apparently cause limitations in the NR usage, particularly for technical and engineering applications. In order to extend the uses of NR, chemical modification of its structure have been envisaged for many years and was shown as an interesting method for producing new NR-derived materials and modifying its intrinsic properties such as chemical resistance, weathering resistance, and thermal stability. Some modified NRs that were reported in the literature are commercially available i.e., liquid natural rubber (LNR) (Ibrahim and Dahlan, 1998), hydrogenated NR, chlorinated NR (CNR), epoxidized NR (ENR) (Bradbury and Perera, 1985; Perera, 1987), maleated NR (MNR) (Nakason *et al.*, 2004 and 2006), graft copolymers of NR and poly(methyl methacrylate) (NR-g-PMMA) (Thiraphattaraphun *et al.*, 2001; Arayapranee *et al.*, 2003), and graft copolymers of NR and polystyrene (NR-g-PS) (Prasassarakich *et al.*, 2001; Chuayjuljit, 2005). Chemical modification of NR can be classified in three main categories:

2.2.1 Modification by bond rearrangement without introducing new atoms other than carbon and hydrogen

Carbon-carbon crosslinking, carbon-carbon isomerization, hydrogenation, cyclization, and depolymerization are among the main examples of this type of modification applied to NR. For instance, hydrogenated NR is thermally more stable than NR, and more resistant to oxidation and radiation effects, because of its

improved tensile strength and fatigue compared to NR, and the bonding to metal and wet grip is also better than with NR (Gelling, and Porter, 1988).

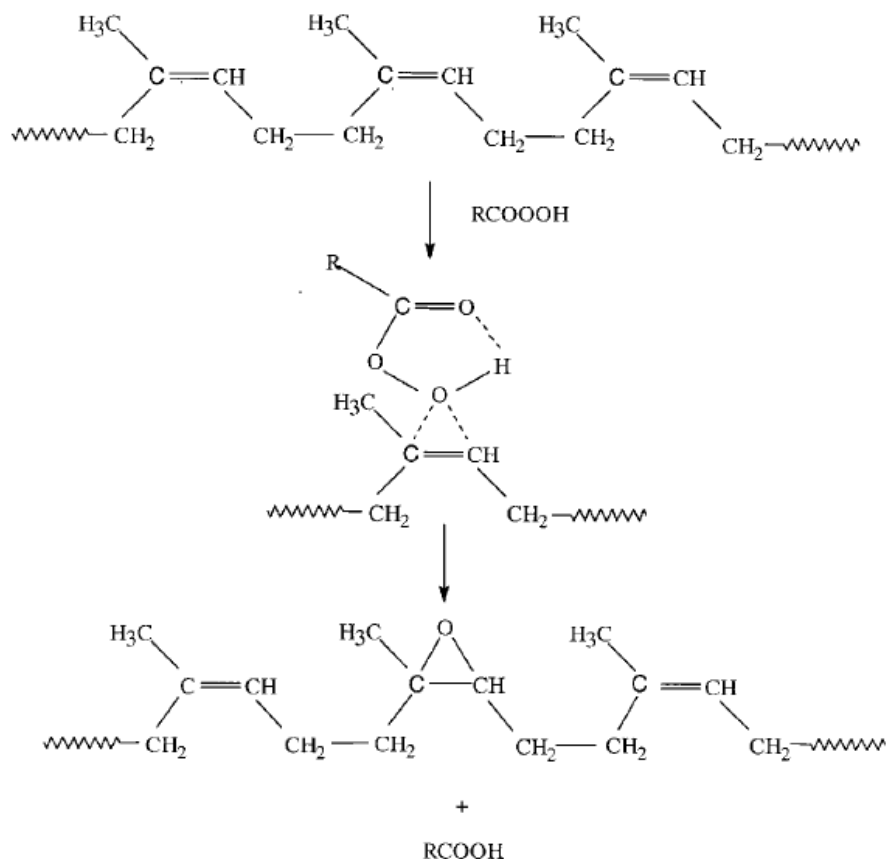


Figure 2.2 Mechanism of the epoxidation of NR by the peracid.

Another interesting chemical modification of NR consisted to incorporate phosphorus-containing groups onto NR backbone to improve its flame and oil resistance (Derouet *et al.*, 2003) but also to incorporate 2-chloroethylphosphonic acid (ethephon), a stimulating compound for the latex production by the *Hevea brasiliensis*, on NR chains (Derouet *et al.*, 2003a). Derouet *et al.* (1995, 2001 and 2003) studied the reaction in solution of dialkyl(or aryl)phosphate onto epoxidized liquid natural rubber (ELNR). They found that 5.2 - 6.8 wt% of phosphorus could be fixed on the NR backbone of a 25 % epoxidized LNR. They also showed that incorporation of the phosphorus-modified liquid natural rubber in a NR formulation decreased the flammability of the NR vulcanizates but unfortunately decreased at the same time their mechanical properties of because vulcanization process was greatly

affected by dibutylphosphate groups (Derouet *et al.*, 1994). More recently, they performed the reaction of dibutylphosphate onto epoxidized natural rubber (ENR) in latex medium and found that the oxirane rings were transformed in 2-butoxy-2-butoxy-2-oxo-1,3,2-dioxaphospholane, β -hydroxyphosphate and side structures (i.e., diol and ethers), as shown in Figure 2.3. (Derouet *et al.*, 2003 and 2005)

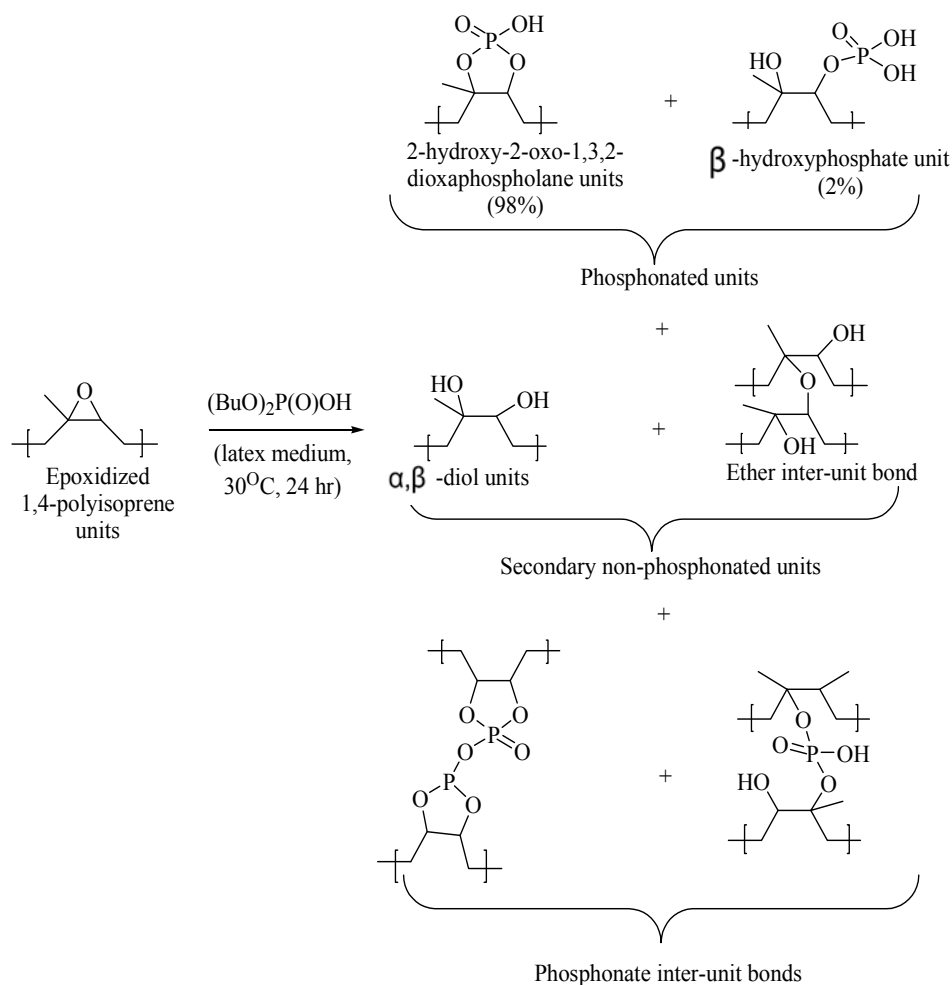


Figure 2.3 Dibutylphosphate reaction with epoxidized 1,4-polyisoprene units of ENR in latex medium.

2.2.3 Grafting of a polymer onto the NR backbone

Grafting has been frequently performed using vinyl monomers like methyl methacrylate and styrene. Graft copolymers of NR and poly(methyl methacrylate) (NR-*g*-PMMA) known as *Heveaplus MG*, are commercially available in two grades: 30 % (MG 30) and 49 % (MG49) of PMMA (Hashim *et al.*, 2002). *Heveaplus MG* shows superior properties like hardness, modulus, abrasion, electrical resistance, and

light color. It has been used to improve the impact properties of polystyrene, and to blend with NR as reinforcing agent. The solution or latex form of *Heveaplus MG* was used as adhesive or bonding agent to bond rubber to poly(vinyl chloride) (PVC), leather, textiles, and metals. Recently, Derouet *et al.* (2008) synthesized well-defined NR-*g*-PMMA by MMA photopolymerization initiated from *N,N*-diethyldithiocarbamate functions previously created along the NR chains (Figure 2.4). They found that the thermal stability of NR was improved after the introduction of PMMA grafts onto NR chains.

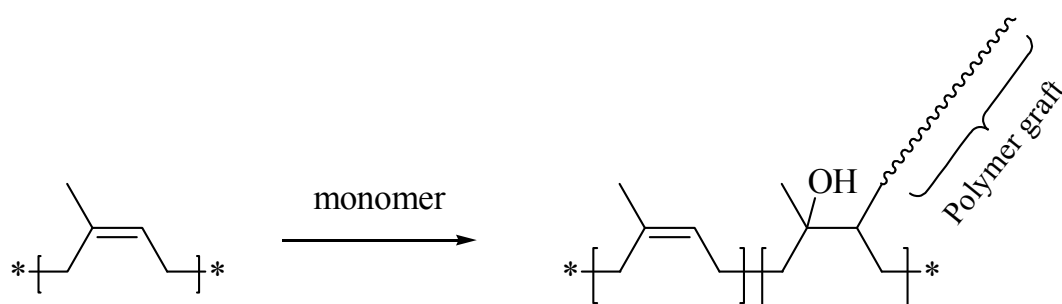


Figure 2.4 Grafting of a second polymer onto the NR backbone. (modified from Derouet *et al.*, 2008)

2.3 Synthesis of graft copolymers

Graft copolymerization is one route that can be used to perform chemical modification of an existing polymer. It consists to link branches (grafts) by covalent bond side along a main polymer backbone. The backbone and grafts can be of different nature and composition, but also of same nature. The grafts are usually of same length and randomly distributed along the backbone because of the specific synthesis techniques used. However, more elaborated methods allowed to synthesize well-defined graft copolymers with grafts equally spaced and of same length, where all the molecular and structural parameters can be accurately controlled, as schematically shown in Figure 2.5. Graft copolymerization has been mainly used to modify polymer properties, i.e., mechanical, thermal, and melt properties.

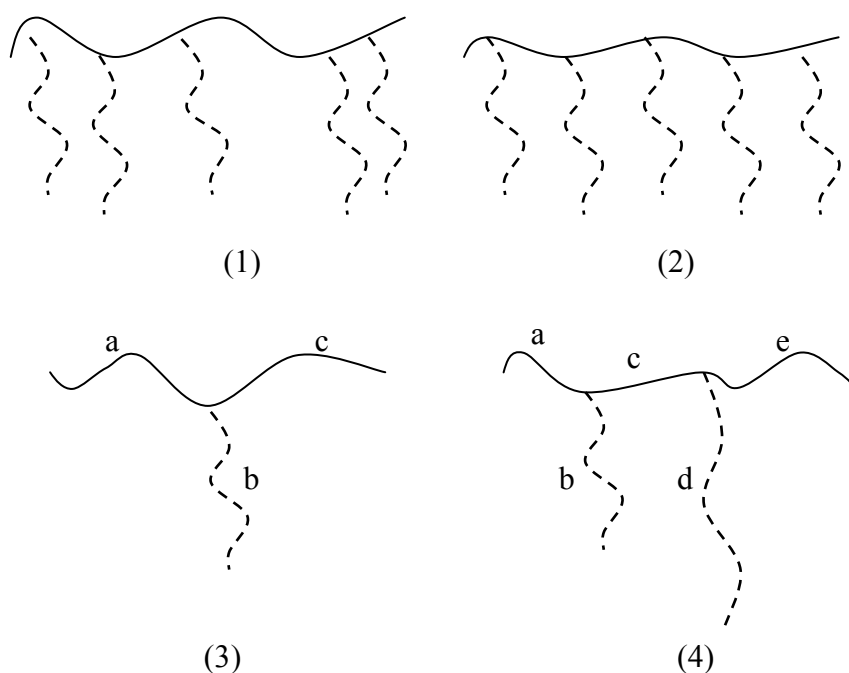


Figure 2.5 Exact graft copolymers (1) random graft copolymer containing identical branches randomly distributed along the backbone; (2) regular graft copolymer containing identical branches equally spaced along the backbone; (3) simple graft copolymer; and (4) graft copolymer with two trifunctional branch points. (Hadjichristidis *et al.*, 2004)

Graft copolymers can be obtained according to three main methods: (1) “grafting onto” in which side chains are preformed, and then chemically bound to the backbone; (2) “grafting from” in which the monomer is grafted from the backbone; and (3) “grafting through” in which macromonomers are copolymerized with monomers.

“Grafting onto” methods involve reactions between functional groups (Y) located at the chain end of a polymer with another functional groups (X) randomly distributed on the main chain of the second polymer, as shown in Figure 2.6.

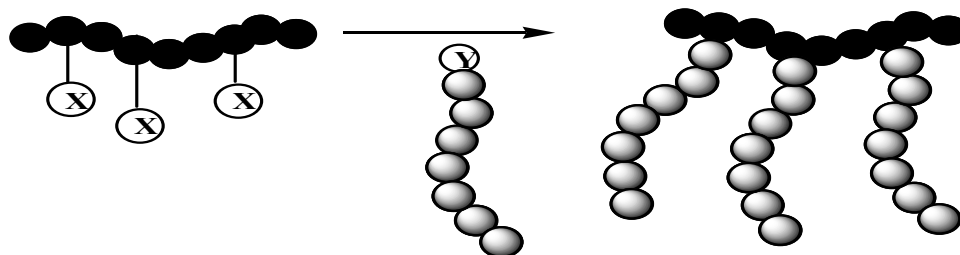


Figure 2.6 Synthesis of randomly graft copolymers according to “grafting onto” method.

Chemical initiation is used in the form of “grafting from” method. In this case, a polymer backbone contains for instance some thermally cleavable bonds (R) such as azo or peroxide linkages (Figure 2.7). If the polymers are heated in the presence of a monomer, initiation of its polymerization takes place. In such systems, homopolymer formation is unavoidable because of the concomitant formation of low molar mass radicals.

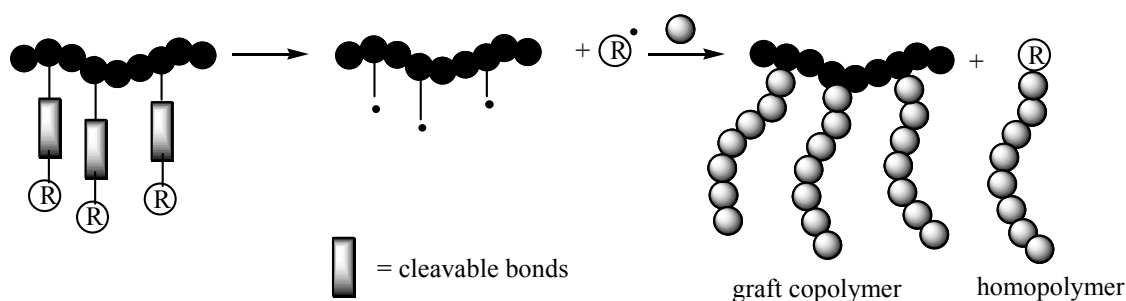


Figure 2.7 Synthesis of randomly branched graft copolymers according to “grafting from” method.

“Grafting through” involves macromonomers that are short polymer chains fitted at chain end with a polymerizable function, as shown in Figure 2.8. This synthesis of well-defined macromonomers owes much to ionic polymerization process.

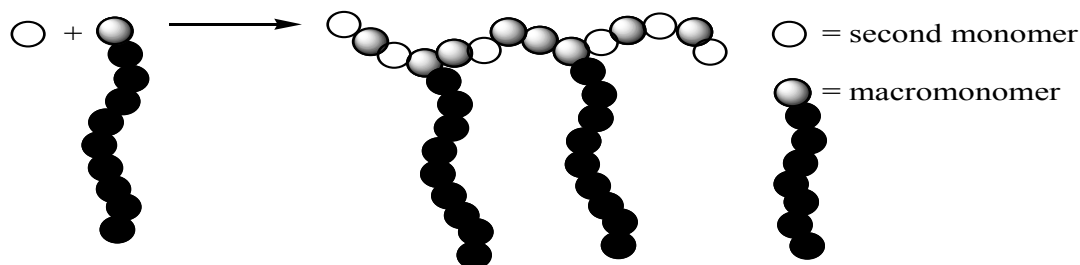


Figure 2.8 Synthesis of randomly branched graft copolymers according to “grafting through” method.

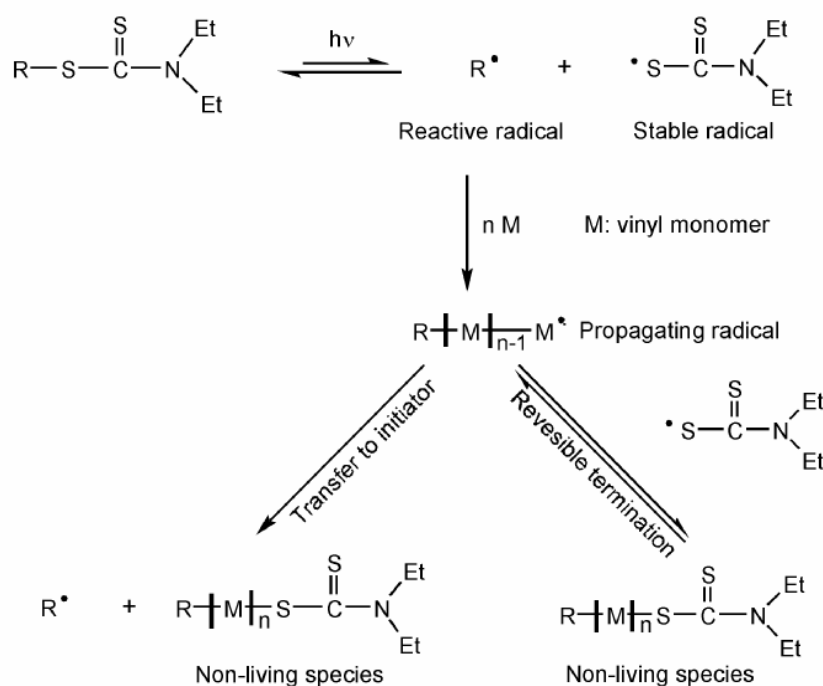
It is interesting to note that in the case of the “grafting from” methods the polymer backbone is chemically modified in order to introduce active sites capable to initiate the polymerization of a monomer, leading to graft copolymers. The number of grafted chains can be controlled by the number of active sites generated along the backbone, assuming that each one participates in the formation of one branch chain (graft). Our purpose will be to use this method to perform the grafting of dimethylphosphonate-functionalized polymers onto natural rubber by photopolymerization of dialkylphosphonate-functionalized monomers initiated from iniferter groups.

Polymerizations of vinyl monomers using iniferters as initiating species are of considerable interest (Otsu *et al.*, 1982 and 1989; Georges *et al.*, 1994). They lead to polymers of relatively low polydispersity and can be used to produce block or graft copolymers. The procedure based on the pioneer works of Otsu *et al* in 1982, was reported as “living” free-radical photopolymerization of vinyl monomers initiated by “iniferters”. Otsu used the term “iniferter” to define compounds capable to act efficiently as **initiator**, **transfer** agent, and **terminator**. Otsu and Yoshida (1982) described the important role of the iniferter in the polymerization process. Under suitable conditions, the iniferter compounds (Scheme 2.1) split (through S-S or C-S bonds) into two radicals, a reactive radical that participates to the initiation of the polymerization and a non-reactive radical (resistant radical) that cannot initiate a polymerization but acts as a primary radical terminator. The linkage, generally a C-S bond, between the growing macroradical and the resistant radical is weak enough to enable repeated scission to the macroradical and resistant radical. The polymers

obtained can be used as macroiniferters for further polymerization with other monomers to form block or graft copolymers. Because termination and other transfer reactions are negligible, these polymerizations occur by successive insertions of monomer molecules through the iniferter bond and are sometimes described as controlled polymerization. The reaction mechanism that is simply considered as an insertion of monomer between C-S bonds is described in Scheme 2.1.

The strategy to achieve such conditions is to find a capping group that reversibly reacts with the propagating chains. In these conditions, the propagating chains are temporarily blocked and prevented from undergoing chain transfer and termination reaction. Some examples of iniferters that are useful for the photochemical synthesis of graft copolymers are diethyldithiocarbamate compounds (TC) (Otsu *et al.*, 1989, 1982 and 1984; Yang and Qiu, 1996; Kongkaewa and Wootthikanokkhana, 1999; Derouet *et al.*, 2007), mercaptobenzothiazole (BT) (Sebenik, 1998), and tetraphenyl biphosphine (Poljanšek *et al.*, 1999).

Derouet *et al.* (2009) studied the synthesis of graft copolymers of natural rubber and poly(dimethyl(acryloyloxymethyl)phosphonate) (NR-g-PDMAMP), and natural rubber and poly(dimethyl(methacryloyloxyethyl)phosphonate) (NR-g-PDMMEP), based on the photopolymerization in latex medium *via* a “grafting from” methodology. The graft copolymerization was initiated from *N,N*-diethyldithiocarbamate groups bound in side position of the rubber chains. It was found that the conversion and grafting rate increased with increasing monomer concentration and reaction time. DMAMP gave higher monomer conversion and grafting rate than DMMMP. Furthermore, grafting of phosphorus-containing monomers along NR chains constitutes a good approach to improve thermal stability and fire retardant of NR.



Scheme 2.1 Mechanism of “living” radical photopolymerization of vinyl monomers initiated from *N,N*-dialkyldithiocarbamate iniferters. (Derouet *et al.*, 2009)

2.4 Thermoplastic elastomers (TPEs)

Thermoplastic elastomers are a family of rubber-like materials that, unlike conventional vulcanized rubber, can be processed and recycled like thermoplastic materials, as defined by ASTM D 1566. The term TPEs sometimes also includes elastoplastic, thermoplastic rubber (TPR), thermoplastic vulcanizate (TPV), and impact modified plastic. In addition, there are a growth of subcategories of TPEs to distinguish between the different types of materials that generally meet in the TPE definition. Several examples are thermoplastic rubber blends, block copolymers, and ionomers. These different terms are used to indicate different morphological structures, different elastomeric performance, and depend on specific application needs.

Normally, a thermoplastic elastomer must have three essential characteristics (Grady and Cooper, 1994):

1. The ability to be stretched to moderate elongations and, after release of the stretch, to return to its original shape
2. The processability as a melt at elevated temperature
3. The absence of significant creep

The classification of the main TPEs of commercial importance is given in Figure 2.9. Also, the structure of three main classes of TPE systems are schematically shown in Figure 2.10

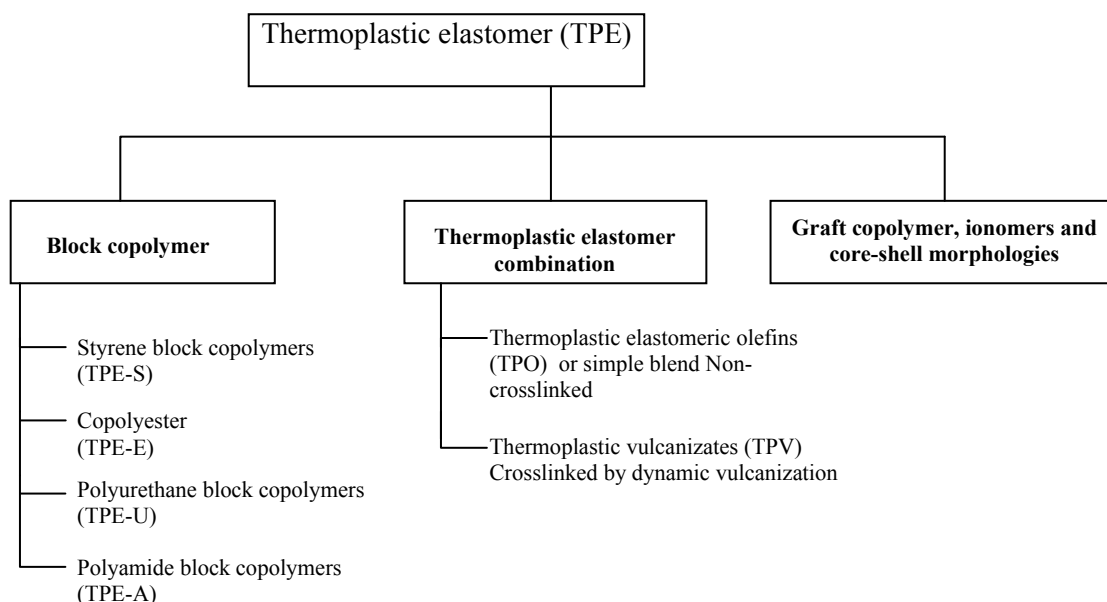


Figure 2.9 Classification of TPEs.

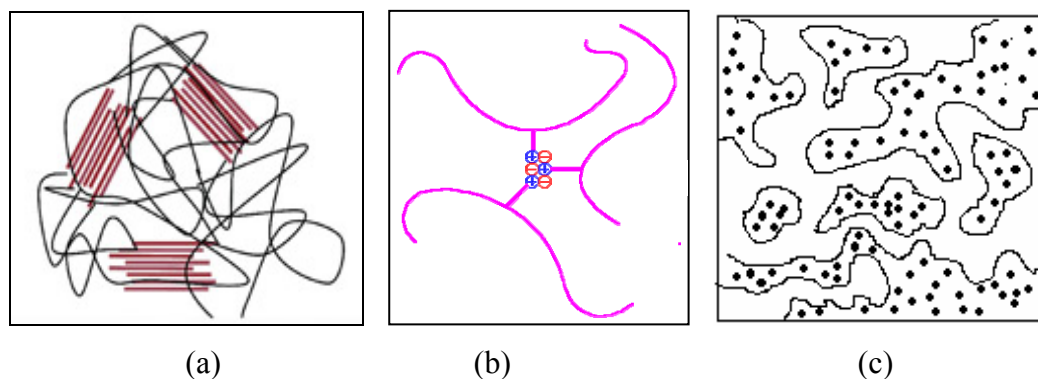


Figure 2.10 Representation of different TPE structures: segmented block copolymer (a), ionomer (b), and hard polymer/elastomer blends (c). (Holden, 2000)

Segmented block copolymers (Figure 2.10a) usually consist of elastomeric segments (soft segments) and crystallizable segments (hard segments). Due to incompatibility between the soft and the hard segments, phase separation occurs and the hard segments crystallize in nano-sized fiber-like crystals. The soft phase gives the material with elastomeric character while the crystallized hard segments serve as physical crosslinks, providing the material dimensional stability and reinforcement of the soft matrix. By heating the polymer above its melting temperature the fiber-like crystals melt and the material can be processed using conventional thermoplastic processing technique.

Ionomers (Figure 2.10b) are polymers with ionic groups that have an electric charge, either positive (+) or negative (-). They contain both non-ionic repeat units, and a small amount of ion containing repeating units. The non-polar chains are grouped together and the polar ionic groups are attracted to each other. This allows thermoplastic ionomers to act in a way similar to that of crosslinked polymers. However, ionomers are not crosslinked polymers. When ionomers are heated, the ionic groups will lose their attractions from each other and the chains will move around freely and the groups cannot stay in their clusters. The clusters cause polymer with the properties of an elastomer and the processability of a thermoplastic.

The blends incorporating hard polymers and elastomers (Figure 2.10c) are produced by mixing the hard polymer and the elastomer together at temperature higher than melting temperature of thermoplastic, using high shear mixing equipment. TPEs based on rubber and plastic blends are among the most interested materials and probably the fastest growing sector in TPE market (Ibrahim and Dahlan, 1998) due to the performances, simple processing and practical productivity, the ease of processing, the recyclability, and the cost effectiveness. TPEs based on plastic and rubber blends can be classified as thermoplastic polyolefin (TPO) or simple blend with a non-crosslinked rubber phase, and dynamic vulcanizate (DV) or thermoplastic vulcanizate (TPV) with crosslinked rubber domains dispersed in a thermoplastic matrix. TPOs are preferably used at lower temperatures without exposition to high mechanical stress. Lower specific gravity than comparable thermoset rubber and TPV containing various additives. On the other hand, the TPVs are widely used in automotive industry with high application temperature.

2.4.1 Simple blends

Thermoplastic elastomer referred as a simple blend (physical blend) can be obtained by uniformly mixing an elastomer with a thermoplastic resin. Many possible morphologies can be observed in a two-phase system. However, morphology of thermoplastic elastomer material is only the co-continuous structures, which is similar to open cells of foam material. That is, the foamed material is one phase dispersed in another phase of air, as illustrated in Figure 2.11. To maintain good fabric ability and a balance of rubber-like performance, this type of morphology yields a product with strength derived from the continuous hard phase, but with flexibility derived from the continuous soft phase. Microstructure in this system enables each phase to share load bearing capability of the material.

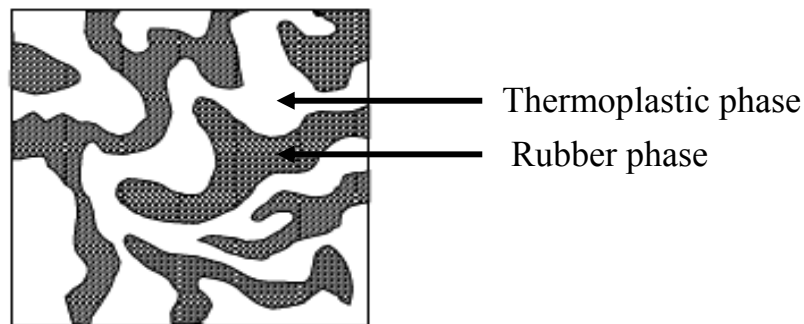


Figure 2.11 Co-continuous structure of TPE based on simple blend of rubber and plastic material. (Holden, 2000)

Co-continuous phase morphology which is a criteria for producing TPE material has been observed in many polymer blend systems under the optimum conditions. Formation of the thermoplastic elastomer material based on simple blend of two-components needs several requirements:

a) The viscosity of polymer pairs must match at the temperature and shear rates of mixing. The temperature during mixing is controlled by adjusting the heating or cooling system on the mixing equipment such as a twin screw extruder or an internal mixer. The optimum viscosity match also depends on the proportions of the two components. Based on experimental observations, the phase with lower

viscosity or higher volume fraction tends to form the continuous phase. Jordhamo *et al* (1986) introduced the semi-empirical expression relation where dual co-continuity phase occurred at a certain viscosity ratio and volume ratio of the blend components. That is, the phase inversion should occur when the viscosity ratio and the volume ratio are about equal, i.e., when:

$$\frac{\eta_1}{\eta_2} = \frac{\phi_1}{\phi_2} \quad (2.1)$$

where η_i is the viscosity of phase i and ϕ_i is the volume fraction of phase i .

The phase inversion is the onset period of changing in morphologies of binary polymer blends. That is, the major phase becomes a minor or dispersed phase while the minor phase becomes form a matrix or major phase. Figure 2.9 shows an ideal plot of viscosity ratio versus composition ratio. The dashed line represents the equality in Equation 2.1 that indicates the midpoint of the phase inversion region. Dual phase co-continuity is expected in a region of viscosity ratio/composition ratio space around the phase inversion line. This region is arbitrarily indicated in Figure 2.12 by the solid lines enclosing the phase inversion line. The exact width and shape of this region will depend upon the system and material under consideration and will have to be determined experimentally. If relation lines below the dual phase region, then phase 1 will be the continuous phase and *vice versa*. In general, for a fixed set of processing conditions, the viscosity ratio will be a constant and phase continuity is most easily obtained by altering the volume fraction of the components. It is also possible to predict the composition ratio required if the viscosities of the components are known using the following relation:

$$\text{Log}_{10}(\eta_A/\eta_B) = 2-4\phi_B \quad (2.2)$$

where η_A and η_B are the viscosities of the components A and B at the processing conditions and ϕ_B is the volume fraction of component B.

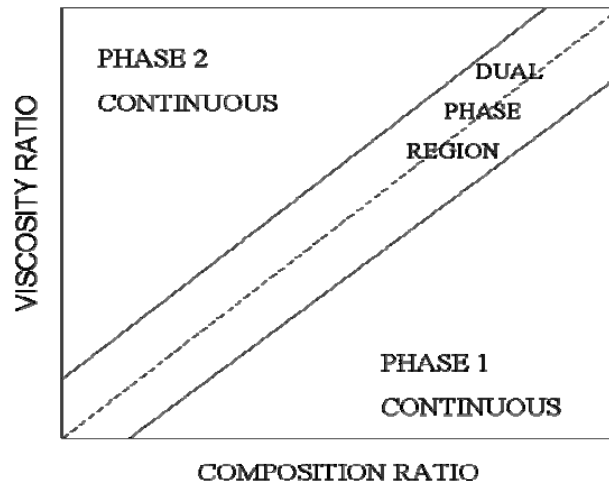


Figure 2.12 Relationship between the ratio of the viscosities of two components and their proportion in the mixture. (Gergen *et al.*, 1987)

b) The compatibility of the two components correlated with the interfacial tension between the two polymers. If two polymers have a large interfacial tension, the formation of a two-phase system with large phase dimensions (i.e., a coarse dispersion) is favored. This coarse dispersion reduces the interfacial area and hence, the interfacial energy. In contrast, polymer pairs with similar solubility parameters or polarity tend to form a finer dispersion. However, if the two polymers have very different solubility parameters, i.e., one is polar while the other is non-polar. They will probably form a coarse dispersion with poor adhesion between the phases. (Gergen *et al.*, 1987)

2.4.2 Thermoplastic vulcanizates (TPVs)

One favorable method of making a TPE material was developed by dynamically vulcanized during blending process. The dynamically vulcanized rubber phase provided the material with good mechanical strength and recovery properties (Tinker *et al.*, 1989). The improvements of various properties of TPVs are:

- Reduce permanent set;
- Improved ultimate mechanical properties;
- Improved fatigue resistance;
- Greater resistance to attack by fluids;
- Improved high temperature utility;

- Greater stability of phase morphology in the melt;
- Greater melt strength;
- More reliable thermoplastic fabricability.

The important factors which cause superior properties of TPVs more than simple blend are listed below:

2.4.2.1 Dynamic vulcanization

Dynamic vulcanization was first discovered by Gessler in 1962 for preparation of high impact compositions containing different amounts of partially vulcanized elastomers in isotactic polypropylene (iPP)/polyisobutylene blends. The first thermoplastic vulcanizate (TPV) introduced in the market in 1973 was a partially crosslinked EPDM phase in EPDM/PP blend. The effects of the size and crosslinking degree of vulcanized rubber particles dispersed in thermoplastic matrix on the materials on properties of TPVs are shown in Figure 2.13. It is seen that the TPV exhibited the superior properties by two important factors: size of vulcanized rubber domains and degree of crosslinking. Generally, the fully vulcanized rubber particles dispersed in the thermoplastic matrix of the TPVs have a size of approximately 0.5-2.0 μm . Smaller rubber domains result in an improvement of mechanical properties. Holden *et al* (1996), Rader (2003), and Coran and Patel (1996), suggested that decreasing size of rubber particles caused an increase in stress and strain at break with the smallest cured rubber particles in a range of 1 - 1.5 μm . In addition, tensile strength, modulus at 100% elongation, and oil resistance were improved abruptly with increasing the degree of crosslinking of the rubber phase, as shown in Figure 2.13(b).

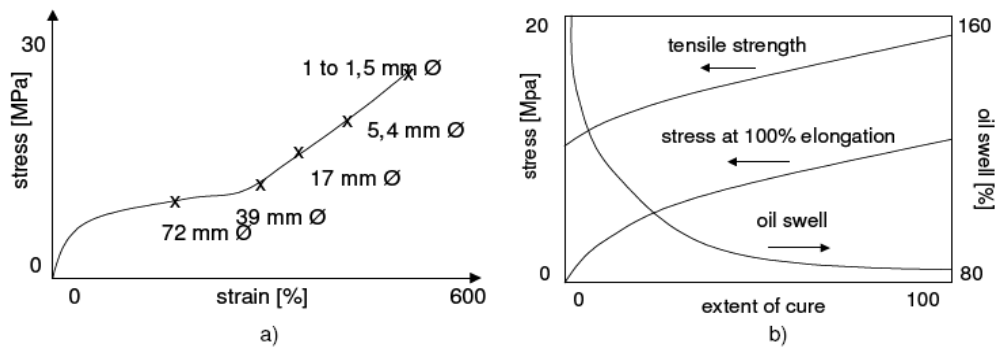


Figure 2.13 Effect of particle size of rubber domains on stress-strain properties of TPVs (a), and effect of extent of cure on mechanical properties and oil swell of TPVs (b). (Coran and Patel, 1996)

2.4.2.2 Morphological development

The morphology of thermoplastic vulcanizates (TPVs) differs from simple blend in a way that the rubber phase is crosslinked by dynamic vulcanization. In general, structure of TPVs consists of a fine dispersion of a crosslinked elastomer phase in hard thermoplastic matrix. During the preparation process, unvulcanized elastomer, vulcanizing ingredients, and thermoplastic are mixed together under high shearing conditions. The mixing temperature must be sufficient to melt thermoplastic and to cause vulcanization that takes place under high shear of dynamic conditions. When vulcanization starts and during crosslinking reaction of the rubber phase, the viscosity of the rubber increases. This causes an increase of the viscosity of the blend, since the melt viscosity of the thermoplastic matrix remains the same. Therefore, the viscosity mismatch between the elastomer and thermoplastic phases occurs and elongational flow is dominant in the flow regime. Hence, the dynamic vulcanizing elastomer phase tends to break up into smaller rubber particles dispersed in the thermoplastic matrix under continuous shearing stress, as the evolution of morphology schematically shown in Figure 2.14. It can be seen that the co-continuous phase of simple blend first occurred. Thereafter, it was gradually modified to dispersion of vulcanized rubber particles in the thermoplastic matrix. The formation of the characteristic matrix-particle morphology is essentially influenced by the kinetics of vulcanization reaction, resulting in

different crosslinking density of the rubber phase. If the crosslinking density of elastomeric phase is very low, it undergoes large deformation under low level of stress. On the other hand, if the crosslinking density is high, the rubber phase deforms under high shear stress without rupture. Therefore, an optimum of the crosslink density was approximately $10\text{-}20 \times 10^{-5} \text{ mol/cm}^3$. (Coran *et al.*, 1978)

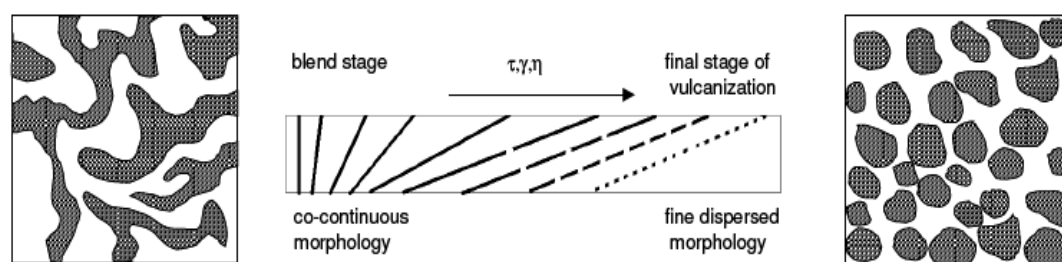


Figure 2.14 Morphology development of dynamic vulcanizates during mixing operation. (Radusch and Pham, 1996)

2.4.2.3 Vulcanization systems

Crosslinking of the rubber phase in heterogeneous blends of thermoplastic and rubber components takes place by introducing of curing agents during the mixing process. This causes crosslinking reactions with formation of covalent bonds between network points. Vulcanization of the rubber phase during mixing or dynamic vulcanization has been used to improve physical properties of thermoplastic elastomers (Coran and Patel, 1983; Fischer, 1973; Strichartzuk, 1977; Goettler *et al.*, 1982). A number of curing systems were used to vulcanize the rubber phase. These include sulphur, phenolic, and peroxide cured systems.

a. Sulphur cured system

Sulphur has been used as a main curing agent. In addition, accelerators such as benzothiazoles, sulfenamides, dithiocarbamates, and amines in combination with activators, such as zinc oxide or stearic acid, are used to shorten curing times and to prevent thermo-oxidative degradation of the rubber. Figure 2.15 shows scheme of the crosslinking reaction of rubber molecules by sulphur vulcanization system. Reactions of accelerator and activator (i.e., ZnO) causes opening of cyclic molecular sulphur (1). Hence, an active sulphurizing complex is formed (2). This complex is

self destroyed, and react with rubber chains leading to a sulphur-bound rubber intermediate (3). The sulphur-bound rubber intermediate thereafter reacts with other rubber chains and causes their crosslinking (4). The polysulphidic links between the rubber chains is consequent.

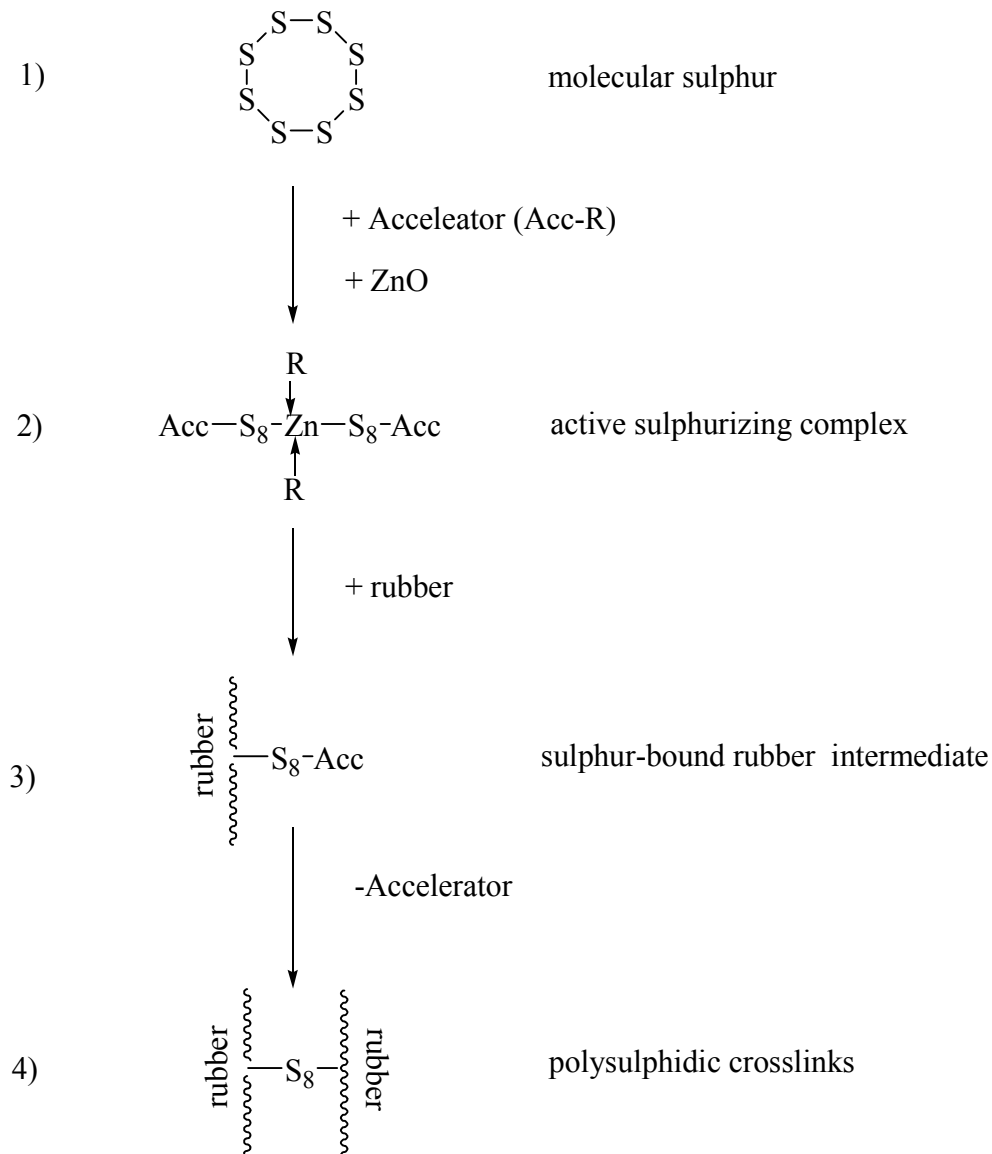


Figure 2.15 Crosslinking of diene rubbers using sulphur cured systems (modified from Coran, 1994).

b. Phenolic cured system

Phenol formaldehyde resins are used to vulcanize diene elastomers such as natural rubber, styrene butadiene rubber (SBR), and butadiene

(BR) in the absence of sulfur, as shown in Figure 2.16. The crosslinking reaction occurs through free phenol groups in presence of stannous or iron chloride catalysts (Van-Duin and Souphanthong, 1995; George *et al.*, 1995; Nakason *et al.*, 2006). Vulcanizates with improved mechanical properties and resistance to moisture and heat are obtained.

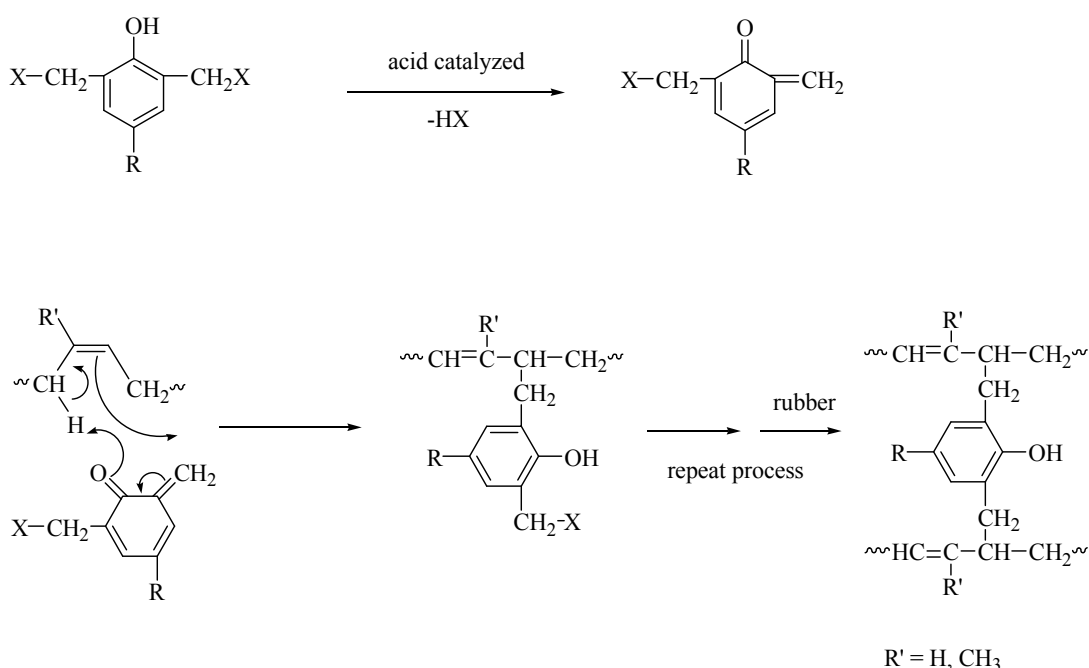


Figure 2.16 Crosslinking of diene rubbers using phenolic cured system. (Coran, 1994).

c. Peroxide cured system.

Peroxides are vulcanizing agents normally used for vulcanization of elastomers that do not contain reactive sites. Some example of elastomers that are vulcanized by peroxide such as ethylene-propylene rubber (EPR), ethylene-vinyl acetate copolymers (EAM), and silicone rubbers. Elastomers such as polyisoprene and polybutadiene can be also readily crosslinked by peroxides, but the properties of the vulcanizates obtained are found lower compared to those of sulphur vulcanizates. On the other hand, peroxide vulcanizates coming from diene rubbers exhibit better thermal ageing and compression set resistance. The mechanism of crosslinking reaction using peroxides is shown in Figure 2.17. At the beginning of the

vulcanization using peroxides, the organic peroxide is decomposed in two organic radicals that can abstract hydrogen atoms on the rubber chains and then convert them in macroradicals. The macroradicals can react together with formation of carbon-carbon intermolecular bridges.

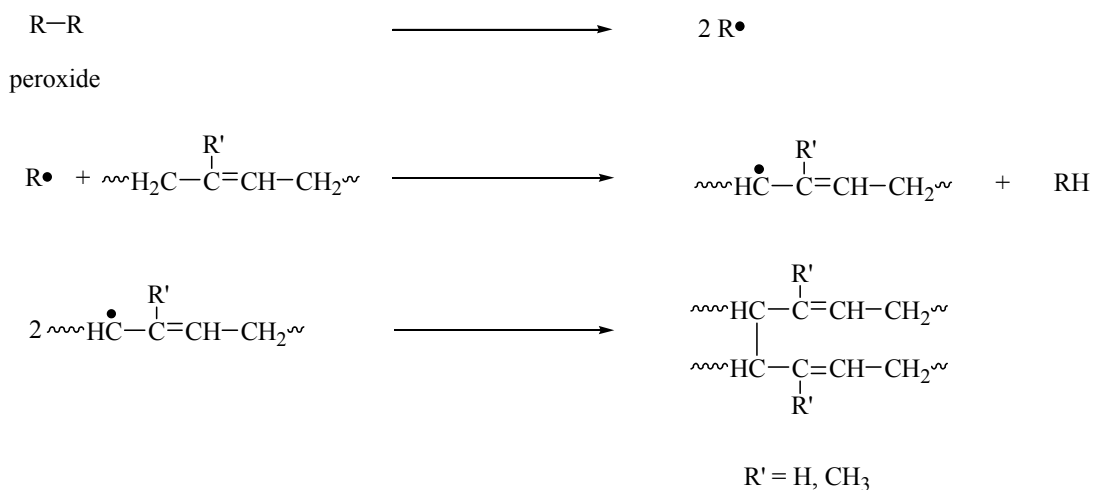


Figure 2.17 Crosslinking of diene rubbers using peroxide cured systems. (Coran, 1994)

The most common types of curing systems, i.e., sulphur, peroxide, and sulphur/peroxide mixed systems, were used for preparation of TPVs. Anyway, the most common vulcanizing method is sulphur which was used in various systems such as NR/HDPE (Nakason *et al.*, 2006b), NR/PS (Asaletha *et al.*, 1999) and NBR/PP (George *et al.*, 1999). It was found that the TPVs prepared using the sulphur curing system showed the highest elongation at break and good elastomeric properties (the lowest tension set). This was explained by the formation of more flexible C-S linkages. In the case of the TPVs prepared from rubber and PP blends using peroxide and mixed cured systems, a degradation of PP was noted due to the presence of peroxide. Moreover, the dynamic vulcanization of rubber and EVA blends carried out using peroxide cured systems caused the crosslinking of the EVA phase (John *et al.*, 2002). This leads to vulcanizates with poor mechanical properties. Other curing agents such as phenolic cured systems (i.e., HRJ-10518 and SP-1045) were also used to perform dynamically curing of ENR/PP blends (Nakason *et al.*,

2008). It was found that TPVs with phenolic containing cured systems exhibited higher viscosity, elastic modulus and tensile strength. Moreover, phenolic cured systems lead to the smallest vulcanized rubber domains dispersed in the thermoplastic matrix.

2.5 Thermoplastic natural rubber blends (TPNRs)

Thermoplastic natural rubber blends are a group of thermoplastic elastomers prepared by blending NR with thermoplastics in various proportions. There are several types of thermoplastic that could be used to prepare TPNRs. They include polystyrene (PS) (Asaletha, 1999), polypropylene (PP) (Pichaiyut *et al.*, 2008; Nakason *et al.*, 2006a and 2007; Akhtar, 1988; Ibrahim and Dahlan, 1998; Choudhury *et al.*, 1989), high density polyethylene (HDPE) (Pechurai *et al.*, 2006; Nakason *et al.*, 2006b and 2006c), linear low density polyethylene (LLDPE) (Dahlan *et al.*, 1992; Abdullah *et al.*, 1995), poly(methyl methacrylate) (PMMA) (Oommen *et al.*, 1996 and 2000; Nakason *et al.*, 2005), and polyamide (PA) (Carone *et al.*, 2000). Ethylene-vinyl acetate (EVA) is also an interesting thermoplastic that can be blend with NR, because of its excellent properties (i.e., excellent ozone resistance, weather resistance, solvent resistance and excellent mechanical properties) and halogen free thermoplastic. (Doak, 1986).

Natural rubber/Ethylene-vinyl acetate blends

Ethylene-vinyl acetate (EVA) copolymers are considered as good partners for NR and several other polymer blends. Blends of natural rubber and EVA have been studied to improve processing characteristics and resistance against the action of degradation agents as thermal aging, γ radiation, and ozone attack (Koshy *et al.*, 1992). An improvement of impact resistance at low temperature and flex crack resistance of NR was noted after blending it with EVA, as well as an increase of melt processing and an enhancement of aging properties.

Several other works were reported on the blending of NR/EVA and the study of the properties of the blends obtained. Sujith and Unnikrishnan (2006) studied the sorption of solvents (i.e., n-alkanes) on crosslinked natural rubber/poly(ethylene-co-vinyl acetate) (NR/EVA) blends at 28, 38, 48, and 58°C,

with respect to the EVA content, curing system, solvent nature, and temperature of sorption. The solvent transport was found to decrease with increase of the EVA content in the blends. Furthermore, using the dicumyl peroxide (DCP) crosslinked blends exhibited the lowest solvent uptake. The transport coefficients, diffusion coefficients, and permeability coefficients, were found to decrease with increasing EVA content in the blends. Lee *et al.* (1993) studied the influence of the blend composition, peroxide content, and Zeosil (or white carbon filler) content on mechanical properties of the dynamically vulcanized NR and EVA blends. It was found that the tensile strength and modulus of the dynamically vulcanized NR/EVA blends were higher than those of the simple NR/EVA blends over the entire blend compositions. The tensile strength decreased but the modulus increased with increasing DCP contents. In addition, the tensile strength decreased with increasing NR content in the NR/EVA blend. The tear strength and hardness properties also decreased with increasing NR content but increased with Zeosil content. Zurina *et al.* (2006) studied the effect of irradiation on tensile strength, dynamic mechanical properties, thermal properties, and morphological properties of ENR-50/EVA blends. Every sample was irradiated using a 3.0 MeV electron beam (EB) irradiation with doses ranging from 20 to 100 kGy. The results indicated that the gel fraction of ENR-50, EVA, and ENR-50/EVA blend increased with increasing the irradiation dose. In addition, the tensile strength increased with increasing dose of the EB radiation. Furthermore, an increase of the elongation at break of ENR-50 and ENR-50/EVA blend, but a decrease of the elongation at break of EVA, was observed with increasing irradiation dose. It was also found that the T_g of all the samples increased with irradiation dose due to the effect of irradiation-induced crosslinking. The compatibility of ENR-50/EVA blend also found to be improved upon increasing irradiation doses. Furthermore, the T_m , T_c , and degree of crystallinity of ENR-50/EVA blends increased with increasing the irradiation dose. This was due to the perfection in the crystal growth occurring during the radiation.

2.6 Compatibilization of Polymer blends

Compatibilization is a process which is used to modify the interfacial properties of the immiscible polymer blends. It causes a reduction of the interfacial

tension coefficient and a stabilization of the desired blend morphology (Utracki, 2003). Most of the polymer blends are found to be incompatible, which are characterized by a two-phase morphology, narrow interface, low physical interactions across the phase boundaries, and poor mechanical properties (George *et al.*, 1995). These problems can be alleviated by addition of a third component into the incompatible polymer blends in order to enhance the degree of compatibility between the components (Bonner and Hope, 1993). The third component is called as a blend compatibilizer that is a macromolecular species exhibiting interfacial activities in heterogeneous polymer blends. Usually, the compatibilizers have a block copolymer structure, one block being miscible with one blend component and a second one miscible with the other blend component (Koning *et al.*, 1998). The mechanical properties of the blends will be determined not only by the properties of its components, but also by the phase morphology and the interfacial adhesion. The phase morphology and the interface adhesion are important from the viewpoint of stress transfer (Bonner and Hope, 1993). From a theoretical perspective, many works studied about the nature of the compatibility and the expected properties of the blends by probing and visualizing its morphology. Figure 2.18(a) shows the morphology of a miscible polymer blend. On the molecular level, the macromolecules of polymer A are intermingle with those of polymer B, and only one phase is observed (i.e., only one value of T_g). Concerning properties and processing, that is like a random copolymer. In order to be miscible, some attractions between the two polymers must be present to overcome the intra-molecular cohesive forces of the individual polymers. Inter-polymer attractions are due to the specific interactions between functional groups on polymer A and different functional groups on polymer B. However, only few polymer blends are totally miscible (Mark *et al.*, 1988b). Figure 2.18(b) shows the morphology of a non-miscible polymer blend. This is a second possible morphology of polymer blend that is more common than the first described in Figure 2.18(a). Generally, the polymer in lower concentration form a discontinuous or discrete phase, while the polymer in high concentration forms a continuous phase. The polymer blends are neither totally miscible nor immiscible. They are called as partially miscible blends. A representation of the morphology of a partially miscible polymer blend is given in Figure 2.18(c). A partially miscible

polymer blend may tend toward a completely miscible blend when one of the two polymers is incorporated in very small amounts. However, when the polymer ratios are almost similar, the phase separation occurs. Partially miscible blends consist of two phases, which may not have a well-defined boundary. The macromolecules of polymer A can significantly penetrate into the phase of polymer B and *vice versa*, but mainly at the interfaces. The domains are stable and a reinforcement of interfacial adhesion occurs. This explains why the two-phase blends usually have good bulk properties (Mark *et al.*, 1988b).

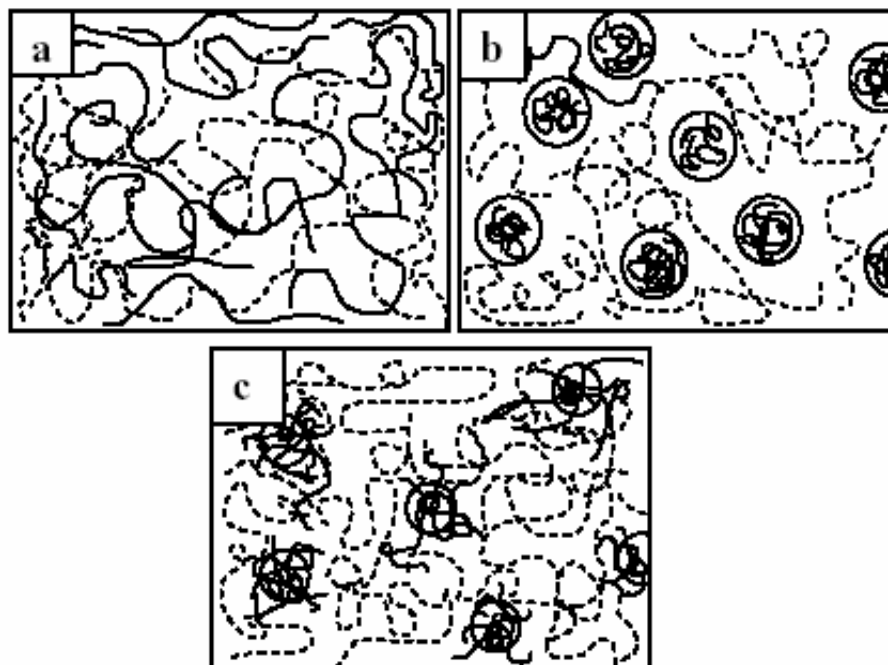


Figure 2.18 Possible morphologies of blends of polymer A (solid lines) and polymer B (dashed lines): (a) miscible, (b) non-miscible, (c) partially miscible. (Mark *et al.*, 1988b)

Compatibilization is therefore required to modify the blends and to produce desired properties. The compatibilization must not only ensure improvement in performance, but it also must be reproducible, improve stress transfer and repeated processings (Ajji *et al.*, 1996). The effects of compatibilization on the properties of binary polymer blends have been widely investigated (Nakason *et al.*, 2008; Oomen

et al, 1996; Jansen and Soares, 1996; Jansen *et al.*, 1996; Asaletha *et al*, 1995; George, 1995 and 1995a; Jansen *et al.*, 1995).

The compatibilization of non miscible polymer blends can be performed using several strategies such as addition of a block or graft copolymer, addition of functional polymers, or inducing *in situ* chemical reactions between the blend components (reactive blending). These strategies play an important role in the development of polymer blends. However, the addition of block or graft copolymers represents the approach the most extensively researched for the compatibilization (Bonner and Hope, 1993). Generally, a suitable block or graft copolymer contains segments that are chemically identical to each of the blend components: one segment is able to form interactions to one of the blend components and another segment interacts with the other blend component. Significant functions in the copolymer are expected to locate at the interface between immiscible blend phases. This causes a reduction of interfacial tension between the blend components and hence a reduction of the resistance to minor phase break up during melt mixing and reducing the size of the dispersed phase. Fine morphologies and high interfacial adhesion usually result in improved physical properties. The effects of copolymers on the morphology of polymer blends, the interfacial adhesion between blend phases, and blend properties depend on parameters such as the type and molecular weight of the copolymer segments, the blend composition, the blending conditions, etc. A classical view of how such copolymers locate at the interfaces is given in Figure 2.19. The most important researched result is that the compatibilizer used to bridge the interface provides a good adhesion between the two phases.

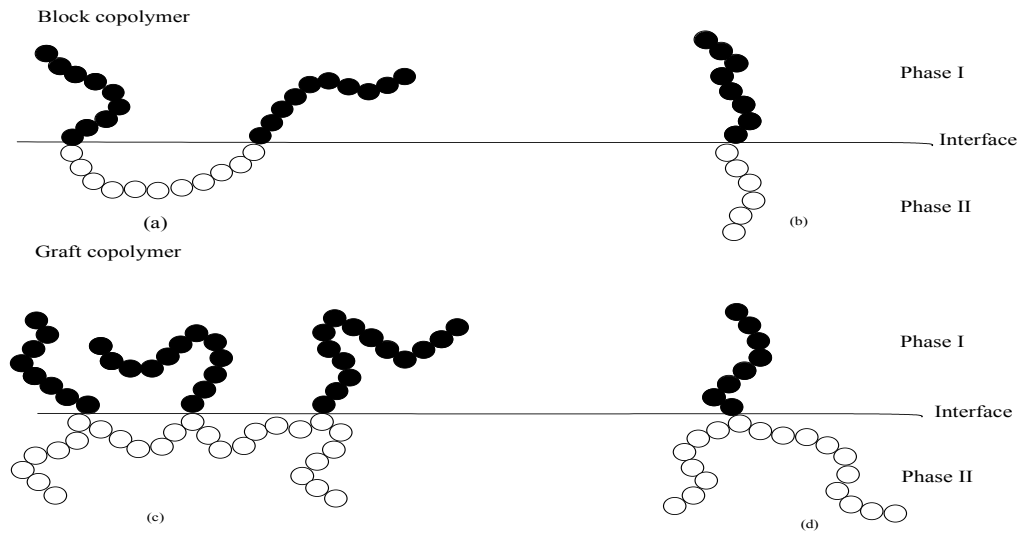


Figure 2.19 Penetration of block or graft copolymers as compatibilizers into I and II phases of a heterogeneous polymer blend: (a) triblock; (b) diblock; (c) multi grafts and (d) single graft. (Koning *et al.*, 1998)

Several research works were successfully performed with the aim to improve the physical properties of non-miscible binary polymer blends, with the purpose to decrease the phase morphology and to enhance the interfacial adhesion by incorporating a block or graft copolymer inside. Phinyocheep *et al.* (2002) studied the influence of various compatibilizers on the mechanical properties of blends containing a dispersed phase of scrap rubber dusts in polypropylene. They found that significant impact strength and elongation at break was reached by using 6 and 10 phr of styrene-ethylene/butylene-styrene (SEBS) and a maleic anhydride-modified styrene-ethylene-butylene-styrene and (SEBS-*g*-MA), respectively, as compatibilizers. The enhancements of the impact strength and the elongation at break are believed to arise from reduction of interfacial tension between the rubber and PP phases, which results in the decrease of the particle size of the fillers. Nakason *et al.* (2006a) studied the effects of phenolic-modified polypropylene (Ph-PP) and of graft copolymers of maleic anhydride and polypropylene (PP-*g*-MA) as blend compatibilizers of ENR/PP blends. Moreover, graft copolymers of HDPE and maleic anhydride (i.e., HDPE-*g*-MA), and two types of phenolic-modified HDPEs (i.e., PhSP-PE and PhHRJ-PE), were tested as compatibilizers for the ENR-

20/HDPE blends (Nakason *et al.*, 2008). The results showed that the blends incorporating compatibilizers exhibited higher tensile strength, hardness, and set properties than the ones without compatibilizer. The blends with compatibilizers also showed smaller phase morphologies than the ones without compatibilizer. Lohse *et al.* (1991) reported the compatibilization of ethylene-propylene rubber (EPR)/polypropylene (PP) blends by addition of up to 10 wt% of EPR-g-PP graft copolymer. The efficiency of the compatibilization was reported to be influenced by the molecular weights of the segments of the block or graft copolymers. When the molecular weight of the compatibilizer segments was low, the depth of penetration of the compatibilizer into the domains was also low. This led to poor interfacial adhesion. On the other hand, the penetration was high when the molecular weight of the compatibilizer segments was very high. Macaúbas and Demarquette (2001) added SBS and SEBS as compatibilizers in PP/PS blends. Morphological, viscosity, and interfacial tension results showed that SEBS was a better compatibilizer for PP/PS blends than SBS. Kunyawut (2006) studied PS/LDPE blends in the absence and presence of SEBSs of different molecular weights as compatibilizers. He found that high molecular weight SEBSs were more effective as coalescence retardation than the low molecular weight ones. The ability to retard coalescence was also found to increase with the increase of SEBS concentration. Galloway *et al.* (2005) studied the effect of symmetric polystyrene–polyethylene block copolymers (PS–PE) of different molecular weights on the morphology of 50/50 PS/PE blends. They found that the presence of 1 % of block copolymer of intermediate molecular weight (i.e., 40,000 g/mol) dramatically decreased the phase size and provided excellent stabilization during annealing process. The addition of high molecular weight block copolymers to the blend did not cause an as much decrease of phase size as the incorporation of block copolymer of intermediate molecular weight. The incorporation of a suitable molecular weight block copolymer caused a balance between the ability of the block copolymer to reach the interface and its relative effectiveness as a compatibilizer.

CHAPTER 3

MATERIALS AND METHODS

3.1 Materials

3.1.1 Materials used for synthesing NR-g-PDMAMP, NR-g-PDMMEP and NR-g-PDMMMP

3.1.1.1 High ammonia (HA) concentrated natural rubber latex

Natural rubber (NR) latex with 60% dry rubber content (DRC) was used as a raw material for preparation of NR-g-PDMAMP, NR-g-PDMMEP and NR-g-PDMMMP, and was manufactured by Yala latex Co., Yala, Thailand.

3.1.1.2 Non-ionic surfactant (Sinnopal NP307)

Sinnopal NP307, $(\text{HO}-(\text{C}_2\text{H}_4\text{O})_n-(\text{C}_6\text{H}_4)\text{C}_9\text{H}_{19})$, was used to stabilize the latex during epoxidation reaction. It was manufactured by Cognis, Meaux, France. It is colourless liquid with a mild odor with specific gravity of 0.99-1.07.

3.1.1.3 Formic acid

Formic acid (H_2CO_2) (99% purity) was used to prepare performic acid by reacting with hydrogen peroxide. The performic acid was used to prepare epoxidized natural rubber (ENR). The formic acid used in this work was manufactured by Riedel De Haën, Seelze, Germany. The molecular weight is 154 g/mol.

3.1.1.4 Hydrogen peroxide

Hydrogen peroxide (H_2O_2) (35 wt%) was used as a co-reagent to prepare *in situ* performic acid for epoxidation reaction of NR latex. It was manufactured by Riedel De Haën, Seelze, Germany.

3.1.1.5 Sodium N,N-diethyldithiocarbamate trihydrate

Sodium N,N-diethyldithiocarbamatetrihydrate ($C_5H_{10}NNaS_2 \cdot 3(H_2O)$) was used as a photoiniferter by introducing in side position of the natural rubber chain. It is light yellow solid powder. It was manufactured by Acros Organics, Geel, Belgium.

3.1.1.6 Tetrabutylammonium bromide (TBAB)

TBAB ($C_{16}H_{36}NBr$) (98% purity) was used as a phase transfer catalyst. It was manufactured by Acros Organics, Geel, Belgium.

3.1.1.7 Methacryloyl chloride

Methacryloyl chloride (C_4H_5OCl) or 2-methyl-2-propenoyl chloride (97% purity) was used to prepare dimethyl(methacryloyloxyethyl) phosphonate (DMMEP) and dimethyl(methacryloyloxymethyl) phosphonate (DMMMP) by reacting with dialkyl(hydroxyalkyl)-phosphonate. It is colorless liquid with density of 1.07 g/ml and a boiling point of 95-96 °C. It was purchased from Aldrich Chemical Company Inc., Milwaukee, USA.

3.1.1.8 Acryloyl chloride

Acryloyl chloride (C_3H_3ClO) (96% purity) or 2-propenoyl chloride or acrylic acid chloride, is a clear, light yellow, flammable liquid with an acid smell. It has density of 1.119 g/cm³ and boiling point of 75.0 °C. It is a commercial product of Aldrich Chemical Company, Inc., Milwaukee, USA.

3.1.1.9 Dimethyl phosphite

Dimethyl phosphite ($C_2H_7O_3P$) or dimethyl hydrogenphosphate (98% purity) was used to prepare dimethyl(2-hydroxymethyl)phosphonate for synthesis of monomer (i.e., DMAMP and DMMMP). It was manufactured by Aldrich Chemical Company, Inc., Milwaukee, USA. It is colorless liquid with boiling point of 170 °C and density of 1.2 g/cm³.

3.1.1.10 Paraformaldehyde

Paraformaldehyde ((CH₂O)_n) was used to react with dimethyl phosphite for a preparation of dimethyl(acryloyloxymethyl) phosphonate (DMAMP) and dimethyl(methacryloyloxymethyl) phosphonate (DMMMP) monomers. It was manufactured by Aldrich Chemical Company, Inc., Milwaukee, USA.

3.1.1.11 Dimethyl(2-hydroxyethyl)phosphonate

Dimethyl(2-hydroxyethyl)phosphonate (C₄H₁₁O₄P) is a colourless liquid with 95% purity. It was used to synthesize dimethyl-(methacryloyloxyethylmethyl)phosphonate (DMMEP) monomer. It is a commercial product of Fluka Chemie (Buchs, Switzerland).

3.1.1.12 Methanol

Methanol (CH₃OH) (95% purity) was used to precipitate NR and graft copolymer from the latex forms, and was distilled before used. It is colorless liquid with density and boiling point at 0.7918 g/cm³ and 64.7 °C, respectively. It was manufactured by Fluka Chemie, Buchs, Switzerland.

3.1.1.13 Dichloromethane

Dichloromethane (DCM) or methylene chloride (CH₂Cl₂) was used as a solvent to synthesize DMAMP, DMMEP and DMMMP monomers, and was distilled under nitrogen atmosphere. It is a colorless liquid with a molecular weight of 84.93 g/mol, a density of 1.3255 g/cm³ and a boiling point of 39 °C. It was purchased from Fluka Chemie, Buchs, Switzerland.

3.1.2 Materials used for preparing of thermoplastic elastomer (TPE) based on NR and EVA blends

3.1.2.1 Natural rubber (NR)

NR, used as a blend component, was an air dried sheet (ADS) grade. It was manufactured by the Khuan PunTae Farmer Co-operative Co., Ltd. Phattalung, Thailand.

3.1.2.2 Ethylene vinyl acetate copolymer (EVA)

EVA, used as another blend component for preparing thermoplastic elastomer, was N8038 grade with 18 wt% vinyl acetate content. It was manufactured by the TPI Polyacrylate Co., Ltd., Rayong, Thailand. Some properties of EVA is shown in Table 3.1

Table 3.1 Some properties of EVA grade N 8038.

Properties	Value
Melt flow index 190 °C (ASTM D1238), g/10 min	2.30
Density (ASTM D1505), g/cm ³	0.941
Tensile strength at yield (ASTM D618), N/mm ²	4.0
Tensile strength at break (ASTM D618), N/mm ²	18
Ultimate elongation (ASTM D638), %	100
Softening temperature (ASTM D1535), °C	58

3.1.2.3 Sulphur

Sulphur (S₈) was used as a vulcanizing agent for NR in dynamic vulcanization. It is a yellow powder with a melting point of 115.21°C. It was manufactured by Siam Chemicals Co., Ltd., Samutprakarn, Thailand.

3.1.2.4 Dicumyl peroxide (DCP)

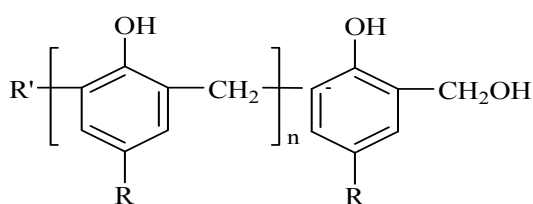
Dicumyl peroxide ($C_{18}H_{22}O_2$) was used as a curing agent in dynamic vulcanization of NR during preparation of thermoplastic vulcanizates (TPVs). It contains 40% active peroxide with melting point in a range of 38-41 °C. It was manufactured by Akzo Nobel Polymer Chemicals BV, Amesfoort, The Netherlands.

3.1.2.5 Triallyl cyanurate (TAC)

Triallyl cyanurate (TAC) was used as a co-agent in peroxide vulcanization system during dynamic vulcanization of NR/EVA blends. It is a colorless viscous liquid which contains 50% of active functional group. This product was purchased from Fluka Chemie, Buchs, Switzerland.

3.1.2.6 Hydroxymethylol phenolic resin (HRJ-10518)

HRJ-10518 was used as phenolic vulcanizing agent to perform dynamic vulcanization of natural rubber/EVA blend. It contains 6-9% active hydroxymethyl (methylol) groups, It was manufactured by the Schenectady International Inc., New York, USA. The molecular structure is shown in Figure 3.9. Some properties of HRJ-10518 are shown in Table 3.3



R: -H or -CH₂OH

R': -C(CH₃)₂CH₂C(CH₃)₃

Figure 3.1 Molecular structure of HRJ-10518

Table 3.2 Properties of HRJ-10518.

Property	Value
Melting Point, (°F)	140-150
Softening Point, (°C)	80-95
Methylol Content, (%)	6-9
Specific gravity	1.05

3.1.2.7 Stannous chloride

Stannous chloride ($\text{SnCl}_2 \cdot 2\text{H}_2\text{O}$) was used as a catalyst in cross-linking reaction of phenolic resin and NR. The molecular weight, density and melting point are 225.63 g/mol, 2.71 g/cm³ and 37-38 °C, respectively. It was manufactured by Schenectady International Inc., New York, USA.

3.1.2.8 Stearic acid

Stearic acid ($\text{C}_{18}\text{H}_{36}\text{O}_2$) was used as an activator in sulphur and mixed (sulphur and peroxide) vulcanization systems. It is a waxy white solid with molecular weight of 284.47 g/mol. The density at 70°C, melting point and boiling point are 0.847 g/cm³, 69.6°C and 383°C, respectively. It was manufactured by Imperial Chemical Co., Ltd., Pathumthani, Thailand.

3.1.2.9 Zinc oxide

Zinc oxide (ZnO) was used as an activator in sulphur and mixed (sulphur/peroxide) vulcanization system. It is a white powder with molecular weight of 81.4084 g/mol, a density of 5.606 g/cm³ and a melting point of 419°C. It was manufactured by Global Chemical Co., Ltd., Samutprakarn, Thailand.

3.1.2.10 N-tert-butyl-2-benzothiazyl sulphenamide (TBBS)

N-tert-butyl-2-benzothiazyl sulphenamide ($C_{11}H_{14}N_2S_4$) was used as an accelerator in sulphur vulcanization system. It is a delayed active accelerator in scorch time. The molecular weight and melting point are 238.37 g/mol and 105 °C, respectively. It was manufactured by Flexsys America L.P., Ohio, USA.

3.1.2.11 Petroleum oil (IRM 903)

IRM 903 was used to characterize oil swelling resistance of the NR/EVA TPVs. It is equivalent to ASTM Oil no.3. It is a light yellow liquid with low viscosity. General properties of IRM 903 are shown in Table 3.3. It was manufactured by DSM Co., Ltd, Rotterdam, Netherlands.

Table 3.3 General properties of Petroleum oil (IRM 903) (ASTM D5964)

Property	Value
Viscosity: cst at 38°C	33.0 ± 1.1
Gravity, API at 16°C	22.0 ± 1.0
Flash point, °C	163 (minimum)
Aniline point, °C	70.0 ± 1.0
Naphthenics, Cn%	40 (minimum)
Paraffinics, Cp%	45 (maximum)
Specific gravity	0.8
Aromatic, Ca%	14
Pour point, °C	-31
Viscosity-gravity constant	0.880 ± 0.005

3.2 Instruments

3.2.1 UV lamps

UV lamp (Philips HPR-125 watt, Turnhout, Belgium) was used as the UV-light source at wavelength of 365 nm for photopolymerization. It is the high-pressure mercury vapor lamps.

3.2.2 Internal Mixer

Internal mixer used in this work was Brabender Plasticorder, model PLE 331 (Brabender OHG Duisburg, Germany) with a mixing chamber of 80 cm³. The mixer consists of an enclosed mixing chamber with two rotors to perform high-speed mixing. The rotor speed and mixing temperature can be adjusted in a range of 0 to 500 rpm and 25 to 300°C, respectively.

3.2.3 Two Roll Mill

Two-roll mill (Chaicharoen Karnchang Ltd., Bangkok, Thailand) was used to compound rubber with additives and to make a thin sheet for subsequent molding. The machine used in this work consist of rollers with a diameter of 160 mm and a length of 360 mm equipped with electrically-heated devices. It is capable of performing or mixing materials at temperatures up to 400°C.

3.2.4 Compression Molding

Compression molding (Chaicharoen Karnchang Ltd., Bangkok, Thailand) was used to fabricate the thermoplastic elastomer material to a thin sheet which was later cut to various types of test specimens. The press is equipped with electric heater (up to maximum temperature of 350°C) and standard electrically heated platens with hydrolic diameter of 8 inches.

3.2.5 Mooney Viscometer

A Mooney viscometer, model VISCAL (Tech Pro Co., Ltd, USA) was used to measure Mooney viscosities of natural rubber and graft copolymers. A

flat serrated disk rotates in the rubber with a fixed rotor speed of 2 rpm. Test temperature is preheated at 100°C for 1 min and testing for 4 min according to ASTM D1646-04.

3.2.6 Fourier Transform Infrared Spectrometer (FT-IR)

FT-IR model Omnic ESP Magna-IR 560 Spectrometer with wave number in a range of 4000-400 cm^{-1} (Nicolet Instrument Corporation, Madison, USA.) was used to characterize a molecular structure of monomers (i.e., DMAMP, DMMEP and DMMMP) and graft copolymers. Liquid samples were analyzed in the form of thin films sandwich between two NaCl disks. Solid samples were analyzed using KBr pellets.

3.2.7 Nuclear Magnetic Resonance Spectrometer (NMR)

NMR spectrometer model Bruker DPX 200 (Bremen, Germany) was used to characterize molecular structures of monomers (i.e., DMAMP, DMMEP and DMMMP) and polymers. The structural information of molecules was detected at 200.13 MHz for ^1H , at 50.32 MHz for ^{13}C , and at 81.01 MHz for ^{31}P . Samples were analyzed in form of solution in deuterated chloroform (99.8% purity, Spectrométrie Spin et Techniques). The ^1H and ^{13}C -NMR, the chemical shifts (δ) as expressed in ppm, were compared with the signal of tetramethylsilane (TMS), as internal standard. The ^{31}P -NMR spectrum was also expressed in ppm (δ), with reference to the phosphoric acid peak, as external standard.

3.2.8 Moving Die Processability Tester (MDPT)

Moving die processability tester (RheoTech MDPT, Tech-Pro, Inc., Cuyahoga Falls, USA) with a conical shape die was used to investigate dynamic properties of TPEs. The uniform shear strain was performed on the test specimen with a dimension of 30x30x3 mm which was loaded onto the lower die. The upper die was then closed to form a constant volume in a conical shape die. The test was performed using frequency sweep mode at constant strain of 7% at 80°C.

3.2.9 Moving Die Rheometer (MD+)

Moving die rheometer (RheoTech MD+, Tech Pro, Inc., Cuyahoya Falls, USA) was used to study curing behaviour of rubber compounds at 150°C. The amplitude of the oscillation was set at 0.5 of arc at a frequency of 1.7 Hz, according to ISO 6502.

3.2.10 Transmission Electron Microscope (TEM)

TEM model: JEOL JEM-2010 (Jeol, Tokyo, Japan), was used to analyze morphological properties of NR latex particles and graft copolymer latices. The polymer-grafted natural rubber latex was diluted to approximately 400 times of its original concentration with distilled water. An aqueous solution (2 wt%) of OsO₄ was added to stain natural rubber macromolecules. The stained latex was then placed on a 400 mesh grid, and dried overnight in a dessicator before characterization. The wide range of magnifications, in this work, of 5,000 time was used.

3.2.11 Scanning Electron Microscope (SEM)

SEM, model: JSM-5800 LV (Jeol, Tokyo, Japan), is used to characterize morphology of the sample surface by scanning with high-energy electron beam in a raster scan pattern. The samples were sputtered with gold before examination. The electrons interact with atoms and producing signals that contain information of surface topography, composition and other properties with a characteristic three-dimensional appearance useful for understanding the surface structure of a sample. The wide range of magnifications could be used however in this work, a magnification of 5,000 time was used.

3.2.12 Tensile Testing Machine

The tensile testing machine, model H 10KS manufactured by Hounsfield Test Equipment Co., Ltd. (Croydon, England) was used at cross head speed of 500 mm/min. The machine consist of load cells (10 kN), grips: pull-rod type wedge action grips 30 kN (thicker and molded polymer specimens) and pneumatic action grips 3 kN (sheet specimens). Tensile test specimen was prepared by cutting the molded sheet using die C, according ASTM D412. Stress-strain tests

(constant deformation rate), modulus, tensile strength, ultimate elongation and visco elastic recovery tests were performed using this machine.

3.2.13 Differential Scanning Calorimeter (DSC)

Differential scanning calorimeter, model DSC Q100 (TA Instruments, New Castle, USA) equipped a TA Universal Analysis thermal analysis data station, and fitted with a mechanical system of cooling by compression (RCS) capable to go down to temperatures as low as $-90\text{ }^{\circ}\text{C}$. A sample (3– 10 mg) was placed in the DSC sample pan, and the heating rate was set at $10\text{ }^{\circ}\text{C min}^{-1}$. The sample was quenched to $-80\text{ }^{\circ}\text{C}$ for 1 min, then heated up to $100\text{ }^{\circ}\text{C}$ and kept at this temperature for 5 min to remove the heat history. Then, the sample was slowly quenched again to $-80\text{ }^{\circ}\text{C}$ and the second heating scan was recorded. This technique was used to measure glass transition temperatures (T_g), melting temperature (T_m), and percentage of crystallinity (X_c) of polymers.

3.2.14 Thermogravimetric Analyzer (TGA)

Thermogravimetric Analysis (TGA) was performed using a TGA Q100 TA Instrument-Walters equipped with an EGA oven furnace. A 10-20 mg sample was placed in a platinum pan. Analyses were carried out under nitrogen or oxygen atmospheres of gas flow = 100 ml.min^{-1} , at a heating rate of $10^{\circ}\text{C.min}^{-1}$ with a temperature range of 30 to 575°C .

3.2.15 Oxygen Index Tester

Flammability behaviour of NR-g-PDMMMP was carried out using Stanton Redcroft Limiting Oxygen Indexer (Tarlin Scientific Co., U.K.) with $100\text{mm}\times 6.5\text{mm}\times 3\text{mm}$ specimens according to ASTM D-2863.

3.2.16 Burning Tester

Burning Tester according to ISO 3582 was built in house. Horizontal burning characteristics was measured in the chamber, having inside dimension of

600±5mm length, 300±5mm width and 760±5mm height, equipped with a gaseous hydrocarbon fuel burner and support holder.

3.2.17 Hardness Tester

Indentation typed shore durometer (Afri, Italy) was used for hardness testing of specimens according to ASTM D 2240.

3.3 Experiments

3.3.1 Preparation of NR-*g*-PDMAMP, NR-*g*-PDMMEP and NR-*g*-PDMMMP

3.3.1.1 Monomer synthesis

DMAMP was first synthesized as follows; Dimethyl(hydroxymethyl)phosphonate (0.2 mol) was first placed in a 500 ml two-necked round-bottom flask equipped with a magnetic stirrer. Distilled triethylamine (0.22 mol) was added, then the mixture was cooled down in an ice bath. A solution of freshly distilled acryloyl chloride (0.2 mol) in 200 ml of dry dichloromethane was then added drop by drop. The mixture was kept at 0 °C for 1 h, then stirred overnight at room temperature. The amine hydrochloride salt was filtered out. The organic phase was washed with small portions of water, treated with anhydrous sodium sulfate, filtered and evaporated solvent. The residue was distilled under vacuum in presence of a small amount of hydroquinone as inhibitor. The obtained monomer was then characterized by ¹H-NMR, ¹³C-NMR, ³¹P-NMR, and FTIR respectively.

DMMEP were prepared using the same procedure as DMAMP. But, methacryloyl chloride and dimethyl(1-hydroxyethyl)phosphonate were used instead of acryloyl chloride and dimethyl(hydroxymethyl)phosphonate, respectively. DMMEP was also characterized by ¹H-NMR, ¹³C-NMR, ³¹P-NMR, and FTIR:

PDMMMP was prepared using, methacryloyl chloride and dimethyl(1-hydroxymethyl)phosphonate using similar procedures for preparation of DMAMP and DMMEP. PDMMMP was also characterized by ¹H-NMR, ¹³C-NMR, ³¹P-NMR, and FTIR.

3.3.1.2 Epoxidation of natural rubber latex

a. Epoxidation of natural rubber latex for NR-g-PDMAMP, NR-g-PDMMEP and NR-g-PDMMMP preparations.

Epoxidized natural rubber (ENR) latex was prepared from NR latex (60% DRC). The latex was first diluted to 20 % DRC with deionized water and stabilized with a non-ionic surfactant (Sinnopal NP 307) at 3.5 wt% of dry rubber content. The NR latex was stirred for 12 h at room temperature to eliminate ammonia and then transferred into a reactor equipped with a mechanical stirrer and a reflux condenser. The mixture was heated to 60°C. Formic acid was added drop by drop, and then hydrogen peroxide was added gradually with continuous stirring for 72 h. The amount of hydrogen peroxide used was calculated in order to obtain a theoretically epoxidation level of 20 mol% for preparation of NR-g-PDMAMP and NR-g-PDMMEP, and epoxidation level of 10, 20 and 30 mol% for NR-g-PDMMMP. Formic acid was used in equimolar quantity in comparison with hydrogen peroxide.

The ENR latex was coagulated in methanol and dried under vacuum. The structure and level of ENR was analyzed by ¹H-NMR.

b. Calculation of epoxidation unit

The epoxidized unit of epoxidized natural rubber was determined by ¹H-NMR technique. This was proposed by many workers (Bradbury and Perera, 1985; Perera, 1987; Burfield *et al.*, 2003 Roy *et al.*, 1993 and Derouet *et al.*, 2005). The epoxidation level was taken from the integrated area of protons corresponding to oxirane ring and protons of carbon-carbon double bond in 1,4-polyisoprene units, by the relationship:

$$\text{epoxidized units (\%)} = \frac{I_{(2.7)}}{I_{(2.7)} + I_{(5.1)}} \times 100 \quad (3.1)$$

Where, $I_{(2.7)}$ and $I_{(5.1)}$ represent the integrations of the signals characteristic of protons of oxirane rings in epoxidized units (at 2.7 ppm) and protons of carbon-carbon double bonds in 1,4-polyisoprene units (at 5.1 ppm), respectively.

3.3.1.3 Synthesis of N,N-diethyldithiocarbamate-functionalized natural rubber (DEDT-NR)

Addition of sodium N,N-diethyldithiocarbamate (DEDT) onto epoxidized natural rubber was carried out in a latex, according to the method previously described by Derouet *et al.*, (2007 and 2008). ENR latex was first diluted to 5 % DRC, Na₂CO₃ was then added to adjust pH to approximately 8 before introduction of sodium N,N-diethyldithiocarbamate trihydrate (DEDT-Na) and tetrabutylammonium bromide (TBAB) as a phase transfer catalyst. The reaction mixture was stirred at 70 °C for 168 h. After reaction, the DEDT-NR was isolated for analysis by coagulation in methanol, and then washed several times with water. It was then dried under vacuum until a constant weight was obtained.

¹H-NMR analysis was used to determine the content of N,N-diethyldithiocarbamate-functionalized 1,4-polyisoprene units. The rate of N,N-diethyldithiocarbamate functionalized units contained in the rubber sample was determined by using the following relationship:

$$\text{DEDT units (\%)} = \frac{I_{(4.35)}}{I_{(2.70)} + I_{(5.20)} + I_{(4.35)}} \times 100 \quad (3.2)$$

Where, $I_{(2.7)}$, $I_{(5.20)}$, and $I_{(4.35)}$ represent the integration of the signals characteristic of protons of oxirane rings in epoxidized units, protons of carbon-carbon double bonds in 1,4-polyisoprene units, and protons on carbons bearing a N,N-diethyldithiocarbamate group [-CH[SC(S)NEt₂]] of N,N-diethyldithiocarbamate functionalized units, respectively.

3.3.1.4 Grafting procedure

a. Grafting procedure of NR-g-PDMAMP, NR-g-PDMMEP and NR-g-PDMMMP

Grafting reactions were performed in latex in 25 ml Pyrex glass tubes equipped with a magnetic stirrer. The glass tubes was closed by a screwed stopper with a teflon covered sealing joint. The reactions were carried out at room temperature under nitrogen atmosphere. An UV lamp with a wavelength of 365 nm

was used as irradiation source to initiate the grafting reaction. Studies were performed using two [monomer]/[DEDT-NR units] molar ratios of 3.5 and 7.0 for prepared NR-g-PDMAMP and NR-g-PDMMEP at DEDT-NR unit of 5.5%. For preparation of NR-g-PDMMMP, three levels of DEDT-NR unit (i.e., 4, 7, 12%, respectively) were studied at the same ratio of concentration in monomer by comparison with the concentration in initiating units at a constant molar ratio [monomer] / [DEDT-NR units] of 1.25. After grafting, the graft copolymer was coagulated in methanol, and then purified by dissolution/re-precipitation with dichloromethane/methanol. The product was then dried at 40°C under vacuum until constant weight was obtained.

b. Calculation of monomer conversion and grafting rate

Monomer conversions, monomer conversions in grafts, and grafting rates (GR is defined as the weight percent of dimethylphosphonate-functionalized grafts in the copolymer) were calculated from the following equations:

$$\text{Monomer conversion (\%)} = \frac{W_c - W_t}{W_m} \times 100 \quad (3.3)$$

$$\text{Monomer conversion in grafts} = \frac{W_s - W_t}{W_m} \quad (3.4)$$

$$\text{Grafting rate (\%)} = \frac{W_s - W_t}{W_s} \times 100 \quad (3.5)$$

where, W_c is the weight of the purified polymer mixture recovered after grafting; W_t is the weight of DEDT-NR before grafting, W_m is the weight of monomer used for the grafting reaction and W_s is the weight of graft copolymer isolated after extraction with methanol

3.3.1.5 Average length of the grafts (degree of polymerization)

Grafting rate (GR), as well as the average length of the grafts, i.e., the degree of polymerization (\overline{DP}_n), were also determined from $^1\text{H-NMR}$ spectra of the graft copolymers obtained after extraction of the dimethylphosphonate functionalized homopolymer that possibly formed. They were calculated by comparing the peak areas of the various signals characteristic of the different types of protons present in the graft copolymer, as follows:

Considering the integration of the rubber chain part in the spectrum of the graft copolymer, I_{rubber} , it includes three different types of units (unsaturated NR units, epoxidized NR units, and DEDT-functionalized NR units) whose units proportions (X, Y, and Z, respectively; $X + Y + Z = 1$), unchanged after grafting, could be determined from the $^1\text{H-NMR}$ spectrum of DEDT-NR used as macroinitiator.

By taking into account the results of the previous studies (Tran, 2008), it was considered in the calculation of I_{rubber} that N,N-diethyldithiocarbamate groups at the end of the grafts have totally disappeared after polymerization. Therefore, I_{rubber} can be determined as follows:

$$I_{\text{rubber}} = (8 \times H_{\text{unsaturated NR units}}) + (8 \times H_{\text{epoxidized NR units}}) + (9 \times H_{\text{DEDT-NR units}}) \quad (3.6)$$

where, $H_{\text{unsaturated NR units}}$ is the I_{uns} integration of the signal at $\delta = 5.0 - 5.2$ ppm on the copolymer spectrum (signal of $=\text{CH-}$ protons of unsaturated NR units), $H_{\text{epoxidized NR units}} = (I_{\text{uns}} \times Y)/X$, and $H_{\text{DEDT-NR units}} = (I_{\text{uns}} \times Z)/X$.

Knowing the integration corresponding to the rubber part in the copolymer spectrum (I_{rubber}), the \overline{DP}_n of PDMAMP, PDMMEP or PDMMMP grafts can be obtained from the following equation:

$$\overline{DPn} = \frac{(I_{total} - I_{rubber})}{A \times H_{DEDT-NR \text{ units}}} \quad (3.7)$$

where, $(I_{total} - I_{rubber})$ is the integration corresponding to the graft protons in the graft copolymer; A is the number of protons in the used monomer (i.e., A = 11 in the case of DMAMP, A = 15 in that of DMMEP, and A = 13 in that of DMMMP).

The number-averaged molecular weight (\overline{Mn}) of phosphorated grafts was obtained by multiplication of \overline{DPn} with the molecular weight of the chosen monomer. Thus, the GR was calculated by applying the following equation:

$$GR = \frac{(M_1 \times \overline{DPn} \times Z)}{(M_1 \times \overline{DPn} \times Z) + (M_2 \times X) + (M_3 \times Y) + (M_4 \times Z)} \times 100 \quad (3.8)$$

where, M_1 = molecular weight of the monomer used (194 g/mol for DMAMP, 222 g/mol for DMMEP or 208 g/mol for DMMMP), M_2 = molecular weight of NR unit (68 g/mol), M_3 = molecular weight of epoxidized NR unit (84 g/mol), M_4 = molecular weight of N,N-diethyldithiocarbamate-functionalized NR in which the N,N-diethyldithiocarbamate group is changed with an hydrogen (considering that the grafts are not terminated by a N,N-diethyldithiocarbamate group).

3.3.1.6 Kinetic studies

Grafting reactions were performed as described in section 3.3.1.4 using two [monomer]/[DEDT-NR units] molar ratios of 3.5 and 7.0 for preparation of NR-g-PDMAMP and NR-g-PDMMEP. For preparation of NR-g-PDMMMP, three levels of macroinitiator of DEDT-NR unit i.e., 4, 7, 12%, respectively, were used to initiate the polymerization at the same ratio of concentration in monomer by comparison with the concentration in initiating units at a constant molar ratio [monomer]/[DEDT-NR units] = 1.25. Different grafting reactions were performed and stopped at various times, and the obtained crude mixtures were treated as described in sections 3.3.1.4 and 3.3.1.5 to determine monomer conversion, monomer conversion in grafts, and grafting rate by weighing, using equations 3.3 to

3.5, respectively. On the other hand, the obtained crude mixtures were also analyzed by ^1H NMR to calculate $\overline{\text{DPn}}$ and grafting rate, by using the equations 3.7 and 3.8 respectively.

3.3.2 Compatibility studies of natural rubber (NR) and ethylene vinylacetate copolymer (EVA) blend.

3.3.2.1 NR-g-PDMMMP compatibilizers

NR-g-PDMMMP was prepared according to section 3.3.1.4(a). Graft copolymer synthesized from 4 % of DEDT-NR unit in the rubber chains (DEDT-NR) with polymerization time of 1 h is denoted as NR-g-PDMMMP 71%. Also, graft copolymer prepared from different DEDT-NR unit such as 4, 7 and 12% with polymerization time for 180 min, are denoted as NR-g-PDMMMP 80%, NR-g-PDMMMP 89% and NR-g-PDMMMP 95%, respectively, as described in Table 3.4. ^1H -NMR, FT-IR and moving die processability tester were used to characterize the obtained graft copolymer. The monomer conversion, monomer conversion in the grafts, grafting rate and $\overline{\text{DPn}}$ were calculated following equation 3.3-3.8.

Table 3.4 Polymerization condition and grafting rate of NR-g-PDMMMP.

NR-g-PDMMMP code	Level of DEDT-NR unit	Polymerization time (min)	$\overline{\text{DPn}}$	Grafting rate* (%)
NR-g-PDMMMP 71%	4	60	26	71
NR-g-PDMMMP 80%	4	180	37	80
NR-g-PDMMMP 89%	7	180	38	89
NR-g-PDMMMP 95%	12	180	38	95

*measurement by weighing

3.3.2.2 Simple blend of NR/EVA

The 50/50 NR/EVA blend with and without blend compatibilizers were prepared. Effect of different types of blend compatibilizer (i.e., NR-g-PDMMMP, NR-g-PDMMEP, NR-g-PDMAMP and ENR-30), various grafting rate (i.e., 70, 80, 89 and 95%) and compatibilizer concentration (i.e., 1, 3, 5, 7, 9, 12 and 15 wt% of NR) of graft copolymer were studied.

a. Effect of different types of blend compatibilizers

Four types of chemical modification of NR i.e., NR-g-PDMMMP, NR-g-PDMAMP, NR-g-PDMMEP containing similar number of active groups (DEDT-NR unit) and grafting length (\overline{DP}_n) of 4 mol% and 37 and 30 mol% epoxidized natural rubber (ENR-30) were used as blend compatibilizers in 50/50 NR/EVA blend with loading level of compatibilizer at 7 wt% of NR. The formulations of the blend and mixing step were shown in Table 3.5. Mechanical and morphological properties of the TPVs are investigated.

Table 3.5. Formulation and mixing schedule of 50/50 NR/EVA blends with different types of compatibilizers.

Polymers	Quantity (wt%)	Mixing time (min.)
EVA	50	2
NR	50	3
Various types of compatibilizers (i.e., NR-g-PDMMMP, NR-g-PDMMEP, NR-g-PDMAMP and ENR-30)	7 wt% of NR	3

b. Effect of grafting rate of NR-g-PDMMMP blend compatibilizers

The graft copolymers with different grafting rates of NR-g-PDMMMP at 71, 80, 89 and 95% were fixed at a constant loading of 7 wt% of NR, as formulation is

shown in Table 3.6. The blended products were later fabricated by compression molding at 120°C under hydraulic pressure of 700 psi for 5 min.

Table 3.6. Formulation and mixing schedule of 50/50 NR/EVA blends with different grafting rate of NR-g-PDMMMP.

Polymers	Quantity (wt%)	Mixing time (min.)
EVA	50	2
NR	50	3
NR-g-PDMMMP 71%, 80%, 89% and 95%	7 wt% of NR	3

c. Effect of loading level of NR-g-PDMMMP blend compatibilizer

The 50/50 NR/EVA blend was prepared by melt-mixing using a Brabender plasticorder at 150°C and a rotor speed of 60 rpm, as formulation and mixing schedule were shown in Table 3.7. The effect of graft copolymer concentration on rheological, dynamic, mechanical and morphological properties of the blends were studied. Various loading level of NR-g-PDMMMP with a grafting rate of 80% at 1, 3, 5, 7, 9, 12 and 15 wt% of NR were investigated.

Table 3.7 Formulation and mixing schedule of 50/50 NR/EVA blends with various loading levels of NR-g-PDMMMP compatibilizer.

Polymers	Quantity (wt%)	Mixing time (min.)
EVA	50	2
NR	50	3
NR-g-PDMMMP 80%	0,1,3,5,7,9,12,15 wt% of NR	3

3.3.3 Thermoplastic vulcanizates (TPVs) based on NR/EVA blends

NR/EVA TPVs with the addition of additives and curing agents were prepared using a Brabender Plasticorder (PLE 330). The mixing was performed at 150°C with a rotor speed of 60 rpm and a fill factor of 80%. All components were incorporated step by step into the mixing chamber of Brabender Plasticorder. At the end of the mixing cycle, the materials were collected and fabricated into a sheet form by a compression molding.

3.3.3.1 Effect of blend ratios

The NR/EVA TPVs with various blend ratios of NR/EVA (i.e., 75/25, 60/40, 50/50, 40/60, 25/75) were prepared using a formulation as shown in Table 3.8. The effect of blend ratios was studied in terms of rheological, dynamic, mechanical and morphological properties.

Table 3.8 Formulation and mixing schedule for preparation of dynamically cured NR/EVA blends with variation of blend ratios.

Materials	Quantity (wt%)					Mixing time (min)
EVA	25	40	50	60	75	2
NR	75	60	50	40	25	3
ZnO	5	5	5	5	5	2
Stearic acid	1	1	1	1	1	1
TMQ	1	1	1	1	1	1
TBBS	1	1	1	1	1	1
Sulphur	2	2	2	2	2	8

3.3.3.2 Effect of vulcanization system

a. Static cure characteristic of NR with various curing systems

Various compounds used in this work was prepared using a formulation and mixing schedule as shown in Table 3.9 and 3.10. The NR was pre-masticated for 5 min. Compounding was carried out using a two-roll mill at a room temperature. The rubber compounds were sheeted and conditioned at room temperature for 24 h in a closed container. The curing behaviour was then characterized at 150°C using a moving die rheometer (RheoTech MD+) at a 1 arc. The scorch time, cure time and cure rate index were calculated based on the curing curve. Furthermore, the minimum and maximum torques of the curing curves were quantified. The rubber compounds were then moulded into test specimens at 150°C according to the respective cure times determined by RheoTech MD+.

Table 3.9 Formulation used to prepare NR compounds with different curing systems.

Ingredients	Quantity (wt%)			
	Sulphur system	Peroxide system	Mixed system	Phenolic system
NR	100	100	100	100
ZnO	5	-	5	1
Stearic acid	1	-	-	5
TMQ	1	1	1	1
TBBS	0.5	-	1	-
Sulphur	2	-	1	-
DCP	-	5	1	-
TAC	-	3	1.5	-
Stannous chloride	-	-	-	0.6
HRJ-10518	-	-	-	5

Table 3.10 Mixing schedule used to prepare NR compounds with different curing systems.

Ingredients	Mixing time (min)			
	Sulphur system	Peroxide system	Mixed system	Phenolic system
NR	5	5	5	5
ZnO	1	-	1	1
Stearic acid	1	-	-	1
TMQ	1	1	1	1
TBBS	1	-	1	-
Sulphur	1	-	1	-
DCP	-	1	1	-
TAC	-	1	1	-
Stannous chloride	-	-	-	1
HRJ-10518	-	-	-	1

b. Effect of dynamic vulcanization of 40/60 NR/EVA blend with various curing system.

Four types of curing system i.e., sulfur, peroxide, mixed (sulfur and peroxide) and phenolic cured system were used in NR and 40/60 NR/EVA TPVs in order to investigate the influence of the curing systems on rheological, dynamic, mechanical and morphological properties of the TPVs. The dynamically vulcanized blends were prepared using the formulations and mixing schedule shown in Tables 3.11 and 3.12, respectively.

Table 3.11 Formulation used to prepare NR/EVA TPVs with different curing systems.

Ingredients	Quantity (wt%)			
	Sulphur system	Peroxide system	Mixed system	Phenolic system
NR	40	40	40	40
EVA	60	60	60	60
ZnO	0.80	-	0.80	0.80
Stearic acid	0.16	-	-	0.16
TMQ	0.16	0.16	0.16	0.16
TBBS	0.08	-	0.16	-
Sulphur	0.32	-	0.16	-
DCP	-	0.80	0.40	
TAC	-	0.48	0.24	-
Stannous chloride	-	-	-	0.096
HRJ-10518	-	-	-	0.80

Table 3.12 Mixing schedule used to prepare NR/EVA TPVs with different curing systems.

Ingredients	Mixing time (min)			
	Sulphur System	Peroxide system	Mixed system	Phenolic system
EVA	2	2	2	2
NR	3	3	3	3
ZnO	1	-	1	1
Stearic acid	1	-	-	1
TMQ	0.5	0.5	0.5	0.5
TBBS	1	-	1	-
Sulphur	8	-	6	-
TAC	-	1	1	-
DCP	-	13	1	-
Stannous chloride	-	-	-	1
HRJ-10518	-	-	-	16

3.3.3.3 Effect of different types of blend compatibilizers

Four types of chemical modification of NR i.e., NR-g-PDMMMP, NR-g-PDMAMP, NR-g-PDMMEP containing similar number of active groups (DEDT-NR unit) and grafting length ($\overline{DP_n}$) of 4 mol% and 37 and 30 mol% epoxidized natural rubber (ENR-30) were used as blend compatibilizers in dynamically cured 40/60 NR/EVA blend with loading level of compatibilizer at 9 wt% of NR. The formulations of the blend and mixing schedule are shown in Table 3.13. Mechanical

and morphological properties of the TPVs were investigated.

Table 3.13 Formulation and mixing schedule used to prepare dynamically cured 40/60 NR/EVA blends with different types of NR-*g*-PDMMMP blend compatibilizer.

Ingredients	Quantity (wt%)				Mixing time (min)
EVA	60	60	60	60	2
NR	40	40	40	40	3
ZnO	0.8	0.8	0.8	0.8	1
Stearic acid	0.16	0.16	0.16	0.16	0.5
TMQ	0.16	0.16	0.16	0.16	0.5
TBBS	0.32	0.32	0.32	0.32	1
Sulphur	0.32	0.32	0.32	0.32	8
NR- <i>g</i> -PDMMMP	3.6	-	-	-	5
NR- <i>g</i> -PDMMEP	-	3.6	-	-	5
NR- <i>g</i> -PDMAMP	-	-	3.6	-	5
ENR-30	-	3.6	-	3.6	5

3.3.3.4 Effect of loading levels of blend compatibilizer

NR/EVA TPV was prepared by blending NR/EVA at a fixed blend ratio of 40/60. The different loading levels of **NR-*g*-PDMMMP 80%** compatibilizer i.e., 0, 1, 3, 5, 7, 9, 12 and 15 wt% of NR were used, as formulation and mixing schedule shown in Table 3.14. Properties of TPVs in terms of rheological, dynamic, mechanical and morphological properties were investigated.

Table 3.14 Formulation and mixing schedule used to prepare NR/EVA TPVs to investigate effect of loading level of NR-g-PDMMMP blend compatibilizer.

Ingredients	Quantity (wt%)								Mixing time (min)
EVA	60	60	60	60	60	60	60	60	2
NR	40	40	40	40	40	40	40	40	3
ZnO	0.8	0.8	0.8	0.8	0.8	0.8	0.8	0.8	1
Stearic acid	0.16	0.16	0.16	0.16	0.16	0.16	0.16	0.16	0.5
TMQ	0.16	0.16	0.16	0.16	0.16	0.16	0.16	0.16	0.5
TBBS	0.32	0.32	0.32	0.32	0.32	0.32	0.32	0.32	1
Sulphur	0.32	0.32	0.32	0.32	0.32	0.32	0.32	0.32	16
NR-g-PDMMMP	0	0.16	0.48	0.8	1.12	1.44	1.92	2.4	5

3.3.3.5 Effect of recyclability

The influence of reprocessability of 40/60 NR/EVA TPVs was performed based on the TPV with sulphur vulcanization system using NR-g-PDMMMP compatibilizer at a loading level of 9 wt% of NR. After each cycle of fabrication, the product was again pelletized using a Bosco plastic grinding machine. The pallet were passed through a two roll mill to obtain a thin sheet. The sample was then fabricated by compression molding. A series of four cycles of alternating compression molding was performed. The mechanical properties in each cycle of reprocessing were investigated compared with the virgin sample.

3.4 Preparation of test specimens

The rubber compounds and the blends after dump from the Brabender were passed to form a thin sheet using a two-roll mill which was kept at room temperature for 24 h in a closed container. The rubber compounds were then compression molded at 150°C according to the respective cure times determined by moving die rheometer. The simple blend and TPVs were also fabricated by compression molding machine at 150°C, 700 psi for 5 min. The polymer was later left in the mold and cooled down to room temperature under high pressure.

3.5 Testing and characterization

3.5.1 Rheological and dynamic properties

Dynamic properties of rubber compounds, NR/EVA simple blends and dynamically cured NR/EVA TPVs were characterized using a rotorless oscillating shear rheometer (RheoTech MDPT). The oscillation frequency was set for the frequency sweeps in the range of 0.38-188.5 rad/s for testing simple blend and 0.3-190 rad/s for TPVs at a constant strain of 3%. The dimension of specimens is around 40x40x2 mm. The storage modulus (G'), loss modulus (G'') and $\tan \delta = G''/G'$ as well as the complex viscosity (η^*) were characterized. All was calculated as follows below:

$$\text{Complex viscosity } (\eta^*), \text{ Pa.s} = \left(\frac{\tau'}{\dot{\gamma}} + \frac{i\tau''}{\dot{\gamma}} \right) \quad (3.9)$$

$$\text{Storage modulus } (G'), \text{ KPa} = \frac{\tau''}{\gamma} \quad (3.10)$$

$$\text{Loss modulus } (G''), \text{ KPa} = \frac{\tau'}{\gamma} \quad (3.11)$$

$$\tan \delta = \frac{G''}{G'} \quad (3.12)$$

Where τ' is viscous stress (Pa)

τ'' is elastic stress (Pa)

γ is shear strain

$\dot{\gamma}$ is shear rate (s^{-1})

3.5.2 Tensile properties

A tensile testing machine (model H 10KS) operating at 500 mm/min cross-head speed was used to determine the tensile properties in terms of tensile strength and elongation at break as well as the tension set of the sample. All tests were carried out at room temperature.

Tensile properties of NR, EVA and their blends were examined at 25 °C according to the ASTM D412 using dumb-bell shape (die c), as test specimen shown in Figure 3.12 and Table 3.15. Dumb-bell samples with a length of 115 mm were cut from a 3 mm thick moulded sheet. Tensile testing is performed by elongating a specimen and measuring the load carried by the specimen. Tensile properties can be extracted from the stress-strain curve. The following calculations are the most common results given:

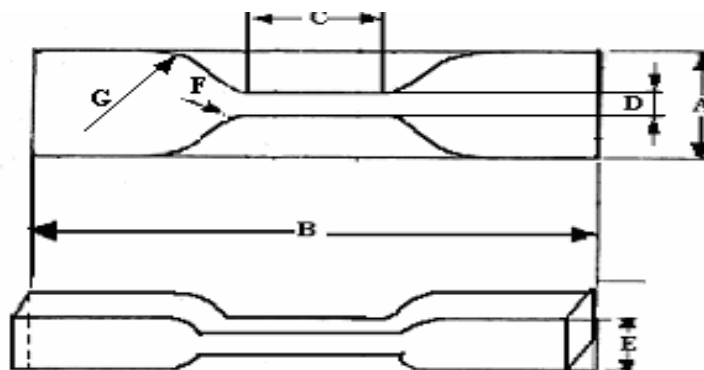


Figure 3.2 Standard Die shape for cutting dumbbell specimens.

Table 3.15 Dimensions of dumbbell die C.

Position	Dimension (mm)	Die C
A	Width of ends	25.0 ± 1.0
B	Overall length	115
C	Length of narrow portion	33.0 ± 1.0
D	Width of narrow portion	6.0 ± 0.1
E	Overall height	2.0 ± 0.1
F	Transition radius inside	25.0 ± 1.0
G	Transition radius outside	14.0 ± 1.0

3.5.2.1 Tensile strength

Tensile strength is the maximum stress on the stress coordinate on the stress-strain curve at the point of rupture. Tensile strength is measured in units of force per unit area as follow (ASTM D412):

$$\text{Tensile strength (MPa)} = \frac{F}{A} \quad (3.13)$$

Where F = the force magnitude at rupture, N.

A = cross section area of unstrained specimen, mm².

3.5.2.2 Elongation at break

Elongation at break is the percentage elongation at the rupture of the test specimen. The increase in length of a test specimen, which results from subjecting it to the breaking force in a tensile test, expressed as a percentage of the

distance between extended at the rupture compared to initial length of the specimen as follows (ASTM D412):

$$\text{Elongation at break (\%)} = \left(\frac{L - L_o}{L_o} \right) \times 100 \quad (3.14)$$

Where L = observed distance between bench marks at the rupture of the test specimen, mm.

L_o = original distance between bench marks of test specimen, mm.

3.5.2.3 Tension set

Tension set is the extent to which specimen is permanently deformed after being stretched at a specified amount (typically 100% elongation) for a short time (10 min). After 10 minutes of elongation, the specimens are allowed to relax for 10 minutes. After the 10 minutes retraction, tension set is measured the distance between bench marks and expressed as a percentage of a final distance between the bench marks after 10 minutes to original distance on the specimens as follows (ASTM D412):

$$\text{Tension set (\%)} = \left(\frac{L - L_o}{L_o} \right) \times 100 \quad (3.15)$$

Where L = final distance between bench marks after 10 min retraction, mm.

L_o = original distance between bench marks, mm.

3.5.3 Oil resistant properties

Swelling test (ASTM D471) were performed on a uniform of rectangular cut from the compression-molded samples with 10x10x2 mm. The test specimens were immersed in IRM 903 oil at room temperature for 168 h. This is to allow the swelling to reach diffusion equilibrium. The test piece was then taken out

and excessive oil was rapidly removed by blotting with filter paper before weighing. The swelling ratio is defined as:

$$\text{Swelling (\%)} = \left(\frac{W_t - W_o}{W_o} \right) \times 100 \quad (3.16)$$

Where W_t = mass of specimen after immersion, g.

W_o = initial mass of specimen after swelling, g.

3.5.4 Hardness properties

Durometer hardness is used to determine the hardness of materials. Hardness tests of rubber and NR/EVA blends samples were reported in Shore A scale. The test specimens are generally 6.4 mm (1/4 in) thick, according to ASTM D2240. The basic test requires applying the force in a consistent manner, without shock measuring the hardness (depth of the indentation). The test procedure was performed at room temperature. The specimen is first placed on a hard flat surface. The indenter for the instrument is then pressed into the specimen, making sure that it is parallel to the surface. Five different positions on the specimen were tested by indentation force that applied for the required time and then read. The hardness is read within one second after firm contact with the specimen.

3.5.5 Thermal properties

Thermal properties in terms of glass transition temperature (T_g) of NR, EVA and their blends were determined using DSC. The samples were first heated to 80°C, cooled to -80°C, and then re-heated to 100°C under nitrogen atmosphere. The heating and cooling rates were 10 °C/min. Melting temperature, crystallization temperature, and degree of crystallinity were also measured by DSC. The degree of crystallinity of pure EVA and their blends were evaluated from the ratio of heat of fusion of EVA to the heat of fusion of the perfectly crystalline polyethylene, as follows:

$$\text{Degree of crystallinity (\%)} = \frac{\Delta H}{\Delta H_0} \times 100 \quad (3.18)$$

Where ΔH = heat of fusion of crystalline of EVA determined from the area of the melting endotherm

ΔH_0 = heat of fusion of the perfectly crystalline polyethylene

($\Delta H_0 = 277.0$ J/g) (Wunderlich and Dole, 1957)

3.5.6 Cure characteristic

Rheological cure characteristic of NR with various vulcanization systems of NR/EVA were investigated using moving die rheometer. The cure rate index (CRI) is a measure of the rate of vulcanization based on the difference between the optimum vulcanization time, t_{c90} , and the incipient scorch time, t_{s2} , as follow:

$$\text{CRI} = \left(\frac{100}{T_{c90} - T_{s2}} \right) \quad (3.19)$$

Where T_{c90} is optimum cure time, min.

T_{s2} is scorch time, min.

3.5.7 Morphological properties

Morphological properties were investigated by scanning electron microscopy (SEM) and transmission electron microscopy (TEM) techniques. Samples were prepared by the cryogenic cracking in liquid nitrogen. To enhance morphological features and to facilitate easy identification of phases, the cryogenically fractured samples were etched with hexane to extract the NR phase for the simple blend. In case of NR/EVA TPVs, samples were etched with tetrahydrofuran (THF) to extract the EVA phase. The dried samples were eventually sputter-coated with gold and scanned under a scanning electron microscope.

Transmission electron microscopy (TEM) was also used to study the morphological properties of the graft copolymers latex (NR-g-PDMAMP, NR-g-PDMMEP and NR-g-PDMMMP). The latices were first diluted to approximately 400 times of its original concentration with distilled water. An aqueous solution (2 wt%) of OsO₄ was added to stain natural rubber macromolecules. The stained latex was then placed on a 400 mesh grid, and dried overnight in a dessicator before characterization.

3.5.8 Flammability

3.5.8.1 Limit oxygen index, LOI

The LOI values of NR and NR-g-PDMMMP were measured according to the ASTM D2863. The flammability of a material can be indicated by the amount of oxygen used in the burning reaction in the atmosphere of a mixture of oxygen and nitrogen gases. LOI values were calculated according to the following equation.

$$\text{LOI \%} = \frac{\text{O}_2}{\text{O}_2 + \text{N}_2} \times 100 \quad (3.20)$$

Where O₂ is volume of oxygen.

N₂ is volume of nitrogen.

3.5.8.2 Burning rate

Burning rate measurements were carried out according to the ISO3582. Test specimens (50x150x13 mm) were conditioned in dessicator at 27°C with humidity of 65% before test at least 24 h. The specimen was marked at 125 mm far from the top, and then placed in gauze which is was clamped in the holder horizontally as shown in Figure 3.13. The top of the specimen was set in order to contact with the center of flame so that the entire top specimen was well burning. The top of the specimen was ignited using a hydrocarbon gas burner for 60 sec. The

specimen was left burning until it extinguished. The burning time which was necessary used to burn from the top to the mark or in a length of 125 mm was recorded. Therefore, the burning rate is defined as:

If the flame front passes the gauge mark,

$$\text{Burning rate} = \frac{125}{t_b} \quad (3.21)$$

Where t_b is the time at which the flame reaches the gauge mark, sec.

If the flame front does not reach the gauge mark,

$$\text{Burning rate} = \frac{L_e}{t_e} \quad (3.22)$$

Where t_e is the time when the flame is extinguished, sec.

L_e is the extent burn, mm.

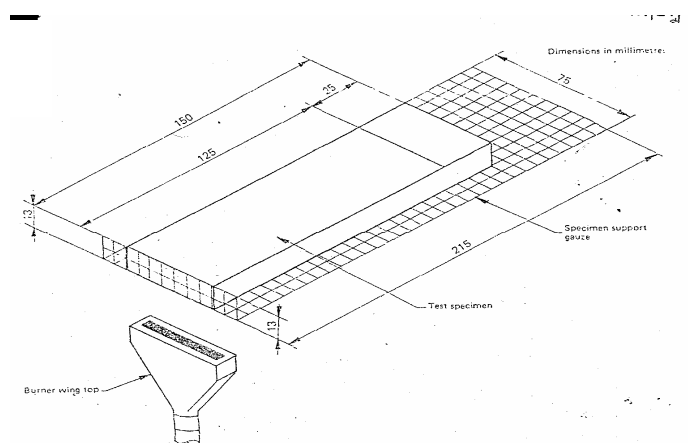


Figure 3.3 Standard specimen shape for testing flammability according to the ISO3582.

CHAPTER 4

RESULTS AND DISCUSSION

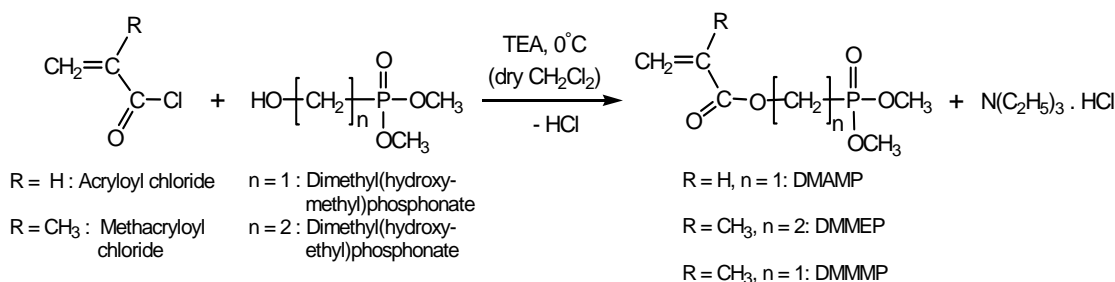
Part A

SYNTHESIS AND CHARACTERIZATION OF NATURAL RUBBER SUPPORT OF DIMETHYLPHOSPHONATE POLYMER GRAFTS

4.1 Monomer synthesis

4.1.1 Synthesis of vinyl dimethylphosphonate monomers

In order to synthesize graft copolymers composed of NR backbone and polymer grafts bearing phosphonate functions *via* a “grafting from” procedure based on the radical photopolymerization of acrylate and methacrylate monomers, three monomers containing dimethylphosphonate functions, i.e., dimethyl(acryloyloxymethyl)phosphonate (DMAMP), dimethyl(methacryloyloxyethyl)phosphonate (DMMEP), and dimethyl(methacryloyloxymethyl)phosphonate (DMMMP) were synthesized. DMAMP was prepared by condensation reaction between acryloyl chloride and dimethyl(hydroxymethyl)phosphonate (Liepins *et al.*, 1978 and Jeanmaire *et al.*, 2002), whilst DMMEP and DMMMP were prepared using methacryloyl chloride with dimethyl(1-hydroxyethyl)phosphonate and methacryloyl chloride with dimethyl(1-hydroxymethyl)phosphonate, respectively (Scheme 4.1). The reactions were performed in dry dichloromethane using triethylamine (TEA) as acid acceptor.



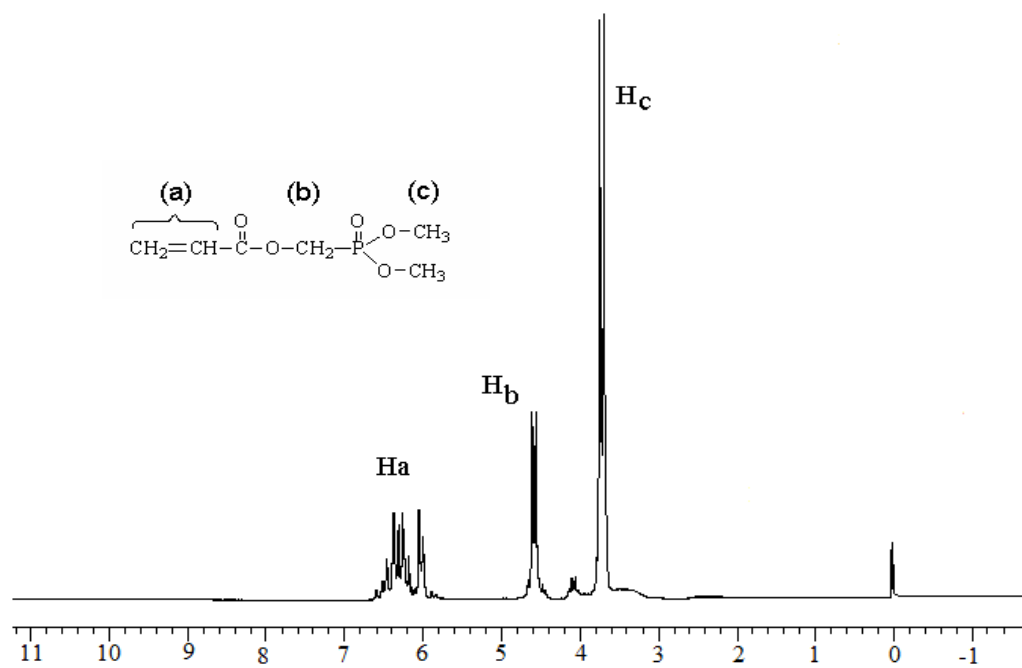
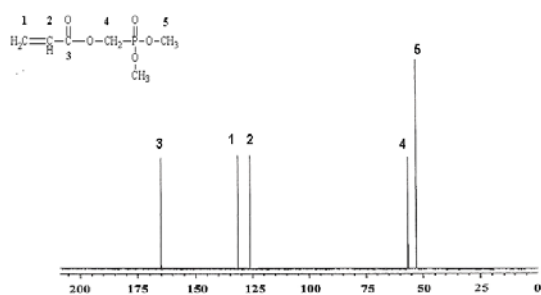
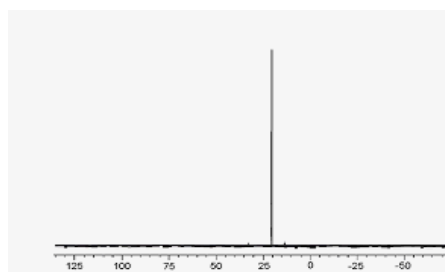
Scheme 4.1 Synthesis of DMAMP, DMMEP, and DMMMP monomers.

4.1.2 Characterization of DMAMP, DMMEP, and DMMMP monomers

Nuclear Magnetic Resonance Spectroscopy (NMR) and Fourier

Transform Infrared Spectroscopy (FT-TR)

Each of the monomers isolated after distillation under vacuum was characterized by $^1\text{H-NMR}$, $^{13}\text{C-NMR}$, and $^{31}\text{P-NMR}$ in CDCl_3 solution, as shown in Figures 4.1–4.3. From $^{31}\text{P-NMR}$, only one single peak was seen on the respective spectra, at $\delta = 21.8$ ppm for DMAMP, $\delta = 28.9$ ppm for DMMEP, and $\delta = 31.5$ ppm for DMMMP, proving the purity of the distilled monomers. On the $^1\text{H-NMR}$ spectrum of DMAMP three doublets were observed at $\delta = 5.84$, 6.09, and 6.37 ppm corresponding to the three protons on the acrylate carbon-carbon double bond. The two protons of the methacrylate double bond in DMMEP and DMMMP were characterized by $^1\text{H-NMR}$ as two singlet signals at $\delta = 5.64$ ppm and $\delta = 6.19$ ppm. $^{13}\text{C-NMR}$ peaks of carbon-carbon double bonds of the dimethylphosphonate monomers were observed at $\delta = 126.7$ ppm ($=\underline{\text{C}}\text{H-}$) and $\delta = 132.8$ ppm ($\underline{\text{C}}\text{H}_2=$) in the case of DMAMP, and $\delta = 125.7$ ppm ($\underline{\text{C}}\text{H}_2=$) and $\delta = 135.8$ ppm ($=\underline{\text{C}}(\text{CH}_3)-$) in that of DMMEP and DMMMP, and those of $\underline{\text{C}}=\text{O}$ at $\delta = 165.7$ ppm and $\delta = 166.7$ ppm, respectively.

(a) $^1\text{H-NMR}$ (b) $^{13}\text{C-NMR}$ (c) $^{31}\text{P-NMR}$ **Figure 4.1** Typical NMR spectra of DMAMP.

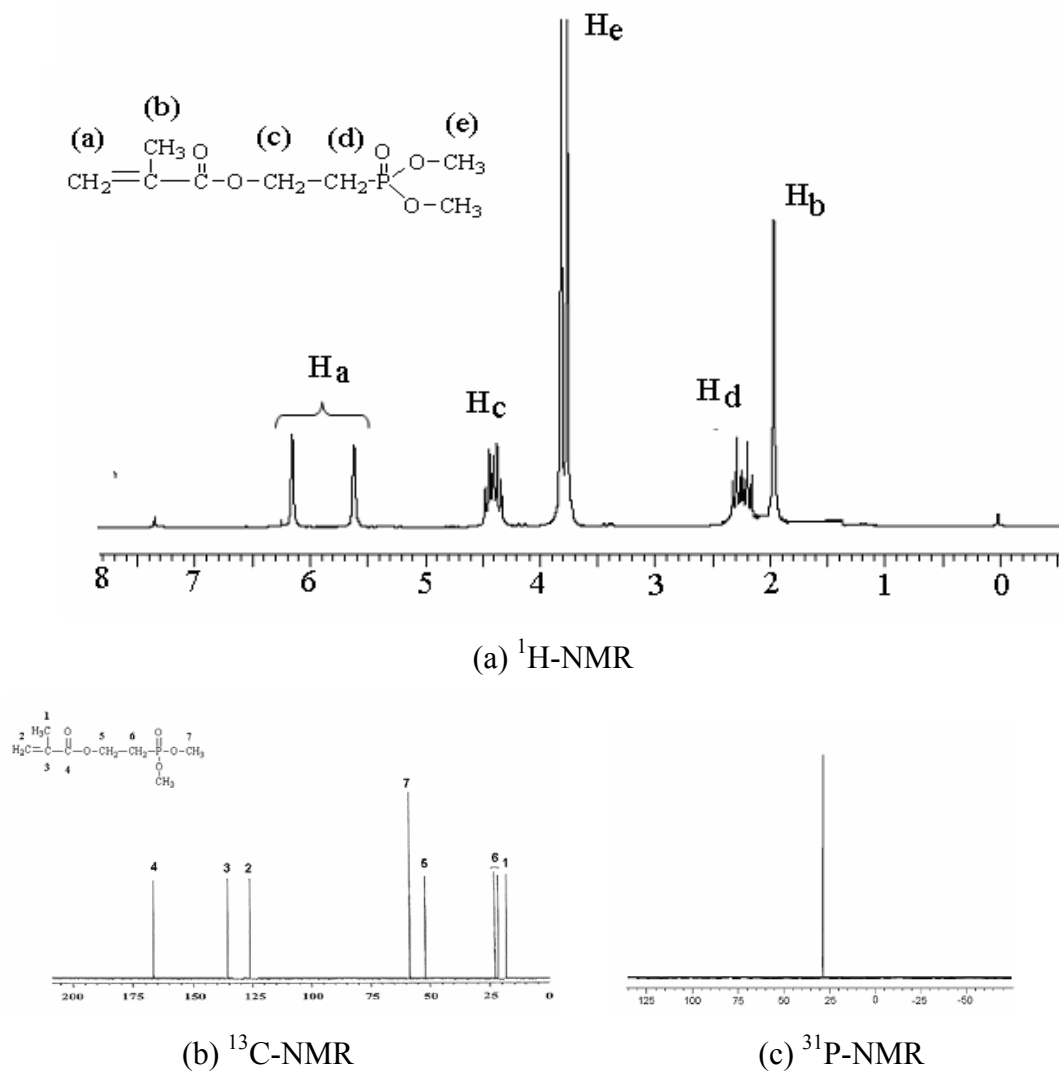


Figure 4.2 Typical NMR spectra of DMMEP.

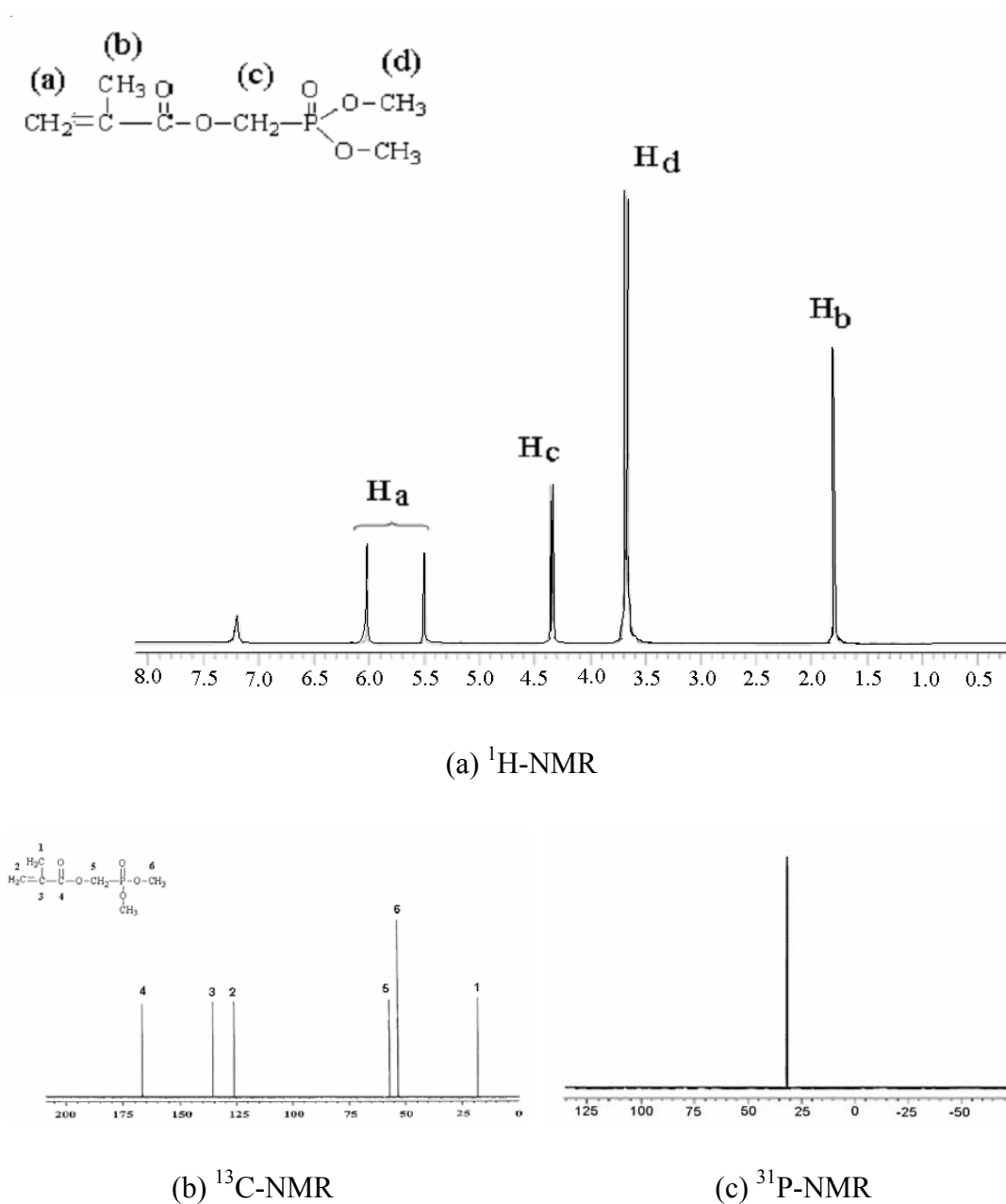


Figure 4.3 Typical NMR spectra of DMMMP.

IR spectra are shown in Figure 4.4. They confirmed the structures of the synthesized monomers with absorption bands characteristic of P=O, C=C, and P-O-C vibrations at 1237, 1632, and 1023 cm^{-1} for DMAMP, at 1240, 1633, and 1030 cm^{-1} for DMMEP, and at 1241, 1638, and 1037 cm^{-1} for DMMMP, respectively.

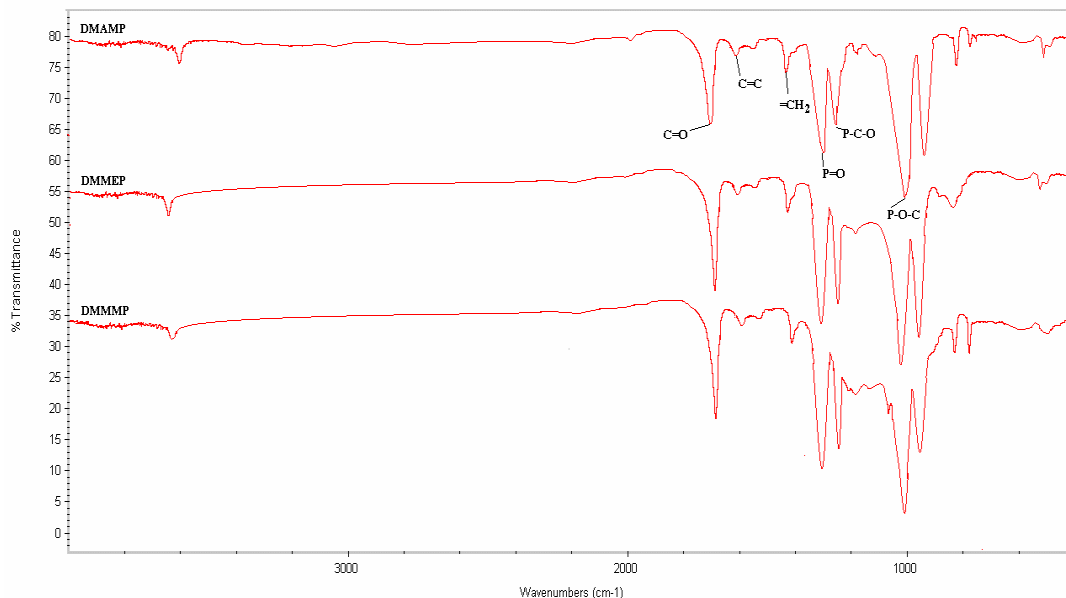


Figure 4.4 Infrared spectra of DMAMP, DMMEP, and DMMMP.

4.2 Synthesis of NR-*g*-PDMAMP, NR-*g*-PDMMEP and NR-*g*-PDMMMP

Three phosphonate monomers (i.e., DMAMP, DMMEP, and DMMMP) were used to perform graft copolymerization *via* photopolymerization initiated from *N,N*-diethyldithiocarbamate-functionalized natural rubber as macroiniferter. Compared with NR-*g*-PDMAMP and NR-*g*-PDMMEP, NR-*g*-PDMMMP was shown particularly interesting for our investigations dealing with the compatibilization of NR/EVA blends, since DMMMP could be easily prepared in high quantities and can be polymerized in the selected conditions. Therefore, in this work, the preparation of NR-*g*-PDMAMP, NR-*g*-PDMMEP and NR-*g*-PDMMMP was presented in two separated parts. The synthesis of NR-*g*-PDMAMP and NR-*g*-PDMMEP was first described, followed by the synthesis of NR-*g*-PDMMMP.

To synthesize graft copolymers of type NR support of dimethylphosphonate-functionalized polymer grafts, the protocol consisted in using a “grafting from” method based on the photopolymerization of a vinyl dimethylphosphonate monomer

poly(dimethyl(methacryloyloxymethyl)phosphonate) (NR-*g*-PDMMP) were synthesized from dimethyl(acryloyloxymethyl)phosphonate (DMAMP), dimethyl(methacryloyloxyethyl)phosphonate (DMMEP), and dimethyl(methacryloyloxymethyl)phosphonate, respectively (DMMMP).

4.2.1 Synthesis and characterization of NR-*g*-PDMAMP and NR-*g*-PDMMEP

a. Epoxidation of natural rubber latex

To characterize the structure of the epoxidized natural rubber unit contained in the ENR latex and to confirm the level of epoxidation, a sample of ENR latex was taken off and isolated after coagulation in methanol and drying under vacuum. The sample was analyzed by $^1\text{H-NMR}$, as result shown in Figure 4.5.

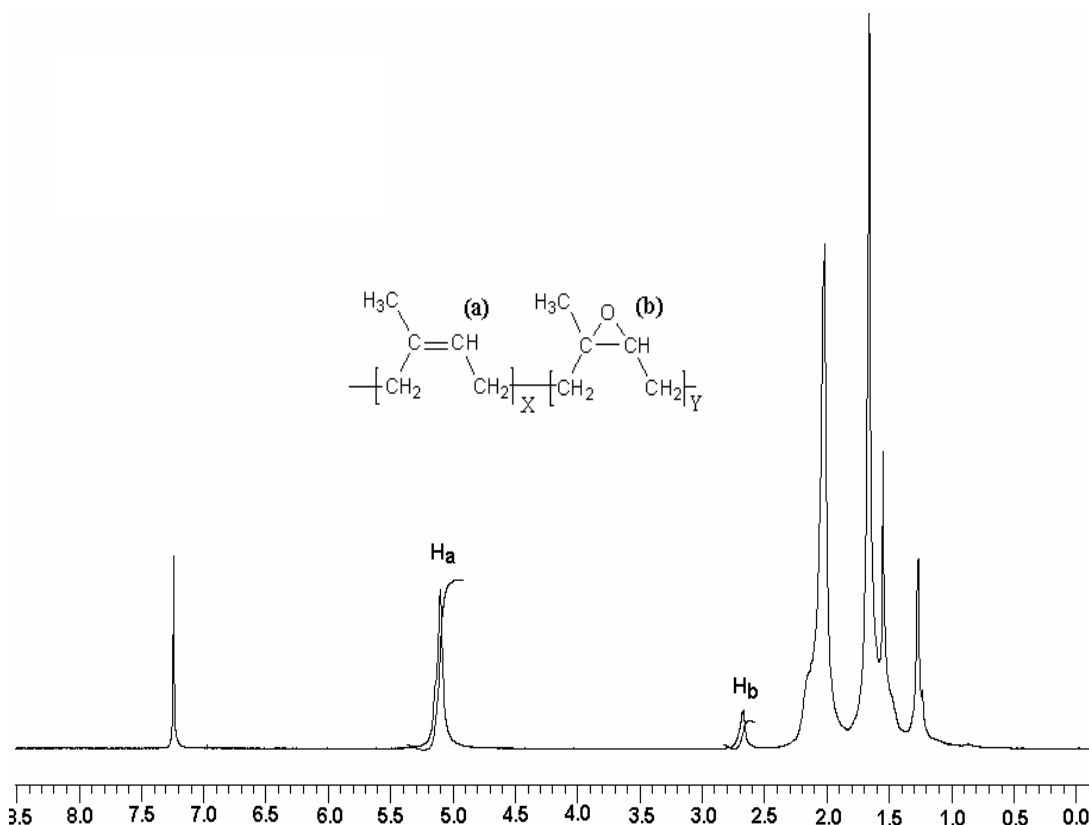


Figure 4.5 $^1\text{H-NMR}$ spectrum of epoxidized natural rubber with 20 mol% epoxide.

proved by addition of DEDT-Na onto 4,5-epoxy-4-methyloctane as a model occurred according to a S_N2 nucleophilic substitution mechanism as shown in Figure 4.7 (Derouet *et al.*, 2007).

The obtained polymer was composed of 80 % of residual NR units, 14.5 % of residual epoxidized NR units, and 5.5 % of DEDT-functionalized NR units.

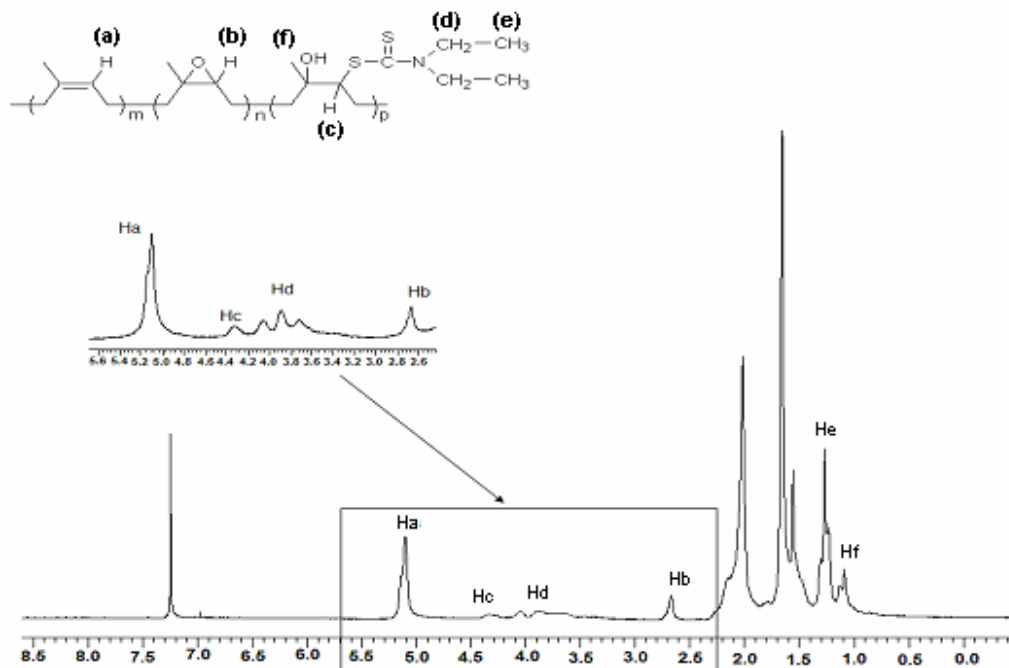


Figure 4.6 ^1H NMR spectrum of NR support of N,N-diethyldithiocarbamate groups with 5.5 mol% DEDT-NR unit.

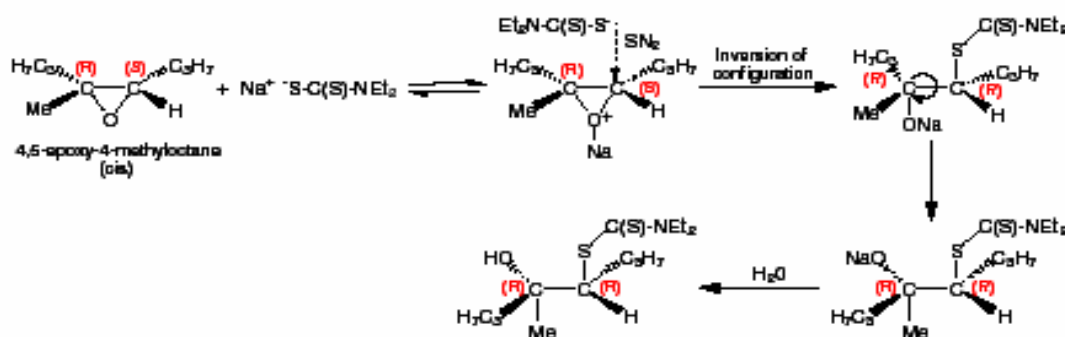


Figure 4.7 Mechanism of the addition of DEDT-Na onto the cis isomer contained in 4,5-epoxy-4-methyloctane. (Derouet *et al.*, 2007)

c. Synthesis and characterization of NR-g-PDMAMP and NR-g-PDMMEP

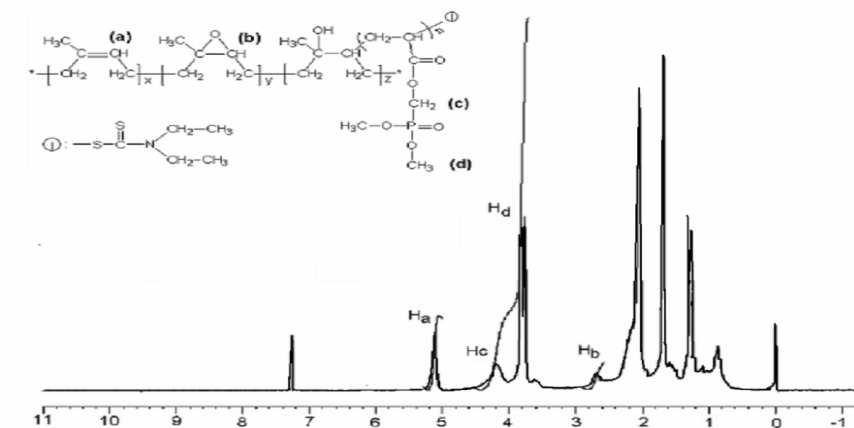
The syntheses of the graft copolymers were performed in latex medium according to the “grafting from” method. For that, photopolymerizations of dimethyl(acryloyloxymethyl)phosphonate (DMAMP) and dimethyl(methacryloyloxyethyl)phosphonate (DMMEP), respectively used as phosphonated monomers, were initiated from *N,N*-diethyldithiocarbamate groups previously bound in side position of the rubber chains. Various conditions were considered to optimize these syntheses. After reaction, the grafts copolymers obtained was coagulated in methanol, and then purified by dissolution/re-precipitation with dichloromethane/methanol, and then dried under vacuum and characterized by ^1H , ^{13}C and ^{31}P -NMR, as well as by FTIR spectroscopy.

c.1. NMR spectroscopy

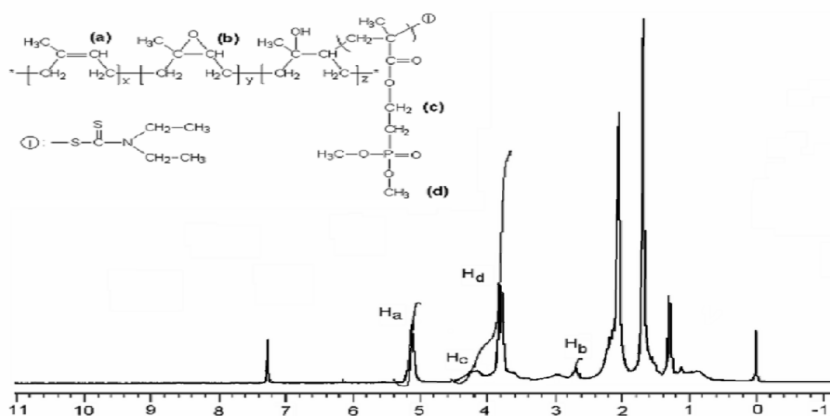
^1H -NMR spectra of NR-g-PDMAMP and NR-g-PDMMEP are shown in Figure 4.8, and the main important signals are summarized in Table 4.1. On NR-g-PDMAMP spectrum (Figure 4.8a), the NR backbone was identified by the signal at $\delta = 5.14$ ppm characteristic of the proton of the carbon-carbon double bond ($-\text{C}(\text{CH}_3)=\text{CH}-$) in unsaturated NR units, and the formation of PDMAMP grafts was confirmed by signals at $\delta = 3.8$ ppm and $\delta = 4.4$ ppm characteristic of the dimethyl ester and methylenoxy protons of the phosphonate functions. In the case of NR-g-PDMMEP (Figure 4.8b), the signal of $-\text{C}(\text{CH}_3)=\text{CH}-$ proton on NR backbone was noted at $\delta = 5.14$ ppm, and those of dimethyl ester and methylenoxy protons of phosphonate function were noted at $\delta = 3.80$ ppm and $\delta = 4.20$ ppm, respectively. In the two families of graft copolymers, the presence of residual epoxidized NR units was also characterized on their ^1H -NMR spectra by the presence of the signal at $\delta = 2.70$ ppm corresponding to the oxirane ring proton of the epoxidized NR units.

^{13}C -NMR characteristics of NR-g-PDMAMP and NR-g-PDMMEP are given in Figure 4.9. The formation of NR-g-PDMAMP was confirmed by the simultaneous presence of signals at $\delta = 125$ ppm and $\delta = 135$ ppm characteristic of $-\text{C}(\text{Me})=$ and $=\text{CH}-$ unsaturated carbons of NR backbone, respectively, and signals at $\delta = 52.9$

ppm and $\delta = 62.1$ ppm characteristic of dimethyl ester and methylenoxy carbons of dimethylphosphonate functions on PDMAMP grafts (Figure 4.9a). In the case of NR-g-PDMMEP (Figure 4.9b), the signals of dimethyl ester and methylenoxy carbons of dimethylphosphonate functions on PDMMEP grafts were characterized at $\delta = 53.2$ ppm and $\delta = 52.0$ ppm, respectively. The formation of dimethylphosphonate-functionalized polymer grafts was also confirmed by the presence of the C=O carbon peak at $\delta = 176.1$ ppm. The C-OH quaternary carbons in NR-g-PDMAMP and NR-g-PDMMEP were noted at $\delta = 74.0$ and $\delta = 74.3$ ppm, respectively.



(a)



(b)

Figure 4.8 Typical $^1\text{H-NMR}$ spectra of (a) NR-g-PDMAMP and (b) NR-g-PDMMEP.

The presence of dimethylphosphonate functions along the grafts was confirmed by ^{31}P -NMR, as the spectra given in Figure 4.10. Only one sharp peak was observed in both cases, at $\delta = 21.6$ ppm for NR-*g*-PDMAMP and $\delta = 29.3$ ppm for NR-*g*-PDMMEP. This indicates that PDMAMP (and PDMMEP) grafts would adopt a stereoregular conformation.

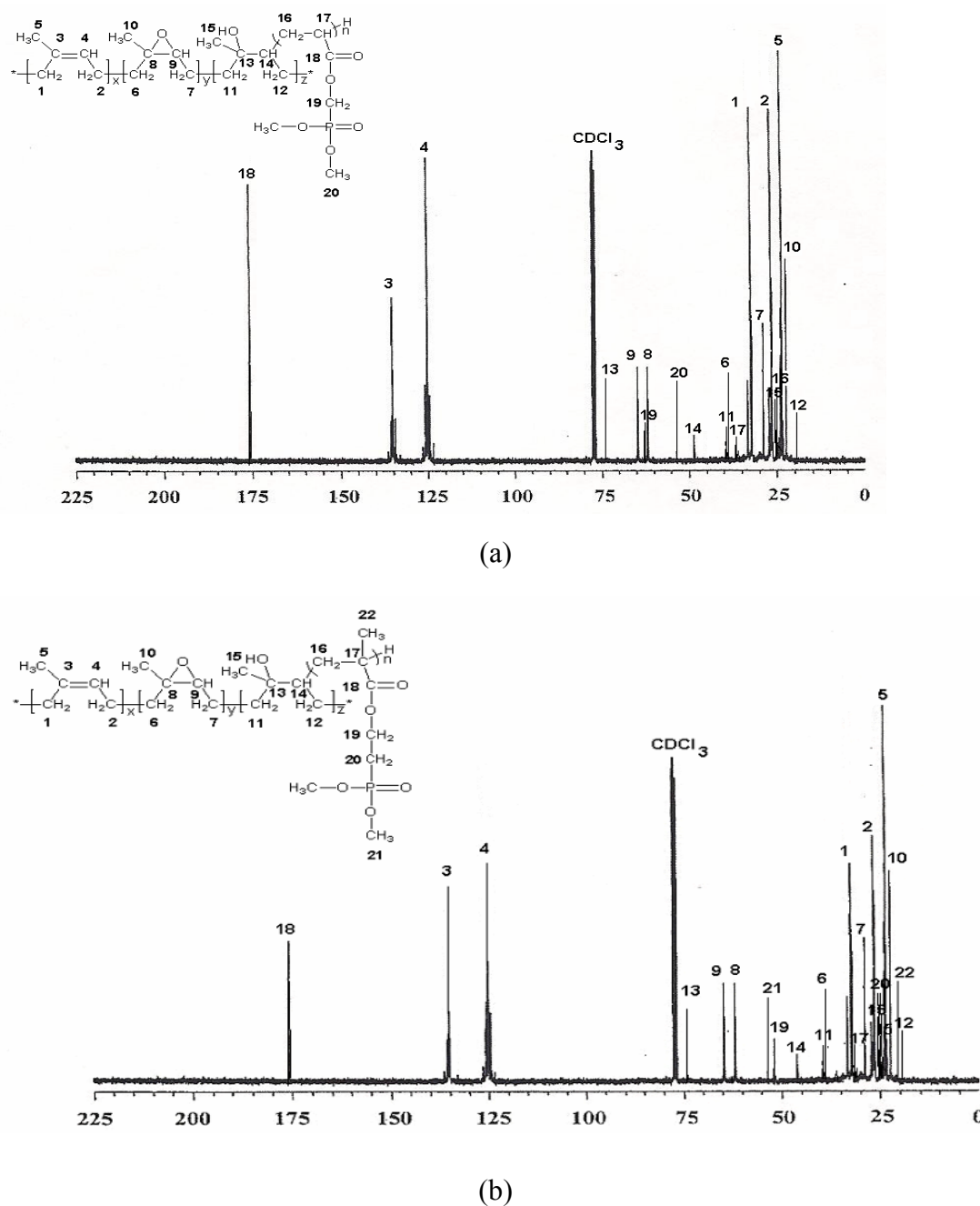
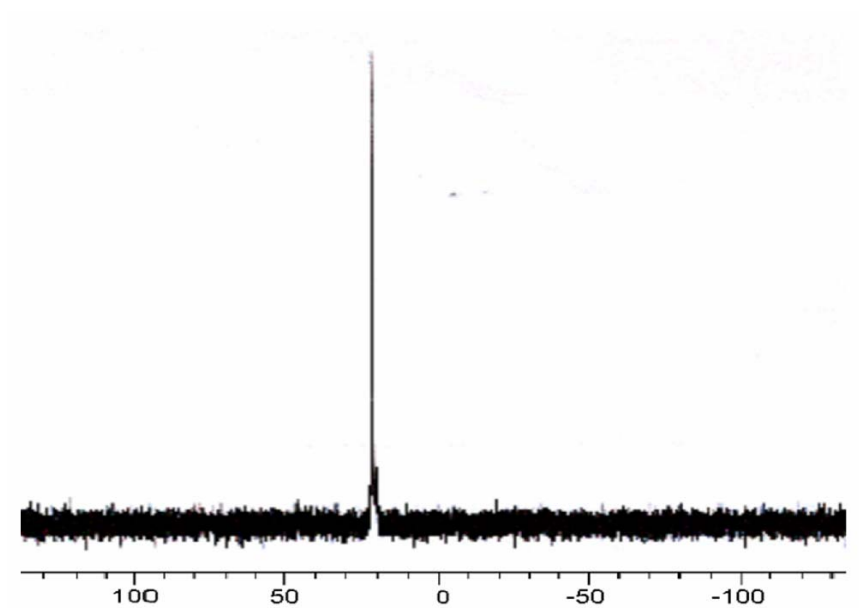
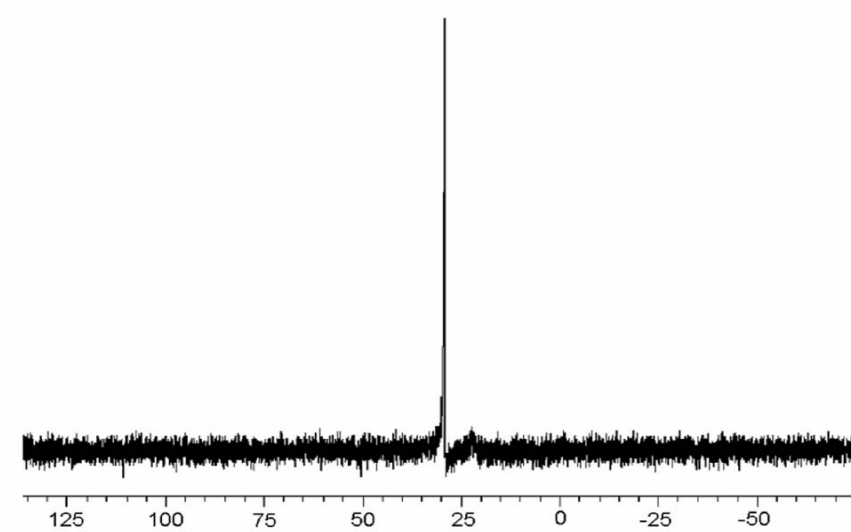


Figure 4.9 Typical ^{13}C -NMR spectra of (a) NR-*g*-PDMAMP and (b) NR-*g*-PDMMEP.



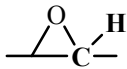
(a)



(b)

Figure 4.10 Typical ^{31}P -NMR spectra of (a) NR-g-PDMAMP and (b) NR-g-PDMMEP.

Table 4.1 Assignment of ^1H -NMR, ^{13}C -NMR and ^{31}P -NMR of NR-*g*-PDMAMP and NR-*g*-PDMMEP.

Graft copolymer	Position	^1H -NMR (ppm)	^{13}C -NMR (ppm)	^{31}P -NMR (ppm)
NR- <i>g</i> -PDMAMP	-C(CH ₃)=CH-	5.14	125.0	
		2.70	64.1	
	(O-CH ₂ -P)	4.40	62.0	21.6
	(P-O-CH ₃)	3.80 ⁺	52.9	
	C-OH	-	74.0	
NR- <i>g</i> -PDMMEP	-C(CH ₃)=CH-	5.14	125.0	
		2.70	64.1	
	(C(O)-O-CH ₂)	4.20	52.0	29.3
	(P-O-CH ₃)	3.80	53.2	
	C-OH	-	74.3	

c.2. Fourier transform infrared spectroscopy (FT-IR)

FT-IR was used to characterize NR-*g*-PDMAMP and NR-*g*-PDMMEP. This was made to verify the chemical structure of the graft copolymers synthesized, in particular the identification of the dimethylphosphonate groups, to confirm the graft formation. IR spectra of NR-*g*-PDMAMP and NR-*g*-PDMMEP are given in Figure 4.11, and the detail of the most important absorption bands is related in Table 4.2. The presence of grafts bearing dimethylphosphonate functions was proved by absorption bands characteristic of P=O and P-O-C vibrations, respectively, at 1238 and 1025 cm⁻¹ for NR-*g*-PDMAMP, and 1265 and 1028 cm⁻¹ for NR-*g*-PDMMEP.

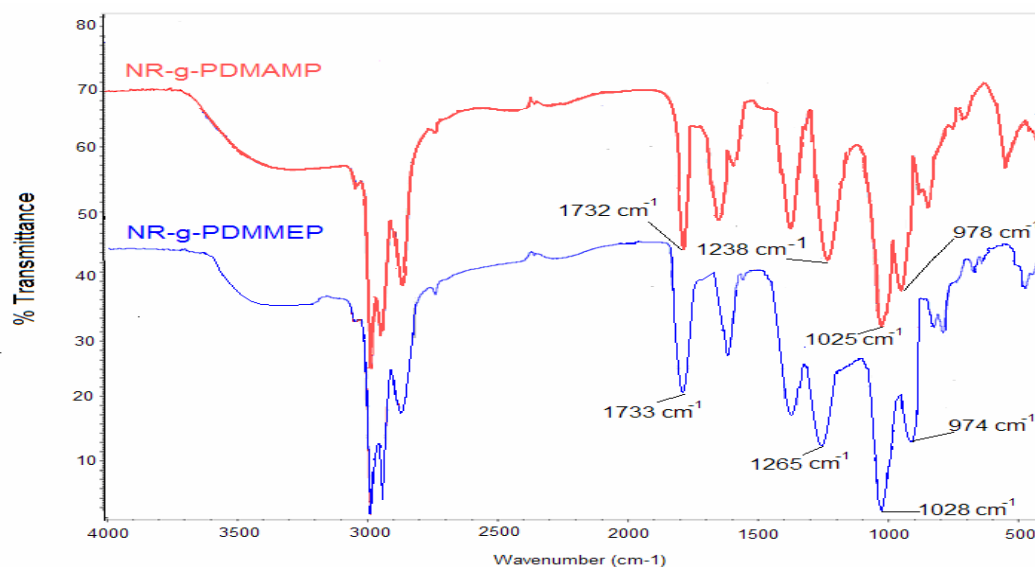


Figure 4.11 FTIR spectra of NR-g-PDMAMP and NR-g-PDMMEP.

Table 4.2 Assignment of FTIR absorption peaks of NR-g-PDMAMP and NR-g-PDMMEP.

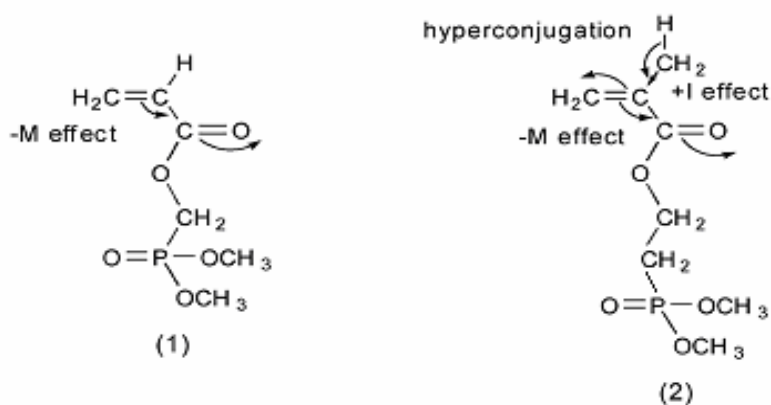
Graft copolymer	Functional groups	Absorption band (cm ⁻¹)
NR-g-PDMAMP	-OH	3425
	-CH ₂ , -CH ₃	2948, 3012
	C=O	1732
	P=O	1238
	P-O-CH ₃	978
NR-g-PDMMEP	-OH	3408
	CH ₂ , -CH ₃	2954, 3015
	C=O	1733
	P=O	1265
	P-O-C ₂ H ₅	974

d. Kinetic studies of the grafting of PDMAMP and PDMMEP onto NR

The kinetics of grafting of PDMAMP and PDMMEP onto NR backbone were studied in terms of influence of monomer structure and monomer concentration.

d.1. Effect of monomer structure

The effect of monomer structure was studied by means of DMAMP and DMMEP, initially chosen as phosphorated monomers (Scheme 4.4).



Scheme 4.4 Influence of DMAMP (1) and DMMEP (2) structures on reactivity.

The kinetics of the photopolymerizations of DMAMP and DMMEP initiated from DEDT-NR chains, using a molar ratio $[\text{monomer}]/[\text{DEDT-NR units}] = 3.5$, showed different reactivities as evidenced from their respective conversions and grafting rates in identical reaction conditions (Figures 4.12 and 4.13). Contrary to the polymerization of DMAMP, which started immediately at the beginning of irradiation, that of DMMEP did not occur until a reaction time of about 20 min. With progress of polymerization, monomers are consumed to form dimethylphosphonate-functionalized polymer grafts, but also homopolymers in low proportions (about 10 % at the grafting end, whatever the structure of the monomer), as shown in Figure 4.12. At each time of the grafting, conversion of DMAMP in grafts is always higher than that of DMMEP. After about 90 min, monomer conversions and grafting rates reached a plateau, indicating that the efficiency of the grafting with DMAMP is higher than that with DMMEP, but also that the propagation step of the “living” radical photopolymerization, (Otsu and Yoshida., 1982; Otsu *et al.*, 1982 and 1995;

Otsu and Matsumoto, 1998; Otsu, 2000), is disturbed by irreversible termination reactions essentially due to the low initiation rate.

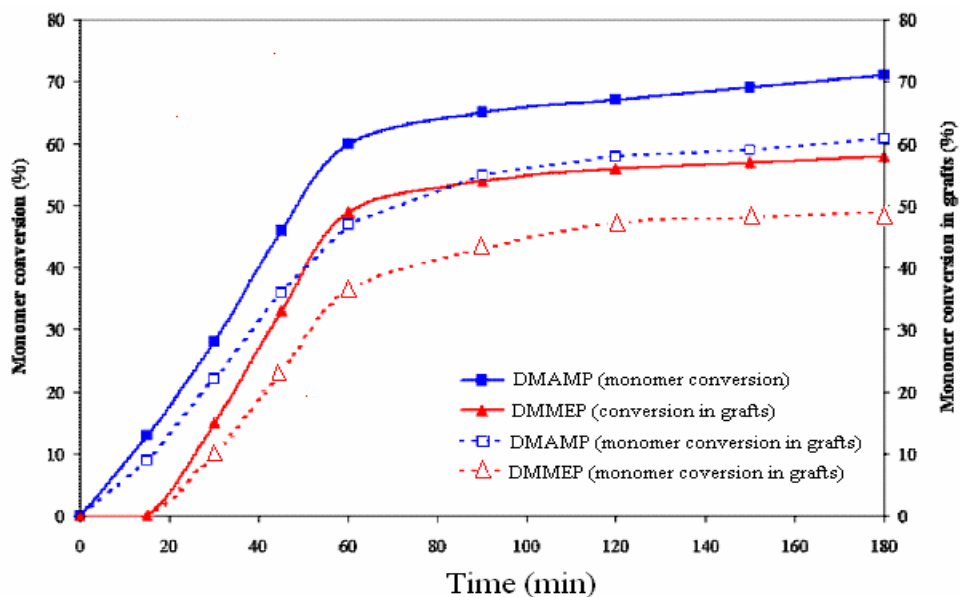


Figure 4.12 Progress of monomer conversion and monomer conversion in grafts (determination by weighing) for the photopolymerizations of DMAMP and DMMEP initiated from DEDT-NR with $[\text{monomer}] / [\text{DEDT-NR units}] = 3.5$.

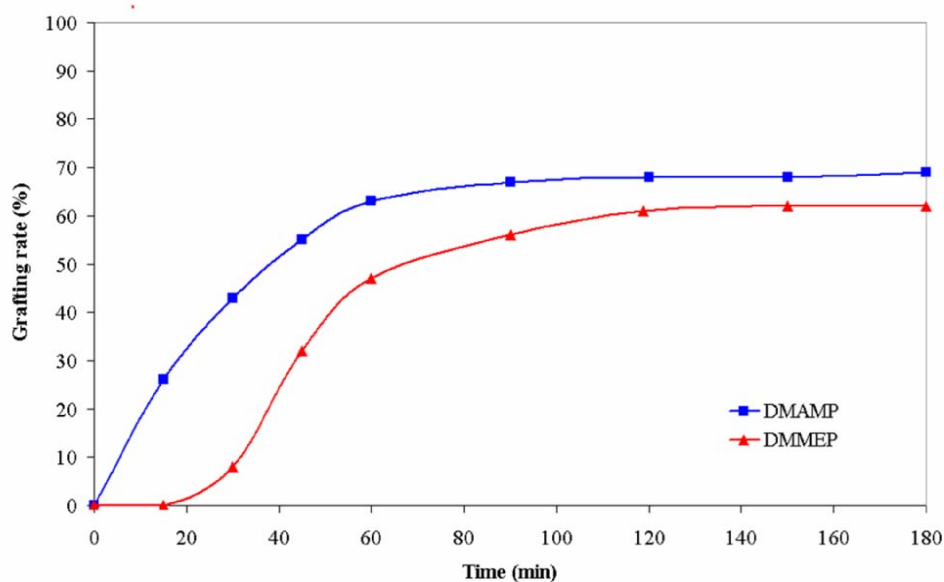


Figure 4.13 Progress of grafting rate (determined by weighing) for the photopolymerizations of DMAMP and DMMEP initiated from DEDT-NR with $[\text{monomer}] / [\text{DEDT-NR units}] = 3.5$.

This was confirmed by the kinetic studies which showed that, whatever the structure of the monomer used, the rate law for the grafting by photopolymerization had not kinetic order of 1 with respect to monomer concentration (Figure 4.14), and the number-averaged molecular weight (\overline{Mn}) of the grafts did not evolve linearly with conversion (Figure 4.15). In Figure 4.15, the fact that the slope of the experimental curve representing the progress of \overline{Mn} versus monomer conversion was lower than that of the theoretical one is significant of the existence of transfer reactions during the photopolymerization step with as a consequence the formation of homopolymer, as already specified. However, the strong increase of \overline{Mn} after 60 % of DMAMP conversion (55 % for DMMEP) is rather surprising because the number of reactive sites is supposed lower at this moment of the reaction, and moreover, the monomer conversion is almost stopped. However, similar effects were already related in literature concerning radical polymerization (Lee *et al.*, 1979). In addition, it was also noted that this strong increase of \overline{Mn} at the moment where the monomer conversion seems stopped (Figure 4.12 and 4.13), begins simultaneously with the increase of latex viscosity (Simionescu and Simionescu, 1984). This result could be explained by recombination reactions (Moad and Solomon, 1995) between growing grafts and growing homopolymers, facilitated by the fact that the initially hydrophobic rubber would become increasingly hydrophilic with the progress of the grafting reaction. As monomer conversion slows down abruptly, the rubber particles of latex, whose polarity is enhanced with the increase of grafting rate, probably disaggregate, and thus the rubbery copolymer would be in part dispersed in the aqueous phase, with for consequence to increase the latex viscosity and thus to favor the approach between growing grafts and growing homopolymers.

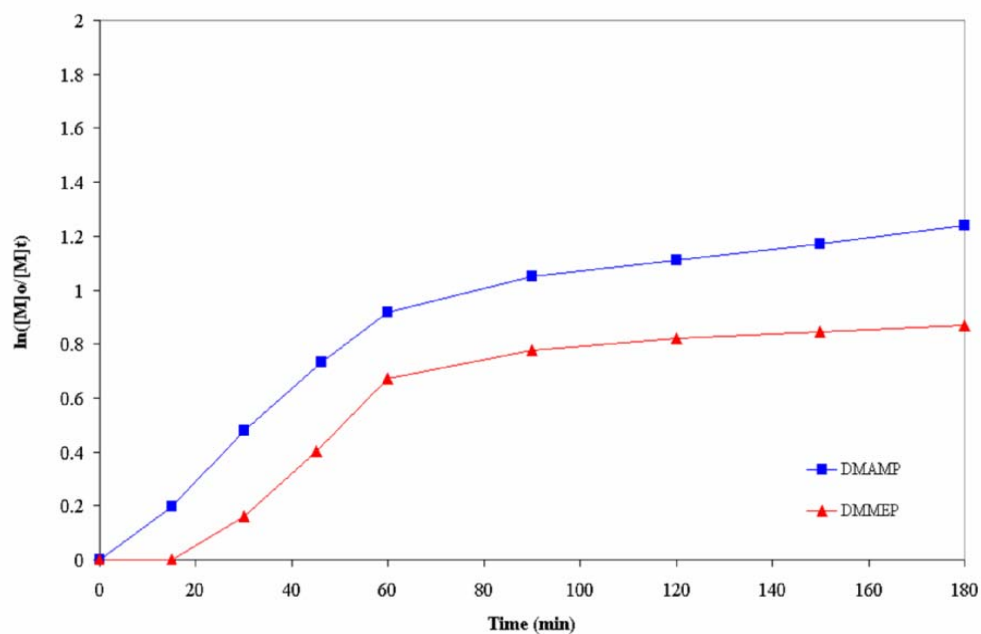


Figure 4.14 First-order kinetic plots for the photopolymerizations of DMAMP and DMMEP initiated from DEDT-NR with $[\text{monomer}] / [\text{DEDT-NR units}] = 3.5$.

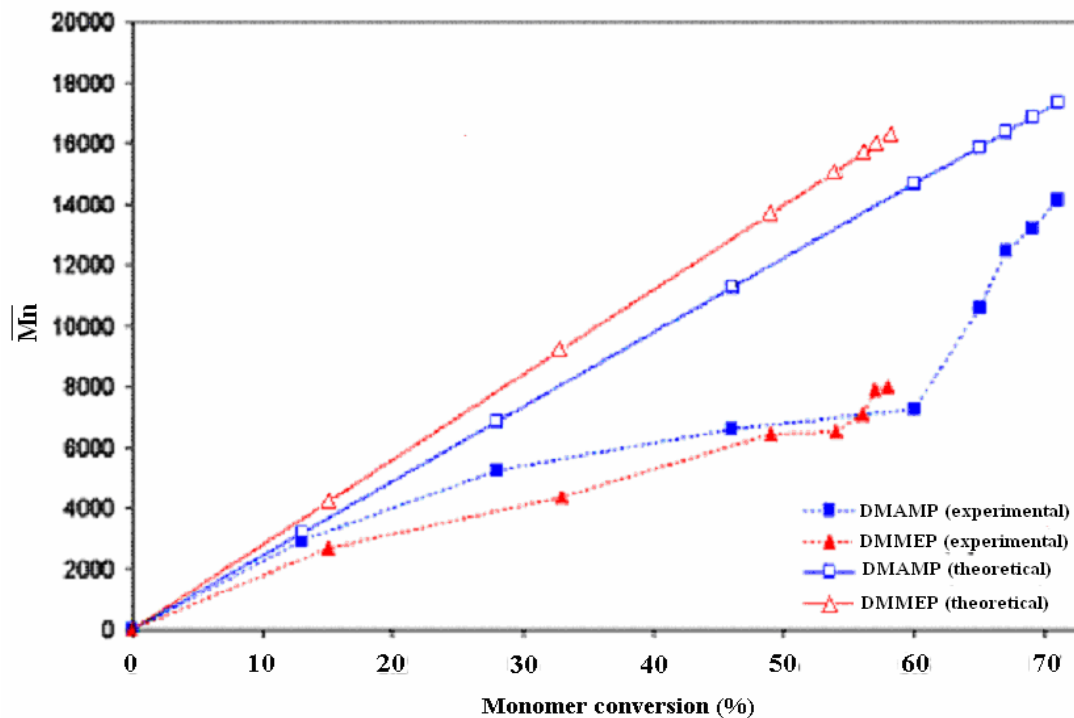


Figure 4.15 Dependence of molecular weight (\overline{M}_n) on monomer conversion for the photopolymerizations of DMAMP and DMMEP initiated from DEDT-NR with $[\text{monomer}]/[\text{DEDT-NR units}] = 7$.

The highest grafting rate obtained with DMAMP by comparison with that obtained with DMMEP is consistent with the general behavior of acrylates and methacrylates (Jiang and Wilkie, 1998). In the two cases the mesomeric effect (-M) of the double bond with the ester function creates a polarization of the double bond, which is compensated in the case of methacrylate by the positive inductive effect (+I) and the hyperconjugation of the methyl. As a consequence, acrylate double bond is more polarized and thus more reactive. The propagation step is also faster with acrylate since the macroradical is less stabilized than methacrylate macroradical (Barson and Benvington, 1987). These factors can account for the observed phenomenon (Nair and Clouet, 1989; Simionescu, 1983).

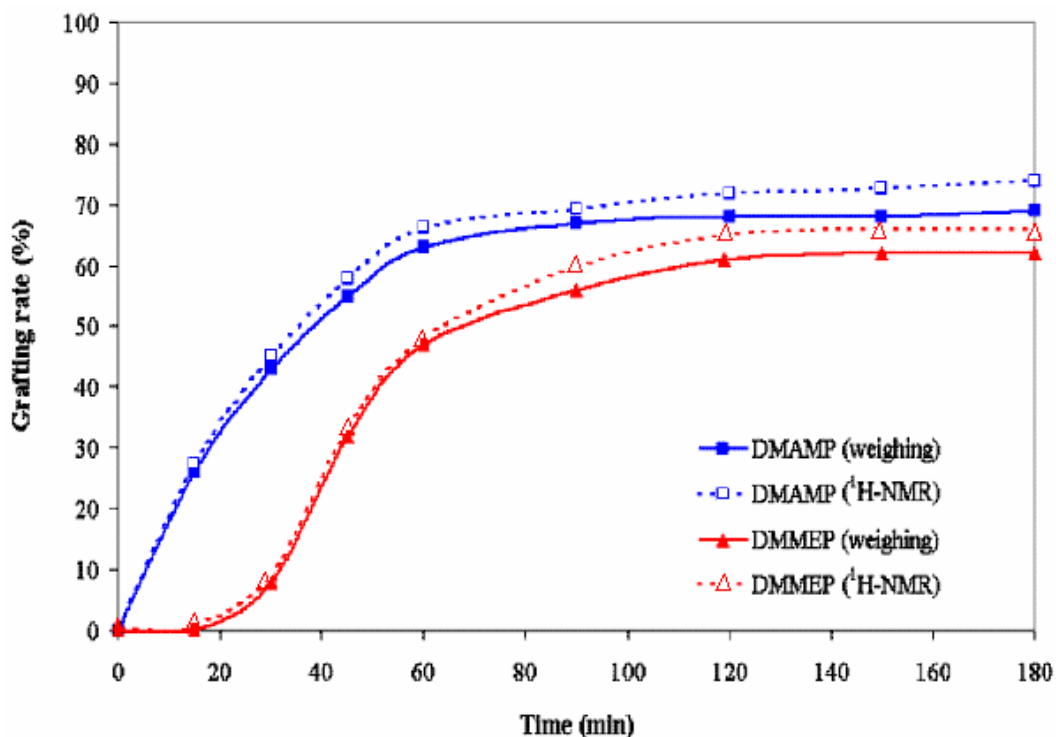


Figure 4.16 Comparison of the progress of the grafting rates determined by weighing with the one of grafting rates obtained from ^1H NMR for the photopolymerizations of DMAMP and DMMEP initiated from DEDT-NR with $[\text{monomer}] / [\text{DEDT-NR units}] = 3.5$.

Figure 4.16 shows the progress of the grafting rates determined by weighing compared with the one of grafting rates obtained from $^1\text{H-NMR}$. It was noted that the grafting rates values determined from $^1\text{H-NMR}$ spectrum of graft copolymers at various times are always higher than the ones measured by weighing. However, an increase of the difference between the respective values obtained is observed with increasing reaction time, but even after high reaction times it remains on the whole very low. The loss of part of products during the different treatments carried out on the crude copolymer obtained after grafting probably explains these little differences.

d.2 Effect of monomer concentration

The effects of monomer concentration on monomer conversion and grafting rate are shown in Figure 4.17. It was noted that the grafting rate increases with increasing monomer concentration. The rate of polymerization, and thus the grafting rate, progresses slowly during the first 100 min of reaction, and finally tends to a plateau whose value increases with monomer concentration. The same trend is observed with monomer conversion: after 90 min irradiation, the proportion of consumed monomer tends to a plateau whose value is dependent on the monomer concentration.

These results show that increasing the monomer concentration can increase the rate of the propagation step, and thus the grafting rate, but effects of irreversible terminations remain unchanged. However, in the present grafting system, another factor must be taken into account: the viscosity of the reaction medium. Indeed, it was observed that the viscosity of the medium obviously not only increased with increasing polymerization time, but also increased with increasing monomer concentration. The mobility of the copolymer-monomer mixture may be affected by this increase of viscosity, so leading to a prematurely end of the radical growing polymerization (Tsafack and Grützmacher, 2006), but not for the recombination reactions between growing homopolymer and grafts, as already explained above.

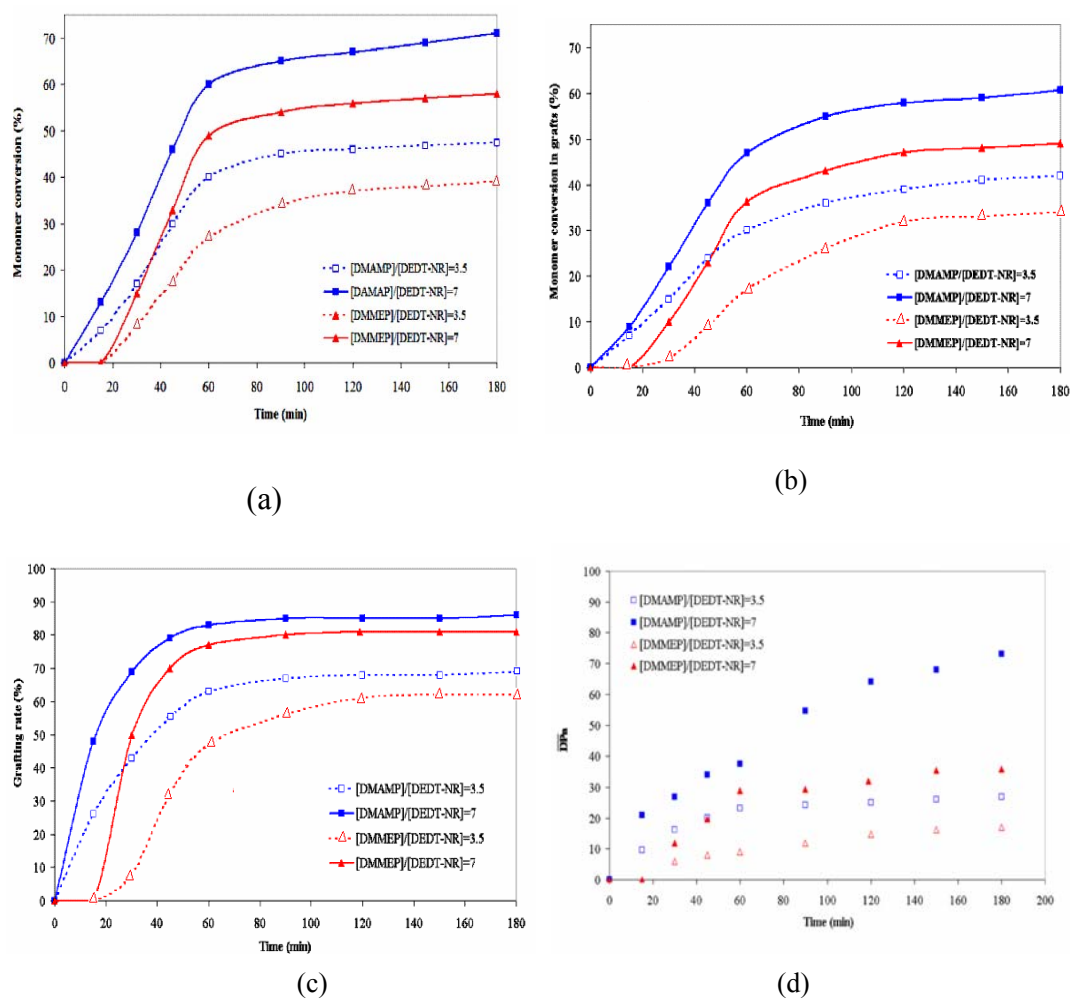


Figure 4.17 Influence of monomer concentration and monomer structure on the progress of (a) monomer conversion, (b) monomer conversion in grafts, (c) grafting rate, and (d) \overline{DP}_n , respectively.

d.3 Average length of the grafts (degree of polymerization)

Degrees of polymerization (\overline{DP}_n) of grafts and grafting rates (GR) of various NR-g-PDMAMP and NR-g-PDMMEP copolymers, prepared under various reaction conditions, are given in Table 4.3.

Table 4.3. Degrees of polymerization (\overline{DP}_n) and grafting rates (GR) of the various graft copolymers obtained.

Type of copolymer	[M]/[DEDT-NR units] (in mol.)	Reaction time (min)	Monomer conversion (%)	Degree of polymerization (\overline{DP}_n)	Grafting rate (GR in wt%)	
					¹ H-NMR	Weighing
NR-g-PDMAMP	3.5	60	40	23	79	63
NR-g-PDMAMP	7.0	60	60	37	87	83
NR-g-PDMAMP	3.5	180	47	27	81	68
NR-g-PDMAMP	7.0	180	71	73	92	86
NR-g-PDMMEP	3.5	60	26	9	62	46
NR-g-PDMMEP	7.0	60	49	29	84	77
NR-g-PDMMEP	3.5	180	39	17	76	62
NR-g-PDMMEP	7.0	180	58	36	86	80

It was noted that \overline{DP}_n and GR increased with increasing monomer concentration and reaction time. Furthermore, when the grafting was carried out in same conditions, the grafting rates of the copolymers coming from DMAMP are always higher than those of the copolymers obtained with DMMEP. As already evoked above (Figure 4.17), one can note similar results concerning the comparison between the GR values determined by weighing and ¹H-NMR, and that, whatever the grafting conditions used. In conclusion, the highest graft lengths ($\overline{DP}_n = 73$) and grafting rates (GR = 86 wt% in dimethylphosphonate-functionalized polymer grafts) were obtained with DMAMP as monomer, using a molar ratio [monomer] / [DEDT-NR units] = 7 and a reaction time of 180 min.

d.4. Thermal stability of the graft copolymers

Thermal stabilities of pure NR, PDMAMP, PDMMEP, NR-g-PDMAMP, and NR-g-PDMMEP were successively characterized by TGA. The various TGA curves obtained within nitrogen atmosphere and oxygen atmosphere are given in Figures 4.18 and 4.19, respectively.

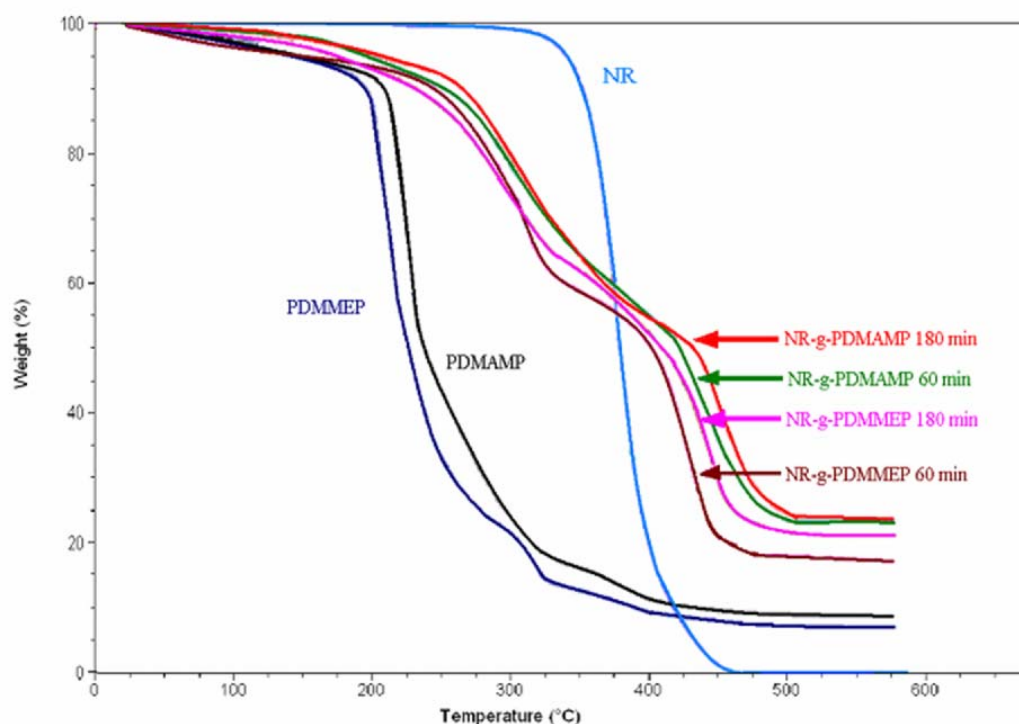
In nitrogen atmosphere (Figure 4.18), it was noted that pure NR showed only single step of weight loss with an onset temperature of approximately

320°C. PDMAMP and PDMMEP homopolymers also showed a single step, but at lower onset temperature of 225°C and 220°C, respectively (Table 4.4). This result agrees with the results reported in previous work (Tsafack and Grützmacher, 2006a). For NR-g-PDMAMP and NR-g-PDMMEP prepared using a ratio [monomer] / [DEDT-NR units] = 7 and isolated at reaction times of 60 min and 180 min, the TGA curves showed double degradation steps. With these graft copolymers, a shift of the TGA curve toward the high temperatures was observed when the grafting rate was increased. Depending on the grafting rate, the first degradation step was noted at onset temperature varying from 260°C to 270°C, corresponding to a weight loss from 46 % to 30 %, and the second one at onset temperature from 400°C to 430°C, corresponding to a weight loss from 37 % to 46 % (Table 4.4). The first decomposition step of the graft copolymers corresponds to the degradation of phosphonate linkages that occurred at lower decomposition temperature than that of NR backbone. On the other hand, the second onset temperature is always higher than that of NR, which shows the ability of dimethylphosphonate-functionalized polymer grafts to improve thermal stability of NR.

Alternatively, TGA analyses were performed under oxygen atmosphere to simulate graft copolymer behavior in commonly used conditions. By comparison with that observed under nitrogen atmosphere, the decomposition under oxygen atmosphere occurred at a lower temperature. That was easily explained by the action of oxygen as oxidant to favor the degradation of the organic materials. Except for NR and homopolymers, the degradation curves of the other analyzed samples were comparable to that obtained in oxygen atmosphere (Figure 4.19). Decomposition of pure NR starts at 179°C, but its main decomposition peak is observed at 260°C. Thermal stability of NR-g-PDMAMP and NR-g-PDMMEP in oxygen also depends on the grafting rate. TGA curves clearly shifts to higher temperature as the grafting rate increases. However, its influence on the thermal stability of the graft copolymer is much more marked. Compared to the values obtained with the same samples in nitrogen atmosphere, the onset temperatures for the first degradation step in oxygen varied from 210°C to 230°C, corresponding to a weight loss from 43 % to 31 %, and that for the second one from 326°C to 396°C, corresponding to a weight loss from 44 % to 50 % (Table 4.4).

Concerning the remaining residues, it was noted that NR is totally degraded at 500°C whatever the surrounding atmosphere. On the other hand, the proportions in carbonaceous residues (or char) observed at this temperature in the case of the degradation of the graft copolymers are always higher than that observed during degradation of PDMMEP and PDMAMP homopolymers. Moreover, they increased with the grafting rate of the copolymer from 17 % to 24 % under nitrogen atmosphere, and 13 % to 19 % under oxygen atmosphere when GR increases from 77 % to 86 %, showing that further oxidation by oxygen of the char formed occurs in oxygen atmosphere.

Figure 4.18 TGA curves under nitrogen atmosphere of NR, PDMAMP, PDMMEP,



NR-g-PDMMEP after 60 min (GR = 77 %) and 180 min (GR = 80 %) of grafting, and NR-g-PDMAMP after 60 min (GR = 83 %) and 180 min (GR = 86 %) of grafting. Grafting conditions: [monomer] / [DEDT-NR units] = 7.

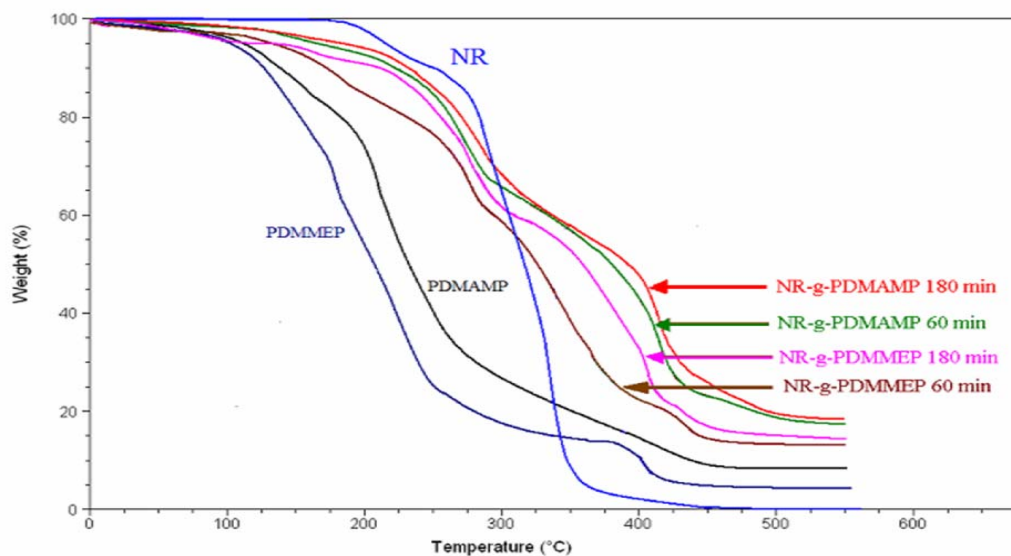


Figure 4.19 TGA curves under oxygen atmosphere of NR, PDMAMP, PDMMEP, NR-g-PDMMEP after 60 min (GR = 77 %) and 180 min (GR = 80 %) of grafting, and NR-g-PDMAMP after 60 min (GR = 83 %) and 180 min (GR = 86 %) of grafting. Grafting conditions: [monomer] / [DEDT-NR units] = 7.

Table 4.4 TGA characteristics of NR, PDMAMP, PDMMEP, NR-g-PDMAMP after 60 min (GR = 83 %) and 180 min (GR = 86 %) of grafting, and NR-g-PDMMEP after 60 min (GR = 77 %) and 180 min (GR = 80 %) of grafting, in nitrogen and oxygen atmospheres, respectively. Grafting conditions: [monomer] / [DEDT-NR units] = 7.

Type of copolymer	Nitrogen atmosphere					Oxygen atmosphere				
	Onset temperature (°C)		Weight loss (%)		Char (%)	Onset temperature (°C)		Weight loss (%)		Char (%)
	1 st	2 nd	1 st	2 nd		1 st	2 nd	1 st	2 nd	
	step	step	step	step		step	step	step	step	
NR	320	-	99.8	-	0.2	193	260	7	92.9	0.10
PDMAMP	225	-	89	-	11	137	190	17	75	8
PDMMEP	220	-	91	-	9	126	170	22	73.3	4.7
NR-g-PDMAMP 83 %*	268	422	40	37	23	225	375	44.5	39	17.5
NR-g-PDMAMP 86 %*	270	430	44	32	24	230	396	46	35	19
NR-g-PDMMEP 77 %*	260	400	37	46	17	210	326	40	47	13
NR-g-PDMMEP 80 %*	262	418	39	40	21	215	343	42	43	15

* grafting rate determined by weighing.

d.5. Thermal behavior of the graft copolymers

The thermal behavior of pure NR, PDMAMP, PDMMEP, NR-g-PDMAMP, and NR-g-PDMMEP were investigated by DSC. Their respective curves are given in Figure 4.20. It can be seen that pure NR as well as PDMAMP and PDMMEP homopolymers showed T_g at -62.1°C , -29.5°C , and -23.8°C , respectively. NR-g-PDMAMP and NR-g-PDMMEP showed two T_g , one corresponding to the glass transition assigned to *cis* 1,4-polyisoprene structures in NR domains (-46°C to -44°C), and the other to the dimethylphosphonate-functionalized polymer graft ones (in a T_g range depending on the nature of the dimethylphosphonate-functionalized polymer grafts: -29.2°C to -29.1°C in the case of PDMAMP grafts, -23.6°C to -23.1°C in that of PDMMEP ones). This result means that, in the range of the considered compositions, with GR between 70 and 90 %, there is phase separation. Moreover, it was seen that when GR increases in this same range of values, the T_g of NR domains increases while that of dimethylphosphonate-functionalized polymer graft ones decreases, showing that the material would tend to become homogeneous when GR is increased. Compared to pure NR, the T_g of NR phase in the graft copolymer is significantly increased with GR.

The formation of a biphasic medium can be explained by the difference of polarity that exists between the NR backbone and the dimethylphosphonate-functionalized polymer grafts. The polar PDMAMP (or PDMMEP) grafts tend to associate between themselves to form polar micro-domains, of which are rejected the non-polar NR structures. Concerning the increase trend of T_g of NR phase with the increase of GR, it can be explained in terms of increase of intermolecular stiffness in the rubber phase, and may be attributed to an increasing trend of the interactions between polar dimethylphosphonate functions within the graft copolymer.

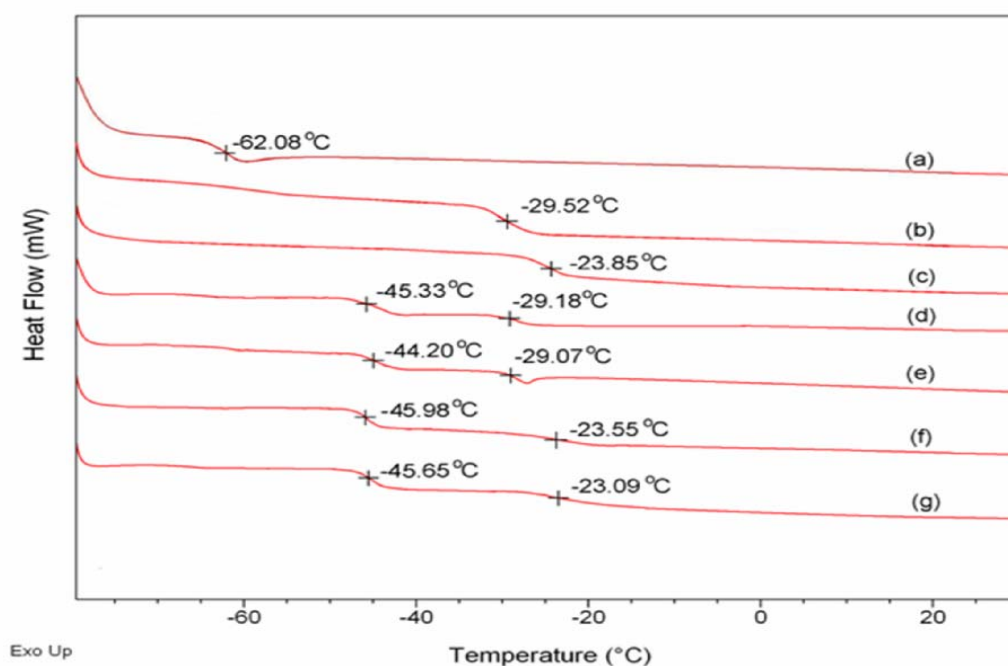


Figure 4.20 DSC curves of (a) NR, (b) PDMAMP, (c) PDMMEP, NR-g-PDMMEP after (d) 60 min and (e) 180 min of grafting, and NR-g-PDMAMP after (f) 60 min and (g) 180 min of grafting. Grafting conditions: $[\text{monomer}] / [\text{DEDT-NR units}] = 7$.

d.6. Morphology of the graft copolymer particles

The grafted natural rubber particles were visualized by TEM technique and the micrographs obtained were compared with that of unmodified NR particles, as shown in Figure 4.21. The lighter areas in the micrographs of NR-g-PDMAMP and NR-g-PDMMEP particles represent the grafted PDMAMP and PDMMEP phases, respectively. This technique does not make it possible to see the core of the latex particles. However, owing to the fact that the penetration of UV rays within the latex particles is restricted (O'dian, 1981), it is obvious that the photopolymerization leading to polar PDMAMP and PDMMEP grafts will be initiated essentially at the surface of the NR particles to form core-shell particles, even if it was already shown that the grafting of dimethylphosphonate-functionalized monomers on NR latex particles could partially take place inside the particles (Schneider, 1996).

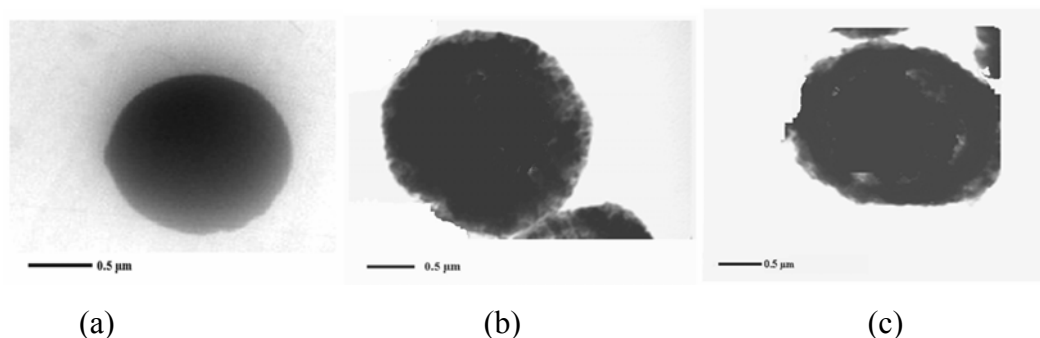


Figure 4.21 TEM micrographs of (a) natural rubber, (b) NR-g-PDMAMP, and (c) NR-g-PDMMEP. Grafting conditions: 60 min with [monomer/[DEDT-NR units] = 7.

4.2.2. Synthesis and characterization of NR-g-PDMMMP

a. Epoxidation of natural rubber latex

NR latex was epoxidized in order to prepare three ENRs with theoretical epoxidation levels of 10, 20, and 30 units%, respectively, by controlling initial amounts of hydrogen peroxide and formic acid (used in equimolar quantities). Molecular structure of ENRs were compared by $^1\text{H-NMR}$ (Figure 4.22), and their real contents in epoxidized 1,4-polyisoprene units were determined by comparing the signal area at $\delta = 2.70$ ppm attributed to the proton of oxirane ring of epoxidized NR units to the one of the signal at $\delta = 5.14$ ppm characteristic of the proton of carbon-carbon double bond ($-\text{C}(\text{CH}_3)=\text{CH}-$) of unsaturated NR units. It was noted that the calculated epoxidation levels for the various ENRs obtained was close to the theoretical ones, as shown in Table 4.5.

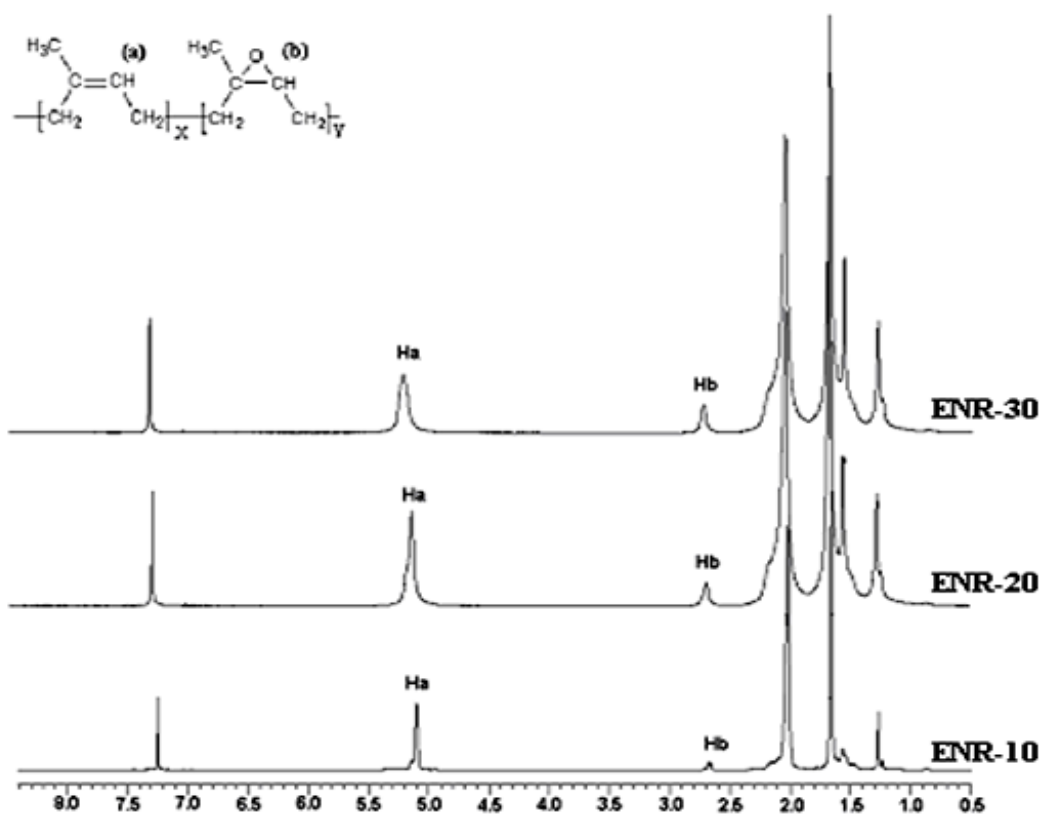


Figure 4.22 ^1H -NMR spectra of ENR with various epoxidation levels.

Table 4.5. Estimation of epoxide content (mol%) of ENR by ^1H -NMR.

Sample	Integrated area		Epoxidation level (%)	
	2.70 ppm	5.20 ppm	Theoretical	Experimental
ENR-10	0.10	1.00	10	9
ENR-20	0.25	1.00	20	20
ENR-30	0.42	1.00	30	30

b. *N,N*-diethyldithiocarbamate-functionalized natural rubber (DEDT-NR)

The addition of DEDT-Na onto the oxirane rings of epoxidized *cis* 1,4-polyisoprene units of the synthesized ENRs was confirmed by the $^1\text{H-NMR}$ signal at $\delta = 4.35$ ppm characteristic of the proton bound to the carbon bearing the *N,N*-diethyldithiocarbamate group ($-\text{CH}[\text{SC}(\text{S})\text{NEt}_2]$) (H_c) (Figure 4.23). On the other hand, the nucleophilic addition was also proved by the presence of two signals at $\delta = 3.7$ ppm and $\delta = 4.0$ ppm which were assigned to the methylenes of diethylamino group ($-\text{N}-\text{CH}_2-\text{CH}_3$) (H_e). However, it was noted that the oxirane rings are not totally transformed during the reaction as shown by the residual signal at $\delta = 2.7$ ppm (H_b). On the other hand, the presence of the signal at $\delta = 5.14$ ppm (H_a) corresponding to the proton of carbon-carbon double bond of NR units showed that NR backbone was not affected during the nucleophilic addition.

The rates of *N,N*-diethyldithiocarbamate functionalized units contained in the synthesized DEDT-NRs were determined from their $^1\text{H-NMR}$ spectra, following equation 3.2. The compositions in units% of the *N,N*-diethyldithiocarbamate-functionalized NRs (DEDT-NR) obtained are given in Table 4.6. The first sample composed of 91 % of NR units, 5 % of residual epoxidized NR units, and 4 % of DEDT-functionalized NR units, will be denoted thereafter as **4% DEDT-NR**, the second sample as **7% DEDT-NR**, and the third as **12% DEDT-NR**.

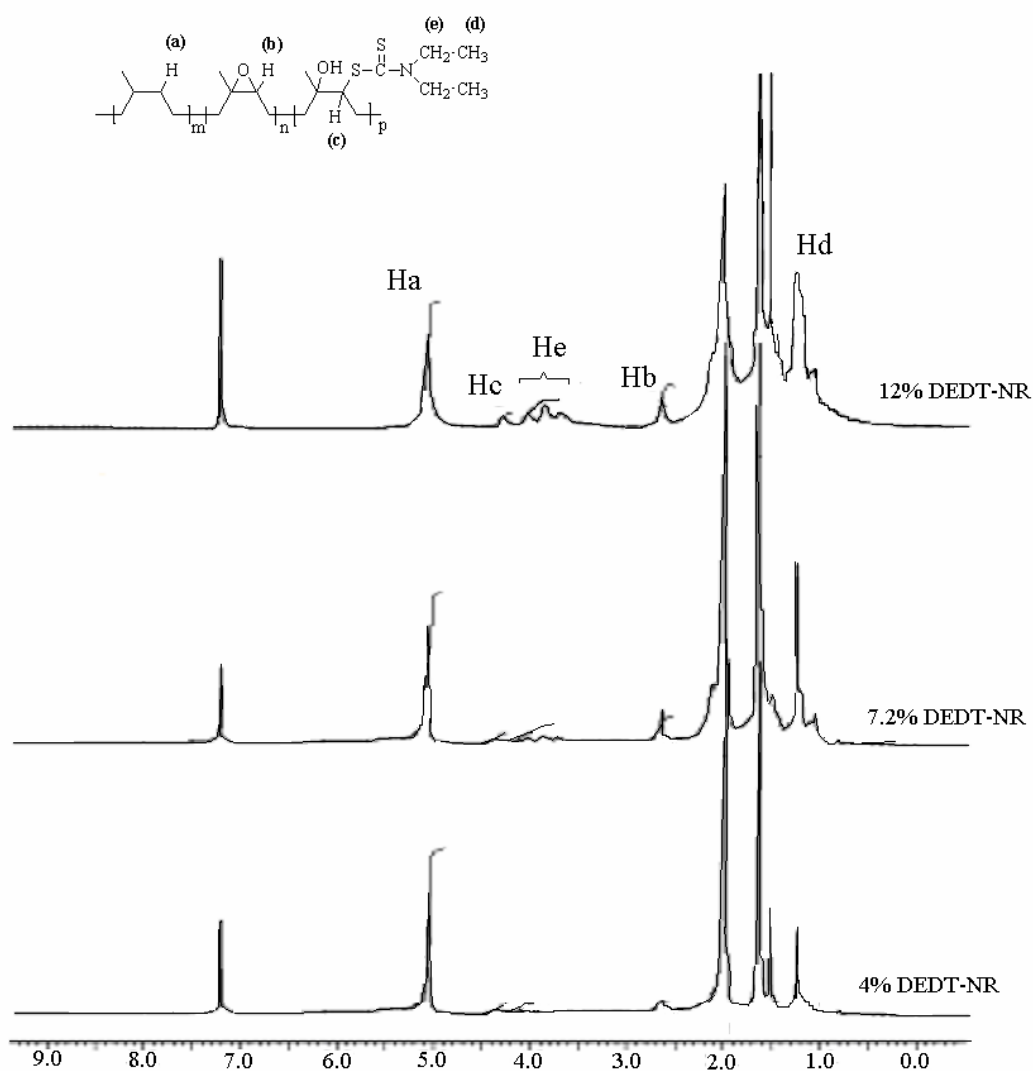


Figure 4.23 ^1H -NMR spectra of *N,N*-diethyldithiocarbamate-functionalized natural rubbers (DEDT-NRs) with various contents in DEDT-NR units.

Table 4.6 Compositions in units% of the *N,N*-diethyldithiocarbamate-functionalized NRs (DEDT-NRs) obtained after addition of DEDT-Na onto oxirane rings of ENRs.

Sample	NR units	Epoxidized NR units	DEDT-NR units
4% DEDT-NR	91	5	4
7% DEDT-NR	80	13	7
12% DEDT-NR	70	18	12

c. NR-g-PDMMMP

c.1. Synthesis and characterization of NR-g-PDMMMP

The synthesis of the NR-g-PDMMMP was performed in latex medium, according to the procedure already described in 4.2.1.c, by using this time dimethyl(methacryloyloxymethyl)phosphonate (DMMMP) as phosphorated monomers. The photopolymerization of DMMMP was initiated from **4% DEDT-NR**, **7% DEDT-NR**, and **12% DEDT-NR**. The purpose was to prepare graft copolymers, different by their density in grafts along NR chains and by their average length of grafts. To confirm the formation of graft copolymers, the crude products were extracted by methanol in order to remove the free homopolymer (i.e., PDMMMP) possibly formed. After the solvent extraction, the NR-g-PDMMMP copolymers obtained by using various conditions were characterized by ^1H , ^{13}C , and ^{31}P -NMR, as well as FTIR spectroscopy.

c.1.1. NMR spectroscopy

Typical ^1H -NMR spectra of NR-g-PDMMMP graft copolymers are shown in Figure 4.24. The peak at $\delta = 5.14$ ppm was assigned to the C=C proton (H_a) of unsaturated units of natural rubber backbone. The signal at $\delta = 2.70$ ppm (H_b) was attributed to the proton of oxirane ring of residual epoxidized NR units. The signals observed at $\delta = 4.40$ (H_c) and $\delta = 3.71$ (H_d) ppm were attributed to the protons of methoxylene and dimethyl of dimethylphosphonate groups along PDMMMP grafts, respectively. These ^1H -NMR analyses confirmed the formation of graft copolymers with PDMMMP grafts bound along NR chains.

The formation of PDMMMP grafts on NR chains was also confirmed in ^{13}C -NMR (Figure 4.25) by peaks at $\delta = 52.9$ ppm and $\delta = 62.3$ ppm, which were assigned to the dimethyl ester and methylenoxy carbons of the dimethylphosphonate functions, respectively. The signal of the C-OH quaternary carbon in NR-g-PDMMMPs was also characterized at $\delta = 74.3$ ppm.

In ^{31}P -NMR a single peak at $\delta = 32.1$ ppm was seen on the spectrum of NR-g-PDMMMPs (Figure 4.26), corresponding to phosphorus atoms of dimethylphosphonate functions of PDMMMP grafts and showing a well-defined structure of the grafts.

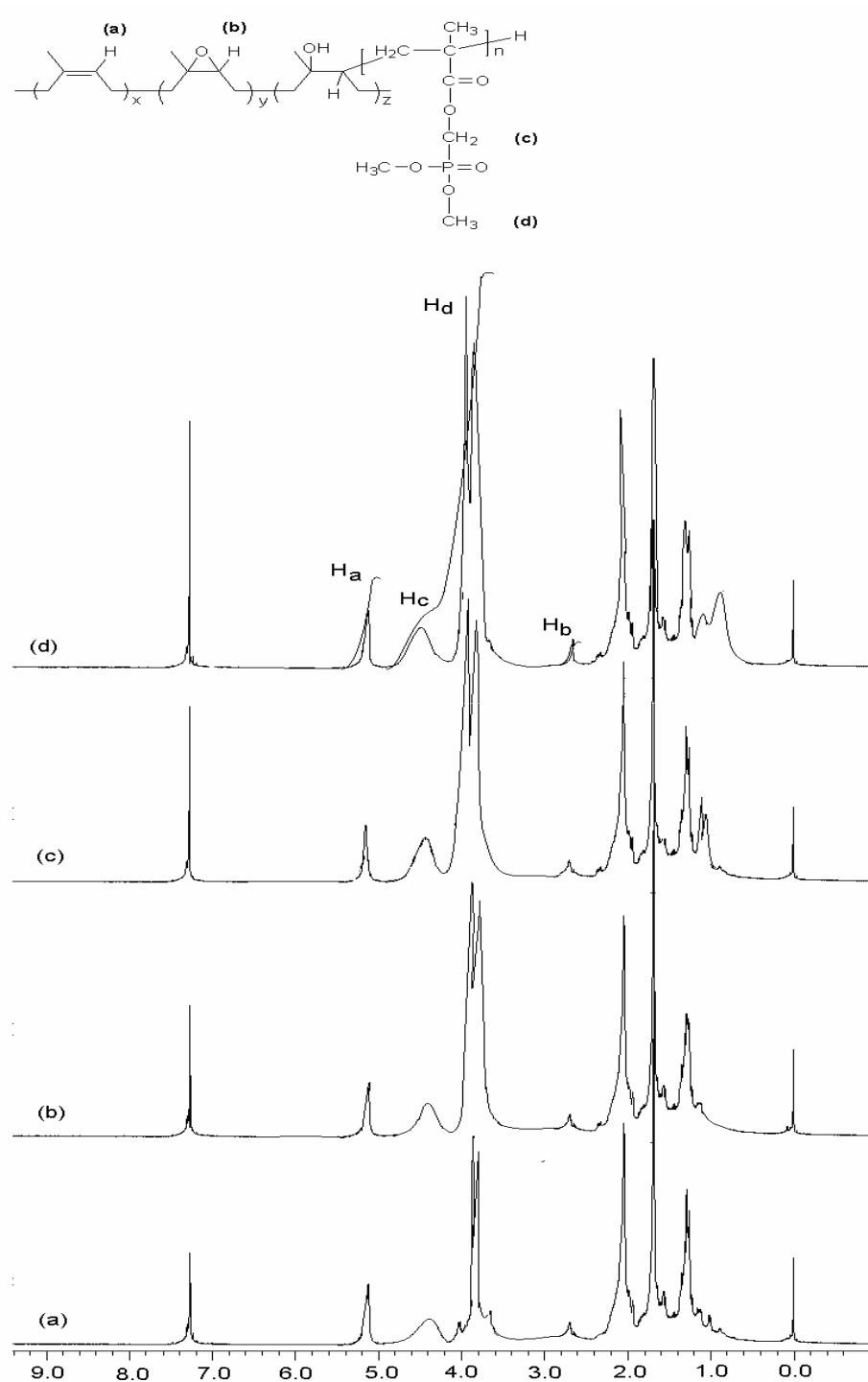


Figure 4.24 $^1\text{H-NMR}$ spectra of NR-g-PDMMMPs obtained after photopolymerization of DMMMP initiated from (a) 4% DEDT-NR during 60 min, (b) 4% DEDT-NR during 180 min, (c) 7% DEDT-NR during 180 min, and (d) 12% DEDT-NR during 180 min.

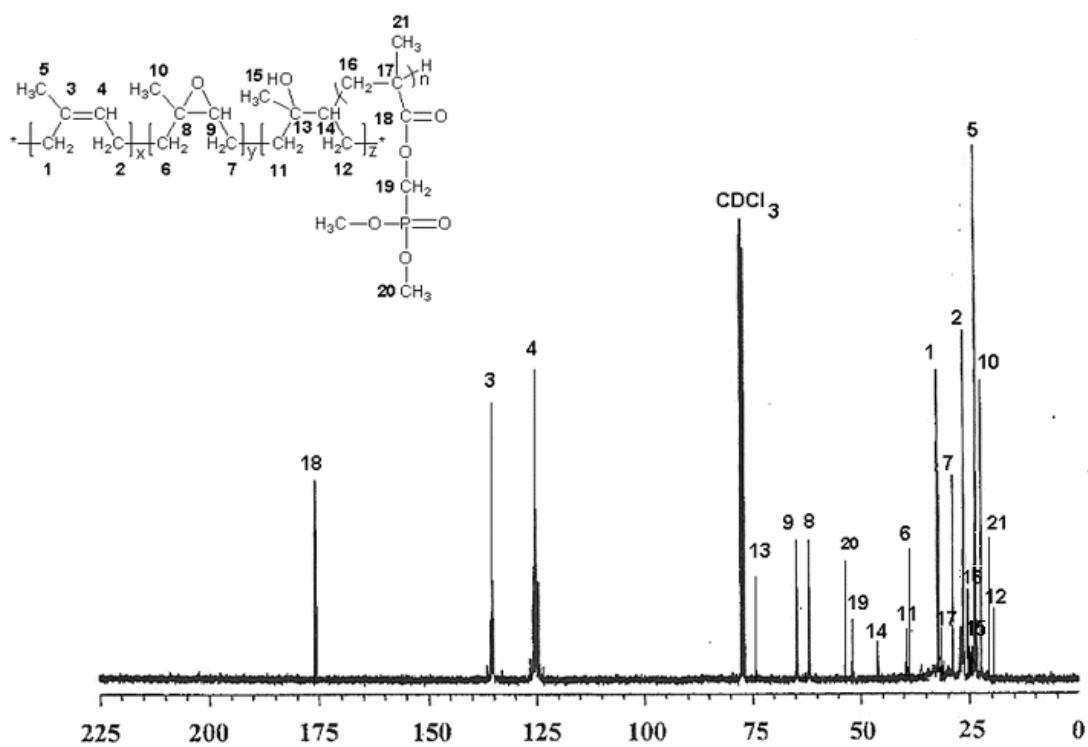


Figure 4.25 Typical ^{13}C -NMR spectrum of NR-g-PDMMMP.

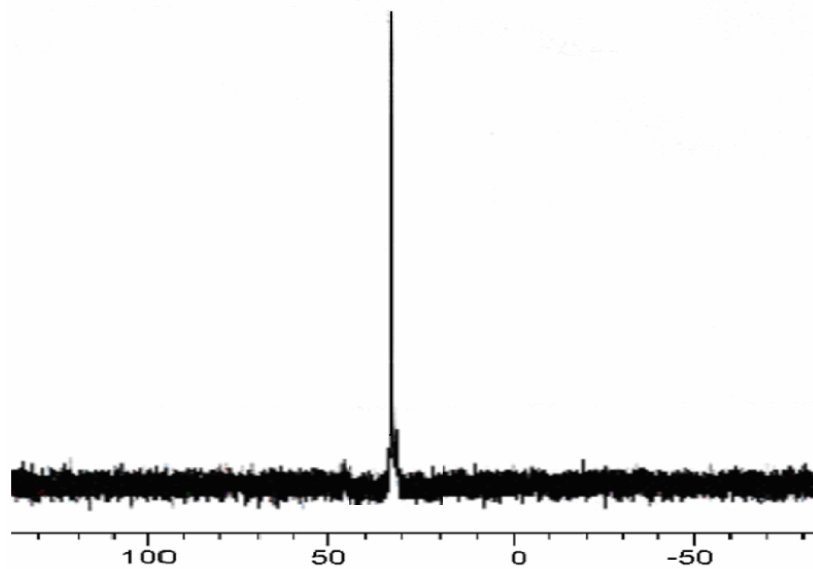


Figure 4.26 Typical ^{31}P -NMR spectrum of NR-g-PDMMMP.

c.1.2. Infrared spectroscopy

IR spectroscopy was used to seek an evidence of the functional groups in NR-g-PDMMMP with the different grafting conditions, as IR spectra shown in Figure 4.27. It can be seen that various absorption bands were observed at 1238, 1050, and 958 cm^{-1} and assigned to the P=O, P-C-O and P-O-CH₃ vibrations of dimethylphosphonate groups in PDMMMP grafts bound to NR backbone, respectively. Furthermore, the absorption band at 1735 cm^{-1} was assigned to C=O of methacrylate structures in PDMMMP grafts. The absorption bands at 1377 and 1451 cm^{-1} were attributed to the aliphatic C-H stretching vibrations in NR backbone. Consequently, because the IR characteristics of monomer functions were observed after the grafting reaction, the occurrence of PDMMMP grafting onto natural rubber backbone was thus confirmed.

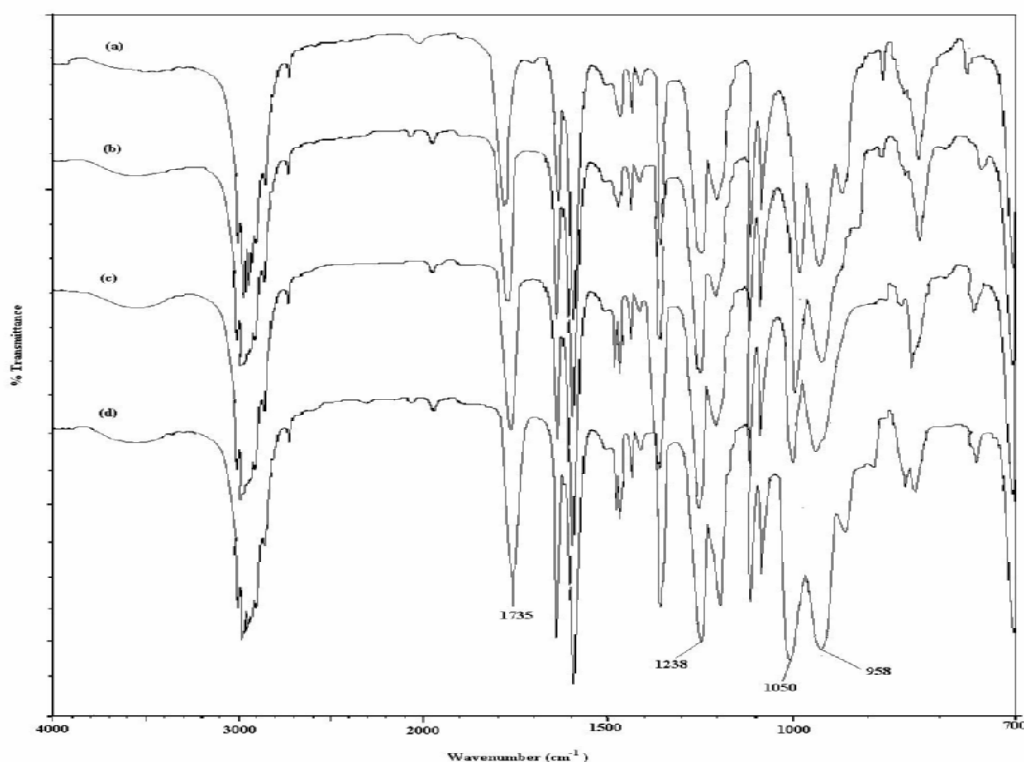


Figure 4.27 IR spectra of NR-g-PDMMMPs obtained after photopolymerization of DMMP initiated from (a) 4% DEDT-NR during 60 min, (b) 4% DEDT-NR during 180 min, (c) 7% DEDT-NR during 180 min, and (d) 12% DEDT-NR during 180 min.

c.2. Grafting kinetics

The kinetic studies of the photopolymerization of DMMMP initiated from three synthesized DEDT-NR, i.e., **4% DEDT-NR**, **7% DEDT-NR**, and **12% DEDT-NR**, respectively, were performed using a constant molar ratio $[\text{monomer}] / [\text{DEDT-NR units}] = 1.25$, whatever the macroinitiator used. The results given in Figure 4.28 show that the curves of monomer conversion and monomer conversion in grafts (determined by weighing) *versus* time were identical whatever the DEDT-NR macroinitiator used, showing that the rate of polymerization did not depend on the density of initiating groups along the rubber chains. After 15 min of retardation period explained by the fact that methacrylate double bond is less polarized and thus less reactive, the polymerization progresses rapidly before reaching a plateau after about 120 min. The difference that exists between the curve of monomer conversion and that of monomer conversion in grafts shows that the grafting copolymerization is always accompanied by the formation of a low amount of PDMMMP homopolymer ($< 10\%$ by comparison with the DMMMP grafted). Figure 4.29 shows the progress of the grafting rate in relation with the density of initiating groups along the rubber chains, which was simultaneously determined by weighing and from $^1\text{H-NMR}$ spectra. It was noted that the grafting rate increases by increasing the concentration of initiating groups on the macroinitiator chains, i.e., **12% DEDT-NR** $>$ **7% DEDT-NR** $>$ **4% DEDT-NR**. On the other hand, it was noted that the grafting rates determined from $^1\text{H-NMR}$ spectra are always slightly higher than those measured by weighing. This can be explained by the tiny loss of products during the different treatments carried out on the crude copolymer obtained after grafting.

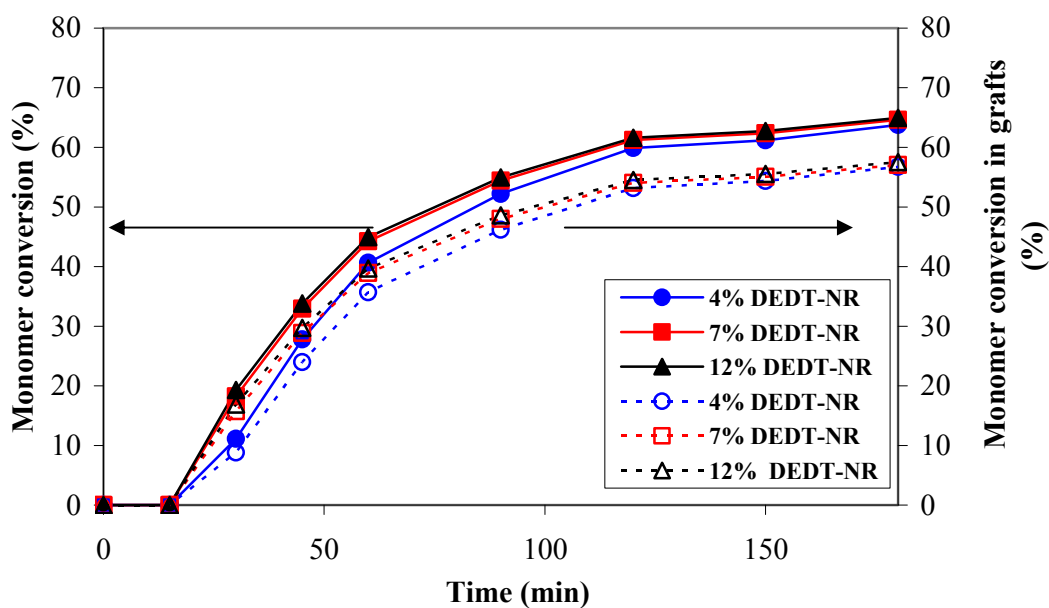


Figure 4.28 Progress of monomer conversion and monomer conversion in grafts (determined by weighing) for the photopolymerizations of DMMMP initiated from 4% DEDT-NR, 7% DEDT-NR, and 12% DEDT-NR, respectively. [monomer] / [DEDT-NR units] molar ratio = 1.25.

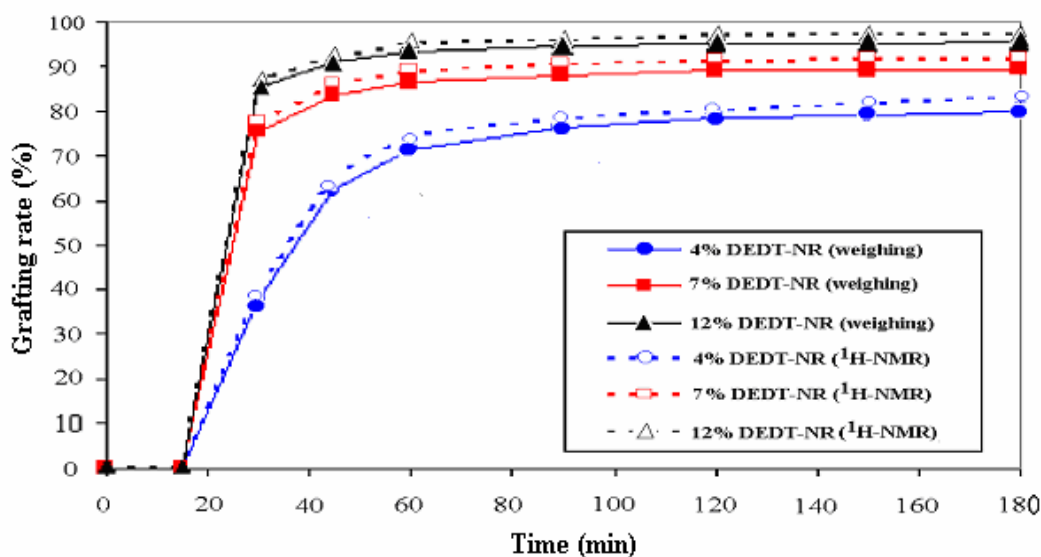


Figure 4.29 Progress of grafting rate (determined by weighing and $^1\text{H-NMR}$ technique) for the photopolymerization of DMMMP initiated from 4% DEDT-NR, 7% DEDT-NR, and 12% DEDT-NR, respectively. [monomer] / [DEDT-NR units] = 1.25.

The kinetic plots given in Figure 4.30 show that the kinetic of the grafting reaction of DMMMP by photopolymerization is not a first-order, which indicates a non-constant radical concentration during the polymerization, and thus that the polymerization do not show the characteristics of living/controlled one. This result was verified whatever the density of initiating groups on the rubber chains and whatever the concentration in DMMMP. Moreover, the fact that the slope of the experimental curve representing the progress of the number-averaged molecular weight (\overline{M}_n) *versus* monomer conversion was lower than that of the theoretical one (Figure 4.31) is also significant of the existence of transfer reactions during the photopolymerization step. However, the slight increase of \overline{M}_n after about 55 % of DMMMP conversion may be noted that this dramatic increase of \overline{M}_n at the moment begins simultaneously with the increase of latex viscosity. This result could be explained with the same phenomena observed with DMAMP and DMMEP by recombination reactions.

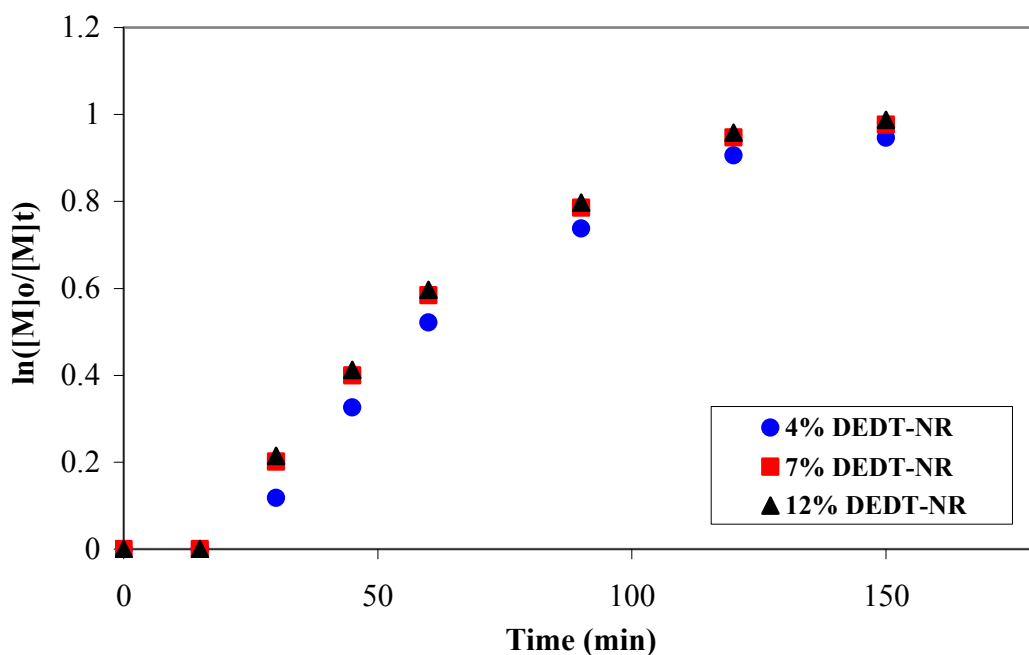


Figure 4.30 First-order kinetic plots for the photopolymerization of DMMMP initiated from 4% DEDT-NR, 7% DEDT-NR, and 12% DEDT-NR, respectively. [monomer] / [DEDT-NR units] molar ratio = 1.25.

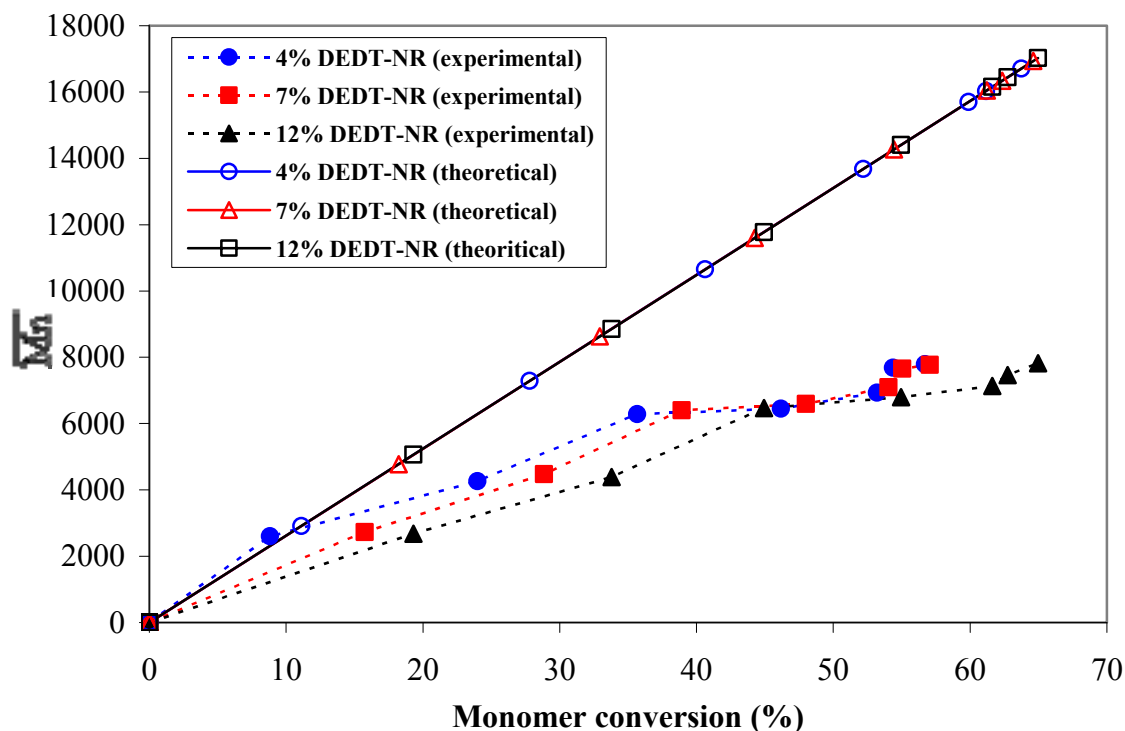


Figure 4.31 Dependence of molecular weight (\overline{M}_n) on monomer conversion for the photopolymerization of DMMMP initiated from **4% DEDT-NR**, **7% DEDT-NR**, and **12% DEDT-NR**, respectively. [monomer] / [DEDT-NR units] molar ratio = 1.25.

c.3. Average length of the grafts (degree of polymerization)

The evolutions of the degree of polymerization (\overline{DP}_n) of PDMMMP grafts in relation with the macroinitiator used, and thus of the concentration of *N,N*-diethyldithiocarbamate groups along the rubber chains, are given in Figure 4.32. It can be seen that \overline{DP}_n increased with reaction time as already stated above, and this increase did not depend on the density of initiating groups on the rubber chains (Figure 4.28). Finally, depending on the reaction conditions, NR-*g*-PDMMMPs bearing PDMMMP graft lengths with \overline{DP}_n of about 30-38 could be synthesized (Table 4.7).

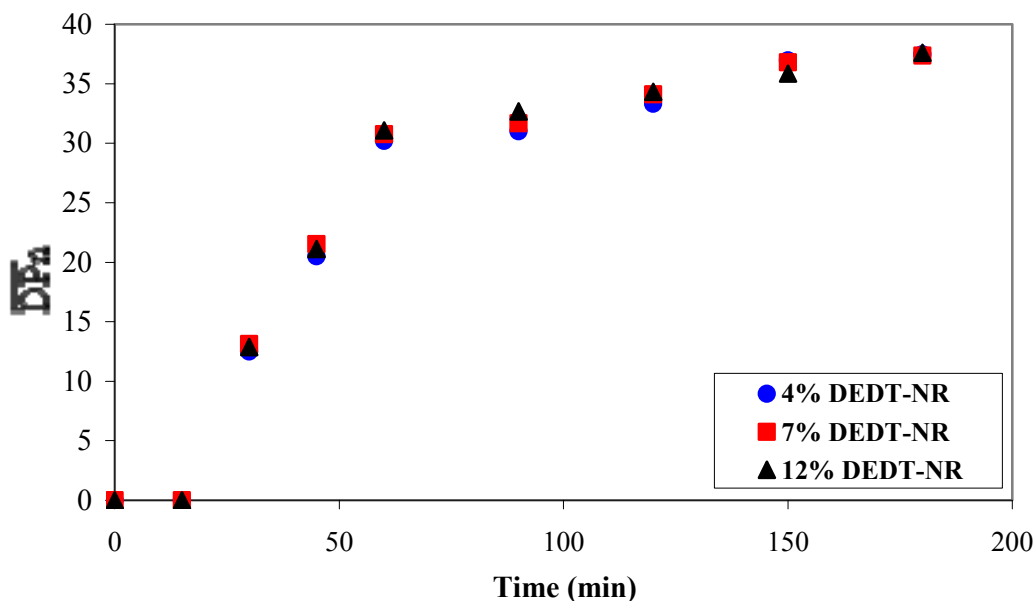


Figure 4.32 Evolution of the degree of polymerization (\overline{DP}_n) of PDMMMP grafts of NR-g-PDMMMPs during DMMMP photopolymerization initiated from **4% DEDT-NR**, **7% DEDT-NR**, and **12% DEDT-NR**, respectively. [monomer] / [DEDT-NR units] molar ratio = 1.25

Table 4.7 Degrees of polymerization (\overline{DP}_n) and grafting rates (GR) of the different NR-g-PDMMMP copolymers coming from **4% DEDT-NR**, **7% DEDT-NR**, and **12% DEDT-NR**, respectively. [monomer]/[DEDT-NR unit] molar ratio = 1.25.

DEDT-NR	Reaction time (min)	Monomer conversion (%)	\overline{DP}_n	Grafting rate (GR in wt%)	
				¹ H-NMR	Weighing
4% DEDT-NR	60	41	30	75	71
4% DEDT-NR	180	64	37	83	80
7% DEDT-NR	180	67	38	91	89
12% DEDT-NR	180	65	37	97	95

c.4. Thermal behavior

Thermal behavior of pure NR and NR-g-PDMMMPs with different grafting rates were investigated by DSC, as shown in Figure 4.33. It is seen that NR showed a

single glass transition temperature (T_g) at approximately -62.1°C . On the other hand, the analyzed NR-g-PDMMMP copolymers showed two T_g s, one at low temperature (i.e., in a range of -53.75°C to -40.60°C) corresponding to the glass transition of *cis*-1,4-polyisoprene backbone of NR domains, and the second at higher temperature (i.e., in range of -22.86°C to -22.50°C) corresponding to the transition of the domains occupied by the dimethylphosphonate-functionalized polymer grafts. Consequently, for NR-g-PDMMMP copolymers whose grafting rates (GR) are between 71 wt% and 95 wt%, a phase separation occurs. It was also seen that the T_g of NR domains increased slightly with the grafting rate of the graft copolymer. This indicates that the material would tend to become homogeneous (i.e., one phase) when GR is increased. The fact that the T_g of NR phase in the NR-g-PDMMMP is higher than the T_g of pure NR can be attributed to a restriction of the chain mobility in the graft copolymer because of the interaction between the polar groups. To prove that interactions occurs in the NR-g-PDMMMP copolymers, Mooney viscosities (MV) of NR-g-PDMMMP with various grafting rates (i.e., 71, 80, 89 and 95 wt%) were measured. It was noted (Figure 4.34 and Table 4.8) that the Mooney viscosity of the NR-g-PDMMMP graft copolymers increases with the increase of GR, the lowest value being obtained with pure NR (ML, 1+4, 100°C). This is an evidence of an increase of interactions and hence of the flow resistance of the material. This correlates well with the restriction of chain mobility.

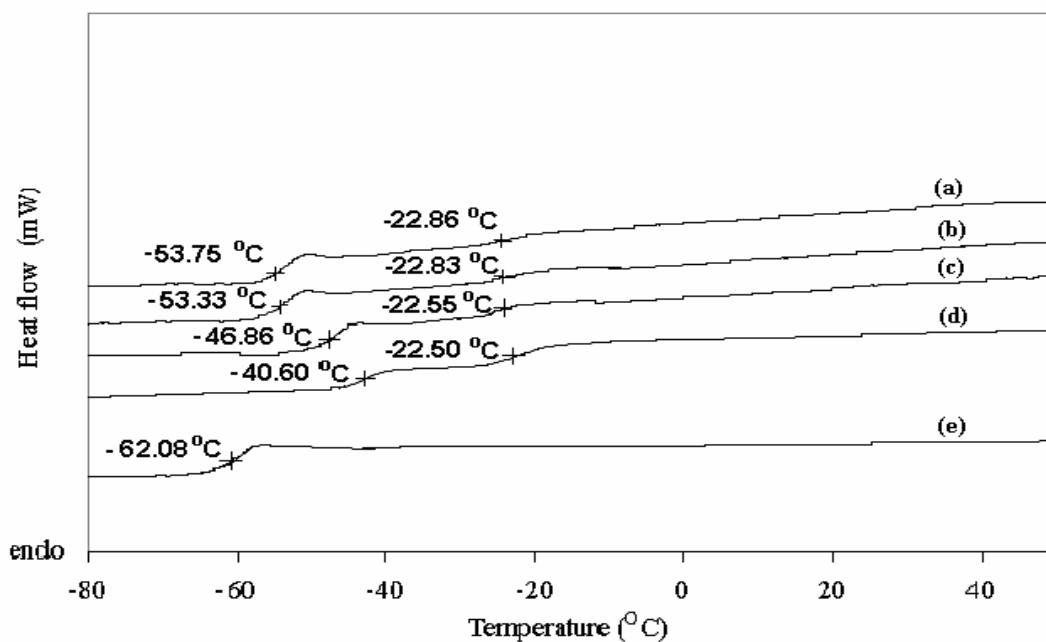


Figure 4.33 DSC curves of NR-g-PDMMMPs with various grafting rates: (a) NR-g-PDMMMP 71%*, (b) NR-g-PDMMMP 80%*, (c) NR-g-PDMMMP 89%*, (d) NR-g-PDMMMP 95%* (e) pure NR. (*grafting rate in wt%)

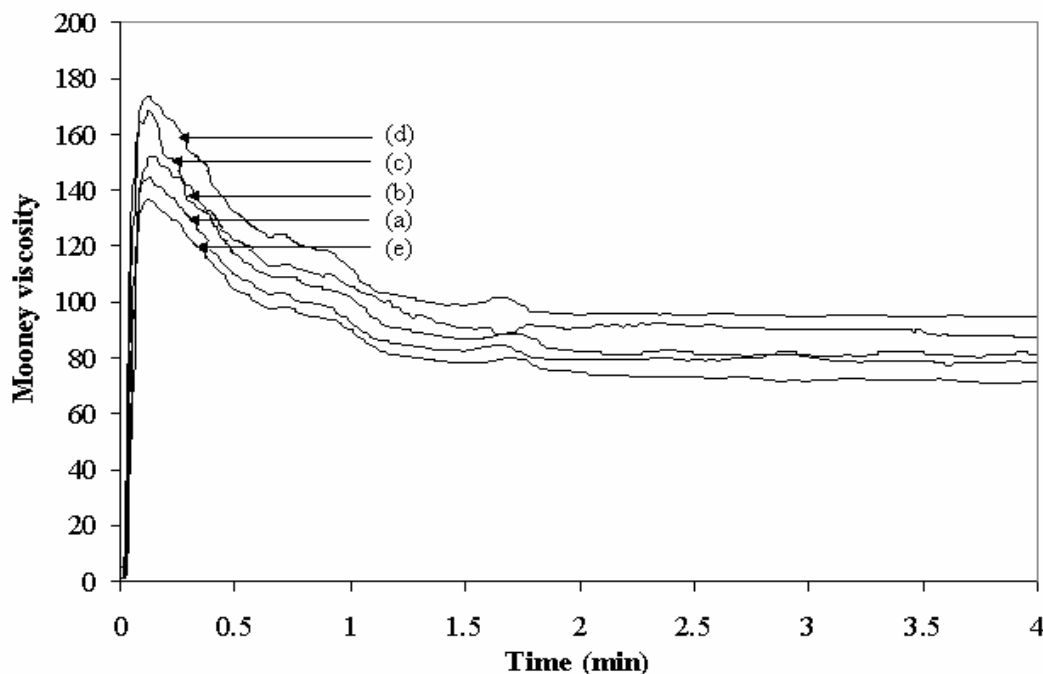


Figure 4.34 Mooney viscosity of NR-g-PDMMMP with various grafting rates: (a) NR-g-PDMMMP 71%*, (b) NR-g-PDMMMP 80%*, (c) NR-g-PDMMMP 89%*, (d) NR-g-PDMMMP 95%* (e) pure NR. (*grafting rate in wt%)

Table 4.8 Mooney viscosity of pure NR and NR-*g*-PDMMMP with various grafting rates.

Sample	Mooney Viscosity (ML (1+4)) 100°C
pure NR	71
NR-<i>g</i>-PDMMMP 71%*	78
NR-<i>g</i>-PDMMMP 80%*	81
NR-<i>g</i>-PDMMMP 89%*	87
NR-<i>g</i>-PDMMMP 95%*	94

*grafting rate in wt%

c.5. Dynamic properties

Figure 4.35 shows the evolution of $\tan \delta$ as a function of frequency of NR-*g*-PDMMMPs with various grafting rates (i.e., 71, 80, 89 and 95 %) compared with pure NR. It was seen that, the $\tan \delta$ increased with increasing grafting rate. At a given frequency, the $\tan \delta$ values of the graft copolymers are greater than that of the pure NR. This is attributed to restriction of the chains because of steric hindrance of the NR chains bearing PDMMMP grafts and increasing of intermolecular forces between the chains with increasing grafting rate. Therefore, higher viscous response or lower elastic response of the graft copolymer (i.e., $\tan \delta = G''/G'$) was observed. This result agrees with the Mooney viscosity (Figure 4.34) of the graft copolymers.

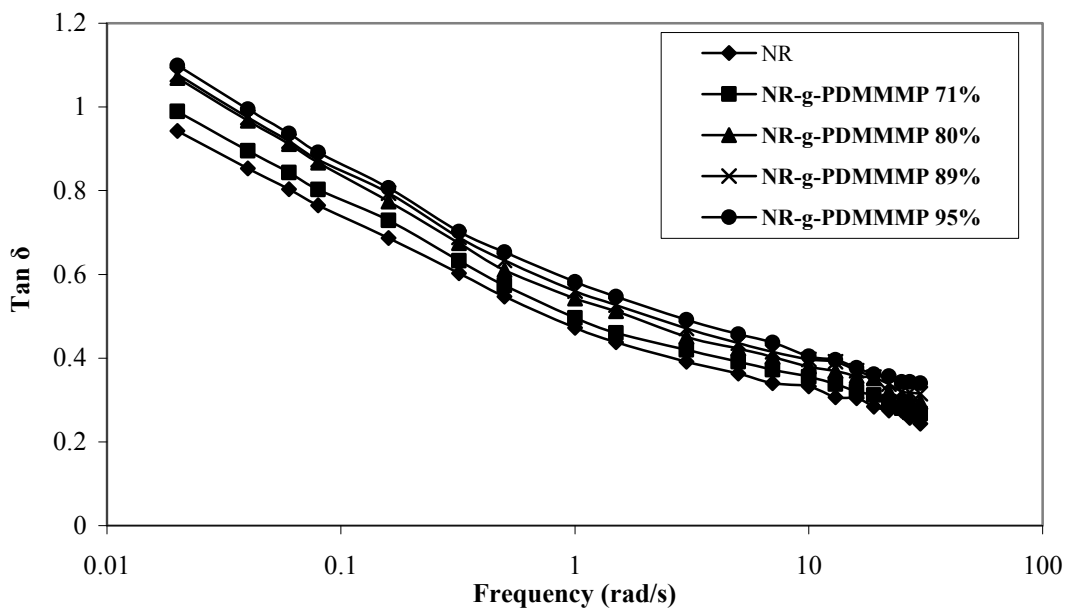


Figure 4.35 $\text{Tan } \delta$ as a function of frequency of pure NR and NR-g-PDMMMP with various grafting rates.

c.6. Thermal stability

Thermal stabilities of pure NR, PDMMMP homopolymer, and NR-g-PDMMMPs with various GR were characterized using TGA technique. Figures 4.36 and 4.37 show TGA thermograms obtained under nitrogen and oxygen atmospheres, respectively.

Under nitrogen atmosphere (Figure 4.36), it can be seen that pure NR and PDMMMP homopolymer exhibited a single step of weight loss with an onset temperature of approximately 320°C and 221°C, respectively (Table 4.9). For NR-g-PDMMMPs with grafting rates in the range of 70 % to 90 %, double degradation steps were observed. The first degradation step occurred at onset temperatures in a range of 258°C to 276°C, corresponding to a weight loss from 37 % to 45 %, while the second step occurred at onset temperatures from 405°C to 445°C, corresponding to a weight loss from 30 % to 47 % (Table 4.9). The first decomposition step of NR-g-PDMMMPs corresponds to the degradation of dimethylphosphonate linkages that occurred at lower degradation temperature than that of the NR backbone. The second decomposition step relates the degradation of

NR structures in the graft copolymer, which occurs at higher temperature than in the case of pure NR. This result proves the ability of dimethylphosphonate-functionalized polymer grafts (i.e., the grafted PDMMMP) to improve thermal stability of natural rubber. This result well correlates with the thermal stability of other graft copolymers of natural rubber bearing dimethylphosphonate-functionalized polymer grafts, including natural rubber-*graft*-poly(dimethyl(acryloyloxymethyl)phosphonate) (NR-*g*-PDMAMP) and natural rubber-*graft*-poly(dimethyl(methacryloyloxyethyl)phosphonate) (NR-*g*-PDMMEP) in section 4.2.1.d.4. The shift of the TGA curves toward higher temperatures when the NR-*g*-PDMMMP grafting rate increases (Figure 4.36) indicates that the thermal stability of the graft copolymer is higher when the content in grafted PDMMMP is higher.

Under oxygen atmosphere, the degradations of the various compounds occurred at lower temperature than in nitrogen atmosphere (Figure 4.37). This is attributed to the activity of oxygen as oxidant to accelerate the degradation of the organic compounds. It was seen that the decomposition of pure NR started at 193°C, but its main decomposition peak was noted at 260°C. On the other hand, the degradation of PDMMMP homopolymer began at lower temperature of approximately 128°C and its main decomposition was observed at higher temperature of 175°C. As under nitrogen atmosphere, NR-*g*-PDMMMPs with grafting rates in the range of 70 % to 90 %, degraded in double stages and their degree of stability in oxygen also depends on the grafting rate. That is, the degradation temperature increased with the grafting rate. The onset temperatures for the first degradation step in oxygen varied from 205°C to 245°C, corresponding to a weight loss from 39 % to 48 %. The degradation temperatures of the second stage are in a range of 335°C to 403°C, corresponding to a weight loss of 49 % to 31 %.

On the other hand, it was also noted that the char residue also depends on the grafting rate of NR-*g*-PDMMMP. The results summarized in Table 4.9 show that an increase of the char residue, from 16 to 25 % in nitrogen atmosphere and from 12 % to 21 % in oxygen atmosphere, was observed when the grafting rate of NR-*g*-PDMMMP was increased from 71 % to 95 %. This clearly proves the essential role of the dimethylphosphonate-functionalized polymer grafts to improve thermal

resistance of the graft copolymer. Higher content of char residue that can act as an insulating protective layer and prevents oxygen transfer to the burning sample which thereafter slow down the degradation process.

The slope of the falling region of the TGA plots was also measured in order to determine the rate of the degradation process (Ramesan, 2004). It was seen that the slopes of the TGA curves of NR-g-PDMMMPs are lower than that of the TGA curve of pure NR (Table 4.9). This indicates that the degradation rates of the graft copolymers are lower than that of pure NR. It was also seen that the slope values for the TGA curves obtained under oxygen were higher than in nitrogen atmosphere, and hence that higher degradation rates are observed in oxygen atmosphere. Therefore, the higher thermal stability with lower degradation rate of NR-g-PDMMMP is attributed to the presence of phosphorus atoms.

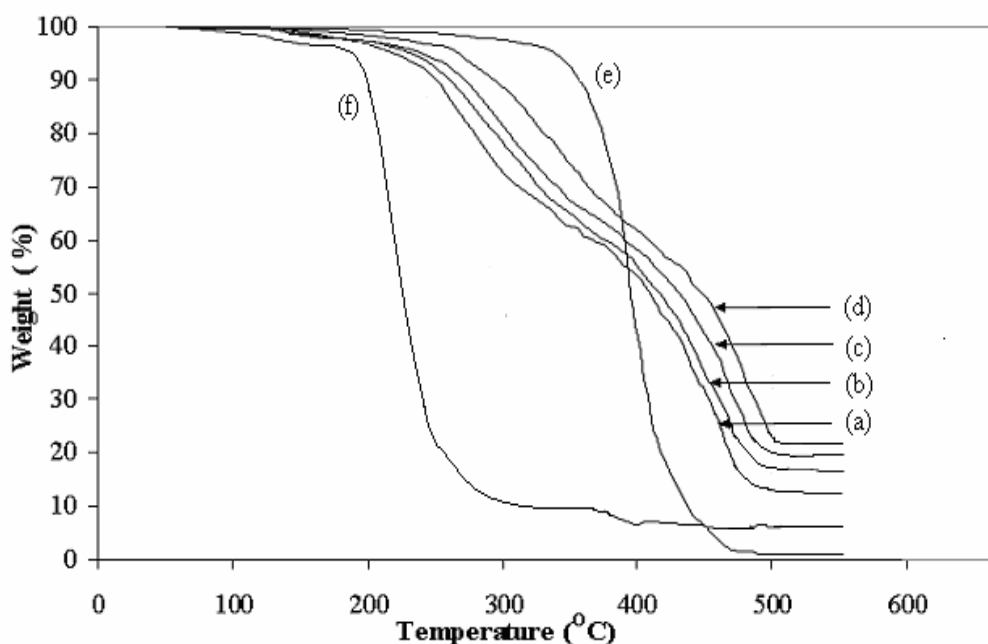


Figure 4.36 TGA thermograms obtained under nitrogen atmosphere of (a) NR-g-PDMMMP 71%, (b) NR-g-PDMMMP 80%, (c) NR-g-PDMMMP 89%, (d) NR-g-PDMMMP 95%, (e) pure NR and (f) PDMMMP homopolymer.

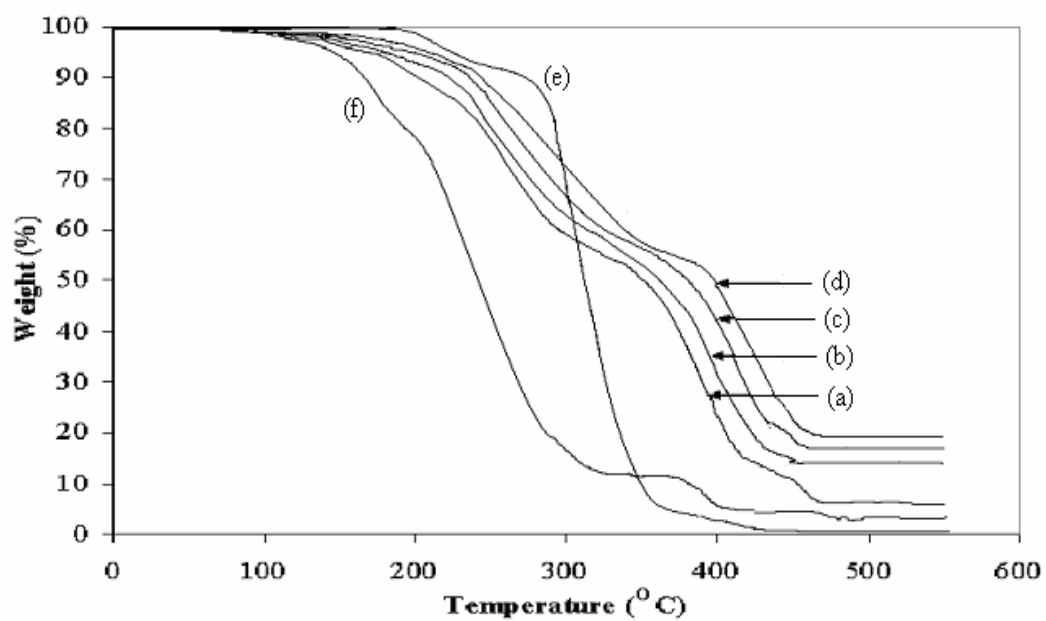


Figure 4.37 TGA thermograms obtained under oxygen atmosphere of (a) NR-g-PDMMMP 71%, (b) NR-g-PDMMMP 80%, (c) NR-g-PDMMMP 89%, (d) NR-g-PDMMMP 95%, (e) pure NR, and (f) PDMMMP homopolymer.

Table 4.9 TGA characteristics of NR, PDMMMP, NR-*g*-PDMMMP with various grafting rates (i.e., 71, 80, 89 and 95%), in nitrogen and oxygen atmospheres.

Type of copolymer	Nitrogen atmosphere						Oxygen atmosphere							
	Onset temperature (°C)		Weight loss (%)		Slope values		Char (%)	Onset temperature (°C)		Weight loss (%)		Slope values		Char (%)
	1 st	2 nd	1 st	2 nd	1 st	2 nd		1 st	2 nd	1 st	2 nd	1 st	2 nd	
	step	step	step	step	step	step	step	step	step	step	step	step		
NR	320	-	99.8	-	0.91	-	0.2	193	260	7	92.9	0.98	-	0.1
PDMMMP	221	-	94	-	0.62	-	6	128	175	12	83	0.75	-	5
NR- <i>g</i> -PDMMMP 71 %	258	405	37	47	0.34	0.61	16	205	335	39	49	0.40	0.65	12
NR- <i>g</i> -PDMMMP 80 %	262	424	40	40	0.30	0.54	20	220	360	44	39.2	0.38	0.62	16.8
NR- <i>g</i> -PDMMMP 93 %	269	440	44	34	0.29	0.48	22	236	383	45	37	0.37	0.58	18
NR- <i>g</i> -PDMMMP 95%	276	445	45	30	0.30	0.45	25	245	403	48	31	0.35	0.53	21

c.7. Flammability behavior

c.7.1. LOI measurements

Limiting oxygen test involves igniting a vertically clamped specimen at its upper end in a controlled, variable oxygen/nitrogen atmosphere. The Limiting Oxygen Index (LOI) is defined as the minimum oxygen concentration that will only support candle-like combustion of the specimen on 50 mm long. It is used to measure flame retardant property of materials. The LOI values of NR and NR-g-PDMMMPs with various grafting rates are shown in Figure 4.38. It can be seen that the LOI of pure NR is lower than that of the graft copolymers. This indicates that pure NR burns at lower oxygen concentration than NR-g-PDMMMPs, and hence shows lower flame retardant property or higher flammability. It was also seen that the LOI of graft copolymer increased with their grafting rates. This indicates increasing tendency of flame resistance. Therefore, the higher LOI index value was observed, the lower the flammability is consequent. The LOI values and char residues based on the TGA analysis could be correlated (Table 4.10 and Figure 4.38). It can be seen that pure NR shows the lowest LOI and char residue. Furthermore, the LOI values and char residues of NR-g-PDMMMPs increase with the increase of the grafting rate, and hence higher flame retardant properties are obtained. This is attributed to the char of phosphorus compounds that behaved as thermal insulation to prevent oxygen gas to enter into the flame, and thus to inhibit combustion. Therefore, the flame resistance of the graft copolymer is as much improved than the volume of char formed during the degradation process is high, which showed that it is well dependent on the grafting rate of NR-g-PDMMMP.

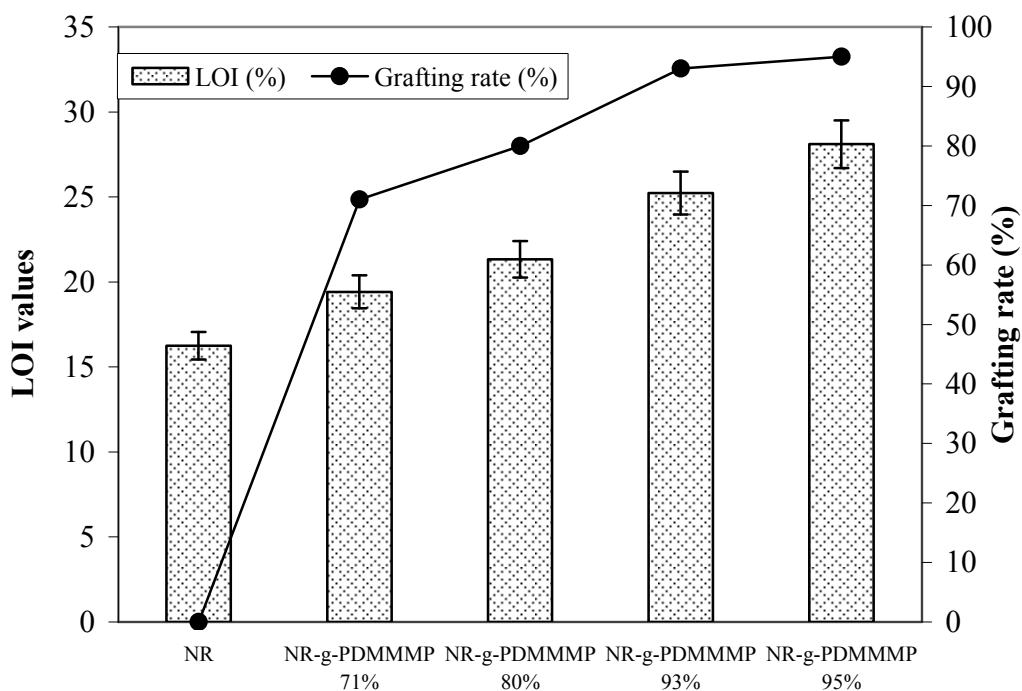


Figure 4.38 LOI values of pure NR and NR-g-PDMMMPs with various grafting rates.

Table 4.10 LOI values and char residue measured by TGA of NR and NR-g-PDMMMPs with various grafting rates.

Sample	Grafting rate (%)	LOI (O ₂ %)	Char residue* (%)	
			Nitrogen atmosphere	Oxygen atmosphere
Pure NR	0	16.25	0.2	0.1
NR-g-PDMMMP 71%	71	19.42	16	12
NR-g-PDMMMP 80%	80	22.33	20	16.8
NR-g-PDMMMP 89%	89	25.12	22	18
NR-g-PDMMMP 95%	95	27.10	25	21

* Measurement by TGA

c.7.2. Burning rates

In the test used to measure the burning rate, a specimen, 50x150x13 mm is clamped horizontally and ignited at its top of the specimen. The burning rate is defined as the time required to the flame to burn a length of 125 mm of the specimen or to extinguish. The burning rates of various NR-g-PDMMMPs, as well as that of pure NR, are given in Figure 4.39. The highest burning rate was observed with pure NR, while a decrease of the burning rate with the increase of the grafting rates was noted in the case of NR-g-PDMMMPs. The results correlated well with what was observed with LOI values and char residues measurement. Therefore, the flame retardant properties of natural rubber can be improved by grafting dimethylphosphonate-functionalized polymers onto NR backbone. The fire retardancy properties of these grafts is attributed to the action of dimethylphosphonate functions that, during thermal degradation, decompose at lower temperature than the degradation temperature of the material studied, which allows to improve its thermal resistance by forming a heat resistant char at the material surface, which acts as a protective thermal barrier to prevent the oxygen transfer to the flame, and then causes the flame extinguishing.

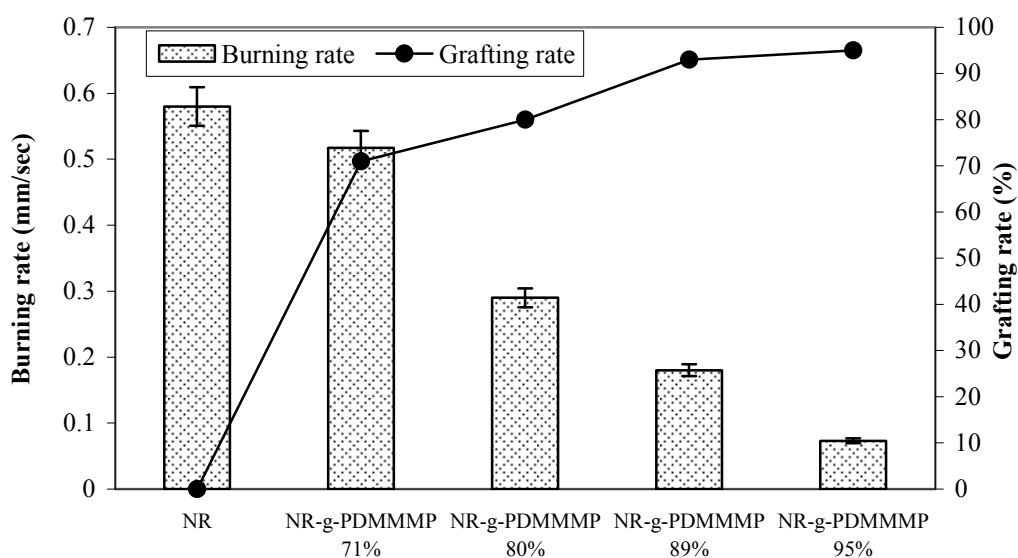


Figure 4.39 Burning rate of pure NR and NR-g-PDMMMPs with various grafting rates.

c.8. Morphology of the graft copolymer particles

The grafted natural rubber latex particles were visualized by TEM technique and the micrographs obtained were compared with that of the unmodified NR latex particles, as shown in Figure 4.40. It can be seen that the surface of NR latex particles is smooth (Figure 4.40a), in contrary to that of the grafted latex particles that shows nodules of PDMMMP (Figure 4.40b-e). This may be due to the growing macroradical chains leading to polar PDMMMP grafts, essentially initiated at the surface of NR particles to form a shell layer. Moreover, it was clearly noted that increasing the grafting rate gives thicker copolymer shells around the NR cores.

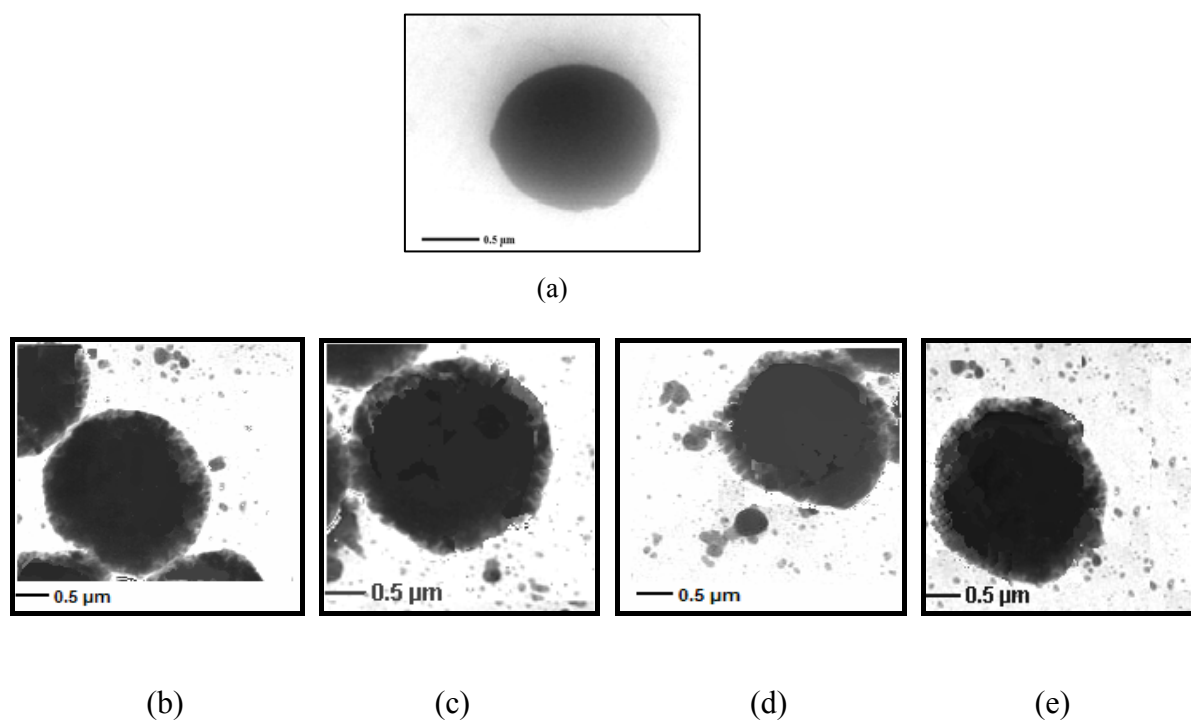


Figure 4.40 TEM micrographs of (a) NR, (b) NR-*g*-PDMMMP 71%, (c) NR-*g*-PDMMMP 80%, (d) NR-*g*-PDMMMP 89%, and (e) NR-*g*-PDMMMP 95%.

PART B

PREPARATION AND CHARACTERIZATION OF SIMPLE BLEND BASED ON NR/EVA

Polymer blend of 50/50 NR/EVA with and without compatibilizer was prepared according to section 3.3.2.2. Effect of different types of graft copolymer, grafting rates and concentration (i.e., 1, 3, 5, 7, 9, 12 and 15 wt% of NR) were studied.

4.3 Thermodynamic of NR/EVA blends

Equation used for calculating heat of mixing for a two component blend system was developed by Schneier, (1973) to approximate the polymer-polymer compatibility, as shown below:

$$\Delta H_m = \left\{ X_1 M_1 \rho_1 (\delta_1 - \delta_2)^2 \left[\frac{X_2}{(1 - X_2)} M_2 \rho_2 + (1 - X_1) M_1 \rho_1 \right]^2 \right\}^{1/2} \quad (4.1)$$

Where X, M, ρ and δ are the weight fraction of the polymer, molecular weight of monomer unit, polymer density and solubility parameter of polymer, respectively.

The heat of mixing of NR/EVA blend was calculated based on Equation 4.1. The heat of mixing value of 50/50 NR/EVA blend was 19.80×10^{-3} cal. This value is higher than the limiting value for compatibility according to Bohn (1968). That is, the compatible polymer pair showed the heat of mixing between approximately 1×10^{-3} to 10×10^{-3} cal. Hence, on the basis of heat of mixing, the NR/EVA blends are incompatible blend. In addition, the heterogeneity of the NR/EVA blend system is emphasized by the difference of the solubility parameter of the two polymers. That is, the solubility parameters (δ) of NR and EVA are $8.34 \text{ cm}^{-3}(\text{cal}/\text{cm}^3)^{1/2}$ and $7.88 \text{ cm}^{-3}(\text{cal}/\text{cm}^3)^{1/2}$, respectively. They were calculated according to Small's equation

$$\delta = \rho \sum F_i/M \quad (4.2)$$

where ρ is the density of the polymer, M is the molecular weight of the repeat unit in the polymer chain and $\sum F_i$ is the sum of the molar attraction constants of all the chemical groups in the polymer repeat unit. As a result, a wide gap of solubility parameters (δ_1 - δ_2) between NR and EVA (i.e., = 0.46) is more than 0.1. This predicted incompatibility of the blend. (Barlow and Paul, 1984)

4.4 Effect of different types of compatibilizers on properties of NR/EVA blends

The effect of the compatibilizer structure on the 50/50 NR/EVA blend was carried out using a loading level in compatibilizer of 7 wt% by comparison with NR. Various types of compatibilizers, i.e., NR-*g*-PDMMMP, NR-*g*-PDMAMP, NR-*g*-PDMMEP, and ENR-30, were considered. The characteristics of the graft copolymers used were similar: same density of grafts on NR backbone and average graft length ($\overline{DP_n}$) of 37. The properties of the blends were studied as follows:

4.4.1 Rheological properties

The effect of the different types of compatibilizers on complex viscosity *versus* frequency is shown in Figure 4.41. On the other hand, the complex viscosity at a constant frequency of 6 rad/s is shown in Figure 4.42. It can be seen that the viscosity decreased with increasing frequency or shear rate (i.e., shear-thinning behavior). Furthermore, at a given frequency or shear rate, the 50/50 NR/EVA blend without compatibilizer showed lower complex viscosity than the ones with compatibilizer. This is the result of a lower compatibility and interfacial interaction between the phases. Among four types of compatibilizers (i.e., NR-*g*-PDMMMP, NR-*g*-PDMMEP, NR-*g*-PDMAMP, and ENR-30), it can be seen that the blend incorporating ENR-30 gave the lowest complex viscosity while NR-*g*-PDMAMP, NR-*g*-PDMMMP, and NR-*g*-PDMMEP, respectively, gave similar values, that is the highest complex viscosity. This result can be explained by the presence of various types of structure (polar and non-polar) in the graft copolymer compatibilizer that can interact with the other ones present in each of the two components of the blend by forming physical interactions (i.e., Van der Waals and dipole-dipole interactions). Indeed, NR-*g*-PDMMMP, NR-*g*-PDMMEP, and

NR-*g*-PDMAMP macromolecules have polar grafts due to the presence of carbonyl and phosphonyl groups, and a non-polar polyisoprene backbone. Furthermore, long chain grafts make more effective entanglement with the EVA matrix. While the NR backbone of graft copolymer is capable to compatibilize with the NR component in the blend NR/EVA. The physical interactions of the graft copolymer macromolecules simultaneously with the two blend components cause higher strength of the blend. As a result, the complex viscosity of the blends was increased. Comparing among graft copolymers, i.e., NR-*g*-PDMAMP, NR-*g*-PDMMEP, and NR-*g*-PDMAMP, it is clear that no difference was noted concerning complex viscosity. This result may be attributed to the fact that the structural characteristics of the considered copolymers are near: grafts with same polar functional groups (i.e., carbonyl and phosphonyl) and same average length. On the other hand, the influence of ENR-30 on NR/EVA blend compatibility was very low, in spite of the presence of oxirane rings along ENR chains that was supposed interact with the acetate groups of the EVA phase. Therefore, the order of the complex viscosity can be ranked as follows: blend without compatibilizer < blend with ENR-30 < blend with NR-*g*-PDMAMP, or NR-*g*-PDMMEP, or NR-*g*-PDMAMP.

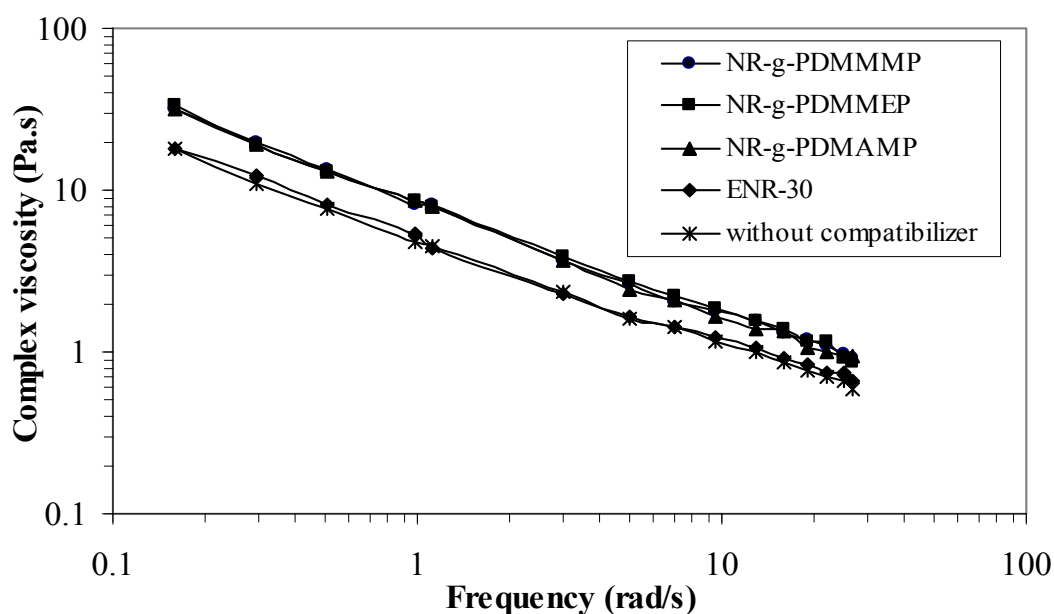


Figure 4.41 Complex viscosity as a function of frequency of 50/50 NR/EVA blends with various types of blend compatibilizers.

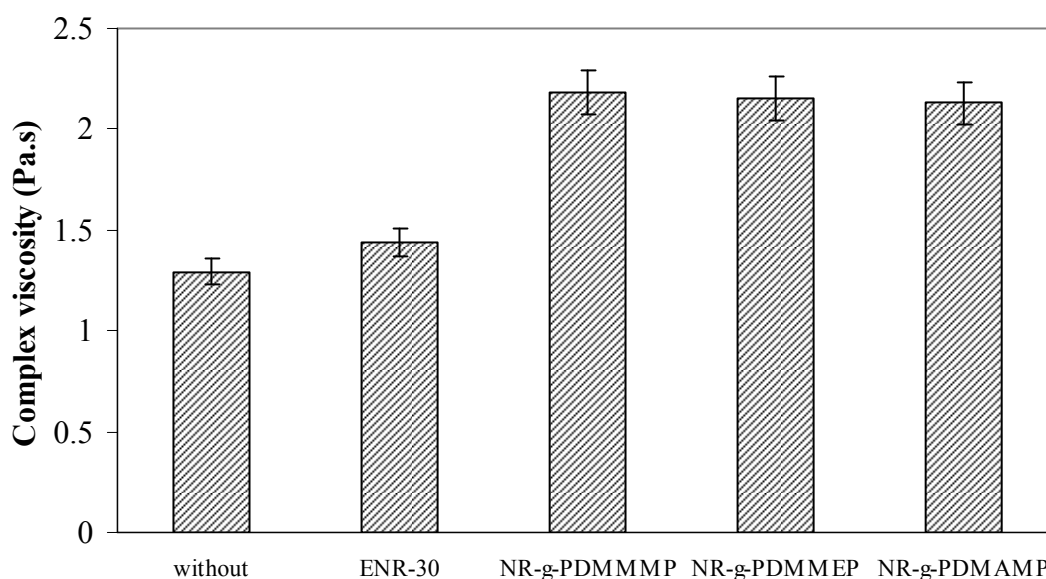


Figure 4.42 Complex viscosity at a constant frequency of 6 rad/s of 50/50 NR/EVA blends with various types of blend compatibilizers.

4.4.2 Dynamic and morphological properties

Figure 4.43 shows the storage modulus (G') of 50/50 NR/EVA blend compatibilized with various types of blend compatibilizers, as a function of frequency. It can be seen that all the blends show an increase in storage modulus with increasing frequency. This is the effect of the decrease in time available for molecular relaxation. At a given frequency of 6 rad/s (Figure 4.44), it is seen that the storage modulus value of the 50/50 NR/EVA blend with the compatibilizer is higher than the one noted without the compatibilizer. Comparing among the four types of blend compatibilizers tested, it is seen that the blends with the graft copolymers, i.e. NR-g-PDMMMP, NR-g-PDMMEP, or NR-g-PDMAMP, showed the highest and similar values of storage modulus while the blend with ENR-30 showed the lowest value that is similar to the one of the blend without compatibilizer. The trend of the storage modulus correlated well with the phase size of the blends, as shown by the SEM micrographs given in Figure 4.45. It can be seen that the blends with NR-g-PDMMMP, NR-g-PDMMEP, or NR-g-PDMAMP compatibilizer, exhibited phases of smaller size and more uniformly dispersed. On

the other hand, the blend with ENR-30 and without compatibilizer revealed larger phase size than that of the blends incorporating the graft copolymer (i.e., NR-g-PDMMMP, NR-g-PDMMEP, or NR-g-PDMAMP). This can be attributed to different effectiveness of interactions, on one hand between the dimethylphosphonate and methacryloyl groups of the polar dimethylphosphonate-functionalized polymer grafts with the acetate groups of EVA blend component, and on the other hand of the non-polar NR backbone of the graft copolymer with the NR blend component. This leads to an entanglement of graft chains with EVA parts and of NR backbone with NR parts, and have as consequence a better mixing of the two blend components. The non-compatibilizing effect of ENR-30 may be probably explained by the low content of oxirane rings along the rubber chains but also by a statistic repartition of these functions on the rubber chains. As a result, NR-g-PDMMMP, NR-g-PDMMEP, and NR-g-PDMAMP exhibited a superior compatibilizing efficiency to 50/50 NR/EVA blends.

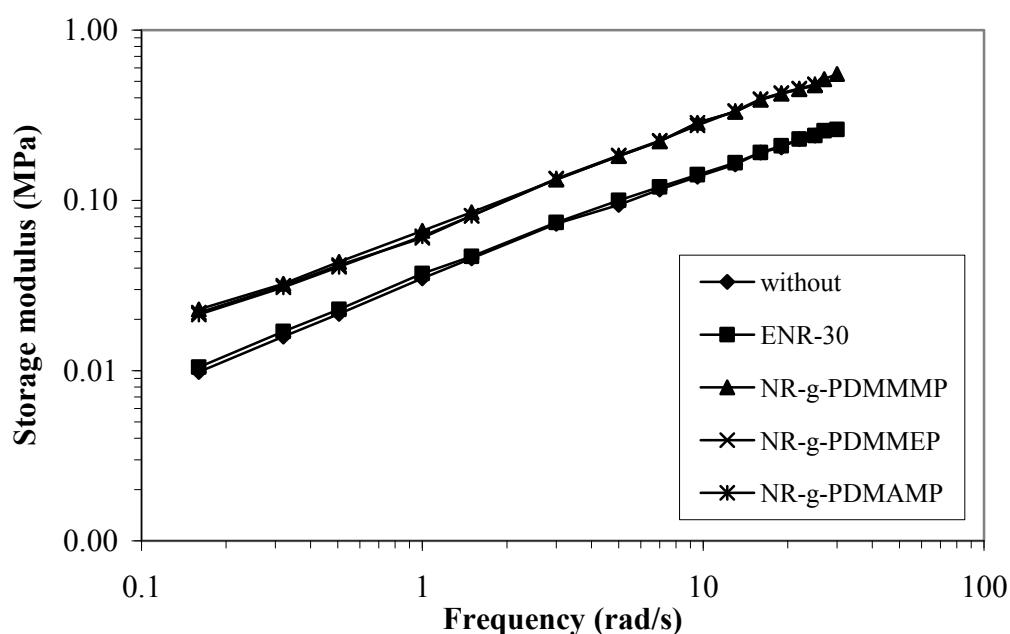


Figure 4.43 Storage modulus as a function of frequency of 50/50 NR/EVA blends with various types of blend compatibilizers.

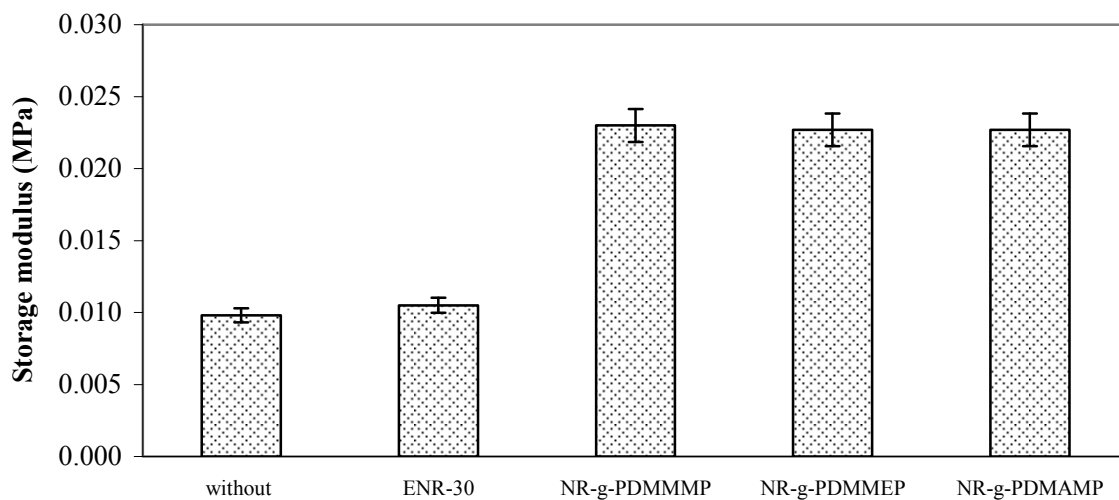
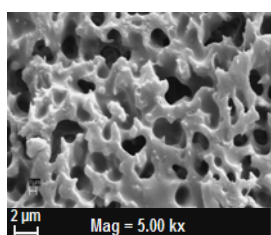
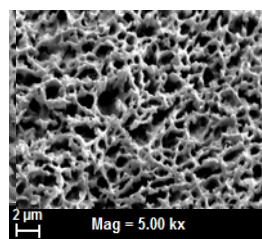


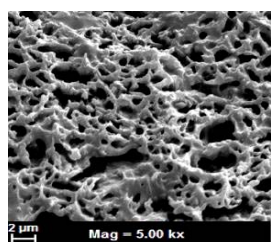
Figure 4.44 Storage modulus at a constant frequency of 0.16 rad/s of 50/50 NR/EVA blends with various types of blend compatibilizers.



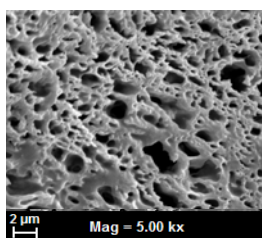
(a) without compatibilizer



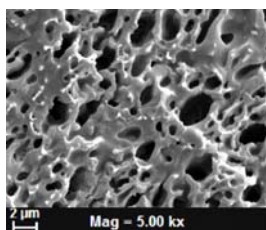
(b) NR-g-PDMMMP



(c) NR-g-PDMMEP



(d) NR-g-PDMAMP



(e) ENR-30

Figure 4.45 SEM micrographs of 50/50 NR/EVA blends with four types of blend compatibilizers: (a) without compatibilizers, (b) NR-g-PDMMMP, (c) NR-g-PDMMEP, (d) NR-g-PDMAMP and (e) ENR-30.

Figure 4.46 shows $\tan \delta$, which is the ratio between loss modulus to the storage modulus or the ratio of viscous to elastic properties ($\tan \delta = G''/G'$). It is seen that the blends with the graft copolymer compatibilizers exhibited higher elastic response with lower value of $\tan \delta$ than the blend without compatibilizer and with ENR-30. This is because higher interaction and increasing interfacial adhesion between rubber and EVA phases. As a result, the blends with the graft copolymers exhibited higher elastic response and lower value of $\tan \delta$. The order of $\tan \delta$ at a given frequency can be ranked as follow: the blend without compatibilizer > the blend with ENR-30 > the blend with NR-g-PDMMMP, NR-g-PDMMEP or NR-g-PDMAMP.

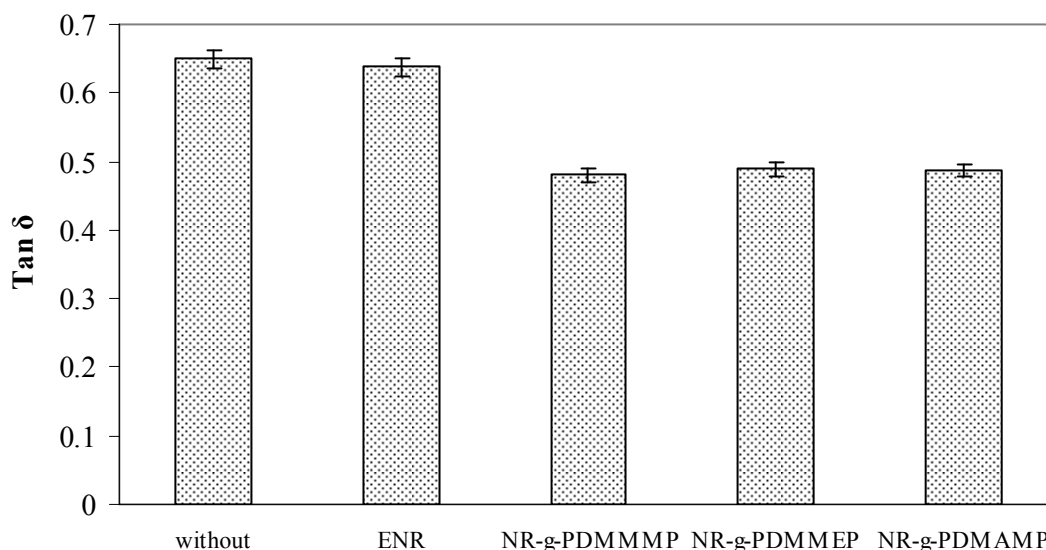


Figure 4.46 $\tan \delta$ at a constant frequency of 0.16 rad/s of 50/50 NR/EVA blends with four types of blend compatibilizers.

4.4.3 Mechanical properties

The stress-strain curves of 50/50 NR/EVA blends with the four types of blend compatibilizers are given in Figure 4.47. It can be seen that the blends compatibilized with NR-g-PDMMMP, NR-g-PDMMEP or NR-g-PDMAMP show similar values of the initial slope at the beginning of the curves. This reflects the similar value of an initial modulus and, hence, stiffness of the material. In

consideration of the area under the curve for toughness, the blend without compatibilizer shows the lowest value. The order of the toughness can be ranked as follows: blends with NR-g-PDMMMP, NR-g-PDMMEP or NR-g-PDMAMP > blend with ENR-30 > blend without compatibilizer. Mechanical properties in term of tensile strength and elongation at break based on the stress–strain curves are summarized in Table 4.11.

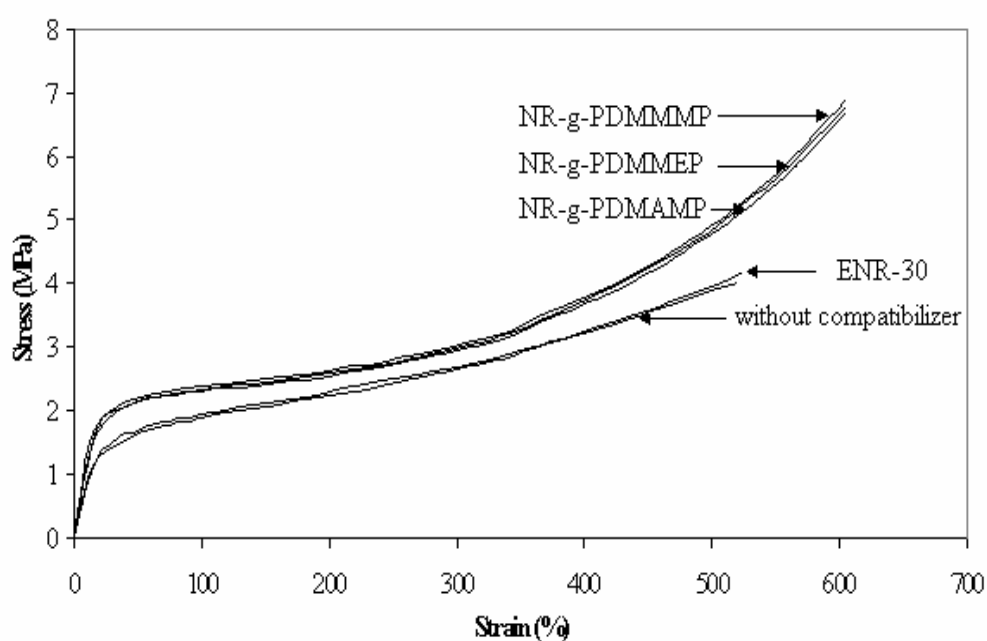


Figure 4.47 Stress-strain behaviours of 50/50 NR/EVA blends with various types of blend compatibilizers.

Table 4.11 Tensile and hardness properties of 50/50 NR/EVA blends without and with various types of blend compatibilizers.

Compatibilizer	Tensile strength (MPa)	Elongation at break (%)	Tension set (%)	Hardness (Shore A)
Without	3.80	520	57	55
ENR-30	4.17	524	55	56
NR- <i>g</i> -PDMMMP	6.89	605	48	56
NR- <i>g</i> -PDMMEP	6.78	605	48	56
NR- <i>g</i> -PDMAMP	6.69	605	49	56

The results in Table 4.11 show that incorporation of blend compatibilizers increased the tensile strength, elongation at break, and slightly hardness. Also, the blends with compatibilizers show tendency to recover from prolonged extension (i.e., lower tension set value). This reveals high elastomeric properties which correspond to the $\tan \delta$ value in Figure 4.46. Therefore, the compatibilizers enhance strength, toughness, and set properties of the NR/EVA blends. Among the four types of compatibilizers used, the mechanical, hardness, and tension set properties of 50/50 NR/EVA blends incorporating the graft copolymers, i.e., NR-*g*-PDMMMP, NR-*g*-PDMMEP, or NR-*g*-PDMAMP, are superior to that of the blend prepared with ENR-30. This is attributed to the compatibilizer macromolecules are capable of linking between the NR and EVA macromolecules with the respective blend components. That is, the non-polar part (NR) of graft copolymer is wetted by the NR phase, while the polar functional groups (i.e., dimethylphosphonate groups and methacrylate (or acrylate) groups) of graft segments in the graft copolymers could interact with polar functional groups (i.e., acetate group) or probably form physical interaction with EVA phase. Also, the

chain entanglement of graft segments in the EVA phase is also possible. This is the reason why the blends with graft copolymers exhibited superior mechanical, hardness, and set properties than the blend without compatibilizer or with ENR-30.

Because its efficiency to compatibilize the 50/50 NR/EVA blends was noted slightly better compared to that of the other compatibilizers tested, and also due to the fact that its preparation is easier and cheaper, NR-g-PDMMMP was finally chosen for the continuation of the studies.

4.5 Effect of grafting rate of NR-g-PDMMMP on properties of NR/EVA blend.

The study was performed with the 50/50 NR/EVA blend using NR-g-PDMMMPs with varied grafting rates, i.e., 71, 80, 89, and 95 %, respectively. Various important properties were studied as follows:

4.5.1 Rheological properties

The relationship between complex viscosity and oscillating frequency of 50:50 NR/EVA blends compatibilized with NR-g-PDMMMPs of various grafting rates, i.e., 71, 80, 89, and 95 %, respectively, at a loading level of 7 wt% is shown in Figure 4.48. It was seen a decreasing trend of complex viscosity with an increase in frequency. This indicates shear-thinning behavior. At a given frequency of 0.16 rad/s (Figure 4.49), the complex viscosity of NR/EVA blend compatibilized with **NR-g-PDMMMP 80%** shows the highest value. This shows a maximum compatibilizing effect when the grafting rate of the graft copolymer is equal to 80 %, which corresponds to the highest physical interactions between the graft copolymer and the NR and EVA phases. Increasing grafting rate from 80 % to 95 % as well as decreasing grafting rate from 80 % to 71 % caused decreasing trend of the complex viscosity. Increasing grafting rate higher than 80 % was less effective to strengthen the interface due to lower diffusion capability of the graft copolymer to reach to the interface. On the other hand, decreasing grafting rate lower than 80 % caused limitation of the physical interactions at the interface.

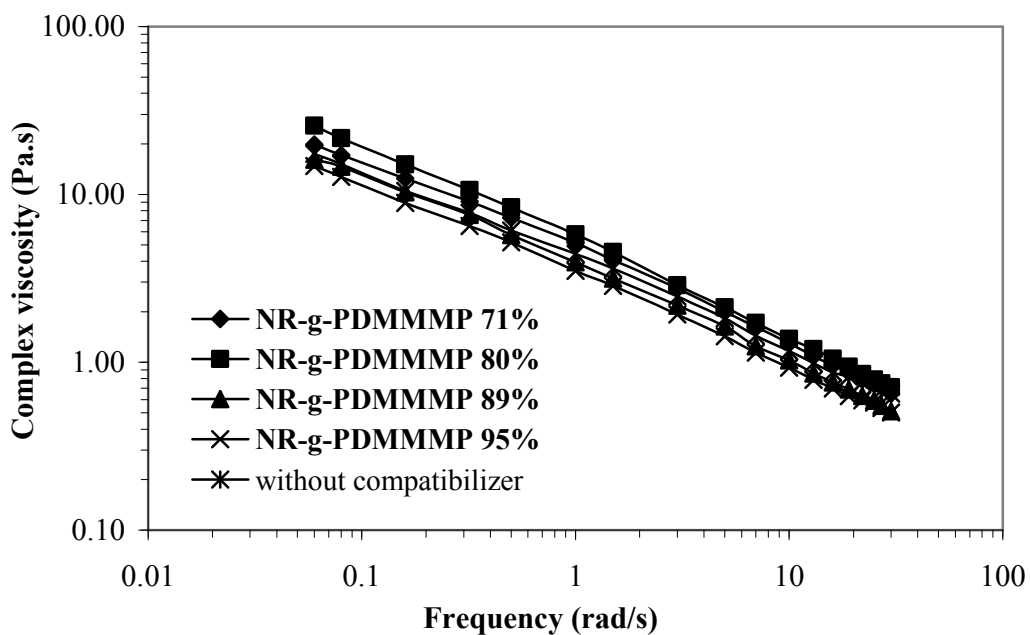


Figure 4.48 Complex viscosity as a function of frequency of 50/50 NR/EVA blends with NR-g-PDMMMP compatibilizer with various grafting rates of 71, 80, 89 and 95 %.

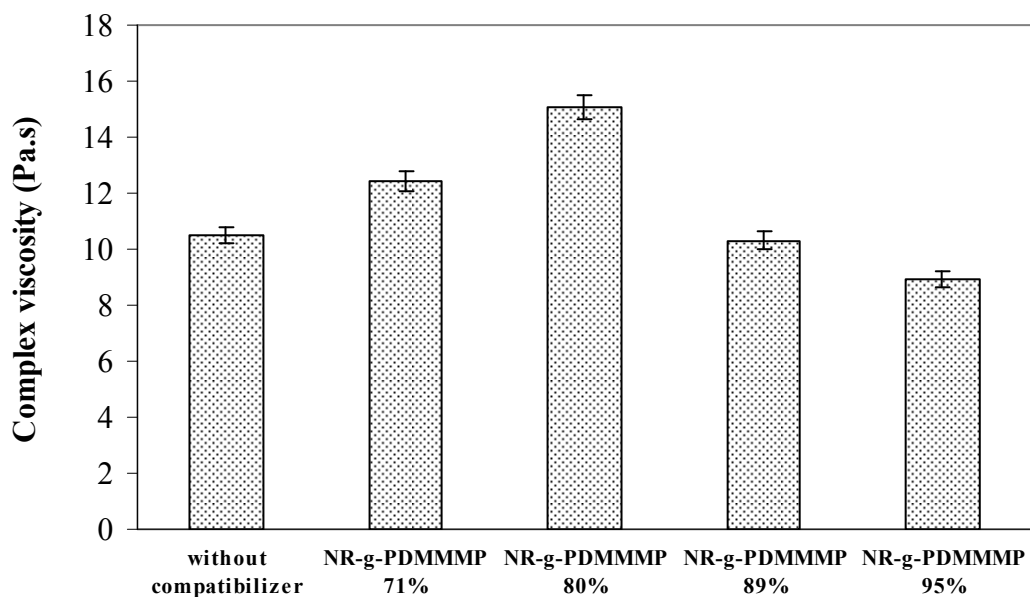


Figure 4.49 Complex viscosity at a constant frequency of 0.16 rad/s of 50/50 NR/EVA blends with NR-g-PDMMMP compatibilizer with various grafting rates of 71, 80, 89 and 95 %.

In this case of the brush-typed NR-g-PDMMMP graft copolymer, it could promote polar interactions with EVA macromolecules and could be miscible with NR component by its non-polar segments during the melt-mixing. Also, the interdiffusion between neighboring polymer chains resulted in the entanglement of polymer chains and hence bonding between phases. This observation suggests that the hydrophilic PDMMMP grafts in NR-g-PDMMMP interact well with the EVA phase while the hydrophobic NR backbone chains could interact with the NR phase in the NR/EVA blend, as schematically described in Figure 4.50.

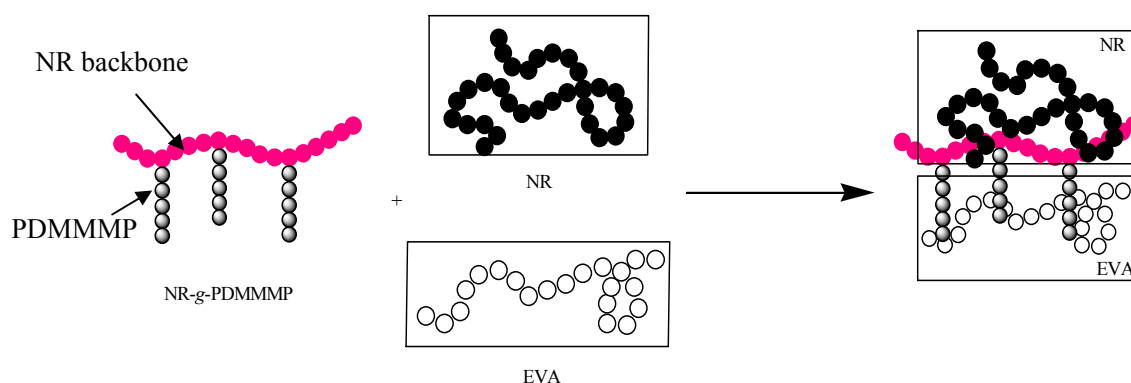


Figure 4.50 Schematic illustration of the physical interaction of the graft copolymer at interfaces.

4.5.2 Dynamic properties

The influence of grafting rates of NR-g-PDMMMP (i.e., 71, 80, 89, and 95 %) on the storage modulus of 50:50 NR/EVA blends at a loading level of NR-g-PDMMMP of 7 wt% is shown in Figures 4.51. It was seen that the storage modulus increased with the increase of NR-g-PDMMMP grafting rate until a optimum value obtained using **NR-g-PDMMMP 80%**, that is with the graft copolymer containing 80 % of PDMMMP grafts. Moreover, at a given frequency of 0.16 rad/s (Figure 4.52), the storage modulus increased also with the grafting rate and reached a maximum value observed at a NR-g-PDMMMP grafting rate of 80 %. Higher grafting rates of NR-g-PDMMMP (i.e., 89 and 95 %) caused a decrease of the storage modulus. The results correspond well with the trend of complex viscosity

shown in Figure 4.49. These results confirm that the highest interactions and adhesion forces between the phases in 50/50 NR/EVA blend are obtained with NR-g-PDMMMP having a grafting rate equal to 80 %.

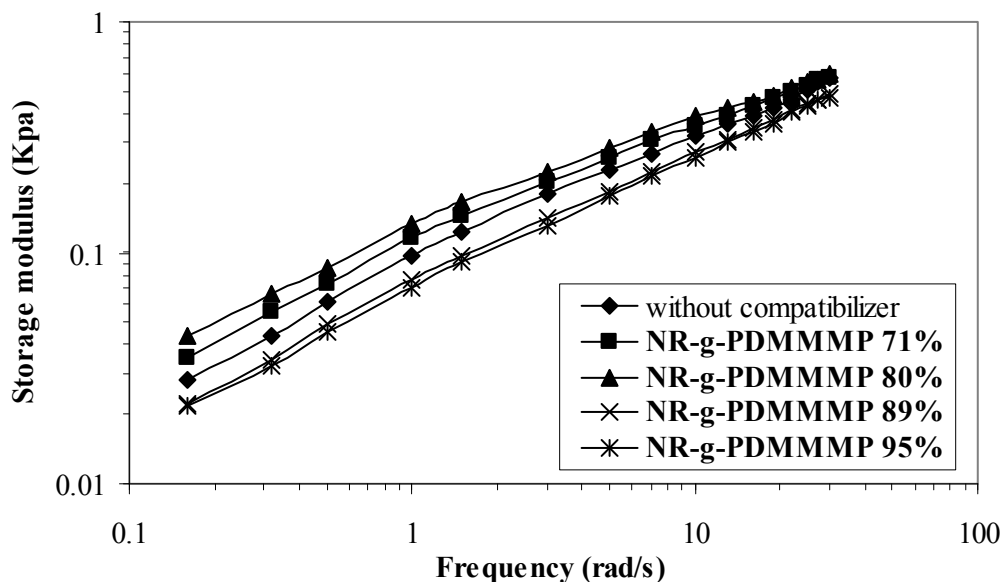


Figure 4.51 Storage modulus as a function of frequency of 50/50 NR/EVA blends with NR-g-PDMMMP compatibilizer with various grafting rates of 71, 80, 89 and 95 %.

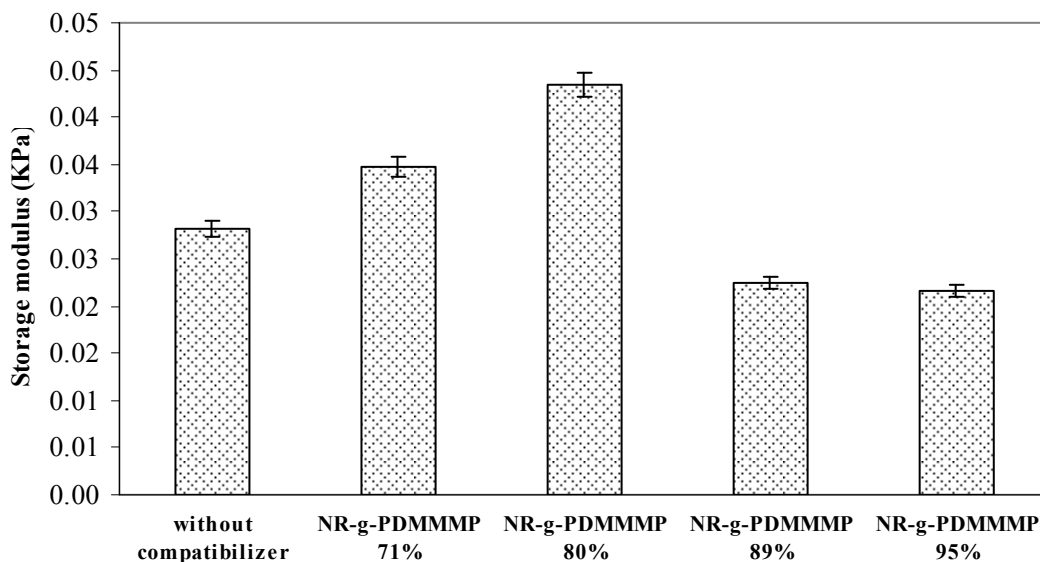


Figure 4.52 Storage modulus at a constant frequency of 0.16 rad/s of 50/50 NR/EVA blends with NR-g-PDMMMP compatibilizer with various grafting rates of 71, 80, 89 and 95 %.

Tan δ as a function of frequency is shown in Figures 4.53. It is seen that tan δ decreased when frequency increased. This is attributed to increasing elastic respond (G') of the material upon increasing of frequency. At a frequency of 0.16 rad/s (Figure 4.54), the lowest value of tan δ was observed with the blend incorporating **NR-g-PDMMMP 80%** at a loading level of 7 wt% of NR. In these conditions, the interactions between NR and EVA phases are optimum. Increasing or decreasing of grafting rates higher or lower than 80 % caused increasing trend of tan δ values, that is to say, a decrease of the elasticity of the blend. This can be attributed to different levels of interfacial forces depending on the degree of anchoring by the graft length and/or the grafting rate. When NR-g-PDMMMPs of grafting rates lower than 80 % (i.e., 71 %) are used, the interfacial forces are not high enough, and hence steric effect are low. The less compatibilizing effect of NR-g-PDMMMPs of grafting rates higher than 80 % (i.e., 89 and 95 %) is explained by its very low critical micelle concentration (Kunyawut, 2006). That is, the ability to immobilize the interface of graft copolymer at high grafting rate is less effective, owing to their higher viscosity. As a result, when 50/50 NR/EVA are compatibilized with NR-g-PDMMMPs of grafting rates higher than 80 %, micelles of graft copolymer are easily formed in the blend. In conclusion, it was shown that the elastic and viscous responds of NR/EVA blend greatly depended on the grafting rate of NR-g-PDMMMP used as compatibilizer, the best elastic and viscous responds being obtained with a NR-g-PDMMMP containing 80 wt% of PDMMMP grafts.

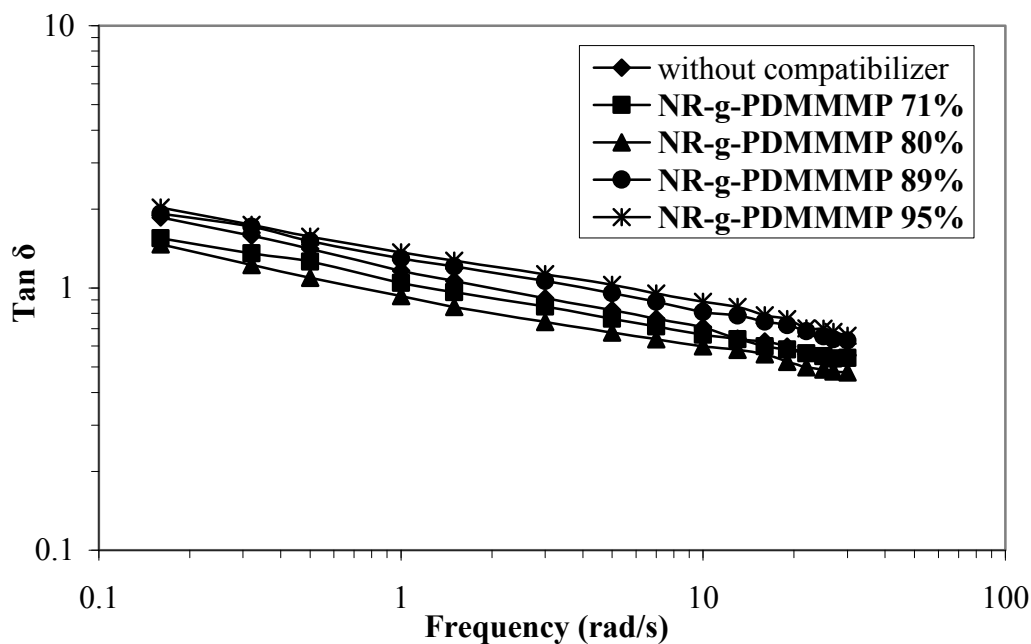


Figure 4.53 $\text{Tan } \delta$ as a function of frequency of 50/50 NR/EVA blends with NR-g-PDMMMP compatibilizer with various grafting rates of 71, 80, 89 and 95%.

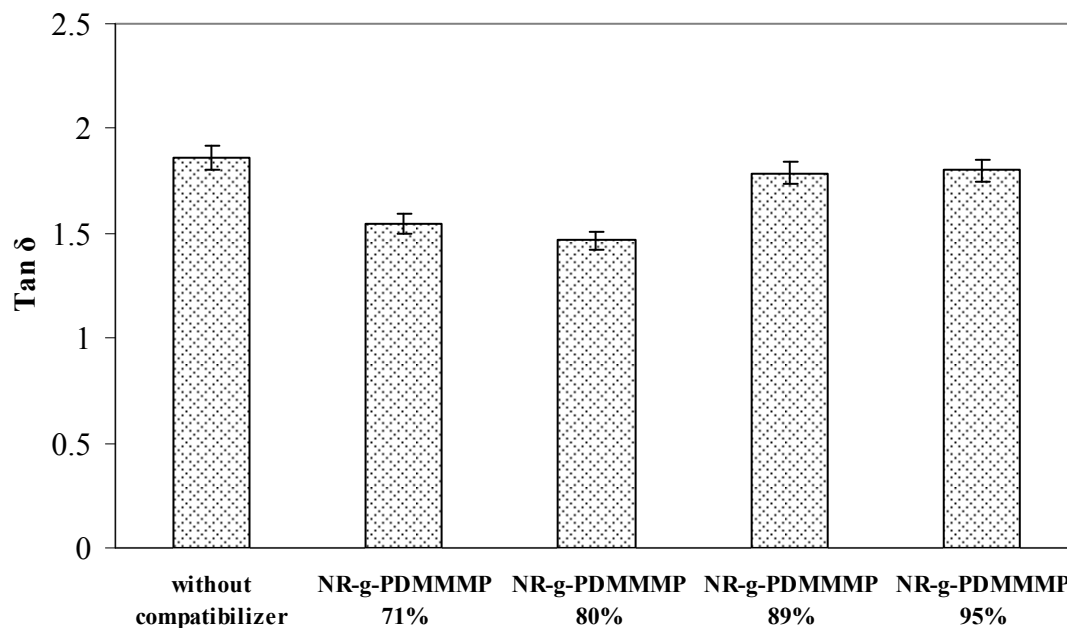


Figure 4.54 $\text{Tan } \delta$ at a constant frequency of 0.16 rad/s of 50/50 NR/EVA blends with NR-g-PDMMMP compatibilizer with various grafting rates of 71, 80, 89 and 95 %.

4.5.3 Mechanical properties

The stress-strain curves of 50:50 NR/EVA blends incorporating NR-g-PDMMMP compatibilizers of various grafting rates, i.e. 71, 80, 89, and 95 %, respectively, at a loading level of 7 wt% are given in Figure 4.55. It was noted that the deformation nature of the blend depended on the grafting rate (i.e., 71, 80, 89, or 95 %) of the NR-g-PDMMMP introduced as compatibilizer. The highest value of the modulus, calculated from the slope of initial linear elastic region, was observed with the NR-g-PDMMMP copolymer having a grafting rate of 80 %. Increasing and decreasing grafting rates higher or lower than 80 % caused decreasing of modulus. This correspond to the trend of complex viscosity (Figure 4.49) and storage modulus (Figure 4.52). In addition, toughness measurements were made by considering the area underneath the stress–strain curves of the blends. It was noted that the 50/50 NR/EVA blend compatibilized with **NR-g-PDMMMP 80%** showed the highest toughness value, with also the highest stress and strain at break.

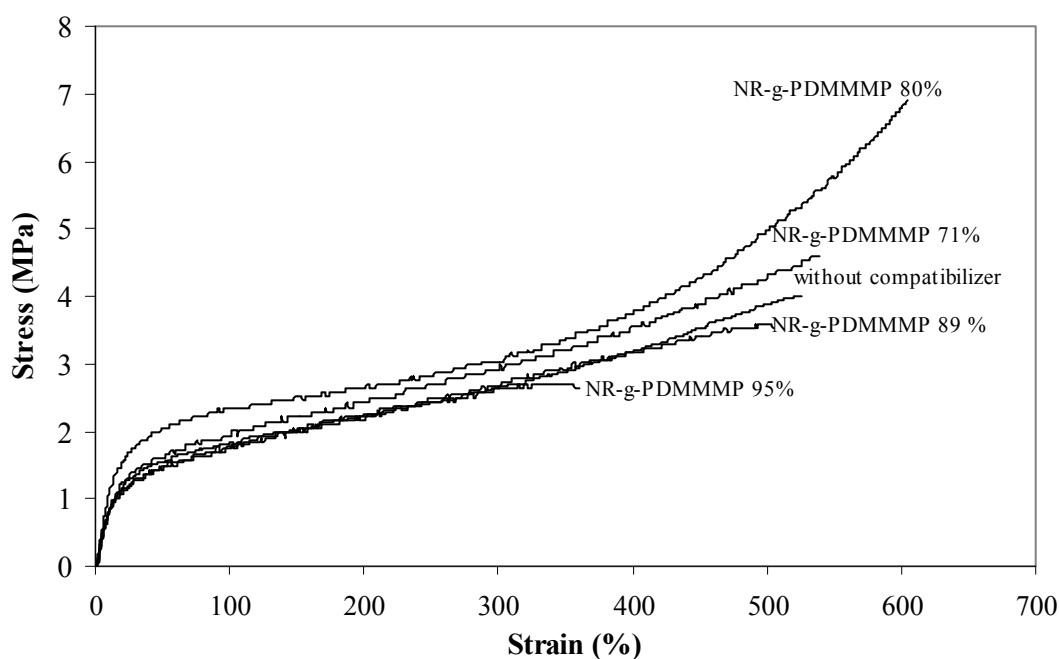


Figure 4.55 Stress-strain behaviours of 50/50 NR/EVA blends with NR-g-PDMMMP compatibilizer with various grafting rates of 71, 80, 89 and 95 %.

The stress and strain at a failure position (i.e., tensile strength and elongation at break) are shown in Figures 4.56 and 4.57, respectively. The tensile strength and elongation at break showed the same trend with the maximum values at 6.89 MPa and 605.25 %, respectively, for the blend compatibilized with **NR-g-PDMMMP 80%**. Increasing and decreasing grafting rate higher and lower than 80 % also caused a decreasing trend of tensile strength and elongation at break. Tension sets of various types of blends are shown in Figure 4.58. Comparing among four levels of grafting rates, the tension sets of the NR/EVA blends with NR-g-PDMMMP at the intermediate grafting rate of 80 % are superior (i.e., the lowest value) than those of the blends with other grafting rates. This suggests that the optimum amount of grafting content corresponds to optimum viscosity, storage modulus, and toughness of the blends. Higher grafting rate with increasing of graft density in graft copolymerization (i.e., **NR-g-PDMMMP 89 and 95 %**) caused lower chain mobility corresponding to higher viscosity and bulky segments. NR-g-PDMMMP 89% and 95 % exhibited lower capability to diffuse into dual phases. Furthermore, there were more possibilities of the graft copolymer to form micelles due to a lower critical micelle concentration (CMC) in the polymer with higher viscosity (i.e., high molecular weight) (Char *et al.*, 1993; Cigana *et al.*, 1997; Hong and Jo, 2000). This leads to the explanation that a lower amount of compatibilizer diffused to the interface and causes a lower compatibilizing effect. Even the diffusion is promoted by the mixing flow field, the long chains are proved to trap in the micelles (Kunyawut, 2006). On the other hand, NR-g-PDMMMPs with lower grafting rates exhibited low viscosity with lower chain entanglements needed to strengthen the interface. 50:50 NR/EVA compatibilized with **NR-g-PDMMMP 80%** showed the best over all performance due to the ability of the graft copolymer to reach the interface and to its relative effectiveness interactions with both phases. Therefore, an optimum level of grafting rate (i.e., 80 %) of the graft copolymer is preferable, especially with a short time scale of mixing process. Fast diffusion of the graft copolymer into a dual components is indeed crucial. This balances the ability of the graft copolymer to reach the interface and its relative effectiveness to function as a blend compatibilizer.

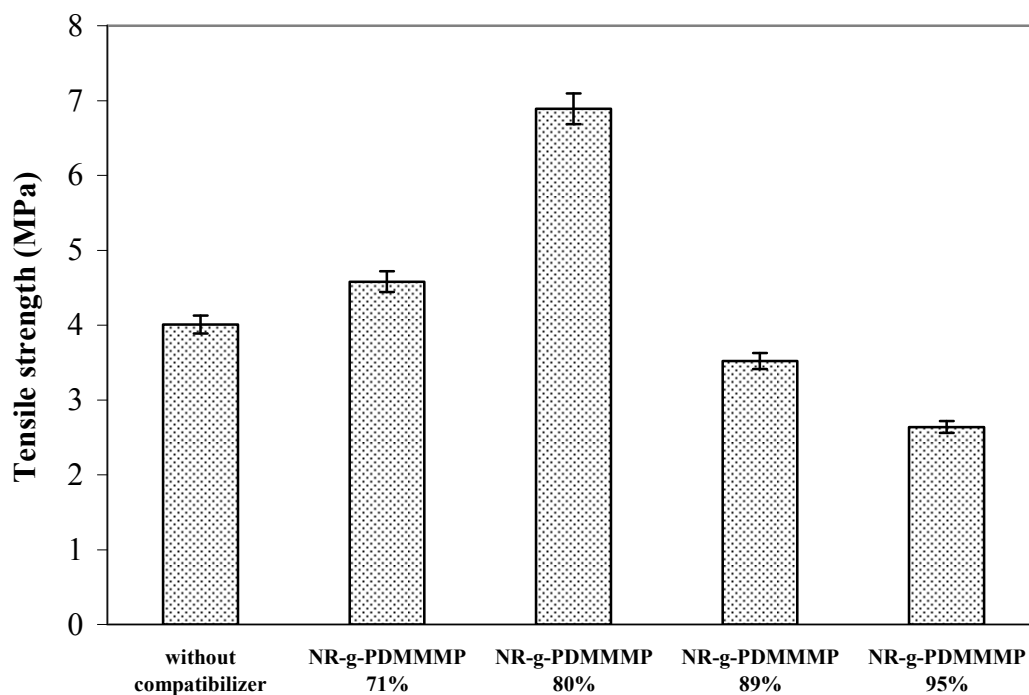


Figure 4.56 Tensile strength of 50/50 NR/EVA blends with NR-g-PDMMMP compatibilizer with various grafting rates of 71, 80, 89 and 95 %.

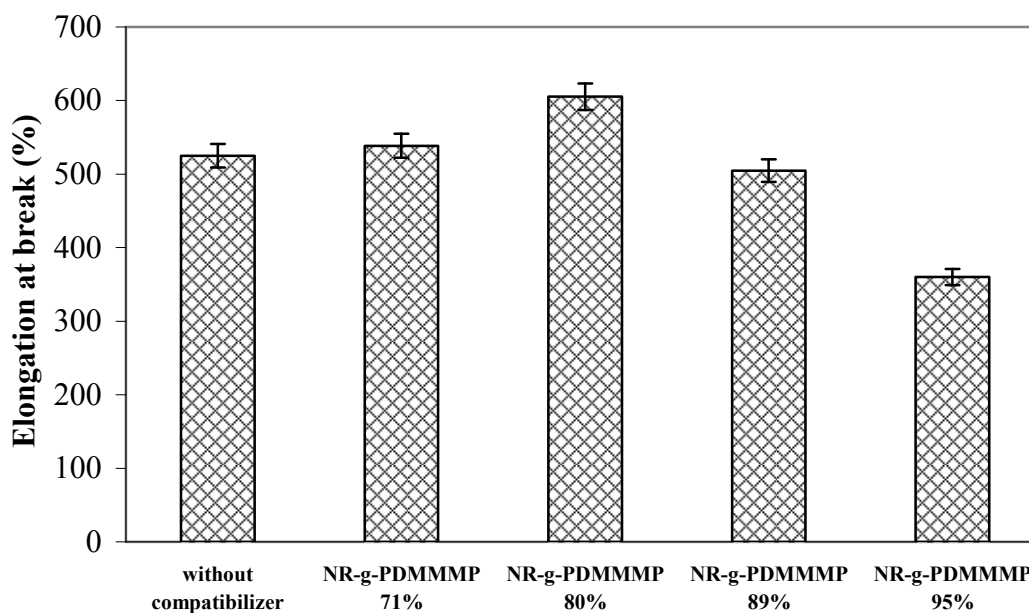


Figure 4.57 Elongation at break of 50/50 NR/EVA blends with NR-g-PDMMMP compatibilizer with various grafting rates of 71, 80, 89 and 95 %.

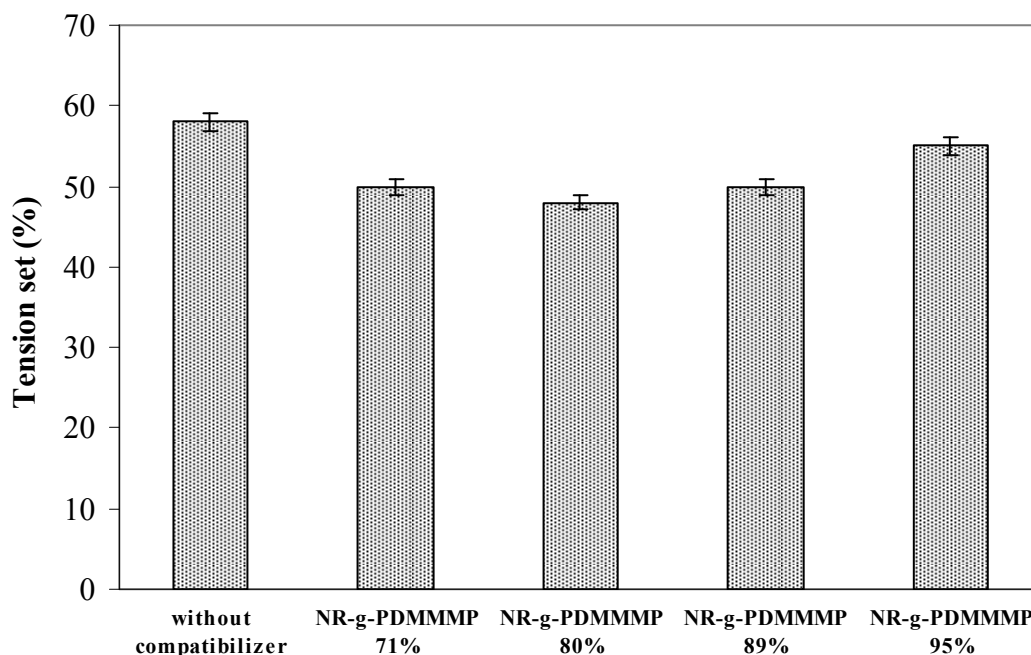


Figure 4.58 Tension set of 50/50 NR/EVA blends with NR-g-PDMMMP compatibilizer with various grafting rates of 71, 80, 89 and 95 %.

4.5.4 Solvent resistance

Solvent resistance of 50:50 NR/EVA blends without and with NR-g-PDMMMP with various grafting rates (i.e., 71, 80, 89, and 95 %) was studied. Rectangular specimens (10 x 10 x 2 mm) were immersed in IRM 903 oil (i.e., former ASTM Oil No.3) at room temperature for 168 hours. Afterwards, they were removed from the oil, wiped with a tissue paper to remove oil excess from the surface, and then weighed. The effect of NR-g-PDMMMP compatibilizer with various grafting rates on mass swell of IRM 903 oil in 50/50 NR/EVA blends is shown in Figure 4.59. It can be seen that an increasing oil resistance (or a decreasing degree of swelling) was observed when increasing grafting rates until 80 %. The oil resistance of the blend thereafter decreased when grafting rate increased. This is due to the fact that the interface becomes stronger as a result of the addition of compatibilizer at grafting rate of 80 %. Hence, lower free volume at the interface restricts oil molecules to enter and to be trapped.

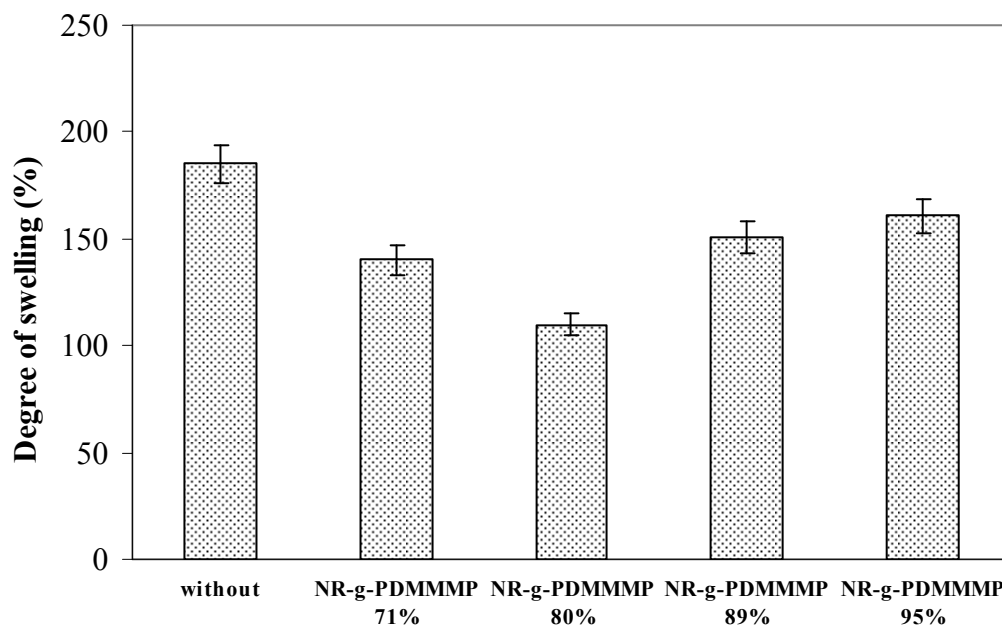


Figure 4.59 Degree of swelling of 50/50 NR/EVA blends with NR-g-PDMMMP compatibilizer with various grafting rates of 71, 80, 89 and 95 %.

4.5.5 Thermal stability

Thermogravimetric plots for NR, EVA, and their 50/50 blends incorporating NR-g-PDMMMP with various grafting rates at a loading level of 7 wt% are given in Figure 4.60, and thermal data are summarized in Table 4.12.

NR degrades in a single step at an onset temperature about 320°C with a weight loss 98.2 %. In the case of EVA, double degradation steps were observed. The first degradation step occurred at about 335°C related to the degradation of acetate groups. The second degradation step occurred at an onset temperature of 437°C and was completed at 512°C. It is assigned to the degradation of EVA polyethylene backbone that occurred at a temperature range higher than that of NR chains. With the 50/50 NR/EVA blend without NR-g-PDMMMP, double degradation steps were also observed.

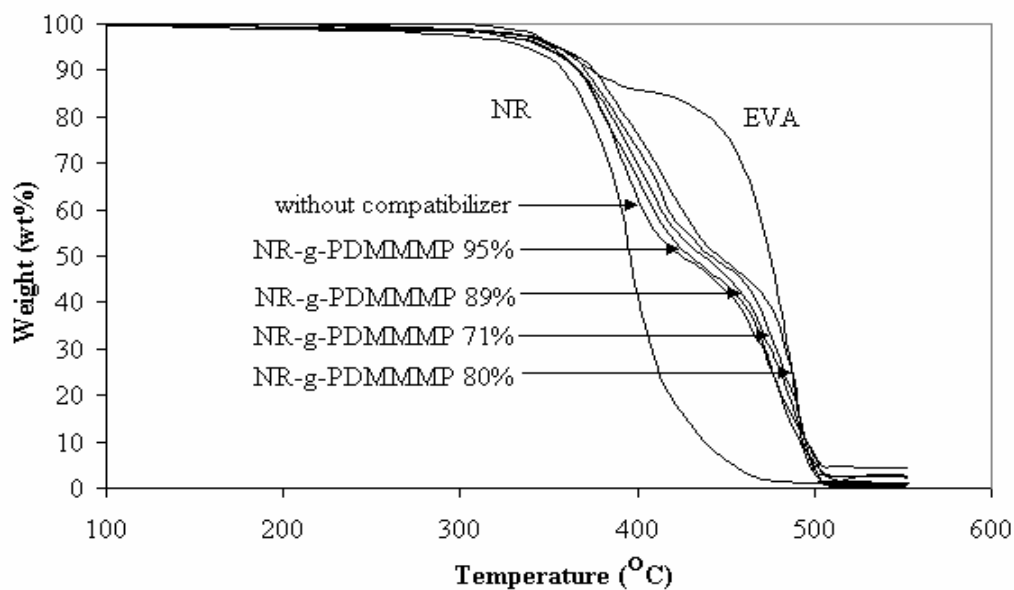


Figure 4.60 TGA curves under nitrogen atmosphere of 50/50 NR/EVA blends.

The first step started at 340°C is attributed to the degradation of NR phase. This onset temperature is higher than that observed in the pure NR. In addition, degradation temperature related to the acetate groups of the EVA backbone was not distinguished. It is probably overshadowed by the degradation of NR. Consequently, because the first onset temperature is higher than that of the pure NR, it can be postulated that EVA contributed to increase thermal stability of NR, as already suggested (Jansen and Soares, 1996). The second degradation step started at 432°C is attributed to the degradation of polyethylene segments in EVA with a total weight loss of 99.3 %.

In the case of 50/50 NR/EVA blends compatibilized with NR-g-PDMMMP, double degradation steps were also observed. However, a slightly shift of the onset degradation temperatures of NR and EVA phases toward higher temperatures was noted, by comparison with the onset temperatures of pure NR and EVA samples. In the case of the blend compatibilized with **NR-g-PDMMMP 71%**, that is the graft copolymer having a grafting rate of 71 %, the onset degradation temperature of the first and second steps were raised to 348.7°C and 459.0°C, respectively, with a total weight loss of 98.1 %. In that of the blend compatibilized with **NR-g-PDMMMP**

80%, the degradation temperature was increased to 350.6°C in the first step and 461.0°C in the second step, with a total weight loss of 97.7 %.

However, in the case of the blends compatibilized with NR-g-PDMMMPs having higher grafting rates (**NR-g-PDMMMP 89%** and **NR-g-PDMMMP 95%**), the degradation temperature was again slightly decreased to approximately 345.1°C to 346.0°C for the first step and 446.5°C to 458.0°C in the second step, with a total weight loss of 97.5 % and 96.3 %, respectively. Finally, the highest thermal stability (i.e. degradation temperature) was obtained with the blend compatibilized with **NR-g-PDMMMP 80%**. These results show that the addition of NR-g-PDMMMP compatibilizer in NR/EVA blend caused improvement of thermal stability of the blend, and also, that its thermal stability directly depends on the compatibilizing effect brought by the NR-g-PDMMMP compatibilizer. The reinforcement of the interfacial forces thank to the action of the graft copolymer in the NR/EVA blend contributes of the improvement of its thermal stability. All that shows that the interactions between the phases can play a major role in controlling the thermal stability of a blend.

Table 4.12 TGA characteristics under nitrogen atmosphere of NR, EVA, 50/50 NR/EVA blends without compatibilizer and with NR-g-PDMMMP containing various grafting rates (i.e., 71, 80, 89 and 95%) as a blend compatibilizer.

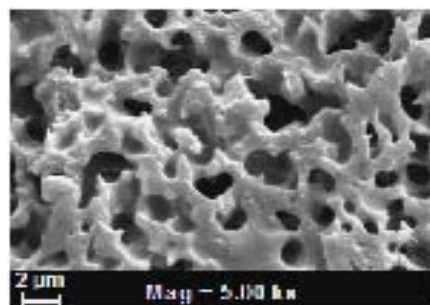
Sample	Onset temperature (°C)		Weight loss (%)		Char (%)
	1 st step	2 nd step	1 st step	2 nd step	
NR	320.0	-	98.2	-	1.8
EVA	335.0	437.0	17.8	82.1	0.1
NR/EVA without compatibilizer	340.0	432.0	49.6	49.7	0.7
NR/EVA+NR-g-PDMMMP 71 %	348.7	459.0	49.0	49.1	1.9
NR/EVA+NR-g-PDMMMP 80 %	350.6	461.0	48.7	49.0	2.3
NR/EVA+NR-g-PDMMMP 93 %	345.1	446.5	48.0	49.5	2.5
NR/EVA+NR-g-PDMMMP 95%	346.0	458.0	47.4	48.9	3.7

On the other hand, an increase of the amount of char formed at the end of the degradation of 50:50 NR/EVA blends compatibilized with NR-g-PDMMMP was observed with increasing the grafting rate of NR-g-PDMMMP. This is explained by the increase of dimethylphosphonate group content in the graft copolymer.

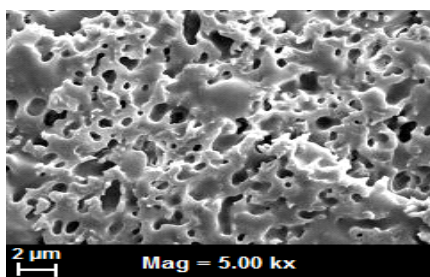
4.5.6 Morphological properties

Effect of graft copolymers of different grafting rates on the morphological characteristics of 50:50 NR/EVA blends is shown in Figure 4.61. It was seen that the analyzed blends exhibited two-phase system with a co-continuous phase morphology at this blend proportion. The black cavitations on the fracture surface correspond to the NR phase that was removed by solvent extraction. The NR/EVA blend compatibilized with **NR-g-PDMMMP 80%** showed smaller phase sizes compared with the blend without compatibilizer. However, the addition of NR-g-PDMMMP with grafting rates of 71, 89, and 95 % lead to lower level of interaction between the interface of the blends. This is revealed by larger phase sizes rather the blend and less uniform dispersion. Therefore, higher interfacial interactions at the interfaces are observed in the blend compatibilized with **NR-g-PDMMMP 80%** than those compatibilized with graft copolymers having higher grafting rates (i.e., **NR-g-PDMMMP 89%** and **NR-g-PDMMMP 95%**) or lower ones (i.e., **NR-g-PDMMMP 71%**). Because the blends compatibilized with NR-g-PDMMMPs having high grafting rates exhibited the highest Mooney viscosities (Figure 4.34), one can expect that a great part of the high viscous graft copolymer does not reach the interfacial area and thus forms micelles more readily in the blend than the low grafting rate or low viscosity ones. This evidence large cavitations in the blend with **NR-g-PDMMMP 89%** and **NR-g-PDMMMP 95%**. However, using NR-g-PDMMMPs with lower grafting rates (i.e., **NR-g-PDMMMP 71%**) also gives low compatibilizing effect. This can be due to the formation of chain entanglements (Galloway *et al.*, 2005) and also low physical interactions between the polar functional groups at the interface. These results are in good agreement with the rheological behavior of the blends in terms of complex viscosity (Figure 4.41) and their mechanical properties (Figure 4.47). According to these results, it is

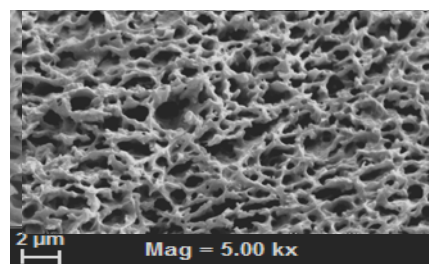
clear that the superior efficiency of **NR-g-PDMMMP 80%** to compatibilize NR/EVA blends was confirmed.



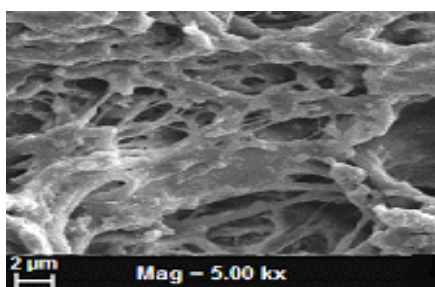
(a) without compatibilizer



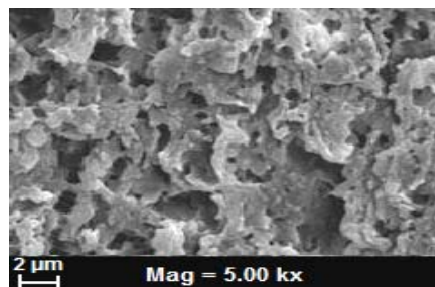
(b) NR-g-PDMMMP 71%



(c) NR-g-PDMMMP 80%



(d) NR-g-PDMMMP 89%



(e) NR-g-PDMMMP 95%

Figure 4.61 SEM micrographs of 50/50 NR/EVA blends with NR-g-PDMMMP compatibilizer with various grafting rates: (a) without compatibilizer, (b) NR-g-PDMMMP 71%, (c) NR-g-PDMMMP 80%, (d) NR-g-PDMMMP 89% and (e) NR-g-PDMMMP 95%.

4.6 Effect of concentration of graft copolymer

Taking into account the results dealing with the effect of the compatibilizer structure on the 50/50 NR/EVA blend was carried out using GR = 80%. It was carried out using a NR-g-PDMMMP copolymer containing 80 wt% of dimethylphosphonate-functionalized grafts (NR-g-PDMMMP 80%), and by considering different loading levels, i.e., 1, 3, 5, 7, 9, 12, and 15 wt%, respectively, by comparison with the NR component. The 50/50 NR/EVA blends incorporating various concentrations of NR-g-PDMMMP 80% were prepared by melt-mixing at 140°C using a rotor speed of 60 rpm, according to the preparation procedure described in section 3.3.2.2.3.

4.6.1 Rheological properties

NR/EVA blends with various concentrations of NR-g-PDMMMP compatibilizer showed pseudoplastic behaviour (Figure 4.62), that is evidenced by the decrease in complex viscosity when increasing oscillating frequency (i.e., shear rate). At a given frequency (i.e., 0.06, 0.08 and 0.16 rad/s) (Figure 4.63), the complex viscosity increased with loading levels of NR-g-PDMMMP 80% until 7 wt% where the maximum value was observed. Further increase of NR-g-PDMMMP higher than 7 wt% caused a decreasing trend of the complex viscosity. The formation of micelles at high concentration may be responsible for the decreasing trend of complex viscosity with the graft copolymer content greater than 7 wt%. It was also found that the complex viscosity of the 50/50 NR/EVA blends with NR-g-PDMMMP compatibilizer indicates positive deviation blends (PDBs) where the blend viscosities showed a synergistic effect, according to the following log additive rule: (Kundu *et al.*, 1996; Nakason *et al.*, 2006)

$$\log \eta_B = \sum_i w_i \log \eta_i \quad (4.2)$$

where η_i and η_B are the viscosity of the i component and that of the blend, respectively, and w_i is the weight fraction of the i component.

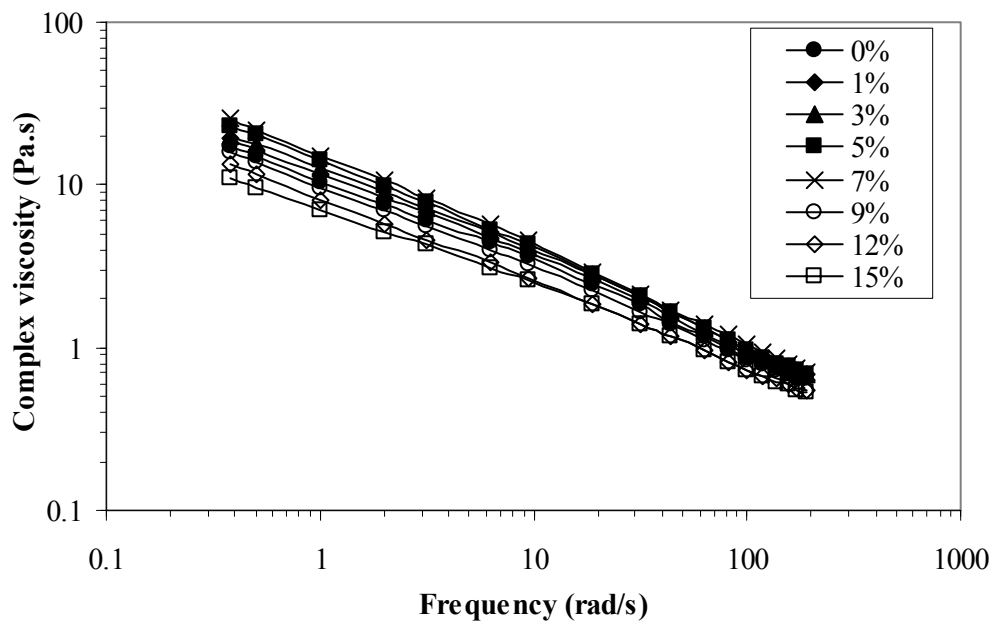


Figure 4.62 Complex viscosity as a function of frequency of 50/50 NR/EVA blends with various loading levels of NR-g-PDMMMP compatibilizer.

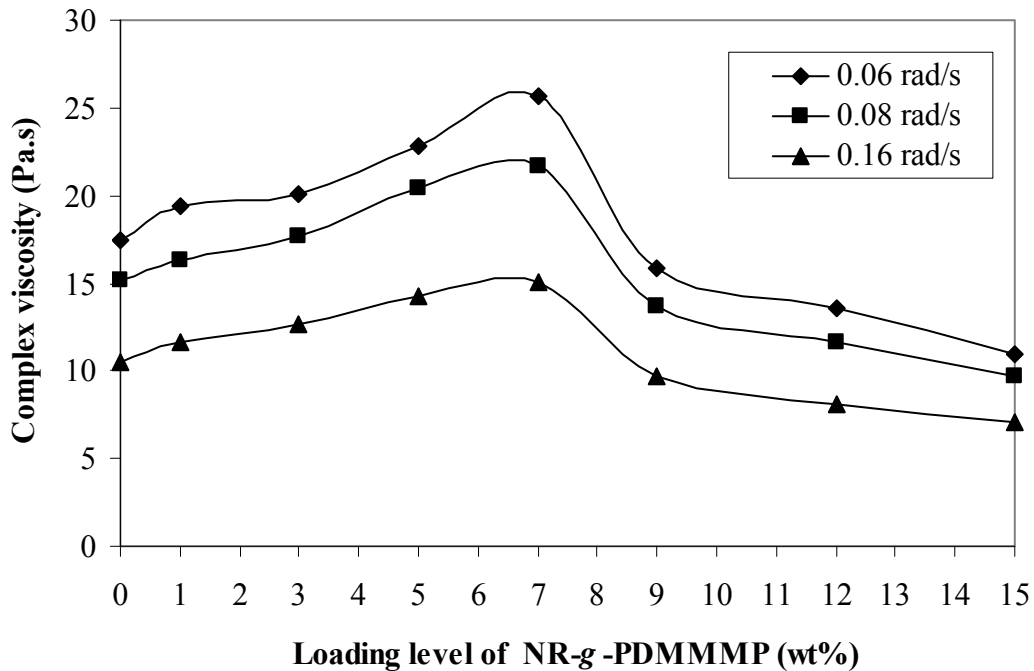


Figure 4.63 Complex viscosity at constant frequencies of 0.06, 0.08 and 0.16 rad/s of 50/50 NR/EVA blends with various loading levels of NR-g-PDMMMP compatibilizer.

During the melt blending, the compatibilizer was forced to locate at the interface between NR and EVA phases. The polar functional groups in NR-*g*-PDMMMP interact with polar functional groups of EVA while the NR backbone is capable of compatibilizing with the NR in the blend component. This leads to a decrease in interfacial tension and an improvement in interfacial adhesion. This causes an increasing trend of physical interactions between the distinct phases (i.e. NR and EVA). Therefore, the increasing trend of complex viscosity was observed. However, a decreasing trend of complex viscosity was observed after the compatibilizer loading of 7 wt%. This may be attributed to the formation of micelles at high concentration of NR-*g*-PDMMMP, as schematically shown in Figure 4.64. The micelles would act as lubricant in the blend system. Nakason *et al.*, (2006a) investigated the influence of PP-*g*-MA and Ph-PP as compatibilizer in 60/40 MNR/PP blends by using the log additive rule to predict the blend compatibility from apparent shear viscosity data. They found that the 60/40 MNR/PP blends with PP-*g*-MA and Ph-PP compatibilizers indicated positive deviation blends (PDB), and behaved as the partially compatible blends. Therefore, in this work, we anticipate that the NR/EVA blend with NR-*g*-PDMMMP as compatibilizer is also the partially compatible blends as evident by positive deviation blend characteristic.

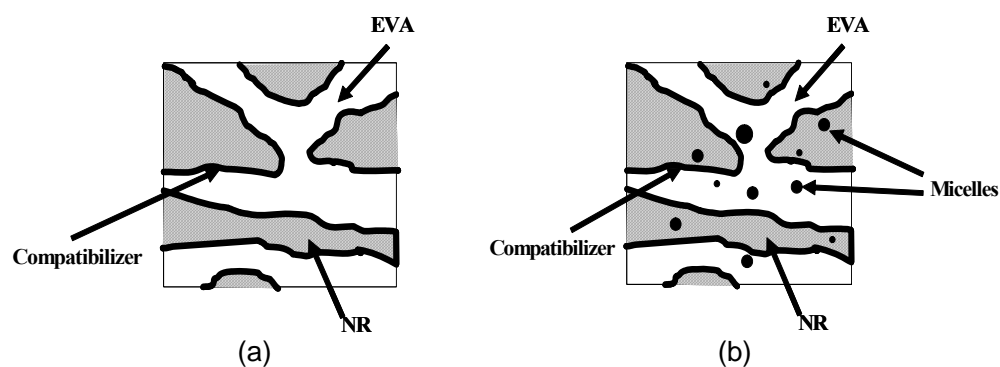


Figure 4.64 Schematic representation of the formation of micelles in 50/50 NR/EVA blend above the critical micelle concentration (CMC): (a) optimum level of blend compatibilizer and (b) concentration of blend compatibilizer higher than CMC.

4.6.2 Dynamic properties

Figures 4.65 and 4.66 depict the variation of storage modulus of 50/50 NR/EVA blends compatibilized with different loading levels of NR-*g*-PDMMMP at a grafting rate of 80% at different frequency. The incorporation of NR-*g*-PDMMMP compatibilizer in the NR/EVA blend causes an increasing trend of storage modulus until a loading level of 7 wt%. Beyond this concentration, a decreased is noted, which showed that the storage modulus of 50/50 NR/EVA blend reaches a maximum value when the NR-*g*-PDMMMP loading level is fixed to 7 wt%. Therefore, at this loading level of NR-*g*-PDMMMP, strong interactions between the phases occurred due to the ability of the graft copolymer to locate at the interface, which thereafter increases the adhesion at phase boundaries. In conclusion, by introducing 7 wt% of NR-*g*-PDMMMP 80% in the 50/50 NR/EVA blend, the compatibilizing effect is maximum. On the other hand, the decreasing trend of the storage modulus observed when loading levels are higher than 7 wt%, can be explained by the formation of micelles (Figure 4.64). The trend of the storage modulus is in good agreement with the complex viscosity (Figure 4.62).

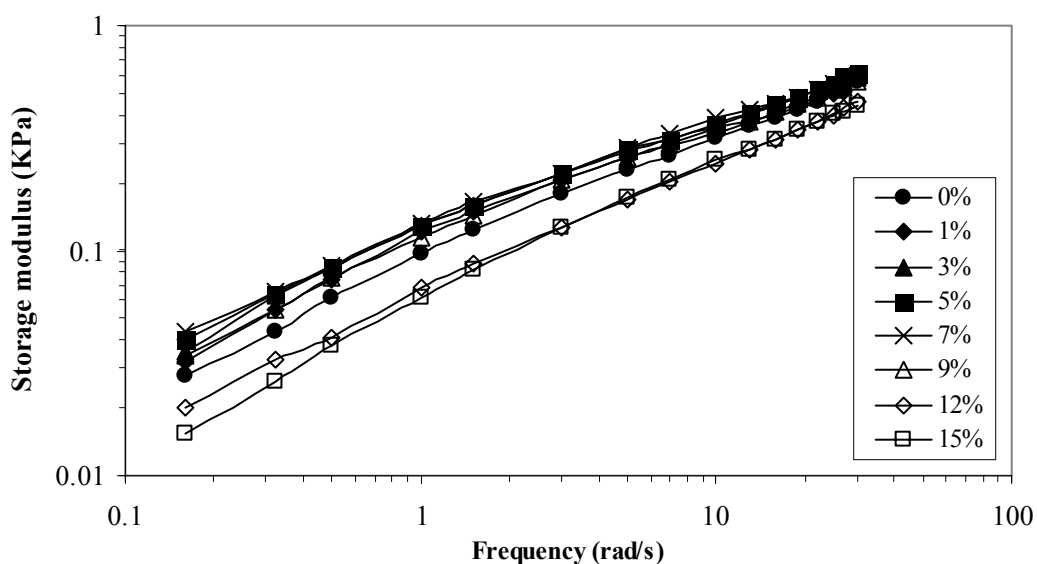


Figure 4.65 Storage modulus as a function of frequency of 50/50 NR/EVA blends with various loading levels of NR-*g*-PDMMMP compatibilizer.

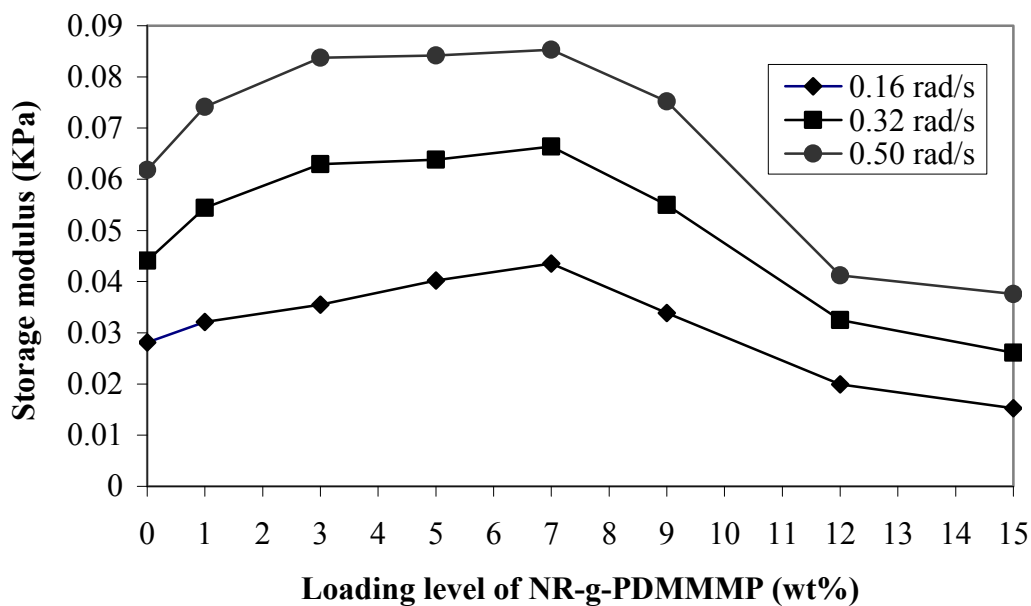


Figure 4.66 Storage modulus constant frequencies of 0.06, 0.08 and 0.16 rad/s of 50/50 NR/EVA blends with various loading levels of NR-g-PDMMMP compatibilizer.

Figure 4.67 and 4.68 show $\tan \delta$ of NR/EVA blend as a function of frequency and various loading levels of compatibilizer. It is seen that the $\tan \delta$ of the blend with 7 wt% of NR-g-PDMMMP showed the lowest value. Which indicated the highest elastic response. This is attributed to stronger interfacial force and hence a strong elasticity of the blend.

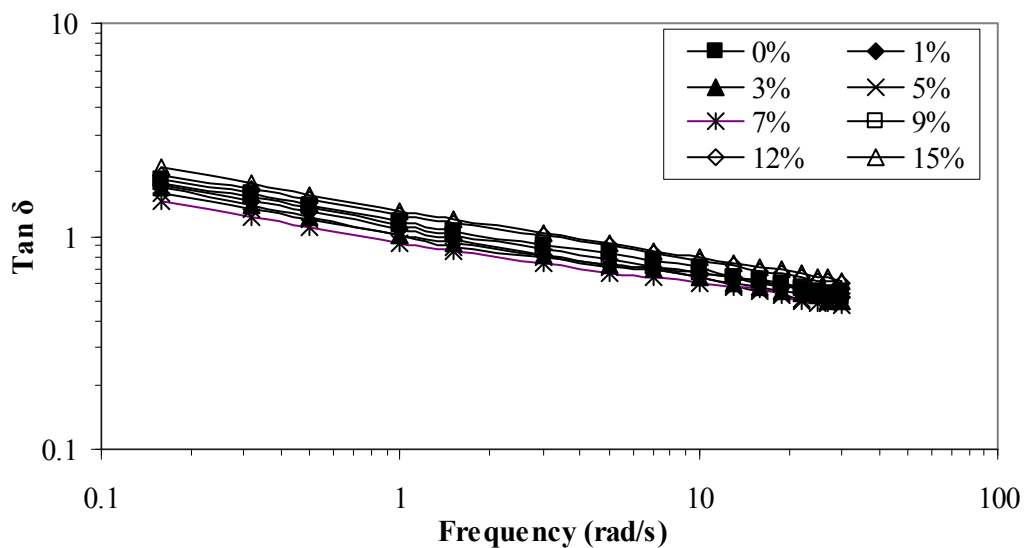


Figure 4.67 $\tan \delta$ as a function of frequency of 50/50 NR/EVA blends with various loading levels of NR-g-PDMMMP compatibilizer.

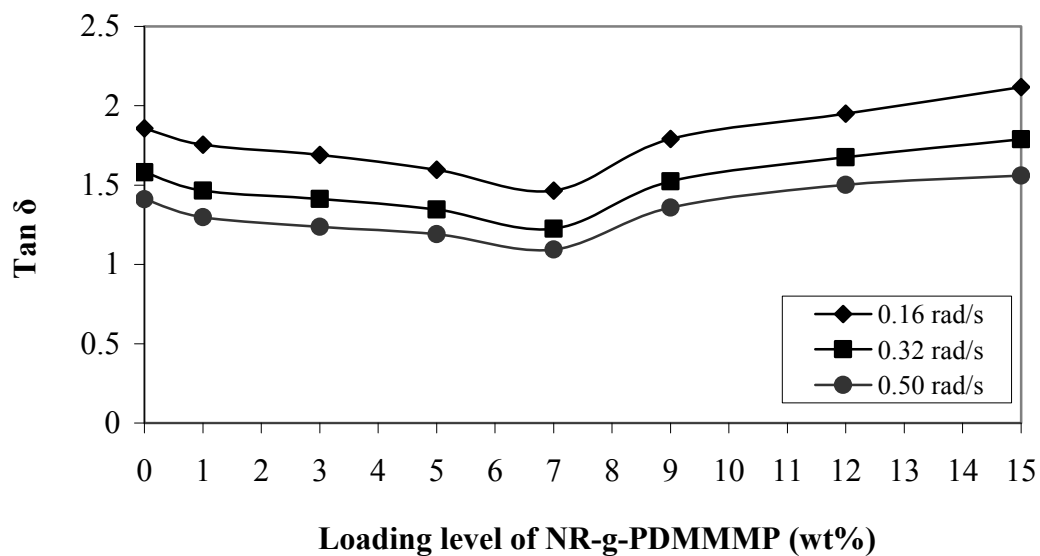


Figure 4.68 $\tan \delta$ at a constant frequencies of 0.06, 0.08 and 0.16 rad/s of 50/50 NR/EVA blends with various loading levels of NR-g-PDMMMP compatibilizer.

4.6.3 Mechanical properties

The stress-strain curves of 50/50 NR/EVA blends with various loading levels of **NR-g-PDMMMP 80%** compatibilizer are given in Figure 4.69. It was noted that the deformation characteristics of the blend are modified after incorporating the graft copolymer in the blend, that is the modulus (initial slope) and toughness of the materials increased with increasing loading level of the compatibilizer until a limit of 7 wt%. Beyond this concentration of NR-g-PDMMMP compatibilizer in the blend, decreasing of the toughness and modulus of the materials were noted. This is in agreement with the trend of tensile properties (Figure 4.70), that is the addition of the graft copolymer in the blend caused increasing of tensile strength and elongation at break until maximum values of 6.89 MPa and 605.25 %, respectively, observed for a blend incorporating 7 wt% of **NR-g-PDMMMP 80%** compatibilizer. For comparison, the values of tensile strength and elongation at break of the blend without compatibilizer were 3.80 MPa and 520 %, respectively. This result indicates an increase of physical interactions at the interface. Further addition of the compatibilizer caused a decreasing trend of tensile strength and elongation at break due to a saturation of the interface by the graft copolymer, that is majority of interfacial areas are occupied by the NR-g-PDMMMP macromolecules, and hence the excess amount of graft copolymer was capable to form a third phase in the blend (i.e., micelles) acting as lubricant and weak point under deformation.

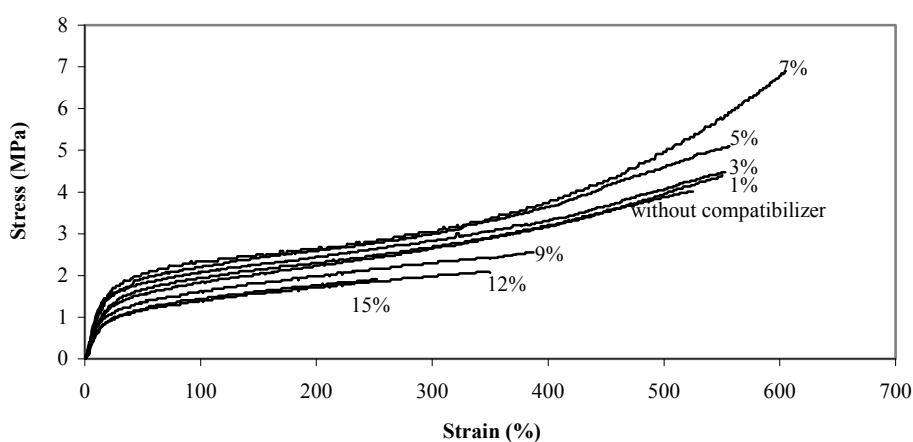


Figure 4.69 Stress-strain behaviours of 50/50 NR/EVA blends with various loading levels of NR-g-PDMMMP compatibilizer.

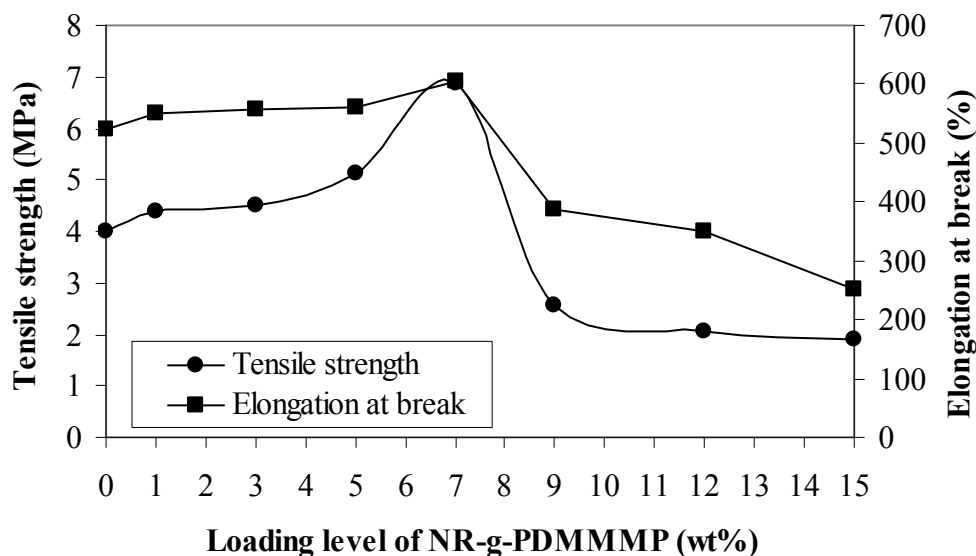


Figure 4.70 Tensile strength and elongation at break of 50/50 NR/EVA blends with various loading levels of NR-g-PDMMMP compatibilizer.

Figure 4.71 shows tension set of the 50/50 NR/EVA blends *versus* the loading level of NR-g-PDMMMP. It was seen that the lowest tension set property was also observed with the blend incorporating 7 wt% of NR-g-PDMMMP compatibilizer. This suggests a good occupation of the interface by the compatibilizer macromolecules. The lower tension set properties observed at loading levels of NR-g-PDMMMP lower than 7 wt% are explained by the fact that the interface is not fully occupied and covered by the compatibilizer, while the lower ones noted at compatibilizer concentrations higher than 7 wt% are explained by the formation of a third phase (i.e., micelles) which act as lubricant and weak point of stress concentration, as stated previously. The trend of tension set values at different loading levels of compatibilizer is rather similar to the trend of $\tan \delta$ (Figure 4.68).

All these results indicate that 50/50 NR/EVA blends incorporating 7 wt% of **NR-g-PDMMMP 80%** exhibits the best elastomeric properties.

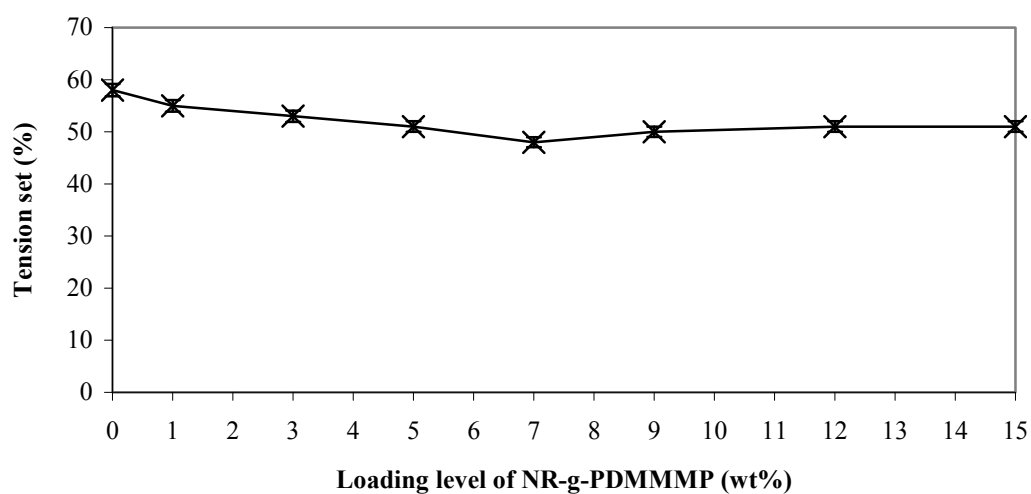
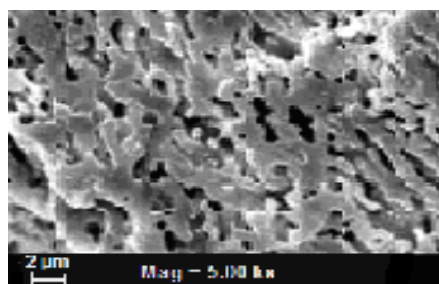


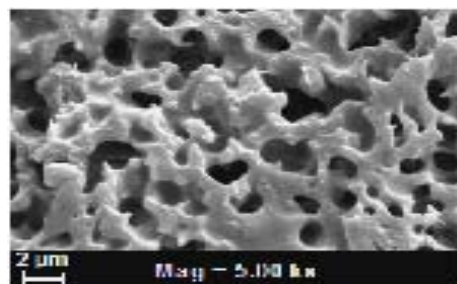
Figure 4.71 Tension set of 50/50 NR/EVA blends with various loading levels of NR-g-PDMMMP compatibilizer.

4.6.4 Morphological properties

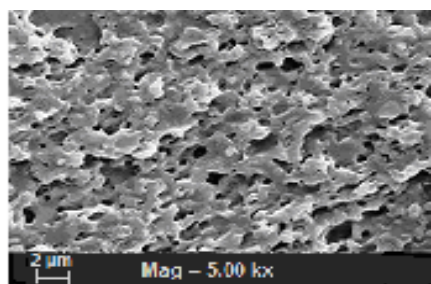
SEM micrographs of 50/50 NR/EVA blends with various loading levels of NR-g-PDMMMP are given in Figure 4.72. These SEM micrographs showed that all types of 50/50 NR/EVA exhibited co-continuous phase morphology where both EVA and NR behave as a continuous phase. On the photographs, the black areas or cavitations represent the NR phases that were previously removed by extraction using n-hexane. It is clear that the incorporation of the compatibilizer at 7 wt% loading level caused the smallest phase morphology due to the penetration of the graft copolymer chain segments into the corresponding adjacent phases. This resulted in an increase of the interfacial adhesion between the NR and EVA phases. Moreover, the graft copolymer contributed to suppress the coalescing of the NR phase, and hence to improve the stabilization the blend. On the other hand, using loading levels of graft copolymer higher than 7 wt% caused a slightly increase of the phase sizes in the blend. This may be attributed to the micelle formation because of excess amount of the graft copolymer, as stated previously. Therefore, the compatibilizer added into the blend system did not perform the task of blend compatibilizer at the interface.



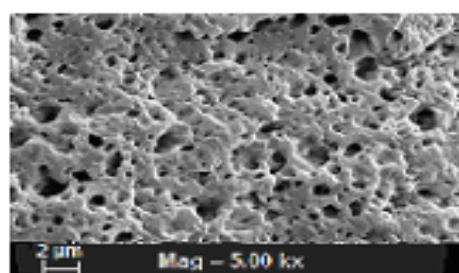
(a) without compatibilizer



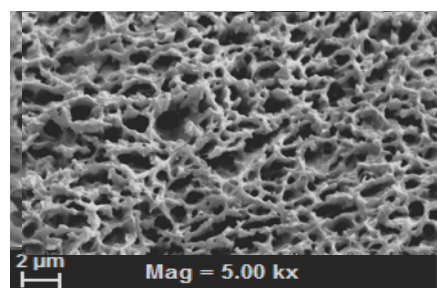
(b) NR-g-PDMMMP =1%



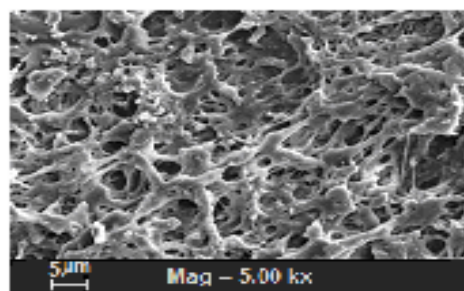
(c) NR-g-PDMMMP =3%



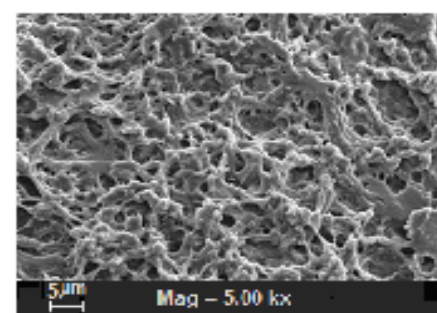
(d) NR-g-PDMMMP =5%



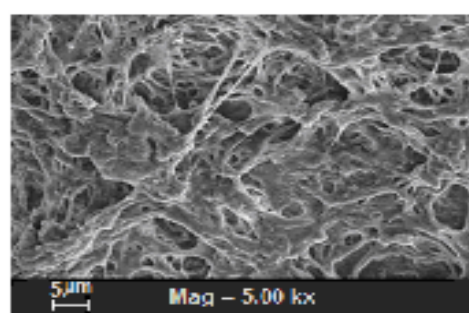
(e) NR-g-PDMMMP =7%



(f) NR-g-PDMMMP =9%



(g) NR-g-PDMMMP =12%



(h) NR-g-PDMMMP =15%

Figure 4.72 SEM micrographs of 50/50 NR/EVA blends with various loading levels of NR-g-PDMMMP compatibilizer : (a) without compatibilizer, (b) with 1%, (c) 3% , (d) 5%, (e) 7%, (f) 9%, (g) 12% and (h) 15% of NR-g-PDMMMP.

PART C

THERMOPLASTIC VULCANIZATES (TPVs)

TPVs are thermoplastic elastomers of two-phase morphology, essentially composed of a fine dispersion of highly vulcanized rubber domains in a continuous thermoplastic phase. The vulcanization of rubber domains occurring during the mixing process is called dynamic vulcanization. At same composition, the properties of TPVs are significantly superior to those of the simple blends (i.e., blend without curatives). However, the obtaining of TPVs with high properties essentially depends on the processing conditions used, and thus on some important parameters such as the blend composition, the mixing conditions, the type of curing system, and the concentration in blend compatibilizer, during the processing, as it will be shown in the following sections for that concerns NR/EVA TPVs.

4.7 Effect of blend compositions on properties of NR/EVA TPVs

NR/EVA TPVs with various NR/EVA ratios were prepared by dynamic vulcanization with a sulphur curing system, according to the experimental procedure described in section 3.3.3.1. Their properties (i.e., rheological, dynamic, mechanical, morphological, and thermal properties) were investigated and compared.

4.7.1 Rheological properties

The complex viscosity as a function of frequency of the dynamically cured NR/EVA blends of various NR contents is shown in Figure 4.73. It was seen that the complex viscosity decreased with increasing oscillating frequency. This indicates shear-thinning nature of the blend systems. It was also seen that at a given frequency (i.e., in Figure 4.74), the complex viscosity increased with increasing the weight fraction of NR in the blend. The viscosity of the blends depends on interfacial thickness and level of interfacial adhesion. Interlayer at the interface was also possible to slip along with the orientation and disentanglement of the

macromolecules on the application of frequency or shear stress. In case of weak interfaces, interlayer slip easily occurs and, as a result, the viscosity of the system decreases. Therefore, increasing complex viscosity with increasing content of NR is attributed to the higher content of vulcanized rubber domains dispersed in the EVA matrix. Generally, increasing rubber content causes an increase of viscosity of the blends, as reported by several authors (Nakason *et al.*, 2006; George *et al.*, 1999 and 2000).

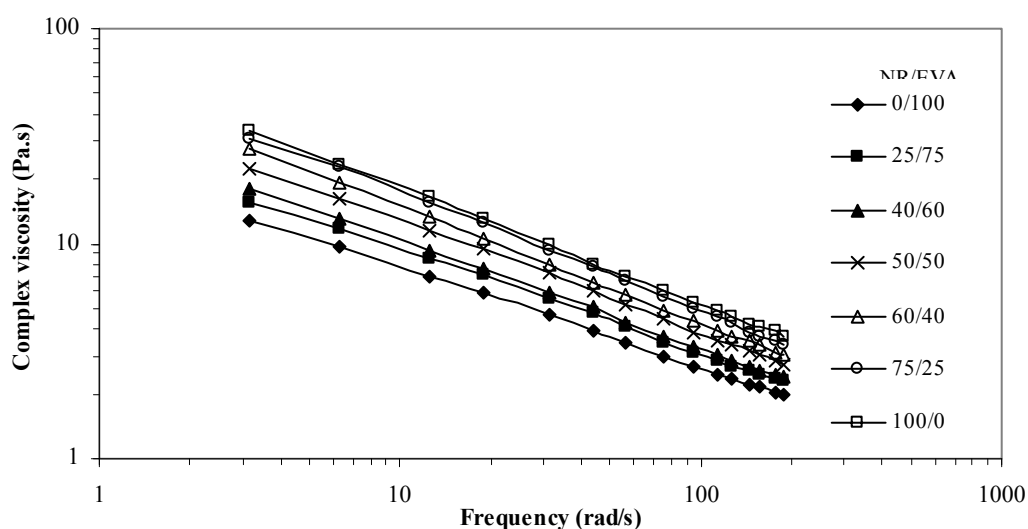


Figure 4.73 Complex viscosity as a function of frequency of dynamically cured NR/EVA blends *versus* NR content.

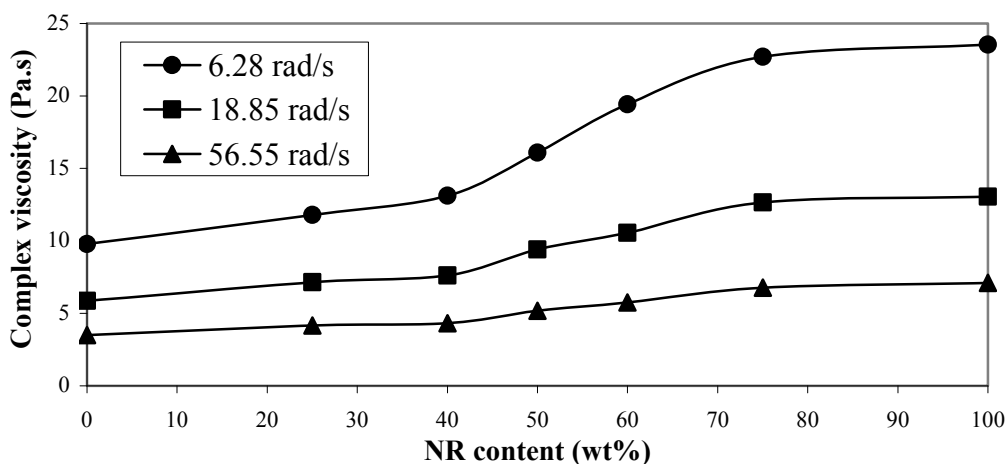


Figure 4.74 Complex viscosity at constant frequencies of 6.28, 18.85 and 56.55 rad/s of dynamically cured NR/EVA blends *versus* NR content.

4.7.2 Mechanical and morphological properties

Nature of deformation of the dynamically cured NR/EVA blends under an applied load can be visualized by the stress-strain curves, as shown in Figure 4.75. It is seen that the Young's modulus based on a slope of the initial curve of pure EVA exhibited the highest value as summarized in Table 4.13. Furthermore, decreasing trend of Young's modulus was observed with increasing the NR content in the blends. It was also clear that the static cured NR without EVA phase exhibited the lowest Young's modulus. Therefore, increasing EVA content in the blends caused deviation nature from ideal elastomer (i.e., the static cured NR to the nature of thermoplastic material (i.e., higher Young's modulus). This was attributed to the crystalline content of EVA provided strength properties to the material. Also, increasing of rubber proportion in the blend caused agglomeration of vulcanized rubber domains dispersed in the EVA matrix. Larger dispersed vulcanized rubber domains with lower interfacial areas and hence higher surface energy were observed. As a result, poor dispersion and lower interfacial adhesion of the NR domains led to poor mechanical strength.

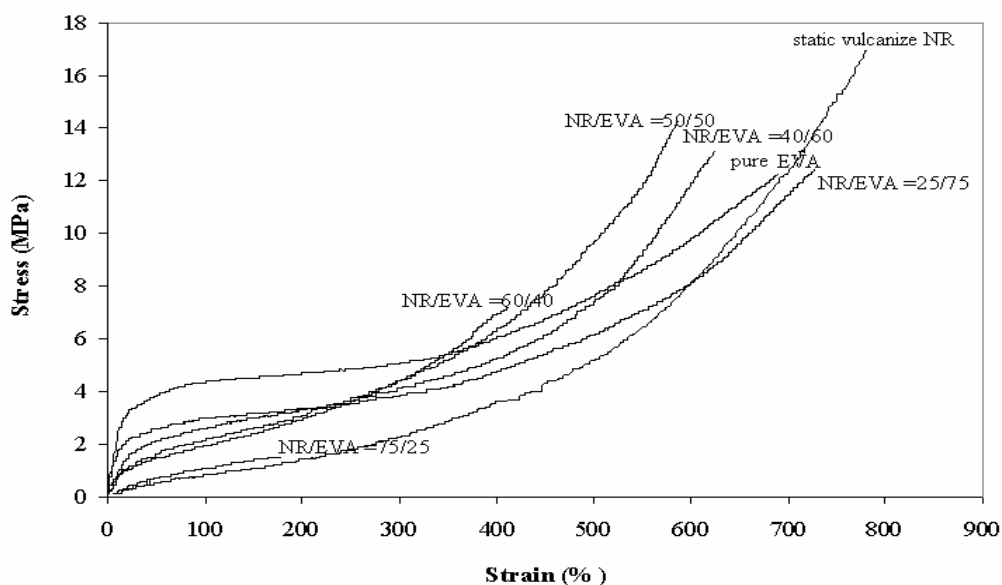


Figure 4.75 Stress-strain curves of dynamically cured NR/EVA blends as a function of NR content.

Table 4.13 Tensile properties of dynamically cured NR/EVA blends with various blend ratios.

Blend ratio (NR/EVA)	Young's modulus (MPa)	Tensile strength (MPa)	Elongation at break (%)	Tension set (%)	Hardness (Shore A)
EVA	15.41	12.25	690	35	85
25/75	10.38	12.47	728	20	80
40/60	7.06	13.15	625	18	74
50/50	5.05	14.29	588	15	62
60/40	4.91	7.16	414	5	55
75/25	1.61	1.50	178	5	46
NR*	1.35	19.06	780	0	32

* prepared by static vulcanization

Tensile strength and elongation at break of different types of dynamically cured NR/EVA blends are shown in Figure 4.76. It can be seen that the strain at rupture of NR/EVA blend decreased slightly with increasing NR content in a range of 25 to 50 wt%, but the tensile stress remains quite constant. However, increasing rubber content higher than 50 wt% caused an abrupt decrease of stress, and strain at break. That is, the elongation at break and strength properties increased with the EVA content, which is in agreement with the results reported previously reported (Lee *et al.*, 1994; Varghese *et al.*, 1995; and Mohamad *et al.*, 2006). This phenomenon occurred because the crystalline regions of EVA underwent rearrangement to accommodate more stress and exhibited the highest elongation at break and tensile strength. Furthermore, in Figure 4.76, it is also seen that the NR statically cured with sulphur system exhibited higher tensile strength than the dynamically cured NR/EVA blends and pure EVA. This is attributed to fully chemical crosslinked structures of the rubber vulcanizates.

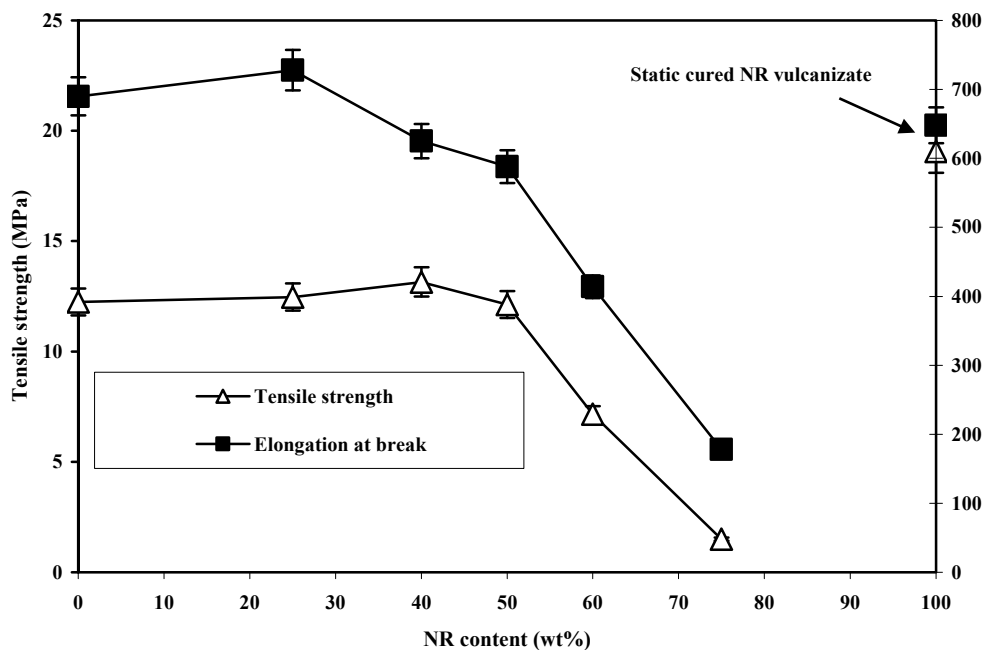
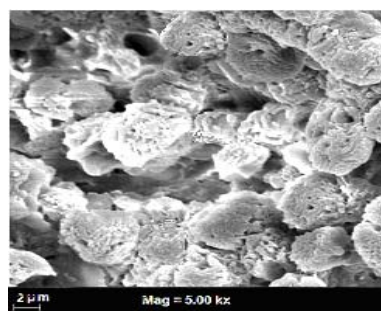
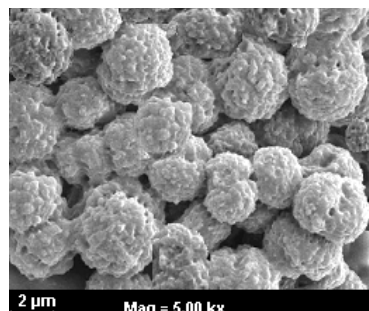


Figure 4.76 Tensile strength and elongation at break of dynamically cured NR/EVA blends *versus* NR content.

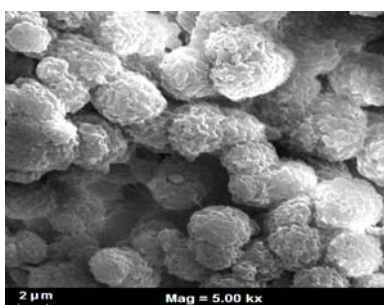
SEM micrographs of dynamically cured NR/EVA blend with various blend ratios are shown in Figure 4.77. A two-phase morphology with spherical vulcanized NR domains dispersed in the EVA matrix was observed in all dynamically cured NR/EVA blends regardless of the blend ratios. However, the particle size of rubber domains were changed with the blend proportions. That is, the size of domains increased with the content of NR in the blends. This may be attributed to an increase of shear and extensional viscosity of the vulcanized rubber domains while the viscosity of EVA phase remained constant. The extensional flow was gradually dominated with increasing mixing time and hence the rubber phase was broken to be droplets dispersed in the EVA phase. In the dynamically cured blends containing high proportion of NR, the newly formed droplets were capable to re-agglomerate or coalesce with as a consequence the formation of larger dispersed rubber particles. This phenomena was already observed in the blends with high contents in rubber (Varghese *et al.*, 1995; Asaletha *et al.*, 1999; Joseph and Thomas, 2003)



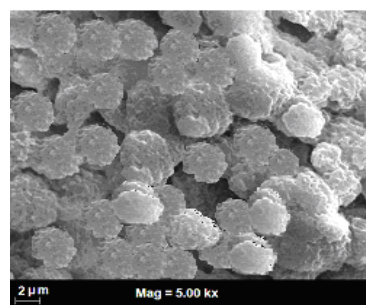
(a) NR/EVA = 75/25



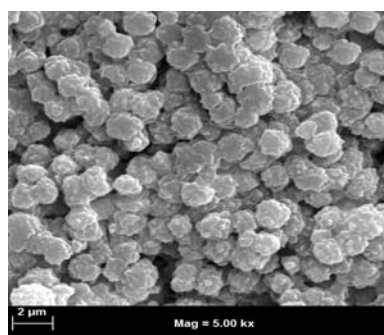
(b) NR/EVA = 60/40



(c) NR/EVA = 50/50



(d) NR/EVA = 40/60



NR/EVA = 25/75

Figure 4.77 SEM micrographs of dynamically cured NR/EVA blends with various blend ratios: (a) 75/25, (b) 60/40, (c) 50/50, (d) 40/60, (e) 25/75.

Figure 4.78 shows a correlation between the tensile strength of the dynamically cured NR/EVA blends and NR domain size (i.e., domain diameter). A slight increase of tensile strength was noted when the NR content in the blend (i.e., the size of rubber domains) increased from 25 to 50 wt%, while beyond 50 wt% (i.e., 60 to 75 wt%) the tensile strength slowed down abruptly. At very low NR contents, very fine vulcanized NR domains are dispersed in the EVA phase. The slight tensile strength increase observed by increasing NR content from 25 to 50 wt%, was

attributed to finer dispersions of vulcanized NR domains in EVA. The NR domain size gradually decreases with the increase of the NR content until 50 wt%, which caused an increase of surface area and hence of the reinforcement effect. On the other hand, the abrupt tensile strength decrease observed beyond 50 wt% abruptly was attributed to a coalescence of the rubber domains, with as a consequence an increased of interfacial tension and thus poor strength properties.

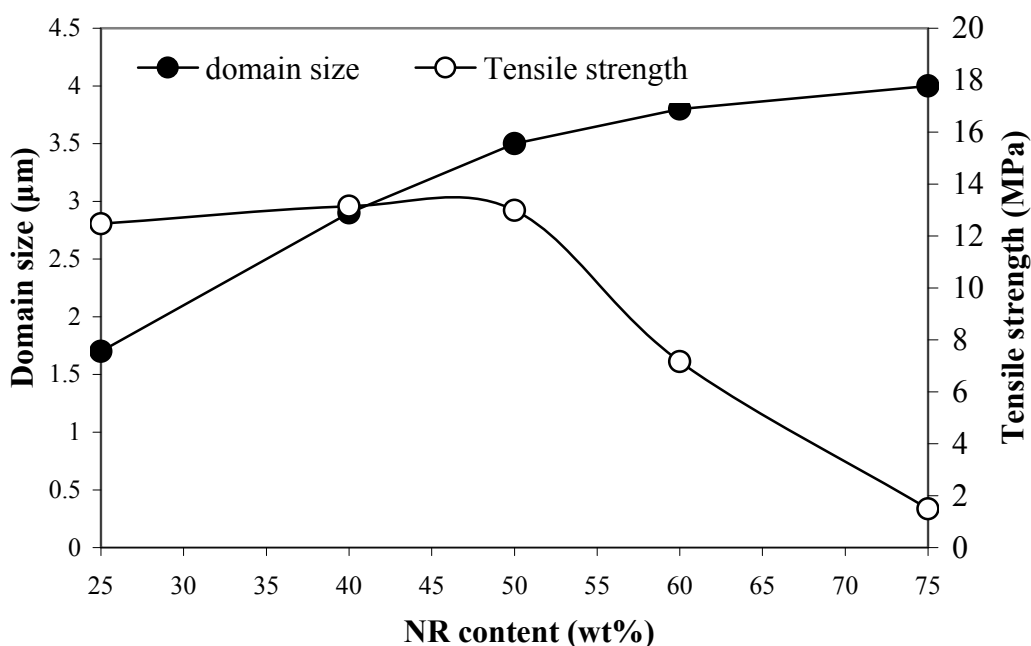


Figure 4.78 Variation of vulcanized NR domain size and tensile strength of the dynamically cured 75/25, 60/40, 50/50, 40/60, 25/75 NR/EVA blend *versus* NR content.

The variation of hardness and tension set with the weight content of NR in the dynamically cured NR/EVA blend is represented in Figures 4.79. It can be seen that the hardness and tension set decreased with increasing NR content. The hardness property of the TPVs material is typically dominated by the thermoplastic component while the elasticity of TPVs is obtained from the rubber phase. The rubber elasticity of the TPVs can be estimated by the tension set property. The decrease of tension set from 20 % to 5 % when NR content in the blend increases from 25 to 75 wt% is significant of an improved elasticity of the material (i.e.,

higher tendency to recover its original shape after prolonged extension). On the other hand, the fact that the static cured NR showed the lowest tension set value is due to the nature of rubber vulcanizate that always exhibits set properties better than those of the TPE materials.

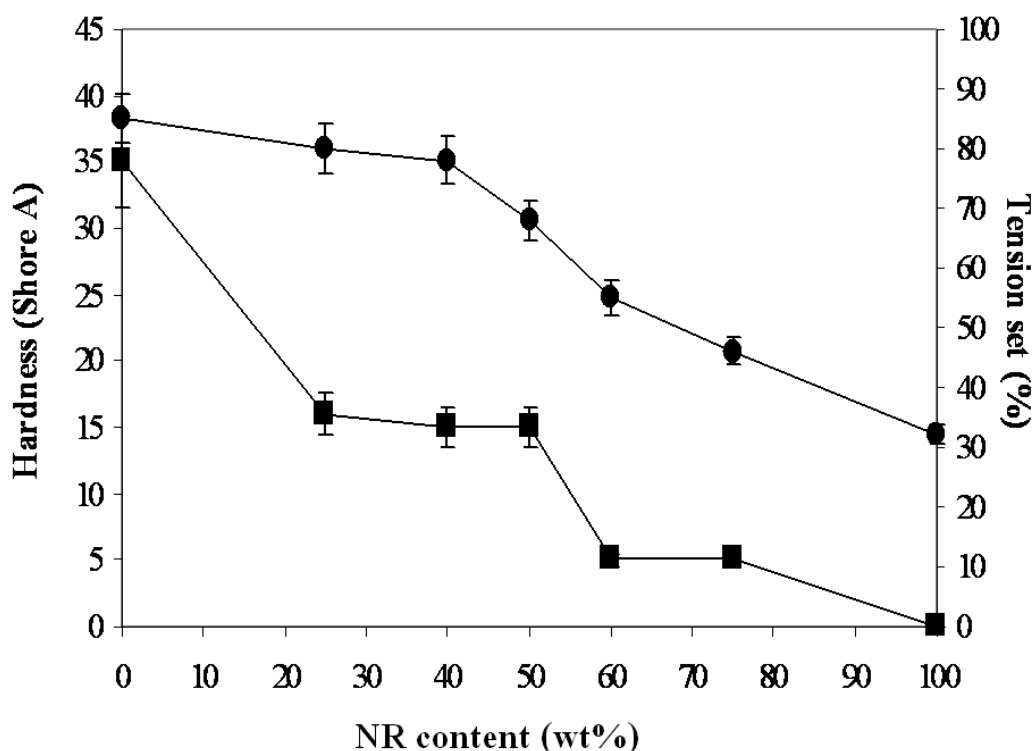


Figure 4.79. Variation of tension set and hardness of dynamically cured NR/EVA blends *versus* NR content, and comparison the ones of pure EVA and static cured NR, respectively.

4.7.3 Solvent resistance

Figure 4.80 shows the swelling behavior of dynamically cured NR/EVA blends with various blend ratios. It is clear that the tendency of oil uptake decreased when increasing the EVA content in the blends. Pure EVA shows the lowest degree of swelling in oil. This is due to the crystalline regions of EVA that contains low free volume for the oil molecules to enter and be trapped. Also, the polarity of EVA caused higher resistance characteristic to non-polar solvents.

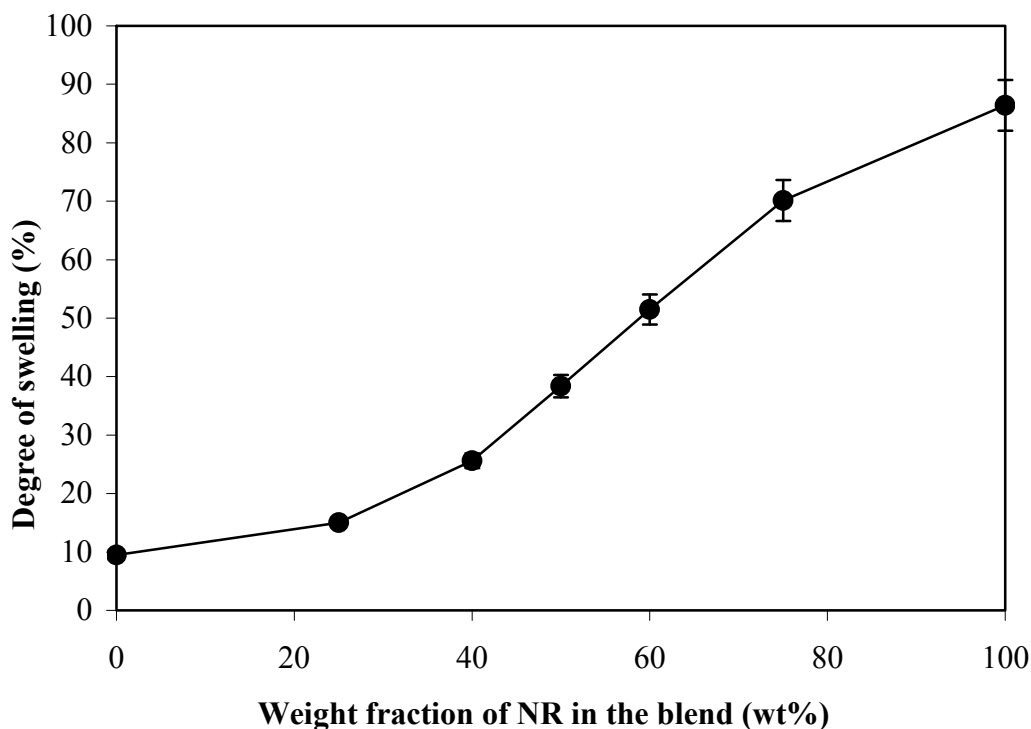


Figure 4.80. Evolution of swelling degree of the dynamically cured NR/EVA blends *versus* NR content, and comparison the one of pure EVA and static cured NR, respectively.

4.7.4 Thermal stability

Figure 4.81 shows TGA thermograms of dynamically cured NR/EVA blends, static cured NR, and pure EVA. The onset degradation temperature and level of weight losses are given in Table 4.14. It is seen that the pure static cured NR showed a single degradation step at an onset temperature of approximately 324°C with a great weight loss of 98.8 %. However, pure EVA shows double degradation stages with an onset temperature at 335°C with a weight loss of 17.8 % in the first stage which corresponds to the degradation of vinyl acetate moieties with emitting acetic acid. The second degradation step was related to the main chain degradation with an onset degradation temperature of 435°C with higher weight loss of 82.1 %. The double degradation stages were also observed in the dynamically cured blends with various blend ratios. That is, increasing proportions of EVA phase in a range of

25 to 75 wt% caused an increase of the onset degradation temperatures from 327 to 338°C with a range of weight loss from 74.9 to 25.1 % for the 1st degradation stage. This is attributed to the degradation of the NR phase that occurs at a higher temperature than in the case of the static cured NR. This proves the ability of EVA to improve thermal stability of dynamically cured NR/EVA blends. Increasing content of EVA in a range of 25 to 75 wt% also caused slight increasing of the onset degradation in the 2nd degradation stage from 429 to 433°C with increasing weight losses in a range of 23.7 to 71.1 %, respectively. This correlates to the degradation of the EVA component in the dynamically cured NR/EVA blends.

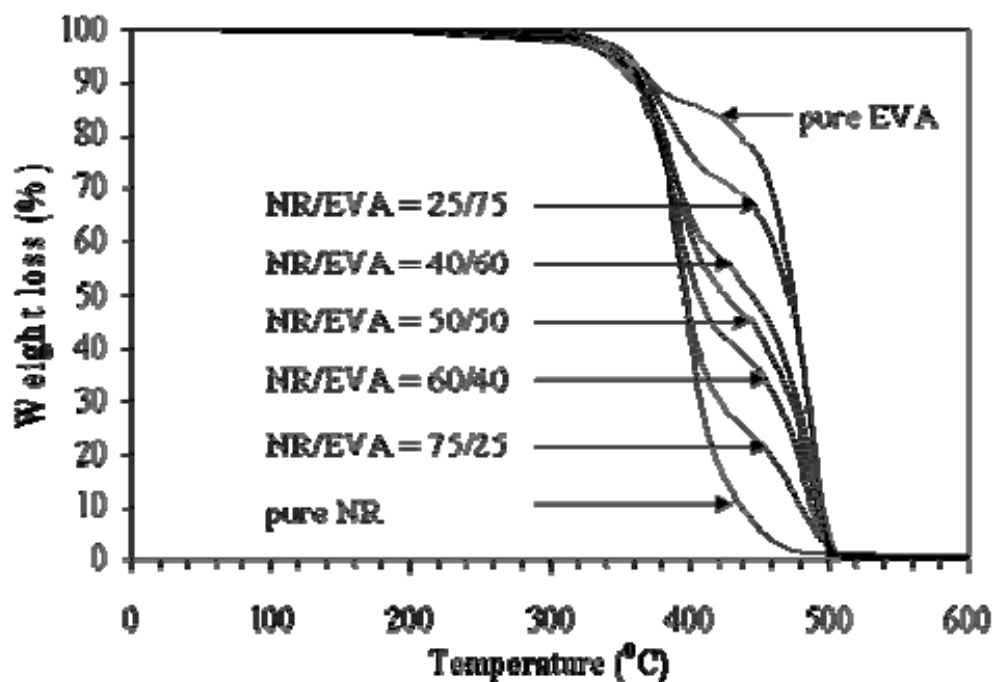


Figure 4.81 TGA thermograms of dynamically cured NR/EVA blends with various blend ratios.

Table 4.14 TGA data of dynamically cured NR/EVA blends with various blend ratio.

Blend ratio of NR/EVA	Onset Temperature (°C)		Weight loss (%)	
	1st step	2nd step	1st step	2nd step
Pure EVA	315	435	17.8	82.0
25/75	338	433	25.1	74.1
40/60	331	432	40.0	59.3
50/50	328	430	48.2	50.3
60/40	327	430	58.7	39.6
75/25	327	429	74.9	23.7
Static cured NR	324	-	98.2	-

4.7.6 Thermal behaviour

Figure 4.82 shows DMTA thermograms in terms of relationship between storage modulus and temperature. It can be seen that the storage modulus of dynamically cured NR/EVA blends with various blend ratios showed three distinct regions: a glassy region, a glass transition region, and a rubbery region. At a lower temperature than the glass transition temperature (i.e., lower than -80°C), the storage modulus of the materials increased with increasing NR content and the static cured NR showed the highest values of storage modulus while the pure EVA exhibited the lowest (i.e., 2.26×10^3 and 0.03×10^3 MPa, respectively), as shown in Table 3. On the other hand, when increasing temperature from -60°C , the static cured NR showed the lowest storage modulus (i.e., 0.007×10^3 MPa) and changed from the glassy state to rubbery state with very sharp decreasing trend of storage modulus at a glass transition temperature of approximately -59.6°C . When increasing amount of EVA in the TPVs, a decreasing trend of the maximum storage modulus was observed. Furthermore, the glass transition is not as sharp as in the blend with higher content of NR. This is attributed to the influence of the crystalline region in the EVA phase. It was also seen that the storage modulus increased

slightly upon increasing the EVA content after increasing temperature above the glass transition region of the rubber phase (i.e., -20°C as shown in Table 4.15). This indicates that the blends become more tough and hard as the EVA content increased.

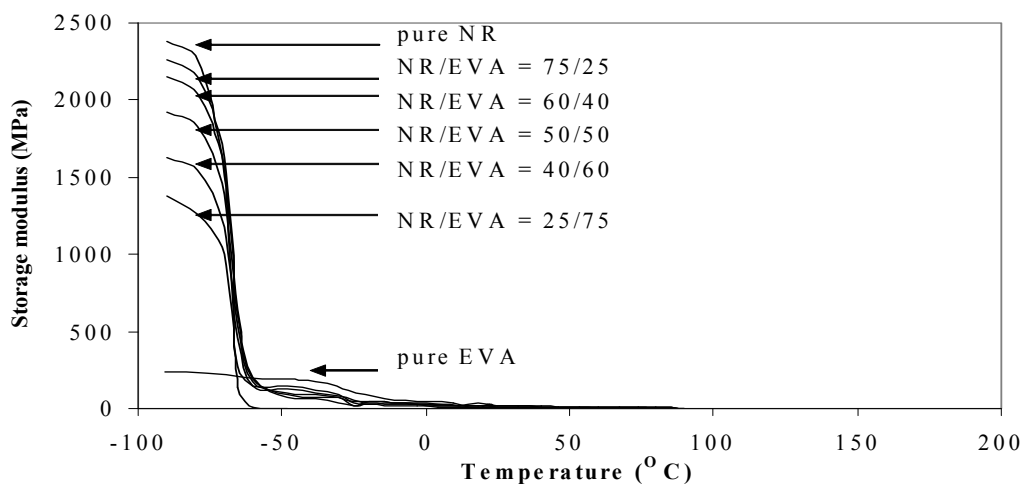


Figure 4.82 Storage modulus (G') of dynamically cured NR/EVA blends of various compositions *versus* temperature, and comparison with that of pure EVA and static cured NR.

Figure 4.83 shows the temperature dependence on $\tan \delta$ of the dynamically cured NR/EVA blends with various blend ratios compared with the static cured NR and pure EVA. It is seen that the static cured NR showed only a single peak of $\tan \delta$ and hence a single value of glass transition temperature at approximately -59.6°C (Table 4.15). On the other hand, the glass transition of EVA was observed at about -14.8°C while the maximum $\tan \delta$ value was significantly lower than that observed in the static cured NR and the blends with NR component. In the dynamically cured NR/EVA blends, two distinct transition temperatures corresponding to the NR and EVA phases were observed. This indicates phase separation or two-phase morphology of the blend components. Also, the $\tan \delta_{\text{max}}$ and the area underneath of $\tan \delta$ curves increased with increasing the NR content, indicating an increase in damping properties of the material. The peak intensity of the EVA phase was not so evident because of the low damping value of this phase.

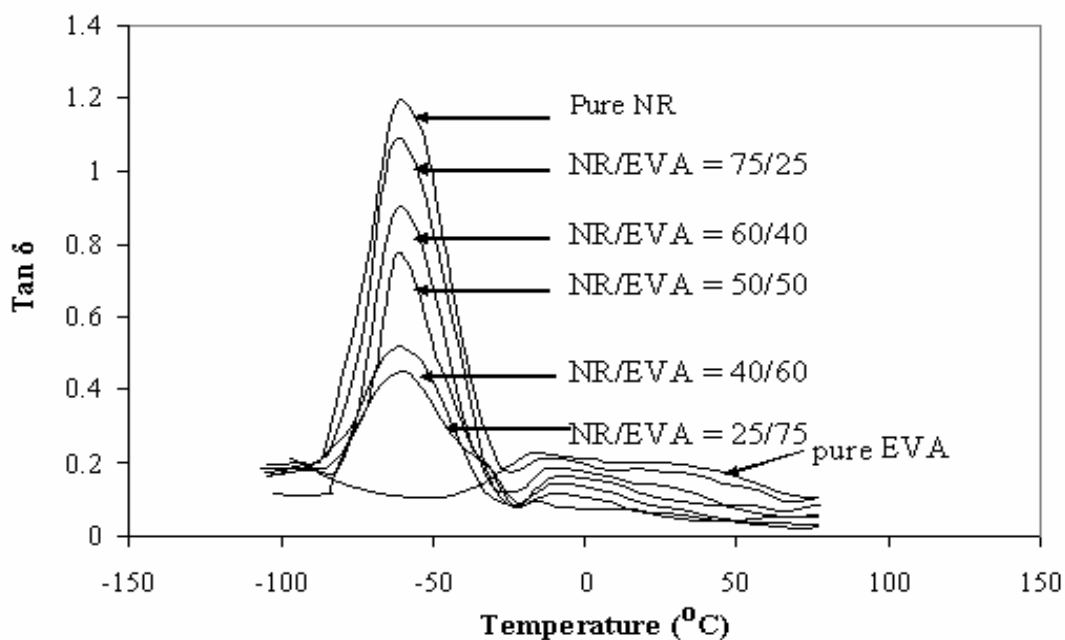


Figure 4.83 Tan δ of dynamically cured NR/EVA blends of various compositions *versus* temperature, and comparison with that of pure EVA and static cured NR.

Table 4.15 DMTA data of dynamically cured NR/EVA blends of various compositions.

Blend component		Storage modulus (G') ($\times 10^3$ MPa)			Maximum tan δ		T _g of NR phase ($^{\circ}$ C)
NR (wt %)	EVA (wt.%)	-80 $^{\circ}$ C	-60 $^{\circ}$ C	-20 $^{\circ}$ C	NR phase	EVA phase	
100	0	2.260	0.007	0.002	0.45	-	-59.6
75	25	2.125	0.153	0.023	0.52	0.10	-60.2
60	40	2.042	0.191	0.047	0.77	0.13	-60.0
50	50	1.825	0.171	0.042	0.91	0.15	-60.2
40	60	1.547	0.150	0.035	1.09	0.17	-60.2
25	75	0.724	0.123	0.050	1.23	0.19	-60.0
0	100	0.230	0.191	0.060	-	0.23	-

4.8 Effect of curing systems in dynamically cured 40/60 NR/EVA blends

NR and dynamically cured 40/60 NR/EVA blends were prepared using various curing systems according to the experimental procedure described in section 3.3.3.2. 40/60 NR/EVA blend was chosen due to its high tensile strength, elongation at break, solvent resistance, and thermal stability, as described in section 4.7. The properties (i.e., cure characteristic, rheological, dynamic, mechanical, morphological, and thermal properties) of NR and dynamically cured 40/60 NR/EVA blends were investigated.

4.8.1 Static vulcanization of NR compounds

4.8.1.1 Cure characteristics

Effect of curing system on static vulcanization of NR was determined by plotting between torque and testing time using a Moving Die Rheometer (MDR) at 150°C, as shown in Figure 4.84 and Table 4.16.

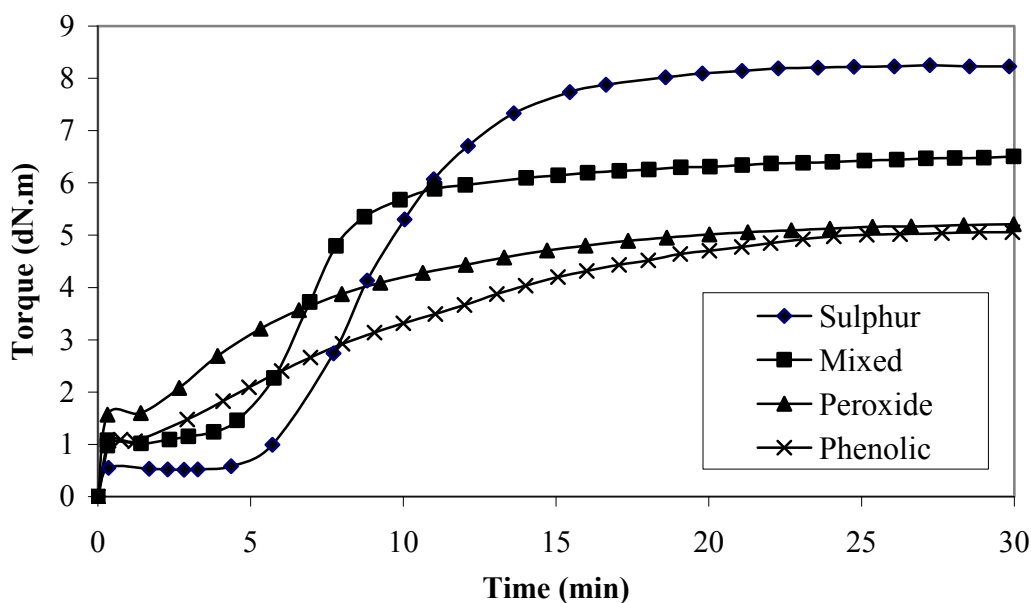


Figure 4.84 Curing curves of the static vulcanization of NR carried out at 150°C using sulphur, peroxide, mixed (sulphur plus peroxide), and phenolic curing systems, respectively.

Table 4.16 Curing characteristics of static vulcanizate of NR carried out at 150°C using sulphur, peroxide, mixed (sulphur plus peroxide), and phenolic curing systems, respectively.

Properties	Curing system			
	Sulphur	Mixed	Peroxide	Phenolic
Min. Torque, dN.m	0.50	1.22	1.40	1.22
Max. Torque, dN.m	8.23	6.51	5.20	5.06
MH-ML, dN.m	7.73	5.29	3.80	3.84
Scorch time, min.	4.36	3.79	1.22	1.40
Cure time, min.	12.12	8.73	14.28	18.86
Cure rate index, min ⁻¹	12.89	20.24	7.76	5.66
Crosslink density, (x10 ⁻⁵ mol/cm ³)	5.21	4.71	4.52	4.68

It was clearly seen that the vulcanization characteristics as evidence from the increase in the maximum torque (Table 4.16) obtained for the sulphur containing compounds (i.e., sulphur and mixed cured systems, respectively). The sulphur curing system exploited carbon-carbon double bonds of NR chains to create links between the rubber chains causing high degree of crosslinking. From the curing curves in Figure 4.84, the effect of curing system on torque difference (MH-ML) of the NR vulcanizate is shown in Figure 4.85. It was seen that the differences of torque related to the level of crosslinking of the rubber vulcanizate, were observed in different curing system. That is, the sulphur cured system showed the maximum torque value that is higher than the mixed, phenolic, and peroxide cured systems, respectively.

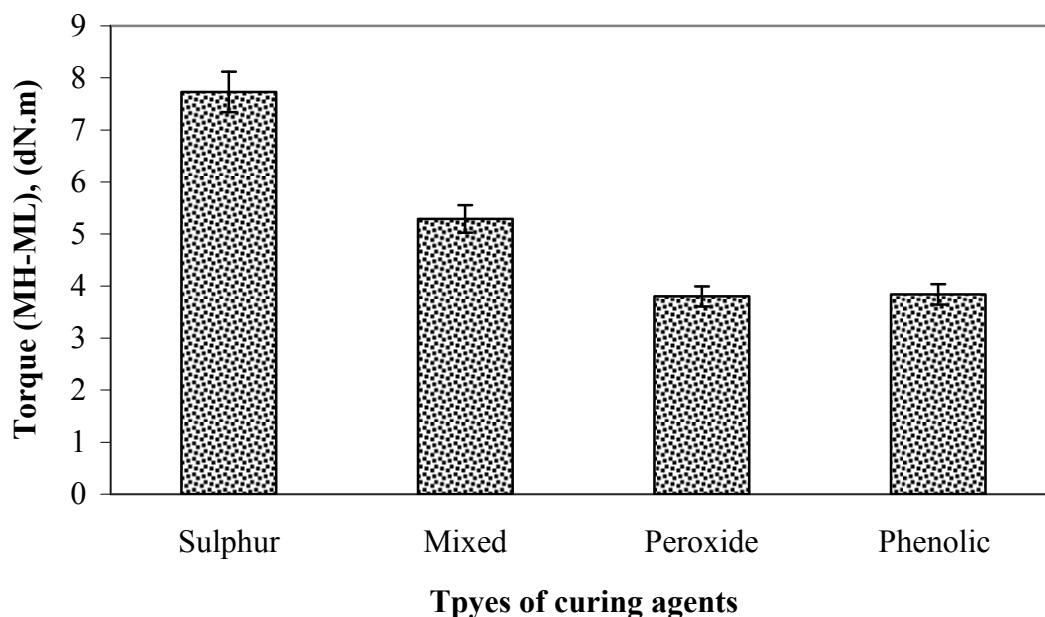


Figure 4.85 Different torque values (MH-ML) of NR vulcanizates according to the curing system used.

In Table 4.16, the phenolic cured system exhibited the highest cure time whilst the peroxide system exhibited the shortest cure time. The scorch time (ts_2) or time to incipient cure is a measure of the time at which premature vulcanization of the material occurs. It was determined from the minimum torque value to increase by two units. The scorch safety of the compound increases with increasing scorch time value. The scorch safety of the sulphur system was the highest whilst the peroxide cured system showed the lowest. This result may be attributed to the fact that peroxides typically react with the elastomer chains by abstracting hydrogen atoms from the NR backbone to create highly active sites or radicals. As a result, carbon to carbon linking occur in the peroxide cured system. The crosslinking reaction is faster than those of the phenolic, mixed, and sulphur vulcanization system, respectively. Therefore, the peroxide cured system shows the shortest scorch time. In phenolic cured system, longer scorch time and cure time than the peroxide system but shorter scorch time and longer cure time than mixed and sulphur cured systems were observed. Scorch time of mixed curing system becomes intermediate between sulphur and peroxide cured systems. Variation of the torque (ML and MH)

of the NR vulcanizate is also shown in Table 4.16. The minimum torque is a measure of the stiffness of the non-vulcanized test specimen by taking the lowest point of the curing curve. It can be seen that the highest minimum torque value was observed in peroxide cured system due to an increase of viscosity. The maximum torque, MH, is a measure of the stiffness or shear modulus of the fully vulcanized specimens at the vulcanization temperature. It can be seen that significant improvement of the vulcanization characteristics as evidence from the increase in the maximum torque obtained from the sulphur vulcanized compounds. This is due to the effectiveness of curing process of the rubber phase by C-Sx-C linkage, resulting in maximum torque values higher than that obtained with mixed, peroxide, and phenolic cured system, respectively.

Figure 4.86 shows the effect of vulcanizing system on the cure rate index (CRI) which is a measure of the rate of the vulcanization based on the difference between the optimum vulcanization time, t_{90} , and the incipient scorch time, t_{s2} . It is seen that the highest value of CRI was observed in the mixed cured system due to a smaller difference of value between cure time and scorch time than in sulphur, peroxide, and phenolic cured systems. It can be explained by the synergistic combination of peroxide (i.e., DCP) and sulfur cured systems. That is, the peroxide cured system offered the fastest scorch while the sulphur cured system exhibited a moderate cure time (t_{c90}) and an higher crosslinking efficiency (i.e., maximum torque). This leads to an enhancement of the cure rate, and decrease of the cure time of NR.

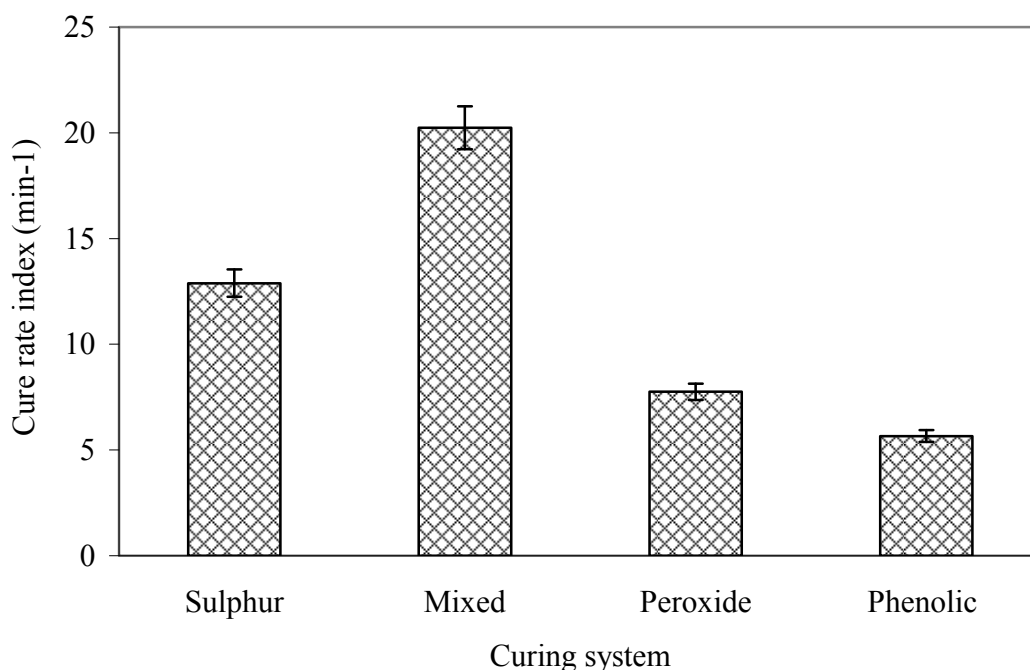


Figure 4.86 Cure rate index (CRI) of NR according to the curing system used.

4.8.1.2 Tensile properties

Stress-strain curves of NR vulcanizates as a function of the curing system used to vulcanize NR are given in Figure 4.87, and the data are summarized in Table 4.16. It was clearly noted that the NR vulcanizate coming from the peroxide system shows higher initial slope at the beginning of the curve (i.e., 20 % modulus) than the ones coming from mixed, sulphur, and phenolic cured systems, respectively. Its tensile properties are strongly different from that of the vulcanizates coming from the other curing system: it showed high modulus (Figure 4.87), but very low tensile strength (Figure 4.88) and elongation at break (Figure 4.89). Highest tensile strength was observed with the sulphur cured system (Figure 4.88) followed in the order by the phenolic, mixed, and peroxide cured systems, respectively. However, the NR vulcanizate coming from the phenolic cured system exhibited the highest elongation at break.

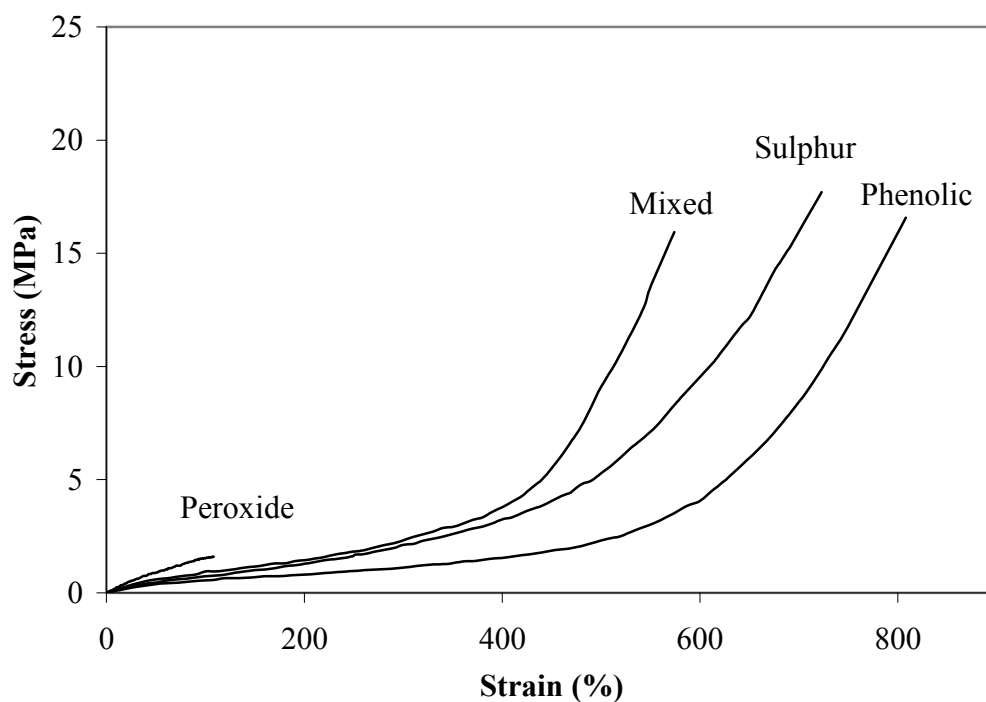


Figure 4.87 Stress-strain curves of NR vulcanizates as a function of the curing system used to vulcanize NR.

Table 4.17 Tensile properties of NR vulcanizates with various vulcanization systems.

Curing system	Modulus (at 200% elongation)	Tensile strength	Elongation at break (%)	Tension set (%) (at 200% elongation)	Hardness (shore A)
Sulphur	0.22	17.71	723	0	33
Mixed	0.28	15.93	574	0	34
Peroxide	0.41	1.60	108	*	36
Phenolic	0.18	16.57	808	0	32

* The sample could not be stretched at a constant elongation at 200%

These results can be explained by the structural characteristics of the different networks formed, which depend on the curing system used, as schematically shown in Figure 4.90. With the peroxide curing system, only C-C bonds are formed, which leads to vulcanizates in which chain flexibility is low. This may be related to the length of the links provided by the curing system (Figure 4.90), which has as a consequence to vary the density and the flexibility of the network formed.

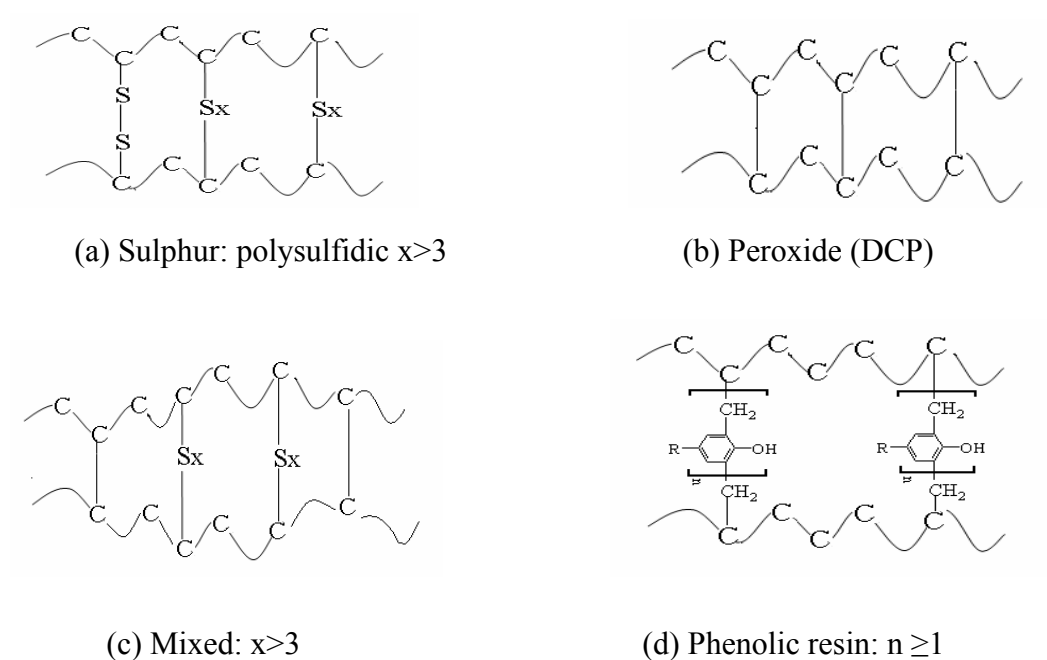


Figure 4.88 Schematic representation of the crosslinked structure of NR vulcanizates in relation with the cured system used.

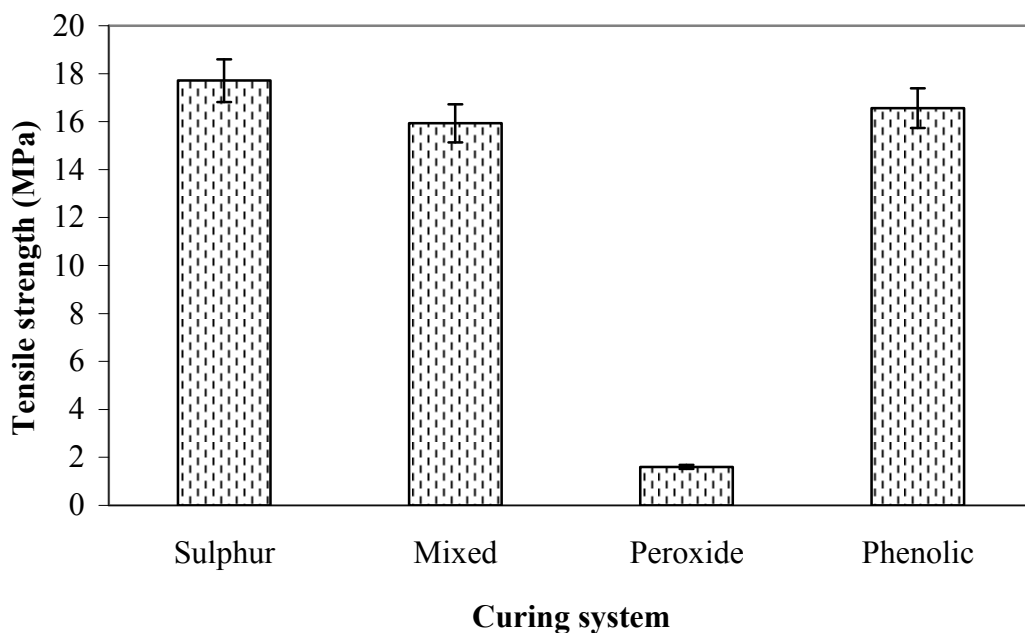


Figure 4.89 Tensile strength of NR vulcanizates according to the cured system used.

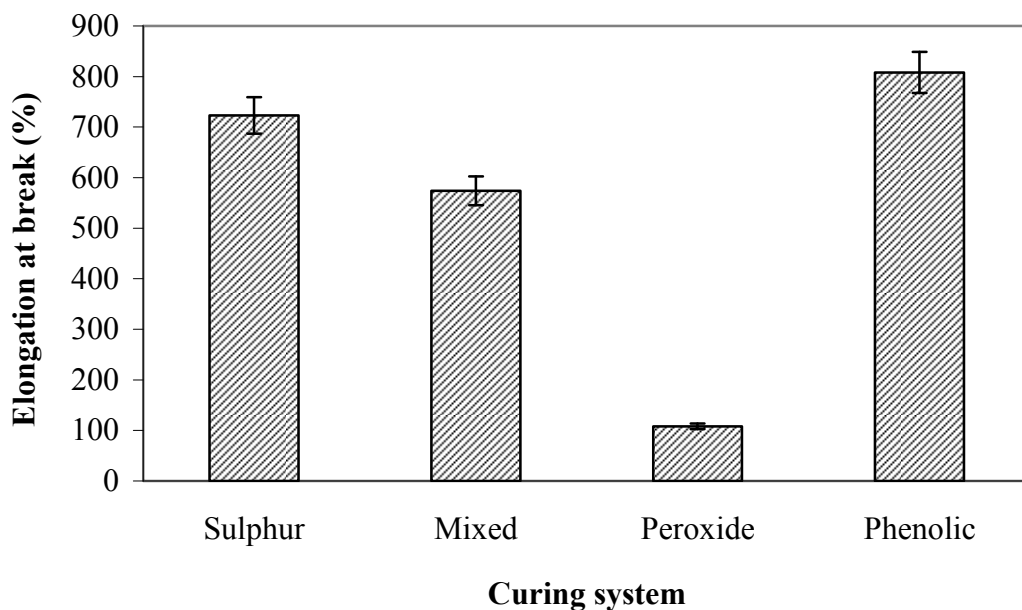


Figure 4.90 Elongation at break of NR vulcanizates according to the cured system used.

Concerning the hardness (shore A) the rubber vulcanizates obtained, it was noted that it also depends on the curing system, and decreases as follows: peroxide cured system > mixed cured system > sulphur cured system > phenolic cured

system (Figure 4.91). This order that relates differences of network rigidity, is also justified by the nature of the links formed between the chains, which depends on the curing system used.

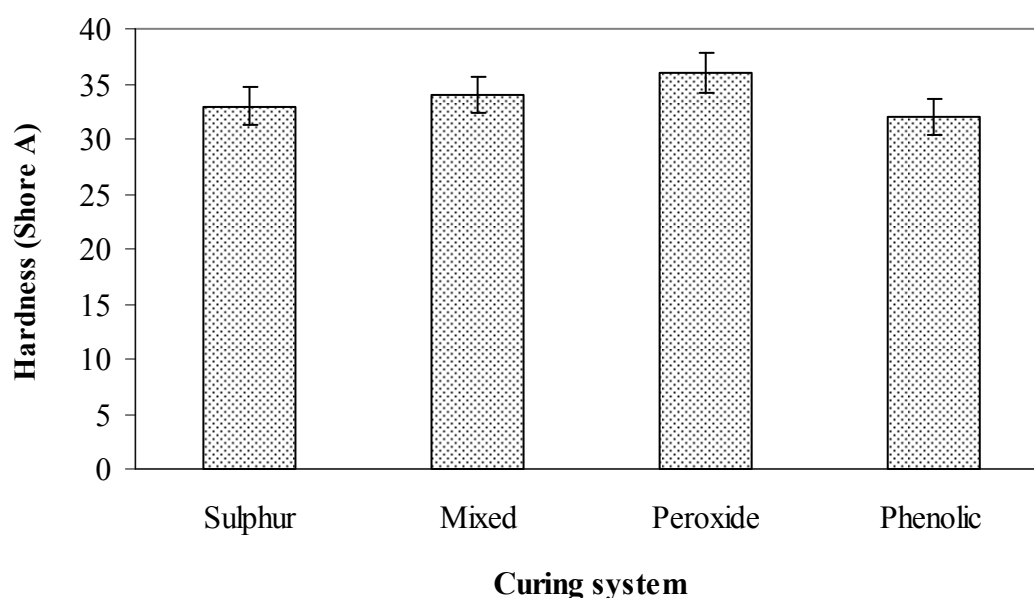


Figure 4.91 Hardness of NR vulcanizates according to the cured system used.

4.8.2 Effect of vulcanization systems on dynamically cured 40/60 NR/EVA blends

40/60 NR/EVA TPVs were prepared using various vulcanization systems, according to the experimental procedures described in section 3.3.3.2. Some of their properties were evaluated, as shown in the following sections.

4.8.2.1 Rheological properties

Plots of complex viscosity as a function of frequency of dynamically cured 40/60 NR/EVA blends using various vulcanizing systems are shown in Figure 4.92. It is clear that the complex viscosity decreased when increasing frequency. This indicates that all TPVs exhibited shear-thinning behavior. At a given frequency of 3.14 rad/s^{-1} (Figure 4.93), the TPV cured with the peroxide system showed the

highest complex viscosity, whilst the lowest value was observed in the case of the TPV cured with the phenolic one. It is well established that peroxide is typically used as a curing agent for EVA (Tai, 1999; Narkis and Miltz, 2003). Incorporation of peroxide in the molten EVA induces a crosslinking reaction of ethylene molecular segments (John *et al*, 2003). Consequently, this can explain why NR/EVA TPVs cured with peroxide system exhibit the highest complex viscosity, and shows that the peroxide curing system cannot be considered as an appropriate curing system for this type of blend. In the mixed curing system, the vulcanization of NR macromolecules and crosslinking of EVA macromolecules took place simultaneously. Diffusion rates of peroxide species in EVA are slightly higher than in the NR phases due to the fact that the solubility parameters of peroxide cured agent (i.e., DCP), NR, and EVA are 7.39 , 8.34 , and 7.88 $(\text{cal}/\text{cm}^3)^{1/2}$, respectively. Therefore, lower loading level of DCP caused lower flow resistance and higher processability.

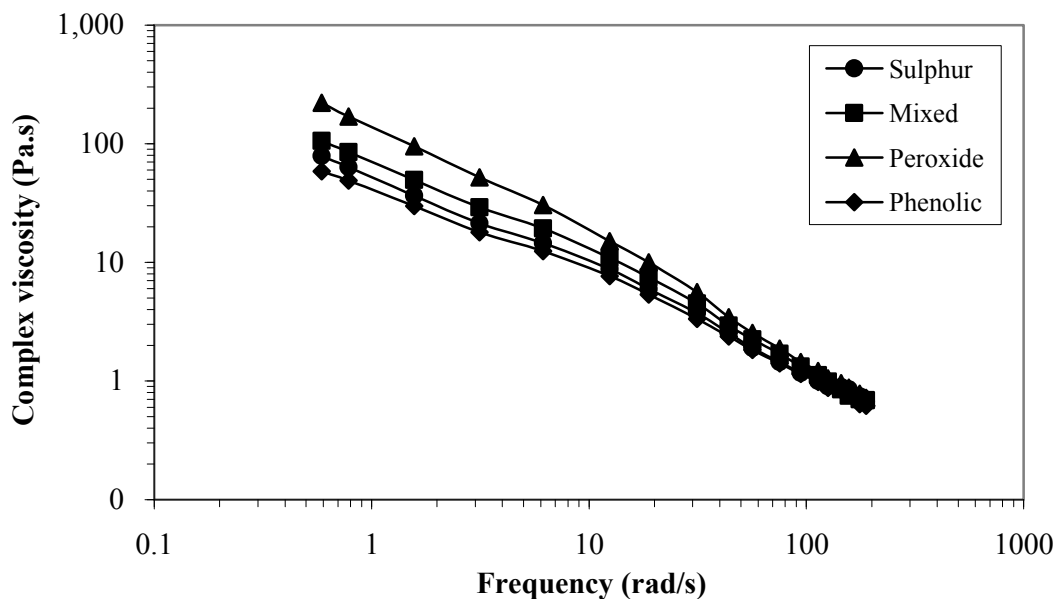


Figure 4.92 Complex viscosity as a function of frequency of the dynamically cured 40/60 NR/EVA blends with various vulcanization systems.

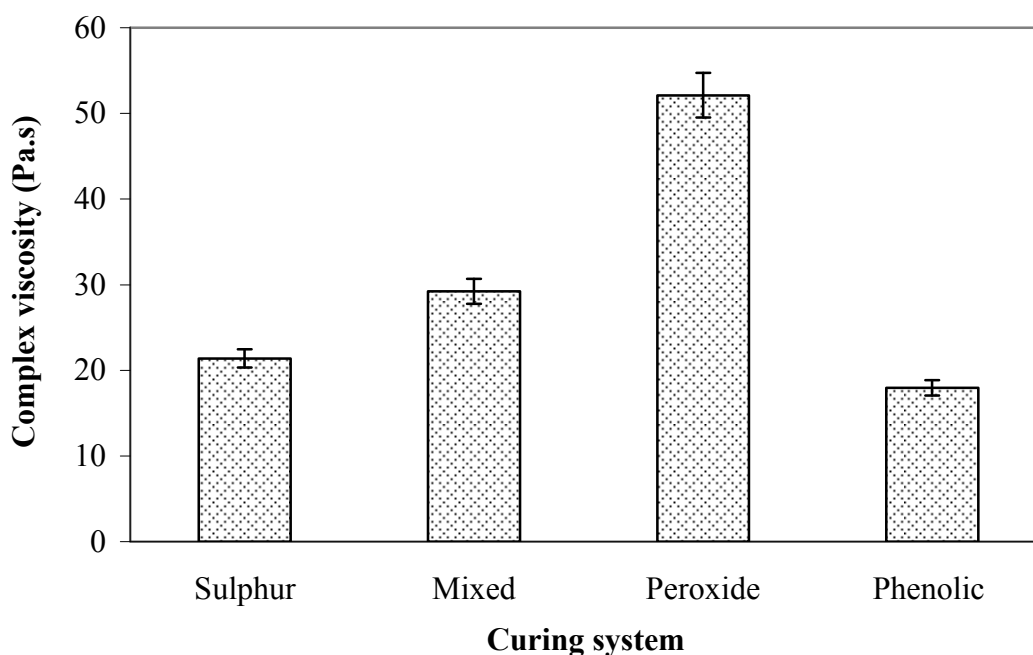


Figure 4.93 Complex viscosity at a constant frequency of 3.14 rad/s of dynamically cured 40/60 NR/EVA blends with various vulcanization systems.

4.8.2.2 Dynamic properties

The storage modulus as a function of frequency of TPVs coming from NR/EVA blends dynamically cured with various curing systems, as well as the one of the uncured sample (i.e., simple blend), is shown in Figure 4.94. It can be seen that the storage modulus, which is the elastic response of the TPVs, increased with increasing frequency because of a decrease in time available for molecular relaxation. Moreover, the storage moduli for all types of TPVs are higher than that of the uncured sample. This is due to the dynamic vulcanization that caused the formation of chemically crosslinked macromolecular networks with higher elasticity and rigidity. On contrary, the unvulcanized sample contains only macromolecular chain entanglements during deformation. Among the four types of curing systems studied, the peroxide cure system showed the highest value of storage modulus at a given frequency, followed by mixed, phenolic, and sulphur cured systems. The increase in storage modulus is more pronounced in the peroxide cured system

because of the crosslinking reaction of EVA phase as evidenced by extraction experiments of NR and EVA (Figures 4.96 and 4.97, respectively). Therefore, the increase of storage modulus is related to the crosslinking of the EVA phase.

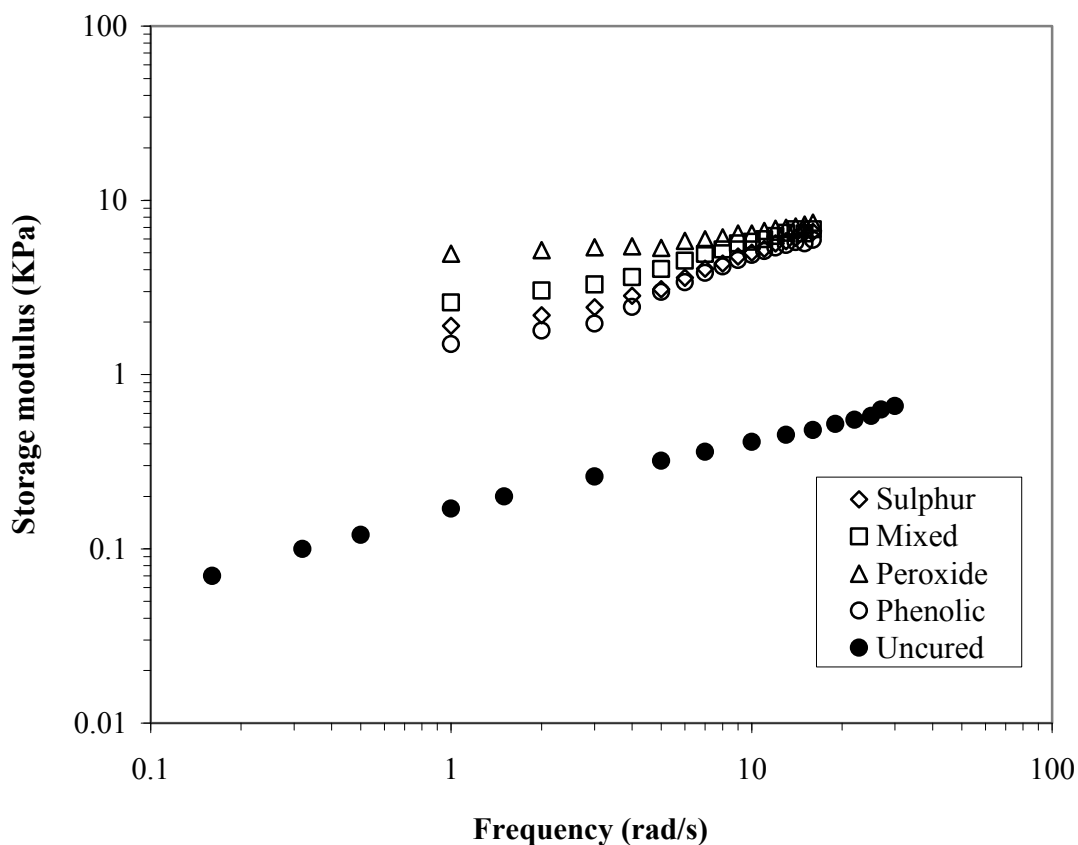


Figure 4.94 Storage modulus as a function of frequency of dynamically cured 40/60 NR/EVA blends with various vulcanization systems.

Figure 4.95 shows $\tan \delta$ as a function of frequency. It can be seen that $\tan \delta$ values of all TPVs are lower than the one of the uncured sample. This indicates higher elastic modulus or elasticity of the TPVs than the uncured sample based on a simple blend. Among the four types of curing systems, the phenolic cured system exhibited the highest value of $\tan \delta$, whilst the mixed and peroxide cured systems exhibited the lowest value. This result confirms a crosslinking of the EVA phase when dynamic vulcanization of NR/EVA blends is carried out with peroxide or mixed curing systems.

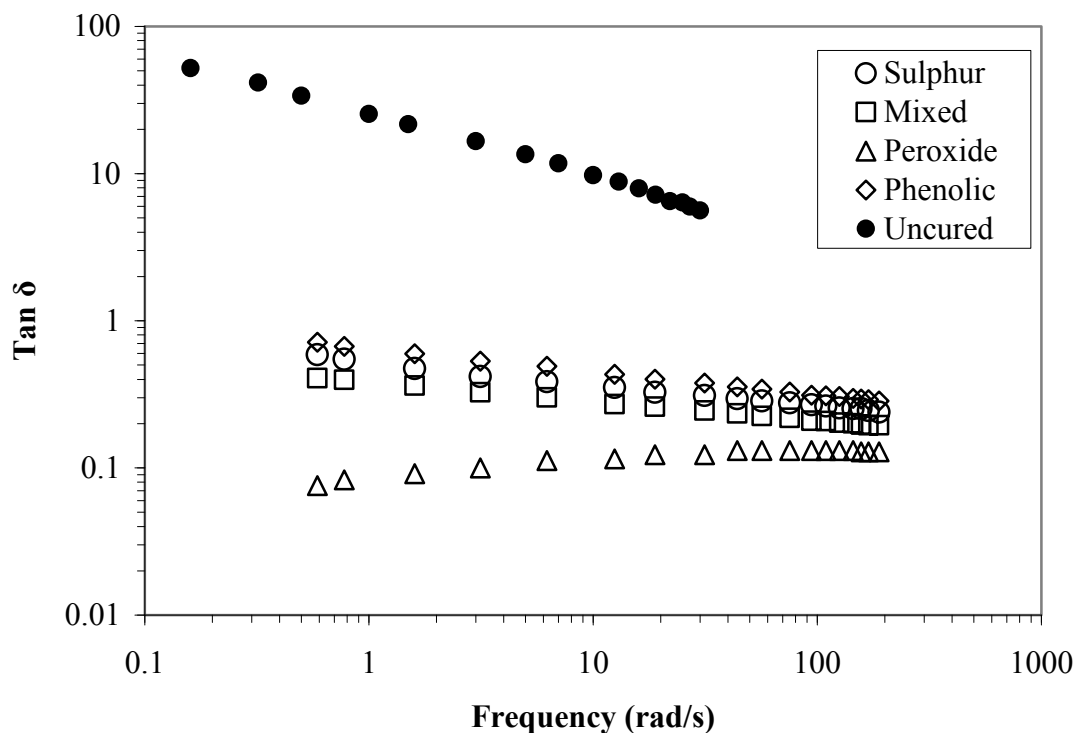


Figure 4.95 Tan δ as a function of frequency of dynamically cured 40/60 NR/EVA blends with various vulcanization systems.

4.8.2.3 Extraction experiment

Non-crosslinked NR phase in the TPVs could be determined by selective extraction of NR with n-hexane. The quantities of NR extracted by n-hexane from TPVs coming from 40/60 NR/EVA blends dynamically cured with various vulcanizing systems are given in Figure 4.96, as well as the one extracted from the uncured sample. As waited, the highest amount of NR extracted was obtained from the uncured sample (i.e., the simple blend) while the quantities extracted from the TPVs depend on the vulcanizing system used. They are ranked as follows: sulphur cured system < phenolic cured system < mixed cured system < peroxide cured systems. On the other hand, experiments involving selective extraction of EVA phase were also carried out using tetrahydrofuran (THF) as extraction solvent, in order to investigate the effect of vulcanizing system on the crosslinking of the EVA phase. The results given in Figure 4.97, show that the

amount of EVA extracted from the TPVs decreased as follows: sulphur cured system = phenolic cured system > mixed cured system >> peroxide cured system. On the other hand, the fact that the quantities of EVA extracted from the TPVs coming from sulphur and phenolic systems are quantitative and similar to the one extracted from the uncured sample indicates that crosslinking of the EVA phase occurs only when peroxide and mixed cured systems are used as vulcanizing systems. This result correlates well with the dynamic property studies (Figures 4.94 and 4.95) that showed that the TPVs coming from the peroxide cured system exhibited the highest storage modulus and the lowest value of $\tan \delta$.

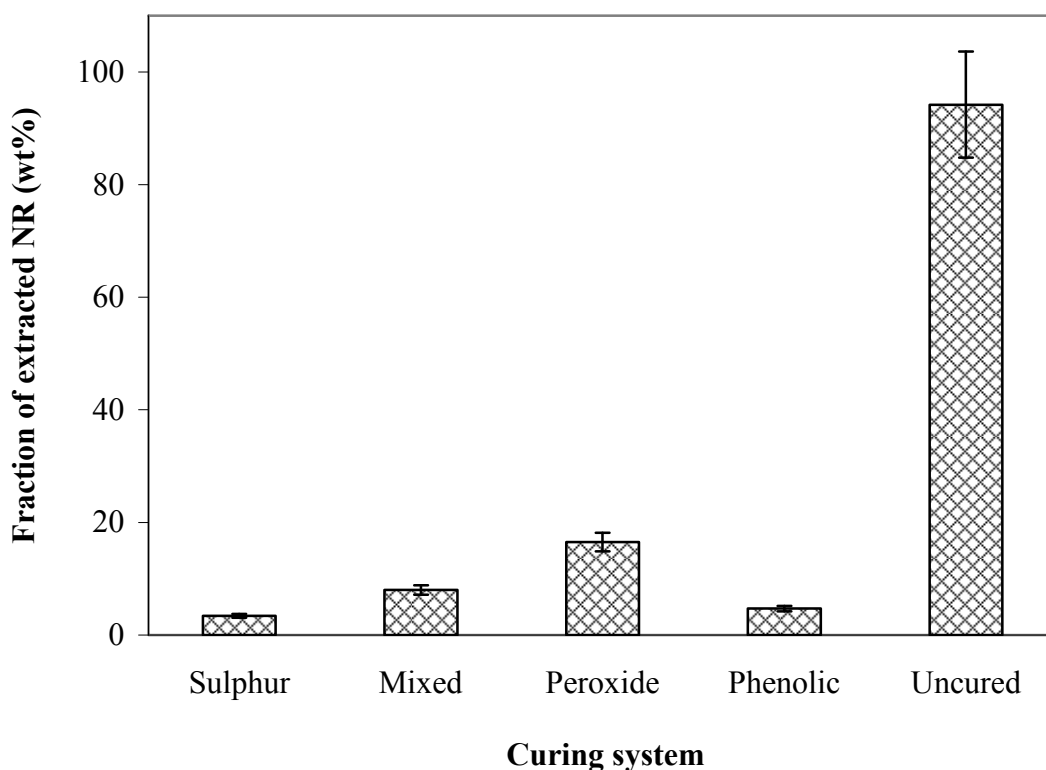


Figure 4.96 Quantity of extractable NR phase of uncured and dynamically cured 40/60 NR/EVA blends with various vulcanization systems.

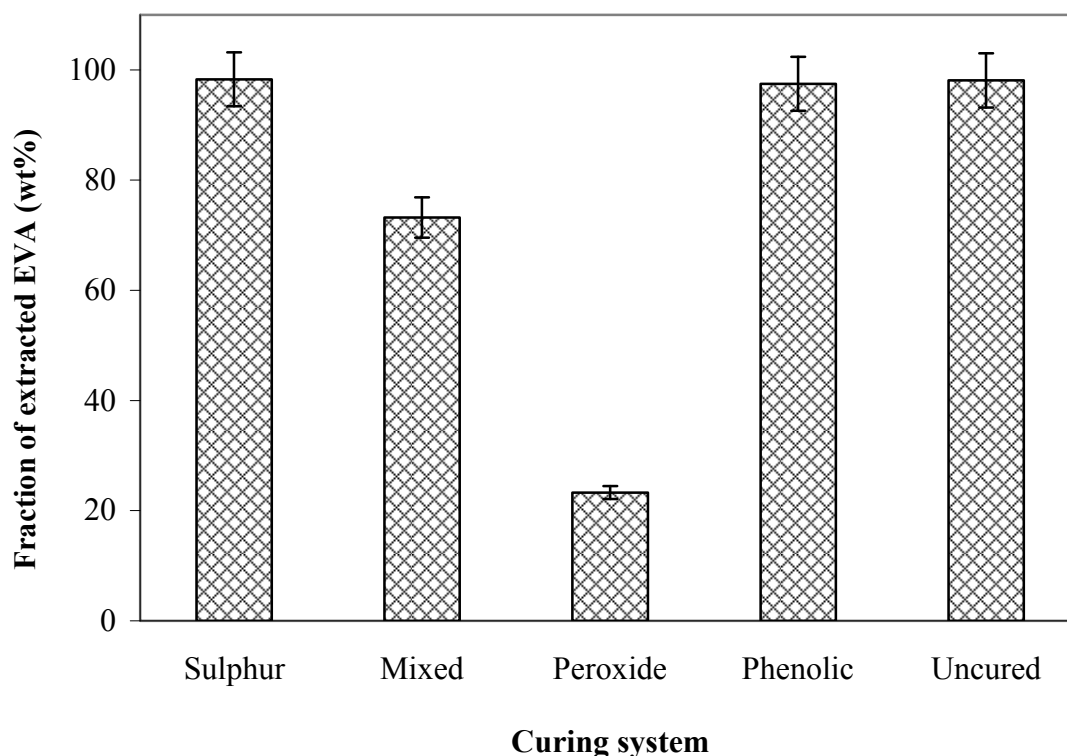


Figure 4.97 Quantity of extractable EVA phase of uncured and dynamically cured 40/60 NR/EVA blends with various vulcanization systems.

4.8.2.4 Solvent resistance

Solvent resistance was evaluated by the determination of the degree of swelling in IRM No.3 oil, a low swelling in oil being significant of a high crosslinking rate, and thus of a high solvent resistance. The degrees of swelling of TPVs coming from 40/60 NR/EVA blends dynamically cured with various vulcanizing systems were compared with the one of non-vulcanized sample (Figure 4.98). According to the curing system used, they can be ordered as follows: uncured > phenolic cured system > sulphur cured system > mixed cured system > peroxide cured system. The low swelling values observed with the mixed and peroxide cured systems is due to the fact that the peroxide caused a crosslinking of EVA phase, as already evidenced by the quantities of EVA phase extracted from the TPVs prepared using these vulcanizing systems (Figure 4.97) and by their dynamic properties (Figures 4.94 and 4.95).

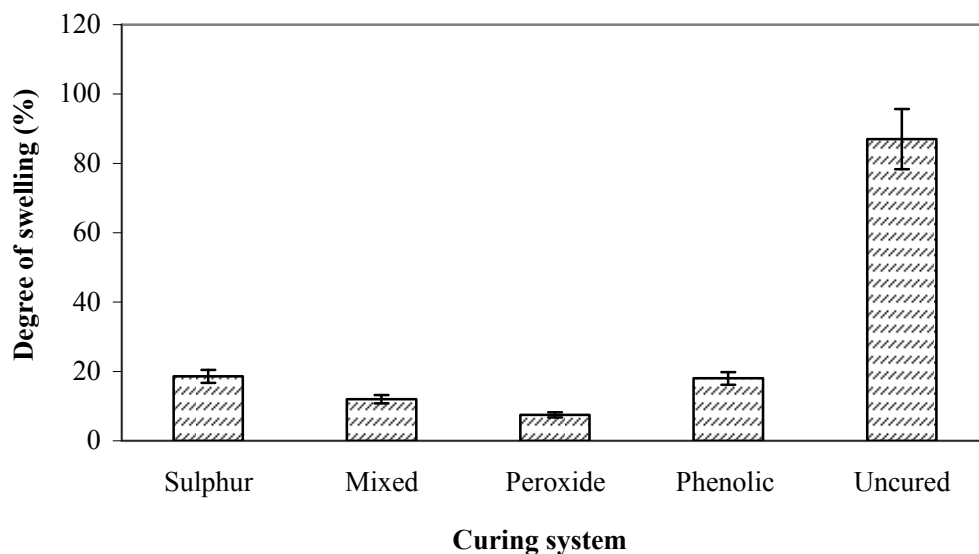


Figure 4.98 Degree of swelling of uncured and dynamically cured 40/60 NR/EVA blends with various vulcanization systems.

4.8.2.5 Mechanical properties

Stress-strain behavior of TPVs coming from 40/60 NR/EVA blends dynamically cured with various vulcanizing systems were compared with the ones of non-vulcanized sample (Figure 4.99; Table 4.18).

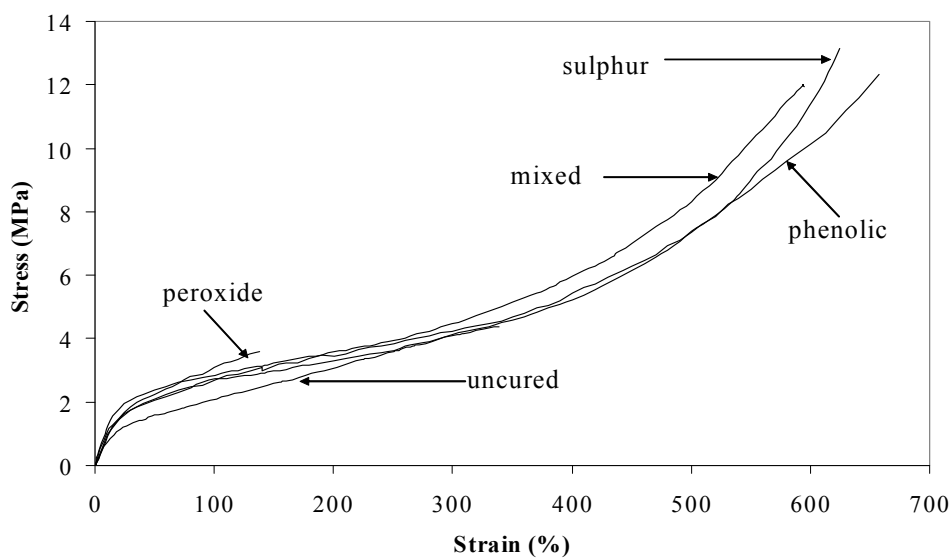


Figure 4.99 Stress-strain behaviours of uncured and dynamically cured 40/60 NR/EVA blends with various vulcanization systems.

Table 4.18 Tensile and hardness properties of uncured and dynamic cured 40/60 NR/EVA TPVs with various types of vulcanization systems.

Curing system	Tensile strength (MPa)	Elongation at break (%)	Tension set (%) at 200% elongation	Hardness (Shore A)
Uncured	4.39	339.2	45	70
Sulphur	13.15	625.5	2	72
Peroxide	3.32	137.8	*	78
Mixed	11.95	592.5	5	75
Phenolic	12.34	658.0	2	72

*The sample could not be stretch at a constant elongation at 200%

It can be seen that the dynamically cured NR/EVA blends show higher initial slope at the beginning of the curve (i.e., 20 % elongation) than uncured sample. This is due to the formation of a chemical crosslink which leads to an increase in modulus of elasticity. It was noted that the TPV coming from the peroxide cured system showed the highest initial slope and hardness, but in same time the lowest tensile strength and elongation at break (Table 4.17), whilst the ones coming from the sulphur and phenolic cured systems showed high tensile strength and elongation at break, but low tension set. Intermediate values were noted with the TPV coming from the mixed cured system.

The mechanical strengths of TPVs generally depend on the type of links formed between the macromolecular chains and on the characteristics of rubber domains dispersed in the thermoplastic matrix. Generally, TPVs composed of very small rubber domains dispersed in the thermoplastic matrix show high tensile strength properties (George et al., 2000; Oommen et al., 2000). Moreover, higher degree of crosslinking in rubber phase results in higher elongation at break, and

enables to the TPV to recover its original shape after prolonged deformation (i.e., the lowest tension set).

The fact that NR/EVA TPVs coming from phenolic cured system showed the highest elongation at break followed in the order by the sulphur, the mixed, and the peroxide cured system, can be explained by the length of crosslinking bridges between NR chains in the TPV. Phenolic and sulphur cured systems lead to longer linkages in the TPV than the systems based on the use of peroxides, which provides higher chain flexibility in rubber domains and thus of the TPV.

On the other hand, NR/EVA TPVs coming from curing systems based on peroxides showed the lowest elongation at break. This may be attributed to a low density in crosslinked structures in NR domains. In addition, the crosslinking of EVA matrix induced by the peroxide, contribute also to increase the TPV rigidity on a whole. This crosslinking of EVA phase also causes the higher permanent set of the TPVs with mixed cured system and the TPV with peroxide cured system could not be determined. Therefore, the TPVs with crosslinked EVA phase showed lower elastomeric properties (i.e., high value of tension set).

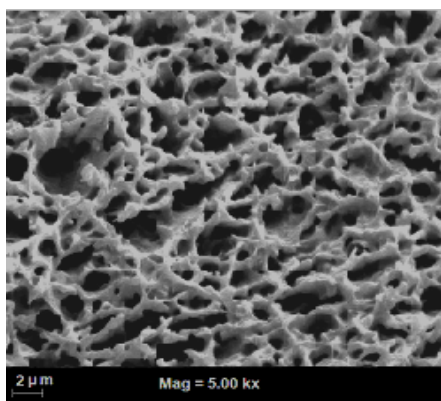
The hardness properties of the TPVs coming from 40/60 NR/EVA blends dynamically cured with various vulcanizing systems are summarized in Table 4.17. The TPVs prepared with peroxide and mixed curing systems showed a marginal increase in hardness over those coming from sulphur and phenolic curing systems. This higher hardness of the TPVs coming from curing systems based on peroxides can be again explained by the crosslinking of EVA phase that also contributes to increase the rigidity of the material.

4.8.2.6 Morphological properties

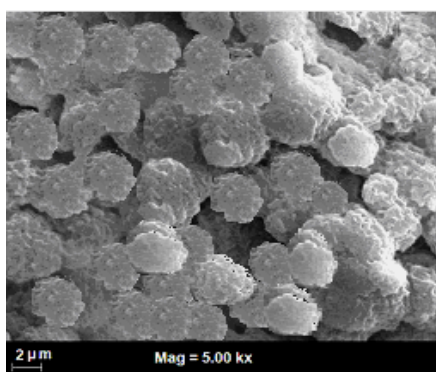
Morphological characteristics of TPVs coming from 40/60 NR/EVA blends dynamically cured with various vulcanizing systems were compared with those of uncured blend. They were investigated by cryogenic cracked and etched the fracture surface by extracting the EVA phase with tetrahydrofuran. The micrographs given in Figure 4.100, show that the uncured sample forms co-continuous phase while dynamically cured blends shows vulcanized rubber domains dispersed in the EVA matrix. That is, during dynamic vulcanization, a co-continuous morphology of EVA

and NR was transferred to a matrix and dispersed-phase morphology, respectively. This is due to the process of dynamic vulcanization performed under high shear condition and the increasing of the viscosity of rubber phase because of crosslinking reaction. It was well established that the elongation flow is dominant at this stage of mixing process (Pechurai *et al.*, 2008). As a result, the rubber phase deforms by the local extensional stress and eventually breaks down into small particles or domains. The mixing conditions also prevent re-agglomeration of the readily formed rubber domains. Therefore, fine distributions of vulcanized rubber particles in thermoplastic matrix are obtained. On the other hand, the morphologies of TPVs coming from sulphur and phenolic cured systems show rubber domains of similar size, i.e., approximately 2.9 μm , that is smaller than those of the TPVs prepared with the mixed curing system. This result can be related to the lower level of crosslinking in the NR phase in the TPV coming from the mixed cured system, because of a small amount of DCP that diffuses in the EVA phase and crosslinks it. As a result, the rubber parts in the TPV of lower viscosity form domains of larger size. In the case of the peroxide cured sample, it is difficult to identify the spherical NR domains due to the crosslinking of EVA phase.

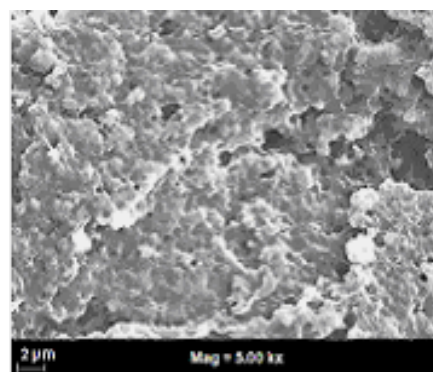
In conclusion, the oil resistance can be related to the size of NR domains dispersed in EVA matrix (Figure 4.100). TPVs with NR domains of small size show high resistance to oil, shown by their low degree of swelling in oil (George *et al.*, 1995 and 2000). This can be explained by the large contact area between the surface of vulcanized NR domains and the EVA matrix. However, the TPVs prepared with the mixed cured system showed larger dispersed rubber domains than the ones obtained with sulphur and phenolic cured systems and exhibited lower degree of swelling, which is in contradiction with the indication given above on the relation NR domain size/resistance to oil. This contradiction with the well-established previous observations, would be explained by the fact that peroxides also induce crosslinking of EVA matrix, which result is to disadvantage the oil penetration.



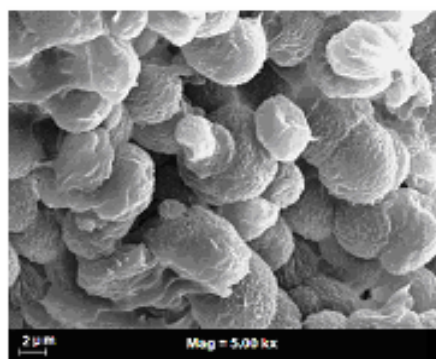
Uncured



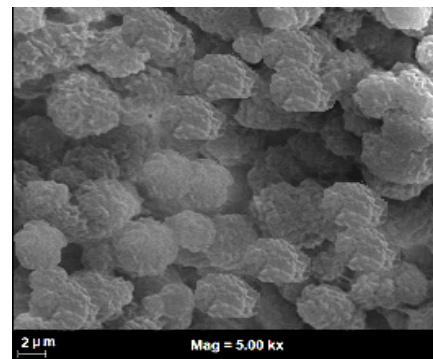
Sulphur



Peroxide



Mixed



Phenolic

Figure 4.100 SEM micrographs of uncured and dynamic cured 40/60 NR/EVA blends with various types of vulcanization systems.

4.9 Effect of different types of compatibilizers

Various types of compatibilizers (i.e., NR-g-PDMMMP, NR-g-PDMAMP, NR-g-PDMMEP, and ENR-30) with a loading level of 9 wt% of NR in dynamically cure 40/60 NR/EVA blends using sulphur cured system was studied.. Various properties of the blends were studied as follows:

4.9.1 Rheological properties

The complex viscosity as a function of frequency is shown in Figure 4.101. Also, the complex viscosity at a constant frequency of 6.25 rad/s is shown in Figure 4.102. It can be seen that the viscosity decreased with increasing frequency or shear rate (i.e., shear-thinning behavior). Furthermore, at a given frequency, the TPV without compatibilizer showed lower complex viscosity than those of the TPVs with compatibilizers. This is a result of a lower compatibility and interfacial interaction between the phases. Four types of compatibilizers (i.e., NR-g-PDMMMP, NR-g-PDMMEP, NR-g-PDMAMP and ENR-30) were studied. The graft copolymers used contained similar number of branching chains (i.e., DEDT-NR unit) and grafting length (\overline{DP}_n) of 4 mol% and 37, respectively. It can be seen that the dynamically cured 40/60 NR/EVA blend with ENR-30 gave the lowest complex viscosity while NR-g-PDMAMP, NR-g-PDMMMP and NR-g-PDMMEP gave similar higher values. This may be attributed to a presence of functional groups that could form interaction (i.e., dipole-dipole interaction). That is, the NR-g-PDMMMP, NR-g-PDMMEP and NR-g-PDMAMP molecules consist of carbonyl and phosphyl groups which can chemically bond to the blend component (i.e., EVA). Also, the graft copolymer contains the grafted segments which cause physical interaction in terms of chain entanglement while the NR backbone is capable of compatibilize with NR component. The interaction of the graft copolymers molecules cause higher strength of the blend. As a result, the complex viscosity of the blends was increased. Comparing among graft copolymers: NR-g-PDMMMP, NR-g-PDMMEP and NR-g-PDMAMP, it is clear that not much difference of complex viscosity was observed. This may be attributed to all graft copolymers contain identical functional groups (i.e., carbonyl and phosphyl groups)

and grafting chain length. On the other hand, ENR-30 molecules consist of epoxy group which should caused the interaction between the phase. However, influence of ENR on compatibility was very low because of the lower anchoring degree of the compatibilizer segments (i.e., chain entanglement) within the corresponding EVA phase. Therefore, the order of the complex viscosity can be ranked as follows: the blend without the compatibilizers < the blend with ENR-30 < the blend with NR-g-PDMMMP, NR-g-PDMMEP and NR-g-PDMAMP. This result showed the same tend as with NR/EVA blend (i.e., simple blend).

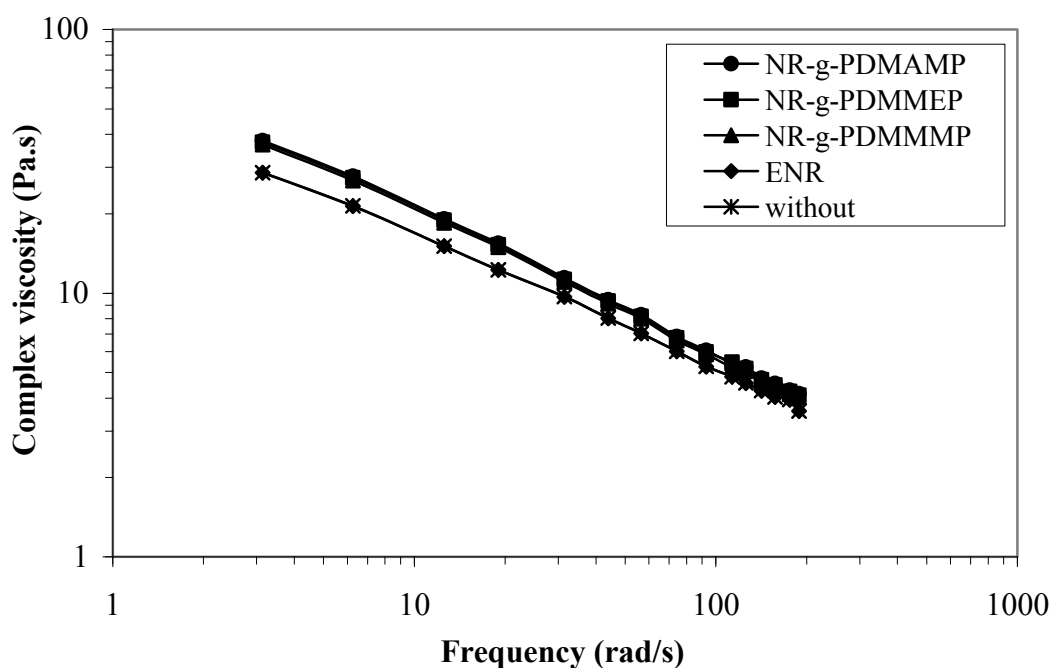


Figure 4.101 Complex viscosity as a function of frequency for the dynamically cured 40/60 NR/EVA TPVs with four types of blend compatibilizers.

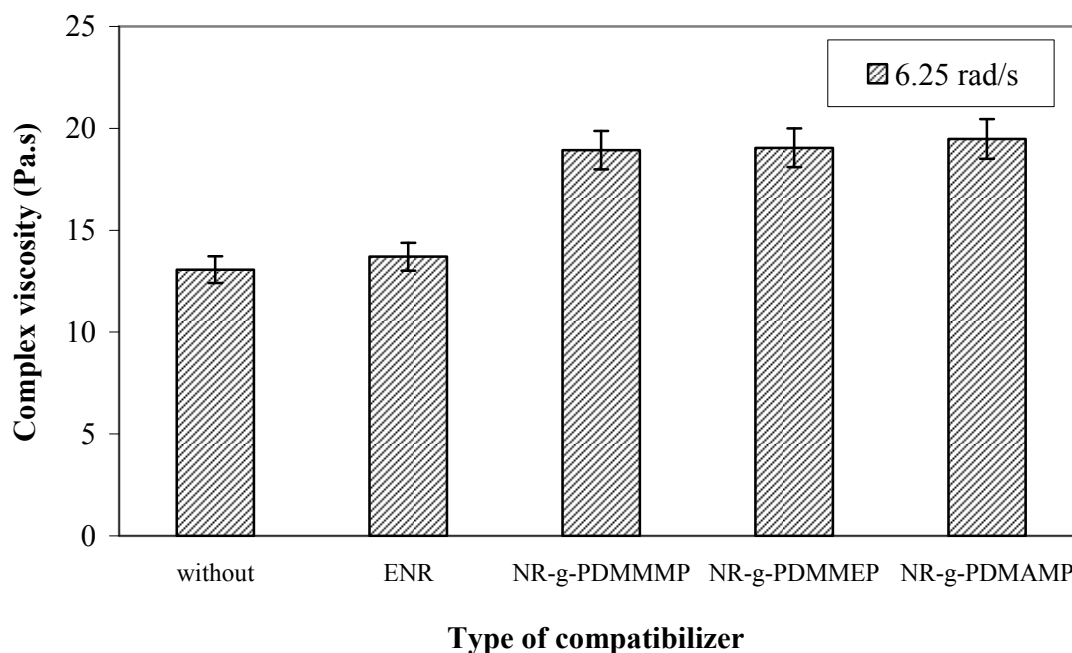


Figure 4.102 Complex viscosity at a constant frequency of 6.25 rad/s for the dynamically cured 40/60 NR/EVA TPVs with four types of blend compatibilizers.

4.9.2 Dynamic properties

Figure 4.103 shows storage modulus (G') as a function of frequency. It can be seen that all TPVs show an increase in storage modulus with increasing frequency. This is due to the decrease in time available for molecular relaxation. At a given frequency at 6 rad/s (Figure. 4.104), the storage modulus values of the TPVs with the compatibilizers are higher than the one without the compatibilizer. Comparing among four types of blend compatibilizers, it is seen that the TPVs with the NR-g-PDMMMP, NR-g-PDMMEP and NR-g-PDMAMP showed the highest and similar values of storage modulus while the TPVs with ENR-30 showed the lowest value which is similar value to the blend without compatibilizer.

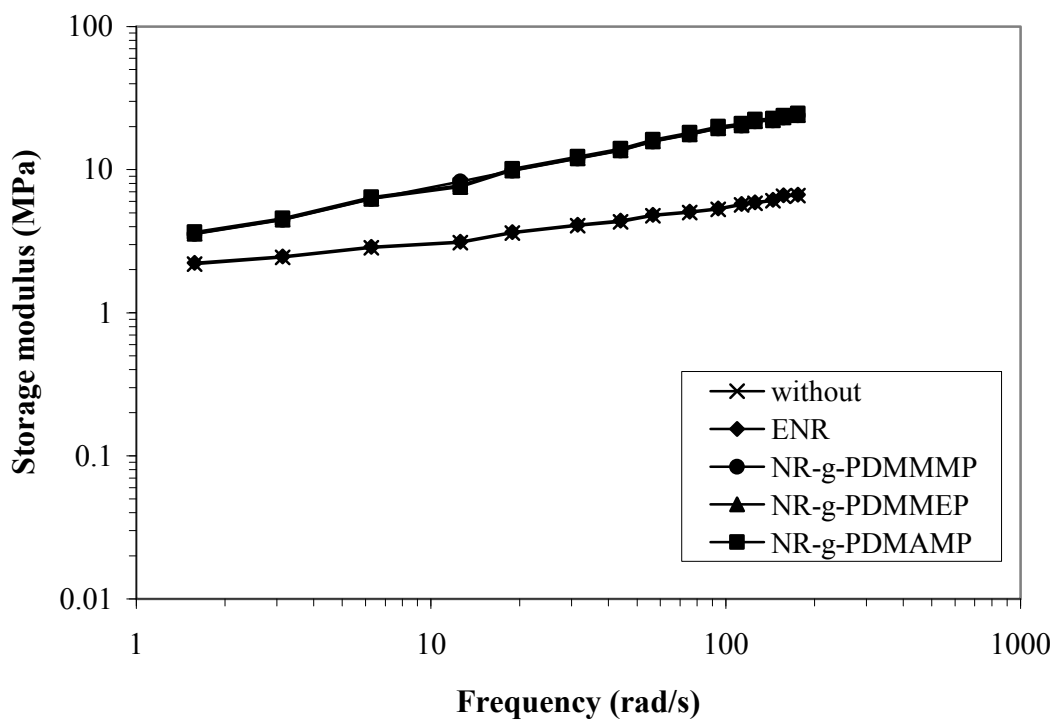


Figure 4.103 Storage modulus as function of frequency in dynamically cured 40/60 NR/EVA TPVs with four types of blend compatibilizers.

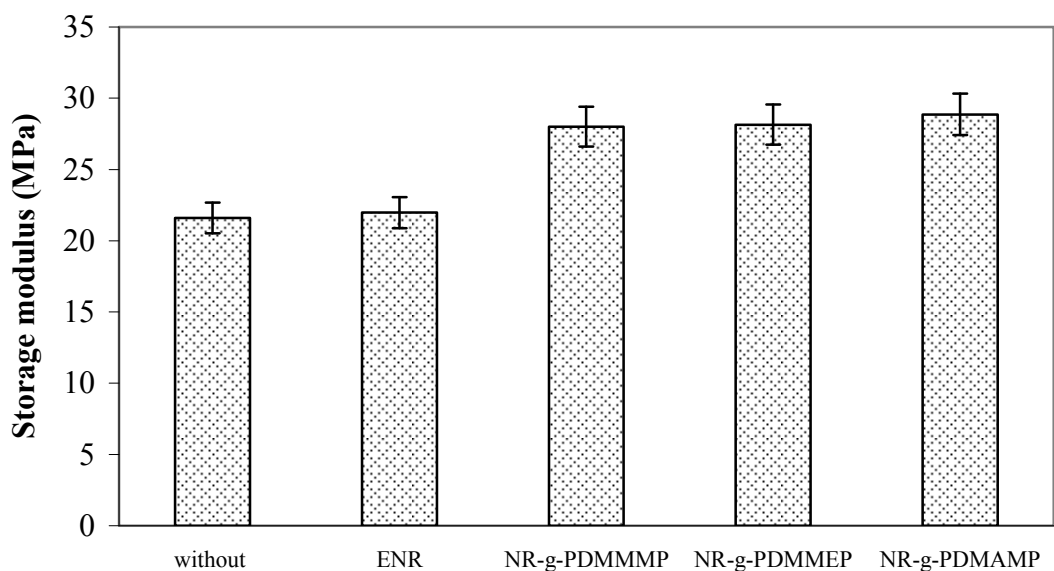


Figure 4.104 Storage modulus at a constant frequency of 6 rad/s of dynamically cured NR/EVA TPVs with four types of blend compatibilizers.

Figure 4.105 shows $\tan \delta$, which is the ratio between loss modulus to the storage modulus or the ratio of viscous to elastic properties ($\tan \delta = G''/G'$). It is seen that the TPV with the graft copolymer compatibilizer exhibited lower value of $\tan \delta$ or higher elastic response than the blend without compatibilizers and ENR-30. This is because of higher interaction and increased interfacial adhesion between NR and EVA phases. Therefore, the trend of $\tan \delta$ at a given frequency can be ordered as: TPV without the compatibilizers $>$ TPV with ENR-30 $>$ TPV with NR-g-PDMMMP, NR-g-PDMMEP and NR-g-PDMAMP.

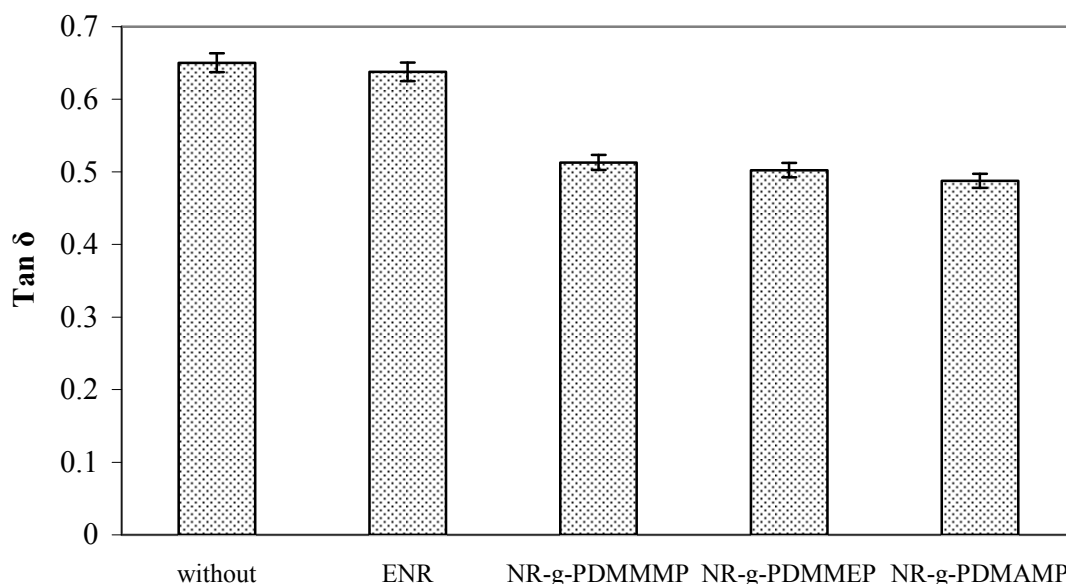
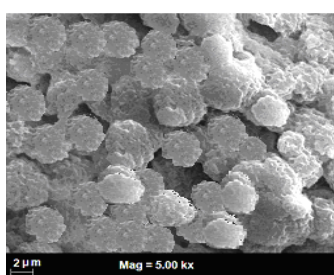


Figure 4.105 $\tan \delta$ as a function of frequency for the dynamically cured NR/EVA TPVs with four types of blend compatibilizers.

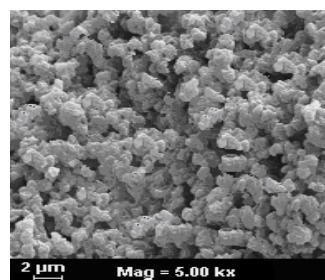
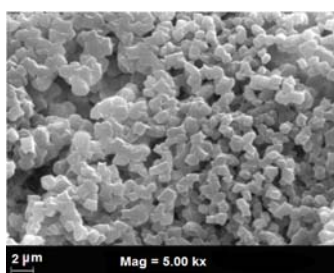
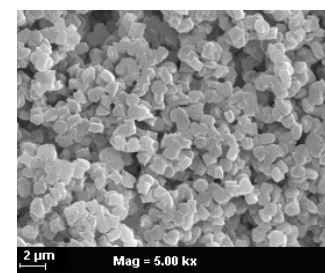
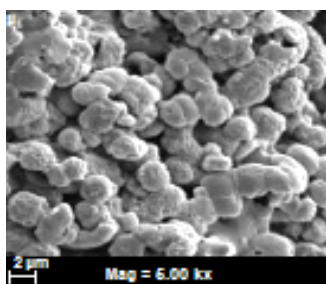
4.9.3 Morphological properties

Influence of various compatibilizers on the morphological properties of dynamically cured 40/60 NR/EVA blends is shown in Figure 4.106. It can be seen that the TPVs with NR-g-PDMMMP, NR-g-PDMMEP and NR-g-PDMAMP compatibilizer exhibited smaller phase size. On the other hand, the TPV with ENR-30 and without compatibilizer revealed a larger NR domain size than that of the TPVs with graft copolymers (i.e., NR-g-PDMMMP, NR-g-PDMMEP and

NR-*g*-PDMAMP). This may be attributed to different effectiveness of interaction between the NR-*g*-polyphosphonate groups. The NR-*g*-polyphosphonate containing molecules consist of epoxide group in rubber backbone, C=O in methacryloyloxy, P=O in phosphonate and entanglement of graft chains, while the ENR molecules consist of only epoxide group with a linear chain structure. As a result, NR-*g*-PDMAMP, NR-*g*-PDMMEP and NR-*g*-PDMAMP exhibited a superior compatibilizing efficiency.



(a) without

(b) NR-*g*-PDMAMP(c) NR-*g*-PDMAMP(d) NR-*g*-PDMMEP

(e) ENR-30

Figure 4.106 SEM micrographs of dynamically cured 40/60 NR/EVA blends: (a) without compatibilizer, (b) NR-*g*-PDMAMP, (c) NR-*g*-PDMMEP, (d) NR-*g*-PDMAMP and (e) ENR-30.

4.9.4 Mechanical properties

The stress-strain curves of dynamically cured 40/60 NR/EVA blends with four types of blend compatibilizers are given in Figure 4.107.

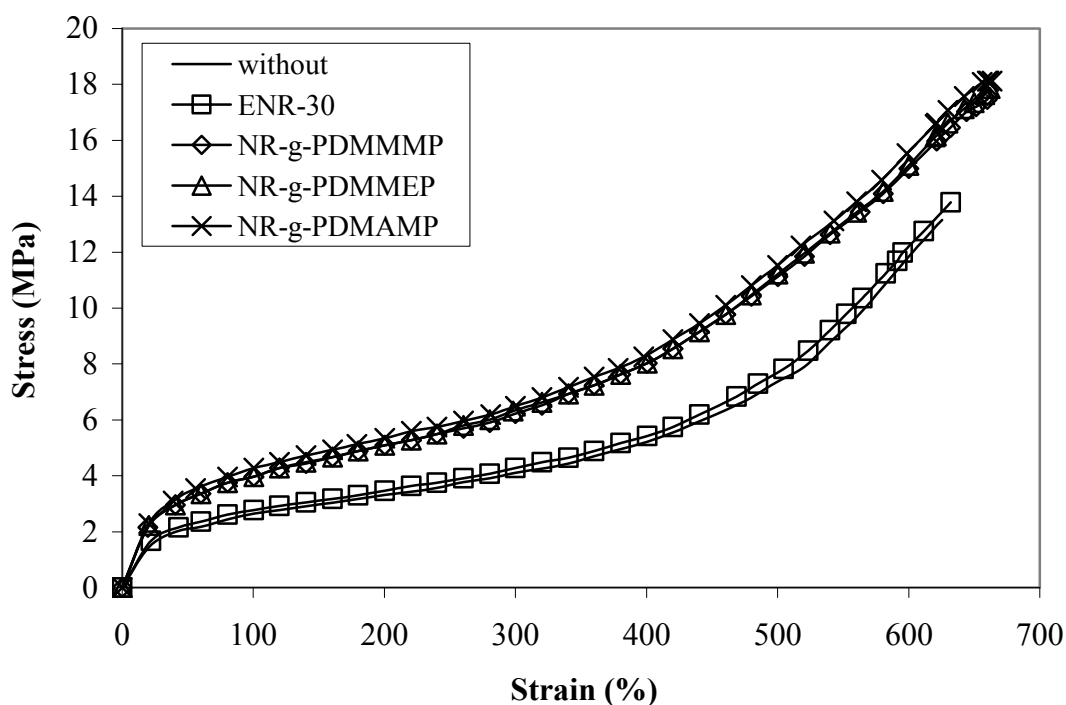


Figure 4.107 Stress-strain behaviours of dynamically cured 40/60 NR/EVA blends with different types of compatibilizers.

It can be seen that TPVs compatibilized with NR-g-polyphosphonate show similar values of the initial slope at the beginning of the curves and higher initial slope at the beginning of the curves. This reflects the value of an initial modulus and hence, stiffness of the material. In consideration of the area under the curve for toughness, the blend without compatibilizer shows the lowest value. The order of the toughness can be ranked as follows: TPV with NR-g-PDMMMP, NR-g-PDMMEP and NR-g-PDMAMP > ENR-30 > without compatibilizer. Mechanical properties in terms of tensile strength and elongation at break of the stress–strain curves in Figure 4.107 are summarized in Table 4.19.

Table 4.19 Tensile properties of dynamically cured 40/60 NR/EVA blends with different types of compatibilizers.

Type of compatibilizers	Tensile strength (MPa)	Elongation at break (%)	Tension set (%)	Hardness (Shore A)
Without	13.15	625	35	72
ENR-30	13.78	632	35	71
NR-g-PDMMMP	17.66	660	25	72
NR-g-PDMMEP	17.60	660	25	72
NR-g-PDMAMP	16.92	660	25	72

The results in Table 4.19 show that incorporation of blend compatibilizers increased the tensile strength, elongation at break and hardness. Also, the blends with compatibilizers show tendency to recover from prolonged extension (i.e., lower tension set value). This indicates high elastomeric properties which correspond to the $\tan \delta$ value in Figure 4.105. Therefore, the compatibilizers contributed to enhancing strength, toughness and set properties of the dynamically cured NR/EVA blends. Among the four types of compatibilizers used, the mechanical, hardness, and tension set properties of the TPVs with the graft copolymer containing polyphosphonate (i.e., NR-g-PDMAMP, NR-g-PDMMEP and NR-g-PDMMMP) are superior to those of the TPV with ENR-30. This is attributed to the compatibilizer molecules which are capable of linking the NR and EVA molecules with the respective blend components as described previously.

4.10 Effect of concentration of compatibilizer

Various loading levels of NR-g-PDMMMP were used in a range of 0, 1, 3, 5, 7, 9, 12 and 15 wt% in dynamically cured 40/60 NR/EVA blend. The effect of compatibilization was studied on dynamic, morphological, rheological, mechanical and thermal properties, as following:

4.10.1 Dynamic properties

Figure 4.108 shows storage modulus as a function of frequency of dynamically cured 40/60 NR/EVA blends with various loading level of NR-g-PDMMMP compatibilizer. It can be seen that storage modulus increase with the frequency. At a given frequency, as shown in Figure 4.109, it can be seen that the storage modulus increased with increasing loading levels of NR-g-PDMMMP and reach the maximum value at 9 wt% of NR-g-PDMMMP. The storage modulus thereafter decreased with increasing loading levels of the NR-g-PDMMMP. This might be attributed to the compatibilizing effect of graft copolymer (i.e., NR-g-PDMMMP) with the blend components (i.e., NR and EVA). During melt blending, the compatibilizer molecules were forced to locate at the interface of NR and EVA blend components. The non polar NR segments in the NR-g-PDMMMP molecules are wetted by the NR of the blend component, while the polar functional groups in the graft copolymer could interact with polar functional groups in EVA molecules (i.e., acetate group), as schematically shown in Figure 4.110.

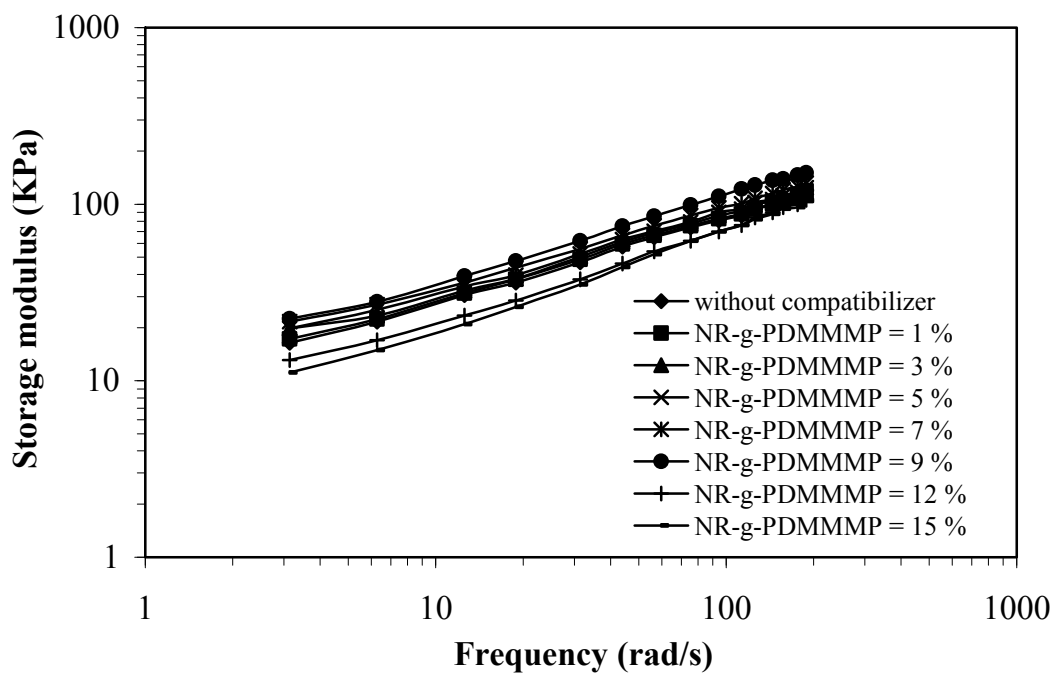


Figure 4.108 Storage modulus as a function of frequency of dynamically cured 40/60 NR/EVA blends with various loading levels of NR-g-PDMMMP compatibilizer.

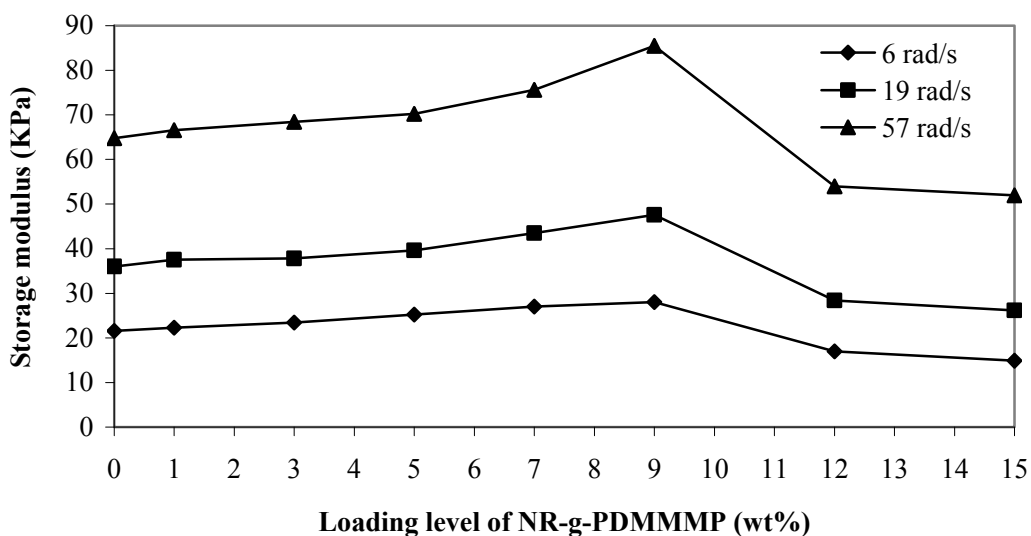


Figure 4.109 Storage modulus at a constant frequency of 6, 19 and 57 rad/s of dynamically cured 40/60 NR/EVA blends with various loading levels of NR-g-PDMMMP compatibilizer.

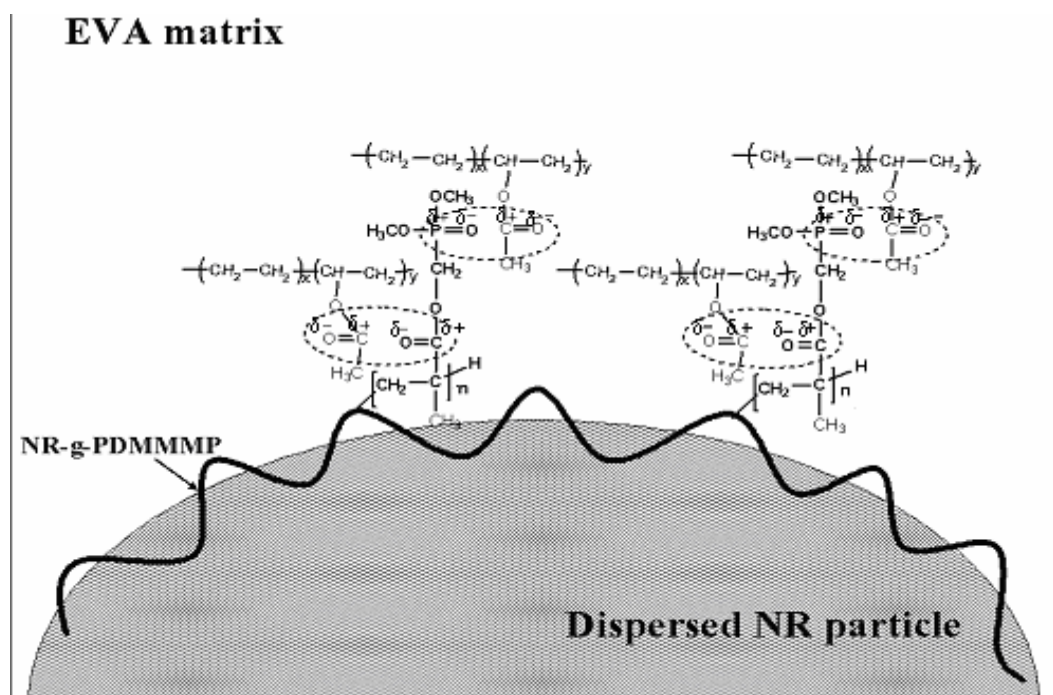


Figure 4.110 Possible interaction of graft copolymer (NR-g-PDMMMP) and natural rubber and EVA in the blend component at the interfacial area.

Interaction in forms of dipole-dipole interaction and chain entanglement of the grafted segments and EVA chains are obvious. This causes increasing trend of storage modulus with increasing loading level of the NR-g-PDMMMP compatibilizer. Decreasing trend of storage modulus in the blends with more than 9 wt% loading levels of the graft copolymer might be attributed to the fact that the quantity of NR-g-PDMMMP compatibilizer covered majority of interfacial areas and reached a critical micelle concentration (CMC). As a consequence, a formation of micelles were formed in the EVA matrix, as previously observed in the PS/EVA, NBR/PP and MNR/PP blends (Tang *et al.*, 2004; George *et al.*, 1999; Nakason *et al.*, 2006), respectively. The small droplets of micelles acted as lubricant in the blend system. A possible location of NR-g-PDMMMP compatibilizer at various loading levels in the dynamically cured NR/EVA blend is schematically shown in Figure 4.111.

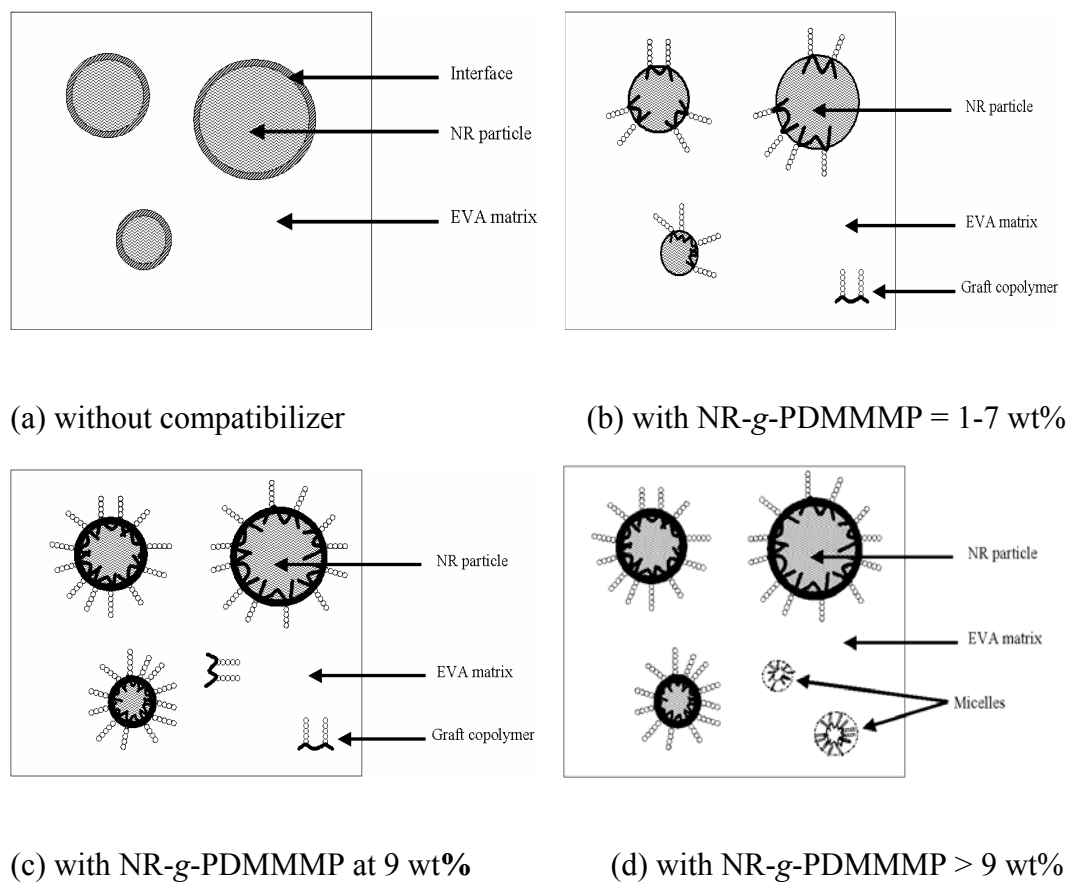


Figure 4.111 Schematic representation of a compatibilization NR-g-PDMMMP compatibilizer at the interface of NR and EVA.

It is seen that the addition of NR-g-PDMMMP in a range of 1-7 wt% caused an increase of the modulus due to a gradually increasing coverage of the interfacial area and hence an increase of the interfacial adhesion between the two phases (Figure 4.111b). However, the interface was not fully occupied as in the case of a loading level of NR-g-PDMMMP at 9 wt% (Figure 4.111c). In the case loading levels of NR-g-PDMMMP greater than 9 wt% (Figure 4.111d), the interface was also fully occupied but the excess amount of the NR-g-PDMMMP caused a formation of micelles. Similar phenomenon was observed in the PP/NBR blends (George *et al.*, 1999). Furthermore, in the maleated natural rubber (MNR)/PP blends with PP-g-MA and Ph-PP compatibilizers, the micelle formation was also observed in the blends with high concentration of compatibilizer (i.e., 10, 15 and 20 wt%) (Nakason *et al.*, 2006). Figure 4.112 shows $\tan \delta$ at given constant frequencies as a function of loading levels of NR-g-PDMMMP compatibilizer. The $\tan \delta$ or loss

tangent is the ratio of loss (G'') to storage modulus (G'). It is seen that the $\tan \delta$ first decreased with increasing concentration of the NR-g-PDMMMP compatibilizer until reaching the lowest value at a loading level of compatibilizer of 9 wt%. It thereafter increased when increasing loading levels of the compatibilizer greater than 9 wt%. At a loading level of NR-g-PDMMMP of 9 wt%, the lowest value of $\tan \delta$ was observed because the highest interaction between NR and EVA and hence the TPV exhibited the highest elastic modulus and complex viscosity but the lowest $\tan \delta$.

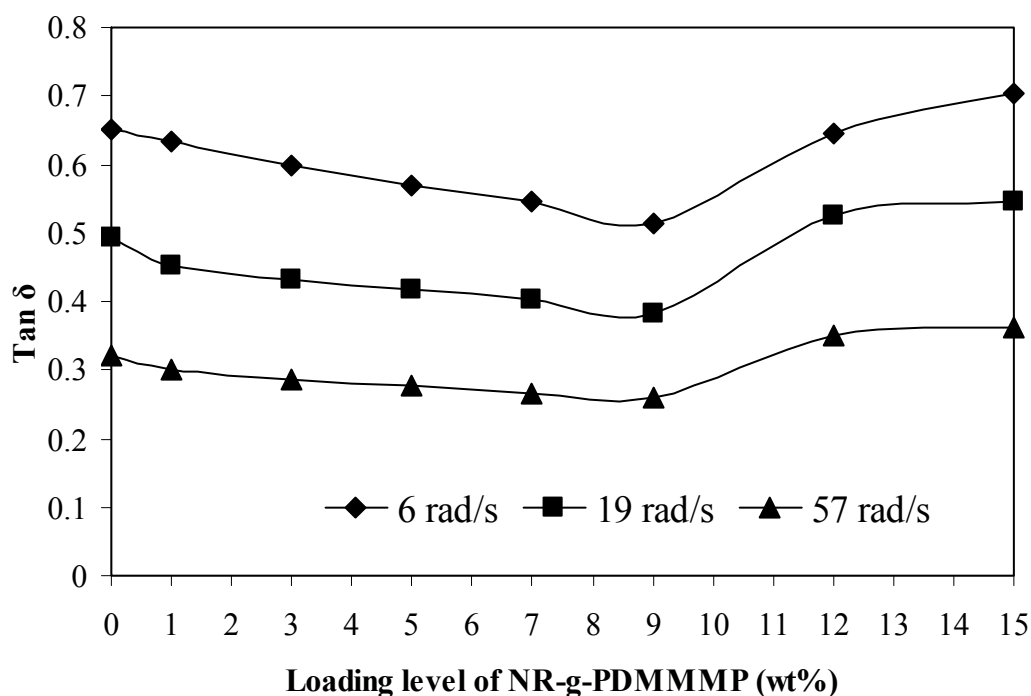


Figure 4.112 $\tan \delta$ at a constant frequencies of 6, 19 and 57 rad/s of dynamically cured 40/60 NR/EVA blends with various loading levels of NR-g-PDMMMP compatibilizer.

4.10.2 Rheological properties

The complex viscosity as a function of frequency of dynamically cured 40/60 NR/EVA blends with various loading levels of NR-g-PDMMMP blend compatibilizer are given in Figure 4.113. It can be seen that complex viscosity decreased when increasing frequency, i.e., shear-thinning behavior. At a given frequency, as shown in Figure 4.114, the complex viscosity increased slightly until reaching the maximum value at a loading level of NR-g-PDMMMP of 9 wt%. The complex viscosity was thereafter decreased when increasing loading level of NR-g-PDMMMP higher than 9 wt%. These results correlated well with the storage modulus as a function of frequency and loading levels of NR-g-PDMMMP in Figures 4.109 and 4.110, respectively. This confirms the interaction between the NR and EVA by compatibilizing effect of the NR-g-PDMMMP compatibilizer.

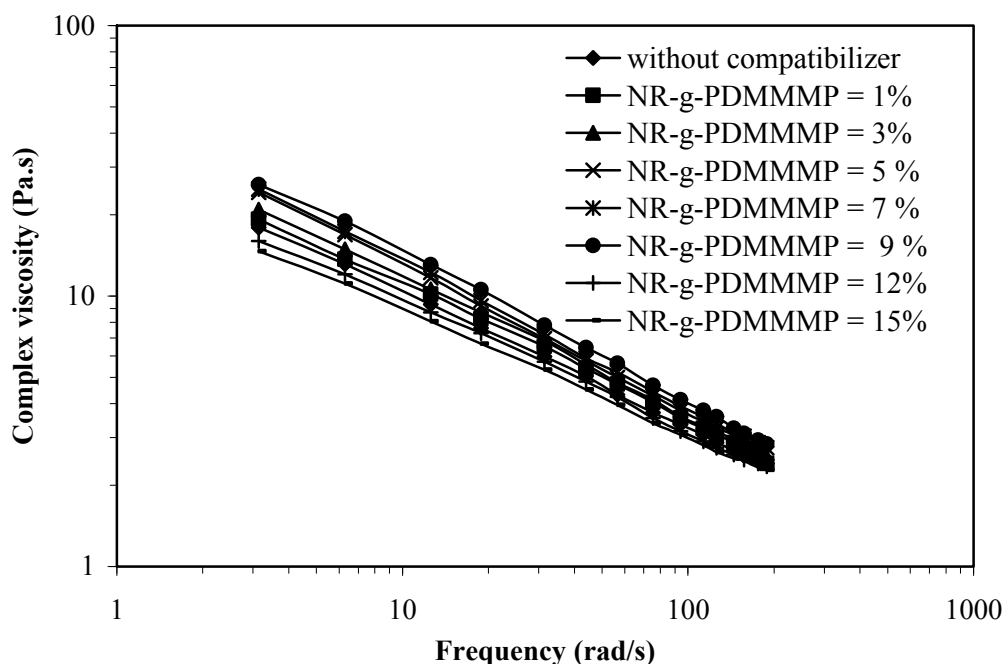


Figure 4.113 Complex viscosity as a function of frequency of dynamically cured 40/60 NR/EVA blends with various loading levels of NR-g-PDMMMP compatibilizer.

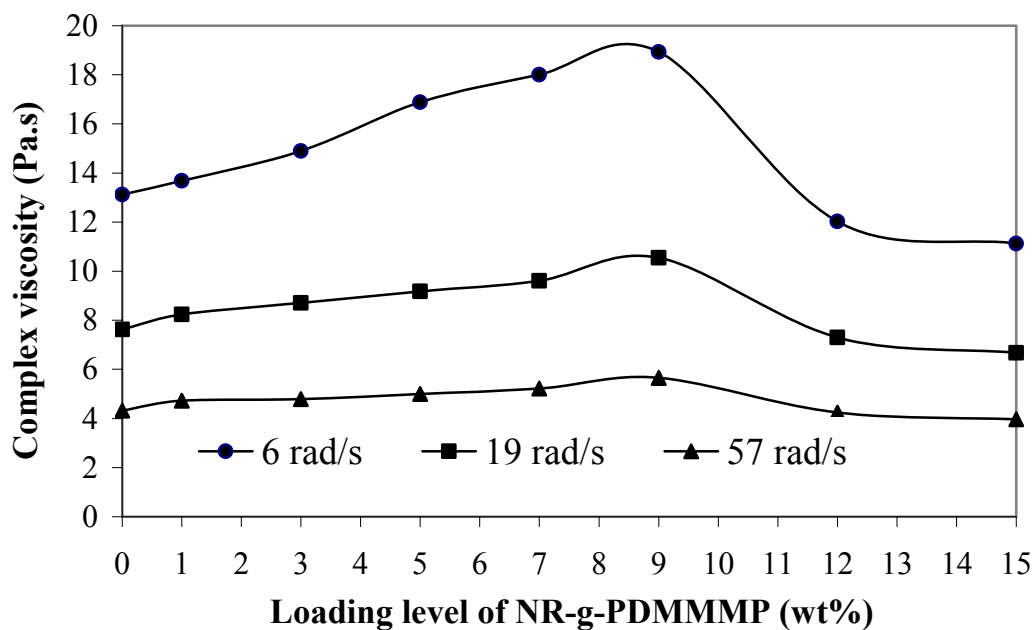
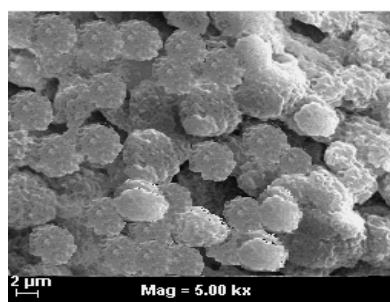


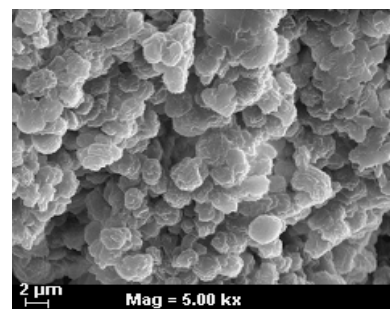
Figure 4.114 Complex viscosity at a constant frequencies of 6, 19 and 57 rad/s of dynamically cured 40/60 NR/EVA blends with various loading levels of NR-g-PDMMMP compatibilizer.

4.10.3 Morphological properties

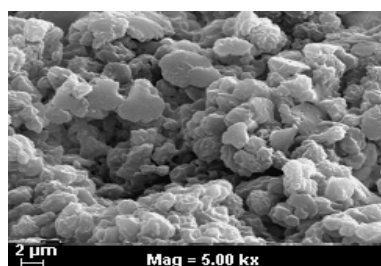
To confirm influence of loading levels of NR-g-PDMMMP compatibilizer on trends of storage modulus and complex viscosity, morphological properties of dynamically cured 40/60 NR/EVA blends were investigated by SEM with cryogenic cracked and etched surface by extracting the EVA phase with tetrahydrofuran, as the SEM micrographs shown in Figure 4.115.



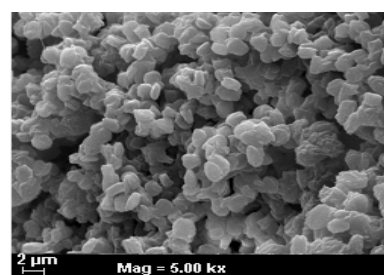
(a) without compatibilier



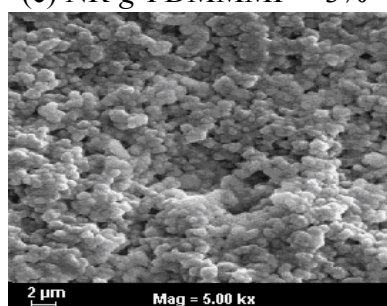
(b) NR-g-PDMMMP = 1



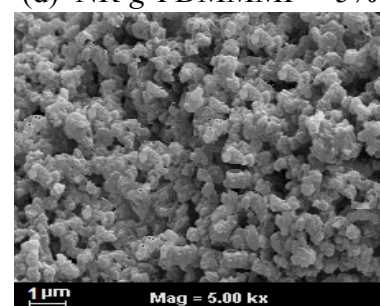
(c) NR-g-PDMMMP = 3%



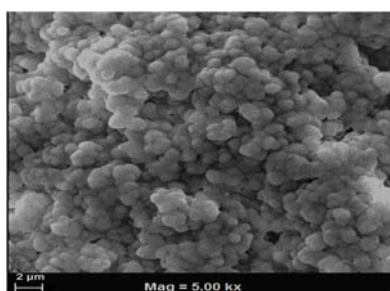
(d) NR-g-PDMMMP = 5%



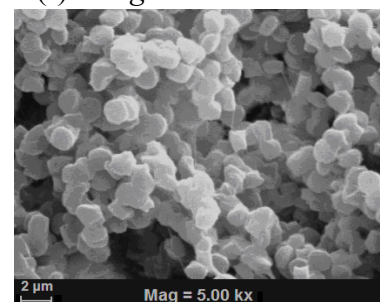
(e) NR-g-PDMMMP = 7%



(f) NR-g-PDMMMP = 9%



(g) NR-g-PDMMMP = 12%



(h) NR-g-PDMMMP = 15%

Figure 4.115 SEM micrographs of dynamically cured 40/60 NR/EVA blends: (a) without compatibilizer, (b) with NR-g-PDMMMP = 1%, (c) with NR-g-PDMMMP = 3%, (d) with NR-g-PDMMMP = 5%, (E) with NR-g-PDMMMP = 7%, (f) with NR-g-PDMMMP = 9%, (g) with NR-g-PDMMMP = 12% and (h) with NR-g-PDMMMP = 15%.

It is seen that the spherical vulcanized rubber domains remained undissolved and adhered at the surfaces. Also, the two phase morphology of micron scale vulcanized NR particles dispersed in the EVA matrix are confirmed. It can be seen that size of vulcanized rubber domains of the dynamically cured NR/EVA blends without compatibilizer are the largest with average particle size of approximately 2.9 μm (Figure 4.115a). Incorporation of the NR-g-PDMMMP compatibilizer caused a decrease of the size of the dispersed vulcanized rubber domains to average diameter at approximately 2.6, 2.4, 1.6, 0.7 and 0.3 μm for the blends with loading levels of the compatibilizer at 1, 3, 5, 7 and 9 wt%, respectively (Figure 4.115b-f). The smallest vulcanized rubber domains (i.e., approximately of 0.3 μm) were observed in the dynamically cured NR/EVA blend with a loading level of graft copolymer at 9 wt%. Increasing loading level of NR-g-PDMMMP higher than 9 wt% to 12 and 15 wt% (Figure 4.115g-4.115h) caused an increase of the size of vulcanized rubber domains to approximately 0.5 and 0.7, respectively. Therefore, average diameter of the dispersed NR particles could correlate negatively to the trend of complex viscosity at a given frequency of 6.28 rad/s., as shown in Figure 4.116.

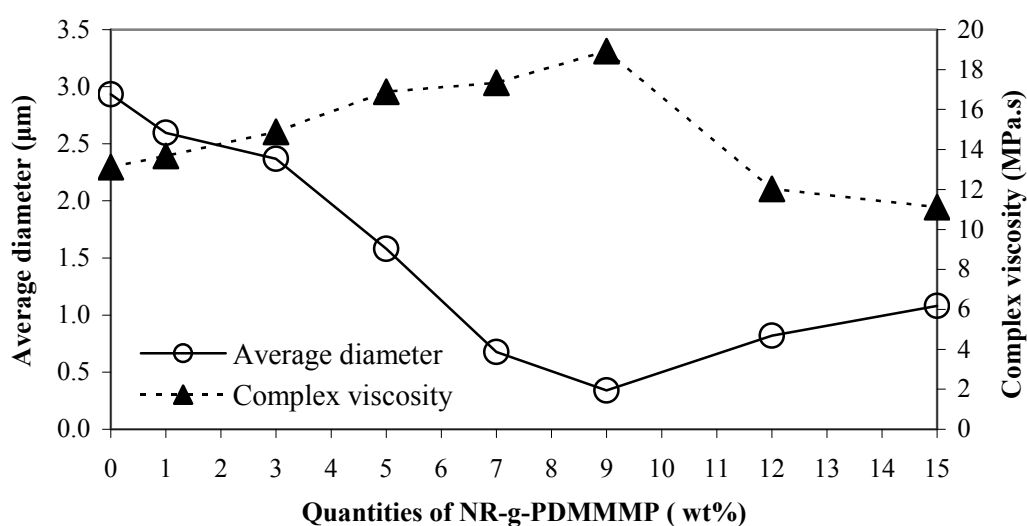


Figure 4.116 Relationship between average diameter of vulcanized rubber domains and complex viscosity at a frequency of 6 rad/s of dynamically cured 40/60 NR/EVA blends with various loading levels of NR-g-PDMMMP compatibilizer.

It can be seen that the complex viscosity increased with the decreasing of the size of vulcanized rubber domains dispersed in the EVA matrix until reached the maximum value at a loading level of NR-g-PDMMMP of 9 wt% where the smallest particles were observed. This proved the highest interaction between rubber and EVA phases. That is, the graft copolymer acted as an interfacial agent and caused a reduction of the size of the dispersed rubber particles.

4.10.4 Mechanical properties

Figure 4.117 shows stress–strain curves of dynamically cured 40/60 NR/EVA blends with various loading levels of NR-g-PDMMMP compatibilizer. It is seen the Young's modulus (i.e., slope at the initial linear region of the curves) of the blends increased with concentration of NR-g-PDMMMP compatibilizer and reached its maximum value at a loading level of 9%wt. This corresponds to the trend of storage modulus (Figure 4.109) and complex viscosity (Figure 4.114) due to the highest compatibilizing effect with this loading level of the blend compatibilizer, as described previously. Mechanical properties in terms of ultimate tensile strength, elongation at break, tension set and hardness of the dynamically cured 40/60 NR/EVA blends are summarized in Table 4.20.

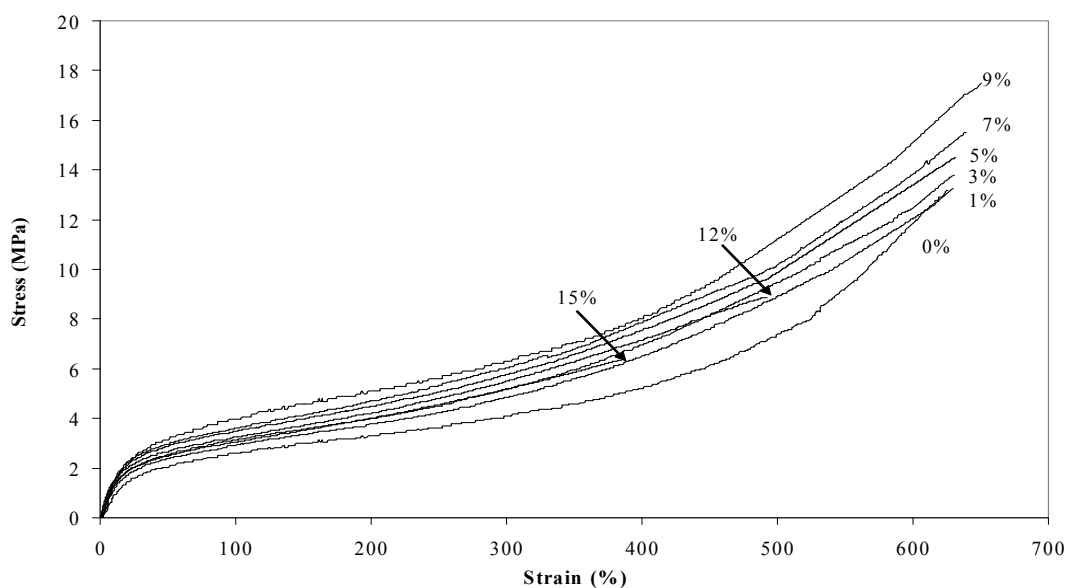


Figure 4.117 Stress-strain behaviours of dynamically cured 40/60 NR/EVA blends with various quantities of NR-g-PDMMMP.

Table 4.20 Mechanical properties of 40/60 NR/EVA blends with various quantities of NR-*g*-PDMMMP.

Loading level of NR- <i>g</i> -PDMMMP (wt%)	Tensile strength (MPa)	Elongation at break (%)	Tension set (%)	Hardness (Shore A)
0	13.15	625	35	72
1	13.25	629	33	72
3	13.80	630	33	71
5	14.50	635	31	72
7	15.53	639	30	72
9	17.65	660	27	72
12	8.88	492	31	72
15	6.34	385	32	72

It can be seen that the blend with a loading level of NR-*g*-PDMMMP compatibilizer at 9 wt% exhibited the highest tensile strength and elongation at break (i.e., 17.65 MPa and 660%, respectively) with the lowest value of the tension set and similar value of hardness compared with other type of blend. The lowest value of tension set revealed the highest tendency to recover to its original shape after prolonged extension of the material. This corresponds to the lowest value of the $\tan \delta$ (Figure 4.112) which revealed the highest elasticity of the material. Therefore, the optimum loading level of the blend compatibilizer was confirmed at a loading level of 9 wt%, as evidenced from the highest mechanical strength due to the highest interaction between different phases. As a consequence, smaller dispersed vulcanized rubber domains (Figures 4.115 and 4.116) were observed and caused higher interfacial

adhesion. In Table 4.20, it is also seen that the blend without compatibilizer exhibited poorer mechanical strength than that of the compatibilized blends. Increasing loading level of the blend compatibilizer in a range of 1 to 9 wt% caused an increasing trend of tensile strength because of the increase of interfacial force between the phases due to the blend compatibilizer. However, when increasing concentration of the blend compatibilizer higher than the optimum dose (i.e., 9 wt%), a decreasing trend of the tensile strength and elongation at break were observed due to the formation of micelles from excess amount of NR-*g*-PDMMMP in the blend system, as described in Figure 4.111.

4.10.5 Thermal behaviour

Figure 4.118 shows DSC thermograms of dynamically cured 40/60 NR/EVA blends and their parent polymer pairs (i.e., pure EVA and pure NR). Single glass transition temperature (T_g) at low temperature was observed in pure NR at approximately -60.3°C . In the pure EVA two glass transition temperatures corresponding to polyethylene and poly(vinyl acetate) segments should be observed. However, in this work a single T_g was observed at approximately at -22.8°C . The crystalline melting temperature of the pure EVA was also clearly observed. In the dynamically cured 40/60 NR/EVA blends, two glass transition temperatures corresponding to NR and EVA components were observed, as summarized in Table 4.21. It is clear that the dynamically cured 40/60 NR/EVA blend without compatibilizer also showed two values of T_g which were very similar to those of each blend component (i.e., NR and EVA). This indicates very low interaction between the EVA and NR phase. However, in the blend with compatibilizer, slight shift of T_g of rubber and plastic phase toward each other (i.e., shift to higher temperature for the rubber phase and lower temperature for plastic phase) was observed. It is also found that the higher shift of T_{gs} was observed in the blend with 9 wt% compatibilizer indicating the highest interaction between the phase. This evidence of interaction between the blend component correlates well with higher storage modulus (Figure 4.109), complex viscosity (Figure 4.114), mechanical

strength (Table 4.19) and smaller size of the vulcanized rubber domains (Figure 4.115) of the blend with 9 wt% of NR-g-PDMMMP compatibilizer.

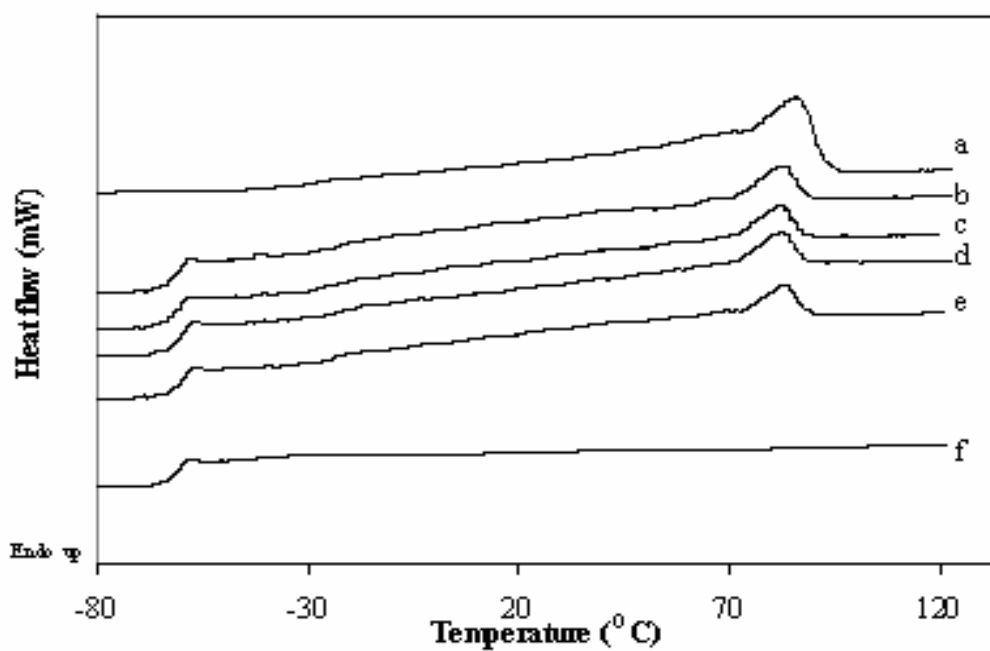


Figure 4.118 DSC thermograms of (a) EVA, (b) 40/60 NR/EVA without NR-g-PDMMMP, (c) 40/60 NR/EVA with 5 wt% of NR-g-PDMMMP, (d) 40/60 NR/EVA with 9 wt% of NR-g-PDMMMP, (e) 40/60 NR/EVA with 15 wt% of NR-g-PDMMMP, (f) NR.

Table 4.21 Glass transition temperature (T_g) of pure EVA, pure NR and their blends with various loading levels of NR-g-PDMMMP.

Sample	T_g (°C) NR phase	T_g (°C) EVA phase
Pure EVA	-	-22.8
NR/EVA blend without compatibilizer	-60.3	-22.7
NR/EVA blend with 5% of NR-g-PDMMMP	-59.3	-22.2
NR/EVA blend with 9% of NR-g-PDMMMP	-58.7	-21.8
NR/EVA blend with 15% of NR-g-PDMMMP	-59.5	-22.1
Pure NR	-60.3	-

Table 4.22 shows heat of fusion (ΔH), degree of crystallinity (X_i) and crystalline melting temperature (T_m) of EVA phase in the pure EVA and dynamically cured 40/60 NR/EVA blends with various quantities of NR-g-PDMMMP compatibilizer. EVA with vinyl acetate content of 18 wt% showed heat of fusion of 62.2 J/mol and degree of crystallinity of 22.4%. It is clear that the EVA in the dynamically cured 40/60 NR/EVA blends exhibited lower heat of fusion, degree of crystallinity and crystalline melting temperature than its one (pure EVA). Increasing loading level of NR-g-PDMMMP compatibilizer caused decreasing trend of heat of fusion, degree of crystallinity and crystalline melting temperature. This might cause a decrease of mechanical strength of the material. However, the dynamically cured 40/60 NR/EVA blend with a loading level of NR-g-PDMMMP of 9 wt% exhibited the highest strength. This might be attributed to the fact that the compatibilizing effect play an higher influence on the overall properties of the blends than on the degree of crystallinity of the EVA matrix phase.

Table 4.22 The melting temperature (T_m), degree of crystallinity (X_i) and heat of fusion (ΔH) of EVA phase in EVA and in 40/60 NR/EVA blends with various quantities of NR-*g*-PDMMMP.

Sample	ΔH (J/mol)	Degree of crystallinity (%)	T_m (°C)
EVA	62.2	22.4	86.5
40/60 NR/EVA	34.1	12.3	84.7
40/60 NR/EVA + 5 % NR- <i>g</i> -PDMMMP	31.5	11.4	84.8
40/60 NR/EVA + 9 % NR- <i>g</i> -PDMMMP	28.6	10.3	84.9
40/60 NR/EVA + 15 % NR- <i>g</i> -PDMMMP	27.5	9.9	84.7
NR	-	-	-

4.10.6 Thermal stability

Thermal stability of dynamically cured 40/60 NR/EVA blends with various loading levels of NR-*g*-PDMMMP compared with pure NR and EVA was characterized by TGA under nitrogen atmosphere, as thermograms shown in Figure 4.119. The onset degradation temperature and char residue of pure NR, EVA and dynamically NR/EVA blends are summarized in Table 4.23.

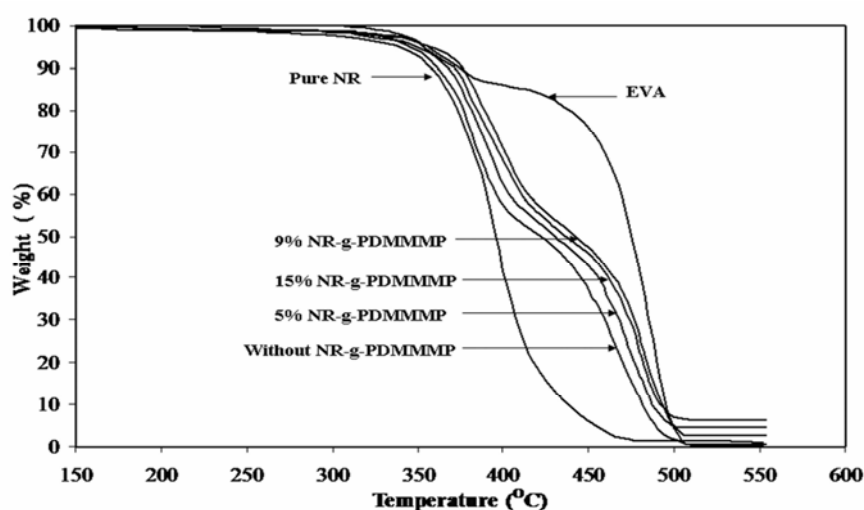


Figure 4.119 TGA thermograms of NR, EVA and 40/60 dynamically cured NR/EVA blends with different loading levels of NR-g-PDMMMP compatibilizer.

Table 4.23 TGA data of NR, pure EVA, and dynamically cured 40/60 NR/EVA blend without and with 5, 9 and 15 wt% of NR-g-PDMMMP 80% compatibilizer.

Sample	Onset temperature (°C)		Weight loss (%)		Char (%)
	1 st step	2 nd step	1 st step	2 nd step	
NR	324	-	98.9	-	1.1
EVA	335	395	17.8	82.1	0.01
NR/EVA with 0 % NR-g-PDMMMP	331	432	40.0	59.3	0.7
NR/EVA with 5 % NR-g-PDMMMP	338	440	39.1	58.4	2.5
NR/EVA with 9 % NR-g-PDMMMP	368	445	38.7	56.6	4.7
NR/EVA with 15% NR-g-PDMMMP	366	442	38.8	54.9	6.3

It is seen that pure NR showed only single step of weight loss with an onset temperature of approximately 324°C with a total weight loss of approximately 98.9%. That is, approximately 1 wt% char residue remained above 500°C indicated insoluble and intractable materials which might be linked to the cyclized rubber (Asaletha *et al.*, 1998). On the other hand, the TGA curve of EVA exhibited double degradation stages where the first stage occurred at higher onset temperature of

approximately 335°C with the weight loss of 17.8%. This is attributed to the degradation of poly(vinyl acetate) segments in the EVA. The second degradation stage occurred with an onset temperature of approximately 437°C with a total weight loss of 82.1%. This corresponds to the degradation of the polyethylene segments in the EVA. In the dynamically cured 40/60 NR/EVA blends without and with various loading levels of NR-*g*-PDMMMP compatibilizer, the double degradation stages were also observed. The degradation of the blend without compatibilizer occurred at lower onset temperatures of 331 and 432°C and higher total weight loss of 40.0 and 59.3% for the 1st and 2nd degradation stages, respectively. Among the dynamically cured 40/60 NR/EVA blends, the material with a loading level of NR-*g*-PDMMMP compatibilizer of 9 wt% exhibited the highest onset temperatures at 368 and 445°C with the low values of the weight loss at 38.7 and 56.6% for the 1st and 2nd degradation stages, respectively. The increase of onset degradation temperature of the blend with compatibilizer might be due to the ability of dimethylphosphonate functionalized grafts to improve thermal stability of the NR/EVA blend. With this reason, the blend with 15 wt% of NR-*g*-PDMMMP compatibilizer should give higher degradation temperature. However, in Figure 4.119 and Table 4.22, it is clear that this type of blend showed lower degradation temperature than that of the blend with the NR-*g*-PDMMMP at 9 %wt. Hence, this phenomena occurred because of a greater compatibilizing effect of NR-*g*-PDMMMP in NR/EVA blends. Concerning the remaining residues, it was noted that the whole NR was almost degraded at 500°C.

On the other hand, the proportions in carbonaceous residues (or char) observed at this temperature in the case of degradation of NR/EVA blends always increase with the loading level of NR-*g*-PDMMMP showing heat stability of the phosphorus compound.

4.11 Recyclability of dynamically cured NR/EVA blends

Dynamically cured 40/60 NR/EVA blends with a loading level of 9 wt% of NR-g-PDMMMP compatibilizer was reprocessed for 5 cycles. Mechanical and morphological properties of virgin and recycled compatibilized and uncompatibilized TPVs were investigated.

4.11.1 Mechanical properties

Stress-strain behaviours of uncompatibilized and compatibilized recycled dynamically cured 40/60 NR/EVA blends compared with the virgin material are given in Figures 4.120 and 4.121, respectively. It can be seen that the compatibilized recycled dynamically cured 40/60 NR/EVA blends showed smaller change of the initial slope and area under the curves than those of the uncompatibilized recycled ones.

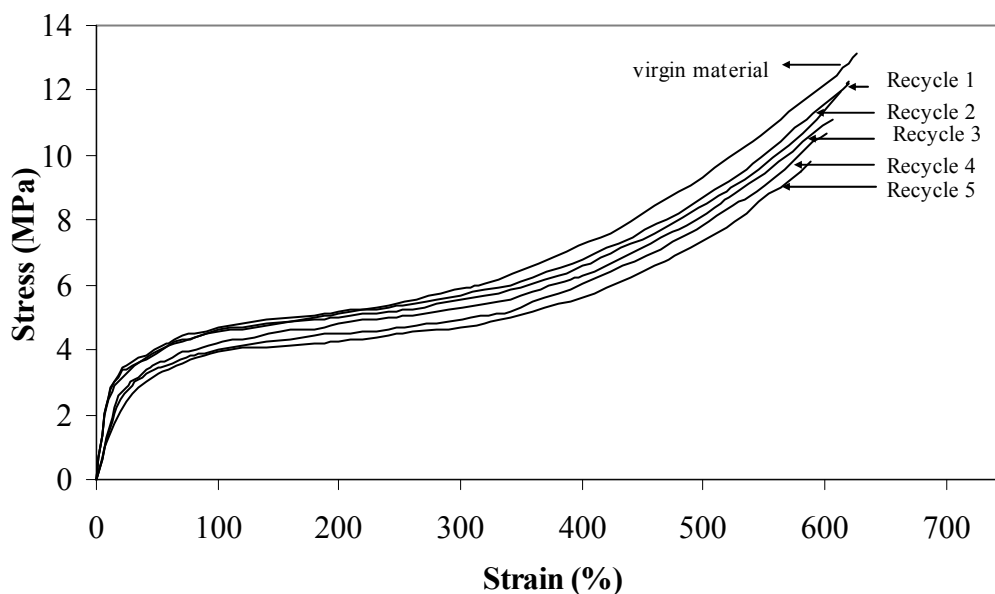


Figure 4.120 Stress-strain behaviours of uncompatibilized recycled dynamically cured 40/60 NR/EVA blends compared with the virgin material.

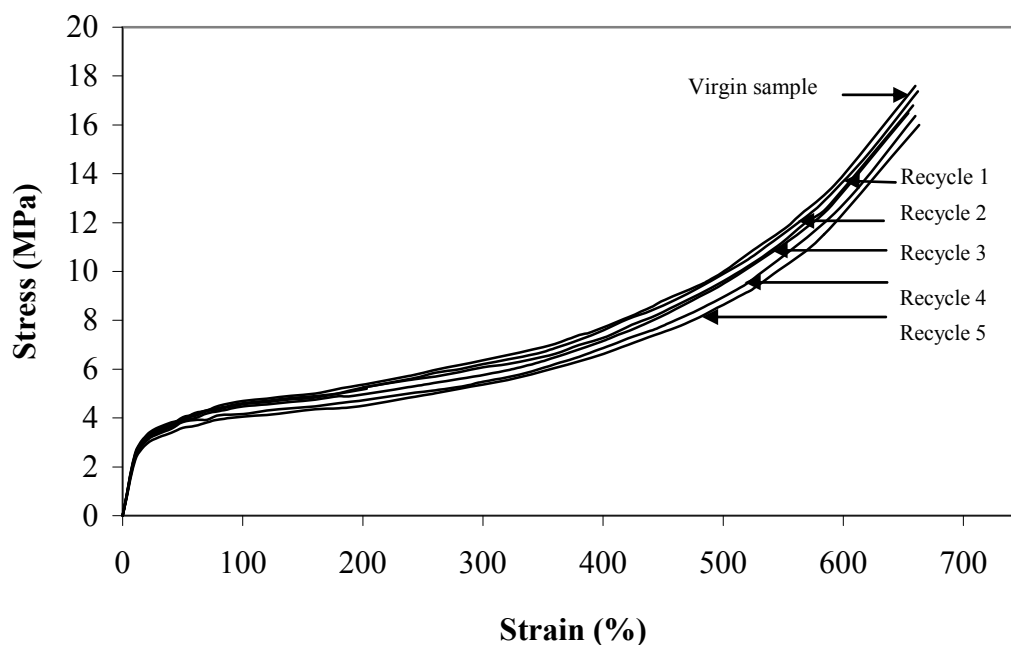


Figure 4.121 Stress-strain behaviours of compatibilized recycled dynamically cured 40/60 NR/EVA blends compared with the virgin material.

Figures 4.122 and 4.123 show tensile strength and hardness of virgin and recycled dynamically cured 40/60 NR/EVA blends with and without NR-g-PDMMMP. It is seen that the strength and hardness properties decreased when increasing the numbers of re-process cycles. This is caused by a degradation of the blend components due to heat and mechanical shearing during reprocess at high temperature. Comparing between dynamically cured 40/60 NR/EVA blends with and without NR-g-PDMMMP compatibilizer, it is clear that the compatibilized blend showed lower gradient or slope of decrease trend of tensile strength and hardness. Figures 4.124 and 4.125 show elongation at break and tension set of recycled dynamically cured NR/EVA blends with and without the graft copolymer. It is clear that a slight decreasing trend of elongation at break and of tendency to recover to the original shape after extension (i.e., increasing trend of tension set) were observed. However, the TPVs without blend compatibilizer show higher gradient of decrease of elongation at break and of increasing trend of tension set. This may be due to a layer of NR-g-PDMMMP which covers around the dispersed

vulcanized rubber domains and caused higher interaction between interfaces which were harder to destroy by heat and shearing action. Also, the coalescence of the rubber domains is suppressed while uncompatibilized blends tend to form phase coalescence during mixing and fabrication processes. The coalescence of dispersed particles and lower interaction leads to poor mechanical properties of the TPVs.

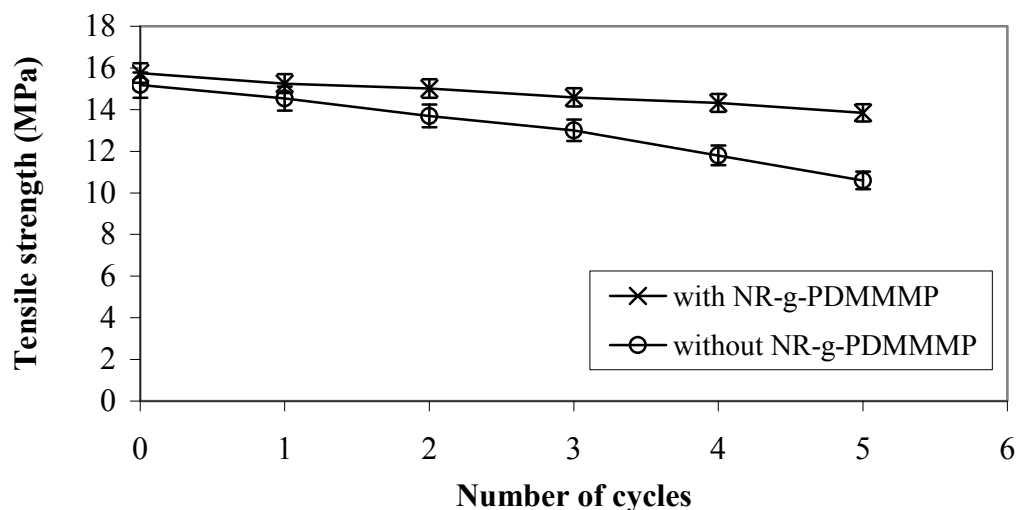


Figure 4.122 Tensile strength of uncompatibilized and compatibilized recycled dynamically cured 40/60 NR/EVA blends compared with the virgin material.

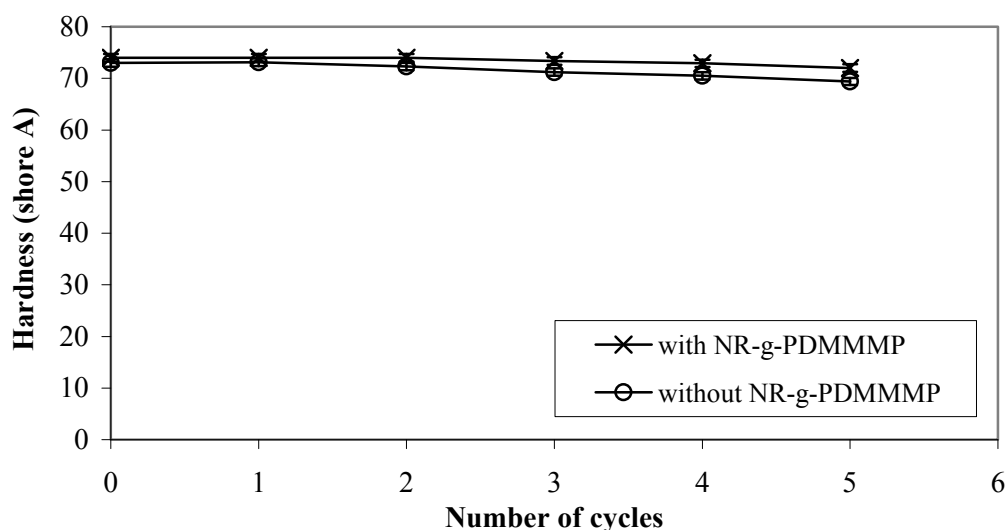


Figure 4.123 Hardness of uncompatibilized and compatibilized recycled dynamically cured 40/60 NR/EVA blends compared with the virgin material.

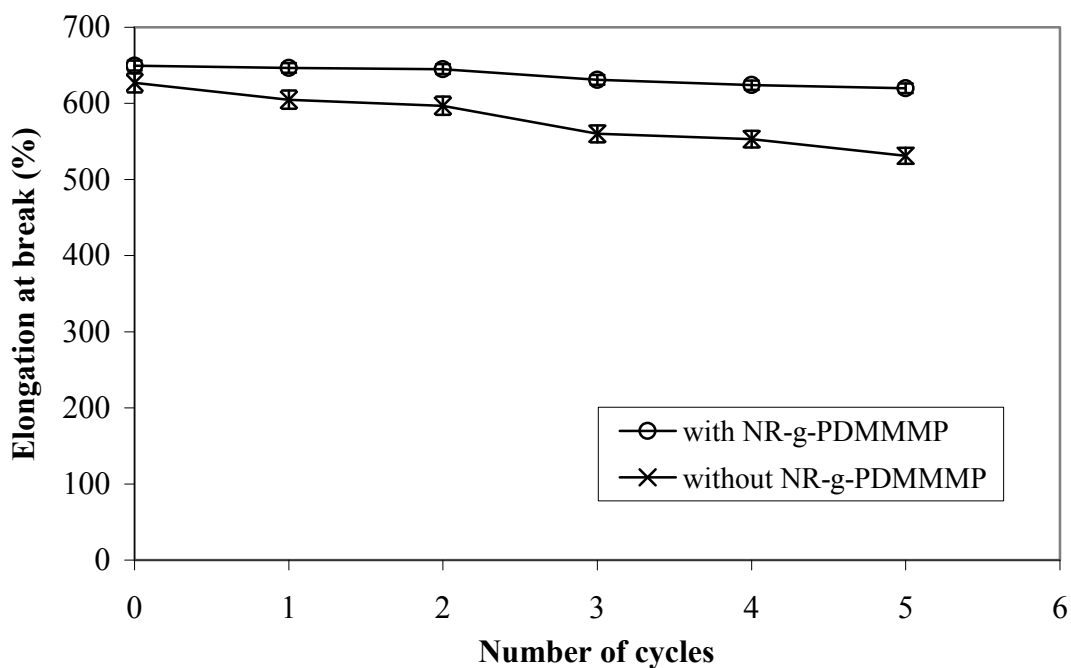


Figure 4.124 Elongation at break of uncompatibilized and compatibilized recycled dynamically cured 40/60 NR/EVA blends compared with the virgin material.

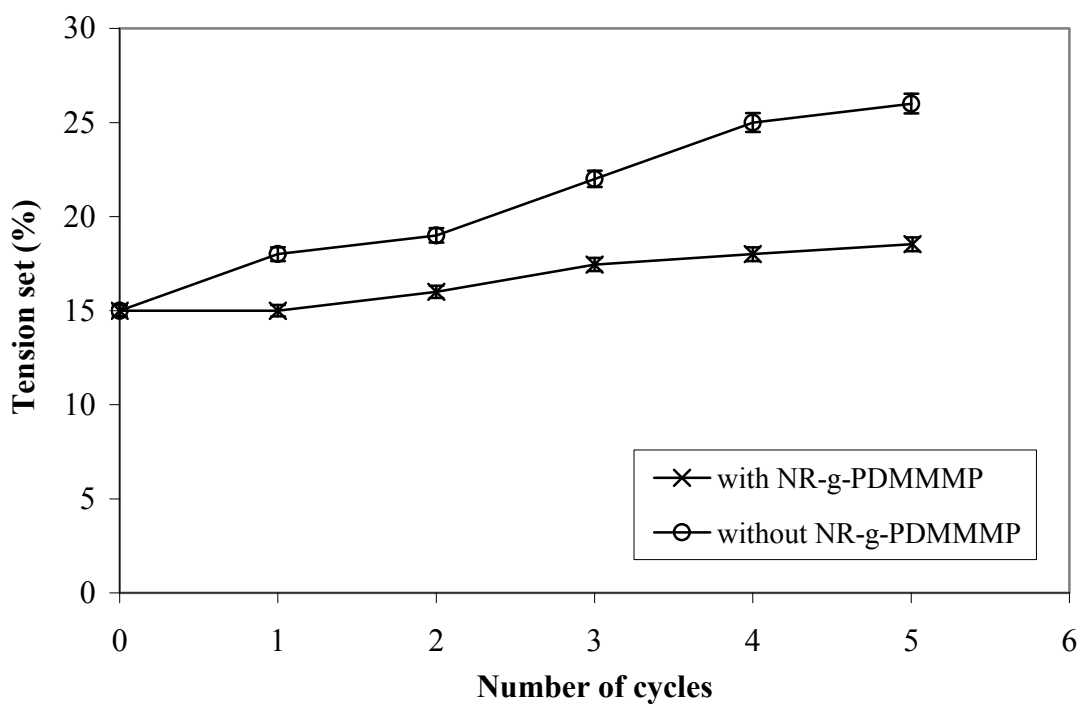
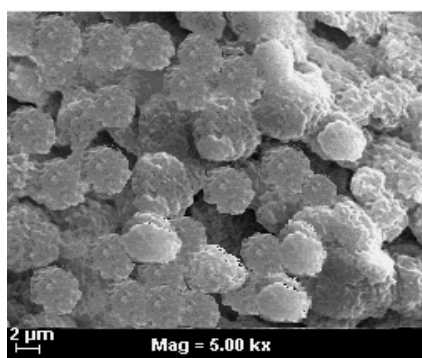


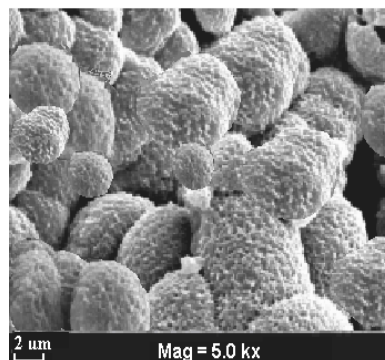
Figure 4.125 Tension set of uncompatibilized and compatibilized recycled dynamically cured 40/60 NR/EVA blends compared with the virgin material.

4.11.2 Morphological properties

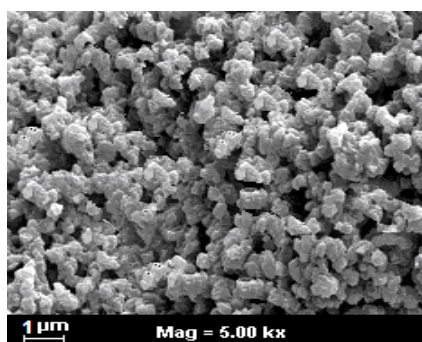
The effect of graft copolymer on morphological properties after 5 reprocess cycles is given in Figure 4.126. It can be seen that there is a dramatic change in the size of vulcanized rubber particles of the recycled material without compatibilizer after 5 cycles (Figure 4.126b) compared with the virgin sample (Figure 4.126a). This is due to heat and shearing action which leads to coalescence of the dispersed NR particles. For the material with NR-g-PDMMMP (Figure 4.126c and d), the size of vulcanized rubber particles was slightly changed after the 5th recycled process. This might be attributed to a shell which surrounds the NR particles and therefore prevents the rubber particles to coalesce and hence stabilized the morphology. It is clearly that in the compatibilized blends, size of the dispersed NR particles was less modified during mixing and fabrication steps. This result is in good agreement with tensile properties (Figures 4.120 and 4.121).



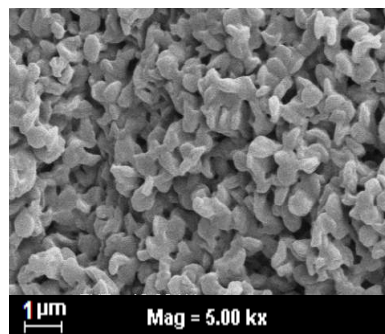
(a) Virgin without compatibilizer



(b) After 5 cycles without compatibilizer



(c) Virgin with NR-g-PDMMMP



(d) After 5 cycles with NR-g-PDMMMP

Figure 4.126 SEM micrographs of dynamically cured 40/60 NR/EVA blends: (a) the virgin without compatibilizer, (b) after 5 cycles without compatibilizer, (c) the virgin with NR-g-PDMMMP and (d) after 5 cycles with NR-g-PDMMMP.

CHAPTER 5
CONCLUSION
PART A: SYNTHESIS AND CHARACTERIZATION OF
NATURAL RUBBER SUPPORT OF
DIMETHYLPHOSPHONATE-FUNCTIONALIZED POLYMER
GRAFTS

5.1 Synthesis and characterization of dimethyl(acryloyloxymethyl)-phosphonate (DMAMP), dimethyl(methacryloyloxyethyl)phosphonate (DMMEP) and dimethyl (methacryloyloxymethyl)phosphonate (DMMMP)

DMMEP was synthesized by esterification reaction between diethylhydroxymethylphosphonate and methacryloyl chloride. DMAMP and DMMMP were prepared by reaction of dimethylhydroxymethylphosphonate upon acryloyl chloride and methacryloyl chloride, respectively. The obtained monomers, i.e., DMAMP, DMMEP, and DMMMP, were characterized by FTIR, $^1\text{H-NMR}$, $^{13}\text{C-NMR}$, and $^{31}\text{P-NMR}$ successively. Typical IR spectra of DMAMP, DMMEP and DMMMP showed the absorption bands characteristic of the stretching vibrations of P=O bonds at $1241\text{-}1237\text{ cm}^{-1}$ and P-O-C bonds at $975\text{-}979\text{ cm}^{-1}$. In addition, the various synthesized monomers showed $^1\text{H-NMR}$ signals at $\delta = 3.80\text{ ppm}$ and $\delta = 4.20\text{ ppm}$, characteristic of dimethyl ester and methylenoxy protons of dimethylphosphonate functions, respectively. $^{13}\text{C-NMR}$ peaks characteristic of carbons in carbon-carbon double bonds of the dimethylphosphonate monomers were observed at $\delta = 126.7\text{ ppm}$ ($=\underline{\text{C}}\text{H-}$) and $\delta = 132.8\text{ ppm}$ ($\underline{\text{C}}\text{H}_2=$) in the case of DMAMP, and $\delta = 125.7\text{ ppm}$ ($\underline{\text{C}}\text{H}_2=$) and $\delta = 135.8\text{ ppm}$ ($=\underline{\text{C}}(\text{CH}_3)\text{-}$) in that of DMMEP and DMMMP. In $^{31}\text{P-NMR}$, only one peak was seen on the respective spectra, at $\delta = 21.8\text{ ppm}$ for DMAMP, $\delta = 28.9\text{ ppm}$ for DMMEP, and $\delta = 31.5\text{ ppm}$ for DMMMP.

5.2 Synthesis and characterization of NR-g-PDMAMP and NR-g-PDMMEP

Graft copolymers of natural rubber and poly(dimethyl(acryloyloxymethyl)phosphonate) (NR-g-PDMAMP), and natural rubber and poly(dimethyl(methacryloyloxyethyl)phosphonate) (NR-g-PDMMEP), were successfully prepared by radical photopolymerization of dialkylphosphonate monomers, i.e., acrylate (DMAMP) and methacrylate (DMMEP), initiated from *N,N*-diethyldithiocarbamate reactive groups previously created along NR chains. The grafting efficiency obtained with the DMAMP monomer was higher than that observed with DMMEP. On the other hand, it was improved by increasing monomer concentration and reaction time. Moreover, the grafting rate was shown very dependent on the viscosity of the reaction mixture. The degree of polymerization (\overline{DP}_n) of the polymer segments that constituted the grafts was in the range of 23-73 for PDMAMP and 9-36 for PDMMEP. Visualization of NR-g-PDMAMP and NR-g-PDMMEP latices by TEM showed that they exhibit core-shell morphologies. Thermal stabilities of NR-g-PDMAMP and NR-g-PDMMEP were performed in nitrogen and oxygen atmospheres, successively. It was observed that under oxygen atmosphere they begin to degrade at a lower temperature than under nitrogen atmosphere, and that the amounts of char residues are decreased. The TGA curves showed that their degradation occurs in two steps. The first degradation step at lower temperature (onset temperature: 258 - 270°C in nitrogen, 210°C - 230°C in oxygen) was attributed to the decomposition of dimethylphosphonate-functionalized polymer grafts, while the second step at higher temperature (onset temperature: 400 - 445°C in nitrogen, 326 - 396°C in oxygen) to the degradation of NR backbone. It was obviously seen that the degradation temperature of the second step was higher than that of the degradation of pure NR (onset temperature: 320°C in nitrogen, 260°C in oxygen), showing that the procedure developed here (i.e., to graft phosphorus-containing monomers along NR chains) constitutes a good approach to improve thermal stability and fire retardancy of NR. Moreover, the measurements made under oxygen atmosphere significantly show that the positive action produced by the dimethylphosphonate-functionalized polymer grafts on the thermal stability is as much more effective than the grafting

rate is high. The DSC results showed that NR-*g*-PDMAMP and NR-*g*-PDMMEP copolymers exhibit two DSC responses, one corresponding to the glass transition of the *cis* 1,4-polyisoprene structures of NR domains, and the other to the dimethylphosphonate-functionalized polymer grafts (PDMAMP and PDMMEP). This result is typical of an heterogeneous material made of two phases, that would tend toward an homogeneous one as shown by the decrease of the threshold between the two T_g when the grafting rate GR of the graft copolymer increases from 75 to 85 %.

5.3 Synthesis and characterization of NR-*g*-PDMMMP

Graft copolymers of natural rubber and poly(dimethyl(methacryloyloxymethyl)phosphonate) (NR-*g*-PDMMMP) were prepared by radical photopolymerization of dimethyl(methacryloyloxymethyl)phosphonate (DMMMP) initiated from *N,N*-diethyldithiocarbamate reactive groups previously created along NR chains, with the aim to prepare graft copolymers different by their density in grafts along NR chains and by their average length of grafts, to be used for the compatibilization studies of NR/EVA blends. They were also characterized by ¹H-NMR, ¹³C-NMR, and ³¹P-NMR and FTIR. The efficiency of the graft copolymerization was studied by considering three starting *N,N*-diethyldithiocarbamate-functionalized NRs as macroinitiators, containing 4, 7, and 12 units% of active initiating units on the rubber chains, respectively. DMMMP grafting rates was found to increase with the increase of initiating group density on NR chains, i.e. **12% DEDT-NR > 7% DEDT-NR > 4% DEDT-NR**, and reaction time. Various degrees of polymerization (\overline{DP}_n) of the polymer segments that constitute the grafts in NR-*g*-PDMMMP, in the range of 12-37, could be obtained by varying the reaction conditions. Visualization of NR-*g*-PDMMMP latices by TEM showed that they exhibit core-shell morphologies, but also that the thick copolymer shells around the NR cores increased with the grafting rate. Measurements of Mooney viscosity (MV) performed on NR-*g*-PDMMMP samples to evaluate the interactions showed that the MVs of NR-*g*-PDMMMPs increased with the increase of grafting rate and were always higher than that of pure NR,

which indicated an increasing level of interactions between the polar functional groups in the graft copolymer. DSC and TGA measurements were also performed on the synthesized NR-g-PDMMMP copolymers, showing thermal behavior and thermal stability similar to that of NR-g-PDMMMPs and NR-g-PDMMMPs. LOI measurements were finally carried out on NR-g-PDMMMP samples to verify their flame resistant properties. An improvement of the flame resistance as much important as the grafting rate was increased was noted, result that is explained by the formation of char residues consisting in phosphorus compounds that act as thermal insulant and barrier against oxygen transfers toward the burning parts.

PART B: Simple blend of NR/EVA

5.4 Effect of different types of compatibilizers on properties of NR/EVA blends

The capability of the different types of graft copolymers synthesized, i.e., NR-g-PDMMMP, NR-g-PDMAMP, and NR-g-PDMMEP, to compatibilize 50/50 NR/EVA blends, was evaluated by considering their contribution to the improvement of the properties of NR/EVA blends. The characteristics of the graft copolymers used, i.e., graft density on rubber chains and average length of grafts ($\overline{DP_n}$), were of same order. By referring to the previous study dealing with the influence of compatibilizer concentration, a loading level in compatibilizer of 7 wt% by comparison with NR was chosen. The best effects on the blend properties were shown independent of the choice of the graft copolymer, i.e., NR-g-PDMMMP, NR-g-PDMMEP, or NR-g-PDMAMP, as blend compatibilizer. In these conditions, whatever the graft copolymer used, NR/EVA blends showed the highest complex viscosity, storage modulus, tensile strength, and elongation at break. For comparison, in same loading conditions, the NR/EVA blend prepared with ENR-30 as compatibilizer showed values similar to that obtained with the blend without compatibilizer, that is the lowest storage modulus. On the point of view morphology, by using NR-g-PDMMMP, NR-g-PDMMEP, or NR-g-PDMAMP as compatibilizer, a decrease of the phase sizes and a more uniform dispersion of NR domains in EVA matrix were noted, in contrary to the blends incorporating ENR-30 as compatibilizer which revealed larger phase sizes.

These morphological characteristics explained why better mechanical, hardness, and tension set properties were observed with 50/50 NR/EVA blends incorporating one of the graft copolymers synthesized, i.e., NR-*g*-PDMMMP, NR-*g*-PDMMEP and NR-*g*-PDMAMP, by comparison with that of the 50/50 NR/EVA blends without compatibilizer or incorporating 7 wt% of ENR-30. This improvement of mechanical, hardness, and tension set properties of the NR/EVA blends can be attributed to the fact that the graft copolymer macromolecules can interact simultaneously with the NR and EVA macromolecules situated at the surface of the respective domains, with creation of physical links. These interesting results led us to continue the investigations by selecting NR-*g*-PDMMMP copolymer as compatibilizer for NR/EVA blends.

5.5 Effect of grafting rate of NR-*g*-PDMMMP on properties of NR/EVA blend.

The study dealing with the effect of grafting rate on the properties of NR/EVA blends was performed with NR-*g*-PDMMMP as compatibilizer, because of its preparation was shown easier and cheaper compared to those of NR-*g*-PDMAMP and NR-*g*-PDMMEP. The influence of the grafting rate of NR-*g*-PDMMMP on the properties of 50/50 NR/EVA blends was studied. For that, four NR-*g*-PDMMMPs with grafting rate equal to 71, 80, 89, and 95 wt%, respectively, were considered. The highest complex viscosity and storage modulus values, accompanied with the lowest $\tan \delta$, were observed by using a NR-*g*-PDMMMP containing 80 wt% of dimethylphosphonate-functionalized polymer grafts. The best mechanical properties of 50/50 NR/EVA blends were also obtained when it was compatibilized with the NR-*g*-PDMMMP copolymer having a grafting rate of 80 %. This was an indication on the interactions existing between the two phases, and proved the role important played by the length of the grafts. The further NR-*g*-PDMMMPs whose grafting rates were upper or lower to 80 %, i.e., 71, 89, or 95 %, the decrease of the phase size was not so much affect as in the case of NR-*g*-PDMMMP of 80 % grafting rate. To conclude on these studies, it can be said that the blends compatibilized with 7 wt% of NR-*g*-PDMMMP 80% show a remarkably decrease of the phase size, which contributes to optimize their mechanical properties.

5.6 Effect of concentration of graft copolymer

It was carried out using a NR-*g*-PDMMMP copolymer containing 80 wt% of dimethylphosphonate-functionalized grafts (**NR-*g*-PDMMMP 80%**), and by considering different loading levels, i.e., 1, 3, 5, 7, 9, 12 and 15 wt%, respectively, by comparison with the NR component. It was noted that the incorporation of 7 wt% of **NR-*g*-PDMMMP 80%** in 50/50 NR/EVA blend gave the blend with the highest complex viscosity, storage modulus, tensile strength, and elongation at break. Furthermore, in same time, the lowest values of $\tan \delta$ and tension set were observed. Morphological characteristics of the 50/50 NR/EVA blends showed co-continuous systems, and the blends compatibilized with 7 wt% of **NR-*g*-PDMMMP 80%** showed the smallest phase sizes. Beyond and below this concentration of 7 wt%, larger phase sizes are observed. In the blend incorporating NR-*g*-PDMMMP concentrations lower than 7 wt%, lower interactions between the phases were observed because of the interface areas were not fully occupied by the compatibilizer, as a result lower mechanical strength. When NR-*g*-PDMMMP concentrations are higher than 7 wt%, an excess amount of compatibilizer might cause the formation of third phase (i.e., micelles) which could possibly acts as a weakening points during deformation process and as a lubricant during the flow. Therefore, the 50/50 NR/EVA blend with a loading level of NR-*g*-PDMMMP compatibilizer of 7 wt%, calculated by comparison with NR component, showed the best over all properties.

PART C: Thermoplastic vulcanizates (TPVs)

5.7 Effect of blend compositions on properties of dynamically cured NR/EVA blends

Uncompatibilized dynamically cured NR/EVA blends with various blend ratios were prepared and their properties were investigated. It was found that the complex viscosity, domain size of vulcanized rubber in the EVA matrix, and degree of swelling of the blend in oil increased with increasing proportion of NR content in the blend. The increasing size of vulcanized rubber domains may be attributed to the tendency of the new dispersed rubber particles formed to re-agglomerate or to coalesce. It was also found that increasing content of NR in a range of 50 to 75 wt% in the blends caused abruptly decreasing trends of the tensile strength and elongation at break. The hardness, tension set properties, and solvent resistance decreased with increasing content of rubber phase. Furthermore, increasing incorporation of EVA from 25 wt% to 75 wt% in the blend caused an increase of thermal stability of the dynamically cured material obtained as shown by the increase of the onset degradation temperature from 327 to 338°C, respectively. The progress of $\tan \delta$ versus temperature of the dynamically cured specimens coming from various blend ratios showed two distinct transition temperature peaks corresponding to glass transition temperatures. The lower glass transition temperature at approximately -59.6°C corresponded to the NR phase, and the glass transition of EVA phase was observed at about -14.8°C in the NR/EVA blends. This confirmed the phase separation of the blend components. Moreover, the maximum intensity of $\tan \delta$ curves ($\tan \delta_{\max}$) and the area underneath of $\tan \delta$ peak could be related to the damping property. It was found that the damping property of blends increased with increasing the proportion of NR.

5.8 Effect of curing systems in dynamically cured 40/60 NR/EVA blends

The efficiency of various curing systems (i.e., sulphur, peroxide, mixed, and phenolic cured systems) for the dynamic vulcanization of 40/60 NR/EVA blend without compatibilizer was tested. It was seen that TPVs coming from peroxide cured system showed the highest complex viscosity and storage modulus. This indicated a crosslinking of the EVA phase as proved by extraction experiments. The efficiency of the cured system that was estimated by the amount of extracted NR increased as follows: sulphur cured system < phenolic cured system < mixed system < peroxide cured systems. On the other hand, experiments of selective extraction of EVA phase from the TPVs prepared using the various curing systems showed that the lowest amount of extracted EVA was obtained with the specimen cured with the peroxide system, followed by the one coming from the mixed cured system. Among the four types of curing systems used, the TPV coming from the phenolic cured system exhibited the highest value of $\tan \delta$, whilst peroxide cured system exhibited the lowest value. This indicates a crosslinking of the EVA phase in the TPVs prepared with the peroxide and mixed cured system. Concerning the solvent resistance, TPVs obtained with peroxide cured system showed the lowest swelling (i.e., the highest solvent resistance), followed in the order by those coming from mixed, sulphur, and phenolic cured systems. In term of mechanical properties, TPVs coming from peroxide cured system gave the highest initial slope but the lowest tensile strength and elongation at break, whilst the ones cured with sulphur and phenolic cured systems showed the highest tensile strengths, elongations at break, and the lowest tension sets, and the ones cured with the mixed cured system showing intermediate properties. For hardness, the TPVs coming from the peroxide and mixed cured systems showed a marginal increase in hardness over those of the TPVs obtained with sulphur and phenolic curing systems. In term of morphology, the TPVs coming from sulphur and phenolic cured systems showed rubber domains of similar size, i.e., approximately 2.9 μm , which are smaller than those of TPVs coming from the mixed cured system. The result of domain size relates to the lower level of crosslinking in the NR phase, because a small amount of dicumyl peroxide diffuse and crosslink the EVA phase. In the case of peroxide cured sample, it was

difficult to see the spherical NR domains due to the crosslinking of EVA phase. They were difficult to dissolve by tetrahydrofuran.

5.9 Effect of concentration of compatibilizer

Dynamically cured 40/60 NR/EVA blends incorporating various loading levels, i.e., 1, 3, 5, 7, 9, 12, and 15 wt% by comparison with NR, of **NR-g-PDMMMP 80%** as blend compatibilizer were prepared using sulphur as curing system and the properties of the TPVs obtained were compared. The compatibilizing effect was characterized by measuring the dynamic, mechanical, thermal, and morphological properties of the different TPVs obtained. Increasing the loading level of NR-g-PDMMMP in the blend caused leads to an increase of the elastic modulus and complex viscosity until reaching a maximum value at a loading level of 9 wt%. This is the result of a maximum compatibilizing effect explained by the covering of the interfacial area by the blend compatibilizer. Thereafter, the elastic modulus and complex viscosity were decreased with increasing the loading level of NR-g-PDMMMP higher than 9 wt%. This is due to the fact that the graft copolymer covers the majority of the interfacial areas, but the excess amount of NR-g-PDMMMP leads to the formation of micelles that act as lubricant, which explains the lower mechanical and rheological properties of the derived materials. The smallest vulcanized rubber domains dispersed in the EVA matrix as a two-phase system and the lowest $\tan \delta$ value were also observed with the TPVs incorporating 9 wt% of NR-g-PDMMMP. Moreover, the superior tensile strength, elongation at break, and tension set, i.e., 17.06 MPa, 660 %, and 27 %, respectively, were also observed in the dynamically cured 40/60 NR/EVA blend incorporating 9 wt% of NR-g-PDMMMP compatibilizer. These good properties were explained by an optimization of the compatibilizing effect brought by NR-g-PDMMMP that is of the physical interactions between the phases. It was also noted that the introduction of NR-g-PDMMMP as compatibilizer in the dynamically cured 40/60 NR/EVA blends leads to an improvement of the thermal stability of the TPVs obtained as compatibilizer as the decomposition temperature was increased with the addition of the graft copolymer. However, the addition of NR-g-PDMMMP in the

blends caused decreasing of the degree of crystallinity of the EVA phase in the TPV but did not cause severe effect on the strength properties.

5.10 Effect of different types of compatibilizers on properties of NR/EVA blends

Dynamically cured 40/60 NR/EVA blends were prepared using compatibilizers of various chemical structures, i.e., NR-g-PDMMMP, NR-g-PDMAMP, NR-g-PDMMEP, and ENR-30, in order to study the effect of the structure parameter on TPV properties. The characteristics of the graft copolymers used, i.e., graft density on rubber chains and average length of grafts ($\overline{DP_n}$), were of same order. By referring to the previous studies dealing with the effects of curing system and compatibilizer concentration, it was chosen to use a sulphur as curing system to cure the blend and a compatibilizer loading level of 9 wt% by comparison with NR. No significant difference was observed in the properties of the TPVs coming from 40/60 NR/EVA blends compatibilized with the grafts copolymers, i.e., NR-g-PDMMMP, NR-g-PDMMEP, or NR-g-PDMAMP. The values of complex viscosity and storage modulus, as well as that of $\tan \delta$ and tension set, were similar. On the other hand, the properties of the TPVs coming from 40/60 NR/EVA blends compatibilized by ENR-30 were strongly decreased. In term of morphology, the TPVs coming from blends compatibilized with the graft copolymers showed decreased phase size and more uniform size dispersion of NR domains in EVA matrix. On the other hand, in the ones coming from blends compatibilized with ENR-30, it was noted that the NR domains were larger. These characteristics related to trend of mechanical properties, that is tensile strength, elongation at break, hardness, and tension set of dynamically cured 40/60 NR/EVA blends compatibilized with the graft copolymers containing, i.e., NR-g-PDMMMP, NR-g-PDMMEP, and NR-g-PDMAMP, were superior to that of the TPVs incorporating ENR-30. These results are explained by the capability of the graft copolymer macromolecules to associate simultaneously with NR and EVA phases, because of the affinity of the polar dimethylphosphonate-functionalized poly(meth)acrylate

grafts with the EVA macromolecules and of that of the non-polar rubber backbone of the graft copolymer with the NR ones.

5.11 Recyclability of dynamically cured NR/EVA blends

Mechanical and morphological properties of uncompatibilized and compatibilized recycled dynamically cured 40/60 NR/EVA blends compatibilized with **NR-g-PDMMMP 80%** at a loading level of 9 wt% by comparison with NR were studied, and compared with that of the virgin materials. It was seen that the strength properties of TPVs incorporating NR-g-PDMMMP or not decreased with increasing the number of re-processings. However, the compatibilized TPVs showed lower gradient or slope of decreasing trend of tensile strength, elongation at break, and hardness than the uncompatibilized ones. Whilst, the TPVs without blend compatibilizer showed higher decreasing trend of tensile strength, elongation at break, hardness, and increasing trend of tension set. On the point of view morphology, a dramatic change in the size of the vulcanized rubber domains was noted after 5 times reprocessing of dynamically cured NR/EVA blend without compatibilizer, while a decrease of their size was noted in the case of the dynamically cured NR/EVA blends compatibilized with **NR-g-PDMMMP 80%**.

REFERENCES

- Annual Book of ASTM D412-00, 2000. Standard test method for vulcanized rubber and thermoplastic elastomers-Tension. Vol. 09.01.
- Annual Book of ASTM D417-00, 2000. Standard test method for Rubber Property-Effect of Liquids. Vol. 09.01.
- Annual Book of ASTM D1566-00, 2004. Standard Terminology Relating to Rubber. Vol. 09.01.
- Annual Book of ASTM D2240-00, 2000. Standard test method for rubber Property-Durometer Hardness. Vol. 09.01.
- Annual Book of ASTM D5289-00, 2000. Standard test method for rubber Property-Vulcanization Using Rotorless Cure Meter. Vol. 09.01.
- Annual Book of ASTM D5964-00, 2000. Standard test method for rubber IRM 902 and IRM 903 Replacement Oils for ASTM No.2 and ASTM No.3 Oils. Vol. 09.01.
- Annual Book of ASTM D2863, 2006. Standard test method for Measuring the Minimum Oxygen Concentration to Support Candle-Like Combustion of Plastic (Oxygen Index). Vol. 08.02.
- Abdou-Sabet, S. and Patel, R.P. 1991. Morphology of elastomeric alloys. *Rubber. Chem. Technol.* 64: 729-796.
- Abdullah, I., Ahmad, S. and Sulaiman, C.S. 1995. Blending of natural rubber with linear low-density polyethylene. *J. Appl. Polym. Sci.* 58(7): 1125-1133.
- Ajji, A., Guèvremont, J., Cole, K.C. and Dumoulin, M.M. 1996. Orientation and structure of drawn poly(ethylene terephthalate). *Polymer* 37(16): 3707-3714.
- Akhtar, S., De, P.P. and De, S.K. 1986. Tensile Failure of Gamma Ray Irradiated Blends of High Density Polyethylene and Natural Rubber, *J. Appl. Polym. Sci.* 32(3): 4169-4183.
- Akhtar, S. and Bhagawan, S.S. 1987. Dynamic mechanical properties of NR-HDPE blends. *Rubber. Chem. Technol.* 60: 591-599.
- Arayaprane, W., Prasassarakich, P. and Rempel, G.L. 2003. Process variables and their effects on grafting reactions of styrene and methyl methacrylate onto natural rubber. *J. Appl. Polym. Sci.* 89: 63-74.

- Asaletha, R., Kumaran, M.G. and Thomas, S. 1995. Effect of casting solvents and compatibilizer loading on the morphology and properties of natural rubber/polystyrene blends. *Polym. Plast. Technol. Eng.* 34: 633-648.
- Asaletha, R., Groeninckx, G., Kumaran, M.G. and Thomas, S. 1998. Melt rheology and morphology of physically compatibilized natural rubber-polystyrene blends by the addition of natural rubber-g-polystyrene. *J. Appl. Polym. Sci.* 69: 2673-2690.
- Asaletha, R., Kumaran, M.G. and Thomas, S. 1998. Thermal behaviour of natural rubber/polystyrene blends: thermogravimetric and differential scanning calorimetric analysis. *Polym. Degrad. Stab.* 61(3): 431-439.
- Asaletha, R., Kumaran, M.G. and Thomas, S. 1999. Thermoplastic elastomers from blends of polystyrene and natural rubber: morphology and mechanical properties. *Eur. Polym. J.* 35(2): 253-271.
- Barlow, J.W. and Paul, D.R. 1984. Mechanical compatibilization of immiscible blends. *Polym. Eng. Sci.* 24(8): 525-534.
- Barson, C.A. and Benvington, J.C. 1987. Copolymerization involving methyl methacrylate, methyl acrylate, stilbene and p.fluorostilbene. *Eur. Polym. J.* 23(3): 251-253.
- Bohn, L. 1968. Incompatibility and phase formation in solid polymer mixtures and graft and block copolymers. *Rubber Chem. Technol.* 41: 495-513.
- Bonner, J.G. and Hope, P.S. 1993. in "Polymer blends and Alloys"; Folkes, M.J. and Hope, P.S., eds. Chapman & Hall Publisher, New York.
- Bradbury, J.H. and Perera, M.C.S. 1985. Epoxidation of natural rubber studied by NMR spectroscopy. *J. Appl. Polym. Sci.* 30(8): 3347-3364.
- Brosse, J.C., Compiston, I., Derouet, D., El Hamdaoui, A., Houdayer, S., Reyx, D. and Ritoit-Gillier, S. 2000. Chemical modifications of polydiene elastomers: A survey and some recent results. *J. Appl. Polym. Sci.* 78(8): 1461-1477.
- Burfield, D.R., Lim, K.L., and Law, K.S. 1984. Epoxidation of natural rubber latices: Methods of preparation and properties of modified rubbers. *J. Appl. Polym. Sci.* 29(5): 1661-1673.

- Burfield, D.R., Lim, K.L. and Law, K.S. 2003. Epoxidation of natural rubber lattices: methods of preparation and properties of modified rubbers. *J. Appl. Polym. Sci.* 29(5): 1661-1673.
- Bywater, S. 1984. Block polymers: characterization and use in polymer blends. *Polym. Eng. Sci.* 24(2): 104-111.
- Carone, E., Kopcak, U., Goncaves, M.C. and Nunes, S.P. 2000. In situ compatibilization of polyamide 6/natural rubber blends with maleic anhydride. *Polymer* 41(15): 5929-5935.
- Chuayjuljit, S., Moolsin, S. and Potiyaraj, P. 2005. Use of natural rubber-g-polystyrene as a compatibilizer in casting natural rubber/polystyrene blend films. *J. Appl. Polym. Sci.* 95(4):826-831.
- Coran, A.Y., Das, B. and Patel, R.P. 1978. US. 4130535, 19 December.
- Coran, A.Y. 1987. in *Thermoplastics Elastomers*, N.R. Legge, G. Holden, and H.E. Schroeder, eds., Hanser Publishers, New York.
- Coran, A.Y. 1995. Vulcanization: conventional and dynamic. *Rubb. Chem. Technol.* 68: 351-375.
- Coran, A.Y. and Patel, R.P. 1996. Thermoplastic elastomers based on dynamically vulcanized elastomer-thermoplastic blends, in *thermoplastic elastomers*, Holden, G., Legge, N.R., Quirk, R. and Schroeder, H.E., Eds., Hanser Publisher, New York.
- Chowdhury, N.R. and Bhowmick, A.K. 1989. Compatibilization of natural rubber-polyolefin. Thermoplastic elastomeric blends by phase modification. *J. Appl. Polym. Sci.* 38(6): 1091-1109.
- Chowdhury, S.R., Mishra, J.K. and Das, C.K. 2000. Structure, shrinkability and thermal property correlations of ethylene vinyl acetate (EVA)/carboxylated nitrile rubber (XNBR) polymer blends. *Polym. Degrad. Stab.* 70(2): 199-204.
- Datta, S. and Lohse, D.J. 1996. in "Polymeric Compatibilizers: uses and benefits in polymer blends", Hanser Publishers, New York.
- Dahlan, H.M., Khairul, Z.M.D. and Ibrahim, A. 2000. Liquid natural rubber (LNR) as a compatibilizer in NR/LLDPE blends. *J. Appl. Polym. Sci.* 78(10): 1776-1782.

- Dahlan, H.M., Khairul, Z.M.D. and Ibrahim, A. 2002. The morphology and thermal properties of liquid natural rubber (LNR)-compatibilized 60/40 NR/LLDPE blends. *Polym. Test.* 21(8): 905-911.
- Derouet, D., Phinyocheep, P., Brosse, J.C. and G. Boccaccio. 1990. Synthèse d'elastomeres photoreticulables par modification chimique du caoutchouc naturel liquide—I. Introduction de l'anhydride maleique sur les structures polyisopreniques. *Eur. Polym. J.* 26(12): 1301-1311.
- Derouet, D., Radhakrishnan, N., Brosse, J.C. and Boccaccio, G. 1994. Phosphorus modification of epoxidized liquid natural-rubber to improve flame resistance of vulcanized rubbers. *J. Appl. Polym. Sci.* 52(9): 1309-1316.
- Derouet, D., Morvan, F. and Brosse, J.C. 1995. Flame resistance and thermal stability of 1,4-polydienes modified by dialkyl(or aryl)phosphates. *J. nat. Rub. Res.* 11(1): 9-15.
- Derouet, D., Morvan, F. and Brosse, J.C. 2001. Chemical modification of 1,4-polydienes by di(alkyl or aryl)phosphates. *Eur. Polym. J.* 37(7): 1297-1313.
- Derouet, D., Brosse, J.C., Cauret, L., Morvan, F. and Mulder Houdayer, S. 2003. Chemical modification of polydienic elastomers by organophosphorated reagents. *J Appl. Polym. Sci.* 87(1): 47-60.
- Derouet, D., Cauret, C. and Brosse, J.C. 2003a. Synthesis of 1,4-polyisoprene support of 2-chloroethylphosphonic acid (ethephon), a stimulating compound for the latex production by the *Hevea brasiliensis*. *Eur. Polym. J.* 39(4), 671 – 686.
- Derouet, D., Mulder-Houdayer, S. and Brosse, J.C. 2005. Chemical modification of polydienes in latex medium: Study of epoxidation and ring opening of oxiranes. *J. Appl. Polym. Sci.* 95(1): 39-52.
- Derouet, D., Tran, Q.N. and Ha Thuc, H. 2007. Synthesis of N,N-diethyldithiocarbamate functionalized 1,4-polyisoprene, from natural rubber and synthetic 1,4-polyisoprene. *Eur. Polym. J.* 43(5): 1806-1824.

- Derouet, D., Intharapat, P., Tran, Q.N., Gohier, F. and Nakason, C. 2009. Graft copolymers of natural rubber and poly(dimethyl(acryloyloxymethyl)-phosphonate) (NR-g-PDMAMP) or poly(dimethyl(methacryloyloxyethyl)-phosphonate) (NR-g-PDMMEP) from photopolymerization in latex medium. *Eur. Polym. J.* 45(3): 820-836.
- Doak, K.W. 1986. Ethylene Polymer, in *Encyclopedia of Polymer. Science and Engineering*, Vol. 6., Mark, H.F., Bikales, N.M., Overberger, C.G. and Menges, G. eds., Wiley, New York.
- El-Sabbagh, S.H. 2003. Compatibility study of natural rubber and ethylene-propylene diene rubber blends. *Polym. Test.* 22(1); 93-100.
- El-Sayed, A.M. and Afifi, H. 2002. Improvement of the compatibility of natural rubber/ethylene-propylene diene monomer rubber blends via natural rubber epoxidation. *J. Appl. Polym. Sci.* 86(11): 2816-2819.
- Fayt, R., Jérôme, R., and Teyssié, Ph. 1987. Characterization and control of interfaces in emulsified incompatible polymer blends. *Polym. Eng. Sci.* 27(5): 328-334.
- Fayt, R., Jérôme, R. and Teyssié, Ph. 1989. *Multiphase Polymers: Blends and Ionomers*. Utracki, L.A. and Weiss, R.A. eds., ACS, Washington DC., 38-66.
- Fischer, W.K. 1973. US. 3758643, 11 september.
- Galloway, J.A., Jeon, H.K., Bell, J.R. and Macosko, C.W. 2005. Block copolymer compatibilization of cocontinuous polymer blends, *Polymer* 46(1): 183-191.
- Gelling, I.R. 1984. Modification of natural rubber latex with peracetic acid. *Rubber Chem. Technol.* 58: 86-96.
- Gelling, I.R. and Porter, M. 1988. *Natural Rubber Science and Technology*. Roberts, A.D. ed., Oxford University Press. UK.
- Gelling, I.R. 1991. Epoxidized natural rubber. *J. Nat. Rubb. Res.* 6: 184-205.
- George, J., Joseph, R., Varughese, K.T. and Thomas, S. 1995. High density polyethylene/acrylonitrile butadiene rubber blends: Morphology, mechanical properties, and compatibilization. *J. Appl. Polym. Sci.*, 57(4): 449-465.

- George, J., Joseph, R., Varughese, K.T. and Thomas, S. 1995a. Blends of isotactic polypropylene and nitrile rubber: morphology, mechanical properties and compatibilization. *Polymer*,36(23): 4405-4416.
- George, S., Ramamurthy, K., Anand, J.S., Groeninckx, G., Varughese, K.T. and Thomas, S. 1999. Rheological behaviour of thermoplastic elastomers from polypropylene/acrylonitrile-butadiene rubber blends: effect of blend ratio, reactive compatibilization and dynamic vulcanization. *Polymer* 40(15): 4325-4344.
- George, J., Varughese, K.T. and Thomas, S. 2000. Dynamically vulcanised thermoplastic elastomer blends of polyethylene and nitrile rubber. *Polymer* 41(4): 1507-1517.
- Gergen, W.P., Lutz, R.G. and Davison, S. 1987. *Thermoplastic Elastomer*, Hanser Publisher, Munich.
- Gessler, A.M., Haslett, J.R. and William, H. 1962. Process for preparing a vulcanized blend of crystalline polypropylene and chlorinated butyl rubber, U.S. Pat 3037954, June.
- Ghosh, P., Chattopadhyay, B. and Sen, A.K. 1996. Thermal and oxidative degradation of PE-EPDM blends vulcanized differently using sulfur accelerator systems. *Eur. Polym. J.* 32(8): 1015-1021.
- Goettler, L.A., Richwine, J.R. and Wille, F.J. 1982. The rheology and processing of olefin-based thermoplastic vulcanizates. *Rubb. Chem. Technol.* 55: 1448
- Hashim, A.S., Ong, S.K. and Jessy, R.S. 2002. A general review of recent developments on chemical modification of NR. 28(40): 3-9. <http://www.rubber-stichting.info/natuurrubber/Natuurrubber%2028.pdf>
- Hoang, D.Q., Kim, J. and Jang, B.N. 2008. Synthesis and performance of cyclic phosphorus-containing flame retardants. *Polym. Degrad. Stab.* 93(11): 2042-2047.
- Hadjichristidis, N., Pispas, S. and Floudas, G. 2003. *Block copolymers: synthetic strategies, physical properties, and applications*. Wiley, New York, USA.

- Hinchiranan, N., Charmondusit, K., Prasassarakich, P. and Rempel, G.L. 2006. Hydrogenation of synthetic cis-1,4-polyisoprene and natural rubber catalyzed by [Ir(COD)py(PCy3)]PF₆. *J. Appl. Polym. Sci.* 100(5): 4219-4233.
- Holden, G., Legge, N.R., Quirk, R. and Schroeder, H.E. 1996. Thermoplastic elastomers, Hanser Publisher, New York, USA.
- Holden, G. 2000. Understanding Thermoplastic Elastomers. Hanser Publisher, Munich, USA.
- Ibrahim, A. and Dahlan, M. 1998. Thermoplastic natural rubber blends. *Prog. Polym. Sci.* 23: 665-706.
- International Organization for Standardization 3582. 2006. Flexible cellular polymeric materials--Laboratory assessment of horizontal burning characteristics of small specimens subjected to a small flame.
- Ismail, H. and Suryadiansyah, S. 2002. Thermoplastic elastomers based on polypropylene/natural rubber and polypropylene/recycle rubber blends. *Polym. Test.* 21(4): 389-395.
- Jansen, P., Amorim, M., Gomes, A.S. and Soares, B.G. 1995. Use of EVA-containing mercapto groups in natural rubber-EVA blends. I. Mechanical, thermal, and morphological properties. *J. Appl. Polym. Sci.* 58(1): 101-107.
- Jansen, P., Gomes, A.S. and Soares, B.G. 1996. The use of EVA-containing mercapto groups in natural rubber-EVA blends. II. The effect of curing system on mechanical and thermal properties of the blends. *J. Appl. Polym. Sci.* 61(4): 591-598.
- Jansen, P. and Soares, B.G. 1996. Effect of compatibilizer and curing system on the thermal degradation of natural rubber/EVA copolymer blends. *Polym. Degrad. Stab.* 52(1): 95-99.
- Jeanmaire, T., Hervaud, Y. and Boutevin, B. 2002. Synthesis of dialkylhydroxymethylphosphonates in heterogeneous conditions. *Phosphorus Sulfur and Silicon* 177(5): 1137-1145.
- Jeong Seok, O.H., Isayev, A.I. and Rogunova, M.A. 2003 Continuous ultrasonic process for in situ compatibilization of polypropylene/natural rubber blends. *J. Appl. Polym. Sci.* 44(8): 2337-2349.

- Jiang, D.D., Wilkie, C.A. 1998. Graft copolymerization of methacrylic acid, acrylic acid and methyl acrylate onto styrene-butadiene block copolymer. *Eur. Polym. J.* 34(7): 997-1006.
- John, B., Varughese, K.T. Oommen, Z., Pötschke, P. and Thomas, S. 2003. Dynamic mechanical behavior of high-density polyethylene/ethylene vinyl acetate copolymer blends: The effects of the blend ratio, reactive compatibilization, and dynamic vulcanization. *J. Appl. Polym. Sci.* 87(13): 2083-2099.
- Jordhamo, G.M., Manson, J.A. and Sperling, L.H. 1986. Phase continuity and inversion in polymer blends and simultaneous interpenetrating networks. *Polym Eng. Sci.* 26(8): 517-524.
- Joseph, S. and Thomas, S. 2003. Morphology development and mechanical properties of polystyrene/polybutadiene blends. *Eur. Polym. J.* 39(1): 115-125.
- Kim, H.T., Kim, H.R., Kim, J.K. and Park, J.Y. 2001. The morphology and mechanical properties of the blends of syndiotactic polystyrene and polystyrene-block-poly(ethylene-co-butylene)-block-polystyrene copolymers. *Kor. Aust. Rheol. J.* 13: 83-90.
- Kongkaewa, A. and Wootthikanokkhan, J. 1999. Polymerization of Isoprene by Using Benzyl Diethyldithiocarbamate as an Iniferter *Science Asia* 25: 35-41
- Koning, C., Van Duin, M., Pagnouille, C. and Jerome, R. 1998. Strategies for compatibilization of polymer blends. *Prog. Polym. Sci.* 23: 707-757.
- Koshy, A.T., Kuriakose, B. and Thomas, S. 1992. Studies on the effect of blend ratio and cure system on the degradation of natural rubber—ethylene-vinyl acetate rubber blends. *Polym. Degrad. Stab.* 36(2):137-147.
- Koshy, A.T., Kuriakose, B., Thomas, S. and Premalatha, C.K. and Varghese, S. 1993. Melt rheology and elasticity of natural rubber - ethylene-vinyl acetate copolymer blends. *J. Appl. Polym. Sci.* 49(5): 901-912.
- Kundu, P.P., Tripathy, D.K. and Gupta, B.R. 1996. Effect of rheological parameters on the miscibility and polymer-filler interactions of the black-filled blends of polyethylene-vinyl acetate and polychloroprene. *J. Appl. Polym. Sci.* 61(11): 1971-1983.

- Kunyawut, C. 2006. A study of droplet coalescence in immiscible PS/LDPE blends under annealing conditions. *Thammasat Int. J. Sc. Tech.* 11(2): 21-33.
- Laokijcharoen., P. and Coran, A.Y. 1998. The evolution of morphology in NR/HDPE blends. Part I. Microscopy for unvulcanized blends. *Rubber Chem. Technol.* 71(5): 966-974.
- Lee, M., Utsumi, K. and Minoura, Y. 1979. Effect of hexamethylphosphorotriamide on the "living" radical polymerization initiated by aged Cr²⁺ BPO. *J. Chem. Soc. Faraday Trans. 1*, 75:1821-1829.
- Lee, J.K., Lee, T.Y., Ha, C.S., Lee, J.O. and Cho, W.J. 1994. Mechanical properties of dynamically vulcanized NR and EVA blends in a roll mill. *Kor. Polym. J.* 18: 61.
- Liepins, R., Surles, J.R., Morosoff, N., Stannett, V., Duffy, J.J. and Day, F.H. 1978. Localized radiation grafting of flame-retardants to polyethylene terephthalate. II Vinyl phosphonates. *J. Appl. Polym. Sci.* 22(9): 2403-2414.
- Lohse, D.J., Datta, S. and Kresge, E. 1991. Graft copolymer compatibilizers for blends of polypropylene and ethylene-propylene copolymers. *Macromolecules.* 24 (2): 561-566.
- Macaúbas, P.H.P. and Demarquette, N.R. 2001. Morphologies and interfacial tensions of immiscible polypropylene/polystyrene blends modified with triblock copolymers. *Polymer* 42(6): 2543-2554.
- Mark, H.F., Bikales, N.M., Overberger, C.G. and Menges, G. Eds., 1988. *Encyclopedia of polymer science and engineering*, 2nd Edn., John Wiley, New York.
- Menon, A.R.R., Pillai, C.K.S. and Nando, G.B. 1996. Thermal degradation characteristics of natural rubber vulcanizates modified with phosphorylated cashew nut shell liquid. *Polym. Degrad. Stab.* 52(3): 265-271.
- Menon, A.R.R. 1997. Flame-retardant characteristics of natural rubber modified with a bromo derivative of phosphorylated cashew nut shell liquid. *J. Fire Sci.* 15(1): 3-13.

- Menon, A.R.R., Pillai, C.K.S. and Nando, G.B. 1998. Modification of natural rubber with phosphatic plasticizers: a comparison of phosphorylated cashew nut shell liquid prepolymer with 2-ethyl hexyl diphenyl phosphate. *Eur. Polym. J.* 34(7): 923-929.
- Mina, M.F., Ania, F., Baltá Calleja, F.J. and Asano, T. 2004. Microhardness studies of PMMA/natural rubber blends. *J. Appl. Polym. Sci.* 91(1): 205-210.
- Moad, G. and Solomon, D.H. 1995. *The chemistry of free radical polymerization*; 1st ed.; Elsevier Science Ltd., Oxford.
- Mohamad, Z., Ismail, H. and Chantara Thevy, R. 2006. Characterization of epoxidized natural rubber/ethylene vinyl acetate (ENR-50/EVA) blend: Effect of blend ratio. *J. Appl. Polym. Sci.* 99(4): 1504-1515.
- Mohanty, S. and Nando, G.B. 1997. Characterization of ionomers formed *in situ* from miscible blends of poly (ethylene-*co*-acrylic acid) (PEA) and epoxidized natural rubber (ENR). *Polymer* 38(6): 1395-1402.
- Mousa, A., Ishiaku, U.S. and Ishak, Z.A.M. 1998. Oil-resistance studies of dynamically vulcanized poly(vinyl chloride)/epoxidized natural rubber thermoplastic elastomer. *J. Appl. Polym. Sci.* 69(7): 1357-1366.
- Nakason, C., Sainamsai, W., Kaesaman, A. and Klinpituksa, P. 2001. Preparation, Thermal and flow properties of epoxidised natural rubber. *Songklanakarini J. Sci. Technol.* 23(3): 415-424.
- Nakason, C., Kaesaman, A. and Supasanthitikul, P. 2004. The grafting of maleic anhydride onto natural rubber. *Polym. Test.* 23(1): 35-41.
- Nakason, C., Pechurai, W., Sahakaro, K. and Kaesaman, A. 2005. Rheological, mechanical and morphological properties of thermoplastic vulcanizates based on NR-g-PMMA/PMMA blends. *Polym. Adv. Tech.* 16, 592-599.
- Nakason, C., Tobprakhon, A. and Kaesaman, A. 2005a. Thermoplastic vulcanizates based on poly(methyl methacrylate)/epoxidized natural rubber blends: Mechanical, thermal, and morphological properties. *J. Appl. Polym. Sci.* 98(3): 1251-1261.

- Nakason, C., Nuansomsri, K., Kaesaman, A. and Kiatkamjornwong, S. 2006. Dynamic vulcanization of natural rubber/high-density polyethylene blends: Effect of compatibilization, blend ratio and curing system. *Polym. Test.* 25(6): 782-796.
- Nakason, C., Saiwari, S. and Kaesaman, A. 2006a. Rheological properties of maleated natural rubber/polypropylene blends with phenolic modified polypropylene and polypropylene-g-maleic anhydride compatibilizers. *Polym. Test.* 25(3): 413-423.
- Nakason, C., Saiwaree, S., Tatun, S. and Kaesaman, A. 2006b. Effect of vulcanization systems on properties of thermoplastic vulcanizates based on epoxidized natural rubber/polypropylene blends. *Polym Test.* 25(5):656-667.
- Nakason, C., Wannavilai, P. and Kaesaman, A. 2006c. Effect of vulcanization system on properties of thermoplastic vulcanizates based on epoxidized natural rubber/polypropylene blends. *Polym. Test.* 25(1): 34-41.
- Nakason, C., Jarnthong, M., Kaesaman, A., and Kiatkamjornwong, S. 2008. Thermoplastic elastomers based on epoxidized natural rubber and high-density polyethylene blends: Effect of blend compatibilizers on the mechanical and morphological properties. *J. Appl. Polym. Sci.* 109(4): 2694-2702.
- Neoh, S.B. and Hashim, A.S. 2004. Highly grafted polystyrene-modified natural rubber as toughener for polystyrene. *J. Appl. Polym. Sci.* 93(4): 1660- 1665.
- Ng, S.C. and Gan, L.H. 1981. Reaction of natural rubber latex with performic acid *Eur. Polym. J.*17(10): 1073-1077
- Odian, G. 1981. *Principles of polymerization*; 2nd ed., John Wiley, New York, USA.
- Oh, J.S., Isayev, I. and Rogunova, M.A. 2003. Continuous ultrasonic process for in situ compatibilization of polypropylene/natural rubber blends. *Polymer* 44(8): 2337-2349.
- Ohlsson, B., Hassander, H. and Törnell, B. 1998. Improved compatibility between polyamide and polypropylene by the use of maleic anhydride grafted SEBS. *Polymer* 39(26): 6705-6714.

- Oommen, Z., Nair, M.R.G. and Thomas, S. 1996. Compatibilizing effect of natural rubber-g-poly(methyl methacrylate) in heterogeneous natural rubber/poly(methyl methacrylate) blends. *Polym. Eng. Sci.* 36: 151-160.
- Oommen, Z. and Thomas, S. 1997. Mechanical properties and failure mode of thermoplastic elastomers from natural rubber/poly(methyl methacrylate)/natural rubber-g-poly(methyl methacrylate) blends. *J. Appl. Polym. Sci.* 65(7): 1245-1255.
- Oommen, Z. and Thomas, S. 1997a. Compatibility studies of natural-rubber poly(methyl methacrylate) blends by viscometry and phase-separation techniques. *J. Mater. Sci.* 32(22): 6085-6094.
- Oommen, Z., Thomas, S., Premalatha, C.K. and Kuriakose, B. 1997. Melt rheological behaviour of natural rubber/poly(methyl methacrylate)/natural rubber-g-poly(methyl methacrylate) blends. *Polymer* 38(22): 5611-5621.
- Oommen, Z., Groeninckx, G. and Thomas, S. 2000. Dynamic mechanical and thermal properties of physically compatibilized natural rubber/poly(methyl methacrylate) blends by the addition of natural rubber-graft-poly(methyl methacrylate). *J. Polym. Sci. Part B.* 38(4): 525-536.
- Otsu, T. and Yoshida, M. 1982. Terminator (iniferter) in radical polymerizations: Polymer design by organic disulfides as iniferters. *Makromol. Chem. Rapid. Commun.* 3(2): 127-132.
- Otsu, T., Yoshida, M. and Tazaki, T. 1982. A model for living radical polymerization. *Makromol. Chem. Rapid. Commun.* 3(2): 133-140.
- Otsu, T., Matsunaga, T., Doi, T. and Matsumoto, A. 1995. Features of living radical polymerization of vinyl monomers in homogeneous system using N,N-diethyldithiocarbamate derivatives as photoiniferters. *Eur. Polym. J.* 31(1): 67-78.
- Otsu, T. and Matsumoto, A. 1998. Controlled synthesis of polymers using the iniferter technique: developments in living radical polymerization. *Adv. Polym. Sci.* 136: 75-137.
- Otsu, T. 2000. Iniferter concept and living radical polymerization. *J. Polym. Sci. Part A: Polym. Chem.* 38(12): 2121-2136.

- Pechurai, W., Nakason, C. and Sahakaro, K. 2008. Thermoplastic natural rubber based on oil extended NR and HDPE blends: Blend compatibilizer, phase inversion composition and mechanical properties. *Polym. Test*, 27(5): 621-631.
- Perera, M.C.S. 1987. Surface modification of natural rubber laces. *J. Appl. Polym. Sci.* 34(7): 2591-2600.
- Phinyocheep, P., Axtell, F.H. and Laosee, T. 2002, Influence of compatibilizers on mechanical properties, crystallization, and morphology of polypropylene/scrap rubber dust blends. *J. Appl. Polym. Sci.* 86(1): 148–159.
- Phinyocheep, P., Pasiri, S. and Tavichai, Orasa. 2003. Diimide hydrogenation of isoprene-styrene diblock copolymers. *J. Appl. Polym. Sci.* 87(1): 76-82.
- Pichaiyut, S., Nakason, C., Kaesaman, A. and Kiatkamjornwong, S. 2008. Influences of blend compatibilizers on dynamic, mechanical, and morphological properties of dynamically cured maleated natural rubber and high-density polyethylene blends. *Polym. Test*. 27(5): 566-580.
- Poljanšek, I., Margon, V. and Šebenik, A. 1999. Synthesis of block copolymers with tetraphenyl biphosphine niferter, *Acta Chim. Slov.* 46(1): 1-13.
- Prasassarakich, P., Sintoorahat, P. and Wongwisetsirikul, N. 2001. Enhanced graft copolymerization of styrene and acrylonitrile onto natural rubber. *J. Chem. Eng. Japan.* 34(2):249-253.
- Rader, C.P. 1988. in *Handbook of thermoplastic elastomers*, B.M. Walker and C.P. Rader, eds., Van Nostrand Reinhold, New York, USA.
- Radhakrishnan, C.K., Sujith, A., Unnikrishnan, G. and Thomas, A. 2004. Effects of the blend ratio and crosslinking systems on the curing behavior, morphology, and mechanical properties of styrene-butadiene rubber/poly(ethylene-co-vinyl acetate) blends. *J. Appl. Polym. Sci.* 94(15): 827-837.
- Radusch, H.J. and Pham, T. 1996. Morphologiebildung in dynamisch vulkanisierten PP/EPDM-Blends, *Kautschuk. Gummi. Kunststoffe.* 49: 249-257.
- Ramesan, M.T. 2004. Thermogravimetric analysis, flammability and oil resistance in natural rubber and dichlorocarbene modified styrene butadiene rubber blends. *React. Funct. Polym.* 59(3): 267-274.

- Ramesh, P. and De, S.K. 1993. Evidence of thermally induced chemical reactions in miscible blends of poly(vinyl chloride) and epoxidized natural rubber. *Polymer* 34(23): 4893-4897.
- Reghunadhan Nair, C.P., Clouet, G. 1989. Effects of solvent and temperature on the copolymerizations of 2-acryloyloxyethyl diethyl phosphate with methyl methacrylate and styrene. *Eur. Polym. J.* 25(3): 251-257.
- Roy, S., Gupta, B.R. and De, S.K. 1993. Epoxidized rubbers, in *Elastomer Technology Handbook*. Cheremisinoff, N.P., Ed. Boca Raton, CRC Press, Florida.
- Samran, J., Phinyocheep, P., Daniel, P. and Kittipoom, S. 2005. Hydrogenation of unsaturated rubbers using diimide as a reducing agent. *J. Appl. Polym. Sci.* 95(1): 16-27.
- Schneier, B. 1973. Polymer compatibility. *J. Appl. Polym. Sci.* 17(10): 3175-3185.
- Schneider, M., Pith, T. and Lambla, M. 1996. Preparation and morphological characterization of two- and three-component natural rubber-based latex particles. *J. Appl. Polym. Sci.* 62(2): 273-290.
- Sebenik, A. 1998. Living free-radical block copolymerization using thio-iniferters. *Prog. Polym. Sci.* 23(5): 875-917.
- Simionescu, C.R., Vasiliu Oprea, C.L and Nicoleanu, J. 1983. Mechanochemically initiated polymerizations-5. Polymerization by vibratory milling of acrylamide and methacrylamide. *Eur. Polym. J.* 19(6): 525-528.
- Simionescu, I.C. and Simionescu, B.C. 1984. Unconventional radical polymerizations. *Pure Appl. Chem.* 56(3): 427-438.
- Singha, N.K., De, P.P. and Sivaram, S. 1997. Homogeneous catalytic hydrogenation of natural rubber using $\text{RhCl}(\text{PPh}_3)_3$. *J. Appl. Polym. Sci.* 66(9): 1647-1625.
- Small, P.A. 1953. Some factors affecting the solubility of polymers. *J. Appl. Chem.* 3: 71-79.
- Strichartzuk, P.T. 1977. US. 4036917, 18 June.
- Sujith, A. and Unnikrishnan, G. 2006. Molecular sorption by heterogeneous natural rubber/poly(ethylene-co-vinyl acetate) blend systems. *J. Polym. Res.* 13: 171-180.

- Sun, L.M., Fan, X.H., Chen, X.F., Liu, X.F. and Zhou, Q.F. 2007. Synthesis and characterization of graft copolymers containing poly(*p*-phenylene) main chains and mesogen-jacketed liquid-crystalline polystyrene side chains. *J. Polym. Sci. Part A: Polym. Chem.* 45(12): 2543-2555.
- Suriyachai, P., Kiatkamjornwong, S. and Prasassarakich, P. 2004. Natural-g-rubber glycidyl methacrylate/styrene as a compatibilizer in natural rubber /PMMA blends. *Rubber Chem. Technol.* 77(5): 914-930.
- Taha, M. and Frerejean, V. 1996. Morphology development of LDPE-PS blend compatibilization. *J. Appl. Polym. Sci.* 61(6): 969-979.
- Tang, L.W., Tam, K.C., Yue, C.Y., Hu, X., Lam, Y.C. and Li, L. 2004. Rheological and mechanical properties of compatibilized polystyrene/ethylene vinyl acetate blends. *J. Appl. Polym. Sci.* 94(5): 2071-2082.
- Tangthongkul, R., Prasassarakich, P. and Rempel, G.L. 2005. Hydrogenation of natural rubber with Ru[CH=CH(Ph)]Cl(CO)(PCy₃)₂ as a catalyst *J. Appl. Polym. Sci.* 97(6): 2399-2406.
- Tinker, A.J. 1984. Preparation of polypropylene/natural rubber blends having high impact strength at a low temperatures, *Polym. Communication* 25: 325-326.
- Thiraphattaraphun, L., Kiatkamjornwong, S., Prasassarakich, P. and Damronglerd S. 2001. Natural rubber-g-methyl methacrylate/poly(methyl methacrylate) blends. *J. Appl. Polym. Sci.* 81: 428-439.
- Thitithammawong, A., Noordermeer, J.W.M., Kaesaman, A. and Nakason, C. 2008. Influence of compatibilizers on the rheological, mechanical, and morphological properties of epoxidized natural rubber/polypropylene thermoplastic vulcanizates. *J. Appl. Polym. Sci.* 107(15): 2436-2443.
- Tran, Q.N. 2007. Synthesis and characterization of thermoplastic-grafted 1,4-polyisoprene. PhD, Université du Maine, Le Mans, France (december).
- Tsafack, M.J. and Levalois-Grützmacher, J. 2006. Plasma-induced graft-polymerization of flame retardant monomers onto PAN fabrics. *Surf. Coat. Technol.* 200(11): 3503-3510.
- Tsafack, M.J. and Levalois-Grützmacher, J. 2006a. Flame retardancy of cotton textiles by plasma-induced graft-polymerization (PIGP). *Surf. Coat. Technol.* 201(6): 2599-2610.

- Udipi, K. 1979. Epoxidation of styrene-butadiene block polymers. *I J. Appl. Polym. Sci.* 23(11): 3301-3309.
- Utracki, L.A. 1989. *Polymers Alloys and Blends*, Hanser Publishers, New York, USA.
- Utracki, L.A. 2002. *Polymer blends handbook: volume 1*. Kluwer Academic Publishers, Netherlands.
- Varghese, H., Bhagawan, S.S., Someswara Rao, S. and Thomas, S. 1995. Morphology, mechanical and viscoelastic behaviour of blends of nitrile rubber and ethylene-vinyl acetate copolymer. *Eur. Polym. J.* 31(10): 957-967.
- Varghese, S., Alex, R. and Kuriakose, B. 2004. Natural rubber-isotactic polypropylene thermoplastic blends. *J. Appl. Polym. Sci.* 92(4): 2063-2068.
- Wang, Z., Zhang, X. and Zhang, Y. 2002. Impact properties of dynamically vulcanized nylon/styrene-acrylonitrile copolymer/nitrile rubber blends. *Polym. Test.* 21(5): 577-582.
- Xie, B.H., Yang, M.B., Li, S.D., Li, Z.M. and Feng, J.M. 2003. Studies on polyamide-6/polyolefin blend system compatibilized with epoxidized natural rubber. *J. Appl. Polym. Sci.* 88(2): 398-403.
- Yang, X.M. and Qiu, K.Y. 1996. Polymerization of styrene using N-(p-tolyl)-N',N'-diethyldithiocarbamoylacetamide as photoiniferter. *J. Apply. Polym. Sci.* 61(3): 513-518.
- Yong, M.K., Ismail, H. and Ariff, Z.M. 2007. Comparison Properties of Natural Rubber (SMR L)/Ethylene Vinyl Acetate (EVA) Copolymer Blends and Epoxidized Natural Rubber (ENR-50)/Ethylene Vinyl Acetate (EVA) Copolymer Blends. *Polym. Plast. Tech. Eng.* 46: 361-366.
- Zurina, M., Ismail, H. and Ratnam, C.T. 2006. Characterization of irradiation-induced crosslink of epoxidised natural rubber/ethylene vinyl acetate (ENR-50/EVA) blend. *Polym. Degrad. Stab.* 91(11): 2723-2730.

APPENDIX

APPENDIX A

Published Article in Eur. Polym. J. 45(3): 820-836 (2009)



Contents lists available at ScienceDirect

European Polymer Journal

journal homepage: www.elsevier.com/locate/europolj

Graft copolymers of natural rubber and poly(dimethyl(acryloyloxymethyl)phosphonate) (NR-g-PDMAMP) or poly(dimethyl(methacryloyloxyethyl)phosphonate) (NR-g-PDMMEP) from photopolymerization in latex medium

Daniel Derouet^{a,*}, Punyanich Intharapat^{a,b}, Quang Ngoc Tran^a, Frédéric Gohier^a, Charoen Nakason^b

^aUCO2M, UMR CNRS 6011, Université du Maine, Faculté des Sciences, Avenue Olivier Messiaen, 72085 Le Mans Cedex 9, France

^bDepartment of Rubber Technology and Polymer Science, Faculty of Science and Technology, Prince of Songkla University, Pattani 94000, Thailand

ARTICLE INFO

Article history:

Received 10 October 2008

Received in revised form 21 November 2008

Accepted 24 November 2008

Available online 10 December 2008

Keywords:

Graft copolymer

Natural rubber

Photopolymerization

Dimethyl (acryloyloxymethyl)phosphonate

Dimethyl(methacryloyloxyethyl)

phosphonate

Latex

ABSTRACT

Graft copolymers of natural rubber and poly(dimethyl(acryloyloxymethyl)phosphonate) (NR-g-PDMAMP), and natural rubber and poly(dimethyl(methacryloyloxyethyl)phosphonate) (NR-g-PDMMEP), were prepared in latex medium via a "grafting from" methodology based on the photopolymerization of dimethyl(acryloyloxymethyl)phosphonate (DMAMP) and dimethyl(methacryloyloxyethyl) phosphonate (DMMEP), respectively, used as phosphorus-containing monomers. The grafting polymerization was initiated from *N,N*-diethyl-dithiocarbamate groups previously bound in side position of the rubber chains. The effects of monomer concentration on monomer conversion and grafting rate were investigated, showing that conversion and grafting rate increased with increasing monomer concentration and reaction time. Highest conversions and grafting rates were obtained with a molar ratio [DMAMP]/[initiating units] = 7 for a reaction time of 180 min. Calculation of the graft average length (\overline{DP}_n) from ¹H NMR spectra of the synthesized graft copolymers showed \overline{DP}_n values were in the range of 9–73. Visualizations of NR-g-PDMAMP and NR-g-PDMMEP latices by Transmission Electron Microscopy (TEM) showed that they exhibit core-shell morphologies. Degradation of NR-g-PDMAMP and NR-g-PDMMEP occurred in two steps: decomposition of dimethylphosphonate-functionalized grafts took place prior to the second step corresponding to the decomposition of NR backbone, but the degradation temperature of this last step was higher than that of pure NR.

© 2008 Elsevier Ltd. All rights reserved.

1. Introduction

Natural rubber (NR) is an interesting material with commercial success due to its excellent physical properties (i.e., high mechanical strength, low heat build up, excellent flexibility, and resistance to impact and tear), but also to the fact that NR is a renewable resource. However, NR has also some drawbacks as, for instance, low flame resistance, sensitivity to chemicals and solvents (ozone and weathering), mainly due to its unsaturated hydrocarbon

chain structure and its non-polar character, which cause limitation in variety of applications. Therefore, chemical modification of NR has been widely studied to improve for instance gas permeability, oil resistance, and flame resistance [1–2]. Various types of well-known modified NR products were thus prepared such as epoxidized natural rubbers [3–4], maleated natural rubbers [5–6], and graft copolymers of NR and PMMA [7–8] and NR and polystyrene [9–10].

Chemical modification of NR macromolecules is one possible approach to prepare new materials. One of the convenient ways is to perform graft copolymerization by incorporating phosphorus-containing monomers onto NR

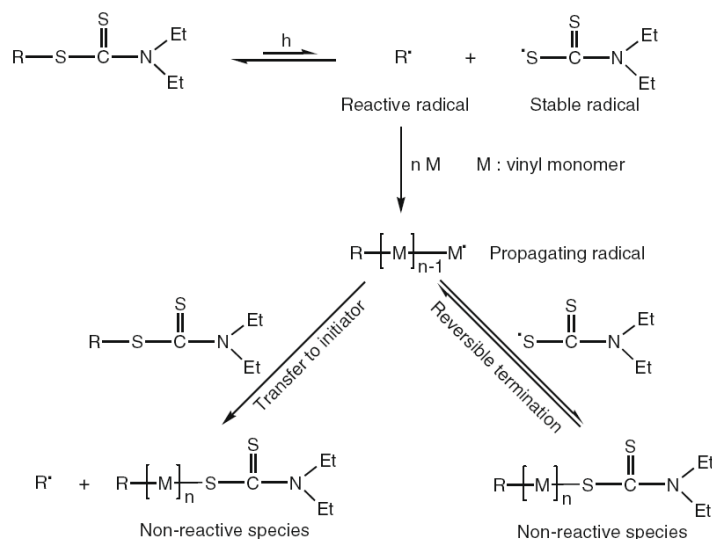
* Corresponding author. Tel.: +33(0)243833326; fax: +33(0)243833754.
E-mail address: Daniel.Derouet@univ-lemans.fr (D. Derouet).

chains. This type of monomer was successfully grafted onto polyethylene terephthalate fiber initiated by gamma radiation [11]. Several types of vinylphosphonate monomers were used including *N*-(dimethylphosphonomethyl)acrylamide, dimethyl(vinylmethoxy)phosphonate, dimethyl(vinylacetoxymethyl)phosphonate, dimethyl(acryloyloxymethyl)phosphonomethyl, dimethyl(vinyl)phosphonate, dimethyl(allyl)phosphonate, and diethyl(vinyl)phosphonate. Furthermore, the low-pressure plasma technique was used to confer a fire-resistant character to polyacrylonitrile (PAN) textiles by grafting and polymerization of various acrylate phosphorus-containing monomers, such as diethyl(acryloyloxyethyl)phosphate, diethyl-2-(methacryloyloxyethyl)-phosphate, diethyl(acryloyloxymethyl)phosphonate, dimethyl(acryloyloxymethyl)phosphonate, diethyl(acryloyloxyethyl)phosphoramidate, and acryloyloxy-1,3-bis(diethylphosphoramidate)propane [12, 13]. All these works found that the flame-retardant effect correlated mostly with the chemical structure of the monomer and the grafted phosphorus amount. Cellulose phosphonate modified with *N,N*-dimethylacrylamide and 4-vinylpyridine was also investigated showing powerful flame-retardant properties [14]. Dialkylphosphate reagents could be introduced onto epoxidized natural rubber (ENR) via a ring opening substitution mechanism on oxiranes [15]. However, the grafting of monomers bearing phosphonate groups onto natural rubber has not been previously reported.

In order to improve NR properties (i.e., flame-retardancy and oil resistance), but also to obtain new NR derivatives being able to be used as blend compatibilizers to promote the compatibility between NR and some polar thermoplastics, the grafting of polymers bearing phosphonate groups have been envisaged on NR by using a “graft-

ing from” methodology we have recently developed [16–18]. The procedure is based on the pioneering works of Otsu et al. in 1982, which were the first to report “living” radical photopolymerization of vinyl monomers initiated by “iniferter” [19–23] (Scheme 1). It consists to introduce *N,N*-diethyldithiocarbamate iniferter groups in side position of the rubber chains [16], and then to use these “iniferter” groups to initiate the photopolymerization of acrylate or methacrylate phosphorus-containing monomers [17,18]. Under UV irradiation the rubbery macroiniferters dissociate to form stable *N,N*-diethyldithiocarbamate radicals and active radicals along the NR chains capable to initiate monomer polymerization. During propagation, there are two major processes based on equilibrium between “living” polymer grafts and “non-living” ones. The reversibility between the growing radical grafts and stable *N,N*-diethyldithiocarbamate radicals cause reversible terminations to form non-propagating polymer grafts. The grafting chain growth can also proceed after chain transfer. Moreover, irreversible terminations such as combination or transfer can occur to stop definitively the chain growth.

The present paper deals with the syntheses of graft copolymers of NR and poly(dimethyl(acryloyloxymethyl)phosphonate) (NR-g-PDMAMP), and NR and poly(dimethyl(methacryloyloxyethyl)phosphonate) (NR-g-PDMMEP), respectively. In a first part, the syntheses of the phosphorus-containing monomers, i.e., dimethyl(acryloyloxymethyl)phosphonate (DMAMP) and dimethyl(methacryloyloxyethyl)phosphonate (DMMEP), will be described. Then, the results of the study of their graft copolymerization onto NR chains carried out in latex medium will be given.



Scheme 1. Mechanism of “living” radical photopolymerization of vinyl monomers initiated from *N,N*-dialkylthiocarbamate iniferters.

2. Experimental

2.1. Materials

Triethylamine and common solvents (acetone and methanol) used were of analytical grade. They were distilled before used. Dichloromethane was distilled under nitrogen atmosphere. The reagents necessary to the synthesis of dimethyl(acryloyloxymethyl)phosphonate (DMAMP) and dimethyl(methacryloylethyl)phosphonate (DMMEP) were prepared according to previous work [11,24]. Dimethyl 2-hydroxyethylphosphonate was purchased from Fluka Chemie AG (Buchs, Switzerland). Dimethyl hydroxymethylphosphonate was synthesized according to the Pudovik reaction in heterogeneous conditions [24]: paraformaldehyde, dimethylphosphite, and anhydrous potassium carbonate were supplied from Acros Organics (Geel, Belgium). Dimethylphosphite, acryloyl chloride, and methacryloyl chloride were obtained from Aldrich (Milwaukee, USA) and used as received. Sodium *N,N*-diethyldithiocarbamate trihydrate (DEDT-Na), tetrabutylammonium bromide (TBAB), and toluene were supplied by Acros Organics (Geel, Belgium). The reagents used for the epoxidation of NR latex, i.e., hydrogen peroxide 35 wt% and formic acid 99 wt%, were obtained from Acros Organics (Geel, Belgium). Natural rubber latex (42% drc, origin: southern part of Thailand) and Sinnopal NP 307 non-ionic surfactant (Cognis, Meaux, France) were used without further purification.

2.2. Monomer synthesis

DMAMP was synthesized as follows: dimethyl (hydroxymethyl)phosphonate (0.2 mol) was placed in a 500 ml two-necked round-bottom flask equipped with a magnetic stirrer. Distilled triethylamine (0.22 mol) was added, and then the mixture was cooled down in an ice bath. A solution of freshly distilled acryloyl chloride (0.2 mol) in 200 ml of dry dichloromethane was then added drop by drop. The mixture was kept at 0 °C for 1 h, and then stirred overnight at room temperature. The amine hydrochloride salt was filtered off, and the organic phase was washed with water and then dried with anhydrous sodium sulfate. After filtration and solvent evaporation, the residue was distilled under vacuum in presence of a small amount of hydroquinone. The obtained monomer was then characterized by ¹H NMR, ¹³C NMR, ³¹P NMR, and FTIR, respectively: ¹H NMR (CDCl₃, δ in ppm): 6.37 (dd, ²J_{HH} = 1.3 Hz, ³J_{HH} = 17.3 Hz, 1H, =CH *trans*); 6.09 (dd, ²J_{HH} = 10.4 Hz, ³J_{HH} = 17.3 Hz, 1H, CH=CH₂); 5.84 (d, ²J_{HH} = 1.3 Hz, ³J_{HH} = 10.4 Hz, 1H, =CH *cis*); 4.40 (d, ²J_{HP} = 8.7 Hz, 2H, —O—CH₂—P); 3.70 (d, ³J_{HP} = 10.8 Hz, 6H, P—O—CH₃). ¹³C NMR (CDCl₃, δ in ppm): 165.7 (C=O); 132.8 (CH₂=CH—); 126.7 (CH₂=CH—); 57.1(—O—CH₂—P); 53.1 (P—O—CH₃). ³¹P NMR (CDCl₃, δ in ppm): 21.8 (s). IR (cm⁻¹): 1729 (C=O), 1632 (C=C), 1237 (P=O), 1167 (P—C—O), 1023 (P—O—C).

DMMEP was prepared using the same procedure as DMAMP. However, methacryloyl chloride and dimethyl(1-hydroxyethyl)phosphonate were used instead

of acryloyl chloride and dimethyl(hydroxymethyl)phosphonate, respectively. DMMEP was also characterized by ¹H NMR, ¹³C NMR, ³¹P NMR, and FTIR: ¹H NMR (CDCl₃, δ in ppm): 6.19 (s, 1H of CH₂=C(CH₃)—); 5.63 (s, 1H of CH₂=C(CH₃)—); 4.48–4.29 (m, 2H, —O—CH₂—CH₂—); 3.71 (d, ³J_{HP} = 10.8 Hz, 6H, P—O—CH₃); 2.12–2.35 (m, —CH₂—P); 1.98 (s, 3H, CH₂=C(CH₃)—). ¹³C NMR (CDCl₃, δ in ppm): 166.7 (C=O); 135.8 (CH₂=C—CH₃); 125.7 (C=C—CH₃); 58.4 (—O—CH₂—CH₂—); 52.2 (P—O—CH₃); 26.1, 23.3 (—CH₂—P); 18.0 (CH₂=CCH₃). ³¹P NMR (CDCl₃, δ in ppm): 28.9 (s). IR (cm⁻¹): 1720 (C=O), 1633 (C=C), 1240 (P=O), 1030 (P—O—C).

2.3. Epoxidation of natural rubber latex

Epoxidized natural rubber (ENR) latex was prepared from NR latex (42% drc). The latex was first diluted to 20% drc with deionized water and stabilized with a non-ionic surfactant (Sinnopal NP 307) at 3.5 wt% of dry rubber content. The NR latex was stirred for 12 h at room temperature to eliminate ammonia and then transferred into a reactor equipped with a mechanical stirrer and a reflux condenser. The mixture was heated to 60 °C. Formic acid was then added drop by drop, and then hydrogen peroxide was gradually added with continuous stirring. The reaction mixture was stirred for 72 h. The amount of hydrogen peroxide used was calculated in order to obtain a theoretical epoxidation level of 20 unit%. Formic acid was used in equimolar quantity by comparison with hydrogen peroxide.

To characterize the structure of the epoxidized rubber contained in the ENR latex and to confirm the level of epoxidation, a sample of ENR latex was taken off and the ENR isolated after coagulation in methanol and drying under vacuum, was analyzed by ¹H NMR.

2.4. Synthesis of *N,N*-diethyldithiocarbamate-functionalized natural rubber (DEDT-NR)

Addition of sodium *N,N*-diethyldithiocarbamate onto epoxidized natural rubber units was carried out in latex medium, according to the method previously described [16]. ENR latex was first diluted to 5% drc. Na₂CO₃ was then added to adjust pH to approximately 8 before introduction of sodium *N,N*-diethyldithiocarbamate trihydrate (DEDT-Na) and tetrabutylammonium bromide (TBAB) as a phase transfer catalyst. The reaction mixture was stirred at 70 °C for 168 h. After reaction, the DEDT-NR formed was isolated for analysis by coagulation in methanol, and then washed several times with water. It was then dried under vacuum until a constant weight. ¹H NMR analysis was used to determine the content in *N,N*-diethyldithiocarbamate-functionalized 1,4-polyisoprene units.

The addition of DEDT-Na onto oxirane rings of epoxidized 1,4-polyisoprene units was confirmed by the ¹H NMR signal at δ = 4.35 ppm. It is characteristic of the proton bound to the carbon bearing the *N,N*-diethyldithiocarbamate group (—CH[SC(S)NEt₂]). On the other hand, the nucleophilic addition was also proved by the presence of ¹H NMR signals at δ = 3.7 ppm and δ = 4.0 ppm which are

assigned to the methylenes of diethylamino group ($-\text{N}-\text{CH}_2-\text{CH}_3$). Moreover, the diastereospecificity of the addition was confirmed by the presence of a single peak characteristic of the $-\text{C}(\text{CH}_3)(\text{OH})-$ methyl protons at $\delta = 1.15$ ppm, as previously reported [16].

The obtained polymer was composed of 80% of residual NR units, 14.5% of residual epoxidized NR units, and 5.5% of DEDT-functionalized NR units.

2.5. Grafting procedure

Grafting reactions were performed in latex medium in 25 ml Pyrex glass tubes equipped with a magnetic stirrer and closed by a screwed stopper with a joint of sealing covered with Teflon. They were carried out at room temperature and under nitrogen atmosphere. An UV lamp with a wavelength of 365 nm was used as irradiation source to initiate the grafting reaction. Studies were performed using two [monomer]/[DEDT-NR units] molar ratios: 3.5 and 7.0. During grafting progress, a very important increase of the latex viscosity was noted after about 60 and 90 min of reaction in the case of DMAMP, and about 90 and 110 min in that of DMMEP, at [monomer]/[DEDT-NR units] molar ratios of 3.5 and 7.0, respectively. After grafting, the graft copolymer was coagulated in methanol, and then purified by dissolution/re-precipitation with dichloro-methane/methanol. The product was then dried at 40 °C under vacuum until constant weight.

After drying, the product was extracted with methanol for 24 h using a Soxhlet extractor to remove the dimethylphosphonate-functionalized homopolymer possibly formed. The residual graft copolymer was recovered by filtration and dried under vacuum at 40 °C until constant weight.

Monomer conversions, monomer conversions in grafts, and grafting rates (GR was defined as the weight percent of dimethylphosphonate-functionalized grafts in the copolymer) were calculated from the following equations:

$$\text{Monomer conversion} = \frac{W_c - W_t}{W_m} \times 100 \quad (1)$$

$$\text{Monomer conversion in grafts} = \frac{W_s - W_t}{W_m} \times 100 \quad (2)$$

$$\text{Grafting rate} = \frac{W_s - W_t}{W_s} \times 100 \quad (3)$$

where, W_c is the weight of the purified polymer mixture recovered after grafting, W_t the weight of DEDT-NR before grafting, W_m the weight of monomer used for the grafting reaction, and W_s the weight of graft copolymer isolated after extraction with methanol.

Grafting rates (GR), as well as the average length of the grafts, i.e., the degree of polymerization ($\overline{\text{DPn}}$), were also determined from ^1H NMR spectra of the graft copolymers obtained after extraction of the dimethylphosphonate-functionalized homopolymer possibly formed. They were calculated by comparing the peak areas of the various signals characteristic of the different types of protons present in the graft copolymer, as follows:

Considering the integration of the rubber chain part in the spectrum of the graft copolymer, I_{rubber} it includes three different types of units (unsaturated NR units, epox-

idized NR units, and DEDT-functionalized NR units) whose units proportions (X , Y , and Z , respectively; $X + Y + Z = 1$), unchanged after grafting, could be determined from the ^1H NMR spectrum of DEDT-NR used as macroinitiator (Scheme 2).

By taking into account the results of the previous studies [18], it was considered in the calculation of I_{rubber} that N,N -diethyldithiocarbamate groups, normally present at the end of the grafts, have totally disappeared after polymerization. Therefore, I_{rubber} can be determined as follows:

$$I_{\text{rubber}} = (8 \times H_{\text{unsaturated NR units}}) + (8 \times H_{\text{epoxidized NR units}}) + (9 \times H_{\text{DEDT-NR units}})$$

where, $H_{\text{unsaturated NR units}}$ is the I_{uns} integration of the signal at $\delta = 5.0 - 5.2$ ppm on the copolymer spectrum (signal of $=\text{CH}-$ protons of unsaturated NR units), $H_{\text{epoxidized NR units}} = (I_{\text{uns}} \times Y)/X$, and $H_{\text{DEDT-NR units}} = (I_{\text{uns}} \times Z)/X$.

Knowing the integration corresponding to the rubber part in the copolymer spectrum (I_{rubber}), the $\overline{\text{DPn}}$ of PDM-AMP (or PDMMEP) grafts can be obtained from the following equation:

$$\overline{\text{DPn}} = \frac{(I_{\text{total}} - I_{\text{rubber}})}{A \times H_{\text{DEDT-NR units}}} \quad (4)$$

where, $(I_{\text{total}} - I_{\text{rubber}})$ is the integration corresponding to the graft protons in the graft copolymer, and A the number of protons in the used monomer (i.e., $A = 11$ in the case of DMAMP, and $A = 15$ in that of DMMEP).

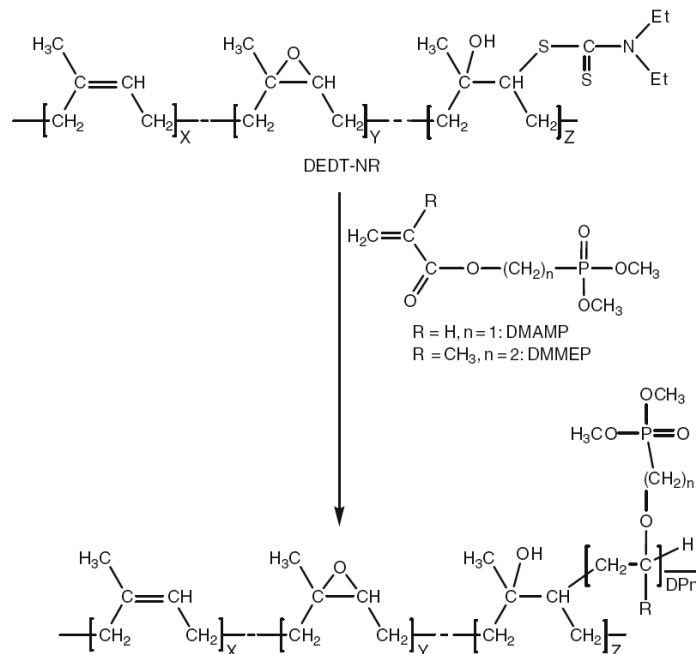
The number-averaged molecular weight (\overline{M}_n) of phosphorated grafts was obtained by multiplication of $\overline{\text{DPn}}$ with the molecular weight of the chosen monomer.

The grafting rate (GR) was obtained by multiplication of $\overline{\text{DPn}}$ with the molecular weight of the chosen monomer. Thus, GR was calculated by applying the following equation:

$$\text{GR} = \frac{(M_1 \times \overline{\text{DPn}} \times Z)}{((M_1 \times \overline{\text{DPn}} \times Z) + (M_2 \times X) + (M_3 \times Y) + (M_4 \times Z))} \times 100 \quad (5)$$

Where, M_1 = molecular weight of the monomer used (194 g mol^{-1} for DMAMP or 222 g mol^{-1} for DMMEP), M_2 = molecular weight of NR unit (68 g mol^{-1}), M_3 = molecular weight of epoxidized NR unit (84 g mol^{-1}), M_4 = molecular weight of N,N -diethyldithiocarbamate-functionalized NR unit in which the N,N -diethyldithiocarbamate group is changed with an hydrogen (considering that the grafts are not terminated by a N,N -diethyldithiocarbamate group).

Kinetic studies. Grafting reactions were performed as described above using two [monomer]/[DEDT-NR units] molar ratios: 3.5 and 7.0. Different grafting reactions were performed and stopped at various times, and the crude mixtures obtained were treated as described above to determine monomer conversion, monomer conversion in grafts, and grafting rate by weighing, using Eqs. (1)–(3), respectively. On the other hand, the crude mixtures obtained were also analyzed by ^1H NMR to calculate $\overline{\text{DPn}}$ and grafting rates, by using the Eqs. (4) and (5), respectively.



Scheme 2. Photopolymerization of DMAMP (or DMMEP) initiated from DEDT-NR as macroinitiator.

2.6. Measurements

Liquid NMR spectra were recorded on a Bruker DPX 200 Fourier-transform spectrometer, at 200.13 MHz for ^1H , at 50.32 MHz for ^{13}C , and at 81.01 MHz for ^{31}P . Samples were analyzed in solution in chloroform- D (99.8% purity; Spectrométrie Spin et Techniques). In ^1H and ^{13}C NMR, the chemical shifts were expressed in ppm in the δ scale, compared with the singlet of tetramethylsilane (TMS), as internal standard. In ^{31}P NMR, they were expressed in ppm in the δ scale, with reference to the phosphoric acid peak, as external standard.

Infrared spectra were recorded on a Fourier Transform InfraRed (FTIR) spectrometer (Omic ESP Magna-IR 560 spectrometer), at a resolution of 4 cm^{-1} , in the spectral range of $4000\text{--}500\text{ cm}^{-1}$. Liquid samples were analyzed in the form of thin films between two NaCl disks. Solid ones were analyzed in KBr pellets.

Thermo Gravimetric Analyses (TGAs) were performed using a TGA Q500 TA Instrument-Waters equipped with an EGA oven. A 10–20 mg sample was placed in a platinum pan. Analyses were carried out under nitrogen and oxygen atmospheres, respectively (gas flow = 100 ml min^{-1}), at a heating rate of $10\text{ }^\circ\text{C min}^{-1}$, on a temperature range of $30\text{--}575\text{ }^\circ\text{C}$.

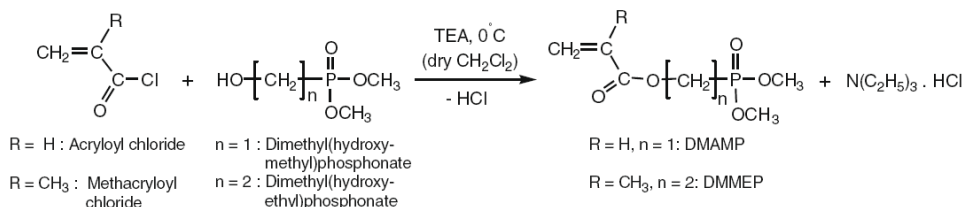
Thermal characterization of the graft copolymers was carried out under nitrogen purge (100 ml min^{-1}) using a Q100 TA Instrument-Waters Differential Scanning Calo-

rimeter (DSC) equipped with a TA Universal Analysis thermal analysis data station, and fitted with a mechanical system of cooling by compression (RCS) capable to go down to temperatures as low as $-90\text{ }^\circ\text{C}$. A sample (3–10 mg) was placed in the DSC sample pan, and the heating rate was set at $10\text{ }^\circ\text{C min}^{-1}$. The sample was quenched to $-80\text{ }^\circ\text{C}$ for 1 min, then heated up to $100\text{ }^\circ\text{C}$ and kept at this temperature for 5 min to remove the heat history. Then, the sample was slowly quenched again to $-80\text{ }^\circ\text{C}$ and the second heating scan was recorded. Tg were taken at the inflexion point.

Transmission Electron Microscopy (TEM) was used on JEOL JEM-2010 to study the morphology of the graft copolymer latices. The polymer-grafted natural rubber latex was diluted approximately 400 times of its original concentration with distilled water. An aqueous solution (2 wt%) of OsO_4 was added to stain natural rubber macromolecules. The stained latex was then placed on a 400 mesh grid, and dried overnight in a desiccator before characterization.

3. Results and discussion

In order to synthesize graft copolymers composed of NR backbone and polymer grafts bearing phosphonate functions via a grafting procedure based on the radical photopolymerization of acrylate and methacrylate monomers, two monomers containing dimethylphosphonate



Scheme 3. Synthesis of DMAMP and DMMEP.

functions, dimethyl(acryloyloxymethyl)phosphonate (DMAMP) and dimethyl(methacryloyloxyethyl)phosphonate (DMMEP), were synthesized. DMAMP was prepared by condensation reaction between acryloyl chloride and dimethyl(hydroxymethyl)phosphonate [13], while DMMEP was prepared using methacryloyl chloride and dimethyl(1-hydroxyethyl)phosphonate (Scheme 3). The reactions were performed in dry dichloromethane in presence of triethylamine (TEA) as acid acceptor.

Each of the monomers isolated after distillation under vacuum was characterized by ¹H, ¹³C, and ³¹P NMR in solution in CDCl₃. In ³¹P NMR, only one single peak was seen on the respective spectra, at δ = 21.8 ppm for DMAMP and δ = 28.9 ppm for DMMEP, proving the purity of the distilled monomers. On the ¹H NMR spectrum of DMAMP, the three doublets observed at δ = 5.84, 6.09, and 6.37 ppm are characteristic of the three protons on the acrylate carbon-carbon double bond. The two protons of the methacrylate double bond in DMMEP were characterized in ¹H NMR as two singlet signals at δ = 5.64 ppm and δ = 6.19 ppm. ¹³C NMR peaks characteristic of carbons in carbon-carbon double bonds of the dimethylphosphonate monomers were observed at δ = 126.7 ppm (=CH-) and δ = 132.8 ppm (CH₂=) in the case of DMAMP, and δ = 125.7 ppm (CH₂=) and δ = 135.8 ppm (=C(CH₃)-) in that of DMMEP, and those of C=O at δ = 165.7 ppm and δ = 166.7 ppm, respectively. IR absorptions confirmed the structures of the synthesized monomers with absorption bands characteristic of P=O, C=C, and P-O-C vibrations, respectively, at 1237, 1632, and 1023 cm⁻¹ for DMAMP, and 1240, 1633, and 1030 cm⁻¹ for DMMEP.

3.1. Synthesis and characterization of the graft copolymers

The syntheses of the graft copolymers were performed in latex medium according to a grafting procedure based on the photopolymerization of dimethyl(acryloyloxymethyl)phosphonate (DMAMP) and dimethyl(methacryloyloxyethyl)phosphonate (DMMEP), respectively, used as phosphorated monomers. The polymerizations were initiated from *N,N*-diethyldithiocarbamate groups previously bound in side position of the rubber chains [16]. The graft copolymers obtained after extraction with methanol were dried and then characterized by ¹H, ¹³C, and ³¹P NMR, as well as by FTIR spectroscopy.

¹H NMR spectra of NR-g-PDMAMP and NR-g-PDMMEP are shown in Figs. 1 and 2, respectively. On NR-g-PDMAMP spectrum (Fig. 1), the NR backbone was identified by the

signal at δ = 5.1 ppm characteristic of the proton of the carbon-carbon double bond (-C(CH₃)=CH-) in unsaturated NR units, and the formation of PDMAMP grafts was confirmed by signals at δ = 3.8 ppm and δ = 4.4 ppm characteristic of the dimethyl ester and methylenoxy protons of the phosphonate function. In the case of NR-g-PDMMEP (Fig. 2), the signal of -C(CH₃)=CH- protons on NR backbone was noted at δ = 5.1 ppm, and those of dimethyl ester and methylenoxy protons of phosphonate function at δ = 3.8 ppm and δ = 4.2 ppm, respectively. In the two families of graft copolymers, the presence of residual epoxidized NR units was also characterized on their ¹H NMR spectra by the signal of the oxirane protons of the epoxidized NR units at δ = 2.7 ppm.

¹³C NMR characteristics of NR-g-PDMAMP and NR-g-PDMMEP are given in Figs. 3 and 4, respectively. The formation of NR-g-PDMAMP was confirmed by the simultaneous presence of signals at δ = 125 ppm and δ = 135 ppm characteristic of -C(Me)= and =CH- unsaturated carbons of NR backbone, respectively, and signals at δ = 52.9 ppm and δ = 62.1 ppm characteristic of dimethyl ester and methylenoxy carbons of dimethylphosphonate functions on PDMAMP grafts (Fig. 3). In the case of NR-g-PDMMEP, the signals of dimethyl ester and methylenoxy carbons of dimethylphosphonate functions on PDMMEP grafts were characterized at δ = 53.2 ppm and δ = 52.0 ppm, respectively. The formation of phosphorated grafts was also confirmed by the presence of the C=O carbon peak at δ = 176.1 ppm. The C-OH quaternary carbons in NR-g-PDMAMP and NR-g-PDMMEP were noted at δ = 74.0 and δ = 74.3 ppm, respectively.

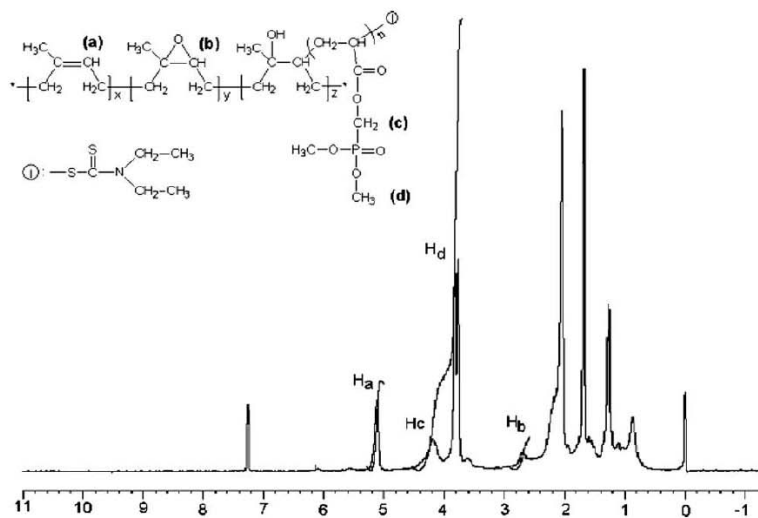
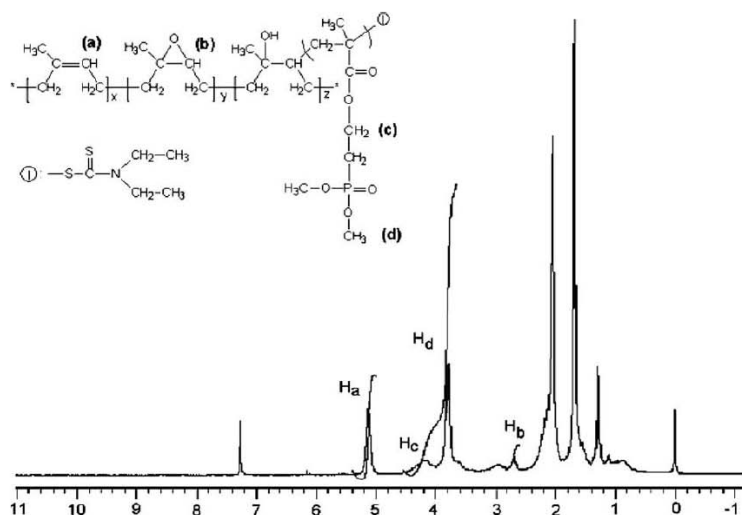
The presence of dimethylphosphonate functions along the grafts was confirmed by ³¹P NMR, as shown on the ³¹P NMR spectra given in Fig. 5. Only one sharp peak was observed in both cases, at δ = 21.6 ppm for NR-g-PDMAMP and δ = 29.3 ppm for NR-g-PDMMEP. This indicates that PDMAMP (and PDMMEP) grafts would adopt a stereoregular conformation.

3.2. Grafting kinetics

The kinetics of grafting of PDMAMP and PDMMEP onto NR chains were studied in terms of influence of monomer structure and monomer concentration.

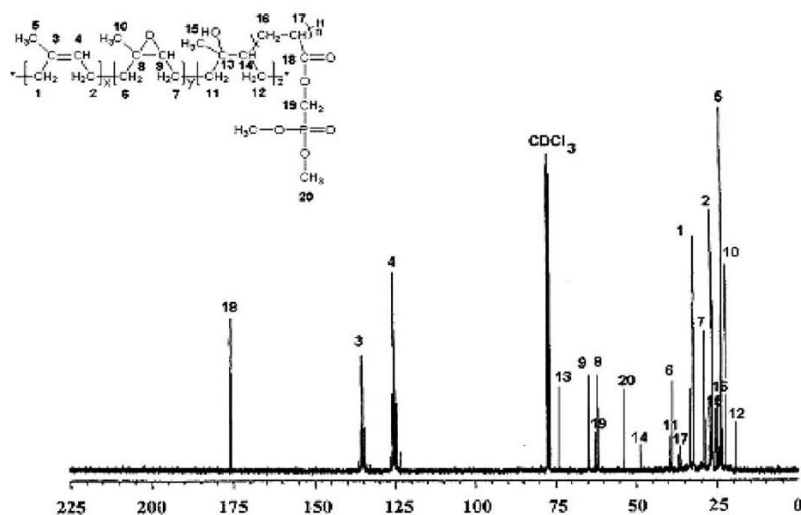
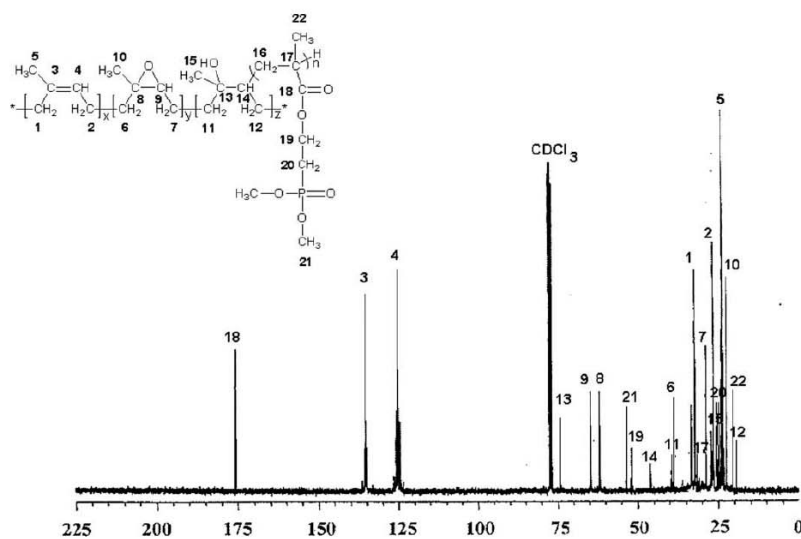
3.2.1. Effect of monomer structure

The effect of monomer structure was studied by means of DMAMP and DMMEP, initially chosen as phosphorated

Fig. 1. Typical ^1H NMR spectrum of NR-g-PDMAMP.Fig. 2. Typical ^1H NMR spectrum of NR-g-PDMMEP.

monomers (Scheme 4). The kinetics of the photopolymerizations of DMAMP and DMMEP initiated from DEDT-NR chains, using a molar ratio $[\text{monomer}]/[\text{DEDT-NR units}] = 3.5$, showed different reactivities as evidenced from their respective conversions and grafting rates in identical reaction conditions (Figs. 6 and 7). Contrary to the polymerization of DMAMP, which started immediately at the beginning of irradiation, that of DMMEP did not oc-

cur until a reaction time of 20 min. With progress of polymerization, monomers were consumed to form phosphorated grafts, but also homopolymers in low proportions (about 10% at the grafting end, whatever the structure of the monomer), as shown in Fig. 6. At each time of the grafting, conversion of DMAMP in grafts is always higher than that of DMMEP. After about 90 min, monomer conversions and grafting rates reached a plateau, indicat-

Fig. 3. Typical ^{13}C NMR spectrum of NR-g-PDMAMP.Fig. 4. Typical ^{13}C NMR spectrum of NR-g-PDMMEP.

ing that the efficiency of the grafting with DMAMP is higher than that with DMMEP, but also that the propagation step of the “living” radical photopolymerization, so-called by Otsu et al. [19–23], is disturbed by irreversible termination reactions essentially due to the low initiation rate. This was confirmed by the kinetic studies which showed that, whatever the structure of the monomer used, the rate

law for the grafting by photopolymerization had not kinetic order of 1 with respect to monomer concentration (Fig. 8), and the number-averaged molecular weight (\bar{M}_n) of the grafts did not evolve linearly with conversion (Fig. 9). In Fig. 9, the fact that the slope of the experimental curve representing the progress of \bar{M}_n versus monomer conversion was lower than that of the theoretical one is

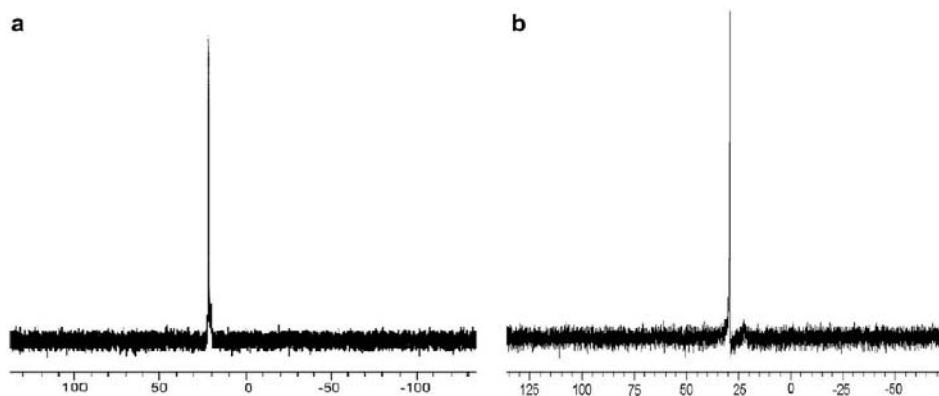
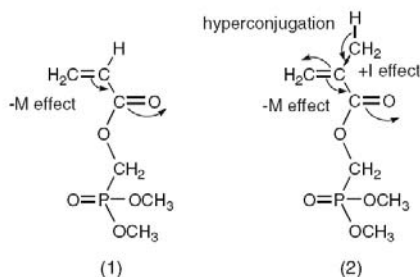


Fig. 5. Typical ^{31}P NMR spectra of NR-g-PDMAMP (a) and NR-g-PDMMEP (b).

significant of the existence of transfer reactions during the photopolymerization step, with as a consequence the formation of homopolymer, as already specified. However, the strong increase of \bar{M}_n after 60% of DMAMP conversion (55% for DMMEP) is rather surprising because the number of reactive sites is supposed lower at this moment of the reaction, and moreover, the monomer conversion is almost stopped. However, similar effects were already related in literature concerning radical polymerization [25]. In addition, it was also noted that this strong increase of \bar{M}_n at the moment where the monomer conversion seems stopped (Figs. 6 and 7), begins simultaneously with the increase of latex viscosity [26]. This result could be explained by recombination reactions [27] between growing grafts and growing homopolymers, facilitated by the fact that the initially hydrophobic rubber would become increasingly hydrophilic with the progress of the grafting reaction. As monomer conversion slows down abruptly, the rubber particles of latex, whose polarity is enhanced with the increase of grafting rate, probably disaggregate, and thus the rubbery copolymer would be in part dispersed in the aqueous phase, with for consequence to increase the latex viscosity and thus to favor the approach between growing grafts and growing homopolymers.

The highest grafting rate obtained with DMAMP by comparison with that obtained with DMMEP is consistent with the general behavior of acrylates and methacrylates [28]. In the two cases the mesomeric effect ($-M$) of the double bond with the ester function creates a polarization of the double bond, which is compensated in the case of methacrylate by the positive inductive effect ($+I$) and the hyperconjugation of the methyl. As a consequence, acrylate double bond is more polarized and so more reactive. The propagation step is also faster with acrylate since the macroradical is less stabilized than methacrylate macroradical [29]. These factors can account for the observed phenomenon [30,31].

The progress of the grafting rates determined by weighing was compared with the one of grafting rates obtained from ^1H NMR (Fig. 10). It was noted that the grafting rates values determined from ^1H NMR spectrum of graft copolymers at various times are always higher than the ones measured by weighing. However, an increase of the difference between the respective values obtained is observed with increasing reaction time, but even after high reaction times it remains on the whole very low. The lost of part of products during the different treatments carried out on the crude copolymer obtained after grafting probably explains these little differences.



Scheme 4. Influence of DMAMP.

3.2.2. Effect of monomer concentration

The effects of monomer concentration on monomer conversion and grafting rate are shown in Fig. 11. It was noted that the grafting rate increases with increasing monomer concentration. The rate of polymerization, and thus the grafting rate, progresses slowly during the first 100 min of reaction, and finally tends to a plateau whose value increases with monomer concentration. The same trend is observed with monomer conversion: after 90 min irradiation, the proportion of consumed monomer tends to a plateau whose value is dependent on the monomer concentration.

These results show that increasing the monomer concentration can increase the rate of the propagation step,

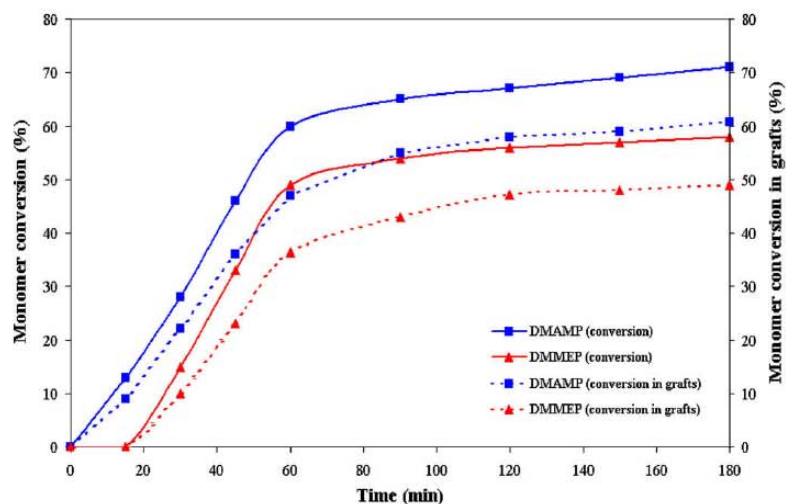


Fig. 6. Progress of monomer conversion and monomer conversion in grafts (determination by weighing) for the photopolymerizations of DMAMP and DMMEP initiated from DEDT-NR with $[\text{monomer}]/[\text{DEDT-NR units}] = 3.5$.

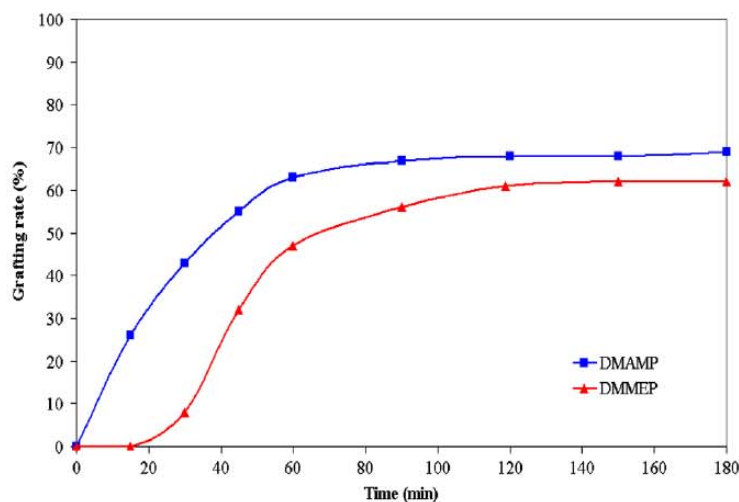


Fig. 7. Progress of grafting rate (determined by weighing) for the photopolymerizations of DMAMP and DMMEP initiated from DEDT-NR with $[\text{monomer}]/[\text{DEDT-NR units}] = 3.5$.

and thus the grafting rate, but effects of irreversible terminations remain unchanged. However, in the present grafting system, another factor must be taken into account: the viscosity of the reaction medium. Indeed, it was observed that the viscosity of the medium obviously not only increased with increasing polymerization time, but also

increased with increasing monomer concentration. The mobility of the copolymer–monomer mixture may be affected by this increase of viscosity, so leading to a premature end of the radical growing polymerization [13], but not for the recombination reactions between growing homopolymer and grafts, as already explained above.

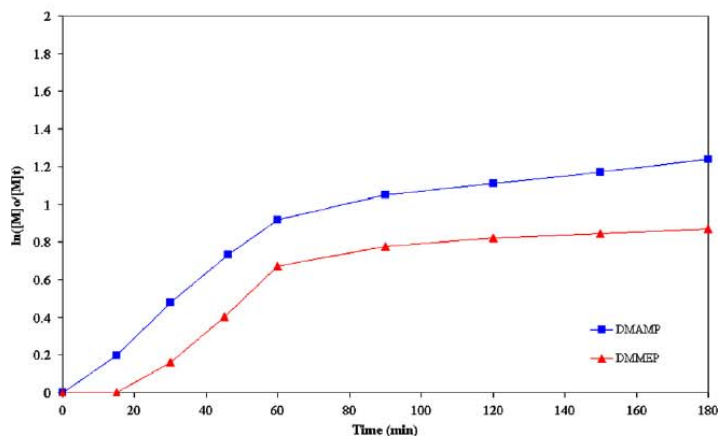


Fig. 8. First-order kinetic plots for the photopolymerizations of DMAMP and DMMEP initiated from DEDT-NR with $[\text{monomer}]/[\text{DEDT-NR units}] = 3.5$.

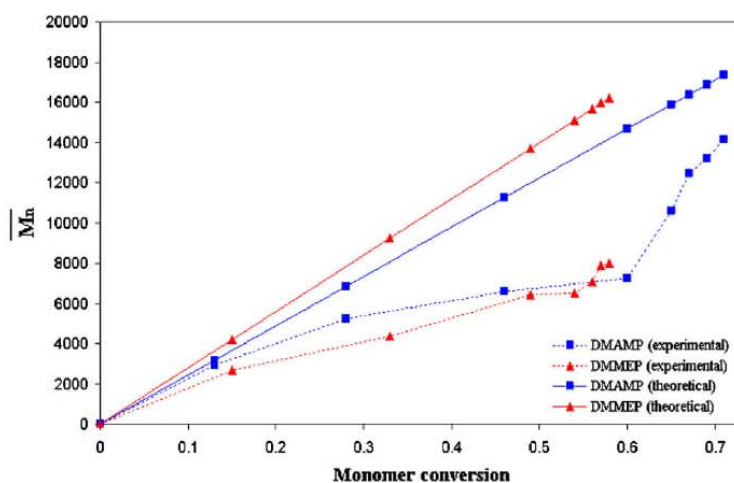


Fig. 9. Dependence of molecular weight (\overline{M}_n) on monomer conversion for the photopolymerizations of DMAMP and DMMEP initiated from DEDT-NR with $[\text{monomer}]/[\text{DEDT-NR units}] = 7$.

3.3. Average length of the grafts (degree of polymerization)

Degrees of polymerization (\overline{DP}_n) of grafts and grafting rates (GR) of various NR-g-PDMAMP and NR-g-PDMMEP copolymers, prepared under various reaction conditions, are given in Table 1. It was noted that \overline{DP}_n and GR increased with increasing monomer concentration and reaction time. Furthermore, when the grafting was carried out in same conditions, the grafting rates of the copolymers coming from DMAMP are always higher than those of the

copolymers obtained with DMMEP. As already evoked above (Fig. 10), one can note similar results concerning the comparison between the GR values determined by weighing and ^1H NMR, and that, whatever the grafting conditions used, the highest graft lengths ($\overline{DP}_n = 73$) and grafting rates (GR = 86 wt% in dimethylphosphonate-functionalized grafts) were obtained with DMAMP as monomer, using a molar ratio $[\text{monomer}]/[\text{DEDT-NR units}] = 7$ and a reaction time of 180 min.

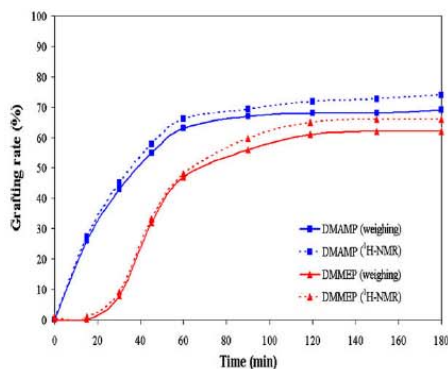


Fig. 10. Comparison of the progress of the grafting rates determined by weighing with the one of grafting rates obtained from ¹H NMR for the photopolymerizations of DMAMP and DMMEP initiated from DEDT-NR with [monomer]/[DEDT-NR units] = 3.5.

3.4. Thermal stability of the graft copolymers

Thermal stabilities of pure NR, PDMAMP, PDMMEP, NR-g-PDMAMP, and NR-g-PDMMEP were successively characterized by TGA. The various TGA curves obtained within nitrogen atmosphere and oxygen atmosphere are given in Figs. 12 and 13, respectively.

In nitrogen atmosphere (Fig. 12), it was noted that pure NR showed only single step of weight loss with an onset temperature of approximately 320 °C. PDMAMP and PDMMEP homopolymers also showed a single step, but at lower onset temperature of 225 °C and 220 °C, respectively (Table 2). This result agrees with the results reported in the previous works [12]. For NR-g-PDMAMP and NR-g-PDMMEP prepared using a ratio [monomer]/[DEDT-NR units] = 7 and isolated at reaction times of 60 min and 180 min, the TGA curves showed double degradation steps. With these graft copolymers, a shift of the TGA curve toward the high temperatures was observed when the grafting rate was increased. Depending on the grafting rate, the first degradation step was noted at onset temperature

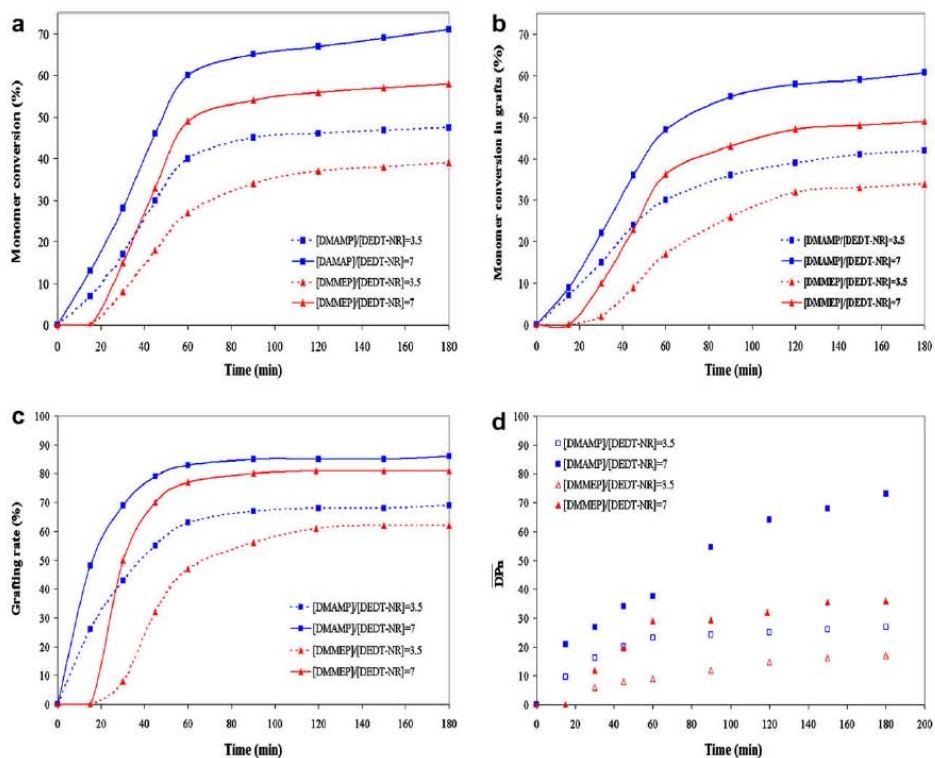


Fig. 11. Influence of monomer concentration and monomer structure on the progress of (a) monomer conversion, (b) monomer conversion in grafts, (c) grafting rate, and (d) DPn, respectively.

Table 1
Degrees of polymerization (\overline{DP}_n) and grafting rates (GR) of the various graft copolymers obtained.

Type of copolymer	[M]/[DEDT-NR units] (mol mol ⁻¹)	Reaction time (min)	Monomer conversion (%)	Degree of polymerization(\overline{DP}_n)	Grafting rate (GR in wt%)	
					¹ H NMR	Weighing
NR-g-PDMAMP	3.5	60	40	23	79	63
NR-g-PDMAMP	7.0	60	60	37	87	83
NR-g-PDMAMP	3.5	180	47	27	81	68
NR-g-PDMAMP	7.0	180	71	73	92	86
NR-g-PDMMEP	3.5	60	26	9	62	46
NR-g-PDMMEP	7.0	60	49	29	84	77
NR-g-PDMMEP	3.5	180	39	17	76	62
NR-g-PDMMEP	7.0	180	58	36	86	80

varying from 260 °C to 270 °C, corresponding to a weight loss from 46% to 30%, and the second one at onset temperature from 400 °C to 430 °C, corresponding to a weight loss from 37% to 46% (Table 2). The first decomposition step of the graft copolymers corresponds to the degradation of phosphonate linkages that occurred at lower decomposition temperature than that of NR backbone. On the other hand, the second onset temperature is always higher than that of NR that shows the ability of dimethylphosphonate-functionalized grafts to improve thermal stability of NR.

Alternatively, TGA analyses were performed under oxygen atmosphere to simulate graft copolymer behavior in commonly used conditions. By comparison with that observed under nitrogen atmosphere, the decomposition under oxygen atmosphere occurred at a lower temperature that was easily explained by the action of oxygen as oxidant to favor the degradation of the organic materials. Except for NR and homopolymers, the degradation curves of the other analyzed samples were comparable to that obtained in nitrogen atmosphere (Fig. 13). Decomposition

of pure NR starts at 179 °C, but its main decomposition peak is observed at 260 °C. Thermal stability of NR-g-PDMAMP and NR-g-PDMMEP in oxygen also depends on the grafting rate: TGA curves clearly shifts to higher temperature as the grafting rate increases. However, its influence on the thermal stability of the graft copolymer is much more marked. Compared to the values obtained with the same samples in nitrogen atmosphere, the onset temperatures for the first degradation step in oxygen varied from 210 °C to 230 °C, corresponding to a weight loss from 43% to 31%, and that for the second one from 326 °C to 396 °C, corresponding to a weight loss from 44% to 50% (Table 2).

Concerning the remaining residues, it was noted that NR is totally degraded at 500 °C whatever the surrounding atmosphere. On the other hand, the proportions in carbonaceous residues (or char) observed at this temperature in the case of the degradation of the graft copolymers are always higher than that observed during degradation of PDMMEP and PDMAMP homopolymers. Moreover, they

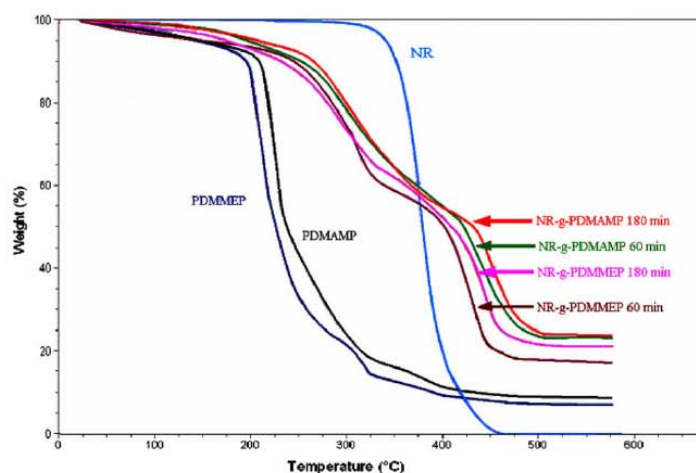


Fig. 12. TGA curves under nitrogen atmosphere of NR, PDMAMP, PDMMEP, NR-g-PDMMEP after 60 min (GR = 77%) and 180 min (GR = 80%) of grafting, and NR-g-PDMAMP after 60 min (GR = 83%) and 180 min (GR = 86%) of grafting. Grafting conditions: [monomer]/[DEDT-NR units] = 7.

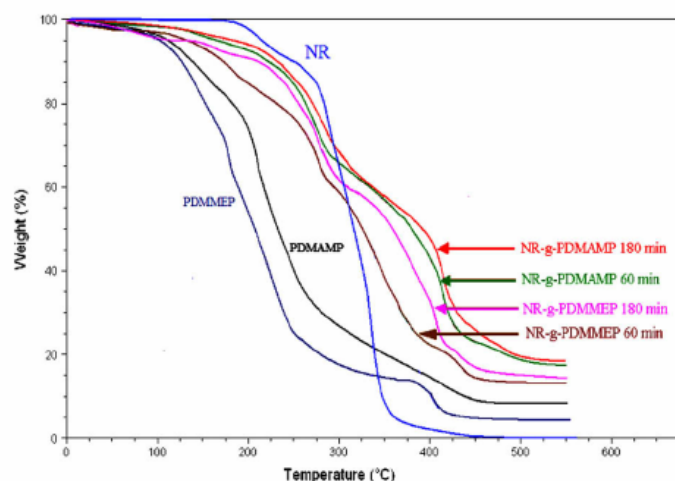


Fig. 13. TGA curves under oxygen atmosphere of NR, PDMAMP, PDMMEP, NR-g-PDMAMP after 60 min (GR = 77%) and 180 min (GR = 80%) of grafting, and NR-g-PDMAMP after 60 min (GR = 83%) and 180 min (GR = 86%) of grafting. Grafting conditions: $[\text{monomer}]/[\text{DEDI-NR units}] = 7$.

Table 2

TGA characteristics of NR, PDMAMP, PDMMEP, NR-g-PDMAMP after 60 min (GR = 83%) and 180 min (GR = 86%) of grafting, and NR-g-PDMMEP after 60 min (GR = 77%) and 180 min (GR = 80%) of grafting, in nitrogen and oxygen atmospheres, respectively. Grafting conditions: $[\text{monomer}]/[\text{DEDI-NR units}] = 7$.

Type of copolymer	Nitrogen atmosphere				Char (%)	Oxygen atmosphere				Char (%)
	Onset temperature (°C)		Weight loss (%)			Onset temperature (°C)		Weight loss (%)		
	1st step	2nd step	1st step	2nd step		1st step	2nd step	1st step	2nd step	
NR	320	–	99.8	–	0.2	193	260	7	92.9	0.10
PDMAMP	225	–	89	–	11	137	190	17	75	8
PDMMEP	220	–	91	–	9	126	170	22	73.3	4.7
NR-g-PDMAMP 83%*	268	422	40	37	23	225	375	44.5	39	17.5
NR-g-PDMAMP 86%*	270	430	44	32	24	230	396	46	35	19
NR-g-PDMMEP 77%*	260	400	37	46	17	210	326	40	47	13
NR-g-PDMMEP 80%*	262	418	39	40	21	215	343	42	43	15

* Grafting rate determined by weighing.

2

increased with the grafting rate of the copolymer: from 17% to 24% under nitrogen atmosphere, and 13% to 19% under oxygen atmosphere when GR increases from 77% to 86%, showing that further oxidation by oxygen of the char formed occurs in oxygen atmosphere.

3.5. Thermal behavior of the graft copolymers

The thermal behavior of pure NR, PDMAMP, PDMMEP, NR-g-PDMAMP, and NR-g-PDMMEP was investigated by DSC. Their respective curves are given in Fig. 14.

Pure NR as well as PDMAMP and PDMMEP homopolymers showed only one Tg at -62.1 °C, -29.5 °C, and -23.8 °C, respectively. NR-g-PDMAMP and NR-g-PDMMEP showed two Tg, one corresponding to the glass transition assigned to cis 1,4-polyisoprene structures in NR domains (-46 °C to

-44 °C), and the other to the dimethylphosphonate-functionalized graft ones (in a Tg range depending on the nature of the dimethylphosphonate-functionalized grafts: -29.2 °C to -29.1 °C in the case of PDAMP grafts, -23.6 °C to -23.1 °C in that of PDMMEP ones). This result means that, in the range of the considered compositions, with GR between 70% and 90%, there is phase separation. Moreover, it was seen that when GR increases in this same range of values, the Tg of NR domains increases while that of dimethylphosphonate-functionalized graft ones decreases, showing that the material would tend to become homogeneous when GR is increased. Compared to pure NR, the Tg of NR phase in the graft copolymer is significantly increased.

The formation of a biphasic medium can be explained by the difference of polarity that exists between the NR backbone and the dimethylphosphonate-functionalized

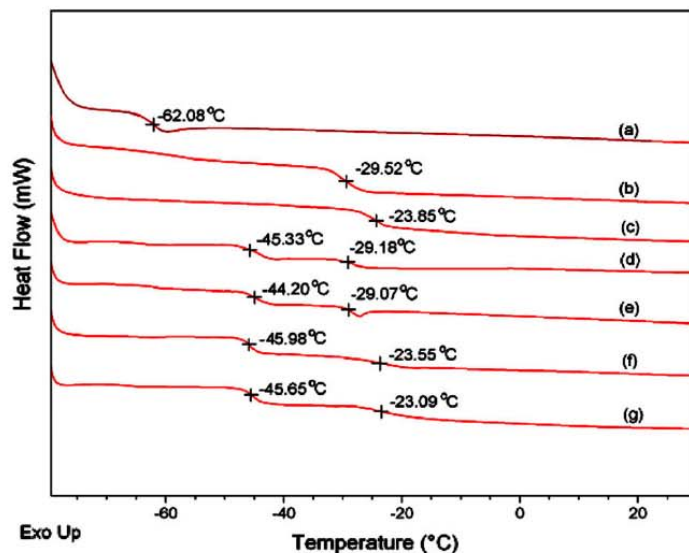


Fig. 14. DSC curves of (a) NR, (b) PDMAMP, (c) PDMMEP, NR-g-PDMMEP after (d) 60 min and (e) 180 min of grafting, and NR-g-PDMAMP after (f) 60 min and (g) 180 min of grafting. Grafting conditions: [monomer]/[DEDT-NR units] = 7.

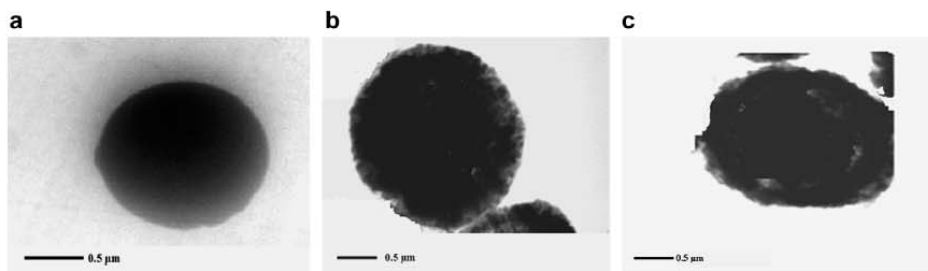


Fig. 15. TEM micrographs of (a) natural rubber, (b) NR-g-PDMAMP, and (c) NR-g-PDMMEP. Grafting conditions: 60 min with [monomer]/[DEDT-NR units] = 7.

grafts. The polar PDMAMP (or PDMMEP) grafts tend to associate between themselves to form polar micro-domains, of which are rejected the non-polar NR structures. Concerning the increase trend of T_g of NR phase with the increase of GR, it can be explained in terms of increase of intermolecular stiffness in the rubber phase, and may be attributed to an increasing trend of the chemical interactions between polar phosphorated grafts within the graft copolymer.

3.6. Morphology of the graft copolymer particles

The grafted natural rubber particles were visualized by TEM technique and the micrographs obtained were com-

pared with that of unmodified NR particles, as shown in Fig. 15. The lighter areas in the micrographs of NR-g-PDMAMP and NR-g-PDMMEP particles represent the grafted PDMAMP and PDMMEP phases, respectively. This technique does not make it possible to see the core of the latex particles. However, owing to the fact that the penetration of UV rays within the latex particles is restricted [32], it is obvious that the photopolymerization leading to polar PDMAMP and PDMMEP grafts will be initiated essentially at the surface of the NR particles to form core-shell particles, even if it was already shown that the grafting of dimethylphosphonate-functionalized monomers on NR latex particles could partially take place inside the particles [33].

4. Conclusion

Graft copolymers of natural rubber with poly(dimethyl(acryloyloxymethyl)phosphonate) (NR-g-PDMAMP), and poly(dimethyl(methacryloyloxyethyl)phosphonate) (NR-g-PDMMEP), were successfully prepared by radical photopolymerization of phosphonate monomers, i.e., acrylate (DMAMP) and methacrylate (DMMEP), respectively, initiated from *N,N*-diethyldithiocarbamate reactive groups previously created along NR chains. Because of the +I effect of methyl group on the carbon-carbon double bond of DMMEP monomer, the grafting efficiency obtained with this last monomer was lower than that observed with DMAMP. On the other hand, it was improved by increasing monomer concentration and reaction time. Moreover, the grafting rate was shown very dependent on the viscosity of the reaction mixture.

¹H NMR spectroscopy was used to determine the average length of the grafts in the synthesized graft copolymers. The calculation consisted to determine the degree of polymerization (\overline{DP}_n) of the polymer segments that constituted the grafts. Depending on the varied conditions used during the present work, this led to \overline{DP}_n in the range of 23–73 and 9–36 with PDMAMP and PDMMEP, respectively.

Visualization of NR-g-PDMAMP and NR-g-PDMMEP latices by Transmission Electron Microscopy (TEM) showed that they exhibit core-shell morphologies.

NR-g-PDMAMP and NR-g-PDMMEP copolymers were analyzed by Thermo Gravimetric Analysis (TGA) in order to evaluate their thermal stabilities. The measurements were performed in nitrogen and oxygen atmospheres. They showed that under oxygen atmosphere they begin to degrade at lower temperature than under nitrogen, and remaining residues at 500 °C are lower. The TGA curves showed that their degradation occurs in two steps. The first degradation step at lower temperature (onset temperature: 260–270 °C in nitrogen, 210–230 °C in oxygen) was attributed to the decomposition of dimethylphosphonate-functionalized grafts, while the second step at higher temperature (onset temperature: 400–430 °C in nitrogen, 326–396 °C in oxygen) to the degradation of NR backbone. It was especially noted that the degradation temperature of the second step was higher than that of the degradation of pure NR (onset temperature: 320 °C in nitrogen, 260 °C in oxygen), showing that the procedure described here to graft phosphorus-containing monomers along NR chains constitutes a good approach to improve thermal stability and fire retardancy of NR. Elsewhere, the measurements made under oxygen atmosphere significantly show that the positive action produced by the dimethylphosphonate-functionalized grafts on the thermal stability is as much more effective than the grafting rate is high.

The DSC results showed that NR-g-PDMAMP and NR-g-PDMMEP copolymers exhibit two DSC responses, one corresponding to the glass transition of the *cis* 1,4-polyisoprene structures of NR domains, and the other to the dimethylphosphonate-functionalized grafts (PDMAMP or PDMMEP). This result is typical of a heterogeneous material made of two phases, that would tend toward an homo-

geneous one as shown by the decrease of the threshold between the two Tg when the grafting rate GR of the graft copolymer increases from 75% to 85%.

Acknowledgements

We are grateful to the Thailand Research Fund (TRF); Grant No. PHD/0068/2547 and French Embassy in Thailand for financial support.

References

- [1] Brosse JC, Compiston I, Derouet D, El Hamdaoui A, Houdayer S, Reyx D, et al. Chemical modifications of polydiene elastomers: a survey and some recent results. *J Appl Polym Sci* 2000;78(8):1461–77.
- [2] Derouet D, Radhakrishnan N, Brosse JC, Boccaccio G. Phosphorus modification of epoxidized liquid natural-rubber to improve flame resistance of vulcanized rubbers. *J Appl Polym Sci* 1994;52(9):1309–16.
- [3] Perera MCS. Surface modification of natural rubber laces. *J Appl Polym Sci* 1987;34(7):2591–600.
- [4] Bradbury JH, Perera MCS. Epoxidation of natural rubber studied by NMR spectroscopy. *J Appl Polym Sci* 1985;30(8):3347–64.
- [5] Nakason C, Kaesaman A, Supasanthitkul P. The grafting of maleic anhydride onto natural rubber. *Polym Test* 2004;23(1):35–41.
- [6] Nakason C, Saiwaree S, Tatun S, Kaesaman A. Effect of vulcanization systems on properties of thermoplastic vulcanizates based on epoxidized natural rubber/polypropylene blends. *Polym Test* 2006;25(5):656–67.
- [7] Arayapraneew W, Prasassarakich P, Rempel GL. Process variables and their effects on grafting reactions of styrene and methyl methacrylate onto natural rubber. *J Appl Polym Sci* 2003;89:63–74.
- [8] Thiraphattaraphun L, Kiatkamjornwong S, Prasassarakich P, Damronglerd S. Natural rubber-g-methyl methacrylate/poly(methyl methacrylate) blends. *J Appl Polym Sci* 2001;81:428–39.
- [9] Prasassarakich P, Sintooorahat P, Wongwisetsirikul N. Enhanced graft copolymerization of styrene and acrylonitrile onto natural rubber. *J Chem Eng Jpn* 2001;34(2):249–53.
- [10] Chuayjuljit S, Moosin S, Potiyaraj P. Use of natural rubber-g-polystyrene as a compatibilizer in casting natural rubber/polystyrene blend films. *J Appl Polym Sci* 2005;95(4):826–31.
- [11] Liepins R, Sures JR, Morosoff N, Stannett V, Duffy JJ, Day FH. Localized radiation grafting of flame-retardants to polyethylene terephthalate. II Vinyl phosphonates. *J Appl Polym Sci* 1978;22(9):2403–14.
- [12] Tsafack MJ, Levalois-Grützmacher J. Flame retardancy of cotton textiles by plasma-induced graft-polymerization (PIGP). *Surf Coat Technol* 2006;201(6):2599–610.
- [13] Tsafack MJ, Levalois-Grützmacher J. Plasma-induced graft-polymerization of flame retardant monomers onto PAN fabrics. *Surf Coat Technol* 2006;200(11):3503–10.
- [14] Inagaki N, Katsuura K. Modification of cellulose phosphonate with *N,N*-dimethylacrylamide and 4-vinylpyridine, and flame retardant properties of the products. *J Appl Polym Sci* 1978;16:2771–9.
- [15] Derouet D, Morvan F, Brosse JC. Chemical modification of 1,4-polydienes by di(alkyl or aryl)phosphates. *Eur Polym J* 2001;37:1297–313.
- [16] Derouet D, Tran QN, Ha Thuc H. Synthesis of *N,N*-diethyldithiocarbamate functionalized 1,4-polyisoprene, from natural rubber and synthetic 1,4-polyisoprene. *Eur Polym J* 2007;43:1806–24.
- [17] Derouet D, Tran QN, Leblanc JL. Physical and mechanical properties of NR-g-PMMA synthesized by MMA photopolymerization initiated from *N,N*-diethyldithiocarbamate functions previously created on NR chains. *J Appl Polym Sci*, in press.
- [18] Tran QN. Synthesis and characterization of thermoplastic-grafted 1,4-polyisoprene. PhD, Université du Maine, Le Mans, France [December 2007].
- [19] Otsu T, Yoshida M. Terminator (iniferter) in radical polymerizations: polymer design by organic disulfides as iniferters. *Makromol Chem Rapid Commun* 1982;3(2):127–32.
- [20] Otsu T, Yoshida M, Tazaki T. A model for living radical polymerization. *Makromol Chem Rapid Commun* 1982;3(2):133–40.
- [21] Otsu T, Matsunaga T, Doi T, Matsumoto A. Features of living radical polymerization of vinyl monomers in homogeneous system using

- N,N*-diethyldithiocarbamate derivatives as photoiniferters. *Eur Polym J* 1995;31(1):67–78.
- [22] Otsu T, Matsumoto A. Controlled synthesis of polymers using the iniferter technique: developments in living radical polymerization. *Adv Polym Sci* 1998;136:75–137.
- [23] Otsu T. Iniferter concept and living radical polymerization. *J Polym Sci Part A: Polym Chem* 2000;38(12):2121–36.
- [24] Jeanmaire T, Hervaud Y, Boutevin B. Synthesis of dialkylhydroxymethylphosphonates in heterogeneous conditions. *Phosphorus Sulfur Silicon* 2002;177(5):1137–45.
- [25] Lee M, Utsumi K, Minoura Y. Effect of hexamethylphosphorotriamide on the "living" radical polymerization initiated by aged Cr²⁺ BPO. *J Chem Soc Faraday Trans 1* 1979;75:1821–9.
- [26] Simionescu IC, Simionescu BC. Unconventional radical polymerizations. *Pure Appl Chem* 1984;56(3):427–38.
- [27] Moad G, Solomon DH. The chemistry of free radical polymerization. 1st ed. Oxford: Elsevier Science Ltd.; 1995.
- [28] Jiang DD, Wilkie CA. Graft copolymerization of methacrylic acid, acrylic acid and methyl acrylate onto styrene-butadiene block copolymer. *Eur Polym J* 1998;34(7):997–1006.
- [29] Barson CA, Benvington JC. Copolymerization involving methyl methacrylate, methyl acrylate, stilbene and *p*-fluorostilbene. *Eur Polym J* 1987;23(3):251–3.
- [30] Reghunadhan Nair CP, Clouet G. Effects of solvent and temperature on the copolymerizations of 2-acryloyloxyethyl diethyl phosphate with methyl methacrylate and styrene. *Eur Polym J* 1989;25(3):251–7.
- [31] Simionescu CR, Vasiliu Oprea CL, Nicolaeu J. Mechanochemically initiated polymerizations-5. Polymerization by vibratory milling of acrylamide and methacrylamide. *Eur Polym J* 1983;19(6):525–8.
- [32] Odian G. Principles of polymerization. 2nd ed. New York: John Wiley & Sons Inc.; 1981.
- [33] Schneider M, Pith T, Lambla M. Preparation and morphological characterization of two- and three-component natural rubber-based latex particles. *J Appl Polym Sci* 1996;62(2):273–90.

APPENDIX B

Published Article in Polym. Advan. Technol. 2009

Dynamically cured natural rubber/EVA blends: influence of NR-*g*-poly(dimethyl(methacryloyloxymethyl)phosphonate) compatibilizer

Punyanich Intharapat^{a,b}, Daniel Derouet^b and Charoen Nakason^{a*}

Graft copolymer of natural rubber and poly(dimethyl(methacryloyloxymethyl)phosphonate) (NR-*g*-PDMMP) was prepared in latex medium via photopolymerization. It was then used to promote the blend compatibility of dynamically cured 40/60 natural rubber (NR)/ethylene vinylacetate copolymer (EVA) blends using various loading levels at 1, 3, 5, 7, 9, 12, and 15 wt%. It was found that the increasing loading levels of NR-*g*-PDMMP in the blends caused the increasing elastic modulus and complex viscosity until reaching the maximum values at a loading level of 9 wt%. The properties thereafter decreased with the increasing loading levels of NR-*g*-PDMMP higher than 9 wt%. The smallest vulcanized rubber particles dispersed in the EVA matrix with the lowest $\tan \delta$ value was also observed at a loading level of 9 wt%. Furthermore, the highest tensile strength and elongation at break (i.e., 17.06 MPa and 660%) as well as the lowest tension set value (i.e., 27%) were also observed in the blend using this loading level of the compatibilizer. Addition of NR-*g*-PDMMP in the dynamically cured NR/EVA blends also improved the thermal stability of the blend. That is, the decomposition temperature increased with the addition of the graft copolymer. However, the addition of NR-*g*-PDMMP in the blends caused the decreasing degree of crystallinity of the EVA phase in the blend. However, the strength properties of the blend are still high because of the compatibilizing effect. Copyright © 2009 John Wiley & Sons, Ltd.

Keywords: compatibilization; dynamic vulcanization; natural rubber; EVA; graft copolymer; poly(dimethyl(methacryloyloxymethyl)phosphonate)

INTRODUCTION

Thermoplastic elastomer (TPE) is a relative new class of polymer and probably fastest growing sector in the polymer market.^[1] TPE based on polymer blend of rubber and thermoplastic also receives considerable success over the years due to it can be manufactured with a relatively low cost with high potential plastic processing equipment. One of the well-known TPE categories is dynamically cured polymer blend termed as "thermoplastic vulcanizates (TPVs)" or dynamic vulcanizates (DVs). Traditionally, TPVs are blends of thermoplastic and elastomeric material with dynamic vulcanization of rubber phase place during mixing operation. As a consequence, small domains of vulcanized rubber disperse in the thermoplastic matrix during dynamic vulcanization.^[2] The final morphology of the TPVs consists of small cross-linked elastomeric domains embedded in a continuous thermoplastic matrix. Combination properties of rubber and thermoplastic are consequent because of the two-phase composition. That is, the elastomer soft phase gives the rubber-like properties while the thermoplastic hard phase gives strength properties including processability and recyclability. It has been well established that the dynamic vulcanization of the blend causes improvement of mechanical, thermal, and impact properties compared with uncured or partly cross-linked materials.^[3–5]

Among the rubber and thermoplastic pairs used to prepare the TPE materials, natural rubber (NR) and ethylene vinylacetate

copolymer (EVA) are the interesting materials because some superior properties of both the blend constituents. NR provides high elasticity to the blend, while the EVA gives superior aging, weathering, chemical resistances, and ease of processability to the blends.^[6–8] NR/EVA blends have been prepared using various blending techniques but incompatibility of NR and EVA has been encountered as the main problem.^[9–12] Therefore, blend compatibilizer has been used to increase blend compatibility. Effect of the compatibilization on the thermal ageing of NR/EVA

* Correspondence to: C. Nakason, Center of Excellence in Natural Rubber Technology, Department of Rubber Technology and Polymer Science, Faculty of Science and Technology, Prince of Songkla University, Pattani 94000, Thailand.
E-mail: ncharoen@bunga.pn.psu.ac.th

a P. Intharapat, C. Nakason
Center of Excellence in Natural Rubber Technology, Department of Rubber Technology and Polymer Science, Faculty of Science and Technology, Prince of Songkla University, Pattani 94000, Thailand

b D. Derouet
LCOM-Chimie des Polymère (UMR du CNRS UCO2M N° 6011), Université du Maine, Faculté des Sciences, Avenue Olivier Messiaen, 72085 LE MANS Cedex 9, France

Contract/grant sponsor: Thailand Research Fund (TRF) through the Golden Jubilee Ph.D. Programme (RGI-PHD); contract/grant number: PHD/0068/2547.
Contract/grant sponsor: French Embassy in Thailand.

blends using EVA containing mercapto groups (i.e., poly(ethylene-co-vinyl alcohol-co-vinyl mercaptoacetate), (EVASH)) as a blend compatibilizer was investigated.^[13] It was found that the blend with the EVASH compatibilizer exhibited better resistance to thermal ageing. Also, the EVASH could possibly promote the cross-linking reaction with the NR phase.^[14] This caused the improvement of thermal stability and mechanical strength of the blend, but the decreasing degree of crystallinity of EVA in the blend.^[14] Dibutyl phosphate supported NR (DSNR) was also used as a blend compatibilizer in the NR/EVA blend.^[15] It was found that the highest mechanical properties was observed in the blend with DSNR at 5 wt%.

Chemical modification of NR molecules is a route to prepare new materials with unique properties. The modified product is possible to be used as blend compatibilizers to promote compatibility between the NR and thermoplastic components, such as EVA. Some well-known modified NR products that have been used as blend compatibilizers such as NR-*g*-PMMA,^[16–17] NR-*g*-glycidyl methacrylate/styrene,^[18] NR-*g*-PS,^[19–21] liquid NR,^[22–23] and epoxidized NR.^[24–26]

In the current work, NR-*g*-polydimethyl(methacryloyloxymethyl)phosphonate (NR-*g*-PDMMP) was prepared and used as a blend compatibilizer in dynamically cured NR/EVA blends. Influence of loading level of NR-*g*-PDMMP compatibilizer on rheological, dynamic, mechanical, morphological, and thermal properties of the blends were investigated.

EXPERIMENTAL

Materials

NR used as a blend component was an air-dried sheet (ADS) manufactured by the Khuan Pun Tae Farmer Co-operation, (Phattaluang, Thailand). EVA grade N8038 used as another blend component was manufactured by the TPI Polyacrylate Co., Ltd. (Rayong, Thailand). This grade of material contains 18 wt% of vinyl acetate content with melt index of 2.3 g per 10 min (2.16 kg, 190 °C) and density of 0.941 g cm⁻³. The zinc oxide and stearic acid used as activators, manufactured by the Global Chemical Co., Ltd. (Samutprakarn, Thailand) and Imperial Chemical Co., Ltd., (Pathumthani, Thailand), respectively. The sulfur used as a vulcanizing agent was manufactured by Ajax Chemical Co., Ltd. (Samutprakarn, Thailand). The *N*-tert-butyl-2-benzothiazole sulphenamides (Santocure TBBS) used as an accelerator was manufactured by Flexsys (USA). The dimethyl(methacryloyloxymethyl)phosphonate (DMMMP) monomer was prepared in-house using methacryloyl chloride and dimethylphosphite (obtained from Aldrich, Milwaukee, USA). Other chemicals used to prepare DMMMP monomer include dimethyl hydroxymethylphosphonate, paraformaldehyde, and anhydrous potassium carbonate, supplied from Acros Organics (Geel, Belgium). *N,N*-diethyldithiocarbamate-functionalized NR (DEDT-NR) was used as starting material to prepare NR-*g*-poly(dimethyl(methacryloyloxymethyl)phosphonate) (NR-*g*-PDMAMP) that was also prepared in-house, as described elsewhere.^[27]

Synthesis and characterization of dimethyl(methacryloyloxymethyl)phosphonate monomer

Graft copolymers of NR backbone and polymer grafts bearing phosphonate functions were synthesized via a grafting procedure based on the radical photopolymerization of methacry-

late monomers containing dimethylphosphonate functions, DMMMP. The DMMMP monomer was first synthesized by reaction of methacryloyl chloride with dimethyl(1-hydroxymethyl)phosphonate.^[28] The reactions were performed in dry dichloromethane in a presence of triethylamine (TEA) acid acceptor. The product was purified and characterized by ¹H-NMR, ¹³C-NMR, and FTIR.

Synthesis of DEDT-NR

Sodium *N,N*-diethyldithiocarbamate (DEDT-Na) was first introduced onto the oxirane ring of epoxidized NR (ENR) in latex medium, according to the method previously described.^[29] ENR with epoxidation level of 20 mol% was first diluted to 5% DRC. Sodium carbonate solution was then added to adjust pH to approximately 8 before introduction of DEDT-Na and tetrabutylammonium bromide (TBAB) as a phase transfer catalyst. The reaction mixture was stirred at 70 °C for 168 hr. After the reaction, the DEDT-NR formed was isolated by coagulation in methanol, and then washed several times with water. It was then dried under vacuum until a constant weight. The addition of DEDT-Na onto oxirane rings of epoxidized 1,4-polyisoprene units was confirmed by ¹H-NMR signal at $\delta = 4.35$ ppm. It is characteristic of proton bound to the carbon bearing the *N,N*-diethyldithiocarbamate (DEDT) group. Furthermore, the nucleophilic addition was also proved by the presence of ¹H-NMR signals at $\delta = 3.7$ ppm and $\delta = 4.0$ ppm that are assigned to the methylenes of diethylamino group.

Preparation NR graft NR-*g*-PDMMP

NR-*g*-PDMMP was synthesized through two steps process. First step is the addition of DEDT-Na onto epoxidized NR units in a latex medium according to the reaction procedure described elsewhere.^[29] This was to create macroinitiators with 4 mol% of DEDT groups in the NR chains (i.e., DEDT-NR). Second step is the grafting reactions of DMMMP monomer with DEDT-NR via photopolymerization in a latex medium. The grafting reaction was performed in 250 ml pyrex kettle equipped with a magnetic stirrer and closed by a screwed stopper with a joint of sealing covered with Teflon. The reaction was carried out at room temperature and under nitrogen atmosphere. Ultraviolet lamp with a wavelength of 365 nm was used as irradiation source to initiate the grafting reaction. After grafting, the graft copolymer was coagulated in methanol, and then purified by dissolution/re-precipitation with dichloromethane/methanol. The product was then dried at 40 °C in vacuum oven until constant weight. The product was later Soxhlet extracted with methanol for 24 hr to remove the NR-*g*-PDMMP. The graft copolymer was recovered by filtration and dried under in vacuum oven at 40 °C until constant weight. ¹H-NMR, ¹³C-NMR, ³¹P-NMR, and FTIR spectroscopies, thermal analysis (i.e., DSC and TGA) as well as transmission spectroscopy (TEM) were used to characterize the graft copolymer.

Preparation of dynamically cured NR/EVA blends

Dynamically cured 40/60 NR/EVA blends was prepared by melt blending of NR and EVA in an internal mixer with a mixing chamber capacity of 80 cm³, Brabender plasticorder, model PLE 331 (Brabender OHG, Duisburg, Germany) at 150 °C and a rotor speed of 60 rpm. EVA was first dried in hot air oven at 45 °C for at least 12 hr and introduced into the mixing chamber before blending for 2 min. The NR was then added and mixed. Other

Table 1. Formulation and mixing schedule used to prepare dynamically cured NR/EVA blends with different loading levels of NR-*g*-PDMMP compatibilizer

Ingredients	Quantity (phr)								Mixing time (min)
	60	60	60	60	60	60	60	60	
EVA	60	60	60	60	60	60	60	60	2
NR	40	40	40	40	40	40	40	40	3
ZnO	2	2	2	2	2	2	2	2	1
Stearic acid	0.4	0.4	0.4	0.4	0.4	0.4	0.4	0.4	0.5
TMQ	0.4	0.4	0.4	0.4	0.4	0.4	0.4	0.4	0.5
TBBS	0.8	0.8	0.8	0.8	0.8	0.8	0.8	0.8	1
Sulfur	0.8	0.8	0.8	0.8	0.8	0.8	0.8	0.8	8
NR- <i>g</i> -PDMMP (wt% of NR)	0	1	3	5	7	9	12	15	5

chemicals (as details shown in Table 1) used to perform dynamic vulcanization of NR phase were incorporated into the mixing chamber, as a mixing schedule shown in Table 1. Various loading levels of NR-*g*-PDMMP compatibilizer (i.e., 1, 3, 5, 7, 9, 12, and 15 wt%) were each incorporated and mixed for 5 min. The TPVs were later fabricated by compression molding at 150 °C for 5 min. Rheological, dynamic, thermal, and morphological properties of the TPVs were characterized.

Dynamic properties

Dynamic properties of the dynamically cured 40/60 NR/EVA blends were investigated by moving die processability tester, RheoTech MDPT, (Tech-Pro, Inc., Cuyahoga Falls, USA). The apparatus consists of a conical shape die, which produce a uniform shear strain on the test specimen. The sample dimension used was 30 mm × 30 mm × 3 mm, which was loaded onto the lower die. The upper die was then closed to conform a constant volume. The test was performed by a frequency sweep mode in the range of 0.3–190 rad/s, with a constant strain at 3%. This was to assure a linear viscoelasticity. The storage (G') and loss shear (G'') moduli, loss factor (i.e., $\tan \delta = G''/G'$) as well as the complex viscosity (i.e., $\eta^* = 3G^*/\omega = \eta'' + i\eta'$) of the TPVs were characterized.

Morphological characterization

Scanning electron microscope (SEM), model JSM-5800 LV (Jeol, Tokyo, Japan) was used to characterize morphological properties of dynamically cured 40/60 NR/EVA blends. The samples were first cryogenic cracked in liquid nitrogen to produce new surfaces. They were then etched by tetrahydrofuran (THF) to preferential extract the EVA phase and dried in hot air oven at 40 °C for 48 hr. They were sputter-coated with gold before examining with a scanning electron microscope.

From the SEM micrographs, particle size of vulcanized rubber in terms of domain diameter was estimated using at least 50 domains. The cross-sectional area (A_i) of each particle in the SEM micrograph was first measured and then converted into the diameter (D_i) of each domains, as follows:^[30]

$$D_i = 2 \left(\frac{A_i}{\pi} \right)^{1/2} \quad (1)$$

Then, the average diameter \bar{D}_i was obtained by

$$\bar{D}_i = \frac{\sum_i D_i}{N} \quad (2)$$

where N is the total numbers of the domains used in the calculation.

Transmission electron microscope (TEM), model JEM-2010 (Jeol, Tokyo, Japan) was used to study the morphology of the graft copolymer latex. The NR-*g*-DMMMP and pure NR lattices were diluted approximately 400 times of their original concentration with distilled water. An aqueous solution (2 wt%) of OsO₄ was added to stain NR molecules. The stained latex was then placed on a 400-mesh grid, and dried overnight before characterization.

Thermal properties

Two types of thermal analysis techniques were used to characterize the dynamically cured 40/60 NR/EVA blends and pure blend components. DSC was performed using DSC Q500, TA Instrument, (New Castle, USA). The sample was first heated to 100 °C with a heating rate of 10 °C min⁻¹ and kept at this temperature for 5 min. This was to eliminate thermal history of the material. Then, the samples were gradually quenched to -80 °C. The second run with the same heating rate was performed and the result was captured.

Degree of crystallinity of the EVA in the pure EVA and dynamically cured NR/EVA blends was calculated based on heat of fusion from the DSC thermograms, as follows:

$$\text{Degree of crystallinity (\%)} = \frac{\Delta H}{\Delta H_0} \times 100 \quad (3)$$

where ΔH is the heat of fusion of samples determined from the area of the melting endotherm, and ΔH_0 is the heat of fusion of the 100% crystalline polyethylene (i.e., $\Delta H_0 = 277.0 \text{ J g}^{-1}$).

Thermogravimetric analysis (TGA) of 40/60 dynamically cured NR/EVA blends and pure blend components were also performed using TGAQ500, TA instrument, (New Castle, USA). The samples were first placed in a platinum pan under nitrogen atmosphere. The test then was performed with a heating rate of 10 °C min⁻¹ with a temperature range of 30–550 °C.

Tensile properties

Tensile strength, elongation at break, and tension set properties of 40/60 dynamically cured NR/EVA blends were tested at 25 °C according to the ASTM D412 using dumb-bell shape (die C) test specimens. Hounsfield Tensometer, model H 10 KS (Hounsfield Test Equipment Co., Ltd, UK) was used at a crosshead speed of 500 mm min⁻¹.

RESULTS AND DISCUSSION

Synthesis and characterization of graft copolymer (NR-g-PDMMMP)

The synthesis of the graft copolymer was performed in latex medium according to a grafting procedure based on the photopolymerization of DMMP used as phosphorated monomer. The polymerization was initiated from DEDT groups previously bound in side position of NR chains (DEDT-NR). The graft copolymer obtained after extraction was dried and then characterized by $^1\text{H-NMR}$, $^{13}\text{C-NMR}$, and $^{31}\text{P-NMR}$ spectroscopy.

$^1\text{H-NMR}$ spectrum of NR-g-PDMMMP is shown in Fig. 1. It is seen that the protons of carbon-carbon double bond $-\text{C}(\text{CH}_3)=\text{CH}-$ of NR backbone was identified by the signal at $\delta = 5.1$ ppm (H_a). The formation of the PDMMMP-grafted site indicated by signals of dimethyl ester and methylenoxy protons of the phosphonate function at $\delta = 3.8$ ppm (H_d) and $\delta = 4.38$ ppm (H_c), respectively. The presence of residual epoxidized NR units was also characterized by the $^1\text{H-NMR}$ spectrum by the signal of the oxirane protons of the epoxidized NR units at $\delta = 2.7$ ppm (H_b).

$^{13}\text{C-NMR}$ spectrum of NR-g-PDMMMP is shown in Fig. 2. The formation of PDMMMP was confirmed by the simultaneous presence of signals at $\delta = 125$ ppm and $\delta = 135$ ppm characteristic of $-\text{C}(\text{CH}_3)=$ and $=\text{CH}$ unsaturated carbons of NR backbone, respectively. Also, the presence of signal at $\delta = 52.9$ ppm and $\delta = 62.3$ ppm characteristic of the dimethyl ester and methylenoxy protons of the dimethylphosphonate functions on PDMMMP grafts. The formation of phosphonated grafts was confirmed by the presence of $\text{C}=\text{O}$ peak at $\delta = 176.2$ ppm. Furthermore, the C-OH quaternary carbons in NR-g-PDMMMP was found at $\delta = 74.3$ ppm.

$^{31}\text{P-NMR}$ spectrum is shown in Fig. 3. It can be seen that only one sharp peak was observed at $\delta = 30.2$ ppm. This confirms the presence of dimethylphosphonate functions along the

grafts. Therefore, the grafting reaction of DEDT-NR and DMMP monomer was confirmed, as a reaction shown in Scheme 1.

The grafted NR particle was also visualized by TEM technique and the micrographs were compared with the unmodified NR particle, as shown in Fig. 4. The lighter areas in the micrograph of NR-g-PDMMMP particles represent the grafted PDMMMP phase. This is clear that the photopolymerization of polar PDMMMP grafts would be initiated essentially at the surface of the NR particles to form core-shell particles. That is, the NR latex grafted with PDMMMP showed irregular in shapes, indicating that the DMMP was distributed continuously on the surface of the graft particles. This phenomenon is probably due to the difference in polarity between hydrophobic NR core and hydrophilic shell of PDMMMP.

Dynamic and morphological properties

Figure 5 shows elastic modulus (G') as a function of frequency for dynamically cured 40/60 NR/EVA blends with NR-g-PDMMMP compatibilizer. It is seen that the elastic modulus increased with the increasing frequency because the decreasing of time available for molecular relaxation. At a given frequency, as shown in Fig. 6, it can be seen that the storage modulus increased with the increasing loading level of NR-g-PDMMMP and reached the maximum value at a loading level of 9 wt%. The elastic modulus thereafter decreased with the increasing loading levels of the NR-g-PDMMMP compatibilizer. This might be attributed to the compatibilizing effect of graft copolymer (i.e., NR-g-PDMMMP) with the corresponding blend components. During the melt blending, the NR-g-PDMMMP molecules were forced to locate at the interface of NR and EVA. The nonpolar NR segments in the NR-g-PDMMMP molecules are wetted by the NR component, while the polar functional groups of the graft copolymer could interact with the polar functional groups in EVA

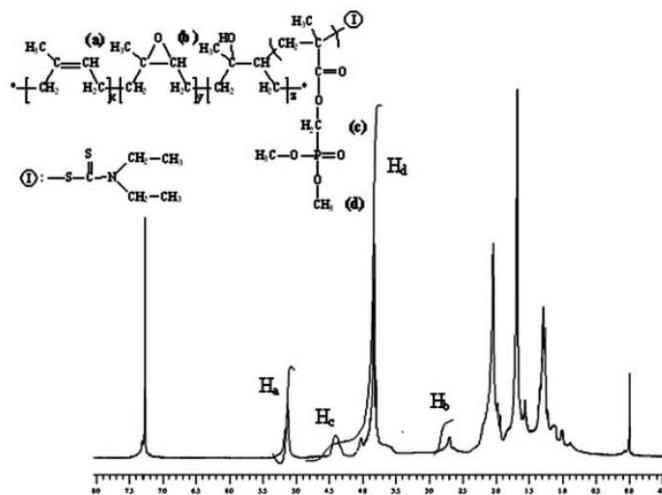


Figure 1. Typical $^1\text{H-NMR}$ spectrum of NR-g-PDMMMP.

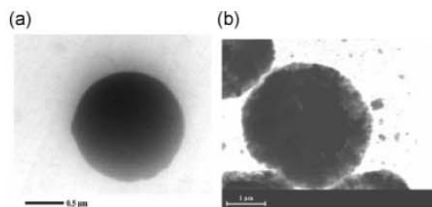


Figure 4. TEM micrographs of (a) NR and (b) NR-g-PDMMMP.

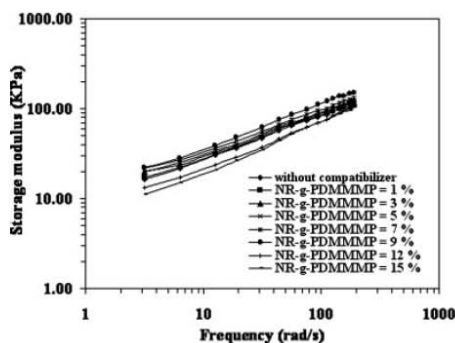


Figure 5. Storage modulus as a function of angular frequency for dynamically cured 40/60 NR/EVA blends with various quantities of NR-g-PDMMMP compatibilizer.

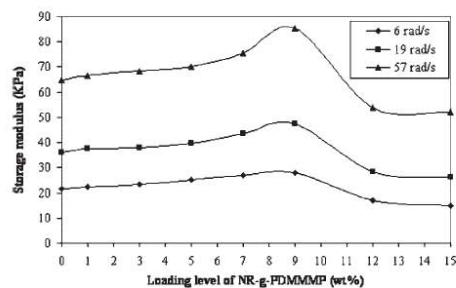


Figure 6. Storage modulus at constant angular frequencies for dynamically cured 40/60 NR/EVA blends with various quantities of NR-g-PDMMMP compatibilizer.

Figure 9 shows complex viscosity as a function of frequency of dynamically cured 40/60 NR/EVA blends with various loading levels of NR-g-PDMMMP compatibilizer. It can be seen that the complex viscosity decreased with the increasing frequency, that is, shear-thinning behavior. At a given frequency, as shown in Fig. 10, the complex viscosity increased until reaching the maximum value at a loading level of NR-g-PDMMMP of 9 wt%. The complex viscosity was thereafter decreased with the increasing loading level of NR-g-PDMMMP higher than 9 wt%. These results correlated well with the trend of the storage modulus as shown in Figs 3 and 4. This confirms the interaction between the NR and EVA phases by compatibilizing effect of the NR-g-PDMMMP compatibilizer.

To confirm influence of NR-g-PDMMMP compatibilizer on elastic modulus and complex viscosity, morphological properties of dynamically cured 40/60 NR/EVA blends were investigated. The

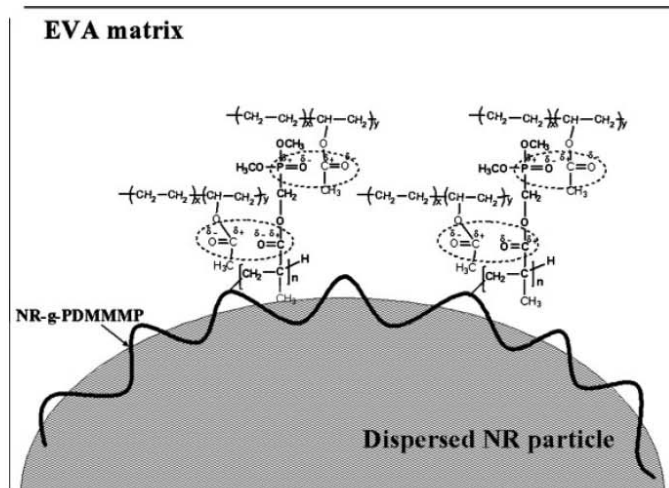


Figure 7. Possible chemical interaction of graft copolymer (NR-g-PDMMMP) with NR and EVA in the blend component at the interfacial area.

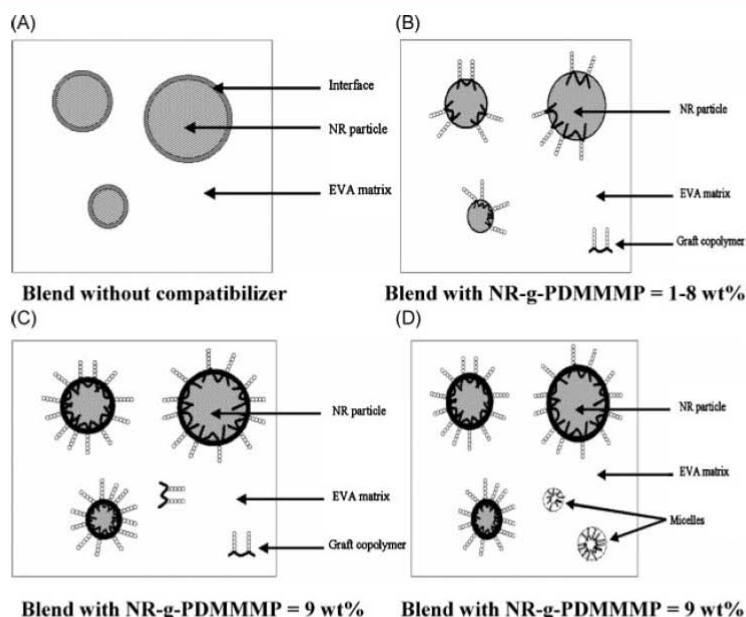


Figure 8. Schematic representation of a compatibilization of various loading level of NR-g-PDMMMP compatibilizer at the interface of NR and EVA.

specimens were first cryogenic cracked and etched the surface by extracting the EVA phase with THF. They were then dried in hot air oven at 40 °C for 48 hr and sputter-coated with gold before examining with a scanning electron microscope. Figure 11 shows SEM micrographs of dynamically cured 40/60 NR/EVA blends without and with various loading levels of NR-g-PDMMMP compatibilizer. It is seen that the spherical vulcanized rubber domains remained un-dissolved and adhered at the surfaces. Also, the two-phase morphology of micron scale vulcanized NR particles dispersed in the EVA matrix was observed. It can be seen that size of vulcanized rubber domains of the dynamically cured NR/EVA blends without compatibilizer are the largest with

average particle size of approximately 2.9 μm , as shown in Fig. 11. Incorporation of the NR-g-PDMMMP compatibilizer caused the decreasing trend of particle size of the dispersed vulcanized rubber domains to the average diameter approximately 2.6, 2.4, 1.6, 0.7 and 0.3 μm for the blends with the loading level of the compatibilizer at 1, 3, 5, 7 and 9 wt%, respectively. The smallest vulcanized rubber domains (i.e., approximately 0.3 μm) were observed in the dynamically cured NR/EVA blend with a loading level of graft copolymer at 9 wt% (Fig. 11F). Increasing the loading level of NR-g-PDMMMP higher than 9 wt% to 12 and 15 wt% (Fig. 13G and H) caused the increasing size of the vulcanized rubber domains to approximately 0.9 μm and 1.2 μm , respectively.

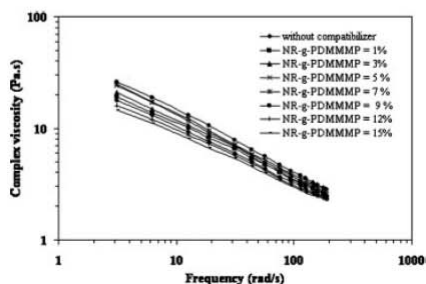


Figure 9. Complex viscosity as a function of angular frequency for dynamically cured 40/60 NR/EVA blends with various quantities of NR-g-PDMMMP compatibilizer.

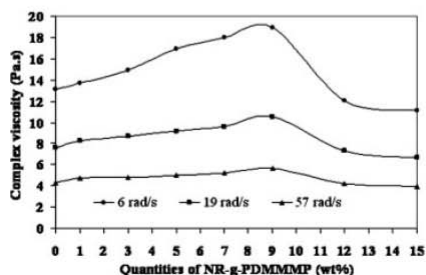


Figure 10. Complex viscosity at a constant angular frequencies for dynamically cured 40/60 NR/EVA blends with various quantities of NR-g-PDMMMP compatibilizer.

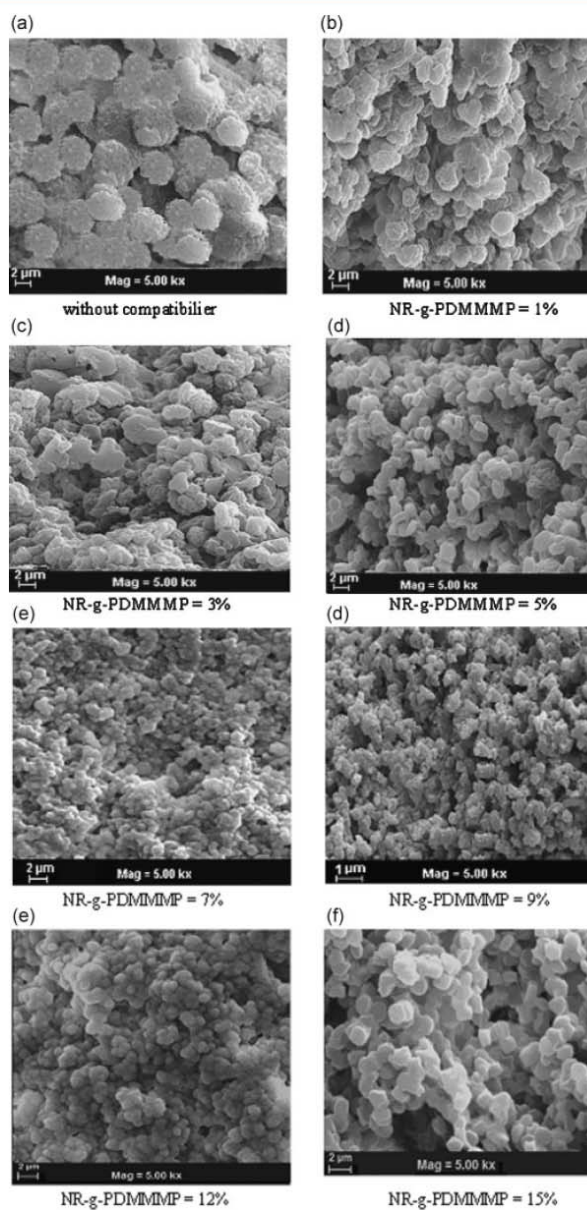


Figure 11. SEM micrographs of dynamically cured 40/60 NR/EVA blends: (A) without compatibilier, (B) with NR-g-PDMMMP = 1%, (C) with NR-g-PDMMMP = 3%, (D) with NR-g-PDMMMP = 5%, (E) with NR-g-PDMMMP = 7%, (F) with NR-g-PDMMMP = 9%, (G) with NR-g-PDMMMP = 12%, and (H) with NR-g-PDMMMP = 15%.

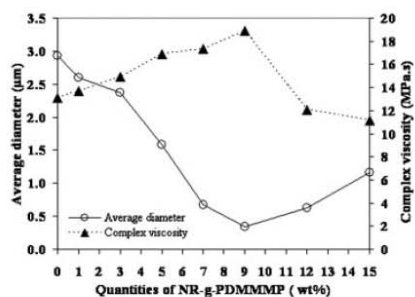


Figure 12. Relationship between average particle diameter of vulcanized rubber domains and complex viscosity at a frequency of 6 rad sec^{-1} of dynamically cured NR/EVA blends with various quantities of NR-g-PDMMMP compatibilizer.

Therefore, average diameter of the dispersed vulcanized NR particles could correlate to the trend of complex viscosity at a given frequency of 6 rad sec^{-1} , as shown in Fig. 12. It can be seen that the complex viscosity increased with the decreasing size of vulcanized rubber domains dispersed in the EVA matrix until reached the maximum value at a loading level of NR-g-PDMMMP at 9 wt% where the smallest particles were observed. This proved the highest interaction between rubber and EVA phases. That is, the graft copolymer acted as an interfacial agent and caused a reduction size of the dispersed vulcanized rubber particles.

Figure 13 shows $\tan \delta$ at a constant frequency and various loading levels of NR-g-PDMMMP compatibilizer. The $\tan \delta$ or loss tangent is the ratio of loss (G'') to storage modulus (G'). It is seen that the $\tan \delta$ first decreased with the increasing concentration of the NR-g-PDMMMP compatibilizer until reaching the lowest value at a loading level of 9 wt%. It thereafter increased with the increasing loading levels of the blend compatibilizer greater than 9 wt%. At a loading level of NR-g-PDMMMP at 9 wt%, the lowest value of $\tan \delta$ was observed because the highest interaction between rubber and EVA phases and caused the highest elasticity of the material. Therefore, the dynamically cured NR/EVA blend with this loading level of NR-g-PDMMMP at 9 wt% exhibited the highest elastic modulus and complex viscosity but the lowest $\tan \delta$.

Mechanical properties

Figure 14 shows stress-strain curves of dynamically cured 40/60 NR/EVA blends with various loading levels of NR-g-PDMMMP

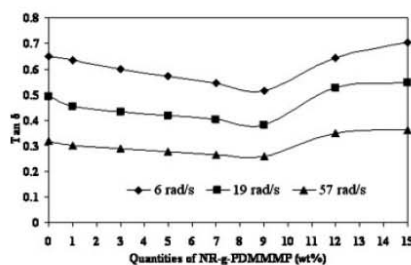


Figure 13. $\tan \delta$ of dynamically cured 40/60 NR/EVA blends with various quantities of NR-g-PDMMMP compatibilizer at constant frequencies.

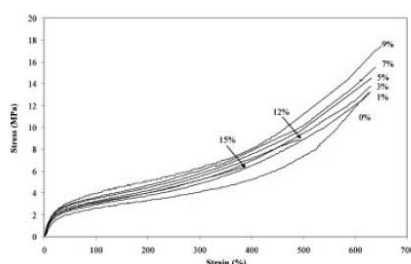


Figure 14. Stress-strain curves of dynamically cured 40/60 NR/EVA blends with various quantities of NR-g-PDMMMP.

compatibilizer. It is seen the Young's modulus (i.e., slope at the initial linear region of the curves) of the blends increased with the increasing concentration of NR-g-PDMMMP compatibilizer and again reached the maximum value at a loading level of 9 wt%. This corresponds to the trends of elastic modulus (Fig. 6) and complex viscosity (Fig. 10) due to the highest compatibilizing effect with this loading level of the blend compatibilizer, as described previously. Mechanical properties in terms of ultimate tensile strength, elongation at break, tension set, and hardness of the dynamically cured 40/60 NR/EVA blends are summarized in Table 2. It can be seen that the blend with a loading level of NR-g-PDMMMP compatibilizer at 9 wt% exhibited the highest

Table 2. Mechanical properties of dynamically cured 40/60 NR/EVA blends with various quantities of NR-g-PDMMMP

Loading level of NR-g-PDMMMP (wt%)	Tensile strength (MPa)	Elongation at break (%)	Tension set (%)	Hardness (Shore A)
0	13.15	625	35	72
1	13.25	629	33	72
3	13.80	630	33	71
5	14.50	635	31	72
7	15.53	639	30	72
9	17.65	660	27	72
12	8.88	492	31	72
15	6.34	385	32	72

tensile strength and elongation at break (i.e., 17.06 MPa and 660%, respectively) with the lowest value of the tension set and similar value of hardness with other type of blend. The lowest value of tension set revealed the highest tendency to recover to its original shape after prolong extension of the material. This corresponds to the lowest value of the $\tan \delta$ (Fig. 13), which revealed the highest elasticity of the material. Therefore, the optimum loading level of the blend compatibilizer was confirmed at a loading level of 9 wt%, as evidence from the highest mechanical strength due to the high interaction between different phases. As a consequence, smaller dispersed vulcanized rubber domains (Figs 11 and 12) were observed and caused higher interfacial adhesion. In Table 2, it is also seen that the blend without compatibilizer exhibited poorer mechanical strength than that of the compatibilized blends. Increasing the loading level of the blend compatibilizer in a range of 1–9 wt% caused the increasing trend of tensile strength because the increasing interfacial force between the phases due to the blend compatibilizer. However, increasing the concentration of the blend compatibilizer higher than that of the optimum dose (i.e., >9 wt%), a decreasing trend of the tensile strength and elongation at break were observed due to a formation of micelles from excess amount of NR-g-PDMMMP in the blend system, as described in Fig. 8.

Thermal properties

Figure 15 shows DSC thermograms of dynamically cured 40/60 NR/EVA blends and their parent polymer pairs (i.e., pure EVA and pure NR). A single glass transition temperature (T_g) at low temperature was observed in the pure NR at approximately -60.3°C . Two values of T_g corresponding to polyethylene and poly(vinyl acetate) segments in EVA should be observed. However, in this work only a single T_g was observed at approximately -22.8°C . This might be due to the chain restriction because of crystalline phase. In the dynamically cured 40/60 NR/EVA blends, two T_g 's corresponding to NR and EVA components were observed, as summarized in Table 3. It is seen that the dynamically cured 40/60 NR/EVA blend without compatibilizer showed two values of T_g with very similar to the T_g of each blend component (i.e., pure NR and pure EVA). This indicates very low interaction between the EVA and NR phases. However, in the

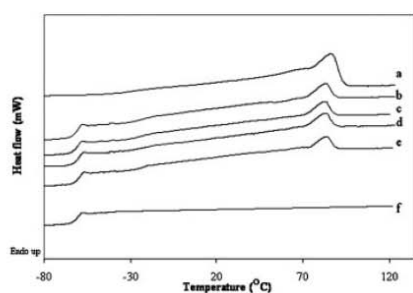


Figure 15. DSC thermograms of (a) pure EVA, (b) NR/EVA blend without compatibilizer, (c) NR/EVA blend with 5 wt% of NR-g-PDMMMP, (d) NR/EVA blend with 9 wt% of NR-g-PDMMMP, (e) NR/EVA blend with 15 wt% of NR-g-PDMMMP, and (f) pure NR.

Table 3. T_g of pure EVA, pure NR, and their blends with various quantities of NR-g-PDMMMP compatibilizer

Samples	T_g ($^\circ\text{C}$) of NR phase	T_g ($^\circ\text{C}$) of EVA phase
Pure EVA	—	-22.8
Blend without compatibilizer	-60.3	-22.7
Blend with 5% of NR-g-PDMMMP	-59.3	-22.2
Blend with 9% of NR-g-PDMMMP	-58.7	-21.8
Blend with 15% of NR-g-PDMMMP	-59.5	-22.1
Pure NR	-60.3	—

blend with compatibilizer, slight shift of T_g of rubber and plastic phase toward each other (i.e., shift to higher temperature for the rubber component and lower temperature for plastic phase) was observed. It can be also seen that the highest shift of the T_g was observed in the blend with compatibilizer of at 9 wt% indicating the highest interaction between the phases. This is evidence of interaction between the blend component that correlated well to higher elastic modulus (Fig. 6), complex viscosity (Fig. 10), mechanical strength (Table 2), and smaller size of the vulcanized rubber domains (Fig. 11) of the blend with 9 wt% of NR-g-PDMMMP compatibilizer.

Table 4. Crystalline melting temperature (T_m), degree of crystallinity (X_c), and heat of fusion (ΔH) of EVA phase in EVA and dynamically cured NR/EVA blends with various quantities of NR-g-PDMMMP

Samples	ΔH (J/mol)	X_c (%)	T_m ($^\circ\text{C}$)
EVA	62.2	22.4	87.7
Without compatibilizer	34.1	12.3	84.7
Blend with 5% NR-g-PDMMMP	31.5	11.4	84.8
Blend with 9% NR-g-PDMMMP	28.6	10.3	84.9
Blend with 15% NR-g-PDMMMP	27.5	9.9	84.7
NR	—	—	—

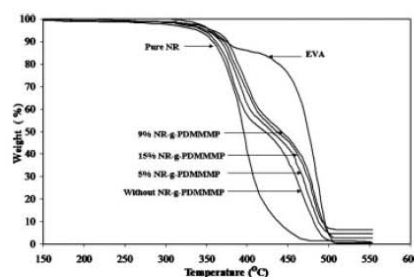


Figure 16. TGA thermograms of NR, EVA, and 40/60 dynamically cured NR/EVA blends with different loading levels of NR-g-PDMMMP compatibilizer.

Table 5. TGA data of NR, pure EVA, and dynamically cured 40/60 NR/EVA blends without and with 5, 9, and 15 wt% of NR-*g*-PDMMMP compatibilizer

Materials	Onset temperature (°C)		Weight loss (%)		Char (%)
	First step	Second step	First step	Second step	
Pure NR	324	—	98.9	—	1.1
Pure EVA	335	395	17.8	82.10	0.01
Without compatibilizer	331	432	40.0	59.3	0.7
Blend with 5% NR- <i>g</i> -PDMMMP	338	440	39.1	58.4	2.5
Blend with 9% NR- <i>g</i> -PDMMMP	368	445	38.7	56.6	4.7
Blend with 15% NR- <i>g</i> -PDMMMP	366	442	38.8	54.9	6.3

Table 4 shows heat of fusion (ΔH), degree of crystallinity (X_c) and crystalline melting temperature (T_m) of EVA phase in the pure EVA and dynamically cured 40/60 NR/EVA blends with various quantities of NR-*g*-PDMMMP compatibilizer. Pure EVA with vinyl acetate content of 18 wt% showed the highest heat of fusion of 62.2 J mol⁻¹ and degree of crystallinity of 22.4%. Furthermore, it is seen that the EVA in the dynamically cured 40/60 NR/EVA blends exhibited lower heat of fusion, degree of crystallinity and crystalline melting temperature than that of the pure polymers. Increasing the loading level of NR-*g*-PDMMMP compatibilizer caused the decreasing trend of heat of fusion and degree of crystallinity while the crystalline melting temperature was more or less constant. This might cause lowering mechanical strength of the blends by incorporating of the blend compatibilizer. However, the dynamically cured 40/60 NR/EVA blend with a loading level of NR-*g*-PDMMMP at 9 wt% exhibited the highest strength. This might be attributed to the compatibilizing effect that plays more significant role on controlling the overall properties of the blends than that of the level of crystallinity of the EVA matrix.

Thermal stability

Thermal stability of dynamically cured 40/60 NR/EVA blends with various loading level of NR-*g*-PDMMMP compared with pure NR and EVA was characterized by TGA under nitrogen atmosphere, as thermograms shown in Fig. 16. The onset degradation temperature of pure NR, EVA, and dynamically NR/EVA blends are summarized in Table 5. It is seen that pure NR showed only single step of weight loss with an onset temperature of approximately 324°C with a total weight loss of approximately 98.9%. That is, approximately 1 wt% char residue remained above 500°C indicated insoluble and intractable materials that might be linked to the cyclized rubber.^[34] On the other hand, the TGA curve of EVA exhibited double degradation stages where the first stage occurred at higher onset temperature of approximately 335°C with the weight loss of 17.8%. This is attributed to the degradation of poly(vinyl acetate) segments in the EVA. The second degradation stage occurred with an onset temperature of approximately 395°C with a total weight loss of 82.1%. This corresponds to the degradation of the polyethylene segments in the EVA. In the dynamically cured 40/60 NR/EVA blends without and with various loading levels of NR-*g*-PDMMMP compatibilizer, the double degradation stages were also observed. The degradation of the blend without compatibilizer occurred at lower onset temperatures of 331 and 432°C and higher total weight loss of 40.0 and 59.3% for the first and second degradation stages, respectively. Among the dynamically cured

40/60 NR/EVA blends, the material with a loading level of NR-*g*-PDMMMP compatibilizer at 9 wt% exhibited the highest onset temperatures at 368 and 445°C with the low values of the weight loss at 38.7 and 56.6% for the first and second degradation stages, respectively. Increasing in onset degradation temperature of the blend with compatibilizer might be due to the ability of dimethylphosphonate functionalized grafts to improve thermal stability of the NR/EVA blend. With this reason, the blend with 15 wt% of NR-*g*-PDMMMP compatibilizer should give higher degradation temperature. However, in Fig. 16 and Table 5, it is clear that this type of blend showed lower degradation temperature than that of the blend with the NR-*g*-PDMMMP at 9 wt%. Hence, this phenomena occurred because greater compatibilizing effect of NR-*g*-PDMMMP in NR/EVA blends. Concerning the remaining residues, it was noted that NR is almost degraded at 500°C.

On the other hand, the proportions in carbonaceous residues (or char) observed at this temperature in the case of degradation of NR/EVA blends always increase with the increasing loading levels of NR-*g*-PDMMMP showing heat stability of the phosphorus compound.

CONCLUSION

NR was chemically grafted with PDMMMP in the presence of DEDT groups previously bound in side position of the rubber. The NR-*g*-PDMMMP with various loading levels (i.e., 1, 3, 5, 7, 9, 12, and 15 wt%) was used as a blend compatibilizer in dynamically cured 40/60 NR/EVA blends. The compatibilizing effect was characterized by dynamic, mechanical, thermal, and morphological properties. Increasing the loading levels of NR-*g*-PDMMMP in the blends caused the increasing elastic modulus and complex viscosity until reaching the maximum values at a loading level of 9 wt%. This is attributed to the compatibilizing effect by covering the interfacial area of the blend compatibilizer. The elastic modulus and complex viscosity were thereafter decreased with the increasing loading levels of NR-*g*-PDMMMP higher than 9 wt%. This is due to the graft copolymer covered majority of interfacial areas with the formation of micelles from the excess amount of NR-*g*-PDMMMP. Therefore, the lubricant effect of the blend system caused the inferior in mechanical and rheological properties of the materials. The smallest vulcanized rubber domains dispersed in the EVA matrix, as two-phase system with the lowest $\tan \delta$ value was also observed in the blend with a loading level of NR-*g*-PDMMMP of 9 wt%. Moreover, the superior tensile strength, elongation at break, and tension set (i.e.,

17.06 MPa, 660 and 27%, respectively) were also observed in the dynamically cured 40/60 NR/EVA blend using this a loading level of NR-g-PDMMMP compatibilizer of 9 wt%. This is attributed to the highest interaction between the phases because of the compatibilizing effect. Incorporation of NR-g-PDMMMP compatibilizer also improved the thermal stability of the blend, as the decomposition temperature was increased with the addition of the graft copolymer. However, the addition of NR-g-PDMMMP in the blends caused the decreasing degree of crystallinity of the EVA phase in the blend but did not cause severe effect on the strength properties.

Acknowledgements

We are grateful to the financial support of Thailand Research Fund (TRF) through the Golden Jubilee Ph.D. Programme (RGJ-PhD) Grant No. PHD/0068/2547 and French Embassy in Thailand.

REFERENCES

- [1] A. Ibrahim, M. Dahlan, *Prog. Polym. Sci.* **1998**, *23*, 665.
- [2] S. Abdou-Sabet, R. P. Patel, *Rubber. Chem. Technol.* **1991**, *64*, 729.
- [3] A. Mousa, U. S. Ishaku, Z. A. M. Ishak, *J. Appl. Polym. Sci.* **1998**, *69*, 1357.
- [4] Z. Wang, X. Zhang, Y. Zhang, *Polym. Test.* **2002**, *21*, 577.
- [5] C. Nakason, P. Wannavilai, A. Kaesaman, *Polym. Test.* **2006**, *25*, 34.
- [6] A. T. Koshy, B. Kuriakose, S. Thomas, C. K. Premalatha, *J. Appl. Polym. Sci.* **1993**, *49*, 901.
- [7] A. T. Koshy, B. Kuriakose, S. Thomas, C. K. Premalatha, S. Varghese, *J. Appl. Polym. Sci.* **1993**, *34*, 3428.
- [8] C. K. Radhakrishnan, A. Sujith, G. Unnikrishnan, A. Thomas, *J. Appl. Polym. Sci.* **2004**, *94*, 827.
- [9] M. K. Yong, H. Ismail, Z. M. Ariff, *Polym. Plast. Tech. Eng.* **2007**, *46*, 361.
- [10] J. K. Lee, T. Y. Lee, C. S. Ha, J. O. Lee, W. J. Cho, *Korea Polym. J.* **1994**, *18*, 61.
- [11] G. G. Bandyopadhyay, S. S. Bhagawan, K. N. Ninan, S. Thomas, *J. Appl. Polym. Sci.* **1999**, *72*, 165.
- [12] A. T. Koshy, B. Kuriakose, S. Thomas, *Polym. Degrad. Stab.* **1992**, *36*, 137.
- [13] P. Jansen, B. G. Soares, *Polym. Degrad. Stab.* **1996**, *52*, 95.
- [14] P. Jansen, M. Amorim, A. S. Gomes, B. G. Soares, *J. Appl. Polym. Sci.* **1995**, *58*, 101.
- [15] S. Songkol, *Chemical modification of epoxidized natural rubber molecules with dibutyl phosphate*. Master of Science Thesis, Prince of Songkla University, Pattani, Thailand, **2007**.
- [16] Z. Oommen, S. Thomas, C. K. Premalatha, B. Kuriakose, *Polymer* **1997**, *38*, 5611.
- [17] Z. Oommen, S. Thomas, *J. Mat. Sci.* **1997**, *32*, 6085.
- [18] P. Suriyachai, S. Kiatkamjornwong, P. Prasassarakich, *Rubber Chem. Technol.* **2004**, *77*, 914.
- [19] S. Chuayijuljit, S. Moosin, P. Potiyaraj, *J. Appl. Polym. Sci.* **2005**, *95*, 826.
- [20] R. Asaletha, M. G. Kumaran, S. Thomas, *Polym. Plast. Technol. Eng.* **1995**, *34*, 633.
- [21] R. Asaletha, G. Groeninckx, M. G. Kumaran, S. Thomas, *J. Appl. Polym. Sci.* **1998**, *69*, 2673.
- [22] H. M. Dahlan, Z. M. D. Khairul, A. Ibrahim, *Polym. Test.* **2002**, *21*, 905.
- [23] H. M. Dahlan, Z. M. D. Khairul, A. Ibrahim, *J. Appl. Polym. Sci.* **2000**, *78*, 1776.
- [24] B. H. Xie, M. B. Yang, S. D. Li, Z. M. Li, J. M. Feng, *J. Appl. Polym. Sci.* **2003**, *88*, 398.
- [25] C. Nakason, W. Sainamsai, A. Kaesaman, P. Klinpituksa, *Songklanakarin J. Sci. Technol.* **2001**, *23*, 415.
- [26] A. M. El-Sayed, H. Afifi, *J. Appl. Polym. Sci.* **2002**, *86*, 2816.
- [27] T. Jeanmaire, Y. Hervaud, B. Boutevin, *Phosphorus Sulfur Silicon Relat. Elem.* **2002**, *177*, 1137.
- [28] M. J. Tsafack, L. Grützmacher, *J. Surf. Coat. Technol.* **2006**, *200*, 3503.
- [29] D. Derouet, P. Intharapat, Q. N. Tran, F. Gohier, C. Nakason, *Eur. Polym. J.* **2009**, *45*, 820.
- [30] H. T. Kim, H. R. Kim, J. K. Kim, J. Y. Park, *Kor. Aust. Rheol. J.* **2001**, *13*, 83.
- [31] L. W. Tang, K. C. Tam, C. Y. Yue, X. Hu, Y. C. Lam, L. Li, *J. Appl. Polym. Sci.* **2004**, *94*, 2071.
- [32] J. Noolandi, K. M. Hong, *Macromolecules* **1984**, *17*, 1534.
- [33] C. Nakason, S. Saiwari, A. Kaesaman, *Polym. Test.* **2006**, *25*, 413.
- [34] R. Asaletha, M. G. Kumaran, S. Thomas, *Polym. Degrad. Stab.* **1998**, *61*, 431.

APPENDIX C

Published Article in e-Polymers. 2009



Compatibilization of NR/EVA blends by natural rubber grafted poly(dimethyl(methacryloyloxymethyl)phosphonate) compatibilizer

Punyanich, Intharapat,^{1,2} Daniel Derouet,² Frédéric Gohier,² Charoen Nakason^{1*}

¹Center of Excellence in Natural Rubber Technology, Department of Rubber Technology and Polymer Science, Faculty of Science and Technology, Prince of Songkla University, Pattani 94000, Thailand; email: ncharoen@bunga.pn.psu.ac.th.

²LCOM-Chimie des Polymère (UMR du CNRS UCO2M N° 6011). Université du Maine, Faculté des Sciences, Avenue Olivier Messiaen, 72085 LE MANS Cedex 9, France.

(Received: 11 October, 2008; published: 15 June, 2009)

Abstract: Graft copolymer of natural rubber (NR) and poly(dimethyl(methacryloyloxymethyl) phosphonate (PDMMMP) (i.e., NR-g-PDMMMP) was prepared and used as a blend compatibilizer in 50/50 NR/EVA simple blends. Influence of various loading levels of NR-g-PDMMMP (i.e., 0, 1, 3, 5, 7, 9, 12 and 15 wt% of NR) on rheological, dynamic, mechanical and morphological properties was investigated. The results showed that the best compatibilization effect was observed in the blend with a loading level of NR-g-PDMMMP at 7 wt%. That is, the highest complex viscosity, tensile strength, elongation at break as well as the lowest values of tension set and $\tan \delta$ value (i.e., damping factor) were observed. This indicates the highest mechanical strength and the supreme elastic response of the material. Morphological properties of 50/50 NR/EVA blends with any loading levels of NR-g-PDMMMP compatibilizer showed co-continuous phase system. However, in the NR/EVA blend with NR-g-PDMMMP at a loading level of 7 wt%, the finest phase morphology was observed. The 50/50 NR/EVA blend with lower and higher loading amounts of NR-g-PDMMMP compatibilizer exhibited inferior dynamic, mechanical properties as well as larger phase morphologies.

Introduction

Blending rubber and thermoplastic is a technique used to prepare materials with desired combinations of properties. However, immiscible polymer blends have been generally encountered. This leads to disadvantages such as poor mechanical properties due to lack of physical and chemical interactions at the interface or phase boundaries as well as poor interfacial adhesion [1]. The immiscible blends are also thermodynamically unstable [2]. It has been well established that the addition of blend compatibilizer such as block or graft copolymers [3-7] makes the immiscible polymer blends more compatible and improves their physical properties [8], creates finer phase morphologies and increases interfacial adhesion [9].

Natural rubber and thermoplastic blends are currently the main interest areas. They have been prepared with various types of blend compatibilizers. For instance, graft copolymer of polypropylene and maleic anhydride (PP-g-MA) and phenolic modified polypropylene (Ph-PP) were used as blend compatibilizers in maleated natural rubber (MNR)/PP blends [10]. The highest shear viscosity, mechanical strength and

elastomeric properties were observed in the TPVs with a loading level of compatibilizers of 5 wt% of PP because of chemical interaction between different phases of MNR and PP in the blend compatibilizers. The phenolic modified polypropylene (Ph-PP) and graft copolymer of maleic anhydride and polypropylene (PP-*g*-MA) were also used as blend compatibilizers in epoxidized natural rubber (ENR)/PP blends [11]. It was found that the blend with compatibilizer exhibited superior mechanical properties (i.e., tensile strength, hardness, and set properties) and showed smaller phase morphology than that of the blend without compatibilizer. Graft copolymer of HDPE and maleic anhydride (i.e., HDPE-*g*-MA) and two types of phenolic modified HDPEs (i.e., PhSP-PE and PhHRJ-PE) prepared by using phenolic resins SP-1045 and HRJ-10518 respectively also showed positive compatibilization in ENR/HDPE blends [12]. Therefore, compatibility of polymer blend depends on the nature of the chemical structure and functional groups presence in the polymer pairs and blend compatibilizers.

Oommen [13] reported the addition of NR-*g*-PMMA as a blend compatibilizer of NR/PMMA blends. It was found that the graft copolymer compatibilized the blend by acting as an emulsifier which locates at the interface and extends the molecular segments into the homopolymer phases. Chattopadhyay [14] studied compatibility of polystyrene (PS) and natural rubber blends by addition of block copolymer of styrene and isoprene (PI-*b*-PS) as a blend compatibilizer using viscometric and phase-separation techniques. It was also claimed that the block copolymer compatibilizer acted as an emulsifier which locates at the interface. Furthermore, El-Sabbagh [15] reported the incorporation of EPDM-*g*-MA compatibilizer in the NR/EPDM blends and found it greatly enhanced blend compatibility.

In the present work, compatibility of NR/EVA simple blends (i.e., the blend without curative) was investigated by the addition of graft copolymer, NR-*graft*-poly(dimethyl(methacryloyloxymethyl)phosphonate) (NR-*g*-PDMMMP). Influence of loading level of NR-*g*-PDMMMP on rheological, dynamic, mechanical and morphological properties of the blends was investigated.

Results and discussion

Preparation of NR-*g*-PDMMMP

¹H-NMR spectrum of NR-*g*-PDMMMP prepared with a level of DEDT-NR unit of 4 mol% with a reaction time of 3 h is shown in Figure 1. It is seen that the proton of carbon-carbon double bond $-\text{C}(\text{CH}_3)=\text{CH}-$ of NR backbone occurred at a chemical shift (δ) of 5.1 ppm (H_a). Also, the presence of the PDMMMP-grafted site indicated by proton of dimethyl and methylenoxy at $\delta = 3.8$ ppm (H_d) and $\delta = 4.25$ ppm (H_c), respectively.

Figure 2 shows infrared spectrum of NR-*g*-PDMMMP. Absorption peaks at 1258, 1052 and 968 cm^{-1} corresponding to the P=O, P-C-O and P-O-CH₃ vibrations in the NR-*g*-PDMMMP, respectively were observed [19]. This confirms the molecular structure of the graft copolymer, NR-*g*-PDMMMP.

Rheological properties

Figure 3 shows complex viscosity as a function of frequency of 50/50 NR/EVA blends with various loading levels of NR-g-PDMMMP compatibilizer. It is seen that the NR/EVA blends showed shear-thinning behaviour. That is evidenced by the decrease in complex viscosity with increasing frequency (or shear rate). The complex viscosity at a given frequency (i.e., 0.38, 0.5 and 1.0 rad/s) is shown in Figure 4. It can be seen that the complex viscosity increased with increasing loading levels of NR-g-PDMMMP until 7 wt% where the maximum value was observed. Further, adding NR-g-PDMMMP higher than 7 wt% caused a decreasing trend of the complex viscosity. It is also seen that the complex viscosity of the 50/50 NR/EVA blends with NR-g-PDMMMP compatibilizer indicates positive deviation blends (PDBs), according to the following log-additive rule [20, 21]:

$$\log \eta_B = \sum_i w_i \log \eta_i \quad (1)$$

where η_i and η_B are the viscosity of the i th component and that of the blend and w_i is the weight fraction of the i th component.

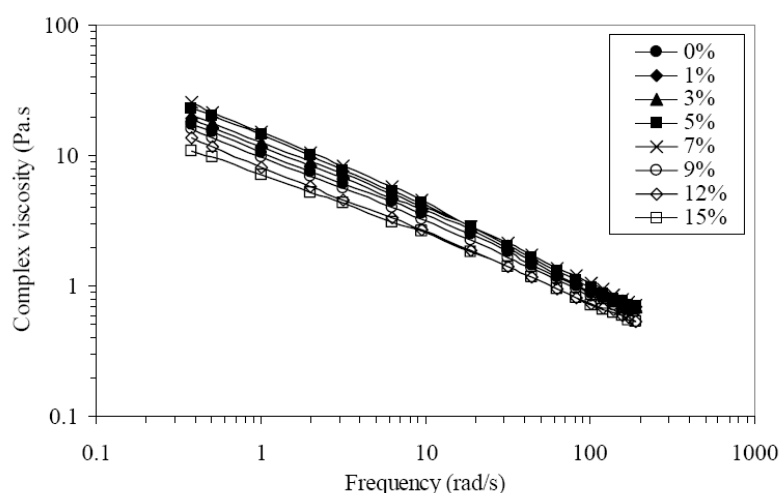


Fig. 3. Complex viscosity as a frequency of 50/50 NR/EVA with various loading levels of NR-g-PDMMMP compatibilizer.

Compatible or partially compatible blends typically lead to a positive deviation in rheological properties, such as viscosity, die swell, etc., and are termed PDBs. It is therefore concluded that the blends of 50/50 NR/EVA with NR-g-PDMMMP compatibilizer were partly compatible blends. This is attributed to interfacial interactions (i.e., polar-polar interaction, H-bonding, dipole-dipole interaction, etc.) between different phases.

During the melt blending, the compatibilizer molecules were forced to locate at the interface of NR and EVA. Therefore, the polar functional groups in NR-g-PDMMMP could interact with polar functional groups in EVA while the NR backbones are

capable of compatibilizing with the NR blend component as the possible interaction shown in Scheme 1.

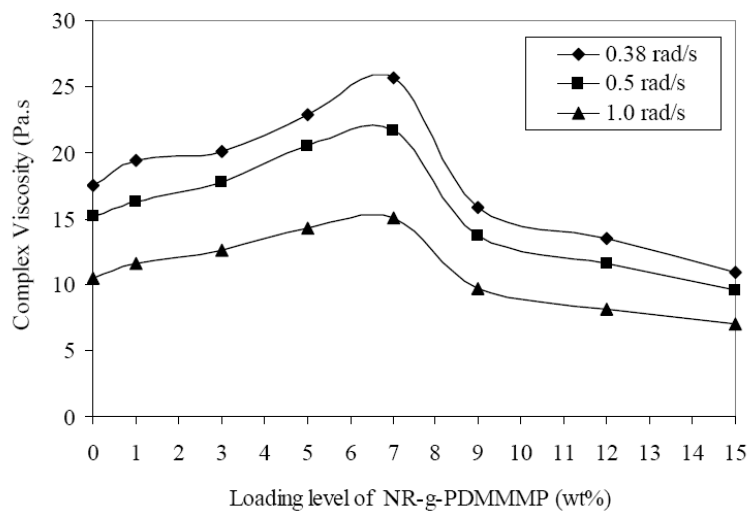
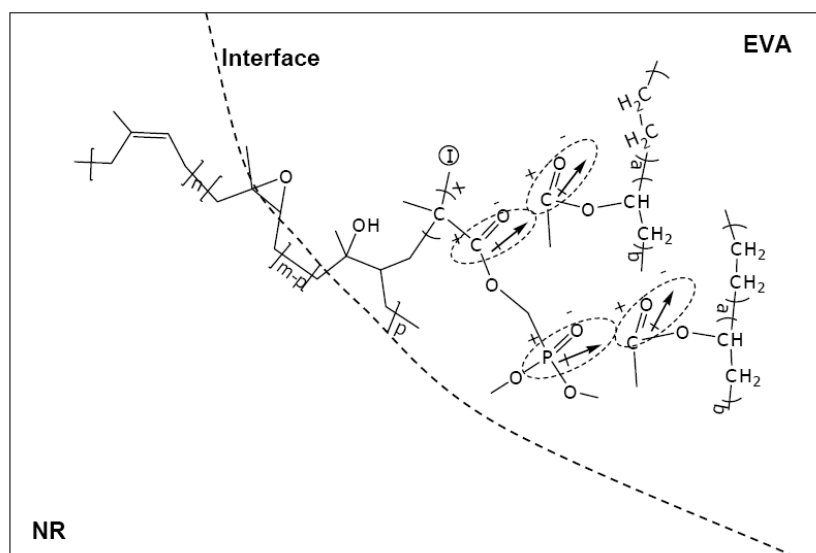


Fig. 4. Complex viscosity of 50/50 NR/EVA blends with various quantities of NR-g-PDMMMP compatibilizer at constant frequencies of 0.38, 0.5 and 1.0 rad/s.



Scheme 1. Possible interaction of NR-g-PDMMMP with EVA and NR at the interface.

This leads to a reduction in interfacial tension and an improvement of interfacial adhesion and hence an increasing level of chemical and physical interaction between the distinct phases (i.e., NR and EVA). Therefore, an increasing trend of complex viscosity was observed with increasing loading level of the NR-g-PDMMMP compatibilizer, as evidenced in Figure 4. However, a decreasing trend of the complex viscosity was observed after loading level of the blend compatibilizer was higher than 7 wt%. This may be attributed to the concentration of the NR-g-PDMMMP reaching above critical micelle concentration (CMC) where the majority of interfacial areas were occupied by the compatibilizer. As a consequence, the formation of micelles or a third component [23-25] was observed at high concentration of NR-g-PDMMMP (i.e., higher than 7 wt%). The micelles could act as lubricant in the blend system, as shown schematically in Figure 5. This could cause a decrease of flow resistance and hence viscosity. Similar phenomena was observed in maleated natural rubber (MNR)/PP blends with PP-g-MA and Ph-PP compatibilizers [10]. In the later case, the log-additive rule successfully predicted the blend compatibility of MNR/PP blends as partially compatible blends.

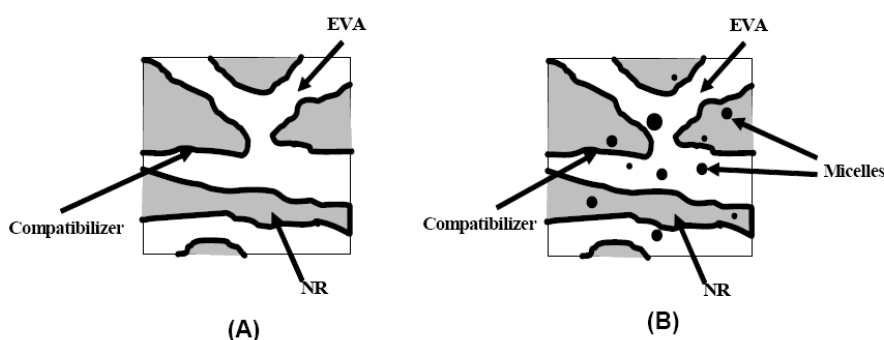


Fig. 5. Schematic representation of the formation of micelles in 50/50 NR/EVA blend above the critical micelle concentration (CMC): (A) optimum level of blend compatibilizer and (B) concentration of blend compatibilizer higher than CMC.

Dynamic properties

Figures 6 and 7 show the variation of storage modulus of 50/50 NR/EVA blends compatibilized with different concentrations of NR-g-PDMMMP. It is seen that the addition of the compatibilizer caused an increasing trend of the storage modulus in the range of 0 to 7 wt% of NR-g-PDMMMP. Increasing concentration of the compatibilizer above 7 wt% caused a decreasing trend of the storage modulus. Therefore, the NR-g-PDMMMP compatibilizer at a loading level 7 wt% exhibited the maximum storage modulus. The result corresponds to the highest complex viscosity in Figure 4. Therefore, the graft copolymer gave the best interaction between the phases at 7 wt% of NR. That is, greater capability of the graft copolymer which located at the interface to interact with both phases and to increase the adhesion between the phases.

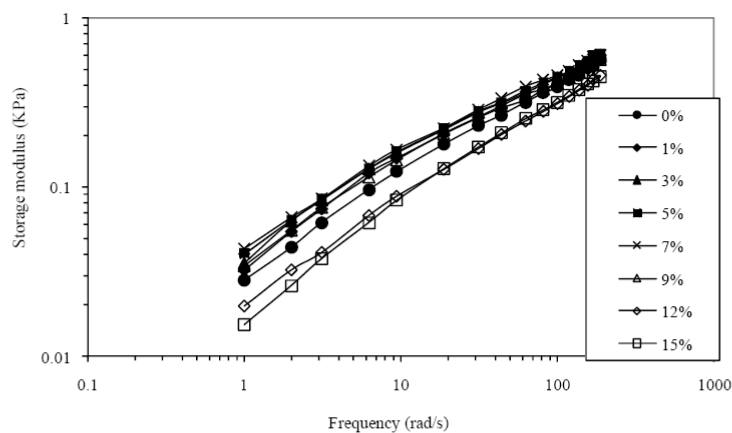


Fig. 6. Storage modulus as a function of frequency for 50/50 NR/EVA blends with various quantities of NR-g-PDMMMP blend compatibilizer.

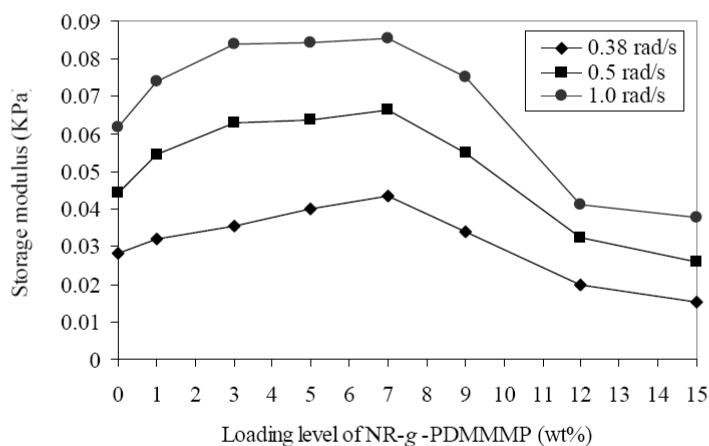


Fig. 7. Storage modulus of 50/50 NR/EVA blends with various quantities of NR-g-PDMMMP compatibilizer at constant frequencies of 0.38, 0.5 and 1.0 rad/s.

Figures 8 and 9 shows $\tan \delta$ values which are the ratio between the loss and the storage modulus (i.e., $\tan \delta = G''/G'$). It is seen that the lowest value of $\tan \delta$ was observed in the blend with 7 wt% of NR-g-PDMMMP compatibilizer. Increasing or decreasing loading level of the NR-g-PDMMMP compatibilizer away from 7 wt% caused an increasing trend of the $\tan \delta$ values. That is, the blend was losing its elasticity or elastic response when higher or lower content of NR-g-PDMMMP than 7 wt% was applied. Therefore, at this loading level of the blend compatibilizer (i.e., 7

wt%), the highest interaction between phases was observed and caused higher elastic response or lower viscous response of the material.

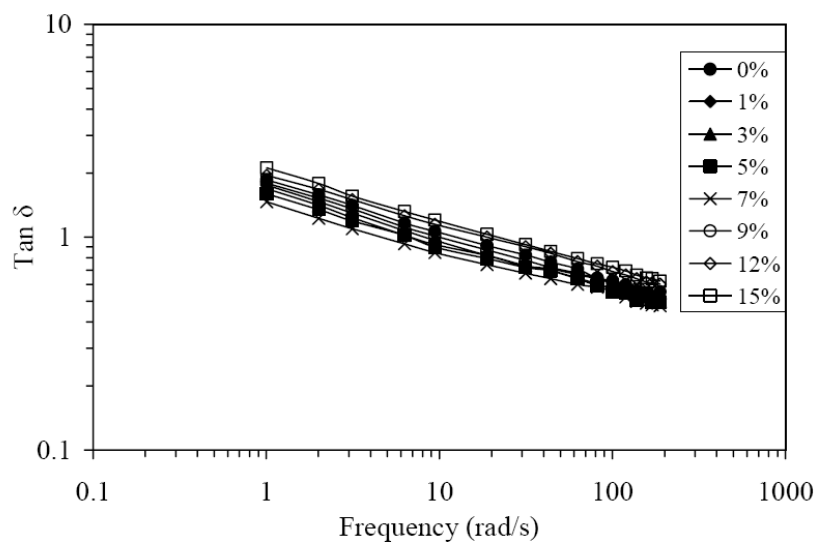


Fig. 8. $\text{Tan } \delta$ as a function of frequency for 50/50 NR/EVA blends with various quantities of NR-g-PDMMMP blend compatibilizer.

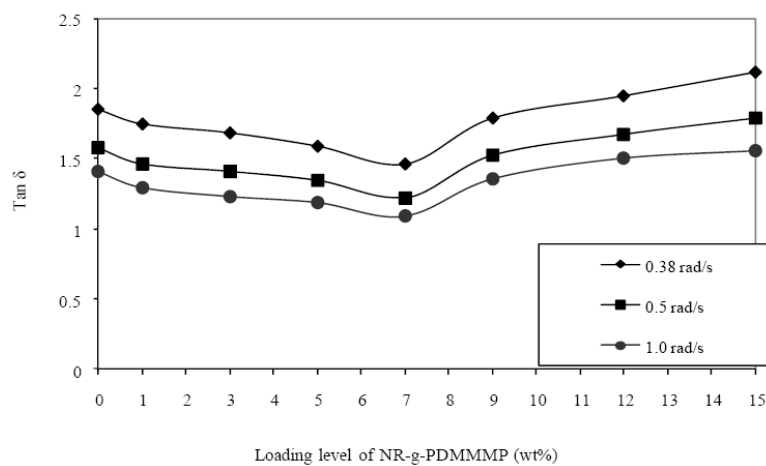


Fig. 9. $\text{Tan } \delta$ of 50/50 NR/EVA blends with various quantities of NR-g-PDMMMP compatibilizer at constant frequencies of 0.38, 0.5 and 1.0 rad/s.

Mechanical properties

The stress-strain curves of 50/50 NR/EVA blends with different loading levels of NR-g-PDMMMP compatibilizer are shown in Figure 10. It is seen that the blend with NR-g-PDMMMP in a range of 9-15 wt% exhibited lower stress and elongation at break as well as area under the curves (i.e., toughness) than that of the blend without compatibilizer. However, the blend with compatibilizer in a range of 1-7 wt% showed higher values of the previous properties with the highest value at a loading level of . NR-g-PDMMMP = 7 wt% of NR. The results correspond to the trend of complex viscosity (Figure 4) and storage modulus (Figure 7). Negative results for the blend with the NR-g-PDMMMP compatibilizer higher than 7 wt% are attributed to formation of micelles as a third blend component, as previously described. They could lubricate and cause the weakness of EVA matrix as evidence from low complex viscosity (Figure 4), storage modulus (Figure 7) and tensile properties (Figure 11), respectively. In Figure 10, it is seen that incorporation of NR-g-PDMMMP in a range of 1-7 wt% caused an increasing trend of stress and elongation at break as well as the area under the curves. Increasing the level of the blend compatibilizer in these ranges possibly allows the blend compatibilizer to gradually cover the interfacial areas. At a loading level of 7 wt%, the blend compatibilizer might have the highest capability to occupy the interface area and creates the highest interfacial force between the NR and EVA interface as a consequence. This is evident from the highest tensile properties, complex viscosity and the lowest $\tan \delta$ (Figure 9) of the blends at this concentration. Figure 11 shows the tensile strength and elongation at break of 50/50 NR/EVA blends with various loading levels of NR-g-PDMMMP compatibilizer. The results confirm the stress-strain at break (Figure 10) where the blend with NR-g-PDMMMP at a loading level of 7 wt% exhibited the highest value of tensile strength and elongation at break (i.e., 6.89 MPa and 605%, respectively). Higher and lower loading levels of the NR-g-PDMMMP than 7 wt% caused a decreasing trend of tensile strength and elongation at break.

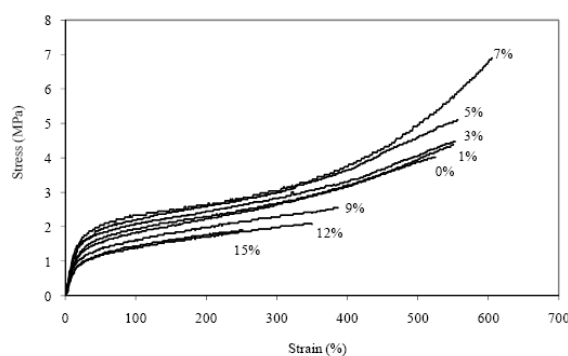


Fig. 10. Stress strain behaviour of 50/50 NR/EVA blends with different quantities of NR-g-PDMMMP.

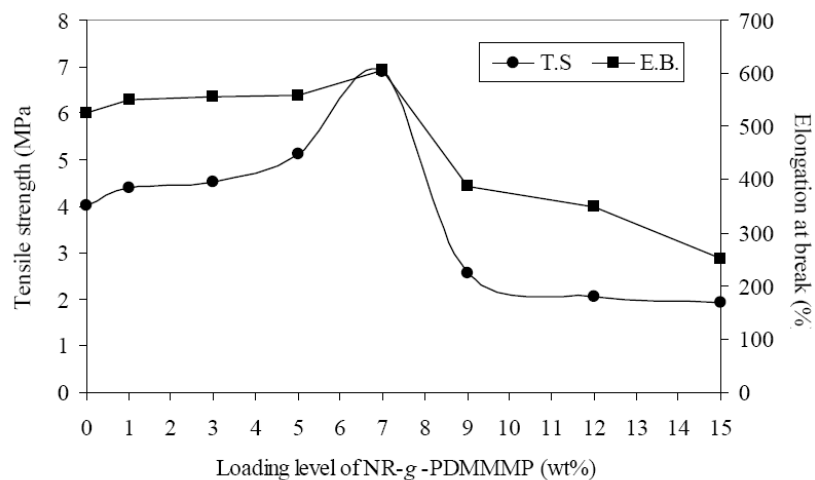


Fig. 11. Tensile strength and elongation at break of 50/50 NR/EVA blend with different quantities of NR-g-PDMMMP compatibilizer.

Figure 12 shows tension set of the 50/50 NR/EVA blends with various loading levels of NR-g-PDMMMP compatibilizer. It is seen that the lowest tension set value was observed in the blend with 7 wt% of NR-g-PDMMMP compatibilizer.

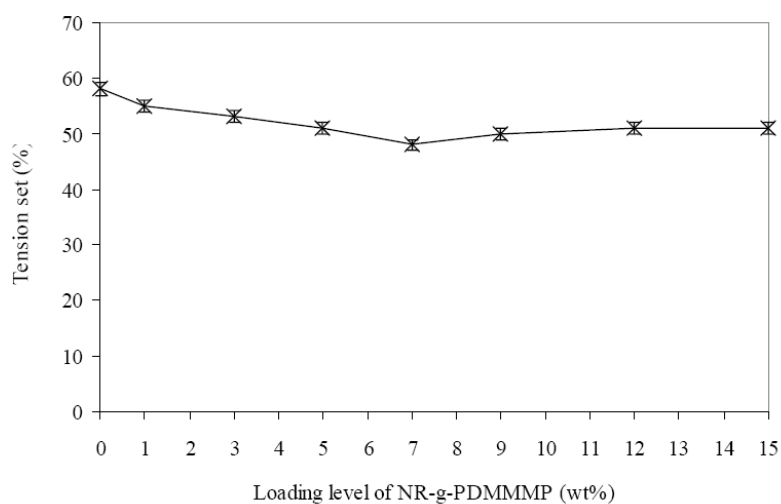


Fig. 12. Tension set of 50/50 NR/EVA blends with different quantities of NR-g-PDMMMP compatibilizer.

This confirms the saturation and occupancy of the interfacial areas by the blend compatibilizer component without generating the third blend component (or micells), as evidenced by the previous properties (i.e., rheological and dynamic properties). Also, inferior levels of the properties were observed at a loading of NR-g-PDMMMP lower than 7 wt%. In the later case, the interface might not be fully occupied and covered by the blend compatibilizers. Therefore, lower interaction between the phases would be a consequence. Also, the addition of compatibilizers higher than 7 wt% showed similar inferior properties due to a formation of a third phase which acts as a lubricant and weak point for stress concentration and hence failure. The trend of tension set values at different loading levels of compatibilizer is similar to the trend of $\tan \delta$ (Figure 9). That is, the greatest elastomeric properties were observed at a loading level of blend compatibilizer of 7 wt% based on NR.

Morphological properties

Effect of loading level of NR-g-PDMMMP compatibilizer on morphological properties of 50/50 NR/EVA blends is shown in Figure 13. It can be seen that all types of 50/50 NR/EVA blends showed co-continuous phase morphology where both phases are continuous phase.

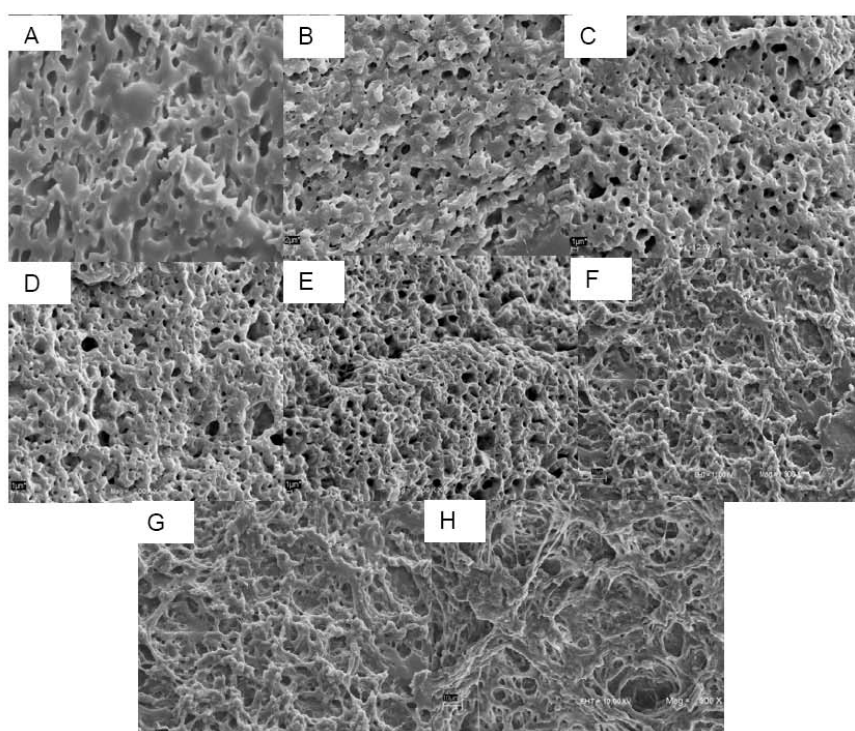


Fig. 13. SEM micrographs of 50/50 NR/EVA blends: (A) without compatibilizer, (B) 1%, (C) 3%, (D) 5%, (E) 7%, (F) 9%, (G) 12% and (H) 15 wt% of NR-g-PDMMMP blend compatibilizer.

The cavitation represents the NR phase which was previously removed by means of extraction. It is clear that the addition of the compatibilizer at a loading level 7 wt% caused the blend to have the smallest phase size. This is attributed to the presence of optimum level of the graft copolymer at the interfacial region through the penetration of the copolymer chain segments into the corresponding adjacent phases. As a result, an increase of the interfacial adhesion between the NR phase and EVA phase was observed. The blend compatibilizer might also play a significant role on suppression of coalescence of new formed particles and cause the stabilization of the blend morphology.

On the other hand, slightly increasing cavitation sizes were observed in the blend with loading levels of NR-g-PDMMMP lower than 7 wt%. It is possibly because of lower interaction between the phases. Therefore, NR phase is more readily removed by means of the extraction. In the case of the blend with NR-g-PDMMMP higher than 7 wt%, the soluble third component of the NR-g-PDMMMP might also cause larger cavitation. Size of phase morphology may be correlated to rheological, mechanical and dynamic properties. It is seen that the blend with NR-g-PDMMMP compatibilizer at a loading level of 7 wt% exhibited the smallest phase morphology. The highest complex viscosity (Figure 4), storage modulus (Figure 7), tensile strength and elongation at break (Figure 11) as well as the lowest $\tan \delta$ (Figure 9) and tension set (Figure 12) were observed.

Experimental part

Materials

Natural rubber (NR) used as a blend component was an air dried sheet (ADS) manufactured by the Khuan Pun Tae Farmer Co-operation, Phattaluang, Thailand. Ethylene vinyl acetate copolymer (EVA) used as another blend component was manufactured by the TPI Polyacrylate Co., Ltd. (Rayong, Thailand). It was N8038 EVA with 18 wt% vinyl acetate content, melt index of 2.3 g /10 min at 190 °C and density of 0.941 g/cm³. Dimethyl(methacryloyloxymethyl)phosphonate (DMMMP) monomer used to prepare the NR-g-PDMMMP was prepared according to the previous work [16,17].

Preparation of NR-g-PDMMMP

NR-g-PDMMMP was prepared through a two step process. First, the addition of sodium N,N-diethyldithiocarbamate (DEDT) onto epoxidized natural rubber units in a latex medium was carried out according to the procedure previously described [18]. This was to create macroinitiators at 4.0 mol% of N,N-diethyldithiocarbamate groups in the rubber chains (DEDT-NR). Second, the grafting reactions of DMMMP monomer onto NR backbone in a form of DEDT-NR were carried out at room temperature under nitrogen atmosphere in 250 ml reactor equipped with a magnetic stirrer and closed by a screwed stopper with a joint seal covered with Teflon. A UV lamp with a wavelength of approximately 366 nm was used to initiate the grafting reaction. A [DMMMP]/[DEDT-NR] ratio used in this study was fixed at 5/1 with a reaction time of 3 h. After reaction, the polymer was coagulated in methanol, and then dried in vacuum oven for 24 h at 40 °C. The phosphonated homopolymer was removed by extraction with methanol. The graft copolymer was then recovered by precipitation with ethanol, filtered, and then dried in vacuum oven for 24 h at 40 °C until a constant

weight. 1H-NMR and FT-IR spectroscopy were later used to characterize the graft copolymer.

Blend preparation

The simple blend (i.e., blend without curative) of 50/50 NR/EVA was prepared by melt-mixing in internal mixer with a mixing chamber of 80 cm³, a Brabender Plasticorder, model PLE 331 (Brabender OHG, Duisburg, Germany) at 140 °C and a rotor speed of 60 rpm. Influence of loading level of blend compatibilizer, NR-g-PDMMMP (i.e., 1, 3, 5, 7, 9, 12 and 15 wt% of NR) was studied. Blend formulations and mixing schedule are shown in Table 1. The blended products were later fabricated by compression molding at 120 °C for 5 min to prepare specimens for various tests and characterization.

Tab. 1. Blend formulation and mixing schedule.

Blend component	Quantities (wt%)	Mixing schedule (min.)
EVA	50	2
NR	50	3
NR-g-PDMMMP	Varied*	3

*0, 1, 3, 5, 7, 9, 12, 15 wt% of NR

Dynamic properties

Dynamic properties were investigated by moving die processability tester (RheoTech MDPT, Tech-Pro, Inc., Cuyahoga Falls, USA) with a conical shape die which produces a uniform shear strain on the test specimen. The sample size of 30x30x3 mm was loaded onto the lower die and then the upper die was closed to form a constant volume. The test was performed using a frequency sweep mode in the range of 0.3-190 rad/s, with a constant strain at 3%. This is to assure a linear viscoelasticity of the test. The storage (G') and loss shear (G'') moduli, loss factor, $\tan \delta = G''/G'$ as well as the complex viscosity (i.e., $\eta^* = 3G^*/\omega = \eta'' + i\eta'$) of the blends were characterized.

Tensile properties

Tensile strength, elongation at break and tension set properties of the 50/50 NR/EVA blends were measured at 25 °C according to the ASTM D412 specification using dumb-bell shape (die c) test specimens at a crosshead speed of 500 mm/min using a Hounfield Tensometer, model H 10 KS (Hounsfield Test Equipment Co., Ltd, UK.).

Morphological characterization

Scanning electron microscopy, model JSM-5800 LV (Jeol USA Inc., Peabody, Massachusetts, USA) was used to perform morphological characterization. The samples were cryogenically cracked to produce new surfaces in liquid nitrogen. The fractured surfaces were then etched with toluene to preferential extract the NR phase. The sample was then dried in hot air oven at 40 °C for 48 h. The dried samples were sputter-coated with gold and examined using a scanning electron microscope.

Acknowledgements

We are grateful to the Thailand Research Fund (TRF): Grant no: PHD/0068/2547 and French Embassy in Thailand for financial support.

References

- [1] George, S.; Ramamurthy, K.; Anand, J.S.; Groeninckx, G.; Varughese, K.T.; Thomas, S. *Polymer*. **1999**, *40*, 4325.
- [2] Utracki, L.A. In: *Polymer blends handbook*, vol.1. Kluwer Academic, Dordrecht, **2002**.
- [3] Oommen, Z.; Thomas, S. *J. Appl. Polym. Sci.* **1997**, *65*, 1245.
- [4] Ohlsson, B.; Hassander, H.; Törnell, B. *Polymer*, **1998**, *39*, 6705.
- [5] Datta, S.; Lohse, D.J., In: *Polymeric Compatibilizers: uses and benefits in polymer blends*. Hanser, Munich, **1996**.
- [6] Nakason, C.; Wannavilai, P.; Kaesaman, A. *J. Appl. Polym. Sci.* **2006**, *100*, 4729.
- [7] Chuayjuljit, S.; Moolsin, S.; Potiyaraj, P. *J. Appl. Polym. Sci.* **2005**, *95*, 826.
- [8] Bonner, J.G.; Hope, P.S. *Polymer blends and Alloys*, In: M.J. Folkes, P.S. Hope. (Eds.), Chapman and Hall. **1993** (Chapter 3)
- [9] George, S.; Joseph, R.; Thomas, S.; Varughese, K.T. *Polymer*. **1995**, *36*, 4405.
- [10] Nakason, C.; Saiwari, S.; Kaesaman, A. *Polym. Test.* **2006**, *25*, 413.
- [11] Nakason, C.; Wannavilai, P.; Kaesaman, A. *Polym. Test.* **2006**, *25*, 34.
- [12] Nakason, C.; Jarnthong, M.; Kaesaman, A.; Kiatkamjornwong, S. *J. Appl. Polym. Sci.* **2008**, *109*, 2694.
- [13] Oommen, Z.; Thomas, S. *J. Mater. Sci.* **1997**, *32*, 6085.
- [14] Chattopadhyay, S. *J. Appl. Polym. Sci.* **2000**, *77*, 880.
- [15] El-Sabbagh, S.H. *Polym. Test.* **2003**, *22*, 93.
- [16] Liepins, R.; Surles, J.R.; Morosoff, N.; Stannett, V.; Duffy, J.J.; Day, F.H. *J. Appl. Polym. Sci.* **1978**, *22*, 2403.
- [17] Jeanmaire, T.; Hervaud, Y.; Boutevin, B. *Phosphorus Sulfur and Silicon*. **2002**, *177*, 1137.
- [18] Derouet, D.; Tran, Q.N.; Ha Thuc, H. *Eur. Polym. J.* **2007**, *43*, 1806.
- [19] Tsafack, M.J.; Levalois-Grützmacher, J. *Surf. Coat. Technol.* **2006**, *201*, 2599.
- [20] Nakason, C.; Saiwari, S.; Kasaman, A. *Polym. Eng. Sci.* **2006**, *46*, 594.
- [21] Kundu, P.P.; Tripathy, D.K.; Gupta, B.R. *J. Appl. Polym. Sci.* **1996**, *61*, 1971.
- [22] Utracki, L.A. *Polym. Eng. Sci.* **1983**, *23*, 602.
- [23] Oommen, Z.; Groeninckx, G.; Thomas, S. *J. Polym. Sci. B: Polym. Phys.* **2000**, *38*, 525.
- [24] George, S.; Ramamurthy, K.; Anand, J.S.; Groenickx, G.; Varughese, K.T.; Thomas, S. *Polymer*. **1999**, *40*, 4325.
- [25] Thitithammawong, A. Noordermeer, J.W.M. Kaesaman, A. Nakason, C. *J. Appl. Polym. Sci.* **2008**, *107*, 2436.

BIOGRAPHY

Name Punyanich Intharapat

Student ID 4748001

Educational attainment

Degree	Name of Institution	Year of Graduation
B.Sc (Rubber Technology)	Prince of Songkla University	2000-2004
First Class Honors		

Scholarship awards during enrolment

1. The Thailand Research Fund (TRF)-the Royal Golden Jubilee (RGJ) Ph.D. Program (Grant No. PHD/0068/2547)
2. French Government via the Embassy in Thailand.
3. The Graduate school, Prince of Songkla University, Pattani.

List of publications and communications

Scientific Papers:

1. Derouet D., Intharapat P, Tran Q N, Gohier F, Nakason C. 2009. Graft copolymers of Natural Rubber and Poly(dimethyl(acryloyloxy-methyl)phosphonate) (NR-g-PDMAMP) or Poly(dimethyl(methacryloyloxy-ethyl)phosphonate) (NR-g-PDMMEP) from photopolymerization in latex medium, European Polymer Journal, volume 45, issue 3, 2009, Pages 820-836.
2. Intharapat P, Derouet D, Gohier F, Nakason C. 2009. Compatibilization of natural rubber and EVA blend with NR-g-PDMMMP: Influence of loading level of compatibilizer, e-Polymers Journal, Volume 75, 2009, Pages 1-14.
3. Intharapat P, Derouet D, Nakason C. 2009. Dynamically cure NR/EVA blends: Influence of NR-g-poly(dimethyl(methacryloylmethyl)phosphonate compatibilizer. Polymers for Advanced Technologies, 2009.
4. Intharapat P, Derouet D, Nakason C. 2009. Thermal and flame resistance properties of natural rubber grafted with polydimethyl(methacryloyloxy-methyl)phosphonate. Journal of Applied Polymer Science, *Inpress*.

5. Intharapat P, Derouet D, Nakason C. 2009. Influence of blend proportion on properties of dynamically cured NR/EVA blends. *Journal of Applied Polymer Science*, submitted.

Conference proceeding:

1. Intharapat P., Nakason C. and Derouet D. 2005. Thermoplastic vulcanizate based on EVA/Dibutyl phosphate supported natural rubber. Proceeding of the RGJ Seminar series XXXV. Faculty of Pharmaceutical sciences, Prince of Songkla university, Songkla, Thailand, 19 August. (Oral presentation)
2. Intharapat P., Nakason C. and Derouet D. 2006. Preparation of Natural rubber/Ethylene vinyl acetate blend compatibilized with natural rubber functionalized dialkyl (or aryl) phosphate. Proceeding of the Second Thai-France seminar Rubber: From Tree to End products under the Thai-France research cooperative program. Century park hotel, Bangkok, Thailand. 1-2 June. (Oral presentation)
3. Intharapat P., Nakason C. and Derouet D. 2006. Thermoplastic natural rubber based on dialkyl (or aryl) phosphates supported natural rubber and ethylene vinyl acetate blends. Proceeding of the 1st World Rubber Summit "Tapping opportunities-Realizing the potential". Impack convention and exhibition center, Bangkok, Thailand. 28 July (Oral presentation)
4. Intharapat P., Nakason C. and Derouet D. 2008. Chemical modification of natural rubber with dimethyl 1-(acryloyloxymethyl)phosphonate and dimethyl 1-(methacryloyloxyethyl)phosphonate by grafting photopolymerization in latex medium. Proceeding of the RGJ-Ph.D Congress IX. Jomtien Palm beach resort, Pattaya, Chonburi, Thailand. 4-6 April. (Poster presentation)
5. Intharapat P., Nakason C. and Derouet D. 2008. Grafting of natural rubber with dimethyl 1-(acryloyloxymethyl)phosphonate and dimethyl 1-(methacryloyloxyethyl)phosphonate by grafting photopolymerization in latex medium. Rubber technology conference, Prince of Songkla university, Songkla, Thailand. 3 March (Oral presentation)